F 1503/2

BULETINUL INSTITUTULUI POLITEHNIC DIN IAȘI

L: 040723

Tomul XXXI (XXXV)

Fasc. 1–4

Secția II

CHIMIE ȘI INGINERIE CHIMICĂ

1985

OMSZÁGOS MŰSZAKI INFORMÁCIÓS KÖZPONT ÉS KÖNYVTÁR 1983

BULETINUL INSTITUTULUI POLITEHNIC DIN IAŞI

Tomul XXXI (XXXV)

Fasc. 1–4

Secţia II

CHIMIE ŞI INGINERIE CHIMICĂ

1985

COLEGIUL DE REDACŢIE

Prof. dr. CAMELUŢA BELDIE (preşedinte)
Prof. dr. ing. ADRIAN RADU
Prof. dr. ing. M. GAFIŢANU
Conf. dr. ing. D. LIUŢE
Prof. dr. doc. D. MANGERON
Prof. dr. ing. GH. MAXIM
Acad. prof. dr. doc. CRISTOFOR SIMIONESCU
Prof. dr. doc. GH. CHIRIŢĂ
Prof. dr. doc. VALERIU BLIDARU

COMITETUL DE REDACŢIE AL SECŢIEI
II. CHIMIE ŞI INGINERIE CHIMICĂ

Prof. dr. doc. RADU TUDOSE
Prof. dr. ANGELA POPA
Conf. dr. ing. I. ROŞCA
Conf. dr. ing. SPIRIDON OPREA

REDACŢIA

Prof. dr. doc. D. MANGERON
(redactor responsabil)
Prof. dr. ing. HUGO ROSMAN
(secretar)
Conf. dr. ing. VICTOR BULACOVSCHI
(redactor)
ECATERINA IRIMIEA
(tehnoredactor)

BULETINUL INSTITUTULUI POLITEHNIC DIN IAŞI
BULLETIN OF THE POLYTECHNIC INSTITUTE OF JASSY
ИЗВЕСТИЯ ЯССКОГО ПОЛИТЕХНИЧЕСКОГО ИНСТИТУТА
Tomul XXXI (XXXV), Fasc. 1—4 1985

Secţia II

CHIMIE ŞI INGINERIE CHIMICĂ

SUMAR

Pp.

N. CALU, A.-R. IORDAN şi I. SANDU, Sistemul Ni(II) — izopropanolamină (I) (franc., rez. rom.) 7

I. ROŞCA, E. ŞTEFANCU şi M. PALAMARU, Studiul formării compuşilor Fe(III) cu derivaţii cloruraţi ai acidului acetic (rom., rez. franc.) . . . 13

A. BOLD, A. POPA şi D. BÎLBĂ, Comportarea unor elemente di- şi trivalente pe vionit CS-3 în sistemul apă—HNO_3 — solvent organic (engl., rez. rom.) 19

L. PĂUNESCU, Complecşi ai 2-metionin fenotiazinei (franc., rez. rom.) . . . 25

O. VICOL, N. HURDUC şi M. NOROC, Combinaţii complexe ale Pd (II) cu histidina (engl., rez. rom.) 29

D. P. ULRICH (R. D. Germană), Influenţa solvenţilor asupra comportării electrozilor (engl., rez. rom.) 35

A. TARHON, N. AELENEI şi M. ŞCHIOPU, Contribuţii la studiul echilibrului chimic pentru formarea oxidului de azot (engl., rez. rom.) 41

AL. SZÉP, C. CALISTRU, L. IFRIM şi GH. MIHĂILĂ, Cercetarea procesului de sublimare a clorurii de amoniu (II) (rom., rez. engl.) 47

C. HAGIU şi I. GRIGORIU, Studiul hidrodinamicii formării bulelor în sistemele apă—aer şi acid fosforic—aer (rom., rez. engl.) 53

R. SMOCOT, A. TALABĂ, I. ENESCU, D. BOTEZATU şi A. BIALUS, Plăci ceramice din argilă de Vlădiceni (fr., rez. rom.) 57

M. CRUCEANU, E. POPOVICI şi M. ALEXANDROAEI, Zeoliţi sintetici în formă de amoniu (engl., rez. rom.) 63

N. NAUM, GH. MIHĂILĂ şi N. BÎLBĂ, Hidrodeclorurarea tetraclorurii de carbon pe catalizatori zeolitici cu nichel (engl., rez. rom.) 67

P. ONU, C. LUCA, V. ABABI şi A. COSĂVEANU, Studiul posibilităţilor de valorificare a subproduselor de la oxidarea ciclohexanului (rom., rez. rus.) 71

GH. SURPĂŢEANU, M. CONSTANTINESCU, I. ZUGRĂVESCU, A. LABLACHE-COMBIER (Franţa) şi J. P. CATTEAU (Franţa), Calculul sarcinilor atomice totale utilizînd iteraţia E.H. şi metoda ESCA (engl., rez. rom.) 77

AL. CAŞCAVAL, Compuşi organici ai sulfului. XV. 2-hidroxicetone. X. O nouă reacţie Mannich aplicată unor derivaţi conţinînd sulf ai 3′, 5′-diclor-2′-hidroxi-acetofenonei (engl., rez. rom.) 81

C. ONISCU, M. CHIRIŢĂ şi FL. IRIMIE, Studiul cinetic al procesului de esterificare a acizilor clorfenoxi-α-propionici (franc., rez. rom.) 87

FL. VITAN şi R. Z. TUDOSE, Curgerea lichidelor în filme subţiri (V) (rom., rez. engl.) 95

RECENZII 101

BULETINUL INSTITUTULUI POLITEHNIC DIN IAŞI
BULLETIN OF THE POLYTECHNIC INSTITUTE OF JASSY
ИЗВЕСТИЯ ЯССКОГО ПОЛИТЕХНИЧЕСКОГО ИНСТИТУТА
Tom XXXI (XXXV), Fasc. 1–4 1985

Section II

CHEMISTRY AND CHEMICAL ENGINEERING

CONTENTS

Pp.

N. CALU, A.-R. IORDAN et I. SANDU, Le système Ni(II) — isopropanolamine (I) (French, Romanian summary) 7
I. ROŞCA, E. ŞTEFANCU et M. PALAMARU, L'étude de la formation des composés Fe(III) avec des acides chloracétiques (Romanian, French summary) 13
A. BOLD, A. POPA and D. BÎLBĂ, Behaviour of certain Di- and Trivalent Ions on Vionit CS-3 from the Wather — Nitric Acid — Organic Solvent Media (English, Romanian summary) 19
L. PĂUNESCU, Complexes du 2-méthionine phénothiazinium (French, Romanian summary) 25
O. VICOL, N. HURDUC and M. NOROC, Complex Compounds of Pd(II) with Histidine (English, Romanian summary) 29
U.P. DECKER (German Democratic Republic), Influence of Solvents on the Behaviour of Electrodes (English, Romanian summary) 35
A. TARHON, N. AELENEI and M. ŞCHIOPU, Contribution to the Study of Chemical Equilibrium in the Formation of Nitrogen Oxide (English, Romanian summary) 41
AL. SZÉP, C. CALISTRU, L. IFRIM and GH. MIHĂILĂ, Study of the Ammonium Chloride Sublimation Process (Romanian, English summary). . . 47
C. HAGIU and I. GRIGORIU, Hydrodynamic Study on Bubble Formation in Air—Water and Air—Phosphoric Acid Systems (Romanian, English summary) 53
R. SMOCOT, A. TALABĂ, I. ENESCU, D. BOTEZATU et A. BIALUS, Plaques céramiques de l'argile de Vlădiceni (French, Romanian summary). 57
M. CRUCEANU, E. POPOVICI and M. ALEXANDROAEI, Synthetic Zeolites in the Ammonium Form (English, Romanian summary). 63
N. NAUM, GH. MIHĂILĂ and N. BÎLBĂ, Hydrodechlorination of Carbon Tetrachloride over Nickel Zeolite Catalysts (English, Romanian summary) . 67
P. ONU, C. LUCA, V. ABABI and A. COSĂVEANU, Research on the Possibilities Waste Recovery from the Ciclohexane Oxidation (Romanian, Russian summary) 71
GH. SURPĂŢEANU, M. CONSTANTINESCU, I. ZUGRĂVESCU, A. LABLACHE-COMBIER (France) and J. P. CATTEAU (France), The Calculus of Total Atomic Charges Using E. H. Iterate and ESCA Methods (English, Romanian summary) 77
AL. CAŞCAVAL, Organic Sulphur Compounds. XV. 2-Hydroxyketones. X. New Mannich Reaction of some Derivatives containing Sulphur of 3′, 5′-Dichloro-2′-hydroxy-acetophenone (English, Romanian summary) . . . 81
C. ONIŞCU, M. CHIRIŢĂ et F. IRIMIE, L'étude cinétique du processus d'estérification des acides chlore-phénoxi-α-propioniques (French, Romanian summary) 87
F. VITAN and R. Z. TUDOSE, Flow of Liquids in Thin Films (V) (Romanian, English summary) 95
BOOK REVIEWS 101

BULETINUL INSTITUTULUI POLITEHNIC DIN IAŞI
BULLETIN OF THE POLYTECHNIC INSTITUTE OF JASSY
ИЗВЕСТИЯ ЯССКОГО ПОЛИТЕХНИЧЕСКОГО ИНСТИТУТА
Том XXXI (XXXV), Вып. 1—4 1985

Секция II

ХИМИЯ И ХИМИЧЕСКАЯ ПРОМЫШЛЕНОСТЬ

СОДЕРЖАНИЕ

Стр.

Н. КАЛУ, А.-Р. ЙОРДАН и И. САНДУ, Система Ni(II) — изопропаноламина (франц., рез. рум.) 7

И. РОШКА, Э. ШТЕФАНКУ и М. ПАЛАМАРУ, Изучение образования соединений Fe(III) с дериватами хлоруксусных кислот (рум., рез. франц.) 13

А. БОЛД, А. ПОПА и Д. БЫЛБЭ, Поведение нескольких би- и тривалентных элементов на Вионите CS-3 системе: вода— HNO_3 — органический растворитель (англ., рез. рум.) 19

Л. ПЭУНЕСКУ, Некоторые комплексы 2-метионин фенотиазины (франц., рез. рум.) 25

О. ВИКОЛ, Н. ХУРДУК и М. НОРОК, Комплексные соединения Pd(II) с чистидином (англ., рез. рум.) 29

У. П. ДЕККЕР (ГДР), Влияние растворителей на проведение электродов (англ., рез. рум.) 35

А. ТАРХОН, Н. АЕЛЕНЕЙ и М. ШКЙОПУ, Достижения в изучении химического равновесия для получения монокиси азота (англ., рез. рум.) 41

АЛ. СЕП, К. КАЛИСТРУ, Л. ИФРИМ и Г. МИХЭИЛЭ, Исследование процесса сублимация хлорида аммония (II) (рум., рез. англ.) . 47

К. ХАДЖИУ и И. ГРИГОРИУ, Изучение гидродинамики образования пузырьев в системах воды — воздуха и фосфорной кислоты — воздуха (рум., рез. англ.) 53

Р. СМОКОТ, А. ТАЛАБЭ, И. ЭНЕСКУ, Д. БОТЕЗАТУ и А. БЯЛУС, Керамические пластинки из глины от Влэдичень (фр., рез. рум.). 57

М. КРУЧЯНУ, Э. ПОПОВИЧ и М. АЛЕКСАНДРОАЕЙ, Синтетический цеолиты в форме аммония (англ., рез. рум.) 63

Н. НАУМ, Г. МИХЭИЛЭ и Н. БЫЛБЭ, Гидродехлорирование четыреххлористого углерода на никеловых цеолитных катализатора (англ., рез. рум.) 67

Г. СУРПЭЦЯНУ, М. КОНСТАНТИНЕСКУ, И. ЗУГРЭВЕСКУ, А. ЛАБЛАШ-КОМБЬЕ (Франция) и Ж. П. КАТТО (Франция), Частот атомных заряд методами E.H. и ESCA (англ., рез. рум.) . . 71

П. ОНУ, К. ЛУКА, В. АБАБИ и А. КОСЭВЯНУ, Изучение возможностей использования побочных продуктов полученных при окисления циклогексаноля (рум., рез. рус.) 77

АЛ. КАШКАВАЛ, Серусодержание соединение. XV. 2-Гидроксикетоны. X. Новые Маннних реакция некоторых серусодержание 3′, 5′-дихлоро -2′- гидроксиацетофенон (англ., рез. рум.) 81

К. ОНИСКУ, М. КИРИЦЭ и Ф. ИРИМИЕ, Кинетика процесса этерификации хлор, феноски - α - протионовы кислот (франц., рез. рум.) . 87

Ф. ВИТАН и Р. З. ТУДОСЕ, Тонко-пеликулярное течение жидкости (V) (рум., рез. англ.) 95

РЕЦЕНЗИЙ 101

BULETINUL INSTITUTULUI POLITEHNIC DIN IAŞI
BULLETIN OF THE POLYTECHNIC INSTITUTE OF IASSY
ИЗВЕСТИЯ ВОСКОГО ПОЛИТЕХНИЧЕСКОГО ИНСТИТУТА
Том XXXI (XXXV), Вып. 1–4 1955

Секция II

ХИМИЯ И ХИМИЧЕСКАЯ ПРОМЫШЛЕННОСТЬ

СОДЕРЖАНИЕ

Стр.

И. КЛАУЗ, А.Р. ВОРЛАЙ и И. САНДУ, Система ZnCl₂ — вопросы образования фаз. (рис., рез. рум.) 7

И. РОШКА, З. ШТЕФАНЕСКУ и М. НАТАНАРЭ, Изучение образования соединений Fe(III) с перманганат-хлорид-ионами (рум., рез., рис.) 13

А. ПОПА, А. ПОНА и Д. БЛАЗИУ, Поведение ионов-ингибиторов би- и тримолибдат-ионов на Бицинте (Cr-3 системе) вода — H₂SO₄ — ортофосфорная кислота (англ., рез., рум.) 19

Д. ПЭУНЕСКУ, Некоторые комплексы 2-метилхинолин-фуксотиазина (франц., рез., рум.) 25

О. ВИРОЛ и К. ХУРДУЗЕ и М. ПОПОВ, Комплексные соединения Pd(II) с тиоэтанолом (англ., рез., рум.) 29

А. И. ЛЕВИЕВ (СЦЕР), Влияние растворителей на проведение электрохимического разложения (англ., рез., рум.) 35

А. ТАРЗОН, И. АЛЕКСЕЕВ и [И. ПЕТРОВ], Построение и изучение химического равновесия для получения молярной доли (англ., рез., рум.) 41

Д.Г. СЕЛЕГЕ, Е. ЛЭЗЭРЕСКУ, Д. ЙОРГА и Г. МИХАЭЛЬ, Исследование процесса сублимации хлорида алюминия (D) (франц., рез., англ.) 47

К. ХАЛЬБАН и П. ГЕРГОРИУ, Изучение гидролитических образований в растворах воды — нитрата и фосфорной кислоты — водорода (франц., рез., англ.) 53

Р. СИМОЛОТ, Х. ТАЛАБА, И. ЭНЕСКУ, Д. ПОТЕЛЯТУ и А. БЕЛЯЕВ, Исследование изотерм на границе со стеклом (франц., рез., рум.) 57

М. ГРЭДИНЯ, Э. ПОПОВИЧ и М. АЛЕКСАНДРОАЕЙ, Синтетическая вода и фарм. валюта (англ., рез., рум.) 63

И. НАУМ, Г. МИХАЭЛЬ и И. ЭЛЕТЕ, Гидрогеохимическое изучение хлоридных источников подземных вод района (англ., рез., рум.) 67

Г. СУЛЮЯНУ, М. ПОПЕСКУ-ЧЕЛЕБУ, И. БУЛЬБУКЭ, Х. ТАЛАБА-ПОПЕСКУ (Франция) и Ж. И. КЛАТТО (Франция), Электрохимическое поведение ванадия в растворах H₂SO₄ (англ., рез., рум.) 71

И. ОНУ, Г. ГУЛЯ, Е. АЛАЛЯ и А. ЛОСЮНУ, Изучение возможности использования подобных пористых пробок при определении [illegible] (франц., рез., рус.) 77

А.Г. ЕЛИНЕАНУ, Спектрографическое определение Zn, Cd, Pb-Германия, [illegible] (англ., рез., рум.) 81

К. ОНИЦЭУ, М. ГИЦЭ и Ф. ШТИНЕ, Влияние пропуска стерилизующего [illegible] (франц., рез., рум.) 87

Ф. ВИТАЛЯ и Г. З. ТЭЛОЕ, Гомогенизирующее тепловое воздействие (франц., рез., англ.) 93

РЕЦЕНЗИИ 101

BULETINUL INSTITUTULUI POLITEHNIC DIN IAŞI
Tomul XXXI (XXXV) Fasc. 1—4, 1985
Secţia II
CHIMIE ŞI INGINERIE CHIMICĂ

C.D. 547.254.4 ; 547.284.3

LE SYSTÈME Ni(II) — ISOPROPANOLAMINE(I)

PAR

N. CALU, ALEXANDRA-RALUCA IORDAN et I. SANDU

1. Introduction

Les complexes du Ni(II) avec amino-alcools sont d'une stabilité moyenne et parfois dans des solutions aqueuses on constate des équilibres entre eux et $Ni(OH)_2$, en cours de formation. Ainsi, en ajoutant les premières quantités d'isopropanolamine à une solution aqueuse avec l'ion Ni^{2+} aq, on obtient une précipitate de $Ni(OH)_2$.

Dans le présent travail sont étudiés certaines conditions de réactions, comme: la nature du milieu, la concentration des réactants, la puissance ionique et d'autres, dans lesquelles les équilibres du système Ni(II) — isopropanolamine sont déplacés vers la formation des ions complexes. Dans la même manière sont déterminées la nature et la stabilité de ces espèces complexes et leurs spectres champ cristallin.

2. Les réactifs

Le générateur de complexes, $NiCl_2$, a été utilisé dans une solution aqueuse de concentration 5.10^{-2} ...1 moles/l.

Le ligand (isopropanolamine) a été utilisé comme solution en alcool éthylique, de concentration 1...10 moles/l.

Le milieu de réaction a été constitué par divers mélanges alcool éthylique—eau.

Les processus de formation des complexes dans le système Ni(II)—isopropanolamine ont été suivis par voie spectrophotométrique et pH-métrique.

3. Résultats et discussions

3.1. Le caractère basique de l'isopropanolamine

La constante de disociation de l'isopropanolamine a été déterminée à l'aide de la courbe :

$$pH = f(HCl) \tag{1}$$

obtenue au titrage de l'isopropanolamine (en solution aqueuse) avec HCl (Fig. 1).

Conformément à la relation

(2) $$pK = pH_{1/2\ échiv.}$$

ont été calculées les constantes de basicité et d'acidité de l'isopropanolamine

$$pK_b = 9{,}78 \text{ et } pK_a = 4{,}22 \text{ (à } 23°C).$$

Avec ces dates on a calculé la fraction molaire en isopropanolamine protonée, en fonction du pH de la solution, conformément à la relation :

(3) $$\eta_{R-\overset{+}{N}H_3} = \frac{[H^+]}{[H^+] + Ka}.$$

Les résultats obtenus de cette manière sont présentés dans la Fig. 2.

Conformément aux dates de la Fig. 2, le processus de la formation des complexes entre le ion Ni^{2+} aq et l'isopropanolamine sera suivi à un $pH > 5$, dans lequel le ligand peut bien se comporter comme base Lewis par la paire des électrons non-participants de la fonction amine $R-\ddot{N}H_2$.

3.2. La réaction entre Ni^{2+} aq et l'isopropanolamine

En solution aqueuse, en ajoutant isopropanolamine (L), le ion Ni^{2+} aq précipite comme $Ni(OH)_2$. Mais si on travaille dans un milieu prépondérent d'alcool éthylique, les produits de la réaction sont les divers espèces complexes Ni(II) — isopropanolamine d'une couleur bleue et un spectre d'absorbtion champ cristallin caractéristique (Fig. 3).

3.3. Composition des ions complexes dans le système Ni(II) — isopropanolamine

La composition des ions complexes Ni(II) — isopropanolamine a été déterminée par voie spectrophotométrique, par la méthode des rapports molaires [1] et la méthode B j e r r u m [2]...[4].

Pour la méthode des rapports molaires on a effectué des mesures d'absorbance sur des séries de solutions avec la concentration constante en Ni^{2+} aq et variable en isopropanolamine. Puis on a représenté le graphique

(4) $$A = f(L : Ni^{2+})$$

comme on observe dans la Fig. 4.

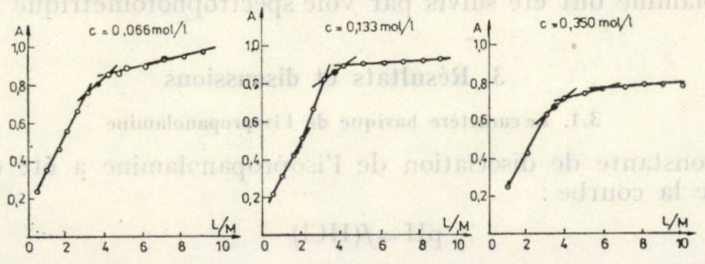

Fig. 4. — Dates concernant la composition des ions complexes du système Ni(II) — isopropanolamine, obtenues par la méthode des rapports molaires[1].

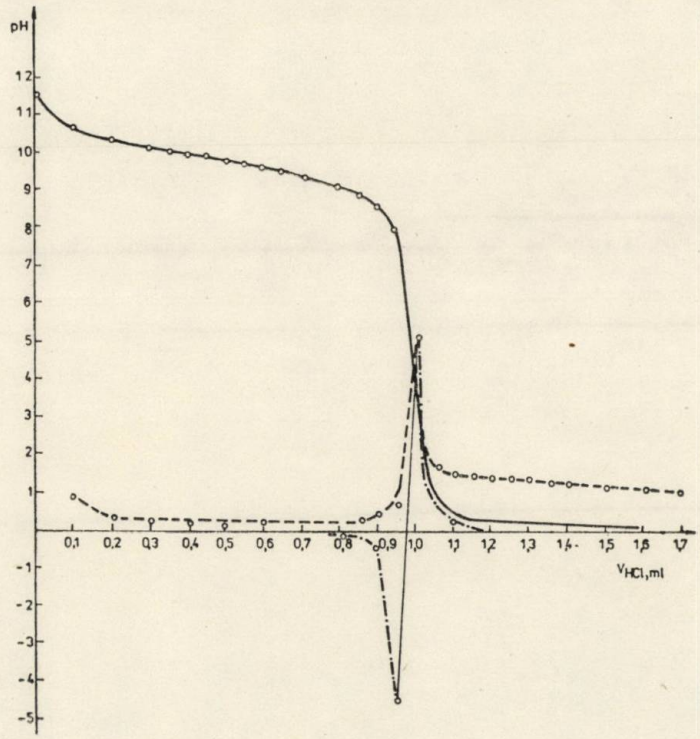

Fig. 1. — La courbe pH = f(HCl), au titrage de l'isopropanolamine (en solution aqueuse).

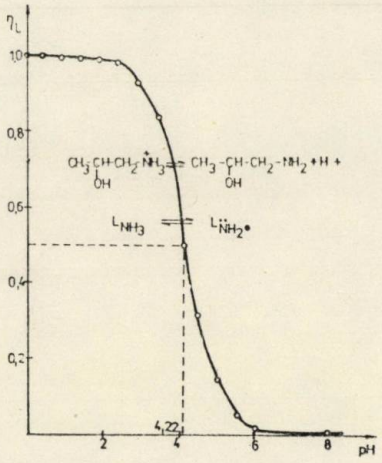

Fig. 2. — La fraction molaire en isopropanolamine protonée en fonction du pH de la solution.

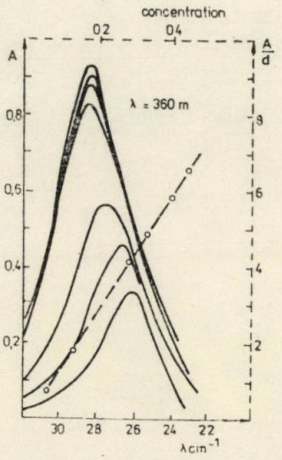

Fig. 3. — une partie des bandes d'absorbtion type champ cristallin aux ions complexes du système NI(II) — isopropanolamine; —o— vérification de la règle de B e e r dans le cas de l'espèce complexe $NiL_4\,aq^{2+}$.

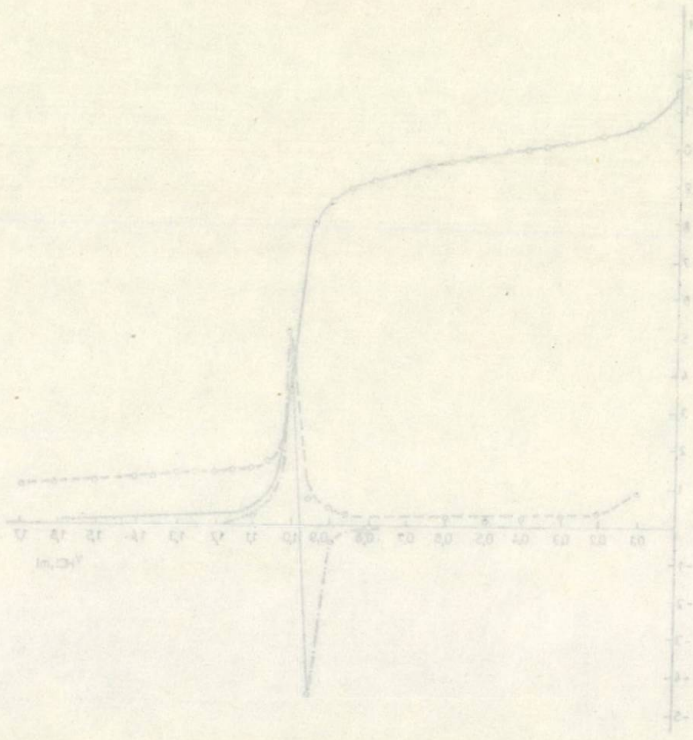

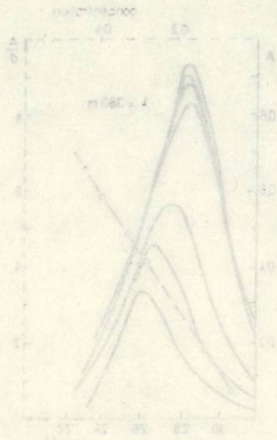

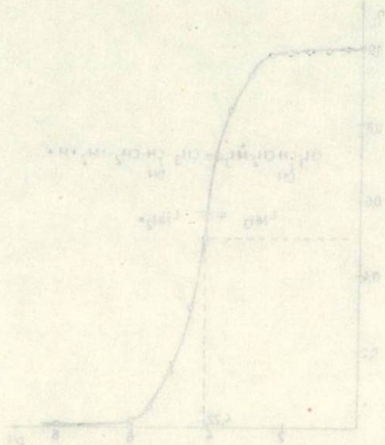

Par cette méthode sont mises en évidence les espèces complexes avec le nombre de coordination $n=2$, 3, 4 et 6.

Dans le cas de la méthode B j e r r u m a été utilisée la variante avec la courbe d'étalonnage :

$$\varepsilon = f(C_L), \tag{5}$$

ou : ε — le coefficient molaire d'absorbation et C_L — la concentration de l'isopropanolamine.

À l'aide des courbes d'étalonnage ont été puis calculés le nombre moyen de coordination $\bar{n}$ et la concentration du ligand libre, L_1, conformément à la méthode B j e r r u m. Avec ces paramètres on a construit la courbe de formation:

$$\bar{n} = f(pL_1), \tag{6}$$

représentée dans la Fig. 5. Par cette méthode sont mises en évidence les espèces complexes avec le nombre de coordination $n=2$, 3 et 4.

En conclusion, les dates obtenues par voie spectrophotométrique permettent à admettre que dans le système Ni(II) — isopropanolamine se forme en degrés plusieurs espèces complexes, avec $n=2$, 3, 4 et 6, à savoir : $[NiL_2]^{2+}$; $[NiL_3]^{2+}$; $[NiL_4]^{2+}$; $[NiL_6]^{2+}$.

La dernière espèce, avec $n=6$, apparaît seulement dans les solutions avec une concentration plus grande que 0,35 moles/l dans le complexe.

3.4. Stabilité de l'ion complexe $[NiL_4]^{2+}$

La constante globale apparente β_4 a été déterminée par voie spectrophotométrique à une concentration de 1.10^{-2} moles/l en complexe, le do-

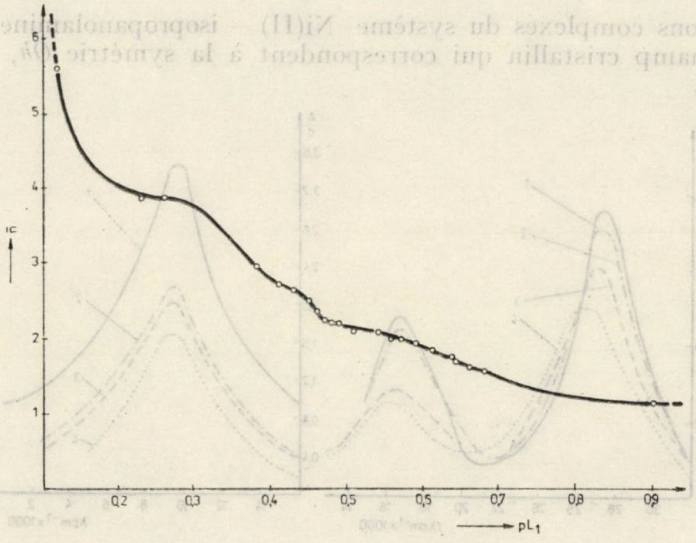

Fig. 5. — La courbe de formation de type B j e r r u m pour le système Ni(II) — isopropanolamine.

maine dans lequel l'espèce avec le nombre maximum de coordination est $[NiL_4]^{2+}$.

On a utilisé la méthode E d m o n d s—B i r n b a u m [5] et les calculs ont été effectués conformément à la relation:

$$K_{(i)} = \frac{C_{L1}^4 C_{L2}^4 (A_1 - A_2)}{A_2 C_{L1}^4 - A_2 C_{L1}^4}, \tag{7}$$

avec $C_{L1}=3{,}0$ moles/l, $C_{L2}=1{,}5$ moles/l, $A_1 = 0{,}375$, $A_2 = 0.355$ d'ou il résulte

$$\beta_4 = \frac{1}{K_{(i)}}. \tag{8}$$

Les valeurs β_4 ainsi obtenues sont centralisées dans le Tableau 1.

Tableau 1

La constante apparente de formation pour l'espèce complexe avec le nombre maximum de ligands à la concentration respective de travail

Ni^{2+} aq moles/l	L moles/l	$NaNO_3$ moles/l	Le ion complexe	β_4
$1 \cdot 10^{-2}$	1,5 3,0	$1 \cdot 10^{-1}$	$[NiL_4\ aq]^{2+}$	3,28
	1,5 3,0	—	$[NiL_4\ aq]^{2+}$	2,22

3.5. Spectres champ cristallin des ions complexes $[NiL_n]^{2+}$

Les ions complexes du système Ni(II) — isopropanolamine sont des spectres champ cristallin qui correspondent à la symétrie *Oh*, (Fig. 6 et Tableau 2).

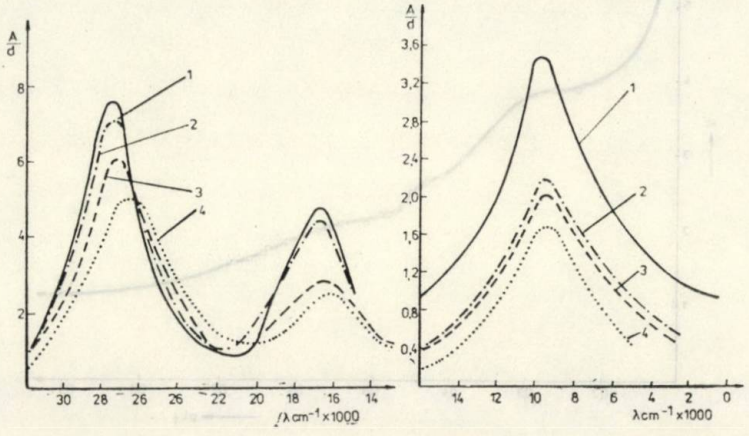

Fig. 6. — Bandes d'absorbtion du type champ cristallin pour les ions $[NiL_n]^{2+}$.

Tableau 2

Données relatives aux spectres d'absorbtion de certains ions complexes $[NiL_w]^{2+}$

Le ion complexe	$^3T_{2g} \xrightarrow{\nu_1} {}^3A_{2g}$ λmax., [cm^{-1}] (ε, [1 cm^{-1}. $moles^{-1}$])	$^3T_{1g}(F) \xrightarrow{\nu_2} {}^3A_{2g}$ λmax., [cm^{-1}] (ε, [1 cm^{-1}. $mole^{-1}$])	$^3T_{1g}(P) \xrightarrow{\nu_3} {}^3A_{2g}$ λmax., [cm^{-1}] (ε, [1 cm^{-1}. $mole^{-1}$])
$[NiL_2aq]^{2+}$	9 524 (5,055)	16 000 (5,2)	26 320 (10,0)
$[NiL_3aq]^{2+}$	9 615 (6,800)	16 600 (7,6)	27 040 (12,2)
$[NiL_4aq]^{2+}$	9 756 (6,900)	16 560 (8,8)	27 200 (14,2)
$[NiL_6]^{2+}$	9 804 (7,000)	16 880 (9,6)	27 280 (15,1)

Seulement le ion complexe $[NiL_6]^{2+}$ présente une microsymétrie *Oh*. D'autres ions complexes (v. tableau 2) présentent une microsymétrie inférieure à celle *Oh* mais à cause de la scission négligeable de leurs niveaux à une microsymétrie inférieure, les bandes d'absorbtion n'apparaissent pas scindées. Les caractéristiques de ces bandes sont données pour comparaison.

Le spectre champ cristallin des ions complexes $[NiL_n]^{2+}$ a été interprété sur la base de la diagramme avec des niveaux énergétiques propres au cas d^8, symétrie *Oh* [6] (Fig. 7).

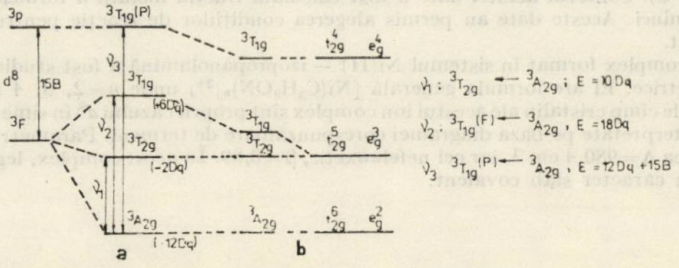

Fig. 7 — Termes spin triplet pour un ion a^8 dans la symétrie *Oh*: *a* — champ faible ; *b* — champ intense.

Le paramètre néphélauxétique β_{35} a été déterminé par voie graphique [4], sur la base de la représentation:

$$\frac{\nu_m}{\nu_n} = f\left(\frac{Dq}{B_c}\right), \tag{9}$$

ou: $m=2,3$ et $n=1,2$, $Dq=980,4$ cm^{-1}, $B_c=1\,041$ cm^{-1} (le paramètre R a c a h) [4].

Les calculs conduisent à $B_c = 928{,}9\ cm^{-1}$ d'où résulte pour le paramètre néphélauxétique:

$$\beta_{35} = \frac{B_c}{B_0} = \frac{928{,}9}{1041} = 0{,}89, \tag{10}$$

valeur approchée de 1 et qui montre que la liaison métal—ligand des complexes $[NiL_n]^{2+}$ est faiblement covalente.

Reçue le 22 avril 1982

Institut Polytechnique, Jassy, Chaire de Chimie anorganique et analytique

BIBLIOGRAPHIE

1. Joe J., Jones A., Ind. Eng. Chem. Anal. Ed., **16**, 11 (1944).
2. Bjerrum J., Kgl. Danske Videnskab. Selskab. mat-phys. medd., **21**, 4 (1944); Ibid., **22**, 18 (1946).
3. Bjerrum J., Chem. Rev., **46**, 381 (1950).
4. Bjerrum J., Jørgensen C. K., Acta Chem. Scand., **7**, 951 (1953); Ibid., **8**, 175 (1954).
5. Edmonds S., Birnbaum N., J. Amer. Chem. Soc., **63**, 147 (1941).
6. Lewer A. B. P., *Inorganic Electronic Spectroscopy*. Elsevier, Amsterdam-London-New York, 1968, 216, 392—400.

SISTEMUL Ni(II) — IZOPROPANOLAMINĂ (I)

(Rezumat)

Se studiază sub aspect structural ionul complex format în sistemul Ni(II) — izopropanolamină. Constanta de bazicitate a izopropanolaminei a fost determinată experimental, $pK_b = 9{,}78$ (la 23°C). Conform acestei date a fost calculată fracţia molară a formelor protonate a izopropanolaminei. Aceste date au permis alegerea condiţiilor de reacţie pentru sistemul mai sus menţionat.

Ionul complex format în sistemul Ni(II) — izopropanolamină a fost studiat prin metode spectrofotometrice. El are formula generală $[Ni(C_3H_9ON)_n]^{2+}$, unde $n = 2$, 3, 4 şi 6.

Spectrele cîmp cristalin ale acestui ion complex sînt proprii cazului d^8 în simetrie octaedrică. Ele au fost interpretate pe baza diagramei corespunzătoare de termeni. Parametrul cîmp cristalin are valoarea $\Delta = 980{,}4\ cm^{-1}$, iar cel nefelauxetic, $\beta = 0{,}89$. În acest complex, legătura metal — ligand are un caracter slab covalent.

BULETINUL INSTITUTULUI POLITEHNIC DIN IAŞI
Tomul XXXI (XXXV) Fasc. 1—4, 1985
Secţia II
CHIMIE ŞI INGINERIE CHIMICĂ

C.D. 546.723 ; 547.292

STUDIUL FORMĂRII COMPUŞILOR Fe(III) CU DERIVAŢII CLORURAŢI AI ACIDULUI ACETIC

DE

I. ROŞCA, ELENA ŞTEFANCU şi MIRCEA PALAMARU

1. Introducere

Ionii CH_3COO^-, CH_2ClCOO^-, $CHCl_2COO^-$ şi CCl_3COO^- sînt cunoscuţi ca liganzi cu capacitate pronunţată de complexare faţă de unii cationi şi în special cei proveniţi de la elementele blocurilor *d* şi *f* [1]... [7]. Această capacitate de complexare se datoreşte grupării carboxilice care, în seria acizilor corespunzători de la care provin, suferă o ionizare diferenţiată funcţie de numărul atomilor de clor din molecula respectivă. Capacitatea de complexare a grupării carboxilice este influenţată de diverşi factori printre care şi efectul inductiv al halogenilor, în special cei care se află în poziţia α faţă de această grupare. Un studiu al capacităţii de complexare al ionilor CH_2ClCOO^-, CH_2BrCOO^-, CH_2KCOO^-, $CHCl_2COO^-$, CCl_3COO^- cu ionii UO_2^{2+} şi stabilitatea combinaţiilor complexe respective în soluţii apoase este efectuat în lucrarea [7].

În cele ce urmează se studiază formarea şi stabilitatea în mediu apos a combinaţiilor complexe obţinute prin interacţiunea Fe^{3+} cu CH_2ClCOO^-, $CHCl_2COO^-$ şi CCl_3COO^-. Studiul s-a efectuat prin analiză chimică şi aplicînd metodele potenţiometrică, pH-metrică şi conductometrică.

2. Rezultatele cercetării

2.1. Echilibre în mediu apos la care participă Fe(III)

În numeroase studii, printre care [8], [9], se remarcă marea capacitate de hidroliză a ionului Fe^{3+} care trece într-o varietate mare de produse, funcţie de temperatură, concentraţie, valoarea pH-ului şi componentele care se găsesc în mediu apos (fig. 1) :

Pînă la pH ≈ 3 produsele de hidroliză sînt formate din specii de ioni, care participă la diferite echilibre [8] şi anume:

(1) $$Fe^{3+} + H_2O \rightleftharpoons [Fe(OH)]^{2+} + H^+, \quad k_1 = (1 \pm 0{,}1).10^{-3};$$

(2) $$Fe^{3+} + 2\,H_2O \rightleftharpoons [Fe(OH)_2]^{+} + 2\,H^+, \quad k_2 = (4{,}9 \pm 1).10^{-7};$$

(3) $$2\,Fe^{3+} + 2\,H_2O \rightleftharpoons [Fe_2(OH)_2]^{4+} + 2H^+, \quad k_3 = (1{,}2 \pm 0{,}1).10^{-3};$$

(4) $$Fe^{3+} + [Fe(OH)]^{2+} \rightleftharpoons [Fe(OH)Fe]^{5+};$$

(5) $$2[Fe(OH)]^{2+} \rightleftharpoons [Fe_2(OH)_2]^{4+}.$$

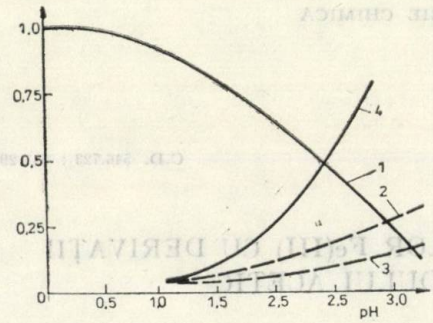

Fig. 1. — Fracțiile molare x ale produselor de hidroliză ale $[Fe(H_2O)_6]^{3+}$ în funcție de pH: *1* — $[Fe(H_2O)_6]^{3+}$; *2* — $[Fe(OH)(H_2O)_5]^{2+}$; *3* — $[Fe(OH)_2(H_2O)_4]^{+}$; *4* — $[Fe_2(OH)_2(H_2O)_8]^{4+}$.

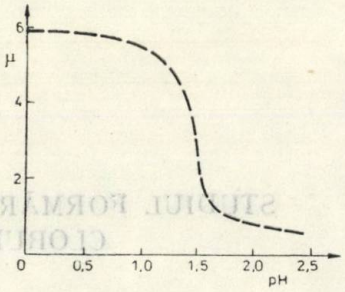

Fig. 2. — Momentele magnetice ale produselor de hidroliză ale $[Fe(H_2O)_6]^{3+}$ în funcție de pH.

Deoarece prin dizolvare se formează mai întîi ioni hidratați și deci în soluție se găsesc numai astfel de ioni este justificat ca aceștia să participe în continuare în mediu apos la procesele de echilibru :

(0) $$Fe^{3+} + 6H_2O \rightleftharpoons [Fe(H_2O)_6]^{3+};$$

(1′) $$Fe(H_2O)_6]^{3+} + H_2O \rightleftharpoons [Fe(OH)(H_2O)_5]^{2+} + H_3O^{+};$$

(2′) $$Fe(OH)(H_2O)_5]^{2+} + H_2O \rightleftharpoons [Fe(OH)_2(H_2O)_4]^{+} + H_3O^{+};$$

(3′) $$2\,[Fe(OH)(H_2O)_5]^{+} \rightleftharpoons [Fe_2(OH)_2(H_2O)_8]^{4+} + 2H_2O.$$

Dacă în mediul apos în care s-a dizolvat o sare de Fe^{3+}, spre exemplu $FeCl_3$, după ce s-au format produsele de hidroliză se adaugă o soluție de $CH_2ClCOONa$, $CHCl_2COONa$ sau CCl_3COONa, toate echilibrele pot fi perturbate, ca urmare a interacțiunii soluției clorurii ferice care creează prin hidroliză un mediu acid și soluției cloracetaților de sodiu care generează prin hidroliză mediu bazic. La aceasta se mai adaugă și coordinarea ionilor de $[Fe(H_2O)_6]^{3+}$ ca anioni proveniți de la sărurile respective și OH^- de la H_2O.

Totalitatea echilibrelor din acest mediu imprimă un anumit pH care determină formarea sau descompunerea complecșilor în aceste condiții. În mediu apos există deci continuu o concurență între anionii proveniți de la acizii cloracetați $(OH)^-$ și moleculele apei de a se uni cu Fe^{3+} pentru a forma produse mai stabile. Neluînd în considerare apa care se leagă slab de ioni, prin hidratare (așa cum se obișnuiește în mod curent) și admițînd că se leagă mai puternic numai ionii OH^- și CH_2ClCOO^-, $CHCl_2COO^-$ sau CCl_3COO^- (X^-) de Fe^{3+} se poate imagina cu ușurință că în termeni generali se stabilește echilibrul:

(6) $$zFe^{3+} + r[Fe_q(OH)_p]^{u} + vX^- + H_2O \rightleftharpoons [Fe_nX_y(OH)_x]^{3n-x-y} + xHX.$$

Deoarece ionii $[Fe(OH)]^{2+}$, $[Fe(OH)_2]^{+}$, $[Fe_2(OH)_2]^{4+}$, provin de la Fe^{3+}, se pot exprima primii în funcție de ultimul și procesul de echilibru va fi descris sub forma :

$$n\,Fe^{3+} + m\,X^- + x\,H_2O \rightleftharpoons [Fe_nX_y(OH)_x]^{3n-x-y} + x\,HX.$$

2.2. Determinări potențiometrice și pH-metrice

Așa după cum s-a arătat anterior, cunoscînd capacitatea Fe^{3+} de a se uni cu ionii OH^- și CH_2ClCOO^-, $CHCl_2COO^-$ sau CCl_3COO^-, se pot forma în mediu apos compuși de tipul $[Fe_nX_y(OH)_x]^{3n-x-y}$.

Prin analiză chimică, potențiometrică și conductometrică s-a determinat compoziția complecșilor care se formează prin interacțiunea în mediu apos a $FeCl_3$ în fiecare soluție de $CH_3ClCOONa$, $CHCl_2COONa$ și CCl_3COONa. Pentru toate probele din mediul apos s-a menținut constantă tăria ionică cu $NaClO_4$.

Modul de lucru este asemănător cu cel prezentat în lucrările [4], [6], [9], [10] și constă în următoarele:

În fiecare soluție de $NaClO_4$ 0,75 M și $CH_2ClCOONa$ 0,1 M, $NaClO_4$ 0,75 M și $CHCl_2COONa$ 0,1 M, $NaClO_4$ 0,75 M și CH_3COONa 0,1 M s-au introdus cantități variabile de $FeCl_3$ 0,5 M măsurîndu-se de fiecare dată potențialul și pH-ul. Deoarece se obțin variații mici de potențial și respectiv de pH, la adăugarea soluției de $FeCl_3$ s-a considerat că ar fi mult mai convenabilă reprezentarea variației diferențiale a potențialului și pH-ului funcție de cantitățile de soluție adăugate (fig. 3). Pentru seria J o b [9] (fig. 4) a soluțiilor de mono-, di- și tricloracetați de sodiu 0,1 M $NaClO_4$ 0,75 M și $FeCl_3$ 0,1 M s-au determinat valorile potențialului și pH-ului.

Se constată că la raportul $|CH_2ClCOO^-|/|Fe^{3+}| = 2{,}6$ se obține variația maximă de potențial și de pH. Deci pentru un ion de Fe^{3+} corespund 2,66 ioni CH_2ClCOO^-, ceea ce înseamnă că pentru trei ioni Fe^{3+} vor corespunde opt ioni CH_2ClCOO^-.

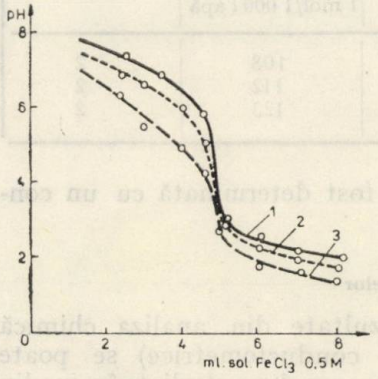

Fig. 3. — Curbele titrărilor pH—metrice ale soluțiilor:
1 — $CH_2ClCOONa$ 0,1 M, $NaClO_4$ 0,75 M;
2 — $CHCl_2COONa$ 0,1 M, $NaClO_4$ 0,75 M;
3 — CCl_3COONa 0,1 M, $NaClO_4$ cu $FeCl_3$ 0,5 M.

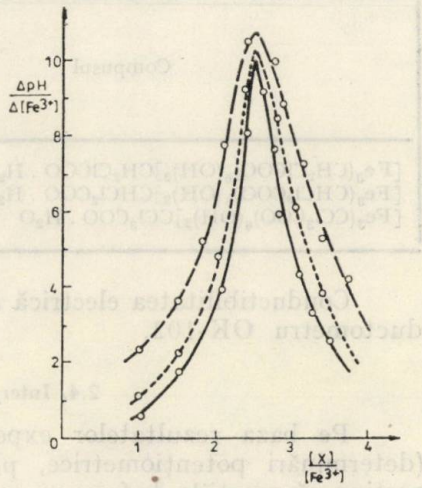

Fig. 4. — Curbele $\Delta pH/\Delta|Fe^{3+}| = f(|X^-|)/|Fe^{3+}|)$: 1 — $X = CH_2ClCOO^-$; 2 — $X = CHCl_2COO^-$; 3 — $X = CCl_3COO^-$.

În mod asemănător se obține același raport de 2,6 pentru cazul în care se lucrează cu soluții de $CHCl_2COONa$ sau CCl_3COONa 0,1 M și respectiv $FeCl_3$ 0,5 M.

Determinarea grupelor OH^- din complex s-a efectuat prin titrare potențiometrică. În acest scop s-au preparat complecșii respectivi din $Fe(OH)_3$ proaspăt obținut și acizii cloracetici corespunzători. Analiza chimică a compușilor obținuți corespunde următoarelor formule:

$$[Fe_3(CH_2ClCOO)_7(OH)_2]H_2O,\ [Fe(CHCl_2COO)_7(OH)_2]H_2O,$$

$$[Fe_3(CCl_3COO)_7(OH)_2]H_2O.$$

Apoi prin solvirea în apă a 1 g din fiecare produs și titrare potențiometrică cu soluție de $HClO_4$ s-au determinat grupele oxidrilice care corespund cu cele determinate prin analiză chimică (la trei ioni de Fe^{3+} corespund două grupări OH^-). Determinările de potențial și de pH s-au efectuat la un pH-metru MV-11.

2.3. Determinări conductometrice

După cum este cunoscut, conductibilitatea electrică a soluțiilor depinde, pentru o anumită concentrație molară, de numărul de ioni în care se disociază molecula compusului respectiv și de mobilitatea acestor ioni. În cazul compușilor studiați conductibilitățile electrice sînt prezentate în tabelul 1, din care rezultă că fiecare moleculă se disociază în doi ioni.

Tabelul 1

Conductibilitățile electrice ale compușilor studiați

Compusul	Conductibilitatea electrică, [ohm^{-1}] sol. de concentrație 1 mol/1 000 l apă	Nr. ioni în care disociază
$[Fe_3(CH_2ClCOO)_6(OH)_2]CH_2ClCOO \cdot H_2O$	108	2
$[Fe_3(CHCl_2COO)_6(OH)_2]CHCl_2COO \cdot H_2O$	112	2
$[Fe_3(CCl_3COO)_6(OH)_2]CCl_3COO \cdot H_2O$	123	2

Conductibilitatea electrică a soluțiilor a fost determinată cu un conductometru OK-102.

2.4. Interpretarea rezultatelor

Pe baza rezultatelor experimentale rezultate din analiza chimică (determinări potențiometrice, pH-metrice și conductometrice) se poate susține că reacțiile de formare a combinațiilor complexe studiate în mediu apos ar putea fi scrise simplificat, neținînd seama de mecanismele de reacție, în modul următor:

$$3Fe^{3+} + 8CH_2ClCOO^- + 2H_2O \rightleftharpoons [Fe_3(CH_2ClCOO)_6(OH)_2]^+ + \quad (7)$$

$$+ 2CH_2ClCOOH\ ;$$

(8) $$3Fe^{3+} + 8CHCl_2COO^- + 2H_2O \rightleftharpoons [Fe_3(CHCl_2COO)_6(OH)_2]^+ + 2CHCl_2COOH;$$

(9) $$3Fe^{3+} + 8CCl_3COO^- + 2H_2O \rightleftharpoons [Fe_3(CCl_3COO)_6(OH)_2]^+ + 2CCl_3COOH.$$

Ținînd cont de hidroliza ionilor $[Fe(H_2O)_6]^{3+}$ și de mecanismul global al acestor procese se poate scrie, în acord cu datele experimentale obținute în această lucrare, următoarea reacție pentru obținerea $[Fe_3(CH_2ClCOO)_6(OH)_2]^+$:

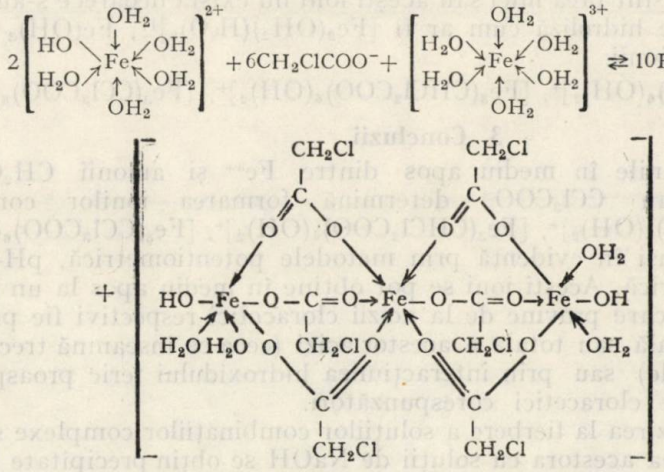

și în mod similar pentru ceilalți compuși.

Ionii $[Fe(OH)(H_2O)_5]^{2+}$ provin din hidroliza $[Fe(H_2O)_6]^{3+}$ (reacția (1')) și din această cauză ei se consumă în reacție cu ionii CH_2ClCOO^-; în consecință ar însemna să se obțină o nouă cantitate de $[Fe(OH)(H_2O)_5]^{2+}$ din $[Fe(H_2O)_6]^{3+}$ și pe această cale să crească concentrația de H_3O^+, mediul devenind din ce în ce mai acid. Totuși, din datele experimentale obținute rezultă că mediul de reacție devine, pe măsura adăugirii $CH_2ClCOONa$ în soluția sării ferice, din ce în ce mai puțin acid ceea ce înseamnă că se consumă în același timp H_3O^+. Ori aceasta se poate explica în felul următor:

a) Reacția de echilibru (1') se poate deplasa spre dreapta pentru a obține o cantitate din ce în ce mai mare de $[Fe(OH)(H_2O)_5]^{2+}$ necesară formării ionului complex $[Fe_3(CH_2ClCOO)_6(OH)_2]^+$ numai dacă o parte din $CH_2ClCOONa$ adăugat în soluție consumă ionii H_3O^+ rezultați prin deplasarea spre dreapta a acestui echilibru (1'):

(11) $$H_3O^+ + CH_2ClCOO^- \rightleftharpoons CH_2ClCOOH + H_2O.$$

b) Pentru fiecare ion $[Fe(OH)(H_2O)_5]^{2+}$ consumat în reacția (2') este necesar să se consume un ion H_3O^+ rezultat din reacția (1') pentru ca acest ultim echilibru se se deplaseze mereu spre dreapta cu scopul de a asigura consumul de $[Fe(OH)(H_2O)_5]^{2+}$ necesar reacției (10).

c) Așadar pentru obținerea unui ion $[Fe_3(CH_2ClCOO)_6(OH)_2]^+$ sînt necesari șase ioni CH_2ClCOO^- în reacția (10) și doi ioni CH_2ClCOO^- pentru consumarea a doi ioni H_3O^+ care să asigure deplasarea echilibrului (1') spre dreapta pentru a obține exact numărul de ioni $[Fe(OH)(H_2O)_5]^{2+}$ care

au intervenit în reacția (10) ceea ce înseamnă că pentru formarea unui singur ion $[Fe_3(CH_2ClCOO)_6(OH)_2]^+$ sînt necesari opt ioni CH_2ClCOO^-, rezultat care concordă cu datele experimentale prezentate în această lucrare.

Din datele experimentale obținute rezultă că în cazul cînd în soluție nu se pot obține în cantități mari ionii $[Fe(OH)(H_2O)_5]^{2+}$ și $[Fe(H_2O)_6]^{3+}$, din cauza mediului prea puternic acid (pH <2) sau prea puternic bazic, nu se poate obține ionul $[Fe_3(CH_2ClCOO)_6(OH)_2]^+$.

În mediile slab acide sau bazice, cînd concentrațiile în $[Fe(OH)(H_2O)_5]^{2+}$ și $[Fe(H_2O)_6]^{3+}$ sînt prea mici sau acești ioni nu există deoarece s-au format alte produse de hidroliză cum ar fi $[Fe_2(OH_2)(H_2O)_8]^{4+}$, $Fe(OH)_3$ etc., nu se pot obține ionii:

$[Fe_3(CH_2ClCOO)_6(OH)_2]^+$, $[Fe_3(CHCl_2COO)_6(OH)_2]^+$, $[Fe_3(CCl_3COO)_6(OH)_2]^+$.

3. Concluzii

Interacțiunile în mediu apos dintre Fe^{3+} și anionii CH_2ClCOO^-, $CHCl_2COO^-$ sau CCl_3COO^- determină formarea ionilor complecși: $[Fe_3(CH_2ClCOO)_6(OH)_2]^+$, $[Fe_3(CHCl_2COO)_6(OH)_2]^+$, $[Fe_3(CCl_3COO)_6(OH)_2]^+$, care au fost puși în evidență prin metodele potențiometrică, pH-metrică și conductometrică. Acești ioni se pot obține în mediu apos la un pH mai mare decît cel care provine de la acizii cloracetici respectivi fie prin neutralizarea parțială sau totală a acestor acizi (ceea ce înseamnă trecerea lor în săruri solubile) sau prin interacțiunea hidroxidului feric proaspăt preparat cu acizii cloracetici corespunzători.

Prin încălzirea la fierbere a soluțiilor combinațiilor complexe studiate sau prin tratarea acestora cu soluții de NaOH se obțin precipitate formate din săruri bazice de Fe(III) cu compoziție variabilă funcție de temperatură și de cantitatea de NaOH introdusă.

Primită la 20 februarie 1982

Institutul politehnic, Iași,
Catedra de chimie anorganică
și analitică

BIBLIOGRAFIE

1. Weinland R., Gusman E., Ber., **42**, 3881 (1909).
2. Weinland R., Buttner E., Z. anorg. chem., **75**, 293 (1912).
3. Golgoțiu T., Roșca I., Bul. Inst. polit., Iași, **XI(XV)**, *1–2*, 107 (1965).
4. Weinland R., Kassler A., Z. anorg. Chem., **152**, 1 (1962).
5. Golgoțiu T., Roșca I., Bul. Inst. polit., Iași, **XI(XV)**, *3–4* (1965).
6. Jezowska – Trzebiatovska, Roczniki chemii, **31**, *3* (1957).
7. Spacu P., Popa F., Lepădatu C., St. cerc. chim., *1* (1965).
8. Biedermenn G., Sillen L., Ark. Kem., **5**, 424 (1953).
9. Milburn R., Vosburgh W., J. Am. Chem. Soc., 77 (1955).
10. Job P., Am. Chem., **9**, 113 (1928).
11. Spacu P., Popa E., St. cerc. chim., **14**, 39 (1965).

L'ÉTUDE DE LA FORMATION DES COMPOSÉS DE Fe(III) AVEC DES ACIDES CHLORACÉTIQUES

(Résumé)

On a déterminé, à l'aide de là potentiométrie, de la pH-métrie et de la conductométrie, l'existence de trois composants complexes qui se forment dans la solution aqueuse de chlorure ferrique et des mono-, di- et trichloracétates de sodium. On a déterminé également le domaine de stabilité de ces complexes et on a proposé un mécanisme de la réaction globale.

BULETINUL INSTITUTULUI POLITEHNIC DIN IAŞI
Tomul XXXI (XXXV) Fasc. 1—4, 1985
Secţia II
CHIMIE ŞI INGINERIE CHIMICĂ

D.C. 661.183.123

BEHAVIOUR OF CERTAIN DI- AND TRIVALENT IONS ON VIONIT CS-3 FROM THE WATER—NITRIC ACID—ORGANIC SOLVENT MEDIA

BY

ANIŞOARA BOLD, ANGELA POPA and DOINA BÎLBA

1. Introduction

At present, the ion exchange chromatography is a procedure more and more employed for separation and concentration of many elements as well as a method of quantitative analysis. Among the factors controlling the separation efficiency increase, an appart atention was paid to the nature and composition of solvent medium. Both the aqueous solutions of complexing agents and mixtures of water with low polarity organic solvents were successfully employed as eluating agents [1] ... [5].

The present paper deals with the experimental results as regards the ion exchange behaviour of Zn(II), Cu(II), Fe(III) and Cr(III) in the water—nitric acid—organic solvent system on the ion-exchanger Vionit CS-3 in order to find out the conditions under which these elements can be separated and recovered from waste catalysts or from other industrial residues.

2. Experimental

Reagents. Aqueous solutions of Zn(II), Cu(II), Fe(III) and Cr(III) nitrates gravimetrically standardized.

Sulfocationit Vionit CS-3, hydrogen form, with exchange capacity of 4.7 ... 5.0 mequiv/g and granule size of 0.50 ... 0.63 mm, purified beforhand by washing with 0.3 N HCl, distilled water, alcohol, acetone and dried in air.

Ion exchange was carried out under statical conditions. The ion-exchanger samples (1 g) were contacted with 50 ml mixture of water—nitric acid—organic solvent containing 100 mg metallic ion to be exchanged.

Concentration of nitric acid range from 0.1 M to 1 M, and that of the organic solvent from 0 to 90%, v/v. Methanol, ethanol, propanol, isopropanol, acetone and ethylenglycol have been employed as organic solvent. The mixture was maintained at room temperature (under periodical stirring) for 24 h, time enough to get steady state, then the phases were separated by filtration. Amount of metallic ion remained in solution at steady state was determined in an aliquot portion from filtrate titrimetrically with EDTA (Zn(II), Cu(II) and Fe(III)) [6] or spectrophotometrically (Cr(III)) [7].

To appreciate the metallic ions repartition at steady state between ion-exchanger and solution, on the basis of the experimental data, distribution coefficients

$$K_d = \frac{\text{amount of retained ion/1 g of dried ion-exchanger}}{\text{amount of remained ion/1 ml of solution}}$$

and separation factors

$$\frac{B}{A} = \frac{K_{dA}}{K_{dB}}$$

have been calculated.

3. Results and Discussions

The experiments as regards sorption and separation of Zn(II) Cu(II), Fe(III) and Cr(III) on Vionit SC-3 allowed to study the influence of both solution acidity and organic solvent presence.

Dependence of the distribution coefficients of studied elements on acidity of the initial aqueous solution is represented in Fig. 1.

As can be seen from Fig. 1, in aqueous solution of 0.1 M HNO_3 retention of cations on Vionit CS-3 increases with ionic radins increasing or with the hydration—solventation tendency decreasing, respectively.

If concentration of nitric acid increases from 0.1 M to 1 M, the distribution coefficients of studied ions decrease, especially for Zn(II) and Cu(II). At the same time, selectivity order of the ion-exchanger against studied cations is modified.

Sorption decrease of the cations with the medium acidity increasing can be explained by competitive action of the hydrogen ions and demotion of the exchange equilibrium.

The separation factors have maximum values in solutions of 0.1 M HNO_3:

$$\alpha_{Zn}^{Cr} = 2.47; \quad \alpha_{Zn}^{Fe} = 1.94; \quad \alpha_{Cu}^{Cr} = 1.53; \quad \alpha_{Cu}^{Fe} = 1.44.$$

Gradual replacing of water, in solution of constant acidity, with organic solvents having lower dielectric constant (ε), leads to some modifications as regards the distribution of ions between ion-exchanger and solutions. Experiments in the presence of organic solvents have been carried out in solutions of 0.3 M HNO_3. Because at this acidity, separation of the ions in aqueous solutions is not possible, the differences between K_d on Vionit CS-3 being very low.

Variation of the distribution coefficients of the studied ions on Vionit CS-3 against methanol content in 0.3 M HNO_3 solution is plotted in Fig. 2.

The Fig. 2 points out that an increase of methanol concentration determines the sorption increase of all cations and growth of the separation factors of divalent ions against those trivalent. Thus, in the system with 90% methanol:

$$\alpha_{Zn}^{Cu} = 1.90; \quad \alpha_{Zn}^{Fe} = 1.54; \quad \alpha_{Cu}^{Cr} = 1.94; \quad \alpha_{Cu}^{Fe} = 1.57.$$

A similar behaviour has been found also in the case of the other employed alcohols: ethanol, propanol iso-propanol and ethylenglycol.

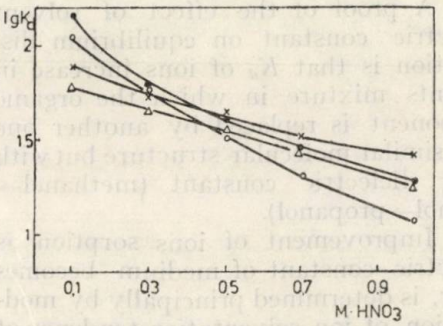

Fig. 1. — Influence of nitric acid concentration : • — Zn(II) ; o — Cu(II) ; × — Fe(III) ; Δ — Cr(III).

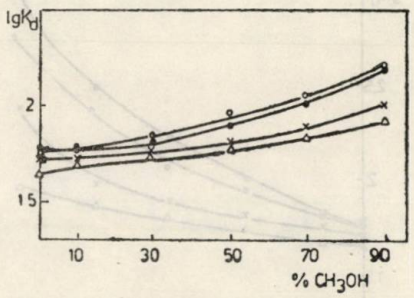

Fig. 2. — Influence of methanol concentration : • — Zn(II) ; o — Cu(II) ; × — — Fe(III) ; Δ — Cr(III).

To exemplify in Table 1 are set out the values of distribution coefficients of Zn(II), Cu(II), Fe(III) and Cr(III) on Vionit CS-3 in the 0.3 M HNO_3 with 90% organic systems.

Table 1

Dependence of K_d for Zn(II), Cu(II), Fe(III) and Cr(III) on Organic Solvent Nature (90%, v/v) *in 0.3M HNO_3 Solution*

Ion and its ionic radius Å	Solvent and its dielectric constant					
	Water	Ethylen-glycol	Methanol	Ethanol	Propanol	Isopropanol
	ε=82.0	ε=41.2	ε=42.0	ε=26.0	ε=22.2	ε=26.0
Zn(II) r = 0.83	59	111.22	158	464	581	640
Cu(II) r = 0.70	58	102.83	163	450	561	709
Fe(III) r = 0.67	53	92.4	102.5	135	145	185
Cr(III) r=0.64	44	60.67	82.8	84	87	88

The data summarized in Table 1 show that for a constant concentration of nitric acid the distribution coeficients of all investigated ions increase as alcohol in solution at equilibrium increases and as dielectric constant (ε) of employed solvent, respectively, decreases, property that controls physico-chemical characteristics of studied ion. The distribution coefficients of ions increase with the carbon atom number in alcohol molecule, with ramification degree of its hydrocarbonate chain and, also, with ionic radius of the investigated elements.

The variation are substantially larger for divalent elements than for trivalente ones, fact that points out an increase of the possibilities to separate the two groups from one another.

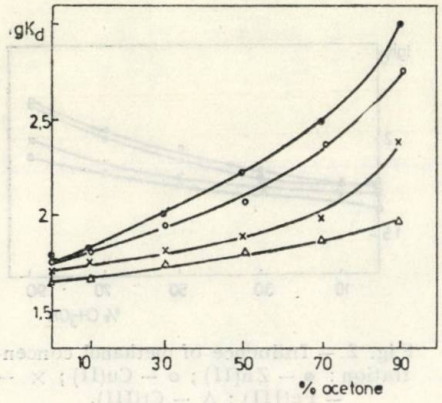

Fig. 3. – Influence of acetone concentration: • – Zn(II); o – Cu(II); × – Fe(III); Δ – Cr(III)

A proof of the effect of solvent dielectric constant on equilibrium distribution is that K_d of ions increase in solvents mixture in which the organic component is replaced by another one with similar molecular structure but with lower dielectric constant (methanol→ethanol→propanol).

Improvement of ions sorption as dielectric constant of medium becomes lower, is determined principally by modification of ion solventation tendency of hydration cloud destroy, depending on charge density of cation. At the same time, the solvents with dielectric constant lower that of water lead to increase of interaction among ions, favouring the ion pairs formation. Besides proper ion exchange, in the solvent mixtures media can take place a strong neutral adsorbtion of electrolyte.

If acetone is exployed as solvent (Fig. 3), values of distribution coefficients of investigated elements increase much more markedly than in the case of alcohols, being more important for divalent elements.

Separation factors become greater too, their values for 0.3 M HNO_3 solution and 90% (v/v) acetone are as follows:

$$\alpha_{Zn}^{Cr}=11.16;\quad \alpha_{Zn}^{Fe}=4.25;\quad \alpha_{Cu}^{Cr}=6.13;\quad \alpha_{Cu}^{Fe}=2.33.$$

On the basis of the obtained data, acetone can be considered the best. suitable eluent for separation of studied elements.

4. Conclusions

1. Nature and concentration of organic solvent influence, by its dielectric constant, ions retention on ion-exchanger Vionit CS-3.

2. Values of distribution coefficients for Zn(II), Cu(II), Fe(III) and Cr(III) increase with organic solvent content.

3. Separation factors of the studied ions on Vionit CS-3 are greater in the water–nitric acid–organic solvent media that in the aqueos ones.

Received, December 1, 1982

Polytechnic Institute, Jassy, Department of Inorganic and Analytical Chemistry

REFERENCES

1. Spiridon S., Sabău C., Korkisch J., J. Radioanalyt. Chem., 3, 5–6, 377 (1969).
2. Simek M., Coll. Czech. Chem. Comm., 39, 3287 (1974).
3. Qureshi M., Rathore H. S., Kaushik R. C., Analyt. Chem., 47, 1710 (1975).

4. Hussain K., Rumean M., Bull. Soc. Chim., *3—4*, 73 (1979).
5. Vlădescu L., Chiru A. F., Rev. Chim. (București), **32**, 64 (1981).
6. Liteanu C., Hopirtean E., *Chimie analitică cantitativă — volumetria*. EDP, Buc., 1972.
7. Пинус А. М., Зав. лаб., **23**, 662 (1957).

COMPORTAREA UNOR ELEMENTE DI- ȘI TRIVALENTE PE VIONIT CS 3 ÎN SISTEMUL APĂ—HNO_3—SOLVENT ORGANIC

(Rezumat)

S-a studiat comportarea la schimb ionic pe Vionit CS-3 a elementelor Zn(II), Cu(II), Fe(III) și Cr(III) din amestecuri apă—HNO_3—solvent organic. S-au determinat coeficienții de distribuție funcție de concentrația HNO_3 și a solventului organic și s-au calculat factorii de separare. La concentrații mari de solvent organic se constată diferențe mari între valorile K_d față de sistemele apoase.

S-au stabilit condițiile de separare a elementelor studiate.

BULETINUL INSTITUTULUI POLITEHNIC DIN IAŞI
Tomul XXXI (XXX V) Fasc. 1—4, 1985
Secţia II
CHIMIE ŞI INGINERIE CHIMICĂ

C.D. 547.869

COMPLEXES DU 2-MÉTHIONINE PHÉNOTHIAZINIUM

PAR

LUMINIŢA PĂUNESCU

1. Introduction

La synthèse du dérivé phénothiazine-méthioninique [1] et ses réactions d'identification [2] ont mis en évidence la formation de composés dans lesquels le 2-méthionine phénothiazinium (FTM) interactionne avec les anions anorganiques et organiques.

Les articles publiés concernant ce type d'interactions laissent apparaître un certain désaccord entre les divers auteurs. Par exemple, les résultats des déterminations effectuées par Mesnard et Lagubeau [3], [4] impliquent l'existence des sels doubles, tandis que Sato, Kinoshita, Sano et Akamatu [5] considèrent les composés obtenus des complexes à transfert de charge. En supposant le transfert d'un électron, appartenant à un donneur vers une molécule d'accepteur, les complexes à transfert de charge des phénothiazines ont été attentivement étudiés [6]...[16].

Afin de préciser la nature des composés formés et antérieurement décrits [2], on a effectué une étude spectroscopique dans les domaines UV, visible et IR pour les composés obtenus ci-dessous: [FTM][HgI_4]; [FTM]H[BiI_6]; [FTM][MoO_4]; [FTM][CdI_4]; [FTM]H[$Fe(CN)_6$]; [FTM][MnO_4]$_2$; [FTM]$_3$[$H_2W_{12}O_{40}$]; [FTM]$_2$[$SiW_{12}O_{40}$]; [FTM][CrO_4]; [FTM][Cr_2O_7]; [FTM]$_x$[ADN]$_y$; [FTM][$C_6H_2(NO_2)_3O$]$_2$; [FTM]$_x$[ARN]$_y$; [FTM][$C_3H_8O_6P$]$_2$.

2. Partie expérimentale

Les spectres IR ont été enregistrés à l'aide d'un spectrophotomètre Perkin-Elmer 577, sous forme de pastilles de KBr, (200...4 000 cm^{-1}) et aussi à l'aide d'un spectrophotomètre Specord 71 Zeiss (700...4 000 cm^{-1}). Quant aux spectres UV et VIS, on a employé un spectrophotomètre Unicam SP-800 B et aussi un Spectrophotomètre Specord UV-VIS 71 Zeiss.

Pour les spectres UV — VIS on a utilisé, comme solvant, le diméthyl sulfoxyde (DMSO) dans lequel la majorité des produits sont solubles, ou un mélange de DMSO/eau.

3. Résultats et discussion

3.1. Spectres IR

On a attribué les caractéristique spectrales de la FTM et des complexes correspondants présentés dans le tableau 1, en les comparant aux donnés de la littérature dans ce domaine [1], [17]...[24].

On peut remarquer que tous les composés synthétisés présentent une ou deux bandes d'absorbtion dans le domaine 1 595...1 470 cm^{-1}. Ces

bandes apparaissent pa
E_{2g}, doublement dégé
survient que lorsqu'il
ou un groupement d'at
d'électrons libres [25].

En ce qui concer
phénothiazinique FTM
serve les déplacements
ainsi que l'apparition

Par exemple, la b
dans le complexe form
apparait à 360 cm^{-1}, d
liaison Cr—N signalée
dans le complexe [FT

Quant au comple
et une modification d
1 629 à 1 600 cm^{-1}, d
correspondantes ν_s(NC
déplacements, moins i
formes tres applaties.
caractéristique pour ν((
que l' OH de l'acide pi
et on remarque aussi
à 3 500...3 420 cm^{-1}, q

On peut considér
mentionnés dans la l
de charge entre le 2-n
En ce qui concerne les
on constate une gran
de leur relative instab
Saucin et Van de
aussi à celles de Gut
posés à transfert de cl

On a obtenu les
complexes et des prod
le Tableau 2, qui cont
lements (entre parenth

On remarque l'a
les complexes, par rap
de nouveaux maximum
Des données similaires
mettent en évidence t
fert de charge [26], q

Le spectre UV—V
présente deux maximu
255 nm ainsi qu'un ép
déplace, fonction de co

bandes apparaissent par suite du dédoublement de la bande fondamentale E_{2g}, doublement dégénérée, appartenant au benzène. Ce phénomène ne survient que lorsqu'il existe une conjugaison entre le noyau et un atome, ou un groupement d'atomes exocycliques, qui possèdent au moins une paire d'électrons libres [25].

En ce qui concerne les produits résultés dans la réaction du dérivé phénothiazinique FTM avec les réactants mentionnés ci-dessus, on observe les déplacements caractéristiques aux composés métalliques utilisés ainsi que l'apparition de la liaison métal—azote.

Par exemple, la bande caractéristique à l'ion CrO_4^{2-} est située à 348 cm^{-1}; dans le complexe formé avec le dérivé phénothiazinique utilisé cette bande apparait à 360 cm^{-1}, donc on a observé un déplacement de 12 cm^{-1} et la liaison Cr—N signalée dans la littérature [23] à 466,44...476 cm^{-1} apparait dans le complexe [FTM][CrO_4] à 475 cm^{-1}.

Quant au complexe avec l'acide picrique, on remarque un déplacement et une modification du doublet caractéristique à l'acide picrique de 1 608, 1 629 à 1 600 cm^{-1}, d'une intensité beaucoup plus réduite. Les bandes correspondantes $\nu_s(NO_2) = 1\,540$ et $\nu_{as}(NO_2) = 1\,350$ [26] présentent des déplacements, moins intenses, à 1 505...1 560 et à 1 310 cm^{-1} ayant des formes tres applaties. La bande intense de l'acide picrique à 3 080 cm^{-1}, caractéristique pour ν(O—H), est déplacée à 3 060 cm^{-1} et applatie, prouvant que l' OH de l'acide picrique est responsable pour la formation du complexe et on remarque aussi l'apparition d'une nouvelle bande, assez applatie, à 3 500...3 420 cm^{-1}, qui prouve la présence des liaisons d'hydrogène.

On peut considérer, en accord avec les données obtenues et les articles mentionnés dans la littérature, l'apparition des complexes à transfert de charge entre le 2-méthionine phénothiazinium et les réactants utilisés. En ce qui concerne les spectres des composés avec mercure et bismuth, on constate une grande ressemblance, ce qui nous conduit à l'hypothèse de leur relative instabilité, en accord d'ailleurs avec les observations de Saucin et Van de Vorst [27], Mercier et Dumont [28] et aussi à celles de Gutmann et Keyser [29] concernant d'autres composés à transfert de charge, obtenus à partie des phénothiazines.

3.2. Spectre UV—VIS

On a obtenu les spectres en UV et VIS des solutions en DMSO des complexes et des produits de réaction. Ces données ont été présentées dans le Tableau 2, qui contient les longueurs d'onde des maximums et les épaulements (entre parenthèses).

On remarque l'apparitions des déplacements des maximums pour les complexes, par rapport aux réactants et à la FTM, ainsi que l'apparition de nouveaux maximums spécifiques, qui prouvent la formation des complexes. Des données similaires ont été aussi publiées pour d'autres produits et elles mettent en évidence tant la formation des complexes moléculaires à transfert de charge [26], que celle des sels [1], [3], [4].

Le spectre UV—VIS du dérivé de phénothiazine (FTM), dans le DMSO, présente deux maximums intenses à 280 nm et 345 nm, un épaulement à 255 nm ainsi qu'un épaulement à 395 nm, qui devient plus intense et se déplace, fonction de concentration (avec l'augmentation de la concentration)

BULETINUL INSTITUTULUI POLITEHNIC DIN IAŞI
Tomul XXXI (XXX V) Fasc. 1—4, 1985
Secţia II
CHIMIE ŞI INGINERIE CHIMICĂ

C.D. 547.869

COMPLEXES DU 2-MÉTHIONINE PHÉNOTHIAZINIUM

PAR

LUMINIŢA PĂUNESCU

1. Introduction

La synthèse du dérivé phénothiazine-méthioninique [1] et ses réactions d'identification [2] ont mis en évidence la formation de composés dans lesquels le 2-méthionine phénothiazinium (FTM) interactionne avec les anions anorganiques et organiques.

Les articles publiés concernant ce type d'interactions laissent apparaître un certain désaccord entre les divers auteurs. Par exemple, les résultats des déterminations effectuées par Mesnard et Lagubeau [3], [4] impliquent l'existence des sels doubles, tandis que Sato, Kinoshita, Sano et Akamatu [5] considèrent les composés obtenus des complexes à transfert de charge. En supposant le transfert d'un électron, appartenant à un donneur vers une molécule d'accepteur, les complexes à transfert de charge des phénothiazines ont été attentivement étudiés [6]...[16].

Afin de préciser la nature des composés formés et antérieurement décrits [2], on a effectué une étude spectroscopique dans les domaines UV, visible et IR pour les composés obtenus ci-dessous: [FTM][HgI_4]; [FTM]H[BiI_6]; [FTM][MoO_4]; [FTM][CdI_4]; [FTM]H[$Fe(CN)_6$]; [FTM][MnO_4]$_2$; [FTM]$_3$[$H_2W_{12}O_{40}$]; [FTM]$_2$[$SiW_{12}O_{40}$]; [FTM][CrO_4]; [FTM][Cr_2O_7]; [FTM]$_x$[ADN]$_y$; [FTM][$C_6H_2(NO_2)_3O$]; [FTM]$_x$[ARN]$_y$; [FTM][$C_3H_8O_6P$]$_2$.

2. Partie expérimentale

Les spectres IR ont été enregistrés à l'aide d'un spectrophotomètre Perkin-Elmer 577, sous forme de pastilles de KBr, (200...4 000 cm^{-1}) et aussi à l'aide d'un spectrophotomètre Specord 71 Zeiss (700...4 000 cm^{-1}). Quant aux spectres UV etVIS, on a employé un spectrophotomètre Unicam SP-800 B et aussi un Spectrophotomètre Specord UV-VIS 71 Zeiss.

Pour les spectres UV — VIS on a utilisé, comme solvant, le diméthyl sulfoxyde (DMSO) dans lequel la majorité des produits sont solubles, ou un mélange de DMSO/eau.

3. Résultats et discussion

3.1. Spectres IR

On a attribué les caractéristique spectrales de la FTM et des complexes correspondants présentés dans le tableau 1, en les comparant aux donnés de la littérature dans ce domaine [1], [17]...[24].

On peut remarquer que tous les composés synthétisés présentent une ou deux bandes d'absorbtion dans le domaine 1 595...1 470 cm^{-1}. Ces

vers des longueurs d'onde plus grandes (395→600 nm). Il est différent du spectre dans l'eau, qui présente les maximums à 237, 277, 337 et 390 nm [1]. Ceci prouve une interaction entre le DMSO et la FTM, ce qui complique l'interprétation des spectres que nous avons enregistré, en utilisant le DMSO comme solvent.

Comme exemple typique, on a pris le complexe moléculaire formé entre la FTM et l'acide picrique (AP), le spectre (dans le DMSO) présente quelques déplacements et l'apparition d'une nouvelle bande, qui ateste la formation d'un complexe à transfert de charge. Donc, l'acide picrique (dans le DMSO) présente des bandes caractéristiques à 260, 377 et un épaulement à 420 nm. Dans le complexe moléculaire FTM.2AP apparaissent trois bandes à 280, 384 et 632 nm (encore une, moins intense, à 260 nm). Les deux premières peuvent être attribuées aux transitions électroniques $\pi_{cycle} \rightarrow \pi^*_{NO_2}$ et $\pi_{NO_2} \rightarrow \pi^*_{NO_2}$ et la troisième, caractéristique au complexe, à la transition $n_{N(FTM)} \rightarrow \pi_{NO_2(AP)}$, ce qui pourrait être attribuée à un transfert intermoléculaire de charge.

Les spectres du complexe $FTM.CrO_4$ et K_2CrO_4 (un des réactants) ont été enregistrés dans un mélange de solvants $DMSO-H_2O$(3:2 v/v), parce que le K_2CrO_4 n'est pas soluble dans le DMSO pur. En comparant avec l'ion CrO_4^{2-}, qui présente des maximums à 273 et 360 nm, dans le complexe les maximums apparaissent à 267, 302, 330 mm ; la nouvelle bande de 302 nm plaide en faveur de la formation d'un complexe à transfert de charge.

Tenant compte de la structure pliée du cycle phénothiazinique [30] ainsi que des données spectroscopiques, on peut formuler les composés mentionnés comme des complexes à transfert de charge, du type des paires ionique.

Reçue le 4 avril 1981

Institut Polytechnique, Jassy,
Chaire de Chimie anorganique
et analytique

BIBLIOGRAPHIE

1. Oiţă N., Airinei A., Surpăţeanu Gh., Rev. Chim. (Bucureşti), **30**, 425 (1979.)
2. Păunescu L., Fişel S., Oiţă N., Farmacia, **27**, 183 (1979).
3. Lagubeau J., Mesnard P., Bull. Soc. Chim. France, *1965*, 2815 (1971).
4. Mesnard P., Lagubeau J., C. r. Ac. Sci., Paris, **260**, 613 (1965).
5. Sato Y., Kinoshita M., Sano M., Akamatu H., Bull. Chim. Soc. Japan, **40**, 2539 (1967).
6. Azzone G. F., Azzi A., Rossi C., Milic G., Biochim. Z., *345*, 322 (1966).
7. Fulton A., Lyons L. E., Austral. J. Chem., **20**, 2267 (1967).
8. Maruchin J. E., Farm. Polska, **22**, 177 (1966).
9. Rubin M., Slonicki A., Neuropsycho-Pharmacol. Proc., 5-th Intern. Congress, Washington, 1966, H. Brilled, Excerpta Medica Foundation, 1967, 661.
10. Yagi K., Ozawa T., Nagatsu T., Biochem. biophys. Acta, **43**, 310 (1960).
11. Eichom G. H., Federation Proc., **20** (supl. 10), 40 (1961).
12. Williams R. J. P., Federation Proc., **20** (supl. 10), 5 (1961).
13. Borg D. C., Cotzias G. C., Federation Proc., **19**, 248 (1960).
14. Briegleb G., *Elektronen – Donatoren – acceptor Komplexe.* Springer, Heidelberg, 1967.
15. Bodea C., Silberg I., *Recent Advance in the Chemistry of Phenothiazines.* Academic Press Inc., New York, 1968.

16. Gutmann F., Keyser H., Agressologie, **9**, 27 (1968).
17. Barbe J., Galy J. P., Hurwic J., Ann. pharm. franc., **30**, 665 (1972).
18. Blažec J., Kračmar J., Cesk. Farm., **24**, 175 (1975),
19. Gutmann F., Keyser H., J. Chem. Phys., **46**, 1969 (1967).
20. Szasz G., Buda L., Hardi P., Lörincz R., Verok M., Acta. Pharm. Hung., **44**, 145 (1974).
21. Thauh Do N., Zsysko E., Farm. Polska, **30**, 499 (1968).
22. Dembinski B., Nowakowski K., Gordizki A., Roczniki Chem., **47**, 1743 (1973).
23. Накамото К., *Инфракрасные спектры неорганических соединении* (пер. с англ.), Изд. Мир, М., 1966, 151, 166, 207, 213, 228.
24. Avram M., Mateescu Gh. D. *Spectroscopia IR. Aplicaţii în chimia organică*. Ed. Tehn., Buc., 1966.
25. Nakanishi K., *Infrared Absorption Spectroscopy*. Holden Day Inc., San Francisco, 1962.
26. Tarasiewicz M., Basinska H., Talanta, **21**, 425 (1974).
27. Saucin M., Van de Vorst A., Biochem. Pharmacol., **20**, 909 (1971).
28. Mercier M., Dumont P., Bull. Soc. Chim. thérap., **6**, 274 (1971).
29. Gutmann F., Keyser H., J. Chem. Phys., **46**, 1969 (1967).
30. Mital R. L., Jaire S. K., Azzaro M., Cambon A., Rosset J. P., Bull. Soc. chim. France, *1970*, 2195 (1970).

COMPLECŞI AI 2-METIONIN FENOTIAZINEI

(Rezumat)

S-a întreprins un studiu spectrofotometric în domeniile ultraviolet vizibil şi infraroşu pentru compuşii obţinuţi între 2-metionin fenotiazină şi anionii: HgI_4^{2-}; BiI_6^{3-}; MoO_4^{2-}; CdI_4^{2-}; $Fe(CN)_6^{3-}$; MnO_4^-; CrO_4^{2-}; $Cr_2O_7^{2-}$; $H_2W_{12}O_{40}^{6-}$; $SiW_{12}O_{40}^{4-}$; acid picric ($C_6H_2(NO_2)_3O^-$), ADN, ARN şi glicerofosfat ($C_3H_8O_6P^-$). Datele spectroscopice obţinute pledează în favoarea formării unor complecşi cu transfer de sarcină.

BULETINUL INSTITUTULUI POLITEHNIC DIN IAŞI
Tomul XXXI (XXXV) Fasc. 1—4, 1985
Secţia II
CHIMIE ŞI INGINERIE CHIMICĂ

D.C. 546.98 ; 547.964.4

COMPLEX COMPOUNDS OF Pd(II) WITH HISTIDINE

BY

OLGA VICOL, NATALIA HURDUC and MARIA NOROC

1. Introduction

The interaction of metallic ions with polypeptides and proteins is a problem of great interest in the chemistry of coordination and in biochemistry.

The imidazol cycle in the molecule of the histidine has a great biological importance ; also it constitutes a possible way of linking of the metallic ions in the albumin serum as well as in the insulin.

A great amount of research was done on metal — histidine complexes. The study of Burk, Shade and Hesselbach reffering to complex compounds of Co with histidine [1] as well as that of Morris [2] reffering to some chelates of Co(II), Ni(II) and Zn(II) with histidine can thus be quoted. More recently, Volstein and his coworkers [3]...[5] published some papers dealing with the preparation and chemical caracterisation of a large series of complex combinations of Pt(II) with histidine.

Taking into account the similarity of behaviour shown by Pd(II) and Pt(II), in the present paper we attempted the synthesis and chemical caracterisation of some complex combinations of Pd(II) with histidine.

Based upon the data found in the literature three new complex compounds of Pd(II) with histidine were prepared.

2. Experimental Part

As a starting point in our synthesis the $K_2[PdCl_4]$ and DL histidine were used.

In order to obtain the $[Pd(hist)_2]$ chelate the molar ratio 1 Pd:4 Histidine and a strong alkaline medium were used.

Heating the solution during two hours in a water bath, holding the volume constant, produced a white-yellow water insoluble precipitate.

It was assumed that the following reaction takes place:

$$K_2[PdCl_4] + 2\,HistH + 2KOH = \underset{(I)}{[Pd(Hist)_2]} + 4KCl + 2H_2O.$$

The compound (I) was later treated with concentrated hidrochloric acid and acetone resulting in separation of yellow-brown crystals, very soluble in water:

$$[Pd(Hist)_2] + HCl_{conc} \rightarrow \underset{(II)}{[Pd(Hist)_2]Cl_2}$$

The aqueous solution of this soluble compound (II) was treated with ammonia (to each 0.2 g of substance 1 ml NH_4OH 1:8 was added) and a complete dissolution of the compound (II) took place:

$$[Pd(Hist)_2]Cl_2 + 2NH_3 \rightarrow [Pd(Hist\ H)_2(NH_3)_2]Cl_2 \text{ (very soluble)}.$$

In order to make evident the formation of this cation, the well-known reaction, from the literature of the complex compounds of platinum, leading to the formation of a Vauquelin type compound by adding $K_2[PdCl_4]$ was used:

$$[Pd(Hist\ H)_2(NH_3)_2]Cl_2 + K_2[PdCl_4] \rightarrow \underset{(III)}{[Pd(Hist\ H)_2(NH_3)_2][PdCl_4]} + 2KCl.$$

This compound has a violet colour and is non-soluble in water as well as in all other usual solvents.

3. Results and Discussions

In order to elucidate the structure of these compounds, their chemical analysis was effected. The results of this analyses, as recorded in Table 1, confirm the proposed formulations.

Table 1

Results of Chemical Analyses

	Compound	$[Pd(Hist)_2]$	$[Pd(Hist\ H)_2]Cl_2$	$[Pd(Hist\ H)_2(NH_3)_2][PdCl_4]$
Pd %	theoretical	25.60	21.74	30.35
	experimental	25.5 ; 24.80	20.80 ; 21.35	30.52 ; 30.25
C %	theoretical	34.85		20.57
	experimental	33.90 ; 34.08		20.80 ; 21.00
H %	theoretical	3.60		3.00
	experimental	3.95		3.17 ; 3.02

In order to elucidate the structure of these three new compounds their IR spectra were determined.

Based upon the data found in the literature [6] the bands were assigned and conclusions upon the coordination of the histidine to the central metallic ion were derived.

One of the most important ranges lies between 1 750...15 550 cm^{-1}, which can give informations about the carboxyl-groups.

Lake most aminoacids, the monochlorhidrate of histidine must not give the carboxylic band.

It was suggested [4] by L a r s o n that this is due to the fact that the pyridinic nitrogen being more basic than the carboxyl group attracts the proton. It is by this reason that the histidine spectrum does not show the —COOH band at 1 750 cm^{-1} but one at 1 630 cm^{-1} assigned to the ionised carboxylic group. The first compound in which the coordination of the histidine to the Pd(II) ion is done by the means of the nitrogen from the $-NH_2$ group and $>N$ shows clearly the band of ionised carboxylic group at 1 625 cm^{-1}.

For the other two compounds where prepared in a strong acid medium (HCl) the band corresponding to the non-ionised carboxyl shows clearly up at 1 740 and 1 745 cm^{-1} respectively.

The free histidine and the first compound show up a band respectively at 1 412 and 1 450 cm^{-1} corresponding to the $-COO^-$ symmetric stretching vibrations.

The three compounds show bands in the range of 3 170... 3 110 cm^{-1} and respectively 3 105 cm^{-1} on one hand and 3 030, 3 045 cm^{-1} on the other hand, which are assigned to the asymmetric and symmetric $-NH_2$ stretching vibrations.

The existence of some strong bands within this range indicates that the histidine is linked to the Pd(II) by means of $-NH_2$ group.

Another strong band shows also up in the range 1 340 ... 1 290 cm^{-1} which is assigned to the $-CH_2$ vibrations (C o r d e s) [7].

The existence of a band in the 1 740 cm^{-1} range for the second and third compound excludes the possibility to the histidine to be bonded by the —COOH group to the Pd(II) ion.

Table 2

Characteristic Group Frequencies for Cmplex Compounds of Pd(II) with Histidine

Compound I $[Pd(Hist)_2]$	Compound II $[Pd(Hist\ H)_2]Cl_2$	Compound III $[Pd(NH_3)_2(Hist\ H)_2][PdCl_4]$	Histidine $C_6H_6N_3O_2$	Assignement of bands
3 190	3 110	3 105		ν_{CH} stretching
			3 140	$\nu_{NH_3}^{+}$ stretching
3 030	3 045			ν_{NH_2} sym. stretching
	1 740			ν_{NH_2} as. stretching
	1 740			$\nu_{C=O}$ stretching
		1 740		$\nu_{C=O}$ as. stretching
1 625			1 630	ν_{COO^-} as. stretching
1 540	1 615	1 610	1 605	$\nu_{NH_3}^{+}$ as. stretching
	1 570	1 580	1 575	$\nu_{C=C}$ stretching
1 512		1 505	1 512	$\nu_{C=N}$ stretching
1 435	1 496	1 480	1 480	$\nu_{NH_3}^{+}$ bending wagging
1 400			1 412	ν_{COO^-} sym. stretching
1 340	1 330	1 290	1 334	ν_{CH_2} wagging

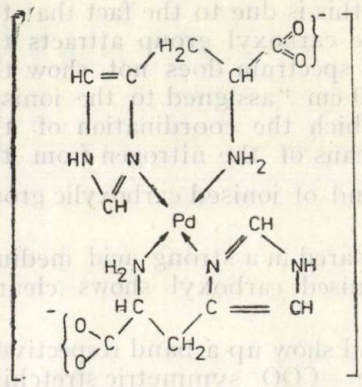

(I)

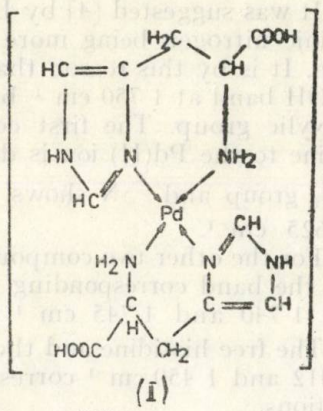

(II)

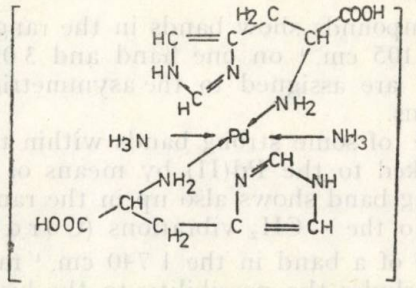

(III)

The following assumptions concerning the structure of the prepared compounds are made based upon the remarks stated above:

a) The proposed formulation were also checked by thermogravimetric analysis.

b) The thermical behaviour of the compounds for a heating rate of 12°C/min, in dynamical conditions of the temperature, was also studied.

c) The effected calculations shows that the weight losses found experimentally are in good agreement with those calculated for the proposed formulations.

Table 3

Thermical Behaviour

Compound	Weight losses, [mg]		Residual, [mg]		Obs.
	calculated	found	calculated	found	
$[Pd(Hist)_2]$	37	37	13	13	Pd met.
$[Pd(Hist)_2]\ Cl_2$	39	40	10.8	10	Pd met.
$[Pd(Hist\ H)_2\ (NH_3)_2]\ [PdCl_4]$	27	25	23	25	$PdCl_2$

The residue for the first and second compound is the metallic paladium, while for the third it is $PdCl_2$.

Received, December 17, 1982

Polytechnic Institute, Jassy,
Department of Inorganic and
Analytical Chemistry
and
Department of Physical Chemistry

REFERENCES

1. Burk D., Shade A. L., Hesselbach M. L., Federation Proc., **5**, 126 (1946).
2. Morris P. Y., Burce Martin R., J. Inorg. Nucl. Chem., 2891 (1970).
3. Вольштейн Л. М., Диканская Л. Д., ЖНХ, **XIX**, *1*, 150 (1974).
4. Вольштейн Л. М., Лукянова Ж. Г., ЖНХ, **XI**, 1327 (1966).
5. Вольштейн Л. М., Диканская Л. Д., ЖНХ, **XIII**, 2524 (1968).
6. Balce V., Theophanides T., J. Inorg. Nucl. Chem., **33**, 1237 (1970).
7. Larson L., Acta chem. Scand., **4**, 27 (1950).
8. Cordes M. M., Walter J. L., Spectrochim. Acta, **24 A**, 1421 (1968).

COMBINAȚII COMPLEXE ALE Pd(II) cu HISTIDINA

(Rezumat)

Se prezintă sinteza și caracterizarea chimică a trei combinații complexe ale Pd(II) cu histidina.

Structura acestor compuși a fost stabilită pe baza spectrelor IR și a analizei termogravimetrice.

BULETINUL INSTITUTULUI POLITEHNIC DIN IAŞI
Tomul XXXI (XXX V) Fasc. 1—4, 1985
Secţia II
CHIMIE ŞI INGINERIE CHIMICĂ

D.C. 66.062 ; 541.135 5

INFLUENCE OF SOLVENTS ON THE BEHAVIOUR OF ELECTRODES

BY
ULRICH P. DECKER

1. Introduction

The investigation of the influence of solvents closely connects the physical chemistry of electrochemical systems with tasks of analytical chemistry through its great practical importance.

A system of the „organic solvent—water" type is converted, by addition of salts, into an electrochemical system. Practical interest is based on the fact, that such systems are of importance as medium of chemical processes.

The following processes may be mentioned as examples: a) distillation and extraction with addition of salts; b) precipitation of salts from aqueous solution by addition of organic solvents; c) electrochemical deposit of metals from the solution of their salts in organic solvents with or without a content of water; d) (continuous) control of electrolyte concentration in a process medium by formation of the electrode potential.

All these processes have some properties in common:

1. they are induced by driving forces;

2. they involve the transport of some kinds of particles through an interface;

3. they are based on the formation of equilibrium after a certain time.

In special cases, a membrane may serve as the phase boundary. This permits the formation of the equilibrium to be modified not only temporally but also with respect to its position.

A simplified description of the situation at such a membrane is presented in Fig. 1. The driving forces give rise to streams and are connected with one another [1]. The individual parameters can be determined and influenced individually.

A simple manifestation of these conditions is the metal—ion-potential on a metal surface. In such cases, one electrode as indicator electrode consists of a metal wire or plate directly connected with one of the poles at the input of the measuring device and immersed into the solution of its corresponding ions. The second electrode is developed as reference electrode, because the potential of one electrode alone cannot be measured. It is only possible to record the potential difference of two electrodes as part of a measuring chain, how it is represented schematically in Fig. 2.

It is possible, however, to insert further materials between the electron-conducting metal of the indicator electrode and the electrolyte solution.

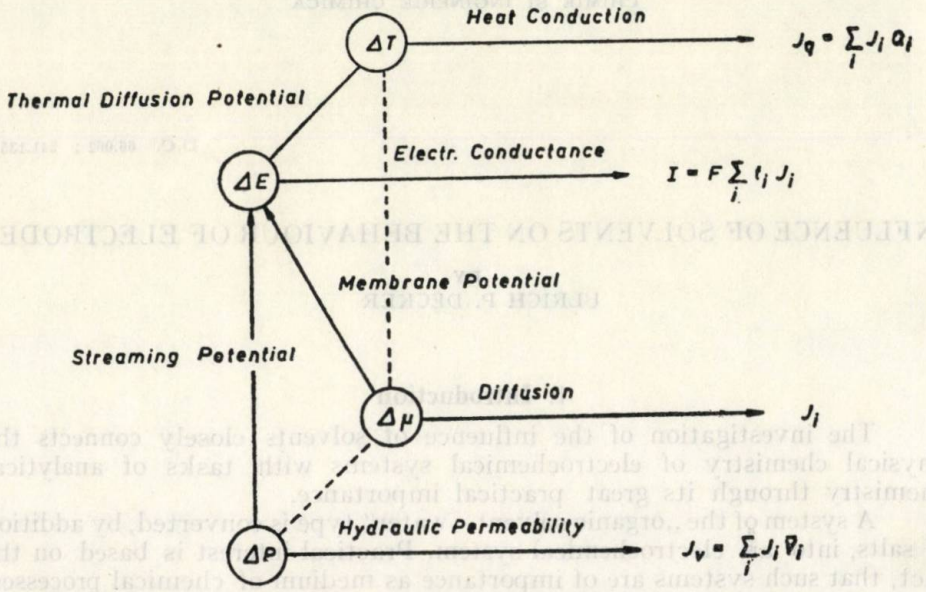

Fig. 1 — Phenomena of transport and potential formation.

Following the division of electrodes into those of the first, second and third kind, a practical classification of electrodes can be established, which also takes account of their applications, how it is shown in Table 1.

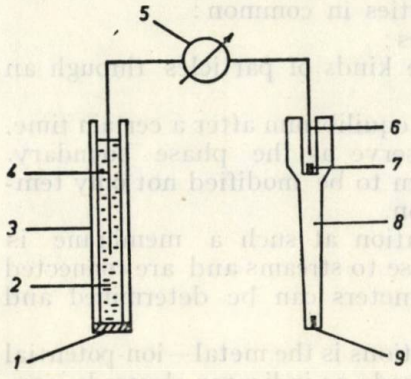

Fig. 2. — Scheme of a measuring chain for potentiometric investigations using electrodes: *1* – sensing element; *2* — inner reference solution; *3* — inert electrode body; *4* — internal reference electrode; *5* — amplifier; *6* — reference electrode; *7* — salt bridge, by; *8*, *9* — conducting element — diaphragm comnnected with sample solution respectively reference electrode.

Table 1

Types of Sensors

Metal (wire) Electrode
Membrane Electrodes
Glas Membrane
Solid State Membrane
Liquid State Membrane
Enzyme Electrode

Nowadays glass, solid and liquid membrane electrodes, in addition to metal electrodes, have found wide applications in practice under the name of ion-selective sensors or electrodes [2]. It appeared that potentiometric measurements are of advantage, as compared with other methods of analysis, if the measurement conditions can be fitted to the conditions necessary for this method to be used [3].

The advantages are the following : a) high sensitivity in a wide range of concentration ; b) great measuring range ; c) small amount of sample solution required; d) convenient measuring technique.

The most important fact is that using electrodes the mean activity of an ion can be converted into an easy measurable electrical quantity. This gives the possibility of signal supervising and automatical controlling of processes.

The measurements preferably are carried out in aqueous solution for a great number of ions which are also of importance for environment protection tasks [4]. But also measurements in mixed solvents are of interest. For application purposes the behaviour of the electrode system under these conditions must be studied [5].

2. Formation of the Electrode Potential

When the electrode is immersed into the solution, the process of charges separation at the electrode—electrolyte phase boundary begins, in order to reduce the equilibrium perturbation. Due to the anisotropy of forces acting directly at the phase boundary rearrangements of the particles within the reach of these forces begins. The aim of these processes is a new state of lowest G i b b 's free energy.

The electrical double layer develops. However, the ions are also able to permeate through the double layer and to migrate into the electrode phase if this can lead to an increase in energy. The opposite process — the migration of an ion into the solution is also possible. Hence, at the phase boundary a state develops which is dependent on the activity of that kind of ions which is present both in the solution phase and the electrode one and can pass through the interface. It is called the potential-determining kind of ions.

This new equilibrium state can be reached under definite condition only:

a) There must be present at least one kind of ions for which this equilibrium can be formed. The electrode is then sensitive to this kind of ions. This is given for a metal electrode by insertion of the ions in question in the lattice under the equilibrium potential.

b) Equilibrium can be formed only if material transport through the interface is not generally hindered. This gives the possibility of controling the selectivity by influencing the transport properties of a phase boundary formed as a membrane.

c) The kind of ions in question must be present in the two phases in such an amount that the identity of the phase does not change when the equilibrium is formed. This point is of importance at extremly low concentrations.

d) Permeation of an ion through the interface involves the necessity of stripping the solvation shell. Here the influence of solvent and counter ions is especially effective.

3. Investigations in Mixed Solvents

In order to determine the influence of solvents on the formation of potential of an electrode, the system:

SCE/0.1 M $KNO_3(H_2O)/Ag^+$, NO_3^- (organic solvent, H_2O)/Ag

was used variing the volume properties of the organic solvent in the mixture.

The influence was studied in such solvents as acetonitrile, dimethylformamide, dimethylsulfoxide, dioxane, acetone, ethylene glykol, methanol, ethanol, propanol.

In the case of acetonitrile it appeared, that the deviation of the whole curve from the N e r n s t-straightline increases with increasing content of organic solvent, how this shows Fig. 3. In mixtures of water with organic nitriles as solvents, the silver ion is specific solvated to a considerable degree, which is due to the specific interaction of the d^{10}-cation with the π-orbital of the nitrile group. Furthermore, a linear behaviour was observed up to an Ag^+-concentration of 10^{-7} mol l^{-1}. This is an extension of the measuring range as compared with the aqueous system.

Direct potentiometric measurements in the presence of protic solvents, how methanol, ethanol, propanol and ethylene glykol, yielded potentials near those of the N e r n s t-curve in aqueous medium. This shows Fig. 4 for the propanol—water-system.

In the presence of the dipolar aprotic solvents, as acetonitrile, dimethylsulfoxide, dimethylformamide, dioxane, acetone, considerable deviations from the N e r n s t-behaviour occur, which increase with increasing solvent content. These deviations can be explained by specific interactions of the silver ion with the molecules of the organic solvent. Fig. 5 shows these deviations in the case of the dimethylformamide — water-system. Furthermore, with DMSO a change of the selective solvation was observed, how this shows Fig. 6. With high DMSO contents, the silver ion is specifical solvated. Hence from DMSO contents of about 60 vol.% upwards, the deviations from the N e r n s t-curve are particularly remarkable.

The AgCl precipitation by KCl has also been investigated in the presence of different solvents. When protic solvents were used, potential jumps were observed, which were almost equal to those in pure water. Extremly high concentrations, near 90 vol. % of the monovalent alcohols, also lead to a distinct increase of the potential jump. The increase is especially great in the presence of acetone and dioxane. Hence for analysis purposes, precipitation titration should be preferably carried out in these solvents.

Furthermore, anions and their behaviour in the solvent mixtures also exert a great influence on the potential formation. The examples presented were intended to describe the effect of different factors on potential formation. These factors are:

1. The solubility product. The lower its value, the lower will be the attainable final activity of Ag^+ in the precipitation titration, and the greater the observed potential jump.

2. The solvation of cations and anions. Both factors are closely connected with each other. According to our opinion, the stability of the solvation shell is of great importance for potential formation in these systems.

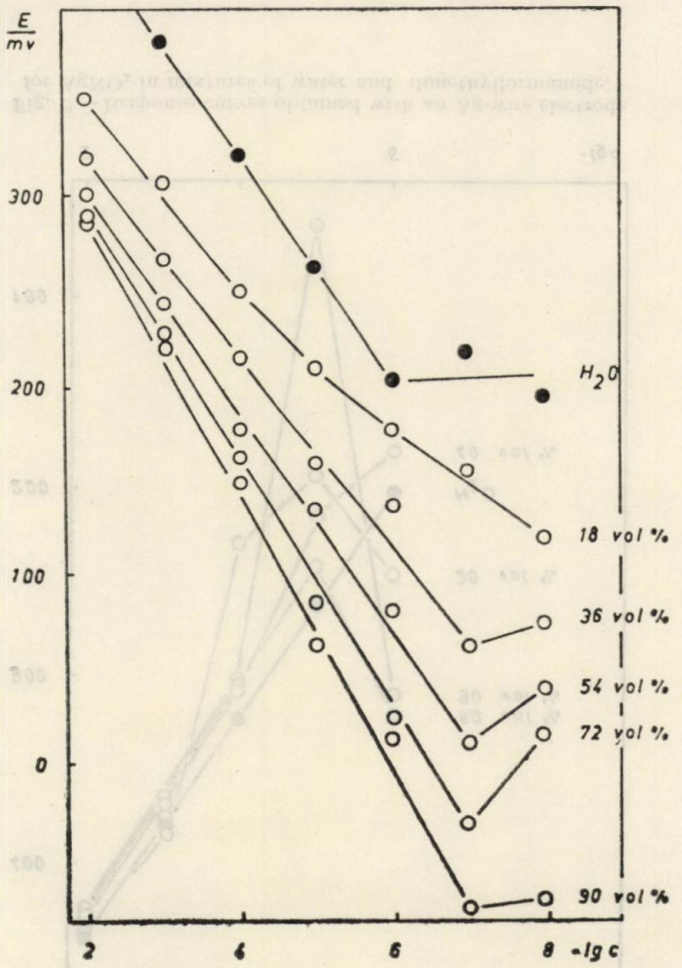

Fig. 3. — Response curves obtained with an Ag-wire electrode for $AgNO_3$ in mixture of water and acetonitrile.

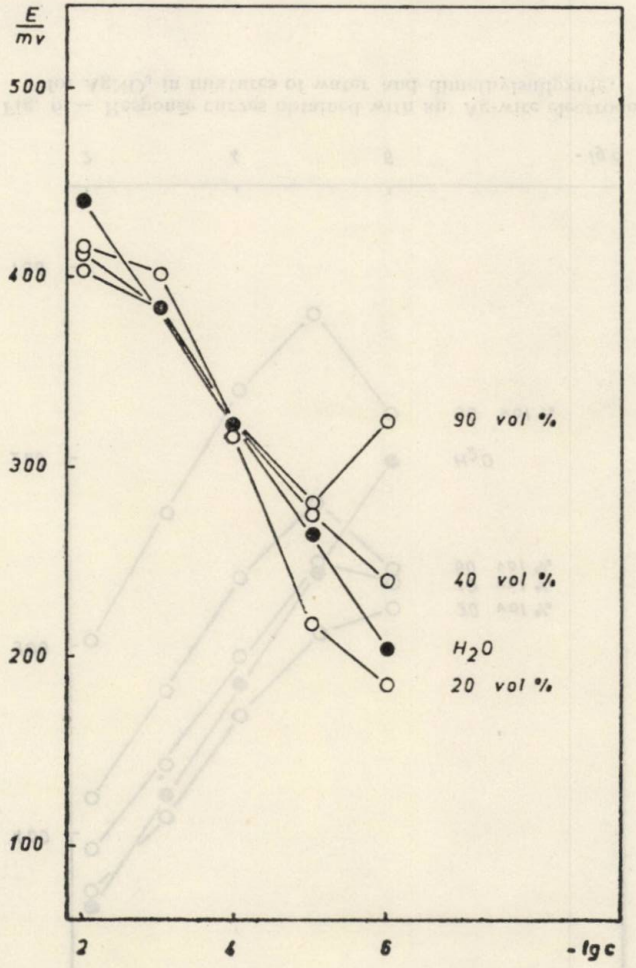

Fig. 4. — Response curves obtained with an Ag-wire electrode for $AgNO_3$ in mixtures of water and *n*-propanol.

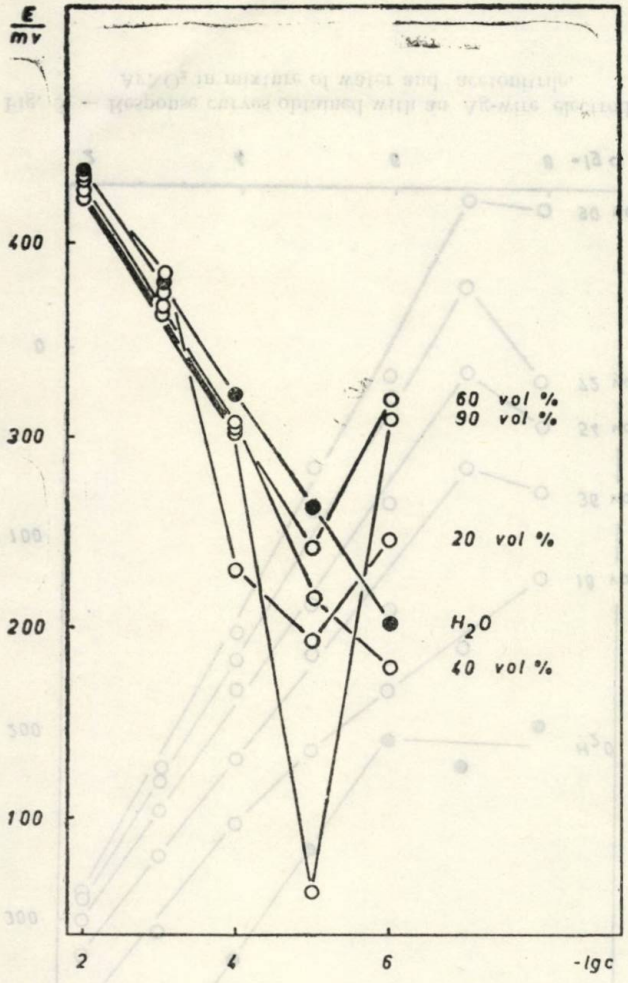

Fig. 5.—Response curves obtained with an Ag-wire electrode for $AgNO_3$ in mixtures of water and dimethylformamide.

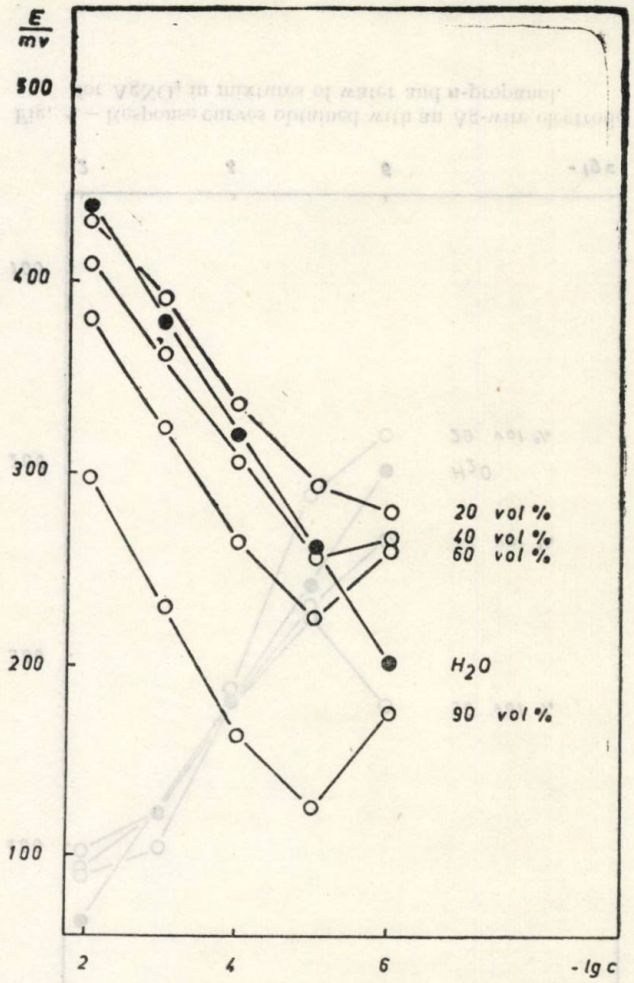

Fig. 6. — Response curves obtained with an Ag-wire electrode for $AgNO_3$ in mixtures of water and dimethylsulfoxide.

A stable solvation shell leads to a decrease of the activity of the cation and causes a decrease of the observed electrode potential. In that manner all negative deviations from the N e r n s t-straightline in various mixtures of water and organic solvent can be interpreted (Fig. 3 and 5 for example).

On the other hand a less stable solvation shell causes an increase of the potential, how it occurs in mixtures of water and propanol or DMSO with high respectively low contents of organic solvent. This opinion serves as a basis for a concept concerning with the influence on the solvation shell of a cation. The aim can be a less stable solvation shell. This can be obtained on the following ways:

a) Steric hindered solvation. Solvents from a great size cannot lead to a stable solvation situation in all cases.

b) Hindered solvation in two cases:

1. favoured solvation of the anion;

2. less stable solvation of the cation, because the interaction ion — molecule of solvent itself is low.

Table 2

Selected Data for Used Solvents and Ions

Classification by HSAB concept				
	aprotic	protic	solvents	
Soft Hard	acetonitrile	water	methanol	ethylene glykol
ε_{rel}	37	78	33	38
R_M/cm^3 . mol^{-1}	11	3	8	15

Classification by HSAB concept		
Weak acids Hard bases	Ag^+ SO^{2-}	Cu^{2+} NO_3^-

Energy of frontier orbitals		
	E_n, [ev]	E_m, [ev]
Cu^{2+}	−0.55	−5.8
Ag^+	−2.82	−4.7

A systematic influence requires the description and discrimination of the particles by quantitative data [6]...[8]. We chose the following procedure for the description: a) the relative strength of interaction between ions and solvents was described by the concept of hard and soft acid and bases, including the calculation of the front orbital energies of the ions; b) additionally, we distinguished between protic and aprotic solvents, deter-

mining them by the relative permittivity and the molecular refraction.

Selected data, which we have used for description, are presented in Table 2.

The described concept and the procedure of description is not only usefull to understand the presented examples. The concept was also succesfull in the case of analysis of potentiometric measurements in systems of Cu^{2+} and various anions in mixed solvents.

Received, April 24, 1984

Technical University „Carl Schorlemmer",
Leuna Merseburg,
German Democratic Republic

REFERENCES

1. Rödicker H., Chem. Techn., **32**, 5, 239 (1980).
2. Koryta J., Anal. Chim. Acta, **91**, 3 (1977).
3. Decker U. P., Geyer R., Acta hydrochim. et hydrobiol., **12**, *1*, 49 (1984).
4. Никольский Б. П., Матерова Е. А., *Ионселективные электроды*. Изд. Химия, Ленинград, 1980.
5. Pungor E., Tóth K., Gábor-Klatsmanyi P., Hungarian Scientific Instruments, **49**, 1 (1980).
6. Geyer R., Decker U. P., Görner W., Z. Chem., **19**, 6, 229 (1979).
7. Pearson R. G., J. Amer. Chem. Soc., **85**, 3533 (1963).
8. Персон Р. Г., Усп., хим., **48**, 1259 (1971).

INFLUENŢA SOLVENŢILOR ASUPRA COMPORTĂRII ELECTROZILOR

(Rezumat)

Dată fiind importanţa indicaţiilor potenţiometrice pentru scopurile tehnologice, se descrie caracterul complex al potenţialului şi legătura sa cu proprietăţile solventului. Sînt demonstrate exemple de cooperare ale ionului de Ag^+ cu solvenţii. Mai mult, s-a făcut o tentativă de sistematizare a rezultatelor măsurătorilor potenţiometrice directe în baza unei concepţii moderne în vederea caracterizării componentelor sistemului.

BULETINUL INSTITUTULUI POLITEHNIC DIN IAȘI
Tomul XXXI (XXXV) Fasc. 1—4, 1985
Secția II
CHIMIE ȘI INGINERIE CHIMICĂ

D.C. 541.121

CONTRIBUTION TO THE STUDY OF CHEMICAL EQUILIBRIUM IN THE FORMATION OF NITROGEN OXIDE

BY

ANA TARHON, N. AELENEI and M. ȘCHIOPU

1. Introduction

The reaction of nitrogen oxide formation :

(1) $$\tfrac{1}{2}O_2 + \tfrac{1}{2}N_2 = NO$$

is endothermic, the thermal effect under standard conditions having values comprised between $\Delta_R H^0_{298K} = 90.37$ KJ mol^{-1} and $\Delta_R H^0_{5\,000K} = 86.63$ KJ mol^{-1}. Qualitatively, one may assert that at high temperatures the chemical equilibrium for the reaction (1) will be shifted towards right. Indeed, rather large amounts of NO can be obtained working only at extremely high temperatures, about 4 000 K, obtained by means of electric arc. At these temperatures the reactions are fast enough for the chemical equilibrium to be attained in an extremely short time, for all possible reactions. For this reason, in a system formed of O_2, N_2 and NO, the chemical composition at equilibrium will be determined exclusively by thermodynamic factors. At temperatures lower than 1 500 K the reaction rates of NO formation and decomposition, respectively, that is of both straight and reverse reactions equal practically zero. That's why the nitrogen oxide can be obtained at low temperatures only in a thermodynamically unstable state, such as in case of catalytic oxidation of NH_3. In this reaction, proceeding commercially at temperatures of about 1 000...1 200 K, the reaction products contain the initial nitrogen amount almost exclusively as nitrogen oxide, although under these conditions it is completely unstable from the thermodynamic point of view.

To calculate the equilibrium composition, in literature [1] one considers only reaction (1), neglecting the other reactions taking place simultaneously. The calculation of composition at equilibrium for simultaneous reactions is not reported in literature in a satisfactory manner. Thus, in many cases, the criteria for establishing the molecular species able really to exist in the considered system are not given, while, on the other hand, the methods for establishing the independent reactions and for solving the system of thermodynamic equations are uselessly complicated [2].

In the following a more reasonable method is proposed, based on the reaction (1).

2. The Proposed Method

Let us note by M the number of molecular species which have a high enough probability of existence at the equilibrium. At high temperatures this probability can be appreciated from the general condition of chemical equilibrium which requires the free enthalpy, at certain values of overall pressure and temperature to be minimum.

Taking by convention the free standard enthalpy of the simple substances equal to zero, in the present case of the molecular species O_2 and N_2, $\Delta_R G^0$ values are to be calculated for the reactions in which one mole O_2 or one mole N_2 distribute as other molecular species.

The more stable molecular species is, that is the higher its probability to exist within the system, the smaller $\Delta_R G^0$ for the reaction of species formation is. By eliminating the molecular species for which $\Delta_R G^0$ is particularly high one may establish the number of molecular species, M. To be able to compare $\Delta_R G^0$ values, that is the existence probabilities or the thermodynamic accesibilities of the molecular species the calculations have to be performed starting every time from one mole O_2 or N_2.

To calculate $\Delta_R G^0$ values, the data given in [3] are used. At 3 500 K the ratio between the standard free enthalpy of formation and temperature, G_f^0/T, has the following values:

	G_f^0/T, [J mol^{-1} grd^{-1}]
O_2, [g]	0
N_2, [g]	0
O, [g]	5.54
N, [g]	69.5
NO, [g]	13.5

For other chemical compounds, such N_2O or NO_2, the much higher values for G_f^0/T indicate them to be completely unstable at this temperature.

One mole O_2 may be distributed between various compounds according to the reactions:

$$O_2 = 2O, \qquad \Delta_R G^0 = 38\,780 \text{ J mol}^{-1};$$

$$N_2 + O_2 = 2NO, \qquad \Delta_R G^0 = 92\,750 \text{ J mol}^{-1}.$$

One mole N_2 may be distributed according the reaction :

$$N_2 = 2N \qquad \Delta_R G^0 = 486\,500 \text{ J mol}^{-1}.$$

The increase of the standard free enthalpy for the formation of the chemical species O, NO and N in comparison to that of simple substances in stable form, O_2 and N_2, is depicted in Fig. 1. The probabilities of

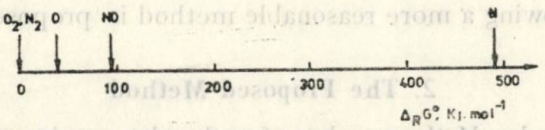

Fig. 1

existence of the molecular species decrease in order O, NO and N. The amount of atomic nitrogen would be so small that it could practically

Taking by convention the free standard enthalpy of the simple substances equal to zero, in the present case of the molecular species O_2 and N_2, $\Delta_R G^0$ values are to be calculated for the reactions in which one mole O_2 or one mole N_2 distribute as other molecular species.

The more stable molecular species is, that is the higher its probability to exist within the system, the smaller $\Delta_R G^0$ for the reaction of species formation is. By eliminating the molecular species for which $\Delta_R G^0$ is particularly high one may establish the number of molecular species, M. To be able to compare $\Delta_R G^0$ values, that is the existence probabilities or the thermodynamic accesibilities of the molecular species the calculations have to be performed starting every time from one mole O_2 or N_2.

To calculate $\Delta_R G^0$ values, the data given in [3] are used. At 3 500 K the ratio between the standard free enthalpy of formation and temperature, G_f^0/T, has the following values:

	G_f^0/T, [J mol^{-1} grd^{-1}]
O_2, [g]	0
N_2, [g]	0
O, [g]	5.54
N, [g]	69.5
NO, [g]	13.5

For other chemical compounds, such N_2O or NO_2, the much higher values for G_f^0/T indicate them to be completely unstable at this temperature.

One mole O_2 may be distributed between various compounds according to the reactions:

$$O_2 = 2O, \qquad \Delta_R G^0 = 38\,780 \text{ J mol}^{-1};$$

$$N_2 + O_2 = 2NO, \qquad \Delta_R G^0 = 92\,750 \text{ J mol}^{-1}.$$

One mole N_2 may be distributed according the reaction :

$$N_2 = 2N \qquad \Delta_R G^0 = 486\,500 \text{ J mol}^{-1}.$$

The increase of the standard free enthalpy for the formation of the chemical species O, NO and N in comparison to that of simple substances in stable form, O_2 and N_2, is depicted in Fig. 1. The probabilities of

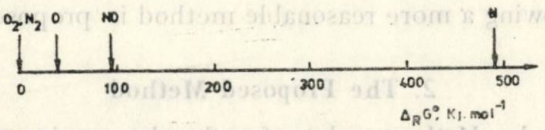

Fig. 1

existence of the molecular species decrease in order O, NO and N. The amount of atomic nitrogen would be so small that it could practically

$$x_2 = x_3 + \frac{K_1}{2}\sqrt{x_3}, \tag{9}$$

$$x_1 = K_2\sqrt{x_3^2 + \frac{K_1}{2}x_3\sqrt{x_3}}, \tag{10}$$

$$x_1 = K_1\sqrt{x_3}, \tag{11}$$

$$f(x_3) = x_3^2 + \frac{12K_1 - K_1K_2^2}{2(4-K_2^2)}x_3\sqrt{x_3} - \frac{16-9K_1^2}{4(4-K_2^2)}x_3 - \frac{3K_1}{4-K_2^2}\sqrt{x_3} + \frac{1}{4-K_2^2} = 0. \tag{12}$$

By calculating the equilibrium constants, at various temperatures, for the reactions:

$$\tfrac{1}{2}O_2 = O, \ (K_1); \qquad \tfrac{1}{2}O_2 + \tfrac{1}{2}N_2 = NO, \ (K_2),$$

the equation (12) may be solved by succesive approximations, simply performed by means of a minicalculator with programme.

From the equations (9)... (11), x_1, x_2 and x_4 are obtained. If interest exist in obtaining the dissociation degree of NO, one calculate q from Eq. (5) and then $\alpha_{NO} = (q-1)/q$.

In the above relations x_1 represent the molar fraction of NO at the equilibrium attained at a high temperature. By cooling sharply the gas mixture the decomposition rate of NO fastly approaches zero so that the equilibrium with respect to NO is „frozen" at low temperatures. The atomic oxygen formed at high temperatures recombines at lower temperatures to form O_2. The mole fraction of NO in cold gases, containing no more oxygen atoms, is:

$$x_{NO}\ (\text{cold gases}) = \frac{x_1}{x_1 + x_2 + x_3 + 0.5x_4}. \tag{13}$$

In this way, the values listed in Table 1 are obtained for x(NO) in „hot" and „cold" gases at different temperatures.

Table 1

T, [K]	K_1	K_2	x (NO) Eq. (10)	x (NO) Eq. (13)	x (O) Eq. (11)
4 000	1.5829	0.2971	0.05640	0.07477	0.49135
3 500	0.5136	0.2032	0.06650	0.07668	0.26564
3 000	0.11898	0.12158	0.05286	0.05497	0.07674
2 500	0.015585	0.05894	0.02832	0.02847	0.01077
2 000	7.344×10^{-4}	0.019847	0.00982	0.00982	5.165×10^{-4}
1 500	4.589×10^{-6}	3.224×10^{-3}	0.00161	0.00161	3.24×10^{-6}

In the last column of the Table 1 the mol fraction is given of atomic oxygen in hot gases. One may notice that the presence of oxygen may be ne lected

at temperatures under 2 000 K but has to be considered at high temperatures. For instance, at 3 500 K, by considering only the reaction:

$$\tfrac{1}{2}O_2+\tfrac{1}{2}N_2=NO,\ K=0.2032,$$

started with pure NO, the value obtained for x(NO) at equilibrium, 0.04621, is considerably different from that obtained for sharply cooled gases (0.07668).

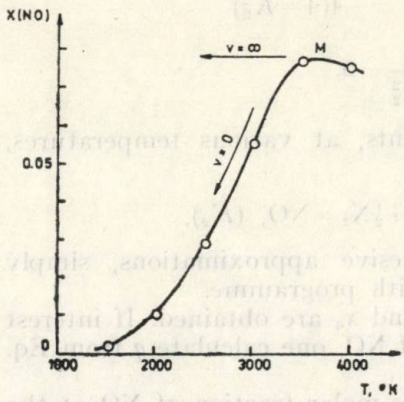

Fig. 2

Due to the different manners in which K_1 and K_2 vary with temperature, x (NO) for cold gases show a maximum a little above 3 500 K, as seen in Fig. 2.

Starting from pure NO or from an equimolecular mixture of N_2 and O_2 and attaining the chemical equilibrium at 3 500 K, the mol fraction of NO calculated by considering that the atomic oxygen was converted subsequently in O_2 molecule will correspond to the point M in Fig. 2.

By cooling the reaction mixture at a theoretically infinite rate in cold gases, 7.668% vol NO would be obtained while at a very small cooling rate (theoretically null) the cold gases would practically contain no NO. In Fig. 2 the variation of composition, by cooling, is indicated by arrows, for the extreme rates $v=\infty$ and $v=0$, respectively.

It might be thus explained the occurence of nitrogen oxide in fuel gases of a fuel in mixture with excess air, if the temperature exceeds 1 500 K and the gases are sharply cooled, by detent, for instance in termal engines.

Received, January 18, 1982

Polytechnic Institute, Jassy,
Department of Physical Chemistry

REFERENCES

1. Dubrisay R., Pascal P., *Nouveau Traité de Chimie Minérale.* Vol. **X**, Paris, 1956.
2. Landauer O., Geană D., Iulian O., *Probleme de chimie fizică.* EDP, Buc., 1978.
3. Landolt-Börnstein, *Zahlenwerte und Funktionen.* **II** Bd., 4 Teil, Springer-Verlag, Berlin, 1961.

CONTRIBUȚII LA STUDIUL ECHILIBRULUI CHIMIC PENTRU FORMAREA OXIDULUI DE AZOT

(Rezumat)

Se studiază echilibrul chimic pentru formarea oxidului de azot, calculîndu-se compoziția la echilibru, prin utilizarea unei metode originale, care ia în considerație nu numai reacția principală ci și alte reacții care au loc simultan în sistem.

BULETINUL INSTITUTULUI POLITEHNIC DIN IAŞI
Tomul XXXI (XXXV) Fasc. 1—4, 1985
Secţia II
CHIMIE ŞI INGINERIE CHIMICĂ

C.Z. 66.049.6 ; 661.321

CERCETAREA PROCESULUI DE SUBLIMARE A CLORURII DE AMONIU

II. INFLUENŢA PARAMETRILOR ASUPRA VITEZEI PROCESULUI DE SUBLIMARE

DE

AL. SZÉP, C. CALISTRU, LIVIA IFRIM şi GH. MIHĂILĂ

1. Introducere

Cercetarea procesului de sublimare a clorurii de amoniu prezintă o importanţă deosebită pentru stabilirea parametrilor tehnologici ai procesului de descompunere a clorurii de amoniu cu carbonat de calciu. Literatura de specialitate consacrată studiului de sublimare [1]...[6] conţine puţine date referitoare la influenţa diferiţilor factori cinetici asupra vitezei procesului.

În cele ce urmează se efectuează un studiu al procesului capabil să permită stabilirea ecuaţiilor care descriu analitic procesul şi a condiţiilor optime de lucru. În acest scop, în cele ce urmează se prezintă rezultatele cercetărilor experimentale privind influenţa temperaturii, volumului stratului şi a debitului agentului de antrenare a fazei gazoase obţinute în urma sublimării, exercitate asupra procesului global.

2. Metodica cercetării experimentale

Pentru cercetarea procesului de sublimare a clorurii de amoniu s-a utilizat o termobalanţă (fig. 1) rezistentă la coroziunea fazei gazoase, prevăzută cu sistem de măsurare şi reglare a temperaturii şi care permite antrenarea cu debit controlat a fazei gazoase.

Modelul hidrodinamic al reactorului experimental corespunde reactorului în strat fix de granule şi antrenare continuă a fazei gazoase.

În studiul procesului s-a utilizat clorură de amoniu, uscată în prealabil într-o instalaţie de uscare la vid prevăzută cu P_2O_5 ca agent de uscare şi avînd dimensiunile granulelor $d_p = 0{,}5...0{,}63$ mm, determinate prin cernere uscată. Determinările au fost efectuate la temperaturi de : 473, 523, 573, 623, 673, 773 K, volumul stratului de granule fiind cuprins între 0,14... 0,64 cm^3 iar debitele de antrenare între 15... 45 l/h.

Pentru determinarea gradului de transformare în procesul de sublimare s-a utilizat relaţia:

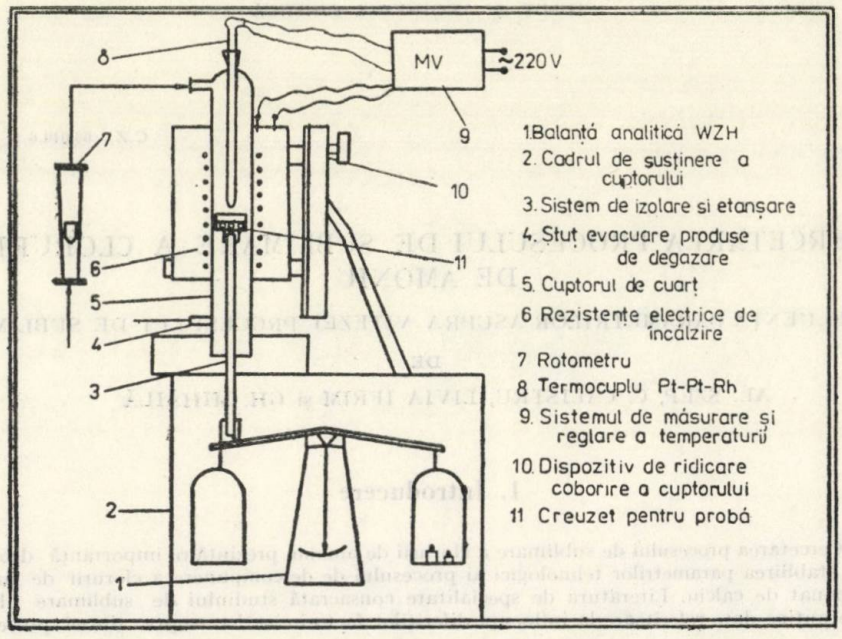

Fig. 1. — Schema instalaţiei experimentale.

$$\eta_{NH_4Cl} = \eta_{[]_s} = \frac{\Delta m_\tau}{m_p^0}, \tag{1}$$

unde: Δm_τ — variaţia masei probei în inventarul $[0, \tau]$, măsurată direct prin cîntăriri la termobalanţă; m_p^0 — masa probei iniţiale supusă analizei; η_{NH_4Cl}; $\eta_{[]_s}$ — gradul de transformare a clorurii de amoniu în procesul de sublimare.

Pentru eliminarea, pe cît posibil, a erorilor experimentale, la fiecare set de valori s-au efectuat mai multe experienţe (2...7 experienţe) iar pe baza acestora s-au calculat valorile medii ale gradelor de transformare.

3. Rezultate obţinute; interpretarea rezultatelor

Rezultatele obţinute sînt prezentate sub forma dependenţelor $\eta_{[]_s} \ldots \tau$ în fig. 2...4, 8...12. Din dependenţele prezentate în fig. 2...4 se poate constata că indiferent de volumul stratului, temperatura exercită o mare influenţă asupra vitezei procesului de sublimare. Pentru a pune mai elocvent în evidenţă influenţa temperaturii, aceste date primare au fost prelucrate prin trasarea dependenţelor specifice obţinute cu ajutorul relaţiei lui Arrhenius:

$$K = K_0 e^{-E_a/RT}, \tag{2}$$

şi anume

$$\lg K = \lg K_0 - \frac{E_a}{R} \cdot \frac{1}{T} \quad (3)$$

Astfel, prin reprezentarea datelor în coordonate specifice $\lg(1/\tau)...(1/T)$, pentru diverse valori ale gradelor de transformare, s-au obținut dependențele prezentate în fig. 5...7.

După cum se poate constata din curbele trasate in fig. 5 temperatura are aceeași influență indiferent de valoarea gradului de transformare (segmentele de drepte sînt paralele). Totodată se poate constata că în cazul volumului mic de strat, ceea ce corespunde unui strat monogranular de substanță, pot fi evidențiate două domenii distincte și anume: la temperaturi mai mici de 523 K energia aparentă de activare indică faptul că procesul se desfășoară pe baza modelului macrocinetic transformare, iar la temperaturi de peste 523 K procesul de desfășoară pe baza unui model macrocinetic combinat.

Creșterea volumului inițial de probă estompează această influență specifică a temperaturii astfel că în cazul $V^0_{strat} = 0{,}32$ cm³ (fig. 6) și $V^0_{strat} = 0{,}64$ cm³ (fig. 7) se evidențiază un singur mecanism indiferent de valoarea gradului de transformare. Energia aparentă de activare obținută în aceste cazuri sugerează faptul că procesul se desfășoară pe baza unui model macrocinetic combinat.

Pe baza dependențelor $\lg(1/\tau)...1/T$ trasate și pentru celelalte condiții experimentale efectuate s-au calculat energiile aparente de activare. Aceste valori sînt prezentate în tabelul 1.

Tabelul 1

Energiile aparente de activare calculate pe baza dependențelor lg $(1/\tau)...(1/T)$

V^0_{strat} cm³	E_a		Obs.
	cal/mol	J/mol	
0,14	16 340	68 464,6	$T \leqslant 523$ K
	7 000	29 330	$T \geqslant 523$ K
0,32	10 430	43 701,7	Pentru întreg intervalul de temperatură studiat.
0,46	9 100	38 129	
0,64	9 200	38 548	

Din datele prezentate în tabelul 1 se poate observa că în cazul unui strat mic, care asigură fiecărei granule recepția unui flux termic unitar, procesul se desfășoară în domeniul cinetic, fapt confirmat și de literatură [6], care indică pentru particule independente, încălzite la temperatură constantă, $E_a = 15\,300$ cal/mol.

Creșterea stratului inițial de granule de la 0,32 la 0,64 nu modifică esențial valoarea energiei aparente de activare.

În ceea ce privește influența volumului inițial de probă se poate observa din fig. 8 și 9 că creșterea volumului probei mărește durata de atingere a gradului de transformare maxim, deci micșorează viteza procesului

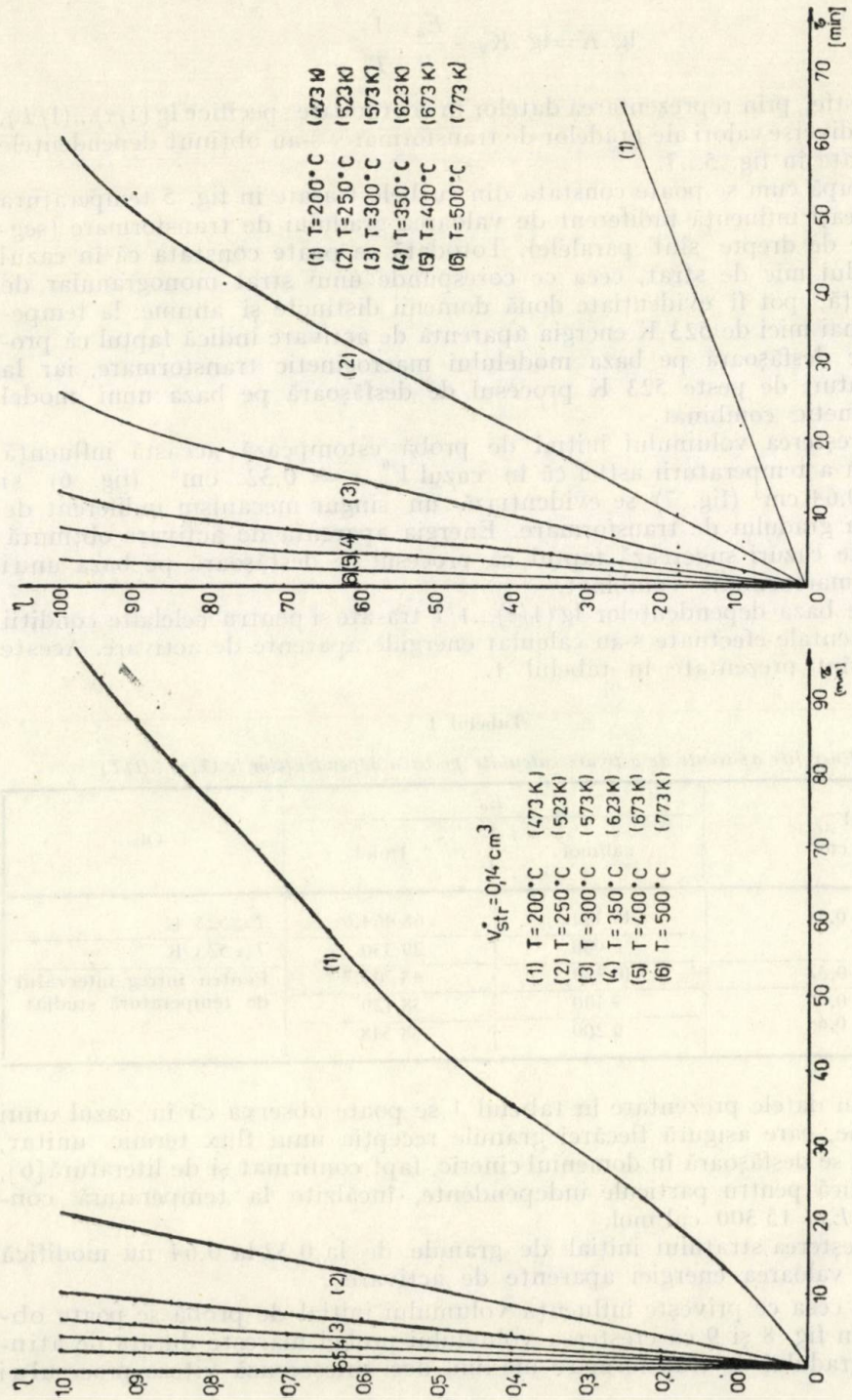

Fig. 2. — Dependența $\eta_{[]s}$ ...τ la diferite temperaturi; $V^0_{strat} = 0{,}14$ cm^3.

Fig. 3. — Dependența $\eta_{[]s}$...τ la diferite temperaturi ; $V^0_{strat} = 0{,}46$ cm^3.

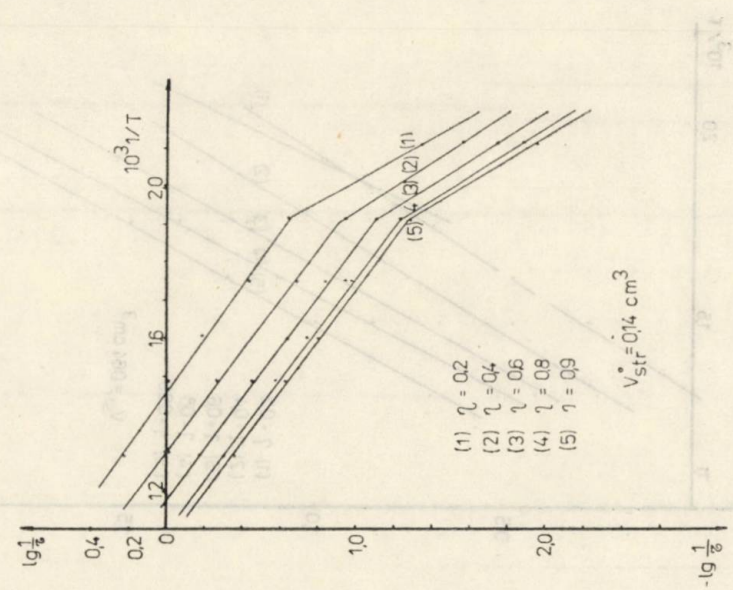

Fig. 5. — Dependența $\lg(1/\tau)...(1/T)$ la diferite valori ale gradului de transformare ; $V^0_{strat} = 0,14$ cm^3.

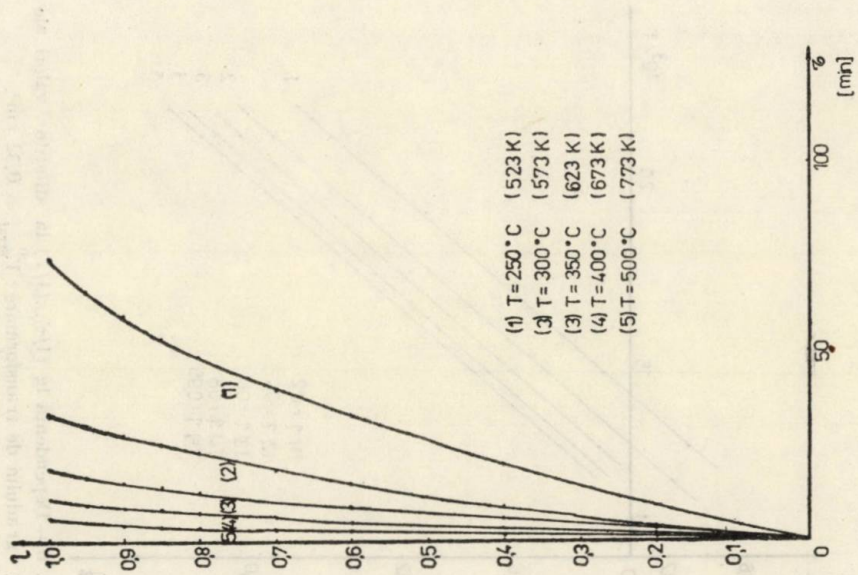

Fig. 4. — Dependența $\eta_{[]s}...\tau$ la diferite temperaturi; $V^0_{strat} = 0,64$ cm^3.

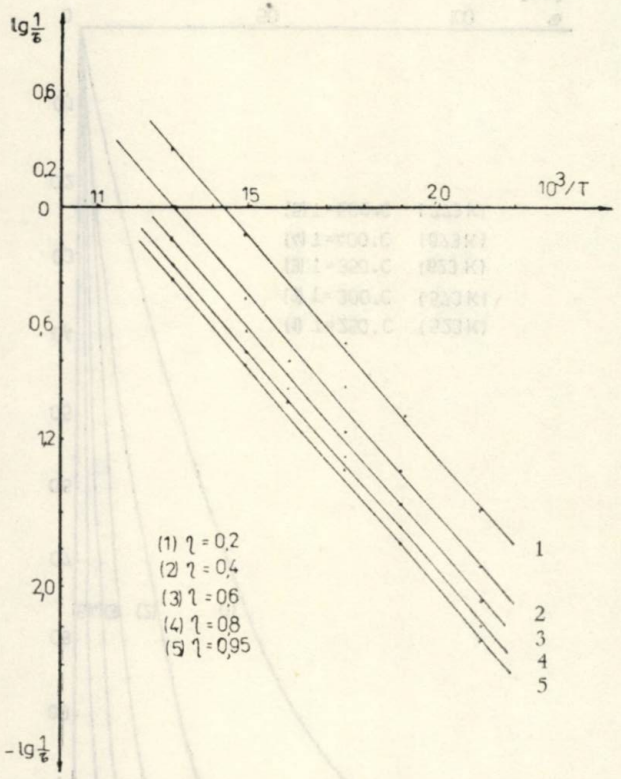

Fig. 6. — Dependența lg $(1/\tau)$...$(1/T)$ la diferite valori ale gradului de transformare ; $V^0_{strat} = 0{,}32$ cm³.

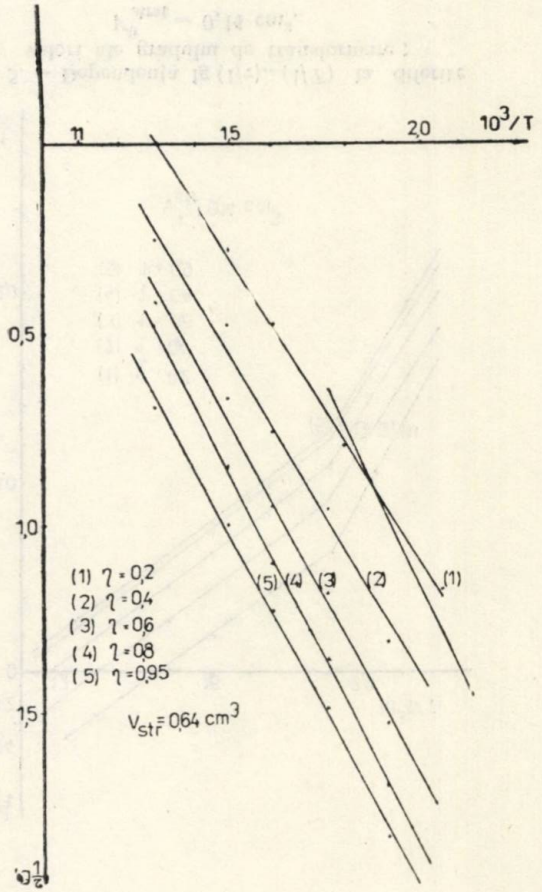

Fig. 7. — Dependența lg $(1/\tau)$...$(1/T)$ la diferite valori ale gradului de transformare; $V^0_{strat} = 0{,}64$ cm³.

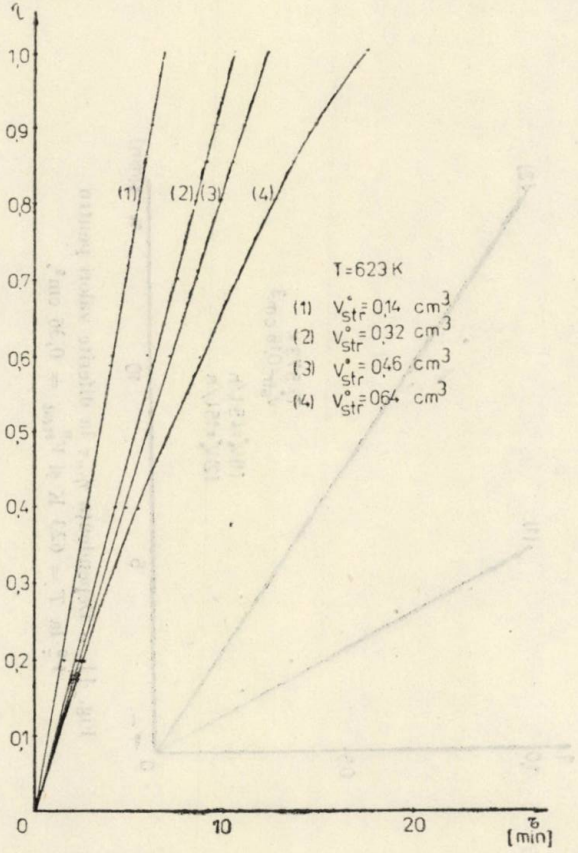

Fig. 8. — Dependența $\eta...\tau$ la diferite valori pentru V^0_{strat} la $T = 623$ K.

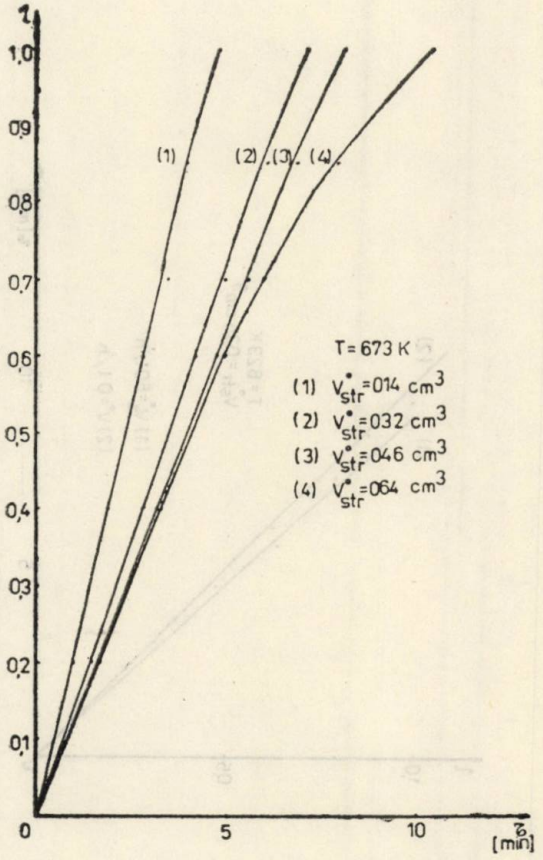

Fig. 9. — Dependența $\eta...\tau$ la diferite valori pentru V^0_{strat} la $T = 673$ K.

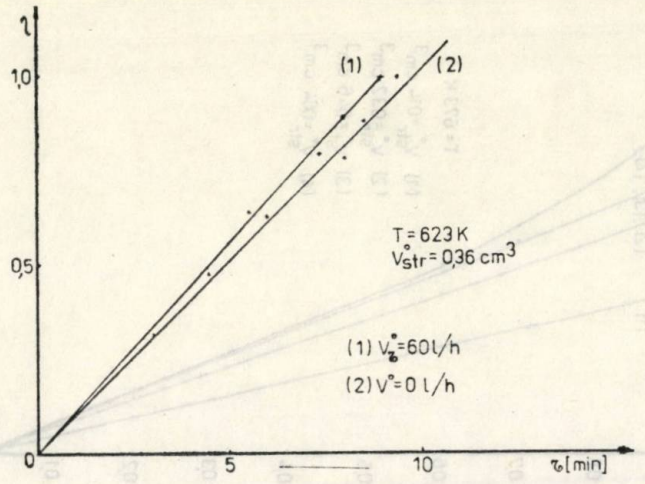

Fig. 10. — Dependenţa $\eta...\tau$ la diferite valori pentru V_τ^0 la $T = 573$ K şi $V_{strat}^0 = 0,16$ cm³.

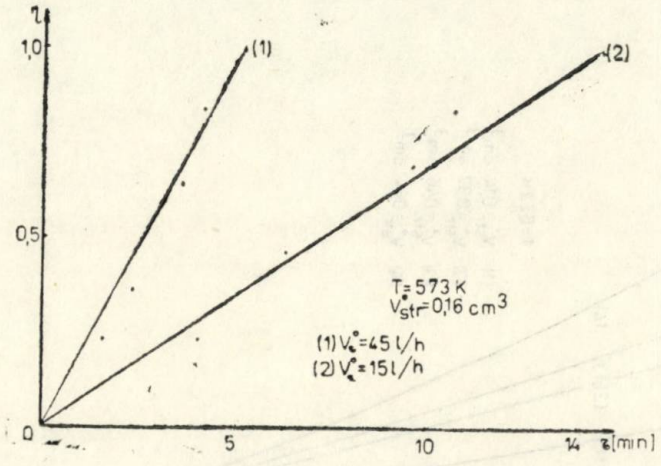

Fig. 11. — Dependenţa $\eta...\tau$ la diferite valori pentru V_τ^0 la $T = 623$ K şi $V_{strat}^0 = 0,36$ cm³.

Tabelul 2

Ecuațiile duratei de consum a clorurii de amoniu în strat fix ($\bar{\tau}$) la diverse temperaturi și volume de strat

V^0_{strat} cm³	T K	$\bar{\tau}=f(\eta_{[]s})$
0,14	473	$\bar{\tau}=97{,}5\ \eta_{[]s}$
	523	$\bar{\tau}=20{,}9\ \eta_{[]s}$
	573	$\bar{\tau}=10{,}8\ \eta_{[]s}$
	623	$\bar{\tau}=6{,}8\ \eta_{[]s}$
	673	$\bar{\tau}=4{,}7\ \eta_{[]s}$
	773	$\bar{\tau}=2{,}49\ \eta_{[]s}$
0,32	473	$\bar{\tau}=194\ \eta_{[]s}$
	523	$\bar{\tau}=61{,}3\ \eta_{[]s}$
	573	$\bar{\tau}=24{,}3\ \eta_{[]s}$
	623	$\bar{\tau}=11{,}22\ \eta_{[]s}$
	673	$\bar{\tau}=7{,}52\ \eta_{[]s}$
	773	$\bar{\tau}=2{,}59\ \eta_{[]s}$
0,46	473	$\bar{\tau}=252\ \eta_{[]s}$
	523	$\bar{\tau}=57{,}8\ \eta_{[]s}$
	573	$\bar{\tau}=23{,}2\ \eta_{[]s}$
	623	$\bar{\tau}=11{,}5\ \eta_{[]s}$
	673	$\bar{\tau}=7{,}11\ \eta_{[]s}$
	773	$\bar{\tau}=3{,}55\ \eta_{[]s}$
0,64	523	$\bar{\tau}=65{,}5\ \eta_{[]s}$
	573	$\bar{\tau}=33{,}15\ \eta_{[]s}$
	623	$\bar{\tau}=18{,}32\ \eta_{[]s}$
	673	$\bar{\tau}=10{,}89\ \eta_{[]s}$
	773	$\bar{\tau}=5{,}42\ \eta_{[]s}$

global. Influența se păstrează pe întregul interval al temperaturilor și pe întreaga gamă a gradelor de transformare studiate. Și acest aspect atestă faptul că procesul se desfășoară pe baza unui model macrocinetic combinat.

Influența specifică a debitului aerului de antrenare se poate constata din dependențele prezentate în fig. 10 și 11. Se poate observa că creșterea de circa 3 ori a debitului aerului de antrenare a produselor gazoase a sublimării duce la creșterea de circa 2...3 ori a vitezei procesului de sublimare, iar dacă se compară vitezele de sublimare obținute la aceleași temperaturi și volume inițiale de strat, realizate cu și fără antrenare, se poate constata că antrenarea duce la creșterea vitezei de circa 1,1...1,2 ori (T=623 K).

Pe baza datelor experimentale obținute s-au determinat expresiile duratei de consum a clorurii de amoniu funcție de temperatură și volumul stratului. Aceste relații sînt prezentate în tabelul 2.

4. Concluzii

Se cercetează influența parametrilor asupra vitezei procesului de sublimare a clorurii de amoniu. Pe baza datelor experimentale se arată că procesul este influențat atît de temperatură cît și de volumul inițial al probei. Energia aparentă de activare determinată indică faptul că procesul se desfășoară pe baza unui model macrocinetic combinat transfer—transformare. Totodată se prezintă influența calitativă și cantitativă a debitului aerului de antrenare asupra vitezei procesului global.

Notații

d_p — diametrul particulelor de clorură de amoniu,
E_a — energia aparentă de activare,
K — constanta vitezei procesului,
R — constanta universală a gazelor,
V^0_{strat} — volumul probei inițiale,
V^0_{τ} — debitul gazului (aer) de antrenare,
$\bar{\tau}$ — timpul de consum mediu a granulelor din strat.

Primită la 1 decembrie 1981

Institutul politehnic, Iași,
Catedra de tehnologia substanțelor anorganice și a materialelor de construcții

BIBLIOGRAFIE

1. Pascal P., *Nouveau Traité de Chimie Minérale*. Vol. **V**, Paris, 1965.
2. * * * *Ullmanns Enziklopädie der tehnischen Chemie*. Bd. **3**, Schwarzenberg, München, 1965, 607.
3. * * * *Gmelins Handbuch der anorganischen Chemie*. Bd. **VII**, Berlin — Heidelberg, 1926.
4. Calistru C., Ifrim L., Szép Al., Bul. celui de al IV-lea Simp. Internaț. de sodă calcinată, Rm. Vîlcea, sept. 1977.
5. Străjescu M. ș.a., Rev. de chimie, **32**, 649 (1981).
6. Печкороский В. В., Звездин Л. Д., Сб. науч. тр. Перм. полит. инст., **18**, 33 41 (1965).
7. Calistru C., Siminiceanu I., Pop Al., Bul. celui de al II-lea Simp. de Ing. proc. chim., P. Neamț, 12—14 oct. 1978.

STUDY OF THE AMMONIUM CHLORIDE SUBLIMATION PROCESS

II. The Influence of the Process Parameters on Overall Rate

(Summary)

The influences of the mains kinetic parameters (temperature, flow rate of carrier gas, size of ammonium chloride bed) upon the overall rate of ammonium chloride sublimation process was studied. Two distinct ranges of temperature has observed, namely: a) $T \leqslant 523$ K, when $E_{app} = 16\,340$ cal/mol and b) $T \geqslant 523$ K, when $E_{app} = 7\,000 \ldots 10\,930$ cal/mol.

BULETINUL INSTITUTULUI POLITEHNIC DIN IAȘI
Tomul XXXI (XXXV) Fasc. 1—4, 1985
Secția II
CHIMIE ȘI INGINERIE CHIMICĂ

C.Z. 532.5 ; 541.012

STUDIUL HIDRODINAMICII FORMĂRII BULELOR ÎN SISTEMELE APĂ—AER ȘI ACID FOSFORIC—AER

DE

CAROLINA HAGIU și I. GRIGORIU

1. Introducere

Realizarea contactului între fazele reactant în sistemele lichid—gaz se face în diferite moduri, după cum cele două faze sînt continue sau dispersate una în alta și anume : a) modele de contact în care ambele faze sînt continue (coloane cu umplutură, strat pelicular) ; b) modele de contact în care faza gazoasă este dispersată în faza lichidă continuă, sub forma bulelor de gaz (talere cu barbotare, reactoare cu barbotare etc.); c) modele de contact în care faza lichidă este dispersată în faza gazoasă continuă, sub forma picăturilor de lichid (coloane cu pulverizare).

Pentru procese care se desfășoară după modele de contact din a doua grupă, mecanismul formării și curgerii bulelor printr-un lichid prezintă deosebită importanță, ceea ce a făcut ca această problemă să fie studiată de numeroși cercetători [1]...[17].

Modelul de contact între fazele reactant în procesul de amonizare a soluțiilor de acid fosforic determină principalele tipuri de reactoare utilizate la scară industrială. Dintre acestea cele mai folosite sînt reactoarele cu un orificiu de barbotare, cu sau fără agitare mecanică, în care se realizează dispersarea amoniacului gazos sub formă de bule în soluții de acid fosforic. În acest caz mecanismul formării bulelor la curgerea gazului printr-un singur orificiu scufundat în lichid constituie o problemă importantă pentru descrierea matematică a procesului de amonizare.

Cercetările experimentale efectuate [6]...[17] arată că principalii factori care pot influența frecvența și dimensiunile bulelor ce se formează în aceste condiții sînt: diametrul orificiului de barbotare, viteza gazului în orificiu, densitatea și vîscozitatea gazului și lichidului, înălțimea de scufundare, unghiul de înclinare a orificiului, diametrul coloanei etc.

La viteze mici ale gazului ($\mathcal{R}_e = 200...300$), diametrul bulelor este dat de relația [6], [7] :

$$d_b = \left(\frac{6\, d_0 \sigma}{\Delta \rho\, g} \right)^{1/3}. \tag{1}$$

Modificarea vitezei gazului influențează mărimea bulelor și frecvența de barbotare ; la creșterea vitezei gazului volumul bulelor rămîne la început aproximativ constant, în timp ce frecvența formării lor crește ; la viteze mai mari ale gazului frecvența rămîne aproximativ constantă iar volumul bulelor crește [8]...[13]. Pentru diferite domenii de curgere ale gazului s-au stabilit, prin prelucrarea datelor experimentale, relații empirice pentru diametrul bulelor. Pentru $\mathcal{R}_e = 200...1\,000$, diametrul bulelor este dat de relația :

$$d_b = k \left(\frac{d_0 \sigma}{\Delta \rho} \right)^{1/3} (v\, \mu_l)^{1/4}. \tag{2}$$

Pentru $\mathcal{R}_e = 1\,000...2\,100$ cercetările experimentale efectuate în sistemul apă—aer arată că frecvența formării bulelor rămîne aproximativ constantă și depinde numai de diametrul orificiului de barbotare [6], [9], [13]. În acest domeniu volumul bulelor crește lent cu creșterea vitezei gazului conform relației [14] :

$$V_b = 1{,}138 \frac{v^{6/5}}{g^{3/5}} \quad (3)$$

În regim turbulent ($\mathcal{R}_e > 2\,100$) apare și predomină fenomenul de dispersare a bulelor datorită turbulenței. Pentru $\mathcal{R}_e > 40\,000$, formarea bulelor este imediat urmată de dispersarea lor în bule cu diametrul mic (5...10 μ), ceea ce determină o modificare considerabilă a suprafeței de contact [17].

Pentru sistemul apă—aer și la $\mathcal{R}_e = 2\,100...10\,000$, Leibson [11] stabilește pentru diametrul bulelor relația :

$$d_b = 0{,}71\ (\mathcal{R}_e)^{-0{,}05}, \quad (4)$$

confirmată și de datele experimentale stabilite de Rennie și Evans [17].

Majoritatea determinărilor experimentale prezentate în literatura citată au fost efectuate în sistemul apă—aer. Ori, după cum s-a arătat, proprietățile fizice (μ, ρ, σ) ale sistemului concret lichid—gaz influențează în mare măsură mecanismul formării și curgerea bulelor. De aceea, în prezenta lucrare ne-am propus cercetarea procesului de formare a bulelor la un orificiu imersat pentru sistemele aer—apă și aer—acid fosforic soluție 45% P_2O_5, acesta din urmă prezentînd interes pentru descrierea matematică a procesului de amonizare a soluțiilor de acid fosforic, proces ce stă la baza obținerii industriale a îngrășămintelor complexe.

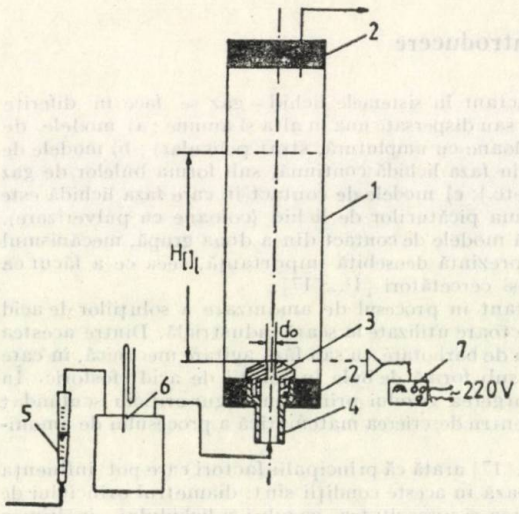

Fig. 1. — Aparat experimental cu barbotare printr-un singur orificiu.

2. Metodica cercetărilor experimentale

Cercetările experimentale au urmărit stabilirea influenței diametrului orificiului de barbotare, a regimului de curgere și a înălțimii coloanei de lichid asupra frecvenței formării bulelor, în sistemele aer—apă și aer—acid fosforic soluție 45% P_2O_5. Programul cercetărilor experimentale este prezentat în tabelul 1.

Instalația pentru experimentare este redată în fig. 1. Aceasta constă dintr-un tub de sticlă (*1*) cu $D_i = 54$ mm și $H = 600$ mm, închis etanș la ambele capete prin dopuri de cauciuc (*2*). La partea inferioară este montat dispozitivul de barbotare (*3*) prin înfiletare într-o piesă metalică fixă (*4*) montată în dopul de cauciuc. S-au utilizat zece dispozitive de barbotare detașabile cu diametrul orificiilor variind între 0,2955 mm și 3,1191 mm. Determinarea diametrelor orificiilor de barbotare (d_9) s-a efectuat cu un micrometru optic. Aerul este introdus în orificiile de barbotare prin intermediul unui rotametru (*5*) și a unui vas tampon prevăzut cu manometru diferențial (*6*). Măsurarea frecvenței bulelor s-a realizat prin iluminarea stroboscopică a sistemului, folosind un stroboscop FEA 0...300 Hz (*7*).

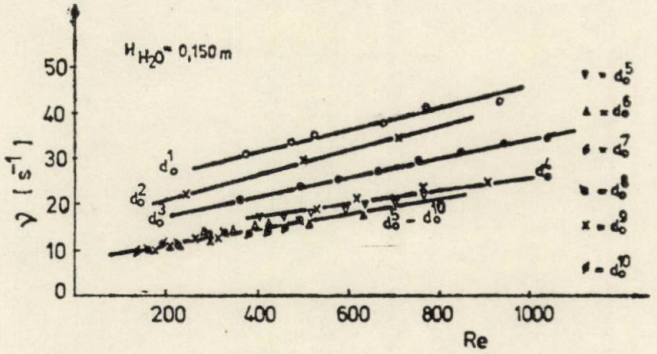

Fig. 2. — Dependența $\nu(\mathcal{R}_e)$ pentru orificiile de barbotare $d_0^1 \ldots d_0^{10}$, $H_{H_2O} = 0{,}150$ m, sistemul aer—apă.

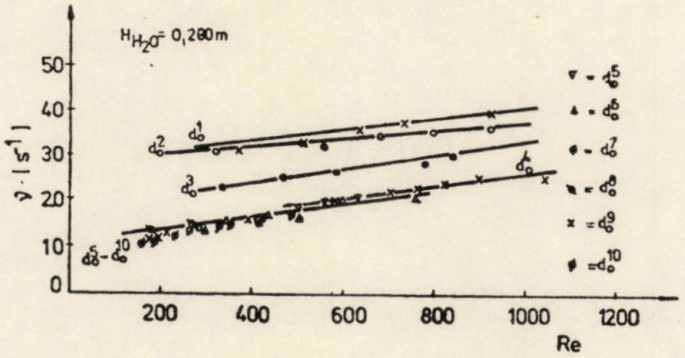

Fig. 3. — Dependența $\nu(\mathcal{R}_e)$ pentru orificiile de barbotare $d_0^1 \ldots d_0^{10}$, $H_{H_2O} = 0{,}200$ m, sistemul aer—apă.

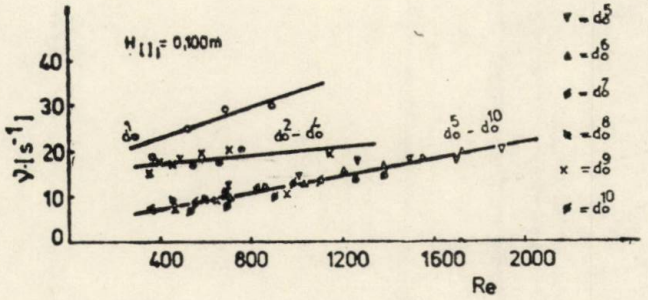

Fig. 4. — Dependența $\nu(\mathcal{R}_e)$ pentru sistemul aer—soluție de acid fosforic 45% P_2O_5, pentru $H_{[]_l} = 0{,}100$ și orificiile de barbotare $d_0^1 \ldots d_0^{10}$.

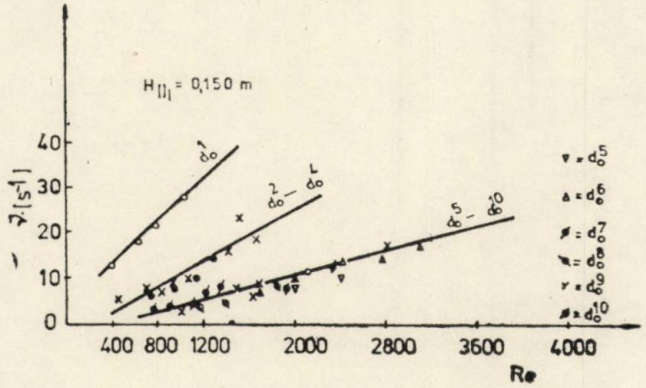

Fig. 5. — Dependența $\nu(\mathcal{R}_e)$pentru sistemul aer—soluție de acid fosforic 45% P_2O_5, pentru $H_{[]_l} = 0{,}150$ și orificiile de barbotare $d_0^1 \ldots d_0^{10}$.

Tabelul 1

Programul cercetărilor experimentale

Sistemul cercetat	Diametrul orificiului de barbotare, $d_0 \cdot 10^3$ m	Înălțimea coloanei de lichid H_{l_l} m	Viteza de curgere a gazului prin orificiu, ω, [m/s]
Apă—aer	0,2955 ; 0,4842 0,6290 ; 0,7725 0,9326 ; 1,3637 1,7018 ; 2,046	0,10 ; 0,15 0,20	0,65... 50
Soluție de acid fosforic 45% P_2O_5 — aer	2,5272 ; 3,1191		3... 150

3. Interpretarea rezultatelor experimentale

Rezultatele experimentale, totalizând peste 350 determinări ale frecvenței în condițiile prezentate în tabelul 1, au fost prelucrate prin trasarea diagramelor frecvență—regim de curgere ($\mathcal{R}e$), prezentate în fig. 2 și 3 pentru sistemul aer—apă și fig. 4 și 5 pentru sistemul aer—acid fosforic, la diferite înălțimi ale coloanei de lichid.

Din diagramele reprezentate în fig. 2 și 3 se constată că pentru sistemul aer—apă, în domeniul $\mathcal{R}e = 200...1\,000$, frecvența formării bulelor crește lent cu creșterea vitezei de curgere a gazului și scade cu creșterea diametrului orificiului de barbotare și înălțimii coloanei de lichid; pentru orificii de barbotare cu $d_0 > 1$ mm, frecvența este independentă de d_0, variind numai funcție de regimul de curgere și de înălțimea coloanei de lichid.

Din diagramele reprezentate în fig. 4 și 5 se constată că variația frecvenței de barbotare funcție de regimul de curgere, diametrul orificiului de barbotare și înălțimea coloanei de lichid pentru sistemul aicid fosforic 45% P_2O_5—aer, urmează aceeași dependență ca și la sistemul apă—aer. Pentru orificii de barbotare cu $d_0 > 1$ mm frecvența este independentă de diametru și variază cu înălțimea coloanei de lichid și regimul de curgere. Pentru $\mathcal{R}e = 400...2\,100$, $H_{l_l} = 0{,}1$ m și $d_0 > 1$ mm s-a stabilit următoarea ecuație pentru frecvența bulelor:

$$\nu = 3{,}5 + 8{,}7329 \cdot 10^{-3} \mathcal{R}e. \tag{5}$$

4. Concluzii

1. S-a cercetat hidrodinamica formării bulelor în sistemul apă—aer și acid fosforic soluție 45% P_2O_5—aer.

2. Rezultatele experimentale, prelucrate sub forma diagramelor ce reflectă dependența frecvenței de regimul de curgere a gazului prin orificiu și înălțimea coloanei de lichid, demonstrează că pentru orificii cu $d_0 > 1$ mm, frecvența de barbotare este independentă de diametru, variind numai cu înălțimea coloanei de lichid și regimul de curgere.

3. Pentru sistemul soluţiei de acid fosforic (45% P_2O_5) — aer, $\mathcal{R}e = 400...$ 2 100 şi $H_{[]l} = 0{,}1$ m s-a stabilit o ecuaţie de dependenţă a frecvenţei de barbotare (ν) de regimul de curgere ($\mathcal{R}e$).

Notaţii

d_0 — diametrul orificiului de barbotare ;
d_b — diametrul bulei ;
g — acceleraţia gravitaţiei;
H — înălţimea coloanei de lichid ;
k — constanta orificiului ;
$\mathcal{R}_e$ — criteriul Reynolds la curgerea gazului prin orificii ;
V_b — volumul bulei ;
v — viteza volumetrică a gazului prin orificiu ;
$\Delta\rho$ — diferenţa de densitate între lichid şi gaz ;
σ — tensiunea superficială a lichidului ;
μ_l — vîscozitatea cinematică a lichidului ;
ν — frecvenţa de barbotare.

Primită la 13 martie 1982

Institutul politehnic, Iaşi,
Catedra de tehnologie a substanţelor anorganice şi a materialelor de construcţii

BIBLIOGRAFIE

1. Kumar R., Kuloor N. R., *Advances in Chemical Engineering*. T. 8, Academic Press, New York, London, 1970.
2. Ramakrishnan S., Kumar R., Kuloor N. R., Chem. Eng. Sci, **24**, 731 (1969).
3. Ramakrishnan S., Kumar R., Kuloor N. R., Chem. Eng. Sci., **24**, 749 (1969).
4. Kumar R., Kuloor N. R., Chem. Technik, **19**, 733 (1967).
5. Pinezewski V. W., Chem. Eng. Sci., **36**, 405 (1981).
6. Valentine F. H. H., *Absorbtion in Gas—Liquid Dispersion ; some Aspects of Bubble Technology*. E.F.N. Spon Ltd., London, 1967.
7. Datta R. L. et al., Trans. Inst. Chem. Eng., **28**, 14 (1950).
8. Coppock P. D., Meicklejohn G. T., Trans. Inst. Chem. Eng., **29**, 75 (1951).
9. Benzing P. J., Myers J. E., Ind. a. Eng. Chem. Engng. Design a. Equipment, **47**, 2087 (1955).
10. Quigley C. J. et al., Chem. Eng. Progr. Symp. Series, **51**, *16*, 31 (1955).
11. Leibson J. et al., Am. Inst. Chem. Eng. J., **2**, 296 (1956).
12. Davidson L., Amick E. H. Jr., Am. Inst. Chem. Eng. J., **2**, 337 (1956).
13. Calderbank P. H., Br. Chem. Eng., **1**, 206 (1956) ; Ibid., **2**, 267 (1956).
14. Davidson J. F., Schüler B.O.G., Trans. Inst. Chem. Eng., **38**, 144 (1960).
15. Davidson J. R., Schuler B. O., Trans. Inst. Chem. Eng., **38**, 335 (1960).
16. Tsuge H., Hibina S., Intern. Chem. Eng., **21**, *1*, 66 (1981).
17. Rennie J., Evans F., Brit. Chem. Eng., **7**, 498 (1962).

HYDRODYNAMIC STUDY ON BUBBLE FORMATION IN AIR—WATER AND AIR—PHOSPHORIC ACID SYSTEMS

(Summary)

The hydrodynamic of bubble formation at an outlet submerged in liquid for air—water and phosphoric acid solution (45% P_2O_5) — air is investigated. The influence of diameter of bubbling inlet and of the liquid height on the bubbling frequency is determined.

For the phosphoric acid—air system an equation for calculating the frequency as a function of flow regime was derived.

BULETINUL INSTITUTULUI POLITEHNIC DIN IAȘI
Tomul XXXI (XXX V) Fasc. 1—4, 1985
Secția II
CHIMIE ȘI INGINERIE CHIMICĂ

C.D. 666.31 ; 666.32

PLAQUES CÉRAMIQUES DE L'ARGILE DE VLĂDICENI

PAR

RODICA SMOCOT, ANA TĂLABĂ, IOLANDA ENESCU, DOINA BOTEZATU et AMEDIU BIALUS

1. Introduction

Les directives du XII-ème Congrès du Parti Communiste Roumain prévoient pour l'étape actuelle de développement de notre pays, une mise en valeur plus complète des resources des matières premières connues aussi que la découverte des quelques nouveaux gisements [1].

Dans ce qui suit on présente les résultats des recherches concernant l'obtention des plaques céramiques de l'argile de Vlădiceni avec les dimensions et les caractéristiques des plaques de faïence.

La mise en valeur de l'argile de Vlădiceni pour obtenir des plaques céramiques se fait inscrire dans le contexte actuel d'une valorification supérieure des matières premières et d'une diversification de la production des entreprises céramiques.

2. La caractérisation de l'argile

La caractérisation chimique et technologique de l'argile de Vlădiceni a prouvé que c'est une argile commune avec une texture fine, située, en ce qui concerne la plasticité, à la limite, entre la plasticité moyenne et supérieure, avec une grande contraction au séchage, une contraction totale moyenne et avec une aptitude de liaison pour les dégraissants, variable, fonction de la nature du dégraissant [2], [3].

En vue de l'utilisation de l'argile de Vlădiceni pour des produits céramiques glaçurés on a étudié le comportement au façonnage, au séchage, au engobage, au glaçuration et à la cuite [3]. Les résultats obtenus ont prouvé la possibilité d'utiliser l'argile de Vlădiceni pour des produits glaçurés.

3, L'obtention des plaques

La recette de fabrication a été établie par recherches de laboratoire dans le but d'obtenir plusieurs échantillons avec une composition différente de la masse céramique.

Dans une première étape ont été confectionnés des échantillons d'argile de Vlădiceni sans addition de dégraissant.

L'argile a été moulue par le procédé humide, le façonnage a été réalisé par coulage en formes de plâtre et le séchage a été effectué à l'étuve à 50°... 100°C pendant 12...14 heures. Les plaques ont été cuites à 900°C et à 1 200... 1 250°C.

La valeur de la contraction et de l'absorbtion d'eau pour les échantillons biscuits d'argile de Vlădiceni apres la calcination à 900°C et à 1 250°C sont présentés dans le Tableau 1 comparativement avec les échantillons de faïence de fabrication courante, cuits dans les mêmes conditions. Les valeurs données représentent la moyenne de cinq essais.

Tableau 1

Les caractéristiques des échantillons biscuits d'argile de Vlădiceni après la calcination à 900°C et 1250°C

Type de l'échantillon	Couleur	Contraction %	Absorbtion d'eau, [%]
$t = 1\,250°C$			
Plaque d'argile de Vlădiceni	brun foncé	fondu	
Plaque de faïence	blanc-jaunâtre	9,8	14
$t = 900°C$			
Plaque d'argile de Vlădiceni	brique	9,7	20,7
Plaque de faïence	jaune-rougeâtre	5,9	25,5

On constate la fusion des échantillons d'argile de Vlădiceni calcinés à 1 250°C et des propriétés différentes des échantillons calcinés à 900°C comparativement aux échantillons de fabrication courante.

On a passé ensuite à la confection des échantillons d'argile de Vlădiceni avec des dégraissants, à savoir : déchets de plaques biscuits et de plaques glaçurés, sable.

La préparation de la masse et le façonnage ont été réalisés d'une façon similaire à la confection des échantillons sans dégraissants. La calcination a été effectuée dans un four Padett à 1 100°C.

Les résultats obtenus, en représentant la moyenne de cinq échantillons pour 20% 25% et 30% déchet de plaques biscuits et de plaques glaçurées sont présentés dans le Tableau 2. Les données du Tableau 2 démontrent que les échantillons avec une proportion de dégraissant de 25% et 30% ont la contraction totale et l'absorbtion d'eau rapprochées aux valeurs des plaques de faïence de fabrication courante.

Les recherches pour l'établissement de la recette de fabrication ont été continuées en utilisant comme dégraissant du sable et du sable ajouté au déchet de plaques biscuits et glaçurées. Les résultats obtenus pour les

Tableau 2

Les caractéristiques des échantillons avec dégraissant et de ceux de faïence calciués

Type de l'echantillon	Contraction au séchage %	Contraction totale %	Absorbtion d'eau %
Échantillon avec 20% dégraissant	6,72	10,04	11,4
Échantillon avec 25% dégraissant	6,50	8,84	12,9
Échantillon avec 30% dégraissant	5,92	8,30	13,8
Échantillon de faïence calciné a 1 100°C	—	8,70	20,0
Échantillon de faïence calciné a 1 250°C	—	9,80	14,0

essais avec 5%, 10% et 15% sable sont présentés dans le Tableau 3. On constate que les échantillons avec 5% sable présentent des valeurs adéquates pour la contraction totale et pour l'absorbtion d'eau, mais on constate aussi pour ces échantillons de même que pour ceux avec 10% et 15 % sable, l'apparition des fissures en S.

Les résultats obtenus pour les essais avec 20% déchet comme dégraissant et avec 10...15% sable, calcinés à 1 100°C (la moyenne pour cinq échantillons) sont présentés dans le Tableau 4. Les données de ce tableau prouvent que les échantillons avec 20% déchet et 10% sable présentent des valeurs de la contraction et de l'absorbtion d'eau très rapprochées aux valeurs des plaques de faïence de fabrication courante, tandis que les échantillons avec 20%

Tableau 3

Les caractéristiques des échantillons de Vlădiceni en mélange avec du sable

Type de l'échantillon	Couleur	Contraction %	Absorbtion d'eau %
t = 1 250°C			
Plaque d'argile de Vlădiceni avec 5% sable	brun	fondu	
Plaque d'argile de Vlădiceni avec 10% sable	brun	fondu	
Plaque d'argile de Vlădiceni avec 15% sable	brun	fondu	
Plaque faïence	blanc-jaunâtre	9,8	14
t = 1 100°C			
Plaque d'argile de Vlădiceni	brique-foncé	10,2	15
Plaque d'argile de Vlădiceni avec 5% sable	brique	7,4	15,9
Plaque d'argile de Vlădiceni avec 10% sable	brique	6,5	18,3
Plaque d'argile de Vlădiceni avec 15% sable	brique	6,2	19,2
Plaque faïence	brique	8,7	20

Tableau 4

Les caractéristiques des échantillons en mélange avec dégraissants et du sable

Type de l'échantillon	Contraction au séchage %	Contraction totale %	Absorbtion d'eau %
Échantillon avec 20% déchet 10% sable 70% argile	5,60	9,1	13,6
Échantillon avec 20% déchet 15% sable 65% argile	3,95	8,0	17,2

déchet et 15% sable présentent des valeurs dans les limites admises pour les plaques de faïence.

En tenant compte de ces résultats on a passé ensuite à l'obtention des plaques d'argile de Vlădiceni d'après le schéma bloc présenté dans la Fig. 1, simultanément aux plaques de faïence de fabrication courante en utilisant les recettes de fabrication présentées dans le Tableau 4.

La diminution de la température de calcination des plaques biscuits, avec 150°C, conduit à une réduction sensible du comburant.

Les plaques biscuits ont été glaçurées une ou deux fois, avec une glaçure en silicate de zirconium et calcinées à 1 000°C...1 060°C. Pour une glaçure avec un contenu diminué en silicate de zirconium, la calcination a été effectuée dans un four électrique à 900°C.

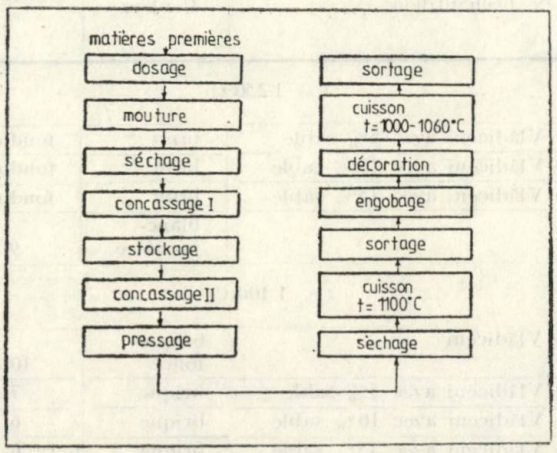

Fig. 1

4. La possibilité de l'utilisation des produits obtenus

L'aspect et les caractéristiques des plaques obtenues sont déterminés d'après les méthodes recommandées pour les plaques de faïence [4]. Les plaques obtenues ont un aspect adéquat et s'encadrent dans la classe de qualité I. Les caractéristiques sont présentées dans le Tableau 5. On constate que les plaques obtenues correspondent aux conditions d'admisibilité prévues pour les plaques de faïence. Le prix de revient des plaques d'argile de Vlădiceni est d'environ 35,50 lei/m^2, ce qui représente une baisse de cca 35 % par rapport au prix actuel des plaques de faïence.

Tableau 5

Les caractéristiques des plaques obtenues

Caratéristique	Valeur
Résistence au courbement (valeur moyenne), [dyN/cm^2]	196
Absorbtion d'eau, [%]	13,5...17,2
Degré de dureté de la glaçure	4
Résistence des plaques murales aux variations de température et adhérence sur mortier	Ne se détachent pas soumises à 10 cycles de + 80°C à + 10°C
Résistence au choc thermique	Ne présentent pas des fissures et des détachements de glaçure
Résistence aux agents chimiques	Ne présentent pas des modifications de la couche de glaçure

Ayant en vue les caractéristiques des plaques obtenues et leur prix de revient plus bas, on apprécie qu'elles peuvent être utilisées au revêtement en placage des murs intérieurs comme remplaçant de la faïence.

5. Conclusions

1. On a étudié la possibilité d'obtention des plaques d'argile de Vlădiceni avec des caractéristiques semblables aux plaques de faïence.
2. On a établi la recette et les conditions d'obtention.
3. On a établi que les plaques céramiques obtenues se placent dans l'intervalle imposé aux propriétés des plaques de faïence.
4. On a proposé l'utilisation des plaques céramiques d'argile de Vlădiceni comme remplaçant de la faïence.

Reçue le 14 juin 1983

Institut Polytechnique, Jassy,
Chaire de Technologie des Substances Anorganiques et des Matériaux de Construction,
Combinat Chimique, Tîrnăveni,
et
Entreprise de Materiaux de Construction, Jassy

BIBLIOGRAPHIE

1. Ceaușescu N., *Directivele Congresului al XII-lea al Partidului Comunist Român*, Ed. Pol., Buc., 1979.
2. Smocot R., Enescu I., Talabă A., Bialus A., Bul. Inst. polit., Iași, **XXIV (XXVIII)**, *3—4*, s. II (1978).
3. Leonte C., Smocot R., Talabă A., Bialus A., Materiale de construcții, **X**, *1* (1980).
4. * * * *Materiale de construcții*. Colecția STAS, vol. II, Ed. Tehn., Buc., 1975.

PLĂCI CERAMICE DIN ARGILĂ DE VLĂDICENI

(Rezumat)

Se prezintă rezultatele cercetărilor privind obținerea plăcilor ceramice din argilă de Vlădiceni, cu caracteristicile plăcilor de faianță.

Pe baza rezultatelor cercetărilor s-a stabilit că plăcile ceramice obținute din argilă degresată cu 10...15% nisip și 20% deșeu (rebut faianță) prin arderea biscuitului la 1 100°C și a glazurii la 1 000°...1 050°C corespund din punct de vedere al aspectului și se încadrează în intervalul de valori impus proprietăților plăcilor de faianță.

Cercetările privind obținerea plăcilor ceramice din argilă de Vlădiceni demonstrează posibilitatea folosirii acestora pentru placarea pereților interiori, ca înlocuitor al faianței.

BULETINUL INSTITUTULUI POLITEHNIC DIN IAŞI
Tomul XXXI (XXXV) Fasc. 1—4, 1985
Secţia II
CHIMIE ŞI INGINERIE CHIMICĂ

D.C. 661.183.48 ; 546.39

SYNTHETIC ZEOLITES IN THE AMMONIUM FORM

BY

M. CRUCEANU, EVELINE POPOVICI and MARIA ALEXANDROAEI

1. Introduction

The ion-exchange on natural and synthetic zeolites is the subject of numerous investigations, justified by practical applications of both the process itself and the cationic forms obtained. One of these species is the hydrogen one, which is characterized by a high thermal stability and a notable catalytical activity [1], [2].

There are several ways to transform the usual zeolites in the hydrogen form [3], namely :

a) by ion-exchange, using the zeolite in silver form, as below

$$Ag\text{-}Z + MeCl + H_2O \rightarrow H\,Z + AgCl + MeOH,$$

where Me is a cation with large radius ;

b) by hydrolysis

$$Na\,Z + H_2O \rightarrow H\,Z + NaOH\ ;$$

c) by their treating with dilute acid solutions

$$Me\,Z + H^+ \rightarrow H\,Z + Me^+\ ;$$

d) by decomposition of zeolites in the ammonium form, at 950°C

$$NH_4\,Z \rightarrow H\,Z + NH_3\ ;$$

The first two methods lead to a low exchange degree and need an excessive long time for process development. The third method has also a degradation of zeolite network. Due to all these facts, the hydrogen form obtention by means of the ammonium form is more and more applied. According to the cited literature [4] there are only a few data available on this process.

The present paper deals with a study on the ion-exchange process of NaA and NaX zeolites, manufactured, currently in our country, using different sources of ammonium, in order to find out the optimal conditions under which the ammonium form zeolite can be obtained.

2. Experimental

The zeolites NaA and NaX molecular sieves, in powdered form, without binder, are produced usually by Sodic Products Works of Govora, S.R. Romania. Prior to ion-exchange, the molecular sieves were activated thermally at 400°C for two hours. The ammonium sources were the 0.1...5.0 M solutions of NH_4OH, NH_4Cl, NH_4NO_3, $(NH_4)_2CO_3$ and $(NH_4)_2SO_4$. The experiments were carried out at 10°...40°C, using a solid to liquid ratio of 1:15. The content

of sodium in solution was determined flamphotometrically, using a Carl Zeiss, Jena, flamphotometer.

3. Results and Discussion

Taking into account the kinetic curves obtained for the two types of molecular sieves, at different temperatures and various concentrations of the exchanging solution, it can be seen that the ion-exchange equilibrium is reached rapidly. To illustrate this fact, were given only the kinetic curves obtained using the 1 M solutions of NH_4OH, NH_4Cl and NH_4NO_3 at 22°C, because no significant differences were obtained for the other ones ammonium sources (Figs. 1...3).

The experimental results allowed to plot the amount of ammonium in zeolite against the ammonium in solution at any moment (Figs. 4 and 5).

The ion-exchange isotherms show the existence of some differences between the exchange capacity of the two types of molecular sieves, differences justified by the Na^+ and NH_4^+ ions positions on the liotrope scale of selectivity of these zeolite species [5[:

a) In NaA zeolite:

$$Ag^+ > Te^+ > Na^+ > K^+ > NH_4^+ > Rb^+ > Li^+ > Cs^+ ;$$

b) In NaX zeolite:

$$Ag^+ > Te^+ > Cs^+ > Rb^+ > NH_4^+ > K^+ > Na^+ > Li^+.$$

The values of the ion-exchange capacity of the two types of molecular sieves are summarized in Table 1. As it can be seen in these Table, the dissociation constant of ammonium salt employed has a notable influence on the ion-exchange capacity.

Table 1

Values of Ion-exchange Capacity of the two Types of Molecular Sieves against Ammonium Sources at Different Temperatures

Ammonium sources	Ion-exchange capacity, [mg Na^+/g zeolite]			
	NaX zeolite		NaA zeolite	
	10°C	22°C	10°C	22°C
NH_4OH	153	191	45	61
NH_4Cl	311	362	183	262
NH_4NO_3	468	531	361	398
$(NH_4)_2CO_3$	571	652	433	511
$(NH_4)_2SO_4$	711	776	557	617

The maximum amount of ammonium ions exchanged can be calculated on the basis of the experimental data. In the case of the investigated ammonium sources, the magnitude of ion-exchange capacity is situated as follows :

$$NH_4OH < NH_4Cl < NH_4NO_3 < (NH_4)_2CO_3 < (NH_4)_2SO_4.$$

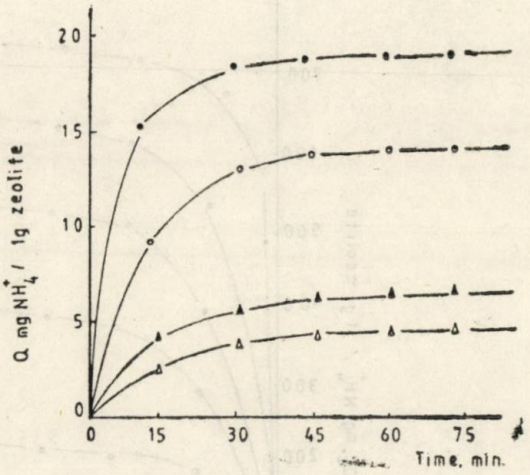

Fig. 1. — Kinetics of ion-exchange in 1 M NH_4OH solution: ● — NaX, 22°C; o — NaX, 10°C; ▲ — NaA, 22°C; Δ — NaA, 10°C.

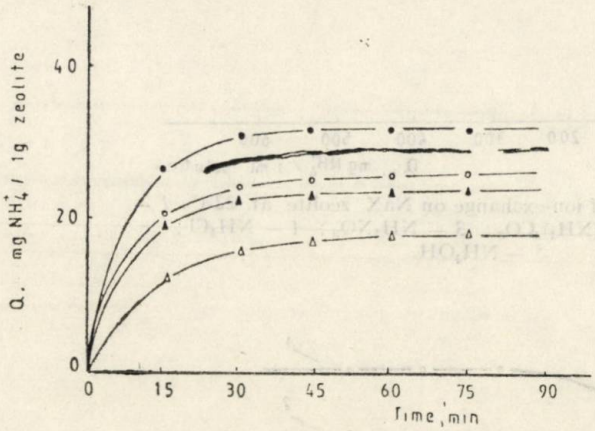

Fig. 2. — Kinetics of ion-exchange in 1 M NH_4Cl solution; same samples and conditions as in Fig. 1.

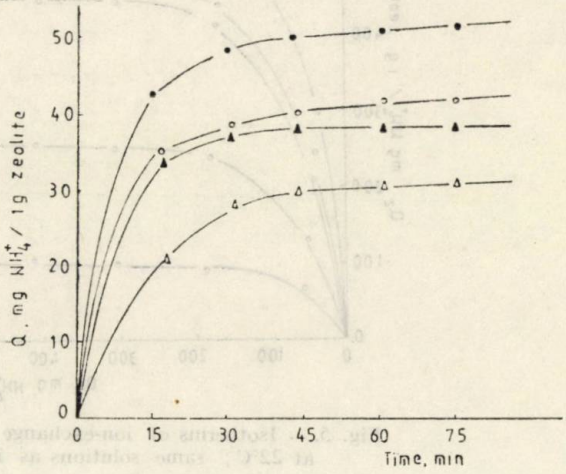

Fig. 3. — Kinetics of ion-exchange in 1 M NH_4NO_3 solution; same samples and conditions as in Fig. 1.

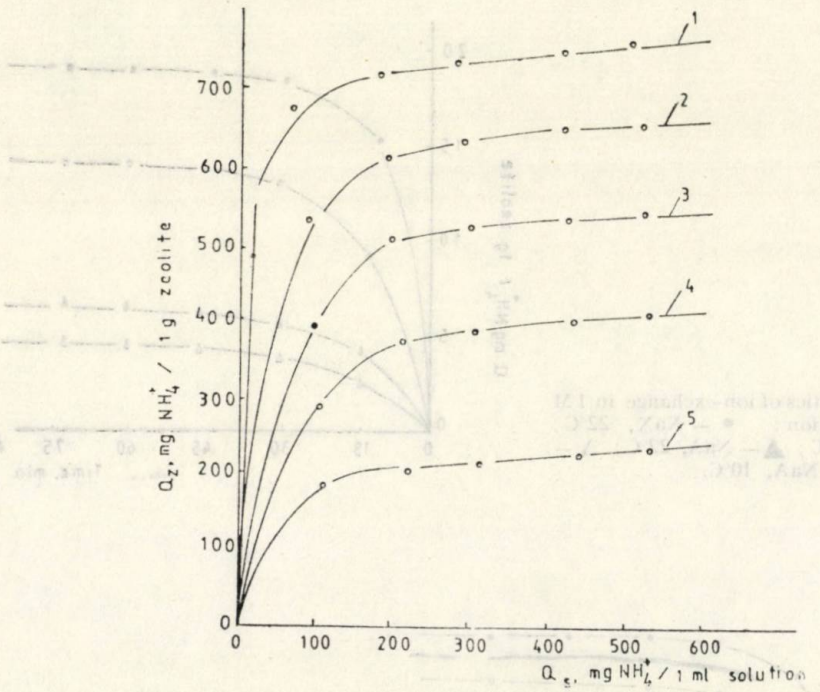

Fig. 4. — Isotherms of ion-exchange on NaX zeolite at 22°C : *1* — $(NH_4)_2SO_4$; *2* — $(NH_4)_2CO_3$; *3* — NH_4NO_3 ; *4* — NH_4Cl ; *5* — NH_4OH.

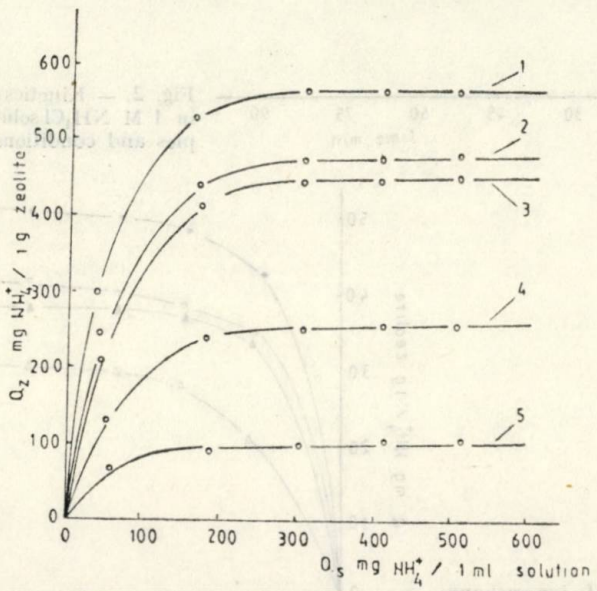

Fig. 5. — Isotherms of ion-exchange on NaA zeolite at 22°C ; same solutions as in Fig. 4.

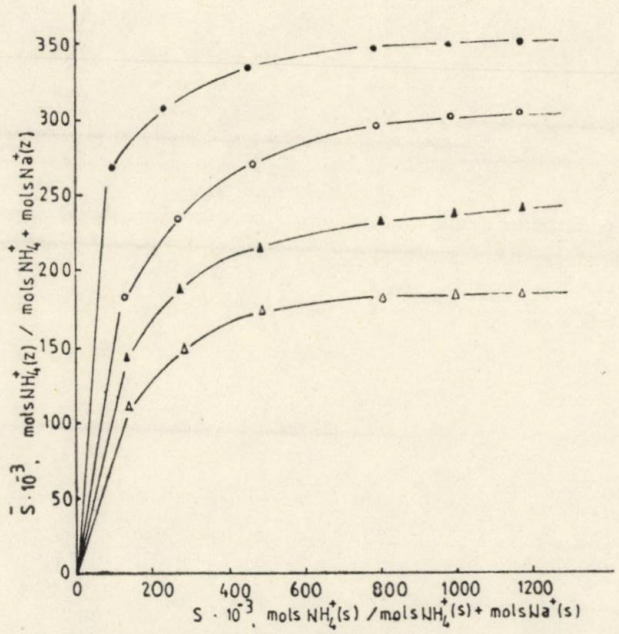

Fig. 6. — Curves of ion-exchange process selecctivity for NH_4Cl ; same samples and conditions as in Fig. 1.

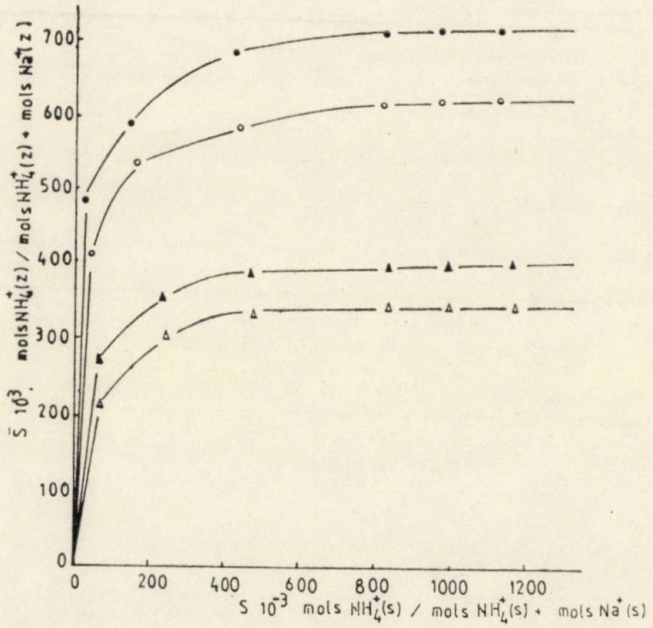

Fig. 7. — Curves of the ion-exchange process selectivity for $(NH_4)_2CO_3$ solution ; same samples and conditions as in Fig. 1.

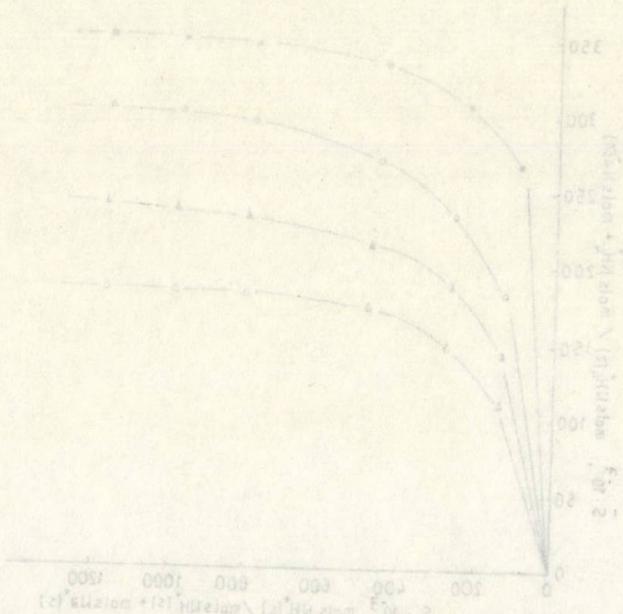

On the basis of the kinetical data, the overall diffusion coefficients were calculated using B o y d and S o l d a n o's equation [6]:

$$\frac{Q}{Q_\infty} = \frac{6}{\pi} \sum_{n=1} \frac{1}{n^2} e^{-\frac{\pi^2 n^2 D}{r^2}}, \quad (1)$$

which under simplified form, proposed by Barrer [7], is

$$\frac{Q}{Q_\infty} = \frac{6}{r\sqrt{Dt/\pi}}, \quad (2)$$

where: Q—amount exchanged at the time t, [mg]; Q_∞—amount exchanged at equilibrium, [mg]; t—time, [s], r—radius of zeolite granule, [μ].

Taking into account the characteristic sizes of the two types of molecular sieves, the relation (2) becomes as below:

a) for the NaA zeolite

$$\frac{Q}{Q_\infty} = 7 \times 10^4 \sqrt{Dt}; \quad (3)$$

b) and for the NaX zeolite

$$\frac{Q}{Q_\infty} = 5.8 \times 10^4 \sqrt{Dt}. \quad (4)$$

The values of the diffusion coefficients calculated are set up in Table 2. As it comes out from Table 2, the NaX zeolite exhibits a more rapid diffusion of ammonium ion than of NaA. The inverse phenomenon that occurs in the case of $(NH_4)_2CO_3$ and $(NH_4)_2SO_4$ solutions proves the influence of anion on the ion-exchange.

Table 2

The Overall Diffusion Coefficient of the Ammonium Ion for 1 M Solutions

Solution	Overall diffusion coefficient, [s^{-1}]			
	NaX zeolite		NaA zeolite	
	10°C	22°C	10°C	22°C
NH_4OH	9.2×10^{-14}	16×10^{-14}	6×10^{-14}	7×10^{-14}
NH_4Cl	11.2×10^{-14}	13×10^{-14}	9.6×10^{-14}	11×10^{-14}
NH_4NO_3	13.2×10^{-14}	16.9×10^{-14}	8×10^{-14}	12.4×10^{-14}
$(NH_4)_2CO_3$	11.4×10^{-14}	12.3×10^{-14}	16×10^{-14}	17×10^{-14}
$(NH_4)_2SO_4$	12×10^{-14}	14.8×10^{-14}	16×10^{-14}	17.2×10^{-14}

Using the B r e c k's procedure [5], the selectivity curves of the two types of molecular sieves against the ammonium sources were worked out and plotted in Figs. 6 and 7, for NH_4Cl and $(NH_4)_2CO_3$.

4. Conclusions

From the experimental results presented above, the following conclusions may be drawn:

1. The highest exchange degrees are exhibited by NaX zeolite against $(NH_4)_2SO_4$ solution and NaA zeolite against $(NH_4)_2CO_3$ or $(NH_4)_2SO_4$.

2. The little differences between amounts of exchanged ions versus operating conditions, determines the utilization of dilute solutions for such a purposes, fact that makes the process economical.

3. Since the temperature does not influence significantly the process rate, the room temperature is the optimal one.

4. The procedure being simple enough, it can be easily applied at industrial scale.

Received, November 17, 1982

Polytechnic Institute, Jassy,
Department of Chemical Technology
and General Chemistry

REFERENCES

1. Gauchi S., Trans. Indian Ceram. Soc., **39**, *2*, 57 (1980).
2. Gárdos K., Péchy R., Hung. J. Ind. Chem., **9**, *1*, 21 (1981).
3. Жданов С. П., Егоров Е. Н., *Химия цеолитов*. Изд. Наука, Ленинград, 1968.
4. * * * Реферативный хурнал, коллекция 1978 — 1983.
5. Breck D. W., *Zeolite Molecular Sieves*. New York, 1973.
6. Boyd D., Soldano V., J. of Colloid Sci., **69**, *2*, 887 (1979).
7. Barrer R. M., *The Properties and Application of Zeolites*. London, 1979.

ZEOLIŢI SINTETICI ÎN FORMĂ DE AMONIU

(Rezumat)

Se studiază procesul de schimb de ioni al zeoliţilor NaA şi NaX fabricaţi în mod curent în ţara noastră, folosind diferite surse de amoniu, cu scopul de a determina condiţiile optime în care zeolitul în formă de amoniu poate fi obţinut.

BULETINUL INSTITUTULUI POLITEHNIC DIN IAŞI
Tomul XXXI (XXX V) Fasc. 1—4, 1985
Secţia II
CHIMIE ŞI INGINERIE CHIMICĂ

D.C. 547.412.133 ; 661.183.6

HYDRODECHLORINATION OF CARBON TETRACHLORIDE OVER NICKEL ZEOLITE CATALYSTS

BY

N. NAUM, GH. MIHĂILĂ and N. BÎLBĂ

1. Introduction

The waste solutions of organic chlcroderivatives, being strong pollutants, raise serious problems as regards either their run-off or separation of certain useful products from them. A new way to turn them to profit is their catalytic hydrodechlorination to hydrocarbons or to other valuable products.

The present paper deals with the results concerning hydrodechlorination of carbon tetrachloride over nickel zeolite catalysts, using the pulse microreactor technique. The effect of catalyst activation temperature as well as of certain cations located in the polycationic forms of the nickel catalysts, prepared from zeolite Y on conversion has been investigated. At low conversion, there were indentified 12 reaction products, principally, chloroforme, hexachlorethane and 1, 1, 1, 2, tetrachlorethane and, at higher conversion, the main product was 1, 1, 1, 2 tetrachlorethane. Since direct chlorination of acethylene leads selectively to 1, 1, 2, 2 tetrachlorethane, it means that hydrodechlorination of carbon tetrachloride over nickel zeolite catalysts is a suitable way to obtain asymmetrical tetrachlorethane. Formation of these C_2-chloroderivatives is due to the reaction between free radicals given by partial catalytic hydrochlorination of carbon tetrachloride.

2. Experimental

Details as regards the preparation and ion-exchange modification of the catalysts employed in this work were already reported in a previous paper [1].

The hydrodechlorination reaction was carried out in chromatographic pulse, using hydrogen carrier for both catalyst reduction and reactant [2], [3]. The quantitative analysis of the reaction products was performed chromatographically, using the same chromatograph to which the microreactor was connected. Conversion was expressed in molar percents of carbon tetrachloride transformed in the reaction products.

Hydrodechlorination of carbon tetrachloride, in chromatographic pulse, was carried out under the following conditions: a) reaction tem-

perature—370°C ; b) hydrogen flowrate—40 cm^3/min ; c) catalyst reduction temperature—370° and 530°C; d) feed pulse—0.05...10 µl; e) mass of catalyst—2 mg.

3. Results and Diseussion

The data obtained under the condition presented above are set out in Figs. 1 and 2.

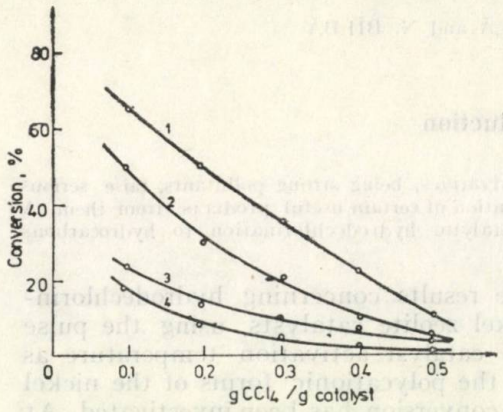

Fig. 1. — Conversion versus the mass ratio, CCl_4/catalyst, at activation and reaction temperature of 370°C for different polycationic forms of nickel zeolite catalyst : *1* — NiNaY ; *2* — NiCuY ; *3* — NiCoY ; *4* — NiCrY.

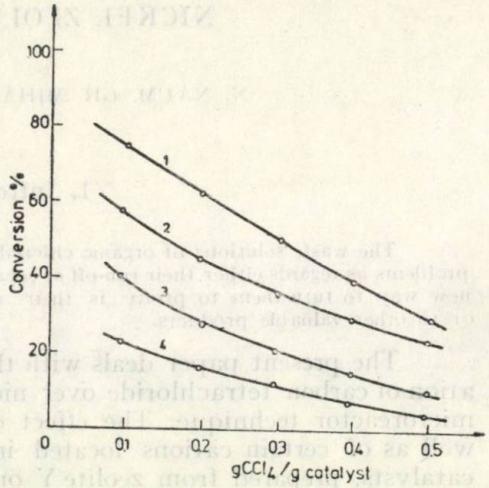

Fig. 2. — Conversion versus the mass ratio, CCl_4/catalyst, at activation temperature of 530°C and reaction temperature of 370°C for different polycationic forms of nickel zeolite catalyst.: *1* — NiNaY ; *2* — NiCoY ; *3* — NiCuY ; *4* — NiCrY.

As shown in Figs. 1 and 2, the catalytical activity of the investigated catalysts decreases with mass ratio, reactant to catalyst. Their activity depends on activation temperature so that at 370°C, it decreases in the order: NiNaY <NiCuY<NiCoY<NiCrY and at 530°C, it decreases in another order, NiNaY<NiCoY<NiCuY<NiCrY.

In addition all catalysts activated at 530°C are more active than those activated at 370°C.

The catalytical activity of the investigated catalysts in the reaction of carbon tetrachloride hydrodechlorination decreases in the same order as in that of chlorbenzene hydrodechlorination [2] except NiCuY activated at 370°C. Their catalytical activity depends on amount of active metal disponible to the reaction contact. At the temperature higher than 370°C, a large amount of nickel is reduced and, at the same time, a part of it migrates to the outer surface of catalytically inactive crystallites.

The lower catalytical activity of NiCrY was almost expected because the Cr^{3+} ions favourise the nickel ions to be localized in the hexagonal

prysmas [4] where they cannot be easily reduced. Reduction of nickel in these polycations zeolites, in hydrogen stream, at 370°C, is approximately 90% for NiNaY and NiCrY, where as at 530°C is over 90% for all polycationic forms [5]. The high percent of reduced nickel determines the existence of a great number of active sites disponible to the reaction.

3. Conclusions

Hydrodechlorination of carbon tetrachloride over nickel zeolite catalysts led selectively to asymmetrical tetrachlorethane obtention. The investigated catalysts present a great catalytical activity for a short time only. Their aging can be due to polymerization of free radicals in pores of zeolite structure. For all cases, catalytical activity decreased with increase of the mass ratio, reactant to catalyst, independent of reduction temperature. The catalytical activity of nikel zeolite catalyst in polycationic forms depends on activation temperature as follows: at 370°C, it decreases in the order NiNaY<NiCuY<NiCoY<NiCrY and at 530°C it decreases in another order, NiNaY<NiCoY<NiCuY<NiCrY.

Received, January 26, 1983

Polytechnic Institute, Jassy,
Department of Chemical Technology,
and General Chemistry

REFERENCES

1. Naum N., Mihăilă Gh., Ababi V., Lucr. șt. ale Inst. inv. sup. Constanța, Ser. Chim., **1**, 3 (1981).
2. Naum N., Ababi V., Mihăilă Gh., Rev. Chim., **28**, 1039 (1977).
3. Mihăilă Gh., Ababi V., Naum N., Brevet R. S. R., *70756* (1979).
4. Bierenbaum H. S., Chiramongkol S., Weiss A. S., J. Catalysis, **23**, 61 (1971).
5. Минашев М. Х., Антошин Г. В., Шапиро Е. С., ИАН СССР, ОХН, 1012 (1974).

HIDRODECLORURAREA TETRACLORURII DE CARBON PE CATALIZATORI ZEOLITICI CU NICHEL

(Rezumat)

S-a cercetat hidrodeclorurarea tetraclorurii de carbon pe catalizatori zeolitici cu nichel și cu alți cationi, folosind tehnica pulsului cromatografic. Reacția cercetată pe acești catalizatori conduce la obținerea de tetracloretan asimetric. Activitatea catalitică a catalizatorilor zeolitici cu nichel și cu alți cationi depinde de temperatura de activare. Astfel, la 370°C, acesta descrește în ordinea: NiNaY<NiCuY<NiCoY<NiCrY iar la 530°C, după cum urmează: NiNaY<NiCoY<NiCuY<NiCrY. Datorită reacțiilor de polimerizare a radicalilor liberi în porii structurii zeolitului, catalizatorii își pierd repede activitatea catalitică.

BULETINUL INSTITUTULUI POLITEHNIC DIN IAŞI
Tomul XXXI (XXXV) Fasc. 1—4, 1985
Secţia II
CHIMIE ŞI INGINERIE CHIMICĂ

C.Z. 66.094.3 ; 547.593.2

STUDIUL POSIBILITĂŢILOR DE VALORIFICARE A SUBPRODUSELOR DE LA OXIDAREA CICLOHEXANULUI

DE

P. ONU, C. LUCA, V. ABABI şi ADRIAN COSĂVEANU

1. Introducere

Procesul de obţinere a caprolactamei plecînd de la ciclohexan a căpătat în ultimul timp o pondere tot mai mare, deşi din punct de vedere practic el implică o serie de incoveniente, printre care gradul redus de utilizare al materiei prime şi formarea unei cantităţi apreciabile de subproduse industriale.

Prin oxidarea catalitică a ciclohexanului la ciclohexanonă şi ciclohexanol rezultă şi o serie de alţi compuşi cu oxigen care formează masa produselor reziduale. Formarea acestor produse se datoreşte faptului că procesul de oxidare a ciclohexanului este neselectiv, din cauza formării unor peroxizi şi radicali liberi, care fac ca oxidarea să se desfăşoare printr-o serie de reacţii paralele şi succesive [1], [2]. Astfel, în instalaţiile industriale care folosesc acest procedeu, pe lîngă produşii de bază, ciclohexanol şi ciclohexanonă, rezultă şi produse reziduale, cunoscute sub denumirea de „fracţia alcooli", „ape acide", „adipaţi" şi „ulei X". Dintre aceste produse cel mai important din punct de vedere cantitativ este uleiul X.

Într-o lucrare anterioră [3] am studiat „fracţia alcooli". Avînd în vedere cantitatea de ulei X şi unele caracteristici fizice ca: punct de inflamabilitate, viscozitate etc., în prezenta lucrare s-a studiat compoziţia chimică a acestuia, precum şi posibilităţile de utilizare ca plastifiant în industria cauciucului.

2. Partea experimentală

Uleiul X este un lichid vîscos, de culoare brun-închis şi are densitatea la 20°C, 0,98...1,061 g/cm^3. O analiză chimică calitativă a produsului brut nu a fost posibilă, deoarece acesta este un amestec complex format din componenţi cu puncte de fierbere apropiate. Ca urmare, produsul brut a fost prelucrat prin distilare fracţionată în intervalul de temperatură de 45°...175°C şi la presiunea de 5...7 mm Hg, evitîndu-se astfel descompunerea termică a componenţilor.

Distilarea fracţionată a fost corelată cu datele analizei cromatografice, în aşa fel încît fracţiunile obţinute să includă un număr cît mai mic de componenţi.

Ca metodă de caracterizare a fracţiunilor, pe lîngă cromatografia în fază gazoasă, s-au folosit: spectroscopia IR, indicele de refracţie, analiza elementară şi extracţia lichid—lichid.

Pentru separarea cromatografică a componenților s-au utilizat diferite faze staționare, ca: dinonilftalat, apeizon L, ulei de silicon și carbowax-20 M. Cele mai bune rezultate s-au obținut cu carbowax-20 M, depus pe cromosorb W.

Drept solvenți în extracția lichid—lichid s-au încercat: metanolul, etanolul, eterul, ciclohexanona, cloroformul, acetona, precum și amestecuri ale acestora cu diferite proporții de apă. Uleiul X s-a dizolvat în agentul de extracție folosit sau s-a emulsionat, încît separarea celor două faze se realizează cu greutate.

În vederea separării unor eventuali fenoli și crezoli s-au folosit pentru extracție și soluții de hidroxid de sodiu, de diferite concentrații.

3. Rezultate și discuții

Prin distilarea fracționată a uleiului X s-au separat patru fracțiuni și a rămas un reziduu. Condițiile de distilare și proporția fracțiunilor obținute în raport cu produsul brut sînt date în tabelul 1.

Tabelul 1

Condițiile de separare a uleiului X în fracțiuni

Fracțiunea	Temperatura °C	Presiunea mm Hg	Proporția, în raport cu produsul brut, [%]
I	45... 86	6...7	8...10
II	87...115	6...7	15...18
III	116...148	5...6	26...28
IV	145...175	5	7... 9
Reziduu	peste 175	5	30...35

Analiza cromatografică a arătat că fiecare fracțiune include 3...4 componenți mai importanți și alți cîțiva sub formă de urme.

Încercările de a realiza prin fracționare o separare mai eficientă nu au dat rezultate. Se pare că separarea componenților este îngreuiată de formarea unor amestecuri azeotrope binare și chiar ternare, cu puncte de fierbere apropiate.

Datele cromatografice indică faptul că în aceste fracțiuni sînt cel puțin 20 componenți. Dintre aceștia au fost identificați, în parte, componenții fracțiunii *I*. Ea reprezintă 8...10% din greutatea produsului brut și include, în principal, ciclohexanona, ciclohexanol, fenol și urme din crezoli. Din acești componenți, ciclohexanolul se găsește în proporție de 40...60% și prin urmare fracțiunea *I* ar putea fi folosită pentru separarea acestui component.

Din cauza dificultăților separării lor în stare pură, componenții din fracțiunile *II*, *III* și *IV* nu au fost încă identificați. Studiile IR indică faptul că aceste fracțiuni conțin derivați hidroxilați ai ciclohexanului, produși de condensare ai ciclohexanonei, mici cantități de acid succinic și acid adipic.

Reziduul rezultat la distilare prezintă un interval de înmuiere în domeniul de temperatură 150°...180°C, în condiții normale fiind sticlos și casant. El este parțial solubil în etanol, cloroform, ciclohexanonă, benzen.

Pentru a face unele considerații asupra naturii chimice a acestor componenți s-a studiat raportul atomic H/C, calculat din analiza chimică elementară și indicele de refracție (tabelul 2).

Tabelul 2

Raportul atomic H/C și indicele de refracție a fracțiunilor obținute

Proba	Raportul atomic H/C	Indice de refracție, n_D^{20}
Fracțiunea *I*	1,7850	1,4590
Fracțiunea *II*	1,5679	1,5090
Fracțiunea *III*	1,5323	1,5125
Fracțiunea *IV*	1,4061	1,5293
Reziduu	1,4064	—

Analizînd datele din acest tabel se constată că atît produsul brut cît și fracțiunile separate au indici de refracție mari, asemănători compușilor aromatici, cu excepția fracțiunii *I*, care are indicele de refracție mai mic. Această observație este în concordanță cu datele analizei cromatografice prin care s-a stabilit că în fracțiunea considerată există o cantitate apreciabilă de ciclohexanol.

De asemenea, se observă că indicii de refracție ai fracțiunilor cresc de la fracțiunea *I* la *IV*, ceea ce ar corespunde cu o creștere a concentrației în derivați aromatici.

Aceeași concluzie ar rezulta și din mărimea raportului atomic H/C, ale cărui valori descresc de la 1,7850 pentru fracțiunea *I*, la 1,4061, pentru fracțiunea *IV*. Această constatare permite să se considere că uleiul X are un caracter preponderent aromatic și slab naftenic. Un argument în plus, în acest sens, este faptul că atît uleiul X cît și fracțiunile obținute au punctele de anilină mici, sub 5°C.

Analizînd caracteristicile fizico-chimice ale uleiului X în raport cu cele ale unor uleiuri utilizate ca plastifianți în industria cauciucului, reiese posibilitatea utilizării lui în acest domeniu (tabelul 3).

Din datele prezentate în tabelul 3 rezultă că proprietățile fizico-chimice ale uleiului X, exceptînd punctul de inflamabilitate, pierderile la încălzire și indicele de refracție, se încadrează în condițiile de calitate impuse. Considerăm că proprietățile uleiului X pot fi îmbunătățite prin îndepărtarea fracțiunii *I*, în care predomină ciclohexanolul. În felul acesta ar crește punctul de inflamabilitate și indicele de refracție și s-ar micșora și pierderile la încălzire.

După cum este cunoscut, plastifianții utilizați în acest scop pot fi introduși în masa de cauciuc în două moduri: fie în faza de obținere a cau-

Tabelul 3

Proprietăți fizico-chimice ale uleiului X și ale unor uleiuri utilizate ca plastifianți în industria cauciucului

Proprietăți	Uleiul X	Extract ulei mediu (valori impuse)	Ulei înalt aromatic
Densitatea la 20°C, [g/cm³]	0,98...1,061	min. 0,96	0,9937
Viscozitatea Engler (100°C), [°E]	2,5 ... 3,01	2,0...3,5	—
Punct de inflamabilitate, [°C]	120...130	min. 200	cca. 210
Punct de congelare, [°C]	9...10	max. 10	10
Conținutul de apă, [%]	0,2 ... 0,4	max. 1	—
Cenușă, [%]	0,3 ... 0,36	max. 0,3	—
Aciditate, alcalinitate, [%]	lipsă	lipsă	lipsă
Indice de refracție, n_D^{20}	1,5200...1,5255	1,5650	1,5655
Indice de brom	13,00...13,40	13,04	—
Pierderi la încălzire, 10 h la 180°C	3,5...4,44	2,26	—

ciucului, de regulă în latexul de la polimerizare, fie în cauciucul brut în faza de prelucrare a acestuia.

Uleiul X, supus în prealabil unor operații de condiționare, a fost testat ca plastifiant prin introducere în masa de cauciuc atît în faza de latex a acestuia cît și în cauciucul brut.

Cantitatea de ulei introdusă într-un latex butadien-α-metil-stirenic a fost de 27% în raport cu greutatea polimerului. După coagulare și uscare, analizele de laborator au indicat că în masa de cauciuc s-a legat aproximativ 15...16% în raport cu polimerul. Acest aspect indică o compatibilitate relativ mică a uleiului în cauciuc, în raport cu alte tipuri de uleiuri utilizate în același scop.

Analizînd indicii fizico-mecanici obținuți (tabelul 4), se constată că deși conținutul de ulei legat este de numai 15...16% totuși ei au valori ce se încadrează destul de bine în condițiile prevăzute de normele de calitate în vigoare.

Tabelul 4

Indicii fizico-mecanici ai cauciucului extins cu ulei X

Nr. crt.	Timpul de vulcanizare min.	Temperatura de vulcanizare, [°C]	Rezistența la tracțiune kg/cm²	Alungirea la rupere %	Alungirea remanentă %	Modulul 300% kg/cm²
1	25	145	200	780	40	76
2	35	145	195	720	32	90
3	50	145	188	680	28	85
Condiții STAS 7 455-75	35	145	min. 180	min. 450	—	70...130

Cercetările de laborator au inclus și studiul indicilor fizico-mecanici ai cauciucului brut supus extinderii cu ulei X. În acest scop s-au folosit compoziții de elastomeri tipice pentru industria de anvelope.

Rezultatele obținute pentru una din compozițiile de elastomeri, tipică pentru coama anvelopelor, în care s-a adăugat uleiul luat în studiu, sînt prezentate comparativ cu cele obținute pentru extractul de ulei și înalt aromatic, în tabelul 5.

Tabelul 5

Caracteristicile fizico-mecanice ale probelor vulcanizate

Caracteristici fizico-mecanice	Condiții de vulcanizare min. °C	Valori impuse	Extract de ulei mediu	Ulei înalt aromatic	Ulei X	Ulei X*)
Rezistență la rupere, [kg/cm²]	20.160	min. 175	202	185	207	222
Alungire relativă, [%]	20.160	420...550	505	493	585	600
Alungire remanentă, [%]	20.160	max. 16	4	8	8	16
Rezistență la sfîșiere, [kg/cm²]	20.160	min. 60	80	82	98	142
Duritate, [°Sh]	20.160	60...65	61	62	61	63
Elasticitate tripsometru, [%]	20.160	—	56,6	57,5	47,9	—
Pierderi abraziune	30.160	—	105	78	125	—

*) vulcanizare 7 min. 160°C.

Din tabelul 5 reiese că indicii fizico-chimici ai vulcanizatelor în care s-a adăugat uleiul X sînt apropiați ca valoare de cei ce caracterizează probele de referință. Excepție fac indicii pierdere la abraziune și alungirea relativă, care pentru proba de ulei X au valori ce depășesc cu puțin valoarea impusă. Totodată se observă că rezistența la sfîșiere a probei cu ulei X este mai mare decît cea corespunzătoare probelor martor, în special pentru proba cu timpul de vulcanizare de 7 minute.

În fig. 1 este prezentată comportarea la vulcanizare a compoziției de elastomer cu ulei X și a compoziției de referință cu un ulei înalt aromatic.

Analizînd curbele care reprezintă viteza procesului de vulcanizare, adică de reticulare în timp, în funcție de temperatură, se constată că proba de ulei X se vulcanizează mai repede decît proba de referință. De asemenea această probă are un înalt grad de reticulare, cu aproximativ

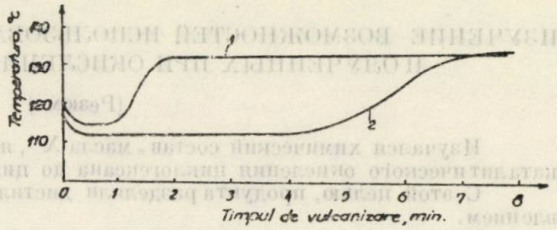

Fig. 1. — Comportarea la vulcanizare: *1* — ulei X; *2* — ulei înalt aromatic.

5...6% mai mic și ca urmare și pierderea la abraziune este mai mare, de aproximativ 20%.

Timpul de vulcanizare mai mic conduce la concluzia că uleiul X ar conține componenți chimici care măresc viteza de vulcanizare, deci ar juca rol de acceleratori de vulcanizare.

Pentru a îmbunătăți indicii fizico-mecanici ai vulcanizatelor extinse cu ulei X, în special gradul de reticulare, s-a căutat să se mărească timpul de prevulcanizare prin schimbarea grupei de vulcanizare, adică a compoziției de elastomeri. Din experiențele efectuate rezultă că există posibilitatea prelungirii timpului de prevulcanizare prin reducerea cantității de accelerator utilizat. Practic s-a găsit un conținut optim de accelerator pentru care timpul de prevulcanizare este redus la jumătate în raport cu cel inițial, dar în aceste condiții unii indici fizico-mecanici ai vulcanizatelor au valori ce se situează în afara limitelor impuse.

4. Concluzii

1. Prin distilare la presiune scăzută (5...7 mm Hg) în intervalul de temperatură 45°...175°C, uleiul X poate fi separat în 65...70% distilat și 30...35% reziduu.

2. Compoziția chimică a uleiului X este complexă, incluzînd peste 20 componenți, avînd un caracter preponderent aromatic și mai slab naftenic.

3. Prin distilarea lui la 45°...90°C și 6...7 mm Hg se obține o fracțiune bogată în ciclohexanol ce poate fi utilizată pentru recuperarea acestuia. Uleiul X astfel condiționat are un punct de inflamabilitate mai ridicat și proprietăți fizico-chimice comparative cu cele ale plastifianților utilizați în industria cauciucului.

Primită la 11 februarie 1982

Institutul politehnic, Iași,
Catedra de tehnologie chimică și chimie generală
și
ICECHIM, Borzești

BIBLIOGRAFIE

1. Березин И. Д., Дзантеев Б. Г., Казанская Н. Ф., Синицкина Л. Н., Эмануел Н. М., ЖФХ, **XXXI**, *3*, 559 (1957).
2. Alagy L., Asselineau L., Busson C., Cha B., Bendler H., Hydrocarbon Processing, **47**, *12*, 131 (1968).
3. Ardeleanu V., Onu P., Luca C., Bul. șt. stud. Inst. polit., Iași, **II**, s. II, 48 (1977).

ИЗУЧЕНИЕ ВОЗМОЖНОСТЕЙ ИСПОЛЬЗОВАНИЯ ПОБОЧНЫХ ПРОДУКТОВ ПОЛУЧЕННЫХ ПРИ ОКИСЛЕНИЯ ЦИКЛОГЕКСАНОЛА

(Резюме)

Изучался химический состав „масла X", являющеися побочным продуктом при каталитического окисления циклогексана до циклогексанола и циклогексанона.

С этой целью, продукта разделяли дистилляцией на фракции при низком давлением.

Физико-химические анализы показали что „масло X", кондиционированный устранением циклогексанола и других летучих составных частей, имеет стравнительные свойства с пластификаторами используемых в пройзводстве резины.

BULETINUL INSTITUTULUI POLITEHNIC DIN IAŞI
Tomul XXXI (XXXV) Fasc. 1—4, 1985
Secţia II
CHIMIE ŞI INGINERIE CHIMICĂ

D.C. 547.321

THE CALCULUS OF TOTAL ATOMIC CHARGES USING E. H. ITERATE AND ESCA METHODS

BY

GH. SURPĂŢEANU, M. CONSTANTINESCU, I. ZUGRĂVESCU,

Corresponding Member of the Romanian Socialist Republic Academy

A. LABLACHE-COMBIER and J. P. CATTEAU

1. Introduction

The study by ESCA (electronic spectra for chemical applications) method of the distribution of the charges in the cycloimonium ylides, allowed to estimate that the negative charge in disubstituted carbanion cycloimonium ylides, traditional writen on the ylide carbon atom, is strongly delocalized [1]...[3]:

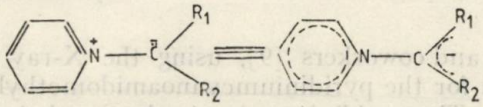

The positive charge in the cycloimonium ylides is delocalized on the all heterocycle (pyridine, quinoline, isoquinoline, pyridazine, etc.). Thus the ylide structures of the type 1 *a* are so far away of the real structures of these systems. Early, the calculus MO — SCF, CNDO/2 method on the pyridinium, quinolinium, isoquinolinium and pyridazinium, ylides carbanion disubstituted [1], [4] permited to obtain the total atomic charges, q_A, of these molecules. By using the equation

$$\Delta B = kq_A + V_A + l, \tag{1}$$

proposed by Siegbahn and coworkers [5], these values with electronic binding energies ΔB have been corelated. In the relation (1) the first term represents the potential created at the atom A by its charge q_A. The potential V_A is given by the following relation:

$$V_A = \sum_{B \neq A} \frac{q_B}{R_{AB}}; \tag{2}$$

V_A represents the potential created at the atom A by the molecular charge; q_B are the total atomic charges on the other atoms than A in the molecule. The constants k and l have different values versus the nature of the atom and of the theoretical method used to obtain the atomic total charges. For the nitrogen atom in CNDO/2 method $k = 21.5$ and $l = 1.7$ [6]. The attempts to calculate the total atomic charges in the pyridinium dicyanomethylide in CNDO/2 method failled [7] because the convergence of the electronic energies using this method are not realized.

2. Results and Discussions

In the first part of this paper we proposed to calculate the total atomic charges using extended Hückel (E.H.) iterative method. The calculus were performed on the two disubstituted carbanion ylides, namely: pyridinium dicyanomethylide and pyridinium cyano amidomethylide. This

two systems were chosen because their geometries are knowen after their determinations by X ray difraction spectra.

Bugg and coworkers [8] have been established the geometry of pyridinium dicyanomethylide (Fig. 1).

The pyridinium ring as well as the trigonal carbon atom are coplanar within ± 0.01 Å. The two cyano groups are inclined with respect to this plane such that the distance from the plane to atoms of carbon and nitrogen in cyano group are 0.08 Å and 0.13 Å respectively. All distances reported in this molecule have an associated estimated standard deviation of ± 0.01 Å.

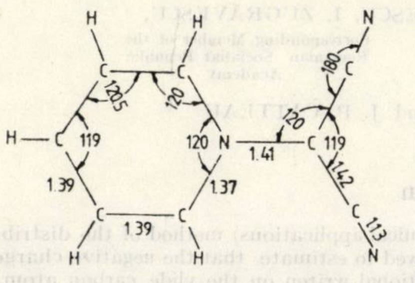

Fig. 1. — Distances and angles in pyridinium dicyanomethylide.

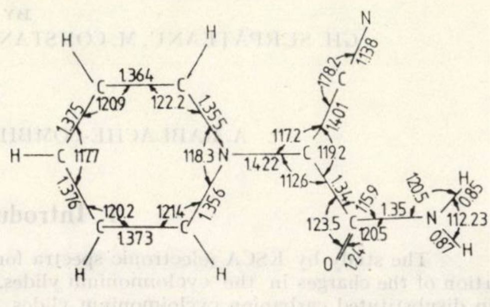

Fig. 2. — Distances and angles in pyridinium cyanoamidomethylide.

L. Devos and coworkers [9], using the X-ray difraction spectra, have been founded for the pyridiniumcyanoamidomethylide the parameters presented in Fig. 2. The pyridinium ring is plane and the ylide carbon atom C_7 is deviated with ± 0.0804 from the plane formed by the atoms N_1, C_8 and C_9.

It must point out that in both studied pyridiniumylides the valences of the ylide carbon atoms are not coplanar.

Using these two geometries in the E. H. iterative method the total atomic charges have been calculated (Figs. 3 and 4).

The calculus with a computer Felix C-256 have been performed. As an interesting fact apears the low positive charges on the yilide carbon atom.

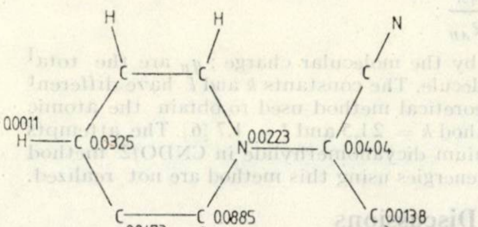

Fig. 3. — The total atomic charges in pyridinium dicyanomethylide.

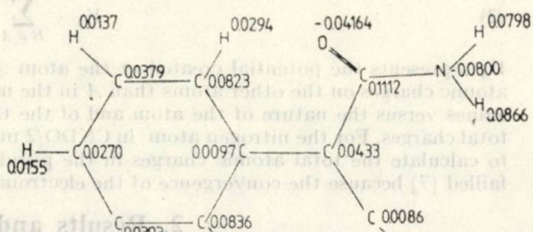

Fig. 4. — The total atomic charges in pyridinium cyano amidomethylide.

Table 1

The Total Atomic Charges and Binding Energies

Ylide	Atom	Charge	V eV	ΔB eV
Dicyanopiridinium methylide	N_1	+0.0223	1.6429	400.2
	N_{10}	−0.2184	1.5753	396.2
Cyano amido-pyridinium methylide	N_1	+0.097	1.4182	399.6
	N_{10}	−0.2278	1.1580	396.3
	N_{12}	−0.0800	1.8113	398.4

In the second part of this paper are presented the electronic binding energies (nitrogen 1 *s*) and the potentials of nitrogen atoms (Table 1), calculated using the relation (2).

The binding energies of the nitrogen 1 *s* electron have been measured with a photometer A.E.J—E.S. 200 B using the ray AlK α. The yilides were deposed simultaneously with sodium nitrate on a sonde cooled at 120°K in order to avoid the fast decomposition of the products by the influence of X ray. The binding energies of nitrogen, 1 *s* electron, with respect to the value of 407.2 eV of sodium nitrate were measured [10].

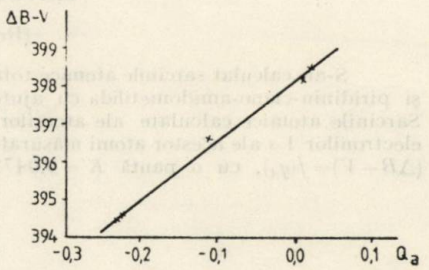

Fig. 5.—The dependence $(\Delta B - V) = f(q_A)$

A graphical representation of $(\Delta B - V) = f(q_A)$ for the nitrogen atoms gives a linear relationship (Fig. 5). The slope of the curve is $K' = 9.0475$. Using this constant we will try to verify it in a next paper for another molecular systems containing different nitrogen atoms.

Received, September 21, 1982

Polytechnic Institute, Jassy,
Department of Organic and Macromolecular Chemistry and Technology,
University „Al. I. Cuza", Jassy,
Computer Center
and
University of Lille, France
Department of Physical Organic Chemistry

REFERENCES

1. Surpățeanu G., Catteau J. P., Karafiloglou P., Lablache-Combier A., Tetrahedron Report, **23** (1976).
2. Catteau J. P., Karafiloglou P., Lablache-Combier A., Lethan N., Surpățeanu G., Tetrahedron, **32** 461 (1976).

3. Catteau J. P., Lablache-Combier A., Grimblot J., Nastasi M. Streith J., Tetrahedron, **31**, 2909 (1975).
4. Surpăţeanu G., Constantinescu M., Zugrăvescu I., Rev. Roum. Chim., **3**, *9—10*, 1449 (1978).
5. Siegbahn K., Johansson G., Hedman J., Heden P. F., Hamrin K., Gelius U., Bergmark, T., Werme L. O., Manne R., Baer Y., *ESCA applied to Free Molecules*. North Holland, Amsterdam, 1969, 108.
6. Schwartz M. E., Switlaski J. D., Stronski R. E., *Photoelectron Spectroscopy*. North Holland, Amsterdam, 1972, 616.
7. Surpăţeanu G., Rev. Roum. Chim., **29**, *11—12*, 877 (1984).
8. Bugg C., Desiderato R., Sass R. L., J. Amer. Chem. Soc., **86**, 3157 (1964).
9. Devos L., Lablache-Combier A., Surpăţeanu G. (unpublished results).
10. Jack J. J., Hercules D. M., Analyt. Chem., **43**, 729 (1971).

CALCULUL SARCINILOR ATOMICE TOTALE UTILIZÎND ITERAŢIA E.H. ŞI METODA ESCO

(Rezumat)

S-au calculat sarcinile atomice totale ale atomilor care compun piridiniu-dicianometilida şi piridiniu-ciano-amidometilida cu ajutorul metodei E.H. (Extended Hückel) iterativă. Sarcinile atomice calculate ale atomilor de azot au fost corelate cu energiile de legătură ale electronilor 1 *s* ale acestor atomi măsurate prin tehnica ESCA. S-a obţinut o dependenţă liniară $(\Delta B - V) = f(q_A)$, cu o pantă $K' = 9.0475$.

BULETINUL INSTITUTULUI POLITEHNIC DIN IAŞI
Tomul XXXI (XXXV) Fasc. 1—4, 1985
Secţia II
CHIMIE ŞI INGINERIE CHIMICĂ

D.C. 661.719.2

ORGANIC SULPHUR COMPOUNDS

XV. 2-HYDROXYKETONES. X. NEW MANNICH REACTION OF SOME DERIVATIVES CONTAINING SULPHUR OF 3′, 5′-DICHLORO-2′-HYDROXY-ACETOPHENONE*)

BY

AL. CAŞCAVAL

1. Introduction

In a comprehensive review M. Tramontini [2] and more recent W. Werner [3] and his co-workers [4] reported new versatile application of the Mannich reaction in the heterocyclic synthesis; in this way *ortho*-hydroxy-acetophenone afforded new chromanones-4 with very promising biological activities. In a recent paper [5] we have reported that 3′, 5′-dichloro-2′-hydroxy-acetophenone (I_a) and 3′, 5′-dichloro-2′-hydroxy-propiophenone (I_b) lead in a facile Mannich-Werner reaction to the new bis-Mannich bases ($V_{a,b}$) and the corresponding mono-Mannich bases ($V_{c,d}$) with chromanone-4 moiety in the molecule. This results encouraged us to generalize of this type of reaction for the obtaining a series of new chromanones-4 which have sulphur in the side chain.

We wish here presented our results in the synthesis of new mono-bases Mannich starting from some sulphur substituted *ortho*-hydroxy-acetophenones and we hope that these compounds will have interesting biological properties.

2. Results

3′,5′-dichloro-2′-hydroxy-α-thiocyanato-acetophenone (I_c) reacts in a aqueous methanolic solution with formaldehyde (solution 35%) and morpholine (II) to leads at the chromanone-4 in a good yield (V_e):

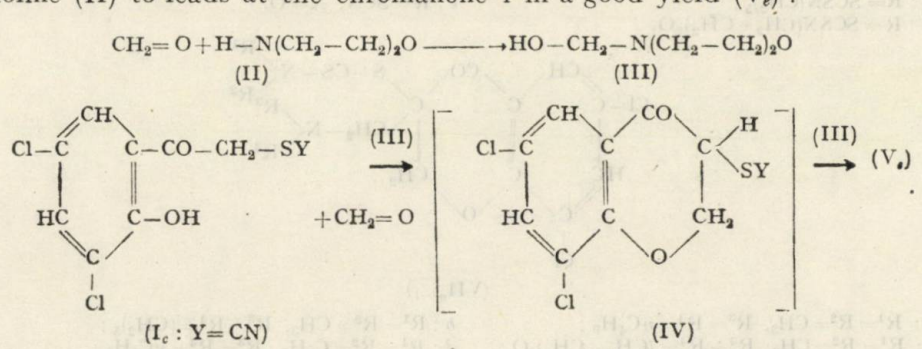

*) s. [1].

It is interesting to note that by the inversion of the adding order of the reactants instead the chromanone-4 (V_e) results 2-morpholino-4-/3,5-dichloro-2-hydroxy-phenyl/1,3-thiazole (VI) by a known reaction to the thiocyanate group [6]. This fact can be explained by a first reaction between morpholine and formaldehyde which afforded [N]-hydroxymethyl-morpholine (III), a basic catalyst in the condensation of *ortho*-hydroxyketone (I_c) with formaldehyde; when morpholine reacts with thiocyanate group, aldol condensation is out and substituted thiazole (VI) was isolated:

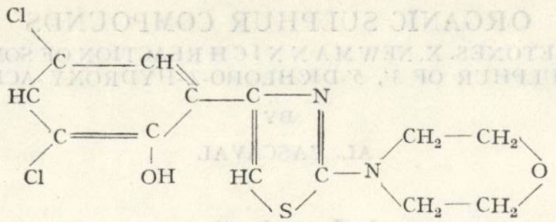

(VI)

3,5-Dichloro-2-hydroxy-phenacyl N,N-dialkyldithiocarbamates ($I_{d\ldots h}$) react in the same cyclocondensation type of reaction with formaldehyde and various secondary amines *via* (IV) intermediate ($Y=CSNR_1R_2$) to new mono-M a n n i c h bases ($VII_{a\ldots l}$) with chromanone-4 moiety in the molecule:

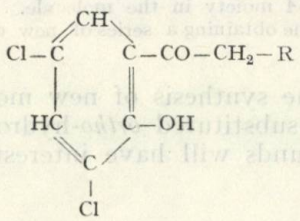

($I_{a\ldots h}$)

a: R= H; *b*: R= CH_3; *c*: R= SCN;
d: R= $SCSN(CH_3)_2$;
e: R= $SCSN(C_2H_5)_2$;
f: R= $SCSN(nC_4H_9)_2$;
g: R= $SCSN(CH_2)_5$;
h: R= $SCSN(CH_2-CH_2)_2O$.

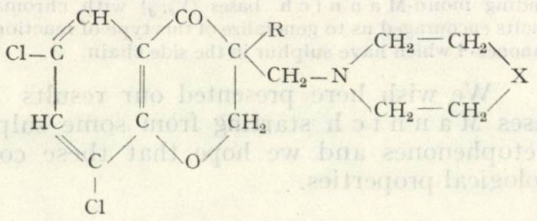

($V_{a\ldots e}$)

a: R= $CH_2-N(CH_2)_5$; X= CH_2;
b: R= $CH_2-N(CH_2-CH_2)_2O$, X= O;
c: R= CH_3, X= CH_2;
d: R= CH_3, X= O;
e: R= SCN, X= O.

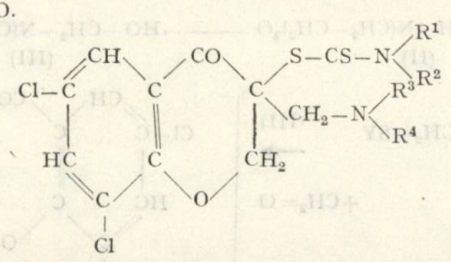

($VII_{a\ldots l}$)

a: $R^1=R^2=CH_3$, $R^3=R^4=nC_4H_9$;
b: $R^1=R^2=CH_3$, $R^3+R^4=(CH_2)_5$;
c: $R^1=R^2=CH_3$, $R^3+R^4=(CH_2-CH_2)_2O$;
d: $R^1=R^2=C_2H_5$, $R^3=R^4=nC_4H_9$;
e: $R^1+R^2=C_2H_5$, $R^3+R^4=(CH_2)_5$;
f: $R^1=R^2=C_2H_5$, $R^3+R^4=(CH_2-CH_2)_2O$;

g : $R^1+R^2=(CH_2)_5$, $R^3=R^4=C_2H_5$, *h* : $R^1+R^2=(CH_2)_5$, $R^3+R^4=(CH_2)_5$;
i : $R^1+R^2=(CH_2)_5$, $R^3+R^4=(CH_2-CH_2)_2O$; *j* : $R^1+R^2=(CH_2-CH_2)_2O$, $R^3=R^4=C_2H_5$;
k : $R^1+R^2=(CH_2-CH_2)_2O$, $R^3+R^4=(CH_2)_5$; *l* : $R^1+R^2=R^3+R^4=(CN_2-CH_2)_2O$.

All experimental data are given in Tables 1 and 2.

Table 1

Data on Elemental Analysis and IR-Characterization of Compounds

Compound	M.p. °C	Yield %	%C Calcd. Found	%H Calcd. Found	%N Calcd. Found	% Cl Calcd. Found	IR (KBr) ν, [cm^{-1}]
(I_c)	143...144	64	41.23 41.63	1.90 2.07	5.34 5.44	27.07 27.50	2 130(SCN), 1 640(CO)
(V_e)	143	77	48.27 48.64	3.72 3.77	7.50 7.23	19.01 18.80	2 130(SCN), 1 690(CO)
(VI)	190...191	29	47.17 47.25	3.62 3.84	8.46 8.54	21.42 21.25	2 850, 1 450
(VII_a)	118	34	52.73 52.74	6.28 6.35	5.87 5.51	14.86 15.09	1 685(CO)
(VII_b)	159	58	49.89 50.04	5.08 5.02	6.88 7.22	16.38 16.66	1 680(CO)
(VII_c)	169	58	46.90 47.12	4.59 4.80	6.44 6.65	16.30 16.64	1 670(CO)
(VII_d)	168	30	54.66 54.34	6.73 6.54	5.54 5.70	14.04 14.25	1 700(CO)
(VII_e)	135...136	25	52.07 52.03	5.64 5.72	6.08 6.28	15.38 15.52	1 690(CO)
(VII_f)	130	62	49.25 49.06	5.18 5.07	6.04 6.10	15.31 15.60	1 690(CO)
(VII_g)	117...118	50	52.07 52.15	5.64 5.72	6.08 6.39	15.38 15.60	1 700(CO)
(VII_h)	146...147	36	53.29 52.81	5.49 5.30	5.92 5.85	14.99 15.02	1 690(CO)
(VII_i)	166	70	50.54 50.72	5.05 5.20	5.89 5.61	14.92 15.02	1 700(CO)
(VII_j)	158...159	57	49.25 49.32	5.18 5.26	6.04 6.09	15.31 15.67	1 690(CO)
(VII_k)	144	55	50.54 50.12	5.05 4.84	5.89 5.94	14.92 15.20	1 680(CO)
(VII_l)	175	80	47.80 47.96	4.61 4.56	5.87 5.66	16.96 16.80	1 690(CO)

Table 2

^{1}H-NMR Characterization of the Prepared Compounds (in $CDCl_3$ at 20°C, TMS)

Compound	Chemical shifts in δ, [ppm], shape*), intensity and assignement of signals
(I$_e$)	4.65 (*s*, 2H, CH_2) ; 7.5...7.7 (*m*, 2H, aromatic) ; 12.8 (*s*, 1H, OH).
(V$_e$)	2.5...2.7 (*t*, 4H, $2CH_2N$) ; 2.8...2.9 (*d*, 2H, CH_2) ; 3.4...3.6 (*t*, 4H, $2CH_2O$) ; 4.6...4.8 (*d*, 1H, H_2) ; 5.4...5.5 (*d*, 1H, H_2); 7.3...7.6 (*dd*, 2H, aromatic).
(VI)	3.3...3.6 (*t*, 4H, $2CH_2N$); 3.6...3.9 (*t*, 4H, $2CH_2O$) ; 6.6 (*s*, 1H, CH) ; 7.05...7.3 (*dd*, 2H, aromatic) ; 12.7...12.8 (*s*, 1H, OH).
(VII$_a$)	0.9...1.05 (*t*, 6H, $2CH_3$) ; 1.3...1.5 (*m*, 8H, $4CH_2C$) ; 2.5...3.1 (*m*, 6H, $3CH_2N$) ; 3.4 (*m*, 6H, $2CH_3N$) ; 4.7...4.9 (*d*, 1H, H-2) ; 5.6...5.8 (*d*, 1H, H-2) ; 7.5...7.7 (*m*, 2H, aromatic).
(VII$_b$)	1.4 (*s*, 6H, $3CH_2C$) ; 2.5...2.9 (*m*, 6H, $3CH_2N$) ; 3.3 (*s*, 6H, $2CH_3N$) ; 4.6...4.8 (*d*, 1H, H-2) ; 5.5...5.7 (*d*, 1H, H-2) ; 7.3...7.6 (*dd*, 2H, aromatic).
(VII$_c$)	2.5...2.7 (*t*, 4H, $2CH_2N$) ; 2.8...2.9 (*d*, 2H, CH_2N) ; 3.3 (*s*, 6H, $2CH_3N$) ; 3.4...3.6 (*t*, 4H, $2CH_2O$) ; 4.6...4.8 (*d*, 1H, H-2) ; 5.5...5.7 (*d*, 1H, H-2) ; 7.3...7.6 (*dd*, 2H, aromatic).
(VII$_e$)	1.0...1.3 (*t*, 6H, $2CH_3$) ; 1.3...1.6 (*m*, 6H, $3CH_2C$) ; 2.4...3.0 (*m*, 5H, $3CH_2N$) ; 3.6...4.0 (*m*, 4H, $2NCH_2CH_3$) ; 4.7...4.9 (*d*, 1H, H-2) ; 5.6...5.8 (*d*, 1H, H-2) ; 7.4...7.7 (*m*, 2H, aromatic)
(VII$_g$)	0.9...1.1 (*t*, 6H, $2CH_3$) ; 1.6...1.8 (*m*, 6H, $3CH_2C$) ; 2.5...3.2 (*m*, 8H, $4CH_2N$) ; 3.8...4.1 (*s*, 2H, CH_2) ; 4.8...5.0 (*d*, 1H, H-2) ; 5.7...5.9 (*d*, 1H, H-2) ; 7.4...7.7 (*m*, 2H, aromatic).
(VII$_h$)	1.3...1.9 (*m*, 12H, $6CH_2C$) ; 2.5...3.0 (*m*, 6H, $3CH_2N$) ; 3.9...4.1 (*m*, 4H, $2CH_2N$) ; 4.7...4.9 (*d*, 1H, H-2) ; 5.6...5.8 (*d*, 1H, H-2) ; 7.3...7.7 (*m*, 2H, aromatic).
(VII$_i$)	1.5...1.8 (*m*, 6H, $3CH_2C$) ; 2.4...2.7 (*t*, 4H, $2CH_2N$) ; 2.85...3.0 (*t*, 2H, CH_2) ; 3.4...3.6 (*m*, 4H, $2CH_2O$) ; 3.8...4.1 (*m*, 2H, CH_2) ; 4.7...4.9 (*d*, 1H, H-2) ; 5.8...6.0 (*d*, 1H, H−2) ; 7.3...7.7 (*m*, 2H, aromatic).
(VII$_j$)	0.9...1.2 (*t*, 6H, $2CH_3$) ; 1.3...1.6 (*t*, 4H, $2CH_2$) ; 2.5...3.1 (*m*, 10H, $5CH_2N$) ; 4.9...5.0 (*d*, 1H, H-2) ; 5.7...5.8 (*d*, 1H, H-2) ; 7.4...7.8 (*m*, 2H, aromatic).
(VII$_k$)	1.5 (*s*, 6H, $3CH_2C$) ; 2.5...2.7 (*m*, 4H, $2CH_2N$); 2.85...2.95 (*d*, 2H, CH_2N); 3.7...3.8 (*t*, 4H, $2CH_2N$) ; 3.9...4.0 (*t*, 4H, $2CH_2O$) ; 4.7...4.9 (*d*, 1H, H-2) ; 5.1...5.3 (*d*, 1H, H-2) ; 7.4...7.7 (*m*, 2H, aromatic).

*) *s*—singlet ; *t*—triplet ; *m*—multiplet ; *dd*—double doublet.

3, Experimental Part

IR-spectra were recorded on a Spekord 71 IR spectrometer as KBr pellets, ^{1}H-NMR spectra on a JEOL—JNM—C—60 HL spectrometer.

a) *2-Morpholino-4[3,5-dichloro-2-hydroxy-phenyl]-1,3-thiazole (VI)*

5.2 g (0.02 mole) 3′, 5′-dichloro-2′-hydroxy-α-thiocyanato-acetophenone (I_c) in methanol (50 ml) with 6 ml morpholine (III) was stirred at room temperature for 2 hours. The reaction mixture was allowed to stand overnight at room temperature. The crystals which separated was filtered, washed with absolute methanol and crystalized from methanol (s. Tables 1 and 2).

b) *General Procedure for the Cyclocondensation of Ortho-hydroxy-acetophenones (I_{c-h}) to the Substituted Chromanones-4 (V) and (VII)*

0.02 mole of (I) in 75 ml methanol, 15 ml aqueous solution of formaldehyde (35%) and 0.025 mole of the corresponding secondary amine was heated on a steam-bath until a clear solution was obtained. After 24 hours at room temperature by adding 250 ml water caused the separation of a crystalline product which was purified by twice crystalizations from methanol. All results are in Tables 1 and 2 given.

* * *

The author is thankfull to „Alexander von Humboldt" Stiftung Bonn-Bad Godesberg for awarding a fellowship to undertake a part of this study in Freiburg i. Br. also BASF—AG/ Ludwigshafen (West-Germany) for a series of intermediate samples.

Received, November 8, 1982

Polytechnic Institute, Jassy, Department of Organic and Macromolecular Chemistry and Technology

REFERENCES

1. Caşcaval Al., XIV and IX parts of this series, Bul. Inst. polit., Iaşi (in press).
2. Tramontini M., Synthesis, 703 (1973).
3. Werner W., Arch. Pharm. (Weinheim, Ger.), *309*, 1011 (1976).
4. Werner W., Hagen H., Schnitzler S., Renner H., German Patent (East). (DDRP) *130 732* (1978), Zentralinstitut für Mikrobiologie; C.A., **90**, 103 834 (1979).
5. Caşcaval Al., Mişcovici E., Chiorean V., Romania Patent (RSRP), *79907* (1982).
6. Schulze B., Mühlstädt M., Schubert I., Z. Chem., **19**, 41 (1979).

COMPUŞI ORGANICI AI SULFULUI

XV. 2-hidroxicetone. X. O nouă reacţie Mannich aplicată unor derivaţi conţinînd sulf_ai_3′, 5′-diclor-2′-hidroxi-acetofenonei

(Rezumat)

Se descrie o reacţie de ciclocondensare de tip Mannich-Werner a 3′,5′-diclor-2′-hidroxi-α-tiocianato-acetofenonei (I_c) precum şi a N, N-dialchilid-tiocarbamaţilor de 3,5-diclor-2-hidroxifenacil ($I_{d...h}$) obţinîndu-se mono-baze Mannich (V_e) şi ($VII_{a...l}$) cu potenţială activitate biologică. De remarcat că, inversînd ordinea adăugării reactanţilor în cazul tiocianatului (I_c) în locul cromanonei-4 aşteptate (V_e), se obţine tiazolul substituit (VI). Sînt prezentate : procedeul general de sinteză, mecanismul de reacţie iar produşii sintetizaţi sînt caracterizaţi din punct de vedere analitic şi spectral.

BULETINUL INSTITUTULUI POLITEHNIC DIN IAŞI
Tomul XXXI (XX XV) Fasc. 1—4, 1985
Secţia II
CHIMIE ŞI INGINERIE CHIMICĂ

C.D. 542.951 ; 547.293

L'ÉTUDE CINÉTIQUE DU PROCESSUS D'ESTÉRIFICATION DES ACIDES CHLORE-PHÉNOXI-α-PROPIONIQUES

PAR

CORNELIU ONISCU, M. CHIRIŢĂ et FLORIN IRIMIE

1. Introduction

Les esters phénoxi-α-propioniques et chlore-phénoxi-α-propioniques sont beaucoup utilisés comme herbicides sélectifs et comme stimulateurs de la croissance des plantes [1]. Ces esters sont aussi des intermédiaires précieux dans la synthèse de certains médicaments anti-infectieux, anti-inflammatoires, hipolipémiants et hypoglycémiques ainsi que dans la synthèse de certains produits ayant une action psycho-énergétique [2], [3].

La littérature de spécialité décrit la technologie d'obtention de certains esters des acides chlore-phénoxi-α-propioniques mais les données cinétiques concernant ce processus n'y sont pas présenteés [4].

Dans ce qui suit on effectue l'étude cinétique du processus d'estérification à l'alcool éthylique des acides chlore-phénoxi-α-propioniques et a en vue la détermination des valeurs cinétiques de la mise en projet et de modélage de ce processus.

2. Données théoriques

On a effectué l'étude cinétique du processus d'estérification des acides chlore-phénoxi-α-propioniques à une température de 78°C, utilisant un rapport molaire de 1:10 entre l'acide phénoxi-α-propionique et l'alcool éthylique; le catalyseur H_2SO_4 est en proportion de 0,5% par rapport à l'alcool. La pureté des acides utilisés a été de 98% et de l'alcool de 95,57%.

Pour déterminer la variation de la concentration des réactants au cours du processus d'estérification on a gelé (bloqué) la réaction et on a titré l'acidité à l'aide d'une solution de NaOH n/10 [5].

L'estérification à l'alcool éthylique des acides phénoxi-α-propioniques se produit suivant la reaction:

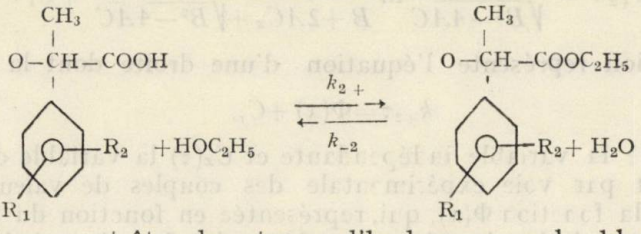

où R_1 et R_2 peuvent être des atomes d'hydrogene ou de chlore.

Pour l'analyse cinétique on emploie les notations suivantes: C_{A0} — la concentration initiale de l'acide, [mol.l^{-1}]; C_{B0}—la concentration initiale de l'alcool, [mol.l^{-1}]; C_{C0}—la concentration initiale de l'eau, [mol. l^{-1}]; C_x—la concentration instantanée de l'ester, [mol^{-1}]; τ—la durée de réaction, [h]; k_{+2}—la constante de vitesse de l'estérification, [l.mol^{-1}.h^{-1}]; k_{-2}—la constante de vitesse de l'hydrolyse, [l.mol^{-1}.h^{-1}]

La vitesse du processus d'estérification est décrite par l'équation

$$\frac{dC_x}{d\tau} = k_{+2}(C_{A0}-C_x)(C_{B0}-C_x) - k_{-2}C_x(C_{C0}+C_x), \tag{1}$$

ou par:

$$\frac{dC_x}{d\tau} = k_{+2}\left[(C_{A0}-C_x)(C_{B0}-C_x) - \frac{k_{-2}}{k_{+2}} C_x(C_{C0}+C_x)\right]. \tag{2}$$

Pour l'équilibre ($\tau \to \tau_{\text{équil.}}$ et $C_x \to C_{x\,\text{équil.}}$) la vitesse du processus d'accumulation de l'ester est nulle. Donc $dC_x/d\tau = 0$, d'ou en résulte:

$$\frac{k_{-2}}{k_{+2}} = \lim_{\substack{\tau\to\tau_{\text{équil.}} \\ C_x\to C_{x\,\text{équil.}}}} \frac{(C_{A0}-C_x)(C_{B0}-C_x)}{(C_{C0}+C_x)}. \tag{3}$$

On détermine la valeur du rapport des constantes des vitesses k_{-2}/k_{+2} en représentant le rapport des concentrations en fonction de temps. Si l'on introduit ce rapport dans l'équation (2) on obtient par intégration:

$$k_{+2}\tau = \int \frac{dC_x}{C_x^2(1-k_{-2}/k_{+2}) - C_x(C_{A0}+C_{B0}+C_{C0}k_{-2}/k_{+2}) + C_{A0}C_{B0}}. \tag{4}$$

En utilisant les notations:

$$1-k_{-2}/k_{+2} = A,\quad -(C_{A0}+C_{B0}+C_{C0}k_{-2}/k_{+2}) = B,\quad C_{A0}C_{B0} = C \tag{5}$$

on obtient:

$$k_{+2}\tau = \int \frac{dC_x}{AC_x^2+BC_x+C}. \tag{6}$$

Si l'on effectue l'intégration de l'équation (6) il est possible à calculer la constante de vitesse de l'estérification des acides phénoxi-α-propioniques, à savoir:

$$k_{+2}\tau = \frac{1}{\sqrt{B^2-4AC}} \ln \frac{B+2AC_x-\sqrt{B^2-4AC}}{B+2AC_x+\sqrt{B^2-4AC}} + C_1. \tag{7}$$

Cette expression représente l'équation d'une droite dont la forme est:

$$k_{+2}\tau = \Phi(x) + C_i, \tag{8}$$

où τ représente la variable indépendante et $C_x(\tau)$ la variable dépendante. Si l'on établit par voie expérimentale des couples de valeurs $C_x(\tau)$, τ on détermine la fonction $\Phi(x)$, qui, représentée en fonction du temps, permet d'obtenir une droite dont la pente détermine la valeur de la constante

de vitesse de l'estérification à l'alcool éthylique des acides phénoxi-α-propioniques.

3. Résultats expérimentaux

3.1. L'estérification à l'alcool éthylique de l'acide 2-chlore-phénoxi-α-propionique.

Pour effectuer l'étude du processus d'estérification à l'alcool éthylique de l'acide 2-chlore-phénoxi-α-propionique, catalysé par l'acide sulfurique monohydré, on a utilisé les concentrations suivantes des réactants :

$$C_{A0}= 1{,}3271 \text{ mol} \cdot 1^{-1},\ C_{B0}= 13{,}6805 \text{ mol} \cdot 1^{-1},\ C_{C0}= 1{,}6205 \text{ mol} \cdot 1^{-1}.$$

Les variations dans le temps de la concentration des réactants et des produits de réaction sont illustrées par le Tableau 1.

Tableau 1

L'estérification à l'alcool éthylique de l'acide 2-chlore-phénoxi-α-propionique

Nr.	τ h	C_x mol/l	$C_{A0}-C_x$ mol/l	$C_{B0}-C_x$ mol/l	$C_{C0}+C_x$ mol/l	$\frac{(C_{A0}-C_x)(C_{B0}-C_x)}{C_x(C_{C0}+C_x)}$	η
1	0	0	1,3271	13,6805	1,6205	11,20	0
2	0,25	0,6675	0,6596	13,013	2,2880	5,62	0,5
3	0,5	0,8519	0,4752	12,8286	2,4724	2,849	0,64
4	1,0	1,0132	0,3139	12,6673	2,6337	1,49	0,76
5	2,0	1,0935	0,2336	12,5870	2,7140	0,99	0,82
6	3,0	1,1479	0,1823	12,5326	2,7684	0,72	0,86
7	4,0	1,1508	0,1763	12,5297	2,7713	0,69	0,865
8	5,0	1,1526	0,1745	12,5279	2,7731	0,684	0,868

En représentant la variation du rapport des concentrations en fonction du temps on trace la courbe de la Fig. 1, de laquelle on obtient, par extrapolation, le rapport des constantes de vitesse $k_{-2}/k_{+2}= 0{,}6$. En introduisant ce rapport dans les équations (4)...(7) on calcule $\Phi(x)$ pour chaque couple de valeurs C_x et τ ; les résultats sont inscrits dans le Tableau 2.

Tableau 2

Les valeurs de la fonction $\Phi(x)$ pour l'estérification de l'acide 2-chlore-phénoxi-α-propionique

Nr.	τ h	C_x mol/l	$\Phi(x)$
1	0	0	0,244
2	0,25	0,6675	0,278
3	0,5	0,8519	0,327
4	1,0	1,0132	0,373
5	2,0	1,0935	0,419
6	3,0	1,1479	0,550
7	4,0	1,1508	0,509
8	5,0	1,1526	0,515

En représentant dans l'abscisse le temps et dans l'ordonnée, la fonction $\Phi(x)$, on trace la droite représentée dans la Fig. 1 dont la pente permet de déterminer la constante de vitesse de l'estérification à l'alcool éthylique de l'acide 2 chlore-phénoxi-α-propionique, à savoir $k_{+2}= 3{,}33 \cdot 10^{-5}$ l . mol^{-1} . s^{-1}.

3.2. L'estérification à l'alcool éthylique de l'acide 3-chlore-phénoxi-α-propionique

Pour effectuer la réaction d'estérification à l'alcool éthylique de l'acide 3-chlore-phénoxi-α-propionique on a utilisé les suivantes concentrations molaires des réactants :

$$C_{A0}= 1{,}3262 \text{ mol} \cdot 1^{-},\ C_{B0}= 13{,}732 \text{ l mol} \cdot 1^{-1}$$
$$C_{C0}= 1{,}6266 \text{ mol} \cdot 1^{-1}.$$

La variation de la concentration des réactants et des produits de réaction est donnée dans le Tableau 3 ; la valeur du rapport des constantes k_{-2}/k_{+2}, déterminée par l'extrapolation de la Fig. 2, est 0,6.

Tableau 3

L'estérification à l'alcool éthylique de l'acide 3-chlore-phénoxi-α-propionique

Nr.	τ h	C_x mol/l	$C_{A0}-C_x$ mol/l	$C_{B0}-C_x$ mol/l	$C_{C0}+C_w$ mol/l	$\frac{(C_{A0}-C_x)\ (C_{B0}-C_x)}{C_x(C_{C0}+C_x)}$	η
1	0	0	1,3262	13,7321	1,6266	11,19	0
2	0,25	0,6896	0,6366	13,0429	2,3162	5,198	0,5
3	0,5	0,9005	0,4257	12,8316	2,5271	2,4	0,68
4	1,0	1,0524	0,2738	12,6797	2,679	1,23	0,79
5	2,0	1,1458	0,1804	12,5863	2,7724	0,71	0,86
6	3,0	1,1577	0,1685	12,5744	2,7843	0,65	0,87
7	4,0	1,1620	0,1642	12,5701	2,7886	0,63	0,876
8	5,0	1,1654	0,1611	12,567	2,7917	0,62	0,878

Tableau 4

Les valeurs de la fonction $\Phi(x)$ pour l'estérification à l'alcool éthylique de l'acide 3-chlore-phénoxi α-propionique

Nr.	τ h	C_x mol/l	$\Phi(x)$
1	0	0	0,233
2	0,25	0,6896	0,290
3	0,50	0,9005	0,329
4	1,00	1,0524	0,386
5	2,0	1,1458	0,517
6	3,0	1,1577	0,6366
7	4,0	1,1620	0,641
8	5,0	1,1651	0,653

Tableau 5

L'estérification à l'alcool éthylique de l'acide 4-chlore-phénoxi-α-propionique

Nr.	τ h	C_x mol/l	$C_{A0}-C_x$ mol/l	$C_{B0}-C_x$ mol/l	$C_{C0}+C_x$ mol/l	$\frac{(C_{A0}-C_x)(C_{B0}-C_x)}{C_x(C_{C0}+C_x)}$	η
1	0	0	1,3260	13,7658	1,6307	11,20	0
2	0,25	0,7001	0,6259	13,0657	2 3308	5,011	0,53
3	0,50	0,9176	0,4084	12,8482	2,5483	2,244	0,69
4	1,0	1,0077	0,3183	12,7581	2,6384	1,527	0,76
5	2,0	1,1138	0,2122	12,652	2,7445	0,878	0,84
6	3,0	1,1523	0,1737	12,6135	2,783	0,68	0,87
7	4,0	1,1549	0,1711	12,6109	2,7856	0,67	0,87
8	5,0	1,1562	0,1698	12,6096	2,7869	0,66	0,87

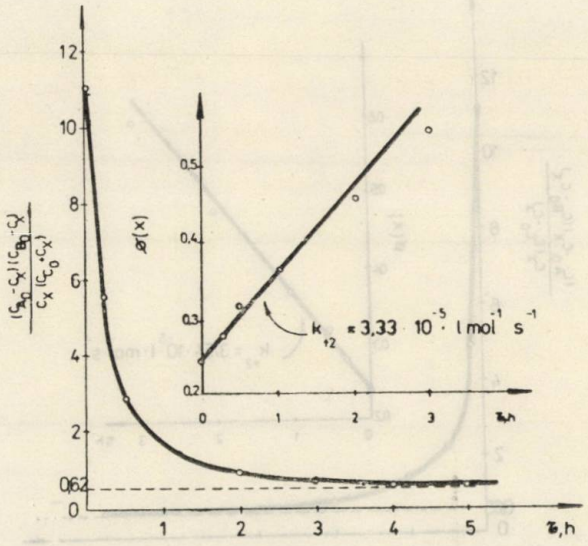

12
10
8
6
4
2
0,62
0
1
2
3
4
5
τ,h
ø(x)
0,5
0,4
0,3
0,2
0
1
2
3
τ,h
k+2 = 3,33 · 10-5 · l mol-1 s-1

Fig. 1

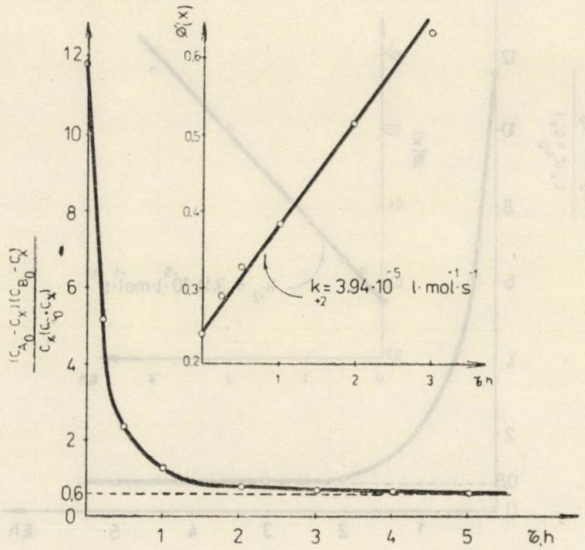

12
10
8
6
4
2
0,6
0
1
2
3
4
5
τ,h
ø(x)
0,6
0,5
0,4
0,3
0,2
1
2
3
τ,h
k+2 = 3,94·10-5 l·mol-1·s-1

Fig. 2

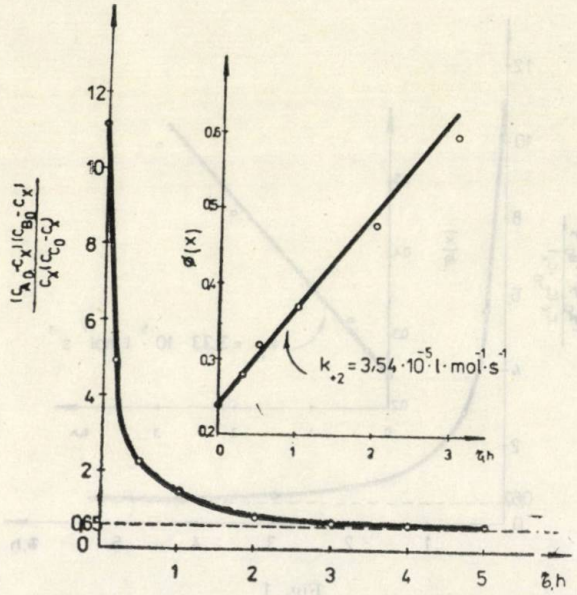
$\frac{[C_{B_0}-C_x]\,[C_{B_0}-C_x]}{C_x\,(C_{C_0}-C_x)}$
12
10
8
6
4
2
0.65
0
1
2
3
4
5
t,h
$\phi(x)$
0.6
0.5
0.4
0.3
0.2
$k_{+2} = 3{,}54 \cdot 10^{-5}\ l \cdot mol^{-1} \cdot s^{-1}$

Fig. 3

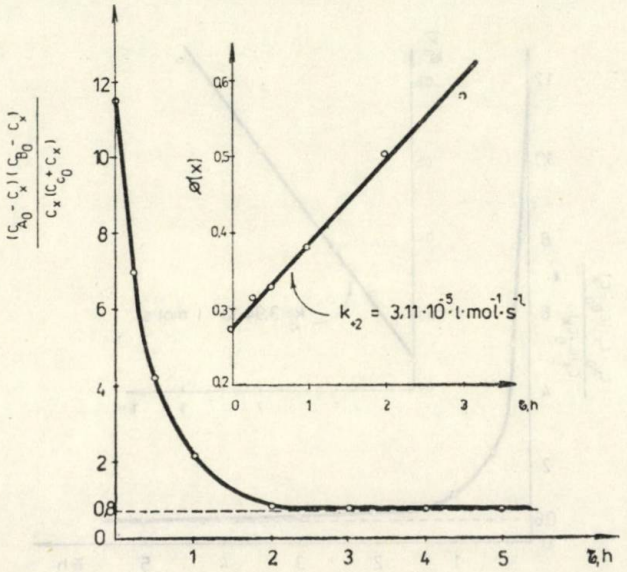
$\frac{[C_{B_0}-C_x]\,[C_{B_0}-C_x]}{C_x\,(C_{C_0}+C_x)}$
12
10
8
6
4
2
0.8
0
1
2
3
4
5
t,h
$\phi(x)$
0.6
0.5
0.4
0.3
0.2
$k_{+2} = 3{,}11 \cdot 10^{-5}\ l \cdot mol^{-1} \cdot s^{-1}$

Fig. 4

A l'aide de cette valeur du rapport, introduite dans les équations (4)...(7), on détermine la fonction $\Phi(x)$ (v. le tableau 4), qui permet, par représentation graphique (Fig. 2), de calculer la constante de vitesse de l'estérification à l'alcool éthylique de l'acide 3-chlore-α-propionique $k_{+2}= 3{,}94 \cdot 10^{-5}$ mol^{-1} . s^{-1}.

3.3. L'estérification à l'alcool éthylique de l'acide 4-chlore-phénoxi-α-propionique

Pour effectuer l'étude cinétique de l'estérification à l'alcool éthylique de l'acide 4-chlore-phénoxi-α-propionique on a utilisé les concentrations suivantes des réactants :

$$C_{A0}= 1{,}3260 \text{ mol} \cdot l^{-1},\ C_{B0}= 13{,}7658 \text{ mol} \cdot l^{-1},\ C_{C0}= 1{,}6307 \text{ mol} \cdot l^{-1}.$$

La variation de la concentration des réactants et des produits de réaction est donnée dans le Tableau 5 ; la valeur du rapport des constantes de vitesse k_{-2}/k_{+2}, déterminée par l'extrapolation de la courbe donnée dans la fig. 3 est de 0,65.

Tableau 6

Les valeurs de la fonction $\Phi(x)$ pour l'estérification à l'alcool éthylique de l'acide 4-chlore-phénoxi-α-propionique

Nr.	τ h	C_x mol/l	$\Phi(x)$
1	0	0	0,238
2	0,25	0,7001	0,286
3	0,5	0,9176	0,329
4	1,0	1,0077	0,370
5	2,0	1,1138	0,480
6	3,0	1,1523	0,582
7	4,0	1,1549	0,622
8	5,0	1,1562	0,657

Introduite dans les équations (4)...(7), cette valeur permet de déterminer la fonction $\Phi(x)$ (v. le tableau 6). En représentant $\Phi(x)$ comme fonction de τ on trace la droite représentée dans la fig. 3 dont la pente rend possible la détermination de $k_{+2} = 3{,}54 \cdot 10^{-5}$ l . mol^{-1} . s^{-1}.

3.4. L'estérification à l'alcool éthylique de l'acide 2,4 dichlore-phénoxi-α-propionique

Pour réaliser l'estérification à l'alcool éthylique de l'acide 2,4-dichlore-phénoxi-α-propionique on a employé les concentrations suivantes des réactants :

$$C_{A0}= 1{,}4030 \text{ mol} \cdot l^{-1},\ C_{B0}= 13{,}490 \text{ mol} \cdot l^{-1},\ C_{C0}= 1{,}5980 \text{ mol} \cdot l^{-1}.$$

La variation dans le temps de la concentration des réactants et des produits de reaction est donnée dans le Tableau 7 ; le rapport des constantes de vitesse k_{-2}/k_{+2}, déterminée par l'extrapolation de la courbe de la Fig. 4, a la valeur 0,8.

À l'aide de cette valeur et en utilisant les équations (4)...(7) on détermine la fonction $\Phi(x)$ dont les valeurs sont données dans le Tableau 8. En représentant graphiquement la fonction $\Phi(x)$ on obtient la droite de la Fig. 4, dont la pente permet de déterminer la valeur de la constante $k_{+2}= 3{,}11 \cdot 10^{-5}$ l . mol^{-1} . s^{-1}.

3.5. L'estérification à l'alcool éthylique de l'acide 2,5-dichlore-phénoxi-α-propionique

On a effectué l'étude du processus d'estérification à l'alcool éthylique de l'acide 2,5-dichlore-phénoxi-α-propionique en employant les concentrations suivantes des réactants :

$$C_{A0}= 1{,}3704 \text{ mol} \cdot l^{-1},\ C_{B0}= 13{,}708 \text{ mol} \cdot l^{-1},\ C_{C0}= 1{,}6238 \text{ mol} \cdot l^{-1}.$$

Tableau 7

L'estérification à l'alcool éthylique de l'acide 2,4 dichlore-phénoxi-α-propionique

Nr.	τ h	C_x mol/l	$C_{A0}-C_x$ mol/l	$C_{B0}-C_x$ mol/l	$C_{C0}+C_x$ mol/l	$\frac{(C_{A0}-C_x)(C_{B0}-C_x)}{C_x(C_{C0}+C_x)}$	η
1	0	0	1,4030	13,490	1,5980	11,84	0
2	0,25	0,6313	0,7717	12,8587	2,2293	7,05	0,45
3	0,5	0,7857	0,6173	12,7043	2,3837	4,187	0,56
4	1,0	0,9680	0,435	12,522	2,566	2,192	0,69
5	2,0	1,1729	0,2301	12,3171	2,7709	0,87	0,83
6	3,0	1,1799	0,2231	12,3101	2,7779	0,838	0,84
7	4,0	1,1806	0,2224	12,3014	2,7786	0,834	0,84
8	5,0	1,1816	0,2214	12,3084	2,7786	0,83	0,84

Tableau 8

Les valeurs de la fonction $\Phi(x)$ pour l'estérification à l'alcool éthylique de l'acide 2,4-chlore-phénoxi-α-propionique

Nr.	τ h	C_x mol/l	$\Phi(x)$
1	0	0	0,276
2	0,25	0,6313	0,323
3	0,50	0,7857	0,351
4	1,0	0,9680	0,381
5	2,0	1,1729	0,512
6	3,0	1,1799	0,575
7	4,0	1,1806	0,580
8	5,0	1,1816	0,587

Tableau 9

L'estérification à l'alcool éthylique de l'acide 2,5-dichlore-phénoxi-α-propionique

Nr.	τ h	C_x mol/l	$C_{A0}-C_x$ mol/l	$C_{B0}-C_x$ mol/l	$C_{C0}+C_x$ mol/l	$\frac{(C_{A0}-C_x)(C_{B0}-C_x)}{C_x(C_{C0}+C_x)}$	η
1	0	0	1,3704	13,708	1,6238	11,56	0
2	0,25	0,5482	0,8222	13,1548	2,172	9,083	0,4
3	0,5	0,7126	0,6578	12,9954	2,3364	5,134	0,54
4	1,0	0,9593	0,4111	12,7487	2,5831	2,115	0,70
5	2,0	1,0826	0,2878	12,6254	2,7064	1,24	0,79
6	3,0	1,1130	0,2574	12,595	2,7368	1,065	0,81
7	4,0	1,1374	0,233	12,57	2,7612	0,93	0,83
8	5,0	1,1442	0,226	12,56	2,769	0,895	0,834

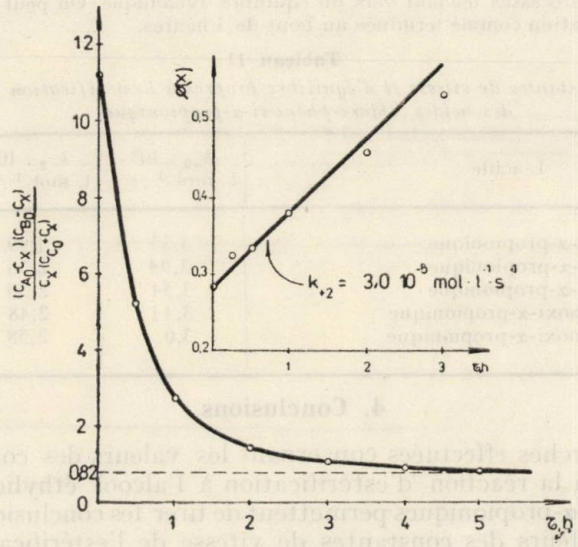

Fig. 5

Le Tableau 9 contient les valeurs de la variation instantanée de la concentration des réactants et des produits de réaction ; l'extrapolation de la courbe de la Fig. 5 permet de déterminer la valeur du rapport k_{-2}/k_{+2}= 0,86.

À l'aide de cette valeur et des équations (4)...(7) on détermine la fonction $\Phi(x)$ (Tableau 10),

Tableau 10

Les valeurs de la fonction $\Phi(x)$ pour l'estérification à l'alcool éthylique de l'acide 2,5-chlore-phénoxi-α-propionique

Nr.	τ h	C_x mol/l	$\Phi(x)$
1	0	0	0,285
2	0,25	0,5482	0,3225
3	0,50	0,7126	0,3403
4	1,0	0,9593	0,3827
5	2,0	1,0826	0,4216
6	3,0	1,1130	0,4359
7	4,0	1,1374	0,4368
8	5,0	1,1442	0,4562

qui, représentée graphiquement, permet de déterminer la constante de vitesse k_{+2}= 3,0 . 10^{-5} l . mol^{-1} . s^{-1}. On a calculé les valeurs des constantes d'équilibre et de hydrolise des esters, en connaissant tant les valeurs des constantes de vitesse d'estérification des acides chlore-phénoxi-α-propioniques que le rapport k_{-2}/k_{+2} (Tableau 11). Ces valeurs représentent les données nécessaires pour modéler le processus d'estérification à l'alcool éthylique des acides chlore-phénoxi-α-propioniques, problème qui fera le sujet d'un autre travail.

Si l'on compare entre eux les résultats obtenus après avoir étudié la réaction d'estérification des acides chlore-phénoxi-α-propioniques, on constate que les valeurs des constantes de vitesse sont du même ordre de grandeur. Les acides monochlorurés, par rapport aux acides dichlorurés, présentent des constantes de vitesse supérieures, dues aux effets inductifs et mésomères des substituts.

Si l'on examine les rendements en ester, on constate que pendant les deux premières heures on a obtenu des valeurs de 83...84% ; l'augmentation des rendements n'ést ensuite

que de 1...2%, le processus tendant vers un équilibre dynamique. On peut donc considérer la réaction d'estérification comme terminée au bout de 3 heures.

Tableau 11

Les valeurs des constantes de vitesse et d'équilibre propres à l'estérification à l'alcool éthylique des acides chlore-phénoxi-α-propioniques

L'acide	$k_{+2} \cdot 10^5$ 1. $mol^{-1} \cdot s^{-1}$	$k_{-2} \cdot 10^5$ 1. $mol^{-1} \cdot s^{-1}$	K
2-Chlore-phénoxi-α-propionique	3,33	1,99	1,67
3-Chlore-phénoxi-α-propionique	3,94	2,36	1,68
4-Chlore-phénoxi-α-propionique	3,54	2,30	1,53
2,4-Dichlore-phénoxi-α-propionique	3,11	2,48	1,25
2,5-Dichlore-phénoxi-α-propionique	3,0	2,58	1,16

4. Conclusions

Les recherches effectuées concernant les valeurs des constantes de vitesse propres à la réaction d'estérification à l'alcool éthylique des acides chlore-phénoxi-α-propioniques permettent de tirer les conclusions ci-dessous :

1. Les valeurs des constantes de vitesse de l'estérification à l'alcool éthylique des acides chlore-phénoxi-α-propioniques sont presques égales est varient entre $3{,}0.10^{-5}...3{,}94.10^{-5}$ $1.mol^{-1}.s^{-1}$.

2. Les rendements obtenus à la suite de l'estérification à l'alcool éthylique des acides chlore-phénoxi-α-propionique où l'alcool éthylique est en rapport molaire de 1:10, varient entre 83...86%.

3. La durée de réaction nécessaire pour obtenir des rendements optima est de 2,5...3 heures.

4. Les valeurs des constantes de vitesse permettent de modéler le processus d'estérification des acides chlore-phénoxi-α-propioniques.

Reçue le 21 avril 1982

Institut Polytechnique, Jassy,
Chaire de Chimie et Technologie
Organique et Macromoléculaire

BIBLIOGRAPHIE

1. Avram M., *Antidăunători*. Ed. Acad. R. S. R., Buc., 1974.
2. Ciorănescu Ec., *Medicamente de sinteză*. Ed. Tehn., Buc., 1966.
3. Oniscu C., Botez Gh., Brevet RSR, *61 526* (1975).
4. Мелников Н. Н., Баскаков И. А, *Химия гербицидов и регуляторов роста растении*, М., 1966.
5. Oniscu C., Bul. Inst. polit., Iaşi, **XIV(XIX)**, *3—4*, s. II (1968).

STUDIUL CINETIC AL PROCESULUI DE ESTERIFICARE A ACIZILOR CLORFENOXI-α-PROPIONICI

(Rezumat)

Studiul cinetic al procesului de esterificare a acizilor clorfenoxi-α-propionici cu alcool etilic de concentraţie 95,57% s-a realizat la 78°C folosind un raport molar alcool : acid de 10 : 1l Reacţia de esterificare a fost catalizată de acidul sulfuric monohidrat luat în proporţie de 0,5% faţă de alcool, iar variaţia concentraţiei reactanţilor s-a determinat prin titrare cu soluţie de NaOH n/10. În urma studiului efectuat s-au stabilit următoarele concluzii :

a) Valorile constantelor de viteză sînt cuprinse între $3{,}0 \cdot 10^{-5}...3{,}94 \cdot 10^{-5}$ $1 \cdot mol^{-1} \cdot s^{-1}$.
b) Randamentele în ester sînt cuprinse între 83...86%.
c) Timpul optim de reacţie este de 2,5...3 ore.

BULETINUL INSTITUTULUI POLITEHNIC DIN IAŞI
Tomul XXXI (XXXV) Fasc. 1—4, 1985
Secţia II
CHIMIE ŞI INGINERIE CHIMICĂ

C.Z. 66.069

CURGEREA LICHIDELOR ÎN FILME SUBŢIRI

V. PARAMETRII ALEATORI ÎN ZONA CU VALURI STABILIZATE

DE

FLORIN VITAN şi RADU Z. TUDOSE

1. Introducere

Curgerea în filme subţiri este un caz special al curgerii lichidelor, caracterizată prin prezenţa unei suprafeţe libere cu o configuraţie geometrică particulară. Peste o anumită valoare a debitului, un film descendent de lichid nu este neted pe întreaga suprafaţă de curgere, verticală sau înclinată, plană sau cilindrică. Curgerea lichidului în film neted are loc pe o porţiune limitată a suprafeţei, după care devine mult mai complexă prin apariţia valurilor la suprafaţa liberă a filmului. Valurile constituie un tip important al instabilităţii hidrodinamice a filmelor subţiri iar apariţia lor reprezintă cauza principală a intensificării transferului de masă şi de căldură. Datorită intensificării deosebite a transferului de masă [1]...[3] şi a transferului de căldură [1], [4], tehnica filmului subţire este frecvent utilizată într-o serie de echipamente din industria chimică sau din alte domenii.

Măsurătorile şi observaţiile experimentale au evidenţiat existenţa, pe suprafaţa unui film descendent, a patru zone distincte în care configuraţia geometrică a suprafeţei libere este diferită [5]...[7] :

a) *zona fără valuri*, denumită şi zona de stabilizare a curgerii ;

b) *zona de apariţie a valurilor*, caracterizată prin valuri transversale lungi, normale la direcţia de curgere, cu profil sinusoidal [8] sau de altă configuraţie [9]. S-a demonstrat că şi această zonă are o lungime limitată, deoarece valurile nu se pot propaga fără a-şi modifica profilul iniţial [6]. Apariţia zonei următoare, denumită

c) *zona de stabilizare a valurilor*, este consecinţa ruperii valurilor transversale din zona anterioară ca urmare a vitezei diferite de propagare pe lăţimea planului. În partea din valul transversal care s-a deplasat cu viteză mai mare are loc o acumulare de lichid din părţile rămase mai în urmă, formîndu-se o „picătură" care generează, lateral, valuri de dimensiuni foarte mici ;

d) *zona de curgere cu valuri stabilizate*, în care valurile din zona precedentă au ajuns la o configuraţie stabilă de picături care se deplasează pe un substrat neted de lichid, de grosime constantă, fără modificarea vitezei şi amplitudinii pe direcţia de curgere.

Cele patru zone pot fi evidenţiate pregnant pentru fluide consistente şi pe lungimi suficient de mari ale planului de curgere.

Pentru zona de curgere cu valuri stabilizate s-a elaborat un model fizic şi matematic [7], verificat pentru lichide newtoniene [10] şi extins şi verificat şi pentru lichide nenewtoniene [11].

Aşa cum s-a constatat experimental, o serie de parametri ai curgerii, cum sînt viteza de deplasare, dimensiunile şi frecvenţa picăturilor în această zonă, au un caracter aleator, iar limitele între care variază aceste mărimi depind de fenomenele din zona anterioară, de consistenţa lichidului şi de debit. Determinarea experimentală a acestor parametri s-a efectuat utilizînd tehnica cinematografică, stabilindu-se repartiţia empirică şi valorile lor medii statistice. Pentru verificarea modelului de curgere în zona cu valuri stabilizate s-a utilizat o instalaţie de laborator prezentată detaliat în lucrarea [10].

În această lucrare se efectuează analiza statistică a unor parametri care intervin în descrierea curgerii în zona cu valuri stabilizate, dintre care cei mai importanți sînt: viteza, dimensiunile și frecvența picăturilor și numărul de picături de pe unitatea de suprafață.

2. Prelucrarea rezultatelor experimentale

Cercetările experimentale s-au efectuat cu glicerină tehnică la temperaturi cuprinse între 25,2°...26,9°C și la debite cuprinse între 1,1749...1,8498 m^3/hm și cu soluții apoase de carboximetil-celuloză (CMC), de concentrații cuprinse între 0,945...1,63% la temperaturi cuprinse între 16...19°C și la debite cuprinse între 0,7844...1,50804 m^3/hm *).

Așa cum s-a precizat, parametrii aleatori studiați sînt: viteza, dimensiunile și frecvența picăturilor, precum și numărul de picături pe unitatea de suprafață. Deoarece între dimensiunile picăturilor, exprimate prin lățimea lor, l, și viteza lor de deplasare, v_p, s-au stabilit corelații de forma generală [10], [11]:

$$v_p = Ml^q, \tag{1}$$

este suficient să se stabilească repartiția dimensiunilor picăturilor pentru a se preciza, prin intermediul relațiilor de tipul (1) și repartiția vitezelor picăturilor. Valorile constantelor M și q, pentru soluțiile utilizate în experimentări, sînt date în tabelul 1.

Tabelul 1

Valorile constantelor M și q din ecuația (1), pentru soluțiile utilizate în experimentări

Soluția	M	q
Glicerină tehnică	$4{,}96060 \cdot 10^{-2}$	0,82807
CMC – 0,945 %	$5{,}17182 \cdot 10^{-4}$	2,15540
CMC – 1,24 %	$1{,}28542 \cdot 10^{-4}$	2,47780
CMC – 1,63 %	$5{,}5449 \cdot 10^{-5}$	2,63780

Numărul picăturilor de aceeași dimensiune raportat la unitatea de lățime a planului de curgere s-a utilizat la calcularea frecvenței acestora, f'. Numărul de picături pe unitatea de suprafață, N_A, s-a determinat prin numărarea picăturilor, la intervale egale de timp, de pe o suprafață de $0{,}2 \times 0{,}3$ m^2, proiectată de pe pelicula cinematografică.

---

[1]) Pentru prepararea soluțiilor s-a utilizat CMC cu gradul de substituție 0,57.

Pentru determinarea experimentală a repartiției statistice a parametrilor menționați s-au reprezentat histogramele, poligoanele de frecvență (punctat, pe aceeași reprezentare cu a histogramelor), și curbele frecvențelor cumulate (funcția de repartiție), utilizînd metodele descrise în literatura de specialitate [12], [13].

Lungimea intervalului de grupare, d, s-a calculat cu relația lui S t u r g e s [13]:

$$d = \frac{x_{max} - x_{min}}{1 + 3{,}232 \lg n}, \tag{2}$$

în care x_{max} și x_{min} reprezintă valorile extreme din selecția considerată, iar n este volumul selecției.

Valorile lui d, calculate cu relația (2), s-au ajustat astfel încît să rezulte un număr întreg de intervale de aceeași lungime. Pentru lățimea picăturilor, l, frecvența raportată la lățimea planului, f' și pentru numărul de picături de pe unitatea de suprafață, N_A, valorile lui d sînt prezentate în tabelul 2.

Pentru caracterizarea statistică a rezultatelor măsurătorilor experimentale s-au calculat și o serie de valori tipice de selecție care servesc la interpretarea calitativă a acestora. Astfel, s-au calculat pentru toate soluțiile și la toate debitele, media aritmetică de selecție, abaterea standard de selecție și coeficientul de variație.

Pentru un șir de valori, x_i, $(i = 1, \ldots, n)$, care formează o selecție, media s-a calculat cu relația:

$$\bar{x} = \sum_i f_i x_i, \tag{3}$$

în care:

$$f_i = \frac{n_i}{\sum_i n_i} = \frac{n_i}{n} \tag{4}$$

este frecvența relativă a valorii x_i, n_i—frecvența absolută a valorii x_i iar n—volumul selecției (numărul total de măsurători asupra variabilei x). Pentru calculul abaterii standard de selecție, s, s-a utilizat relația:

$$s = \sqrt{\frac{\sum_i (x_i - \bar{x})^2}{n}} \tag{5}$$

Deoarece abaterea standard se exprimă prin unitatea de măsură a mărimilor care alcătuiesc selecția, pentru a se aprecia mai corect gradul de împrăștiere a valorilor care alcătuiesc selecția se utilizează coeficientul de variație, C_v, dat de raportul dintre abaterea standard și media aritmetică:

$$C_v = \frac{s}{\bar{x}}. \tag{6}$$

Acesta indică fracțiunea din media aritmetică pe care o reprezintă abaterea standard. Valori mici ale coeficientului de variație indică o grupare avan-

Tabelul 2

Valorile intervalului de grupare, mediei aritmetice, abaterii standard și a coeficientului de variație

Parametrul aleator	Lichidul utilizat	$\mathcal{R}_e$	d	Media	Abaterea standard	Coeficientul de variație
l, [mm]	Glicerină tehnică	11,06 15,90 18,79	1,496 1,606 2,195	17,49 19,76 20,64	2,569 2,984 4,868	0,146 0,151 0,235
	CMC 0,945%	26,67 33,08 41,22	1,785 2,431 2,500	20,06 20,94 22,91	3,580 4,450 4,990	0,178 0,212 0,217
	CMC 1,24%	7,63 9,43 13,13	1,398 1,562 2,138	20,19 20,54 22,15	3,079 3,544 3,858	0,152 0,172 0,174
	CMC 1,63%	1,57 2,18 2,61	1,027 1,645 1,285	23,32 24,18 24,55	2,317 3,350 2,790	0,099 0,138 0,113
f', [s^{-1} m^{-1}]	Glicerină tehnică	11,06 15,90 18,79	2,823 3,052 2,416	5,975 6,311 6,442	4,432 4,660 3,609	0,741 0,738 0,560
	CMC 0,945%	26,67 33,08 41,22	1,507 2,838 1,811	4,008 4,183 4,581	2,265 2,892 2,550	0,565 0,691 0,556
	CMC 1,24%	7,63 9,43 13,13	0,708 0,974 1,531	2,384 2,892 2,983	1,163 1,227 1,172	0,487 0,424 0,392
	CMC 1,63%	1,57 2,18 2,61	0,502 0,939 1,219	1,877 1,949 2,325	0,749 1,132 1,368	0,399 0,580 0,588
N_A, [m^{-2}]	Glicerină tehnică	11,06 15,90 18,79	25,00 16,66 22,23	214,58 186,07 169,41	46,98 26,20 32,51	0,218 0,140 0,191
	CMC 0,945%	26,67 33,08 41,22	27,76 25,00 25,00	223,00 214,10 207,81	49,67 33,85 42,44	0,222 0,158 0,204
	CMC 1,24%	7,63 9,43 13,13	13,88 22,21 13,88	144,08 138,68 137,70	24,88 33,75 26,28	0,172 0,243 0,190
	CMC 1,63%	1,57 2,18 2,61	13,32 13,32 10,00	85,75 80,36 75,97	20,65 24,40 16,76	0,240 0,303 0,220

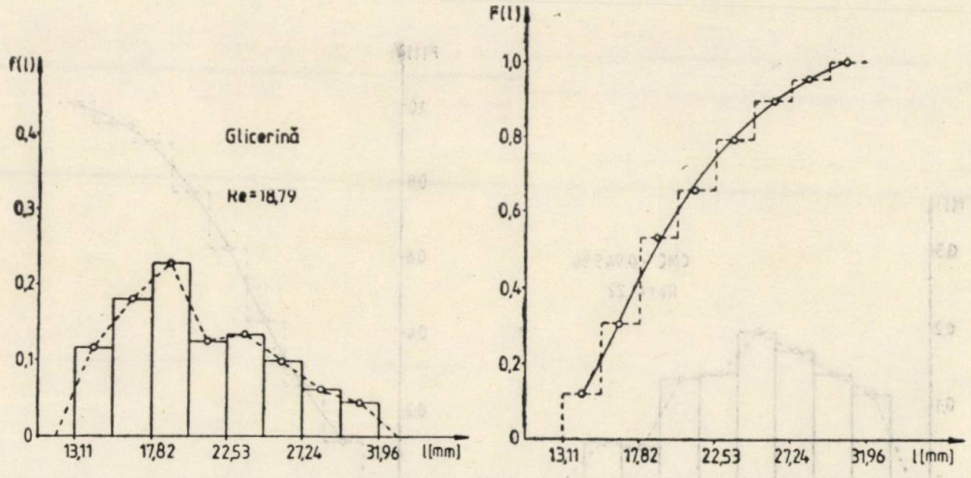

Fig. 1. — Repartiția lățimii picăturilor, pentru glicerină, la $\mathcal{R}_e = 18,79$.

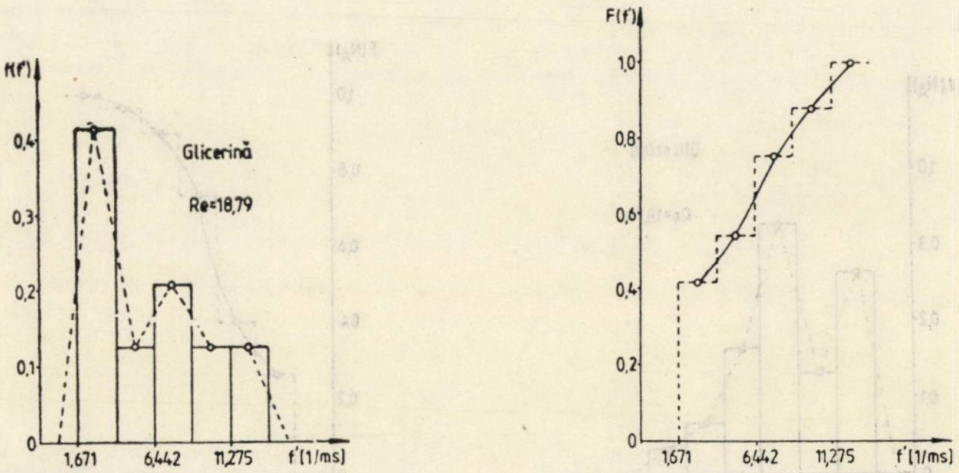

Fig. 2. — Repartiția frecvenței raportată la unitatea de lățime a planului de curgere, pentru glicerină, la $\mathcal{R}_e = 18,79$.

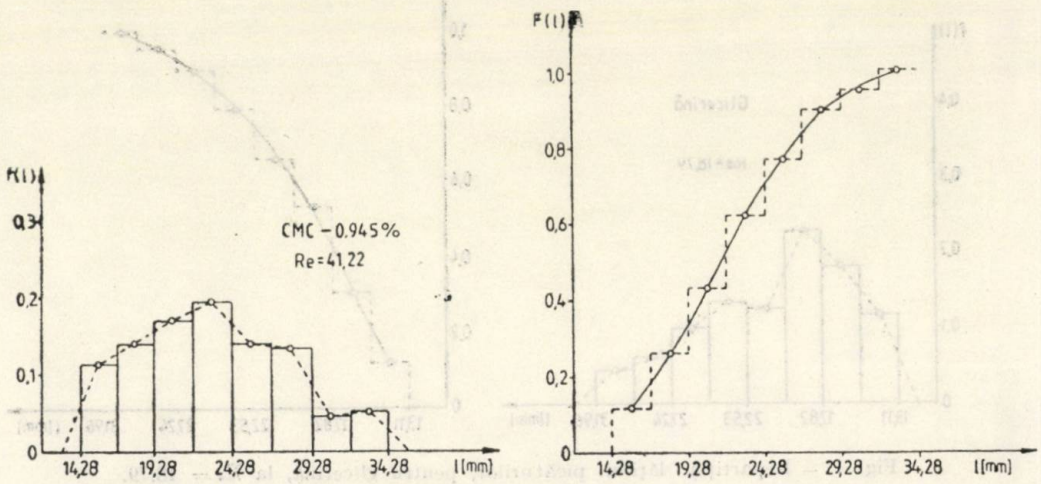

Fig. 3. — Repartiția numărului de picături de pe unitatea de suprafață, pentru glicerină, la $\mathcal{R}_e = 18,79$.

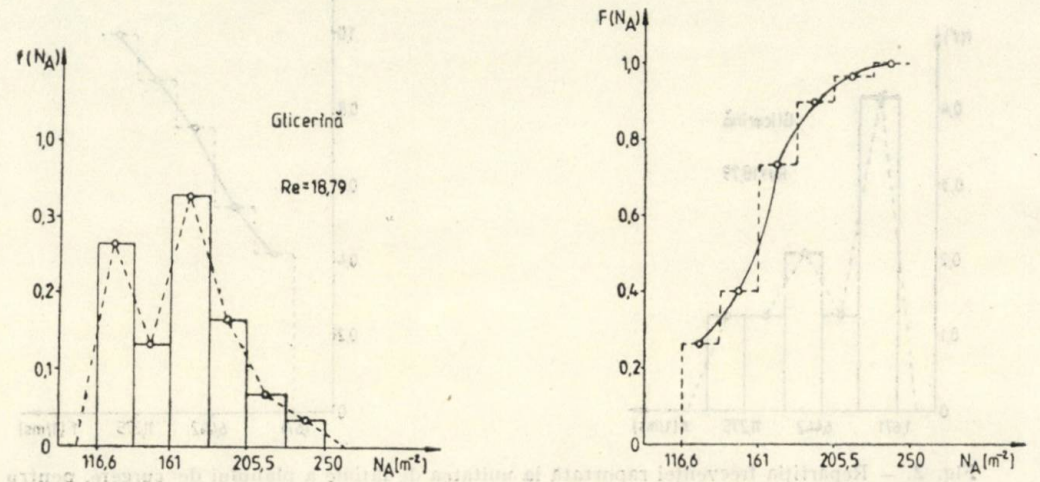

Fig. 4. — Repartiția lățimii picăturilor, pentru soluția CMC – 0,945%, la $\mathcal{R}_e = 41,22$.

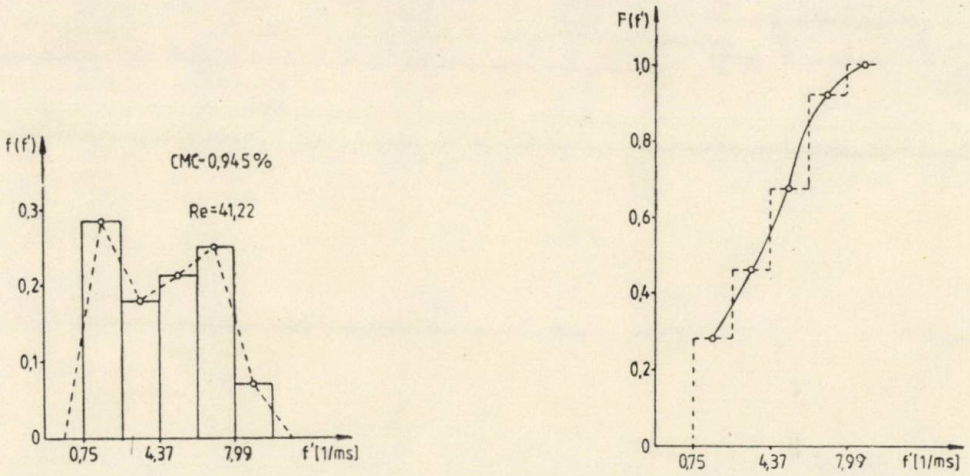

Fig. 5. — Repartiția frecvenței raportată la unitatea de lățime a planului de curgere, pentru soluția CMC—0,945%, la $\mathcal{R}_e = 41{,}22$.

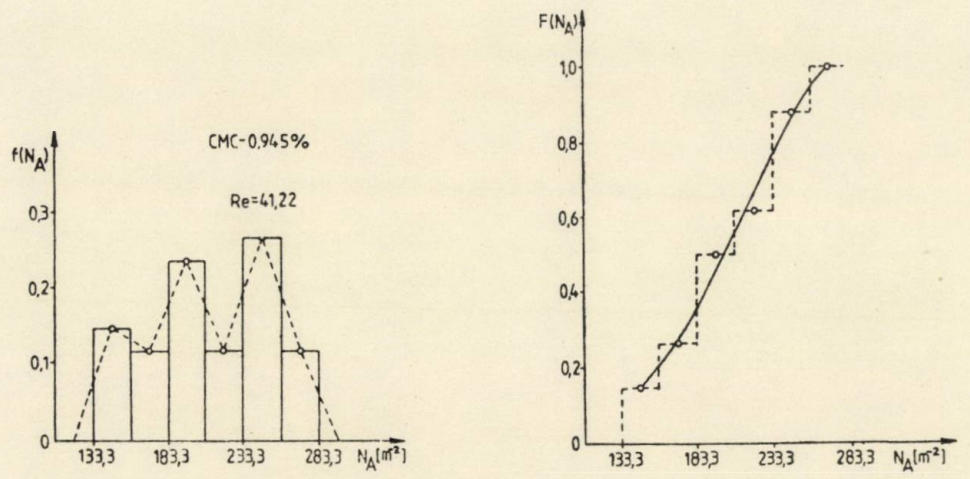

Fig. 6.—Repartiția numărului de picături de pe unitatea de suprafață, pentru soluția CMC—0,945%, la $\mathcal{R}_e = 41{,}22$.

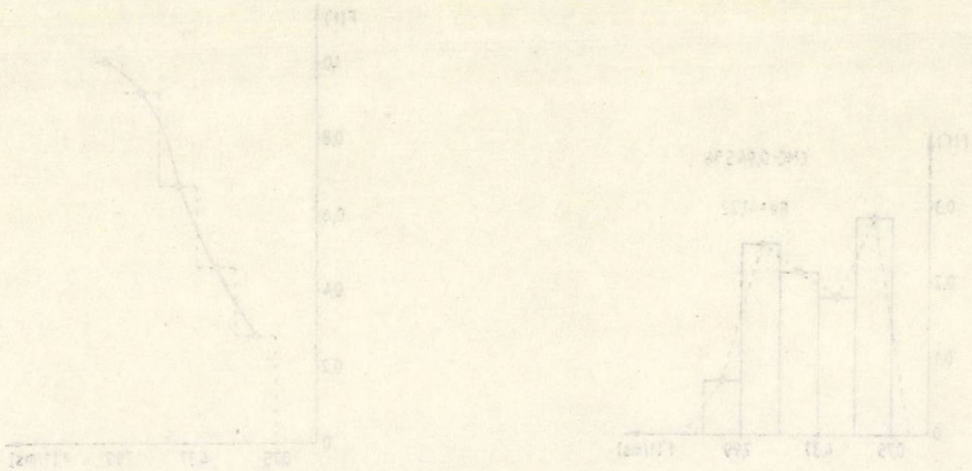

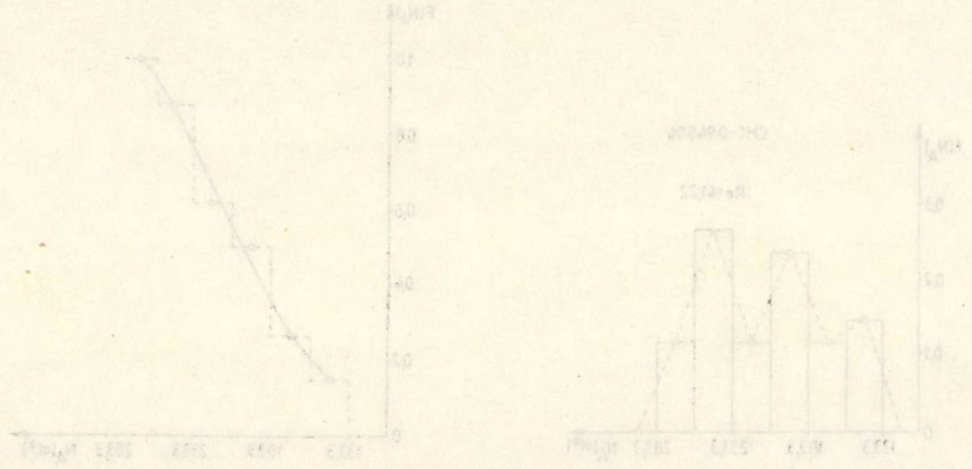

sată în jurul valorii medii (o dispersie redusă) iar valorile mari ale coeficientului de variație indică o împrăștiere avansată a datelor măsurate. Valorile mediilor, abaterilor standard și ale coeficientului de variație, pentru lățimea picăturilor, frecvența raportată la unitatea de lățime a planului și pentru numărul de picături de pe unitatea de suprafață, din zona cu valuri stabilizate, calculate cu relațiile (3)...(6), sînt prezentate în tabelul 2.

3. Interpretarea rezultatelor

Analizînd datele din tabelul 2 se poate constata că pentru o soluție dată, fără excepție, lățimea picăturilor și frecvența raportată la unitatea de lățime a planului, cresc cu creșterea criteriului R e y n o l d s, pe cînd numărul de picături de pe unitatea de suprafață scade ușor cu creșterea debitului. Pentru soluții diferite, dimensiunile picăturilor depind de consistență, lățimea lor fiind cu atît mai mare cu cît consistența lichidului este mai mare, deși diferențele dintre valorile medii nu variază între limite prea largi. Spre deosebire de lățimea picăturilor frecvența scade cu creșterea consistenței, diferența dintre valorile medii fiind mult mai mare decît în cazul lățimii. Numărul de picături de pe unitatea de suprafață, pentru o soluție de un anumit tip, scade cu creșterea debitului și cu creșterea consistenței lichidului. Diferențele dintre valorile medii ale numărului de picături pe unitatea de suprafață, pentru aceeași soluție, sînt relativ mici, dar diferă semnificativ în funcție de consistență.

Examinînd valorile coeficientului de variație se constată că lățimea picăturilor prezintă gruparea cea mai avansată în jurul valorii medii, urmată de numărul de picături de pe unitatea de suprafață. Valorile relativ mari ale coeficientului de variație pentru frecvență indică o împrăștiere apreciabilă în raport cu media.

Pentru soluțiile și pentru valorile criteriului R e y n o l d s din tabelul 2 s-au reprezentat histogramele, poligoanele de frecvență și curbele frecvențelor cumulate, pentru lățimea picăturilor, frecvența raportată la unitatea de lățime și pentru numărul de picături de pe unitatea de suprafață. O parte din aceste reprezentări sînt date în fig. 1...6[2]). S-a constatat că repartiția frecvențelor relative ale mărimilor l, f' și N_A este, în general, plurimodală, cel mai adesea bimodală sau trimodală și nu respectă nici una din repartițiile teoretice cunoscute în literatură. Acest fapt ar putea fi explicat prin aceea că limitele între care fluctuează mărimile aleatoare depind de fenomenele din zonele anterioare zonei de curgere cu valori stabilizate, care au un caracter întîmplător, nerespectînd o lege anume.

4. Concluzii

Pentru curgerea în zona cu valuri stabilizate s-au efectuat determinări experimentale referitoare la unii parametri ai curgerii care au caracter aleator. Folosind tehnica cinematografică s-a determinat experimental repartiția statistică a lățimii picăturilor, l, a frecvenței raportată la unitatea

[2]) Reprezentări identice s-au trasat pentru toate soluțiile și la toate debitele din tabelul 2, care nu sînt prezentate în lucrare din motive de spațiu. Concluziile însă s-au tras în urma analizării tuturor distribuțiilor determinate experimental.

de lățime a planului, f' și a numărului de picături pe unitatea de suprafață, N_A. În general, densitatea de repartiție a acestor variabile aleatoare are un caracter plurimodal, adesea bimodal sau trimodal. Pentru aceleași variabile aleatoare s-a calculat media aritmetică, abaterea standard și coeficientul de variație, pentru a se aprecia gradul de dispersare a valorilor selecției în jurul mediei aritmetice, constatîndu-se că cea mai mare împrăștiere o prezintă frecvențele iar cea mai bună grupare o prezintă lățimea picăturilor.

Primită la 4 mai 1982

Institutul politehnic, Iași,
Catedra de inginerie chimică

BIBLIOGRAFIE

1. Emert R. E., Pigford R. L., Chem. Eng. Prog., **50**, 84 (1957).
2. Jepsen J. C., Crosser D. K., Perry R. H., A. I. Ch. E. J., **12**, 186 (1966).
3. Oliver D. R., Atherinos T. E., Chem. Eng. Sci., **23**, 525 (1968).
4. Chand R., Rossen H. F., Ind. Eng. Chem., Fundam., **4**, 356 (1965).
5. Tudose R. Z., Năforniță C., Rev. Roum. Chim., **25**, 155 (1980).
6. Vitan F., Tudose R. Z., Bul. Inst. polit., Iași, **XXVIII (XXXIII)**, *1—4*, s. I, 75 (1982).
7. Tudose R. Z., Vitan F. Rev. de chimie, **37**, 132 (1986).
8. Капица П. Л., ЖЕТФ, **18**, 3 (1948).
9. Tudose R. Z., Zăinescu C., Rev. de chimie, **35**, 810 (1984).
10. Tudose R. Z., Vitan F., *Curgerea lichidelor în filme subțiri* (III), Rev. de chimie (sub tipar).
11. Tudose R. Z., Vitan F., *Curgerea lichidelor în filme subțiri* (IV). Rev. de chimie (sub tipar).
12. Ceaușescu D., *Utilizarea statisticii matematice în chimia analitică*. Ed. Tehn., Buc., 1982.
13. Tiron M., *Prelucrarea statistică și informațională a datelor de măsurare*. Ed. Tehn., Buc., 1977.

FLOW OF LIQUIDS IN THIN FILMS.

V. Aleatory parameters in zone with stabilized waves

(Summary)

Above a certain value of flow rate on the free surface of a falling film wave occurs whose configuration is modified along the flow plane. On this surface four distinct zones are evidenced namely : zone without waves, zone of wave inception, zone of wave stabilization and zone of flow with stabilized waves.

For the zone with stabilized waves a physical and mathematical model was derived and checked for newtonian fluids which was then extended and checked also for nonnewtonian fluids. A series of flow parameters necessary in the model of zone with stabilized waves have proved to exhibit an aleatory character. In the paper the statistical analysis of these parameters by means of experimental distributions and some typical selection values such : mean value, standard deviation and coefficient of variation is effectuated.

BULETINUL INSTITUTULUI POLITEHNIC DIN IAŞI
Tomul XXXI (XXX V) Fasc. 1—4, 1985
Secţia II
CHIMIE ŞI INGINERIE CHIMICĂ

RECENZII

BOOK REVIEWS РЕЦЕНЗИИ

* * * JOURNAL OF CONTROLLED RELEASE. Official Journal of the Controlled Release Society. Editors: Jorge Heller, Director, Polymer Sciences Department, S.R.I. International, Menlo Park. C.A. 94025, U.S.A.; Jan Feijen, Department of Chemical Technology, Twente University of Technology, 0.0. Box 217, A. E. Enschede, The Netherlands.

The Journal of Controlled Release is a new international journal dealing with the science and technology of the controlled release of active agents. The term „controlled release" is used in its broadest sense to include control over rate of release using — either singly or in combination — diffusion, chemical reactions, dissolution, osmosis or mechanical devices, as well as control over the site of action of the active agent using pro-drugs or carriers such as water-soluble polymers, microcapsules or liposomes.

Although the major emphasis of the journal is controlled release, relevant work dealing with toxicology, pharmaco-kinetics and biocompatibility is also included.

The journal is intended to serve a wide range of specialists and to bring together high quality papers dealing with various aspects of controlled release of therapeutic agents for human and animal use, as well as those dealing with insect and other pest management, fertilizers, weed control and marine antifouling applications.

In addition to original papers, technical reviews and short communications, the journal includes book reviews, reports of meetings, descriptions of new controlled release products, announcements pertaining to activities of the Controlled Release Society, and other announcements.

Severian Dumitriu

P. TRAMBOUZE, H. VAN LANDEGHEM, J. P. WAUQUIER, *Les réacteurs chimiques* (conception calcul, mise en oeuvre). Editions Technic — Paris, 1984, VIII + 652 pp.

Cet ouvrage comprend quatorze chapitres et quatre annexes. A la fin de chaque chapitre est insérée la nomenclature spéciale ainsi que la bibliographie.

Le premier chapitre (pages 9 à 57) est un *rappel des notions fondamentales* et des définitions concernant la stoéchiométrie, la thermodynamique chimique et la cinétique chimique formelle. Dans l'annexe de ce chapitre on traite plus en détail le comportement cinétique global des „groupements" de composés. C'est le cas particulièrement rencontré dans les processus pétrochimiques (reforming catalytique, cracking catalytique, hydro-cracking) où le nombre de réactifs et de produis peut être très élevé.

Dans le *deuxième chapitre* (pages 59 à 89), les réacteurs chimiques rencontrés en pratique *sont classifiés* selon deux critères : la nature des phases du milieu réactionnel (monophasiques et polyphasiques) et le mode d'opération. D'après ce dernier, les réacteurs peuvent être continus ou discontinus (avec la variante semi-continue). Les réacteurs continus, à leur tour, sont de trois types : tubulaires, parfaitement agités et étagés. Le réacteur étagé est un cas intermédiaire entre les deux premiers modèles idéaux ; il est constitué par une série de zônes parfaitement agitées. Les équations générales des bilans pour différents types de réactions idéalisés sont ensuite établies dans le cas où le milieu réactionnel est monophasique. Dans les deux derniers paragraphes de ce chapitre on traite de notions très importantes, concernant l'écoulement d'un fluide à travers un réacteur à savoir : la distribution des temps de séjour et micromélange.

Les trois types de réacteurs idéaux sont présentés dans les chapitres 3 à 5 en se limitant à des processus chimiques homogènes. On commence avec le plus simple type de réacteur que l'on puisse envisager pour réaliser un processus chimique : le *réacteur discontinu monophasique* (chapitre 3, pages 91 à 120). Les équations différentielles, décrivant le fonctionnement d'un tel réacteur sont intégrées analytiquement dans quelques cas simples, en supposant toujours le processus isotherme et isochore. Les auteurs utilisent, dans ce but, les avancements molaires

en tant que variables. Dans les systèmes complexes, les notions de *sélectivité* et de *rendement* jouent un rôle important. On indique, brièvement, la manière de calculer ces deux grandeurs dans deux cas : réactions jumelles et réactions consécutives.

Lorsque le processus est exothermique, un phénomène d'instabilité thermique peut apparaître dans un réacteur discontinu. Les auteurs présentent, d'une manière bien claire, comment ce phénomène peut apparaître, tout en indiquant les critères de stabilité thermique.

Les *réacteurs semi-continus* sont présentés comme une variante des réacteurs discontinus. Le cas le plus fréquent est celui où un réactif est injecté progressivement, surtout lorsque la réaction est fortement exothermique ou quand peut apparaître le problème de la sélectivité.

Le quatrième chapitre (pages 121 à 139) présente les réacteurs continus tubulaires. C'est le type de réacteur le plus simple que l'on puisse imaginer pour un processus continu. Les équations différentielles des bilans massiques et énergétiques sont, d'abord, établies pour le modèle idéal d'écoulement-piston qui est souvent qualifié de réacteur tubulaire idéalisé. L'influence du *rétromélange* est ensuite prise en considération, afin de délimiter le domaine d'applicabilité du modèle idéal.

Le chapitre 5 (pages 141 à 163) est consacré aux réacteurs continus parfaitement agités. On suppose qu'en tout point d'un tel type de réacteur la concentration et la température ont la même valeur. Par la suite, les équations des bilans sont les plus simples ; elles peuvent être intégrées pour des cas assez complexes. Les auteurs analysent, plus en détail, le fonctionnement autothermique d'un tel type de réacteur et les problèmes de stabilité qui se posent en pratique, dans ce cas. Le réacteur étagé est défini comme une association en série de plusieurs réacteurs parfaitement agités. Chaque étage de la cascade est traité comme un réacteur parfaitement agité.

Dans le *sixième chapitre* (pages 165 à 196) *on compare les trois types de réacteurs* idéaux afin de bien mettre en lumière leurs avantages et inconvénients respectifs. Le choix du réacteur à adopter pour réaliser un processus donné se fera, d'après les auteurs, sur la base des critères de sélection suivants : la capacité de production, les conditions opératoires (mode d'opération, les variables intensives P et T, le temps moyen de séjour), la conversion et la sélectivité. Dans le cas où le processus est assez simple (une seule relation stoéchiométrique) seules la capacité et la conversion seront fixées en tant qu'objectifs à atteindre ; le problème de la sélectivité ne se pose pas.

Le septième chapitre (pages 197 à 267) présente les caractères généraux des *réacteurs à deux phases fluides* (gaz — liquide et liquide — liquide). On commence par un rappel de la théorie du transfert de masse et du transfert de masse accompagné de réaction chimique. L'influence de la réaction chimique sur la vitesse d'absorption d'un gaz par un liquide est évaluée quantitativement à l'aide des grandeurs spécifiques, à savoir : nombre de Hatta, efficacité, facteur d'accélération. Le même problème est ensuite abordé d'une manière différente, en considérant la réaction chimique accompagnée de transfert de masse (cinétique apparente). Les méthodes de calcul des réacteurs à deux phases fluides sont ensuite presentées, dans les deux cas extrêmes (réaction lente et réaction rapide), pour chacun de ces trois types d'appareillage : réacteur discontinu, réacteur tubulaire, réacteur parfaitement agité.

Le *chapitre 8* (pages 269 à 319) rassemble les données expérimentales et les corrélations permettant le calcul complexe des réacteurs gaz — liquide. Un tableau final peut servir de base à un choix rationnel du contacteur gaz — liquide parmi les appareils suivants : colonnes à bulles, appareils à agitation mécanique, colonnes à plateaux, colonnes à garnissage, scrubbers.

Le *neuvième chapitre* (pages 321 à 356) présente les mêmes aspects pour les réacteurs liquide — liquide : colonnes à garnissage, colonnes avec agitateur rotatif, mélangeurs — décanteurs. Pour chacun de ces types on donne des informations concernant : l'hydrodynamique (rétention des phases, aire interfaciale, rétromélange), les coefficients de transfert et même des details technologiques.

Les chapitres 10 à 12 sont consacrés aux réacteurs mettant en jeu des catalyseurs solides.

Le dixième chapitre (pages 357 à 411) présente la théorie des processus catalytiques au niveau d'un grain poreux de catalyseur ainsi qu'au niveau de l'ensemble des grains, en finissant par les diverses techniques pour „contacter" les phases : lit fixe, lit mobile, agitation mécanique, lit fluidisé, lit entrainé.

Dans *le chapitre 11* (pages 413 à 469) sont examinés en détail les trois types de réacteurs catalytiques mettant en jeu une seule phase fluide : réacteurs à lit fixe, à lit mobile, à lit fluidisé.

Le chapitre 12 (pages 471 à 511), présente les mêmes aspects pour les réacteurs catalytiques triphasiques ; la colonne à bulles, la cuve agitée mécaniquement, le réacteur à lit fixe, le réacteur à lit fluidisé à trois phases.

Le chapitre 13 (pages 513 à 546) est consacré à l'examen des processus solide — fluide où le solide est un réactif. Les auteurs présentent, tout d'abord, les problèmes macrocinétiques

spécifiques en analysant le comportement d'une particule solide isolée en tant que microréacteur discontinu. Ils examinent, ensuite, les réacteurs utilisables pour effecteur les processus solide — fluide non-catalytiques : à lit fixe, à lit mobile (fours rotatifs, grilles transporteuses, hauts-fourneaux), à lit fluidisé.

Dans *le chapitre 14* (pages 547 à 576), l'aspect méthodologique de l'extrapolation d'un réacteur chimique est présenté à l'aide d'exemples concrets. On constate que l'élaboration d'un modèle mathématique représente la façon la plus efficace pour réussir une extrapolation.

Les quatre annexes donnent des corrélations et des données expérimentales très importantes, concernant : les techniques d'agitation et de mélange (A 1 — pages 577 à 605) ; les fluides de transfert thermique (A 2 — pages 607 à 610) ; les appareils à couche mince en tant que réacteurs chimiques (A 3 — pages 611 à 627) ; matériaux et techniques de construction des réacteurs chimiques (A 4 — pages 629 à 639).

Cet ouvrage s'adresse d'une part aux ingénieurs de conception (recherche et développement), de conduite des installations de production ou d'ingénierie et d'autre part, aux enseignants et étudiants en génie chimique. Il se distingue par sa présentation claire, sa documentation abondante en cas réels et sa facilité d'usage.

L'aspect pratique de ce livre découle, en grande partie, de l'expérience acquise par les auteurs au sein d'un groupe de travail a l'Institut Français du Pétrole (I.F.P.), où ils ont effectué des mises au point des procédés industriels de raffinage et de pétrochimie.

Ceci est à la fois un ouvrage de réflexion, un traité académique et le résultat des stages dans l'enseignement supérieur que les auteurs ont été invités à effectuer dans divestes institutions de France, Algérie, et Tunisie.

Ilie Siminiceanu

ATWOOD J. L., DAVIES J. E., MAC NICOL D. D., *Inclusion Compounds*. Vol. 1, 2, 3, Academic Press, Inc. (Harcourt Brace Jovanovich, Publishers), 1984.

Initiative of the editors to write a book concerning inclusion chemistry is a remarkable one. The book was written by a great group of authors from numerous countries, each of them being an expert with firsthand knowledge and information in the area, having own research too. For the first time, all scientific information published worldwide on the inclusion compounds is collected in one convenient reference source, that consists in three volume book of 420, 499 and 669 pages and 895, 1223 and 1449 references, respectively.

Volume 1, entitled *Structural Aspects of Inclusion Compounds Formed by Inorganic and Organometallic Hosts*, was structured in nine chapters.

The first chapter covers crystal chemistry embraces inclusion compounds, the spread of inclusion chemistry, present and prospective elaboration of inclusion structures.

The second chapter is devoted to the Hofmann-type and related inclusion compounds.

The third chapter deals with the structure and composition of the inclusion compounds formed by MX_2A_4 hosts, the role of steric effects in intramolecular (host) and intermolecular (guest — host) interactions in Werner type inclusion compounds und kinetics of the sorption — desorption processes.

The fourth chapter describes the inclusion compounds of diisothiocyanatotetrakis (α-arylalkyl-amine) nickel (II) complexes as regards their preparation and inclusion results, the driving forces in inclusion compound formation, influence of the optical isomerism of α-arylalkylamines and their applications.

The fifth chapter is dedicated to the hydrate inclusion compounds. The structural basis of the hydrate inclusion compounds formation, clathrate hydrate structures, per alkylonium salt hydrate structures, position of the anions, alkylamine hydrate structures and miscellaneous hydrate inclusion structures are given.

The sixth chapter presents the zeolite inclusion complexes. The intrazeolitic channels and cavities, distributions of guest molecules, a comparison between zeolitic sorption and clathration, metal — zeolite complexes, salt — zeolite complexes and molecule — zeolite complexes are reported.

The seventh chapter treats the intercalation compounds and the eighth chapter, cyclophosphazene inclusion compounds.

The nineth chapter covers the main aspects on liquid clathrates, i.e. definition of liquid clathrate behaviour, synthesis and structure of parent compounds, $M[Al_2R_6X]$, preparation and composition of liquid clathrates, liquid clathrates from parent compounds which do not contain aluminium alkyls and applications.

Volume 2, entitled *Structural Aspects of Inclusion Compounds Formed by Organic Host Lattices*, was structured in 11 chapters.

The first chapter is referring to the structure and design of the clathrates of hydroquinone, phenol, D i a n i n's compound and related systems.

The second chapter covers the inclusion compounds of urea, thiourea and selenourea and their industrial applications

The third chapter describes the main aspects of the inclusion compounds of perhydrotriphenylene, as regards their preparation, composition and structure and the phase diagrame of binary systems perhydrotriphenylene — guest.

The fourth chapter discusses the inclusion compounds of cyclotriveratrylene, trithiacyclotriveratrylene and oxocyclotriveratrylene.

The fifth chapter is devoted to the hexa-host analogy, hexa-hosts and related systems and design of hosts with trigonal symmetry.

The sixth chapter treats the inclusion compounds of the trianthranilides and the seventh chapter those of deoxycholeic acid.

The eighth chapter describes the structural aspects of cyclodextrins and their „channel type" and „cages type" inclusion complexes with numerous chemical compounds.

The nineth chapter deals with the complexes of crown ethers with molecular guests. The host — guest complexes of the macrocyclic 18 — crown — 6 system, the inclusion of alkylammonium guests within crown ether hosts, other types of complexes with monocyclic hosts and inclusion compounds of oper-chain polyether ligands are reported.

The tenth chapter is devoted to macrobicyclic ligands — cryptates, macrotricycles, macrotetracycles, mononuclear and dinuclear cryptates, functionalized macrocycles, anion complexation and cryptate applications and the 11th chapter deals mainly with inclusion compounds formed by trimesic acid, substituted methanes and ethanes, cyclophanes, 4,4′-dinitrobiphenyl etc.

Volume 3, entitled *Physical Properties and Applications*, was structured in 16 chapters.

The first chapter summarizes the theoretical and experimental methods on decomposition pressures of the inclusion compounds, enthalpies of clathration, heat capacity measurements and thermal anomalies of urea and thiourea inclusion compounds and β-quinol clathrates.

The second chapter is dedicated to the spectroscopic studies of inclusion compounds, such as infrared and R a m a n, inelastic neutron scattering, electron spin resonance, M ö s s b a u e r and photoelectron and high resolution solid state NMR.

The third chapter treats identification and characterization of clathrates by NMR, NQR and dielectric methods.

The fourth chapter presents the crystallographic studies of inclusion compounds such as experimental techniques, crystal packing, description of cavities, channels and layers.

The fifth chapter is dedicated to the host — guest molecule energy transfer processes.

The sixth chapter presents applications of inclusion compounds of W e r n e r type, urea, thiourea and cyclodextrins in chromatography and the seventh chapter the sorptive abilities of tetracyanocomplexes as stationary phases in gas chromatography.

The eighth chapter deals with uses of zeolites and crown ethers as hosts in isotopic fractionation and nineth chapter, enantiomeric selectivity of host lattices : cyclodextrins, deoxycholic acid, tri-*ortho*-thymotide, etc.

The tenth chapter describes the inclusion polymerization of some vinylic and dienic monomers in urea, thiourea and perhydrotriphenylene. Control phenomena at the molecular and supermolecular level, significance and prospects of the study of inclusion polymerization are reported.

The 11th chapter covers the industrial applications of cyclodextrins in foods, cosmetics and toiletry, in tabacco products, in pharmaceuticals, in analytical chemistry, in the chemical industry and agricultural applications.

The 12th chapter discusses cycloamyloses and their inclusion complexes and the 13th chapter the reactions of inclusion complexes formed by cyclodextrins and their derivatives.

The last three chapters, i.e. 14, 15 and 16, treats the enzyme models related to inclusion compounds, enzyme — substrate interactions, and cation transport in liquid membranes mediated by macrocyclic crown ether and cryptand compounds, respectively.

The book is written at a highly scientific level being particulary useful to the researchers working in the field of clathrate compounds and molecular inclusion phenomena. This book edited by J. L. A t w o o d, J. E. D a v i e s, D. D. M a c N i c o l, can undoubtedly be recommended as an invaluable tool in the work of a large circle of chemists.

C. Luca

Combinatul de Fibre Sintetice Săvinești produce și livrează :

- **Fire și fibre sintetice :**

— fibre acrilice Melană (R) ;
— fibre poliamidice Relon (R) ;
— fire poliamidice textile Relon (R) ;
— fire poliamidice covor Relontex (R) ;
— fire poliamidice tehnice și cord Relon (R) ;
— corzi perii.

- **Produse chimice :**

— caprolactamă ;
— acid adipic ;
— tetracloretan ;
— clorură de cianuril ;
— dibenzildiizocianat DBDI ;
— polietilenglicoladipat PEGA ;
— granule poliamidice pentru mase plastice ;
— bare și plăci poliamidice.

- **Utilaje și piese de schimb pentru industria de fibre sintetice :**

— linii complete de fabricare a firelor și fibrelor sintetice ;
— pompete de filare pentru fibre sintetice ;
— filiere pentru filare din topitură ;
— pompe de presiune pentru curățiri de vase în industria chimică ;
— mașini de bobinat fire ;
— mașini de sculuit ;
— fuse pentru mașini textile ;
— mașini de tăiat fibre ;
— diverse piese de schimb din industria de fibre chimice.

Producător : Combinatul de Fibre Sintetice, Săvinești, Piatra Neamț
Telex 025221-222 ; telegraf C.F.S. Săvinești

Exportatori :

— **Fire și fibre sintetice : ICE Danubiana, București,**
Spl. Independenței 202 A
Telex 11489 ; PO BOX 3915 DANAZ

— **Produse chimice : ICE Chimimportexport, București,**
Bd. Republicii 10
Telex 11184 ; PO BOX 1—74

— **Utilaje și piese de schimb : ICE Industrialexport, București,**
Str. Scaune 1—3
Telex 10052 ; PO BOX 768

Synthetic Fibers Factory, Săvinești produces and delivres :

- **Synthetic Yarns and Fibers :**

— Melana (R) acrylic fibers ;
— Relon (R) polyamidic fibers ;
— Relon (R) polyamidic textile yarns ;
— Relontex (R) carpets polyamidic yarns ;
— Polyamidic technical yarns and Relon (R) cord ;
— Brush strings.

- **Chemical Products :**

— Caprolactam ;
— Adipic acid ;
— Tetrachlorethane ;
— Cyanuril chloride ;
— Dibenzyldiisocyanate DBDI ;
— Polyethyleneglycoladipate PEGA ;
— Polyamidic grains for plastic materials ;
— Polyamidic rods and plats.

- **Implements and Spare Parts for Synthetic Fibers Industry :**

— Full operation lines for producing synthetic yarns and fibres ;
— Spinning pumps for synthetic fibers ;
— Dies for melt spinning ;
— Pressure pumps for vessel claning in chemical industry ;
— Warp winding machines ;
— Shuttle sprindles ;
— Fiber-cutting machines ;
— Different spare parts for chemical fibers industry.

Producer : Combinatul de Fibre Sintetice Săvinești, Piatra Neamț
Telex 025221-222 ; telegraph C.F.S. Săvinești.

Exporters :

— **Syntetic Yarns and Fibres : ICE Danubiana, București,**
Spl. Independenței 202 A
Telex 11489 ; PO BOX 3915 DANAZ

— **Chemical Products : ICE Chimimportexport, București**
Bd. Republicii 19
Telex 111184 ; PO BOX 1—74

— **Implements and Spare Parts : ICE Industrialexport, București,**
Str. Scaune 1—3
Telex 10052 ; PO BOX 768

L'Usine de Fibres Synthétiques, Săvinești, produit et fournit :

- **Fils et fibres synthétiques :**

— fibres acryliques Melana (R) ;
— fibres polyamidiques Relon (R) ;
— fils textiles polyamidiques Relon (R) ;
— fils polyamidiques tapis Relontex (R) ;
— fils polyamidiques techniques et corde Relon (R).

- **Produits chimiques ;**

— caprolactame ;
— acide adipique ;
— éthane tétrachlorure ;
— chlorure de cyanurile ;
— dibenzylediisocyanate DBDI ;
— polyéthylèneglycoleadipate PEGA ;
— granules polyamidiques pour matériaux plastiques ;
— barres et plaques polyamidiques.

- **Outillages et pièces de réchange pour l'industrie des fibres synthétiques :**

— lignes technologiques pour la fabrication de fibres et fils synthétiques ;
— pompes de filage pour fibres synthétiques ;
— filières pour filage des mélanges coulées ;
— pompes à pression pour nétoyage de l'outillage de l'industrie chimique ;
— machines à bobiner ;
— brochettes de navette ;
— machines à trancher des fibres ;
— différentes pièces de réchange pour l'industrie des fibres chimiques

Producteur : Combinatul de Fibre Sintetice, Săvinești, Piatra Neamț
Telex 025221-222 ; télégraphe C.F.S. Săvinești

Exportateurs :

— **Fibres et fils synthétiques : ICE Danubiana, București,**
Spl. Independenței 202 A
Telex 11489 ; PO BOX 3915 DANAZ

— **Produits chimiques : ICE Chimimportexport, București,**
Bd. Republicii 10
Telex 11184 ; PO BOX 1—74

— **Outillages et pièces de rechange : ICE Industrialexport, București,**
Str. Scaune 1—3
Telex 10052 ; PO BOX 768

Moldoplast

The „MOLDOPLAST" factory from Jassy offers to his customers processed products from polyvinyl cloride, polyethylene, polystyrene, ABS, polypropylene, technopolymers, in a large variety of assortments and dimensions :

Products from :

PVC	*Polyethylene*	*Polypropylene*	*ABS and polystyrene*	*Technopolymers*
● carpets	● films and sheets	● fabric sacks	● plates	● tubes
● plates		● threads	● profiles	● profiles
● granules	● articles from films	● plates		
● tubes	● havy sacks	● granules		
● pipes	● tubes			
● bars	● containers			
● electrodes	● plates			
● profiles	● high pressure hoses			
● films				

New products :

- **Granules from PVC in TH, THA and F conditions**
- **Aspiration pipes with insertion**
- **Thermocontractible profiles**
- **Pipes for irrigation purposes**
- **Films for hydroisolation purposes**
- **Modified rigid films**
- **Coextruded bags**
- **Bags with thickened handle**
- **Marketing bag of undervest type in two colors**
- **Films and fabrics from EVA**
- **Boxes for bread, vegetables and fruits**
- **High pressure pipes**
- **Pieces for cars**
- **Plates from polypropilene**
- **Fabric sacks from polypropilene**
- **Stretchet threads from polypropilene**

Moldoplast

Учреждение ,,Молдопласт", г. Яссы, предлагает своим заказникам готовые изделия из полихлорвинила, полиэтилена, полистирола, АБС, полипропилена, технополимеров в широкой гамме асортиментов и типоизмерений :

Изделия реализованы из :

ПВЦ	*Полиэтилен*	*Пропилен*	*АБС и полистирол*	*Технополимеры*
• ковёры	• фольги и фильмы	• метки	• плиты	• трубы
• плиты	• изготовления	• нати	• профили	• профили
• зерна	из фольг	• плиты		
• трубы	• мешки	• зерна		
• трубки	• трубы			
	• плиты			
• пластины	• рукавы			
• шины	• прочные на высокие			
• электроды	• давления			
• фольги				
• профили				

Новые изделия :

- зерна РВЦ в режиме ТХ; ТХА и Ф
- трубы-аспираторы
- профили термопроводимые
- трубки для орошения
- фольги для гидроизолирования
- твёрдые фольги
- мешки
- сетки
- фольги и конфекции
- прочные трубам
- нити из пропилена

Tiparul executat sub cd. 281 la
Întreprinderea Poligrafică Iași.
Str. 7 Noiembrie nr. 49.

Tiparul executat sub cd. 281 la
Întreprinderea Poligrafică Iași.
Str. 7 Noiembrie nr. 43.

1997 FEB 2

40822

F 1503/2 L: 040723

BULETINUL INSTITUTULUI POLITEHNIC DIN IAȘI

Tomul XXXI (XXXV)

Fasc. supl.

Secţia II

CHIMIE ŞI INGÌNERIE CHIMICĂ

1985

BULETINUL INSTITUTULUI POLITEHNIC DIN IAŞI

Tomul XXXI (XXXV)

Fasc. supl.

Secţia II

CHIMIE ŞI INGINERIE CHIMICĂ

1985

COLEGIUL DE REDACŢIE

Prof. dr. CAMELUŢA BELDIE (preşedinte)
Prof. dr. ing. ADRIAN RADU
Prof. dr. ing. M. GAFIŢANU
Conf. dr. ing. D. LIUŢE
Prof. dr. doc. D. MANGERON
Prof. dr. ing. GH. MAXIM
Acad. prof. dr. doc. CRISTOFOR SIMIONESCU
Prof. dr. doc. GH. CHIRIŢĂ
Prof. dr. doc. VALERIU BLIDARU

COMITETUL DE REDACŢIE
AL SECŢIEI
II. CHIMIE ŞI INGINERIE CHIMICĂ

Prof. dr. doc. RADU TUDOSE
Prof. dr. doc. ANGELA POPA
Conf. dr. ing. I. ROŞCA
Conf. dr. ing. SPIRIDON OPREA

REDACŢIA

Prof. dr. doc.
DUMITRU MANGERON
(redactor responsabil)
Prof. dr. ing. HUGO ROSMAN
(secretar)
Conf. dr. ing.
VICTOR BULACOVSCHI
(redactor)
ECATERINA IRIMIEA
(tehnoredactor)

BULETINUL INSTITUTULUI POLITEHNIC DIN IAŞI
BULLETIN OF THE POLYTECHNIC INSTITUTE OF JASSY
ИЗВЕСТИЯ ЯССКОГО ПОЛИТЕХНИЧЕСКОГО ИНСТИТУТА
Tom XXXI (XXXV), Fasc. supl. 1985

Secţia II

CHIMIE ŞI INGINERIE CHIMICĂ

SUMAR

Pag.

AL. DUCA, M. GĂBURICI, AL. CECAL şi M. SURPĂŢEANU, Studiul unor complecşi aminici ai cobaltului prin voltametrie anodică (engl., rez. rom.) 9

N. CALU, A. BOLD, O. VICOL, E. SAVIUC, L. BOSNEA, I. BERDAN şi I. SANDU, Metode de caracterizare fizico-chimică a coloranţilor în amestec (franc., rez. rom.) 15

C. BELDIE, A. ONU, N. AELENEI, GH. NEMŢOI, AL. RADOVICI şi AL. SAVIN, Relaţia vîscozitate—masă moleculară pentru poli(etilentereftalat) modificat cu 1,2-propandiol (engl., rez. rom.) 23

I. ROŞCA, E. ŞTEFANCU şi M. PALAMARU, Compuşi de coordinaţie ai La (III) şi Ce (IV) cu acidul dibutilfosfinic (engl., rez. rom.) 29

E. POPOVICI, M. CRUCEANU, A. POPA, A. VASILE şi M. ALEXANDROAEI, Zeoliţi sintetici pentru condiţionarea detergenţilor (I) (engl., rez. rom.) . . 35

AL. SZÉP, L. IFRIM, C. LEONTE şi C. CALISTRU, Studiul procesului de descompunere a carbonatului de calciu cu clorură de amoniu solidă (engl., rez. rom.) 41

M. PETROVANU, GH. SURPĂŢEANU, M. CONSTANTINESCU şi A. LABLACHE-COMBIER, Izomerii *E* şi *Z* ai ilurilor de 1.2-4H triazol (franc., rez. rom.) 47

GH. MIHĂILĂ, C. CIUGUREANU, N. BÎLBĂ, P. ONU, C. LUCA şi N. NAUM, Esteri şi eteri ai amidonului cu proprietăţi aglutinate (engl., rez. rom.) . . . 53

C. VASILIU-OPREA, M. POPA, AL. CONSTANTINESCU şi A. IOANID, Caracterul treptiform al procesului de rupere a polimerilor în condiţiile fluajului la tracţiune (germ., rez. rom.) 59

N. ASANDEI, M. NICU, M. RUSU, S. PETROVAN, V. NICU şi M. LUNGU, Copolimeri (VIII) (engl., rez. rom.) 65

N. FOCA, V. GORDUZA şi L. WAGNER, Complecşi ai 5-amino-benzimidazolonei-2 cu unii cationi ai metalelor tranziţionale (engl., rez. rom.) . . . 73

I.I. NEGULESCU, A.A. POPA şi C. MIHĂILESCU, Polimerizarea cationică a 4-vinil-1-ciclohexenei (engl., rez. rom.) 79

C. VASILE, FL. POPESCU, O. PETREUȘ, M. SABLIOVSCHI, A. AIRINEI și I. AGHERGHINEI, Influența ignifuganților asupra comportării poliolefinelor la temperaturi ridicate (engl., rez. rom.) 87

I. DIACONU și C. CHELARU, Sinteza și proprietățile unor noi copolimeri acrilici (I) (engl., rez. rom.) 91

S. OPREA, E. DUMITRIU și V. HULEA, Reactivitatea monomerilor acrilici (XII) (engl., rez. rom.) 101

M. DUMITRIU, M. PĂSTRĂVANU și T. LIXANDRU, Sinteza și caracterizarea unor noi poliazometine (II) (engl., rez. rom.) 105

V. BULACOVSCHI, M. GROVU-IVĂNOIU, M. DĂRÂNGĂ și S. DUMITRESCU, Polimerizarea 3-metilpent-1-in 3-olului catalizată de $PdCl_2$ și complecșii acesteia (engl., rez. rom.) 111

S. IOAN, C. SAVA și B.C. SIMIONESCU, Proprietățile soluțiilor de polimeri cu mase moleculare foarte mari (9) (engl., rez. rom.) 117

M. GRIGORAȘ, G. ONOFREI, E. BÎCU și I. RABIA, Tranziții conformaționale în tribloccopolimeri de tip *ABA* (franc., rez. rom.) 123

V. BĂRBOIU, G.E. GRIGORIU, E. RUSU, T. MARCU și E. BURUIANĂ, Proces de fotoreticulare în filme solide (I) (engl., rez. rom.) 129

R.Z. TUDOSE, E. MERICĂ și ȘT. UNGUREANU, Studiul transferului de masă la curgerea în filme subțiri a suspensiilor (engl., rez. rom.) 135

BULETINUL INSTITUTULUI POLITEHNIC DIN IAŞI
BULLETIN OF THE POLYTECHNIC INSTITUTE OF JASSY
ИЗВЕСТИЯ ЯССКОГО ПОЛИТЕХНИЧЕСКОГО ИНСТИТУТА

Том XXXI (XXXV), Supl. Fasc. 1985

Section II

CHEMISTRY and CHEMICAL ENGINEERING

CONTENTS

Pp.

AL. DUCA, M. GĂBURICI, AL. CECAL and M. SURPĂŢEANU, The Study of some Complex Amines of Cobalt by Anodic Stripping Voltammetry (English, Romanian summary) 9

N. CALU, A. BOLD, O. VICOL, E. SAVIUC, L. BOSNEA, I. BERDAN et I. SANDU, Méthodes pour la caractérisation physico-chimique des mélanges de colorants (French, Romanian summary) 15

C. BELDIE, A. ONU, N. AELENEI, GH. NEMŢOI, AL. RADOVICI and AL. SAVIN, Viscosity—Molecular Weight Relationship for Poly(ethyleneterephtalate) Modified with 1,2-Propanediol (English, Romanian summary) . . 23

I. ROŞCA, E. ŞTEFANCU and M. PALAMARU, Complexes of La (III) and Ce (IV) with Dibutylphosphinic Acid (English, Romanian summary) 29

E. POPOVICI, M. CRUCEANU, A. POPA, A. VASILE and M. ALEXANDROAEI, Synthetic Zeolites for Detergents Conditioning (I) (English, Romanian summary) 35

AL. SZÉP, L. IFRIM, C. LEONTE and C. CALISTRU, Study of the Calcium Carbonate Decomposition Process with Solid Ammonium Chloride (English, Romanian summary) 41

M. PETROVANU, GH. SURPĂŢEANU, M. CONSTANTINESCU et A. LABLACHE COMBIER, Isomères *E* et *Z* d'ylures de 1.2-4H triazolum (French, Romanian summary) 47

GH. MIHĂILĂ, C. CIUGUREANU, N. BÎLBĂ, P. ONU, C. LUCA and N. NAUM, Starch Esters and Ethers as Thickeners in Textile Printing (English, Romanian summary) 53

C. VASILIU-OPREA, M. POPA, AL. CONSTANTINESCU und A. IOANID, Der stufenweise Charakter des Bruchprozesses bei Polymeren durch Zugkraft unter Kriechbedingungen (German, Romanian summary) 59

N. ASANDEI, M. NICU, M. RUSU, S. PETROVAN, V. NICU and M. LUNGU, Copolymers (VIII) (English, Romanian, summary) 65

N. FOCA, V. GORDUZA and L. WAGNER, Complex Compounds of 5-Aminobenzimidazolone-2 with certain Cations of Transitional Metals (English, Romanian summary) 73

I.I. NEGULESCU, A.A. POPA and C. MIHĂILESCU, Cationic Polymerization of 4-Vinil-1-cyclohexene (English, Romanian summary) · · · · · · · · 79

I. DIACONU and C. CHELARU, Synthesis and Properties of certain New Acrylic Copolymers (I) (English, Romanian summary) · · · · · · · · · · · · 87

C. VASILE, FL. POPESCU, O. PETREUȘ, M. SABLIOVSCHI, A. AIRINEI and I. AGHERGHINEI, Influence of Flame-retardants on the Behaviour of Polyolefines at high Temperatures (English, Romanian summary) · · 91

S. OPREA, E. DUMITRIU and V. HULEA, Reactivity of Acrylic Monomers (XII) (English, Romanian summary) · 101

M. DUMITRIU, M. PĂSTRĂVANU and T. LIXANDRU, Synthesis and Properties of new Polyazomethines (II) (English, Romanian summary) · · · · · · 105

V. BULACOVSCHI, M. GROVU-IVĂNOIU, M. DĂRÂNGĂ and S. DUMITRESCU, Polymerization of 3-Methylpent-1-yn-3-ol by $PdCl_2$ and its Tryphenylphosphine Complexes as Catalysts (English, Romanian summary) · 111

S. IOAN, C. SAVA and B.C. SIMIONESCU, Solution Properties of Ultrahigh Molecular Weight Polymers (9) (English, Romanian summary) · · · · 117

M. GRIGORAȘ, G. ONOFREI, E. BÎCU et I. RABIA, Transitions Conformationnelles des tribloccopolymères du type *ABA* (French, Romanian summary) 123

V. BĂRBOIU, G.E. GRIGORIU, E. RUSU, T. MARCU and E. BURUIANĂ, Photocrosslinking Processes in Solid Films (I) (English, Romanian summary) · 129

R.Z. TUDOSE, E. MERICĂ and ȘT. UNGUREANU, Mass Transfer during Thin Film Flow of Suspensions (English, Romanian summary) · · · · · · · · 135

BULETINUL INSTITUTULUI POLITEHNIC DIN IAŞI
BULLETIN OF THE POLYTECHNIC INSTITUTE OF JASSY
ИЗВЕСТИЯ ЯССКОГО ПОЛИТЕХНИЧЕСКОГО ИНСТИТУТА
Том XXXI (XXXV), Доп. вып. 1985

Секция II

ХИМИЯ И ХИМИЧЕСКАЯ ПРОМЫШЛЕНОСТЬ

СОДЕРЖАНИЕ

Стр.

АЛ. ДУКА, М. ГЭБУРИЧ, АЛ. ЧЕКАЛ и М. СУРПЭЦЯНИУ, Поведение некоторых комплексных амин кобальта методом инверсионной вольтаметрии (англ., рез. рум.) 9

Н. КАЛУ, А. БОЛД, О. ВИКОЛ, Е. САВИУК, Л. БОСНЯ, И. БЕРДАН и И. САНДУ, Методы физико-химического характеризования смешаных красителей (франц., рез. рум.) 15

К. БЕЛДИЕ. А. ОНУ, Н. АЕЛЕНЕЙ, Г. НЕМЦОЙ, АЛ. РАДОВИЧ и АЛ. САВИИ, Отношение вязкость—молекулярную массу для модифицированного поли(этилентерефталала) 1, 2-пропандиолом (англ., рез. рум.) 23

И. РОШКА, Е. ШТЕФАНКУ и М. ПАЛАМАРУ, Координационные La (III) и Ce (IV) дибутилфосфиновой кислотой (англ., рез. рум.) 29

Е. ПОПОВИЧ, М. КРУЧЯНУ, А. ПОПА, А. ВАСИЛЕ и М. АЛЕКСАНДРОАЕЙ, Синтетический цеолиты для моющес вещество обусловленные (I) (англ., рез. рум.) 35

АЛ. СЕП, Л. ИФРИМ, К. ЛЕОНТЕ и К. КАЛИСТРУ, Исследование процесса разложения карбоната калция с хлористым аммонием (англ., рез. рум.) 41

М. ПЕТРОВАНУ, Г. СУРПЭЦЯНУ, М. КОНСТАНТИНЕСКУ и А. Лаблаш-КОМБИЕ, Изомеры *E* и *Z* 1-2-4Н триазол илуридов (франц., рез. рум.) 47

Г. МИХЭИЛЭ, К. ЧУГУРЯНУ, Н. БЫЛБЭ, П. ОНУ, К. ЛУКА и Н. НАУМ, Эстеры и эфиры крахмала сгустители в текстильной набивке (англ., рез. рум.) 53

К. ВАСИЛИУ-ОПРЯ, М. ПОПА. АЛ. КОНСТАНТИНЕСКУ и А. ИОАНИД. Ступенчатный характер преломления полимеров в условиях рэстяжения (нем., рез. рум.) 59

Н. АСАНДЕЙ, М. ИНКУ, М. РУСУ, С. ПЕТРОВАН, В. НИКУ и М. ЛУНГУ, Сополимеры (VIII) (англ., рез. рум.) 65

Н. ФОКА, В. ГОРДУЗА и Л. ВАГНЕР, Комплексы 5-амино бензимидазолоны-2 с катионов переходных металлов (англ. рез. рум.) . . . 73

И.И. НЕГУЛЕСКУ, А.А. ПОПА и К. МИХЭИЛЕСКУ, Катионная полимеризация 4-винил-1-циклогексана (англ., рез. рум.) 79
И. ДИАКОНУ и К. КЕЛАРУ, Синтезис и свойства новых акриловых сополимеров (I) (анлг., рез. рум.) 87
К. ВАСИЛЕ, ФЛ. ПОПЕСКУ, О. ПЕТРЕУШ. М. САБЛИОВСКИЙ, А. АЙРИНЕЙ и И. АГЕРГИНЕЙ, Влияние затушителей на свойствах полиолефинов в переделах высоких температур (англ. рез. рум.) 91
С. ОПРЯ, Е. ДУМИТРИУ и В НУЛЯ, Реактивность акриловых мономеров (XII) (англ., рез. рум.) 101
М. ДУМИТРИУ, М. ПЭСТРЭВАНУ и Т. ЛИКСАНДРУ, Синтез и характеризование полиазометин (II) (англ., рез. рум.) 105
В. БУЛАКОВСКИЙ, М. ГРОВУ-ИВЭНОЮ, М. ДЭРЫНГЭ, С. ДУМИТРЕСКУ, Полимеризация 3-метилпент-1-ин-3-ола в присуствии $PdCl_2$ и его комплексов с трифенилфосфином (англ., рез. рум.) . 111
С. ИОАН, К. САВА и Б. К. СИМИОНЕСКУ, Свойства растворов полимеров с очень болшие молекулярные веса (9) (англ., рез. рум.) . . 117
М. ГРИГОРАШ, Г. ОНОФРЕЙ, Е. БЫКУ и И. РАБИА, Конформационные переходы в триблоксополимеры типа *ABA* (франц., рез рум.) 123
В. БЭРБОЙ, Г.Е. ГРИГОРИУ, Е. РУСУ, Т. МАРКУ и Е. БУРУИАНЭ, Фотостивающие процессы в твердых плёнкак (I) (англ., рез. рум.) 129
Р.З. ТУДОСЕ, Е. МЕРИКЭ и ШТ. УНГУРЯНУ, Исследование масс передачи в течение суспензий в тонких фильмах (англ., рез. рум.) 135

BULETINUL INSTITUTULUI POLITEHNIC DIN IAȘI
Tomul XXXI (XXXV), Fasc. supl., 1985
Secția II
CHIMIE ȘI INGINERIE CHIMICĂ

D.C. 546.73 ; 537.741.3

THE STUDY OF SOME COMPLEX AMINES OF COBALT BY ANODIC STRIPPING VOLTAMMETRY

BY

AL. DUCA, MARIA GĂBURICI, AL. CECAL and MIOARA SURPĂȚEANU

1. Introduction

Anodic stripping voltammetric technique has been little used for the determination of low contents of cobalt, firstly, because the anodic stripping peaks are not well reproducible and secondly, because incomplet data are reported in literature as regards the products obtained by cobalt reduction on mercury.

The investigation of the mechanism and kinetics of Co (II) reduction is rather difficult due to the low solubility of this metal in mercury. Similar to all metals having low solubility in mercury, cobalt has the tendency to form mercuric compounds [1] :

$$Co^{2+} + 2e^- \rightleftharpoons Co(Hg),\ Co(Hg) \rightarrow CoHg_x,\ CoHg_x \rightarrow Co(Hg) \rightarrow Co_2Hg_x.$$

The first reaction is reversible, the latest two wich lead to binary or higher order compounds are not reversible.

Ivanov and Yofa [2] have indicated that dispersed cobalt is formed on mercury electrode, the process being dependent on voltage.

Perone and Gutknecht [3] studied the electroreduction of Co (II) in thiocyanate solutions and suggested the amalgamation of reduced cobalt at pre-electrolysis voltage of $-1{,}45$ V.

Janiszewska and Galus [4] have been found that the reduction of Co (II) on hanging mercury drop electrodes with initially deposited metallic cobalt proceeds faster than on pure mercury.

This paper deals with the influence of experimental parameters on voltammetric behaviour of low amounts of cobalt, as well as with the $[Co(NH_3)_6]^{3+}$, $[Co(en)_3]^{3+}$ (en-ethylene diamine) complexes. Ammonia buffer, Na_2SO_4, KSCN and NH_4SCN were employed as supporting electrolytes.

2. Experimental

The experiments were carried out using a mercury film stationary electrode, obtained by electrolytic deposition from a solution of $Hg(NO_3)_2$ [5].

The possibility of reproducing of the same surface depends on the obtaining of homogeneous mercury thin films. Since the width of the anodic curves depends on the thickness of the mercury film, it must be rigorously standardised in order to get some sharp and easy separable peaks. All potential measurements have been made using a saturated calomel electrode. The recording of anodic stripping curves has been carried out on the LP-60 and OH-102 polarographs. The solutions were prepared using tridistilled water, carrying out a rigorous control of supporting electrolytes.

3. Results and Discussion

3.1. The Behaviour of Co^{2+}

In order to establish the optimum conditions for the determination of low contents of cobalt, the influence of voltage, preelectrolysis time, nature and concentration of supporting electrolyte have been investigated.

The optimum voltage according to experimental data is of −1.2 V (Fig. 1). At this pre-electrolysis voltage the dependence of the anodic stripping peak on Co^{2+} concentration in solution has been studied. In Fig. 2, etalonated curves for Co^{2+} in the concentration range of 5×10^{-8} to 10^{-6} M in several supporting electrolytes are represented.

For concentrations higher than 10^{-5} M, even for low pre-electrolysis times, the anodic wave is de-doubled.

There is a weak difference as regards the behaviour of Co^{2+} in both KSCN and NH_4SCN solutions 0.1 M as supporting electrolytes. The disadvantage of the latter consists in fact that it pemits the degradation of the electrode surface in a short time. This fact was established experimentally, using the same electrode for several series of determinations, without its surface area regeneration. Between experiments, the electrode was kept in tridistilled water.

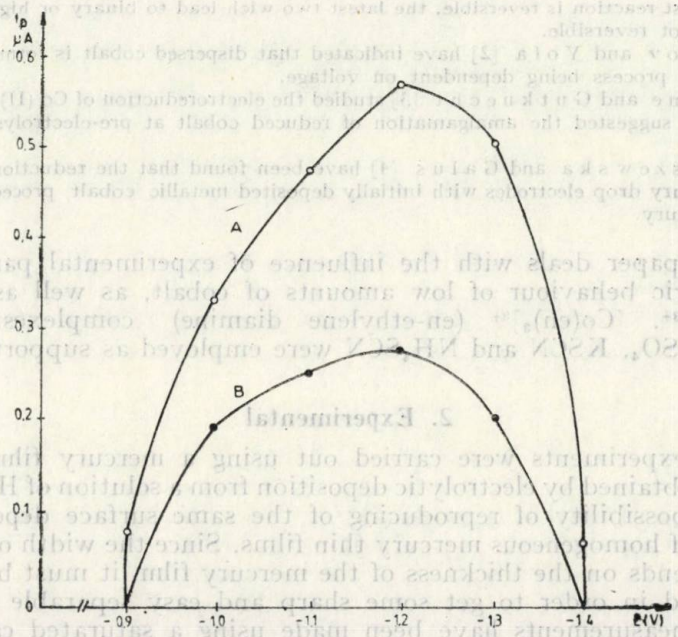

Fig. 1. — Influence of the pre-electrolysis potential over the anodic stripping peak height of Co^{2+} ($t_e=3$ min ; supporting electrolyte : KSCN 0.1 M ; $A-c=5\times10^{-7}$ M ; $B-c=2.5\times10^{-7}$ M.

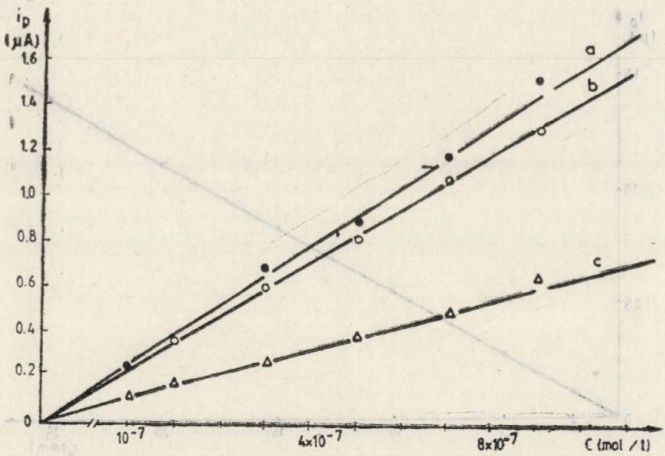

Fig. 2. — The calibration curves for determination of Co^{2+} in the concentration range $10^{-7}...10^{-6}$ M (a — KSCN 0.1 M ; b — NH_4SCN 0.1 M ; c — $NH_4Cl + NH_4OH$ 0.1 M ; $E_e = -1.2$ V, $t = 2$ min.).

The verification of the electrode surface area reproductibility was proved in the same solution for several days, as it can be seen in Table 1.

Table 1

The Reproductibility of the Electrode Surface Area against the Nature of the Supporting Electrolyte

Working time	Anodic stripping peak, h, [mm]		
	KSCN 0.1 M	NH_4SCN 0.1 M	Ammonia buffer
Fresh surface	41.5	39.2	24.0
5 hours	41.5	30.4	24.0
2 days	41.3	0	23.8
5 days	40.5	0	21.0

Another parameter that influences the anodic stripping peaks height of cobalt is the pre-electrolysis time. As it comes out from Fig. 3, as the pre-electrolysis time increases, the anodic stripping peak height increases. For pre-electrolysis times superior to 10 min. and for concentrations higher than 10^{-6} M, the anodic curves get out of shape.

The kinetics of the electrolytical deposition of Co^{60} from solutions of different concentrations on the mercury film electrode was investigated (Fig. 4).

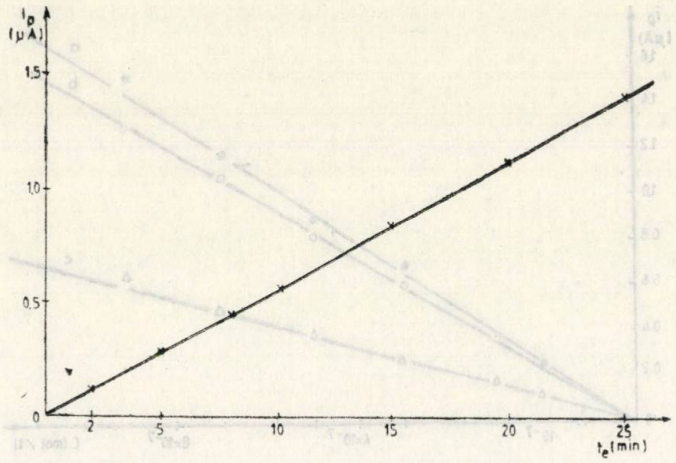

Fig. 3. — Influence of the pre-electrolysis time on the anodic stripping peak height of Co^{2+}, $C = 10^{-7}$ M, supporting electrolyte : KSCN 0.1 M.

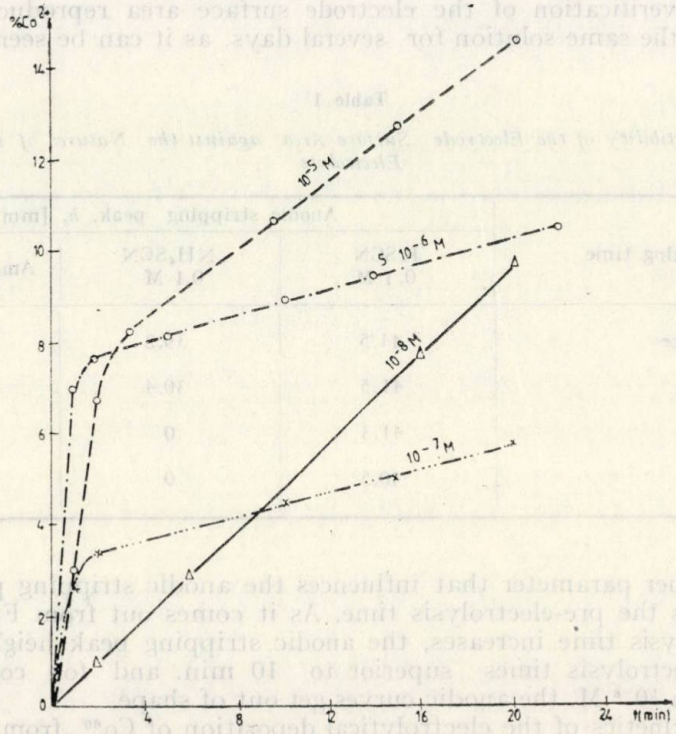

Fig. 4. — The kinetics of the electrolytical deposition of Co^{60} from the KSCN 0.1 M solution.

In order to reveal the nuclear radiations emited by Co^{60} in analysed samples, a scintilation sound with NaI (Tl) crystal connected to a NK-150 monochannel analyser apparatus was employed.

3.2. The Behaviour of $[Co(en)_3]^{3+}$

This complex has been studied in the same supporting electrolytes (KSCN, NH_4SCN) and ammonia buffer, under different concentrations. The nature of supporting electrolyte influences the potential corresponding to the maximum anodic current, as it can be seen in Table 2. This fact is of great importance, because in the case of coexistence of other foreign ions wich are reduced at potentials, other than that of complex, the basis solution allows to obtain the distinct anodic curves.

Table 2

The Potentials Corresponding to the Maximum Anodic Current against the Nature of Supporting Electrolytes Employed for Determination of $[Co(en)_3]^{3+}$

Supporting electrolyte	KSCN 0.5 M	NH_4SCN 0.5 M	Ammonia buffer
E_{an}, [V]	−0.35	−0.41	−0.42

For high concentrations of supporting electrolytes, the anodic peaks are diminished because the increasing of solution viscosity modifies the value of the diffusion coefficient and on the other hand, due to the adsorptions of ions on electrode surface take place under these conditions. Referring to the pre-electrolysis time, the linearity is not maintained for long times, when on the electrode is deposited a relatively more quantity of metal.

The optimum pre-electrolysis voltage is −1.3 V.

3.3. The Behaviour of $[Co(NH_3)_6]^3$

For this complex, the anodic peak depends on the nature of the supporting electrolyte, as observed from Table 3.

In the KSCN 0.1 M solution, the optimum pre-electrolysis voltage is −1.1 V ; for more negative potentials the anodic curves get out of shape.

Table 3

The Potentials Corresponding to the Maximum Anodic Current against the Nature of Supporting Electrolyte for Determination of $[Co(NH_3)_6]^{3+}$

Supporting electrolyte	KSCN 0.1 M	NH_4SCN 0.1 M	Ammonia buffer	Na_2SO_4 0.1 M
E_{an}, [V]	−0.42	−0.41	−0.46	−0.49

If Na_2SO_4 0.1 M solution is employed as supporting electrolyte, the optimum pre-electrolysis-potential is -1.5 V.

In Fig. 5 etalonated curves for $[Co(NH_3)_6]^{3+}$ in several supporting electrolytes are represented.

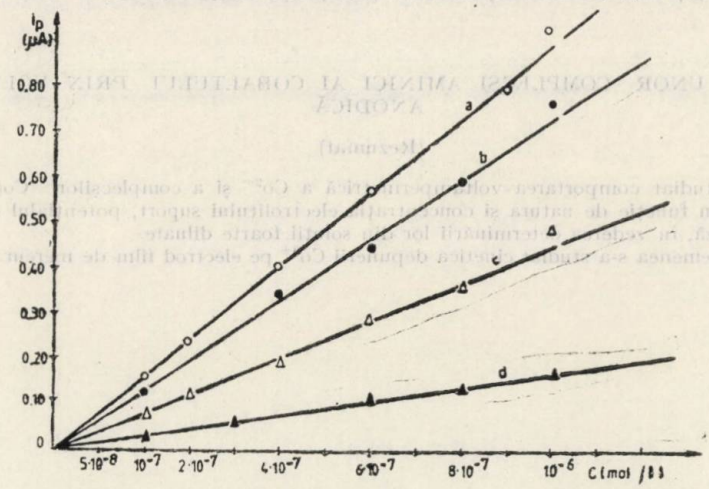

Fig. 5. — The calibration curves for determination of $[Co(NH_3)_6]^{3+}$ in the concentration range of $5\times10^{-8}...10^{-6}$ M in the following electrolytes: a — KSCN 0.1 M($E_e=-1.1$ V); b — NH_4Cl+NH_4OH 0.1 M($E_e=-1.2$ V); c — NH_4SCN 0.1 M($E_e=-1.1$ V); d — Na_2SO_4 0.1 M($E_e=-1.5$ V); $t_e=5$ min.

Although the sensitivity of determinations in Na_2SO_4 0.1 M solution is much smaller as compared to other employed electrolytes, Na_2SO_4 exhibits the advantage that the anodic curves are well defined with peaks easy to be estimated.

4. Conclusions

From the obtained results, the following conclusions can be drown:

1. Low amounts of both free and complexed cobalt can be selectively determined in the chosen concentration range on mercury film electrode.

2. In order to get a high sensitivity of the method, the optimum experimental parameters, wich alow to obtain well shaped anodic curves, have been established.

3. As regards the shape of the anodic curves obtained under the same concentration, the supporting electrolyte and other parameters being maintained constant, the differences can be explained on the basis of the different stabilities of the investigated complexes.

Received, March 18, 1985

Polytechnic Institute, Jassy,
Department of Inorganic and Analytical Chemistry and Technology

REFERENCES

1. Neeb R., *Polarographie und Voltammetrie*. Akad.-Verlag, Berlin, 1969. 139.
2. Иванов В. Ф. Иофа З. А., ДАН СССР, **140**, 1368 (3961).
3. Perone S.P., Gutknecht W.F., Anal. Chem., **39**, 892 (1967).
4. Janiszewska L., Gallus Z., Chemia Analityczna, **17**, 691 (1972).
5. Duca Al., Găburici M., Bul Inst. polit., Iași, **XXIII** (**XXVII**), *1—2*, s. II, 13 (1977).

STUDIUL UNOR COMPLECȘI AMINICI AI COBALTULUI PRIN VOLTAMETRIE ANODICĂ

(Rezumat)

S-a studiat comportarea voltampermetrică a Co^{2+} și a complecșilor $[Co(NH_3)_6]^{3+}$ și $[Co(en)_3]^{3+}$ în funcție de natura și concentrația electrolitului suport, potențialul și timpul de pre-electroliză, în vederea determinării lor din soluții foarte diluate.

De asemenea s-a studiat cinetica depunerii Co^{2+} pe electrod film de mercur.

BULETINUL INSTITUTULUI POLITEHNIC DIN IAŞI
Tomul XXXI (XXXV), Fasc. supl., 1985
Secţia II
CHIMIE ŞI INGINERIE CHIMICĂ

C.D. 667.21

MÉTHODES POUR LA CARACTÉRISATION PHYSICO-CHIMIQUE DES MÉLANGES DE COLORANTS

PAR

N. CALU, ANIŞOARA BOLD, OLGA VICOL, EUGENIA SAVIUC, LUCIA BOSNEA, I. BERDAN et I. SANDU

1. Introduction

D'une manière générale, l'état des mélanges de colorants, avec les composants auxiliaires ainsi que leur action dans le processus de teinture pose de nombreux problèmes d'interactions physiques et chimiques, de systèmes disperses, de thermodynamique et de cinétique.

Tout d'abord, les colorants, grâce a leurs groupements polaires, actifs (chromophores, auxochrômes, ionisables—solubilisants) mais aussi par la partie hydrophobe des molécules, conduisent à des interactions entre eux avec la formation de complexes H, complexes moléculaires, ions, polymères, etc. [1].

Par exemple, les complexes H se forment par l'établissement des liaisons d'hydrogène entre les molécules des colorants :

$$\begin{array}{c} R-H+R-H \rightleftarrows (R-H) \\ \qquad\qquad \downarrow\uparrow RH \\ \qquad\qquad (R-H)_3 \text{ etc.,} \end{array} \tag{1}$$

$$(R-H)_n + S_{\text{excès}} \rightleftharpoons nR-H.S \; ; \; S-\text{solvant.} \tag{2}$$

Les complexes moléculaires impliquent des liaisons de type donneur—accepteur :

$$R+R' \rightleftharpoons R \leftarrow R', \tag{3}$$

ou

$$R \leftarrow R' + S_{\text{excès}} \rightleftharpoons R \leftarrow S + R'. \tag{4}$$

Les équilibres ci-dessus sont considérablement influencés par l'excès de solvant, S, le pH et la concentration de la solution, etc.

Dans de tels équilibres, parmi les produits de réaction, ceux formés à base de liaisons plus fortes seront dominants.

D'autre part, le processus de teinture, réversible du point de vue thermodynamique, implique une série de phénomènes tels que la diffusion, le potentiel d'interface, l'échange ionique, les interactions physico-chimiques colorant—fibre etc. Les interactions colorant—fibre peuvent être de différents types : van der Waals, liaisons de hydrogène, etc. Quelquefois il arrive que ces interactions soient plus fortes en se manifestant dans le cadre des liaisons ioniques ou covalentes. Par conséquant les associations résultées à la suite des réactions (1)...(4) dépendent de la nature des interactions colorant—fibre et peuvent devenir transitoires dans le processus de teinture. Les colorants peuvent se fixer sur la fibre au niveau moléculaire, comme particules colloïdales, etc.

De toute manière, les associations des colorants ainsi que la charge électrostatique des colorants-ions et de la fibre — de même signe — diminuent la vitesse de teinture.

Évidemment, le problème de l'état des colorants et leur action dans le processus de teinture, présentent un intérêt particulier, surtout dans la perspective de l'assimilation de nouveaux colorants et fibres.

Dans une série de travaux antérieurs nous avons étudié quelques colorants se trouvant dans des mélanges, le dosage de ceux-ci, etc. [2] ... [4]. En poursuivant nos recherches, dans cette Note on présente de nouvelles données qui définissent les techniques de séparation et caractérisation physico-chimique des colorants préparés pour la teinture.

2. Partie expérimentale

Les déterminations ont été effectuées sur différents mélanges industriels de colorants (Tableau 1).

Tableau 1

Mélanges industriels des colorants étudiés

No.	Dénomination technique
1	Rouge de Dispersion *RR*
2	Jaune de Dispersion *G*
3	Bleu Marine de Dispersion *RE*
4	Palanyle Scharlach *RR*
5	Palanyle Violet 3 *B*
6	Cottestren Scharlach *G*
7	Cottestren Violett 3*B*
8	Cottestren Blau *SBC*
9	Indantren Brillanviolett 3*B*

Tableau 2

Les valeurs ND et NA de certains solvants [5], [6]

No.	Solvant	ND	NA
1	Benzène	0,1	8,2
2	Acétone	17,0	12,5
3	Diméthylesulfoxyde	29,8	19,3
4	Eau	33,0	54,8

Pour dissolution, les suspensions aqueuses des mélanges de colorants ont été repris par du diméthylesulfoxyde (DMSO). Les solutions ainsi obtenues ont la concentration 0,5% v/v.

On a préferé le DMSO comme solvant, puisqu'il possède une capacité donneuse comparable à celle de l'eau, conformément à ND, d'après Gutmann [5]...[6] (Tableau 2). En conséquence, il est probable que les processus de type (1)...(4), se passant en solution aqueuse (qui vise, à l'équilibre, la partie soluble) soient semblables aux processus qui ont lieu en DMSO.

Les constituants de ces mélanges de colorants ont été séparés par chromatographie en couche mince (CCM), alors que leur caractérisation a été réalisée par spectrophotométrie d'absorption dans le visible [2]...[4], [7]...[10].

2.1. Séparations par CCM

On a utilisé comme phase stationnaire le silicagel RG, auquel on y ajoute 5% $CuSO_4$. 1,5 H_2O, avec une granulation de 10...40 μ.

Les plaques pour CCM ont été préparées d'après la technique usuelle, en déposant uniformément une suspension de silicagel sur des plaques en

verre de dimensions 20 × 20 cm. La suspension avait été préparée en mélangeant 5 g de phase stationnaire avec 12 ml eau distillée. Après séchage pour une durée de 24 h à température ordinaire, les plaques ont été activées par échauffement à 110°C durant 30 min.

Comme phase mobile nous avons utilisé les mélanges d'éluants $M_i - M_j$..., dont la composition est présentée dans le Tableau 3.

Tableau 3

La composition de la phase mobile dans la séparation par CCM des mélanges industriels de colorants

No.	Mélange de solvants	Rapport des constituants (v/v)
1	Benzène – Acétone	9 : 1
2	Benzène – Chloroforme – Acétone	5 : 2 : 1
3	Benzène – Acétone – HCl	9 : 1 : 0,5
4	Toluène – Acétone	20 : 1
5	Éthanol – Eau	4 : 1
6	Benzène – Méthanol	9 : 1

On a procédé au développement ascendent – les variantes simple et double, avec le séchage intermédiaire des plaques. Les taches chromatographiques obtenues à la suite de la séparation sont colorées et par conséquent on n'a pas recouru à des réactions d'identification.

2.2. Spectres d'absorption

Les colorants, en tant que constituants des taches chromatographiques de la séparation par CCM, ont été élués par DMSO et les solutions ainsi obtenues ont été analysées par spectrophotométrie dans le visible. Parallèlement ont été analysés par voie spectroscopique et les mélanges industriels de colorants, nonséparés, dans des conditions opératoires identiques.

Les spectres ont été enregistrés à l'aide d'un spectrophotomètre Spekord UV–VIS, Carl Zeiss Jena.

3. Résultats et discussions

Parfois dans un système de colorants, une série d'interactions peuvent être estompées par le solvant à la suite de la formation de certaines associations colorant–fibre ; ceci vise surtout les processus (2) et (4). Les interactions colorant–colorant, plus fortes, restent inchangées mais elles peuvent afaiblir au fur et à mesure que le caractère donneur ou accepteur du solvant augmente et le système tend à s'uniformiser avec associations colorant–solvant.

L'état des colorants d'un système donné est donc fortement influencé par la nature du solvant. Par conséquent, dans des conditions données de pH, concentration, etc., l'état actuel des colorants d'un système est apprécié par „le niveau donneur", (ND), ou par le „niveau accepteur", (NA), imposé par le solvant.

3.1. Séparation des colorants des mélanges

En utilisant le silicagel comme phase stationnaire et le mélange benzène—acétone comme phase mobile, on a réalisé une séparation nette des colorants des mélanges. Les données expérimentales indiquent une séparation des colorants caracterisée par un grand nombre de taches chromatographiques (Fig. 1).

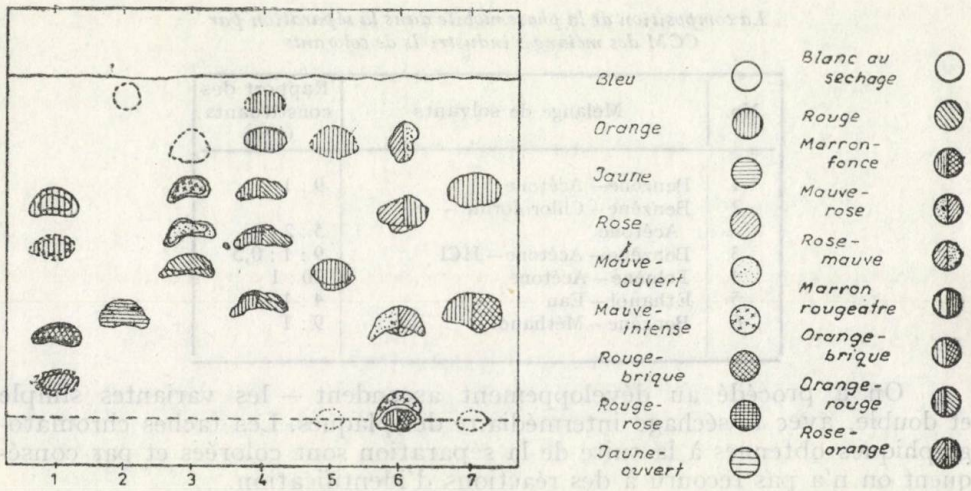

Fig. 1—Aspects de la séparation par CCM de certains colorants préparés pour la teinture: *1*—Rouge de Dispersion *RR* ; *2*—Jaune de Dispersion *G* ; *3*—Bleu Marine de Dispersion *RE* ; *4*—Palanyle Scharlach *RR* ; *5*—Palanyle Violet 3 *B* ; *6*—Cottestren Scharlach *G* ; *7*—Cottestren Violet 3*B*.

Lors de ces séparations, la dissociation des aggrégations de colorants a lieu sous l'influence de différents processus. Ainsi, le DMSO, par dissolution, favorise les processus (2) et (4). À l'équilibre, établi entre la phase stationnaire— phase mobile et les colorants constituants, le silicagel interactionne par des processus acido-basiques ou par des liaisons d'hydrogène en formant des complexes π, etc. Les deux solvants, l'acétone et le benzène, donnent lieu à des interactions plus faibles, de type donneur – accepteur (Tableau 2).

3.2. Caractérisation spectrophotométrique des mélanges de colorants

Les produits résultés lors de l'interaction des colorants, tels que les dimères et autres associations plus complexes, constituent des nouveaux systèmes d'absorption de la lumière, ce qui explique les nombreux écarts des solutions aqueuses de colorants à la loi générale de l'absorption [1].

Par exemple, pour deux molécules équivalentes, *A* et *B*, avec les fonctions d'onde Φ_a et Φ_b ou en états excités, Φ'_a et Φ'_b, l'état d'un dimère AB, formé à base de forces de dispersion L o n d o n, est donné par l'équation :

(5) $$\psi_0 = \Phi_a \Phi_b .$$

Pour ses formes excitées on aura les états :

$$\Psi_{\pm} = \frac{1}{\sqrt{2}} (\Phi'_a \Phi_b \pm \Phi_a \Phi'_b), \tag{6}$$

dont les énergies sont différentes entre elles et par rapport à celle de l'état excité du monomère, ce qui explique l'apparition des modifications dans le spectre d'absorption [1].

Pour un complexe à transfert de charge, DA, l'interaction entre l'état fondamental nonliant Φ_{DA} et celui excité polaire, Φ_{D+A^-}, conduit à un état fondamental stabilisé :

$$\Psi_0 = \Phi_{DA} + \lambda \Phi_{D+A^-}, \tag{7}$$

auquel correspond l'état (sous forme excitée, par transfert de charge) :

$$\Psi' = \Phi_{D+A^-} + \mu \Phi_{DA}. \tag{8}$$

Le complexe moléculaire présente une bande à transfert de charge spécifique, associée à la transition électronique $\psi_0 \rightarrow \psi'$ [11].

Les investigations spectrophotométriques concernent la longueur d'onde et le coefficient molaire d'absorption de la bande caractéristique et sont effectuées plus récemment avec de la lumière polarisée [1]. Les données ainsi obtenues permettent de mettre en évidence les interactions chimiques entre les colorants, l'établissement de la composition et de la stabilité des produits formés et le dosage des colorants des mélanges.

Ces déterminations reposent sur les lois générales de l'absorption [11] :

$$A = \varepsilon c d \tag{9}$$

et

$$A_t = \sum_i A_i = d \sum_i \varepsilon_i c_i, \tag{10}$$

où : A_t — absorbance totale de la solution ; d — épaisseur de la couche de solution ; ε_i — coefficient molaire d'absorption de l'espèce i et c_i — concentration (moles/l) de l'espèce i.

a) *L'état des colorants des mélanges.* D'une manière générale, en absence des interactions entre les constituants d'un mélange de colorants, les grandeurs A_t et ΣA_i, dans des conditions expérimentales identiques, obéissent à l'équation (10). En échange, lors des interactions entre les colorants, apparaissent des effets batôchromes, hipsochromes ou hyperchromes en provoquant des écarts par rapport l'équation (10).

Dans ce qui suit on présente les données obtenues concernant l'analyse spectrophotométrique de certains mélanges de colorants dont les constituants ont été séparés par CCM (Fig. 2 et 3).

Ainsi, pour le mélange Cottestren Scharlach *G* (Fig. 2), on a :

$$A \approx \sum_i A_i \tag{11}$$

dans les limites des erreurs admises. L'effet hipsochrome qui apparait à 22...23 000 cm^{-1} sur A_t suggère que lors de la dissolution de ce mélange dans le DMSO, les interactions entre les colorants constituants n'ont pas été entièrement estompées ; mais ce dernier phénomène est réalisé lors de la séparation par CCM.

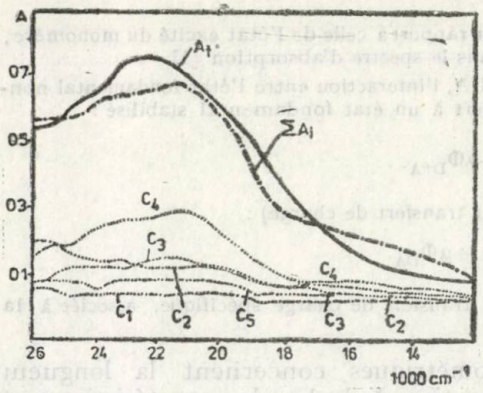

Fig. 2.— Spectres d'absorption dans le visible enregistrés sur le Cottestren Scharlach *G*(*CSG*) : A_t — spectre d'absorption enregistré sur le mélange technique CSG ; $C_1 ... C_5$ — spectres d'absorption des constituants du mélange technique CSG, séparés par CCM ; $\sum_i A_i$ — spectre résulté comme somme des absorbances des constituants $C_1 ... C_5$.

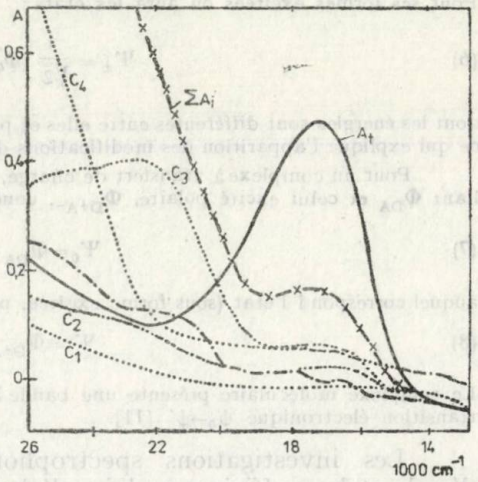

Fig. 3.— Spectres d'absorption dans le visible energistrés sur le Bleu Marine de Dispersion *RE*(AMDRE) : A_t — spectre d'absorption enregistré sur le mélange technique AMDRE ; $C_1 ... C_4$ — spectres d'absorption des constituants du mélange technique AMDRE, séparés par CCM ; $\sum_i A_i$ — spectre résulté comme somme des absorbances des constituants $C_1 ... C_4$.

En revanche, pour le mélange Bleu Marine de Dispersion *RF* (Fig. 3) :

$$A_t \neq A_i, \tag{12}$$

ce qui indique qu'à la dissolution de celui-ci dans le DMSO, l'établissement des interactions entre les colorants se poursuit tout en permettant la séparation des constituants par CCM.

Tous ces résultats peuvent s'intégrer dans un test d'appréciation de l'état des colorants des mélanges, par rapport à un niveau donneur (ND), éventuellement accepteur (NA), imposé par le solvant. Ainsi, les mélanges qui obéissent à l'équation (10) s nt considérés des systèmes summatifs pour la valeur de ND caractéristique au solvant utilisé. Dans ces mé.anges le colorants se trouvent à l'état associé avec le solvant, sous forme de monomères, etc. Les mé anges pour lesquels s'applique l'inégalité (12) présentent un caractère intégral. Ces mélanges exigent des solvants à ND plus élevé qui peuvent diminuer les interactions entre les constituants.

b) *Paramètres* R_F *et* λ_{max}. De nombreux colorants avec la même formule et la même structure moléculaire ont des appélations techniques différentes. Dans une première étape ils peuvent être investigués par l'intérmediaire des paramètres R_f et λ_{max}, obtenus par l'étude des colorants par CCM et, respectivement, par spectroscopie d'absorption. Dans ce but on peut construire des diagrammes en coordonnés R_f et λ_{max} à base de valeurs déterminées dans des conditions standards (Fig. 4). Dans un tel

diagramme, parmi les colorants concentrés dans des domaines étroits on y trouve tant les colorants semblables du point de vue chimique que des colorants semblables du point de vue optique. Cet aspe t peut représenter une première étape de sélection pour mieux choisir les colorants substituants et pour définir les recettes de teinture.

c) *Dosage des colorants des mélanges.* La classification des mélanges de colorants comme summatifs et intégrals présente un grand intérêt dans le dosage spectrophotométrique des colorants des bains de teinture. Ainsi, les colorants des mélanges summatifs peuvent être simultanément dosés à base de leurs spectres d'absorption. En échange, ceux à caractère intégral nécessitent le choix d'un autre solvant à ND plus élevé qui peut diminuer les interactions du système.

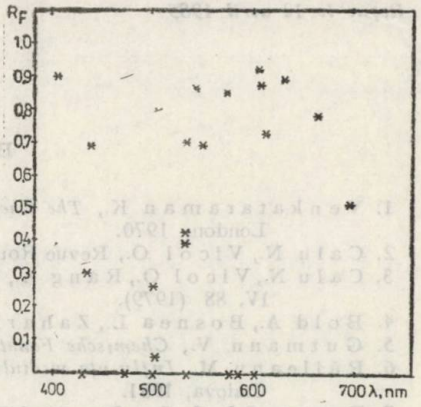

Fig. 4.— Diagramme $R_F - \lambda_{max}$ avec les paramètres caractéristiques des constituants des mélanges techniques : Rouge de Dispersion *RR* ; Bleu Marine de Dispersion *RE* ; Palanyle Violett *3B* ; Cottestren Scharlach *G* ; Cottestren Violett *3B* ; Cottestren Blau *SBC* et Indantren Brillantviolett *3B*.

Concernant le dosage, pour calculer la concentration des colorants nous avons proposé un système d'équations algébriques, avec une validité générale [2]. Ainsi, pour un mélange de deux colorants, les équations de calcul ont la forme :

$$(13)\quad \frac{A'}{d} = \operatorname{tg}\alpha_{1\lambda'} x \pm n_{1\lambda'} + \operatorname{tg}\alpha_{2\lambda'} y \pm n_{2\lambda'}, \quad \frac{A''}{d} = \operatorname{tg}\alpha_{1\lambda''} x \pm n_{1\lambda''} + \operatorname{tg}\alpha_{2\lambda''} \pm x_{2\lambda''},$$

où : $\operatorname{tg}\alpha_i$ et n_i représentent la pente et respectivement l'ordonnée à l'origine des droites $A = f(c)$ caractéristiques de chacun des constituants i ; A' et A'' —les absorbances du mélange de colorants à λ' et respectivemment λ'' (on prend le signe + pour $n > 0$ et le signe — pour $n < 0$) ; x et y — les concentrations des deux colorants du mélange.

4. Conclusions

a) L'état des colorants d'un système est apprécié à base du caractère donneur, éventuellement accepteur des solvants.

b) Les mélanges de colorants pour lesquels l'absorbance totale A_t est égale à la somme des absorbances des constituants $(\sum_i A_i)$ sont considérés, au niveau donneur imposé par le solvant, comme systèmes summatifs. Les autre mélanges, avec $A_t \neq \sum_i A_i$, à caractère intégral, peuvent devenir summatifs par rapport aux solvants avec des propriétés donneur—accepteur plus fortes.

c) Les colorants des mélanges summatifs peuvent être simultanément dosés par voie spectroscopique, à l'aide d'un système d'équations algebriques en tg α et n.

d) Les paramètres R_f et λ_{max} interviennent dans la sélection des colorants remplaçants et à l'élaboration des recettes de teinture.

Reçue le 12 avril 1985

Institut Polytechnique, Jassy,
Chaire de Chimie et Technologie
anorganique et analytique

BIBLIOGRAPHIE

1. Venkataraman K., *The Chemistry of Synthetic Dyes*. Acad. Press, New-York—London, 1970.
2. Calu N., Vicol O., Revue Roumaine de Chimie, 26, 5, 783—792 (1981).
3. Calu N., Vicol O., Rang A., Saviuc E. et collab., Bul. Şt. Stud., Inst. polit., Iaşi, IV, 88 (1979).
4. Bold A., Bosnea L., Zaharia E., Revista de chimie, **33**, *10*, 953 (1982).
5. Gutmann V., *Chemische Fonktionslehre*. Springer Verlag, 1971.
6. Răileanu M., *Influenţa mediului asupra reactivităţii chimice*. Ed. Scrisul Românesc Craiova, 1981.
7. Brown C.J., J. Soc. Dyers and Col., **80**, 185 (1964); Ibid., **85**, 137 (1969).
8. Johnson D.C., Telesz A.L., J. Soc. Dyers ans Col., **78**, 496 (1962).
9. Sweeny D.C., American Dyestuff Reports, **61**, 70 (1972).
10. Beer A., Ann. Phys. Chem., *163*, 78 (1852).
11. Rose J., *Molecular Complexes*. Pergamon Press, Oxford-London, 1967.

METODE DE CARACTERIZARE FIZICO CHIMICĂ A COLORANŢILOR ÎN AMESTEC

(Rezumat)

În sistemul de coloranţi pregătiţi pentru vopsire au loc diverse interacţiuni fizice şi chimice între coloranţi, cu implicaţii în procesul de vopsire. În acelaşi timp, solventul produce asociate colorant—solvent. Ca urmare, în lucrare este folosit conceptul de nivel donor, eventual acceptor, al solventului pentru a aprecia starea asociatelor colorant—solvent, din sistemele luate în studiu.

În fapt, coloranţii din amestecuri, separaţi prin cromatografie în strat subţire, au fost caracterizaţi pe baza benzilor de absorbţie în vizibil. Astfel, amestecurile la care absorbanţa totală, A_t, este egală cu suma absorbanţelor coloranţilor componenţi, $\sum_i A_i$, sînt apreciate ca sumative, la nivelul donor—acceptor impus de solvent. Pentru celelalte amestecuri, cu $A_t \neq \sum_i A_i$, se admite un caracter integral. Ele pot deveni sumative în solvenţi cu o capacitate donor—acceptor mai ridicată. Coloranţii din amestecurile sumative pot fi dozaţi pe cale spectrofotometrică, folosind un sistem de ecuaţii în tgα şi n.

Pe de altă parte, parametrii R_f şi λ_{max} sînt utili în selectarea unor coloranţi înlocuitori, la elaborarea reţetelor de vopsire.

BULETINUL INSTITUTULUI POLITEHNIC DIN IAȘI
Tomul XXXI (XXXV), Fasc. supl., 1985
Secția II
CHIMIE ȘI INGINERIE CHIMICĂ

D.C. 532.13 ; 541.24

VISCOSITY — MOLECULAR WEIGHT RELATIONSHIP FOR POLY (ETHYLENETEREPHTALATE) MODIFIED WITH 1,2-PROPANEDIOL

BY

CAMELUȚA BELDIE, ANA ONU, NICOLAE AELENEI, GH. NEMȚOI, AL. RADOVICI and AL. SAVIN

1. Introduction

To obtain certain peculiar properties (optical effects, dye adsorption, good resistance for technical use, etc.), the studies on poly(ethyleneterephtalate) were applied more and more on its copolyesters, too. Features as solubility, crystallinity, melting point, etc., can be changed inserting small amounts of a comonomer, in the chain.

The obtaining of a polyester sample with optimal properties intended to be used in a certain application depends on the molecular weight, and molecular weight distribution, so that any investigation should search these features. The value of the molecular weight polydispersity due to the existence of some low molecular weight fractions, can lead to an important modification of copolyester properties.

The evaluation of the molecular weights as well as the molecular weight distribution was performed in solution.

In our case, the solubility of these copolyesters was limited due to a high crystallinity which reduces the number of the used solvents, and it is necessary to use high temperatures in order to prepare the solutions.

This paper deals with the study of the relation between $[\eta]$ and $\overline{M}_n$ for poly(ethyleneterephtalate) modified with 1,2-propanediol on unfractionated and fractionated samples in two solvents : *o*-chlorophenol (OCPh) and phenoltetrachloroethane (Ph—TCE) mixture.

2. Experimental

Samples of poly(ethyleneterephtalate) modified with 1,2-propanediol (5.0...10.0% of 1,2-propanediol) of different molecular weights, as well as fractions obtaind from a copolyester having 10.0% 1,2-propanediol were investigated from the physico-chemical point of view.

In order to choose a proper solvent corresponding to the copolyester, the following solvents were searched: *m*-cresol, *o*-chlorophenol, and phenol/tetrachlorethane (3/2 w/w).

The solubility of the copolyester samples were studied in comparison with poly(ethyleneterephtalate). It was noticed that inserting 1,2-propanediol results in an increase of the solubility of the copolyester samples in all listed solvents. From the three investigated solvents, *m*-cresol is less proper, so the viscosimetric studies of the copolyester samples were performed using

o-chlorophenol and the phenol/tetrachloroethylene (3/2 w/w) while the cryoscopic measurements were carried out in *o*-chlorophenol.

The viscosimetric measurements of the fractions performed by the fractionation technique of copolyester were carried out using only *o*-chlorophenol, small amounts of copolyester being available.

The fractionation of poly(ethyleneterephtalate) modified with 1,2-propanediol was performed applying the known technique [1], [2] based on the distribution of copolyester between two liquid phases with reduced miscibility. The fractionation was performed at 56°C using phenol as solvent and the phenol – n-heptane mixture as eluent. The percent of phenol was increased from 45.0% up to 70.0%. The fractions were precipitated from the solution by adding acetone in exces, at 40°C.

The viscosimetric measurements were carried out on a Ubbehlode viscosimeter at 25°C. The limit viscosity index of the fractions 2...10 and unfractionated samples was determined by the H u g g i n s method [3], carrying out measurements on four different concentrations. The limit viscosity index of the fractions 1 and 11...14 was determined using the S o l o m o n - C i u t a's relation [4] when the measurements of viscosity were performed for one concentration.

The number average molecular weights were measured by the cryoscopic method on a Knauer cryometer apparatus fitted with thermoelectric cooling unit. The cooling of the sample was performed applying the Peltier's effect. The cooling degree and the cooling velocity depends on the „warm welding" thermoelement temperature and as consequence it depends on the room temperature and the working time of the apparatus. This phenomenon is not quite important for solvents which show small or moderate undercoolings ($\Delta T \leqslant 5°C$), but it is important in the case of solvents having high undercoolings (for instance, *o*-chlorophenol used in our case). In order to perform the same undercooling for all samples and solvents, the „warm welding" of the thermoelement was thermostated. For this purpose, cold water (0°C) was circulated through the thermostatic mantle of the thermoelement by means of a MK-70 Ultracryostate apparatus.

For each sample, measurements were carried out at least five different concentrations ; 20 measurements were performed for each concentrations. Polystyrene was used as standard sample (Arro Laboratories Inc., Illinois, USA), of which molecular weight (20.450) was in the average range of the measured values

3. Results and Discussion

A copolyester sample having a content of 10.0% 1,2-propanediol and $\overline{M}_n = 23\,100$ g/mol was fractionated. The experiemental data were processed and plotted as distribution curves in Fig. 1.

The results of the viscometric and cryoscopic determinations, performed in *o*-chlorophenol, at 25°C, are shown in Table 1.

The coefficients of the M a r k – H o u w i n k – S a k u r a d a (M-H-S) equation $[\eta] = KM^{\alpha}$ were calculated using these experimental data applying the least squares method :

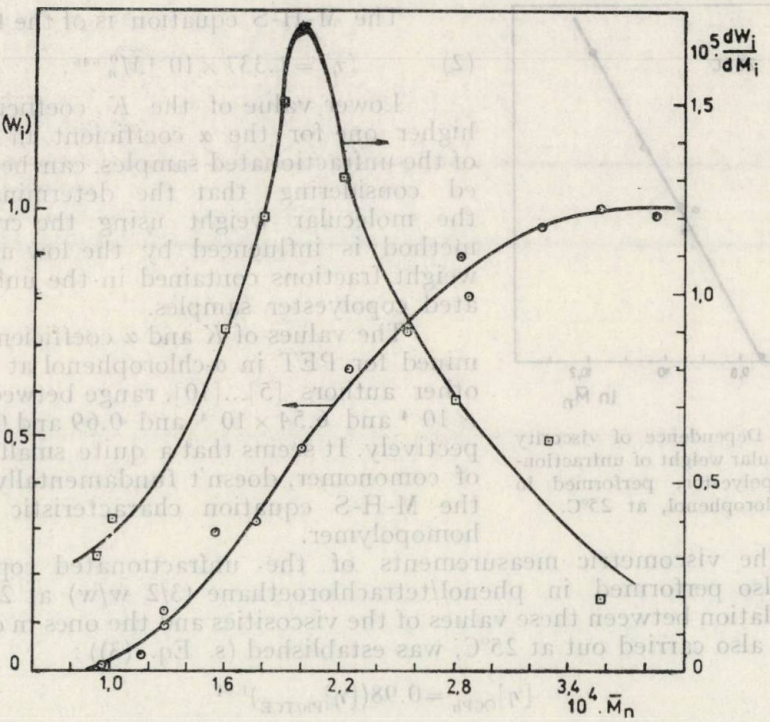

Fig. 1. — The distribution of the molecular weights for copolyester sample which contains 10.0% 1,2-propanediol.

Table 1

Number Average Molecular Weights ($\overline{M}_n$) and the Limit Viscosity Indexes ([η]) of the Copolyester Fractions, Determined in o-Chlorophenol, at 25°C

Fraction	$\overline{M}_n \times 10^{-4}$ g/mol	[η] dl/g	Fraction	$\overline{M}_n \times 10^{-4}$ g/mol	[η] dl/g
1	0.970	0.289	8	2.27	0.543
2	1.35	0.430	9	1.30	0.361
3	2.50	0.590	10	1.77	0.454
4	1.38	0.395	11	1.10	0.402
5	1.79	0.510	12	3.25	0.726
6	2.56	0.697	13	3.86	0.810
7	1.48	0.361	14	3.55	0.942

$$[\eta] = 3.12 \times 10^{-4} \overline{M}_n^{0.75} \quad (1)$$

The viscometric and cryoscopic studies of unfractionated copolyester samples with 5.0...10.0% 1,2-propanediol, in *o*-chlorophenol, at 25°C show the dependence of viscosity on molecular weight represented in Fig. 2.

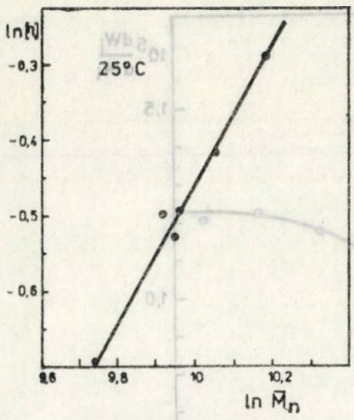

Fig. 2 — Dependence of viscosity on molecular weight of unfractionated copolyester, performed in *o*-chlorophenol, at 25°C.

The M-H-S equation is of the form:

$$[\eta] = 1.337 \times 10^{-4} \bar{M}_n^{0.846}. \quad (2)$$

Lower value of the K coefficient and higher one for the α coefficient in the case of the unfractionated samples can be explained considering that the determination of the molecular weight using the cryoscopic method is influenced by the low molecular weight fractions contained in the unfractionated copolyester samples.

The values of K and α coefficients determined for PET in *o*-chlorophenol at 25°C, by other authors [5]...[10], range between $1.6 \times \times 10^{-4}$ and 6.54×10^{-4} and 0.69 and 0.83, respectively. It seems that a quite small percent of comonomer, doesn't fundamentally change the M-H-S equation characteristic to the homopolymer.

The viscometric measurements of the unfractionated copolyester were also performed in phenol/tetrachloroethane (3/2 w/w) at 25°C and a correlation between these values of the viscosities and the ones in *o*-chlorophenol also carried out at 25°C, was established (s. Eq. (3)):

$$[\eta]_{OCPh} = 0.98([\eta]_{Ph/TCE})^{1.04} \quad (3)$$

By measuring the viscosity of the industrial copolyester samples in Ph/TCE (3/2 w/w) (the most used solvent in the laboratories of the chemical industry) and knowing the relation between this solvent mixture and *o*-chlorophenol (Eq. (3)), one can calculate $\bar{M}_n$ of the investigated sample, according to the dependence $[\eta]_{OCPh}$ vs. $\bar{M}_n$, given by Eq. (2). The experimental results are in good agreement.

The knowledge of this dependence between the viscosities in different solvents answers to a practical need, because the viscometric measurements can be easily performed in solvent mixtures, while the molecular weight measurement methods assume the utilization of a single solvent. Our results allow to widen the application possibilities of the viscosity — molecular weight relations established by different authors.

4. Conclusions

The performed studies pointed out the following conclusions:

1. The copolyester presents a better solubility than poly(ethyleneterephtalate) in *m*-cresol, *o*-chlorophenol and Ph/TCE mixture (3/2 w/w) as proved by the solubility tests as well as by viscometric determinations; *o*-chlorophenol was the best solvent for the copolyester samples.

2. The fractionation of 1,2-propanediol-ethyleneterephtalate copolyester applying the known methods for poly(ethyleneterephtalate) is not entirely adequately, because using the same solvent/nonsolvent ratio and

elution velocity, inversion of the fraction separation succession are obtained.

3. The experimental date, performed in *o*-chlorophenol at 25°C, for the 14 fractions and unfractionated copolyester, lead to a linear dependence between viscosity and molecular weight given by Eqs. (1) and (2). The K coefficient is smaller for the unfractionated samples as compared to that of the fractionated copolyester while the α exponent is higher. This behaviour is due to the existence of low molecular weight fractions which influence the number average molecular weight, while the viscosimetric measurements are influenced by the high molecular weight fractions existing in the polydisperse copolyester.

4. The determined correlation between viscosity in *o*-chlorophenol and Ph/TCE (3/2 w/w) allows the experimental determination of viscosity, in Ph/TCE (used by chemical industrial laboratories), and the calculation of $\overline{M}_n$ value by means of the viscosity—molecular weight relation. This study offers the possibility to widen the application field of the equation (2).

Received, April 18, 1985

Polytechnic Institute, Jassy,
Department of Physical and
General Chemistry

REFERENCES

1. Duveau M., J. Polymer Sci., **57**, 375 (1962).
2. Feldman D., Theil I., Călugăru E.M., Faserforschung-Textiltechnik, **23**, 123 (1972).
3. Huggins M.L., J.Am. Chem. Soc., **64**, 2716 (1942).
4. Solomon O.F., Ciuta I.Z., J. Appl. Polym. Sci., **6**, 683 (1962).
5. Ward I.M., Trans. Faraday Soc., **53**, 1406 (1957).
6. Ravens D.A.S., Ward I.M., Trans. Faraday Soc., **57**, 150 (1961).
7. Moore W.R., Sanderson D., Polymer (London), **9**, 153 (1968).
8. Marshall J., Todd A., Trans. Faraday Soc., **49**, 65 (1953).
9. Meyerhoff G., Shimotsuma S., Makromol. Chem., *135*, 195 (1970).
10. Hergenrother W.L., Nelson Ch.J., J. Polym Sci., Polymer Chem. Ed., **12**, 2905 (1974).

RELAȚIA VÎSCOZITATE—MASĂ MOLECULARĂ PENTRU POLIETILENTEREFTALAT MODIFICAT CU 1,2-PROPANDIOL

(Rezumat)

S-au determinat coeficienții K și α din ecuația Mark-Houwink-Sakurada în *o*-clorfenol (OCF) pentru poli(etilentereftalat) modificat cu 1,2-propandiol atît nefracționat cît și pentru fracțiuni. La 25°C, $[\eta]=3{,}12.10^{-4}\overline{M}_n^{0,75}$ dl/g pentru fracțiuni și $[\eta]=1{,}337.10^{-4}\times\overline{M}_n^{0,846}$ dl/g pentru probele nefracționate. Pentru probele nefracționate s-a obținut între vîscozitatea în OCF și în amestecul de solvenți fenol/tetracloretan (F/TCE) : (3/2), la 25°C relația $[\eta]_{OCF}=0{,}98[(\eta]_{F/TCE})^{1,04}$. Masele molare au fost determinate prin metoda crioscopică, utilizînd un crioscop tip Knauer prevăzut cu o unitate de răcire termoelectrică bazată pe efectul Peltier.

elution velocity, inversion of the fraction separation succession are obtained.

3. The experimental date, performed in o-chlorophenol at 25°C, for the 14 fractions and unfractionated copolyester, lead to a linear dependence between viscosity and molecular weight given by Eqs. (1) and (2). The K coefficient is smaller for the unfractionated samples as compared to that of the fractionated copolyester while the α exponent is higher. This behaviour is due to the existence of low molecular weight fractions which influence the number average molecular weight, while the viscosimetric measurements are influenced by the high molecular weight fractions existing in the polydisperse copolyester.

4. The determined correlation between viscosity in o-chlorophenol and Ph/TCE (3/2 w/w) allows the experimental determination of viscosity, in Ph/TCE (used by chemical industrial laboratories), and the calculation of $\overline{M}_n$ value by means of the viscosity—molecular weight relation. This study offers the possibility to widen the application field of the equation (2).

Received, April 18, 1985

Polytechnic Institute, Jassy,
Department of Physical and
General Chemistry

REFERENCES

1. Duveau M., J. Polymer Sci., 57, 375 (1962).
2. Feldman D., Thell I., Câlugăru E.M., Faserforschung Textiltechnik, 23, 123 (1972).
3. Huggins M.L., J. Am. Chem. Soc., 64, 2716 (1942).
4. Solomon O.F., Ciuta I.Z., J. Appl. Polym. Sci., 6, 683 (1962).
5. Ward I.M., Trans. Faraday Soc., 53, 1406 (1957).
6. Ravens D.A.S., Ward I.M., Trans. Faraday Soc., 57, 150 (1961).
7. Moore W.R., Sanderson D., Polymer (London), 9, 153 (1968).
8. Marshall J., Todd A., Trans. Faraday Soc., 49, 65 (1953).
9. Meyerhoff G., Shimotsuma S., Makromol. Chem., 135, 195 (1970).
10. Hergenrother W.L., Nelson Ch.J., J. Polym. Sci., Polymer Chem. Ed., 12, 2905 (1974).

RELAŢIA VÎSCOZITATE—MASĂ MOLECULARĂ PENTRU POLIETILENTEREFTALAT MODIFICAT CU 1,2-PROPANDIOL

(Rezumat)

S-au determinat coeficienţii K şi α din ecuaţia Mark-Houwink-Sakurada în o-clorfenol (OCF) pentru poli(etilenterftalat) modificat cu 1,2-propandiol atît nefracţionat cît şi pentru fracţiuni. La 25°C, $[\eta]=3{,}12\cdot10^{-4}\overline{M}_n^{0{,}75}$ dl/g pentru fracţiuni şi $[\eta]=1{,}337\cdot10^{-4}\times\overline{M}_n^{0{,}848}$ dl/g pentru probele nefracţionate. Pentru probele nefracţionate s-a obţinut între viscozitatea în OCF şi în amestecul de solvenţi fenol/tetracloretan (P/TCE) (3/2), la 25°C relaţia $[\eta]_{OCF}=0{,}98[\eta]_{P/TCE}^{1{,}04}$. Masele molare au fost determinate prin metoda crioscopică, utilizînd un crioscop tip Kunner prevăzut cu o unitate de răcire termoelectrică bazată pe efectul Peltier.

BULETINUL INSTITUTULUI POLITEHNIC DIN IAŞI
Tomul XXXI (XXXV), Fasc. supl., 1985
Secţia II
CHIMIE ŞI INGINERIE CHIMICĂ

D.C. 546.654 : 546.36

COMPLEXES OF La(III) AND Ce(IV) WITH DIBUTYLPHOSPHINIC ACID

BY

I. ROŞCA, ELENA ŞTEFANCU and MIRCEA PALAMARU

1. Introduction

Development of investigation in the field of the compounds prepared from cations of the block *d* metals with derivatives of phosphinic acid resulted, last years, in the synthesis and study of numerous compounds with special properties [1] ... [10].

The studies performed on these compounds have proved their high thermal stability and elastic properties which maintain at very low temperature. Besides high thermostability, some of these compounds are semiconductors or insulators, resistent in corossive media [5] ... [14]. An uncommon application of these products is their utilization in aeronautics and artificial satellites [9].

The present paper deals with some new syntheses and studies on the properties of the compounds prepared from cations of the block *d* metals with derivatives of phosphinic acid, especially complexes of La(III) and Ce(IV).

2. Experimental

2.1. Synthesis and Characterization

The studied compounds have been o' tained in melt or by refluxing in benzene, toluene, butanol or ethanol of respective reagents. For this reason, stoichiometrical amounts of La(III) o Ce(IV) acetya'cetonate and dibutylphosphinic acid have been introduced in a flask fitted with a refluxing condenser. Both La(III) and Ce(IV) acetylacetonate and dibutylphosphinic acid have been obtained, as in [15], [16].

The flask containing the reagents was heated up to the boiling temperature of the solvent or over melting temperature of the reagents for melt syntheses. The reagents concentration was 0.2...0.02 mole/L. The reagents are soluble but products are only partially soluble in the employed solvents. Separation of the products was carried out by filtration and the soluble fractions by solvent evaporation.

From the chemical composition of the obtained complexes, it appears that for each La^{3+} or Ce^{4+} cation correspond three, respectively four anions of dibutylphosphinic acid (Table 1).

Table 1

Composition and Molecular Weight of the Obtained Compounds

Compound	Molecular Weight	Composition, [%]							
		M		C		P		H	
		teor.	exp.	teor.	exp.	teor.	exp.	teor.	exp.
$\{La[(C_4H_9)_2PO_2]_3\}_n$	6 110	20.7	20.2	43.2	43.6	13.9	13.5	8.06	8.32
$\{Ce[(C_4H_9)_2PO_2]_4\}_n$	8 620	16.5	16.3	45.3	45.8	14.6	14.2	8.49	8.76

The molecular weights of the soluble fractions, determined cryoscopically in benzene are summarized in Table 1.

2.2. Thermogravimetrical Analysis and Kinetics of the Thermal Decomposition Reaction

Thermogravimetrical analysis of the samples has been carried out on a Paulik-Paulik-Erdey derivatograph with amounts of 50 mg at a heating rate of 10°C/min from 20°...700°C.

The derivatograms show that the thermal decomposition occurs gradually, by releasing gaseous products (Fig. 1).

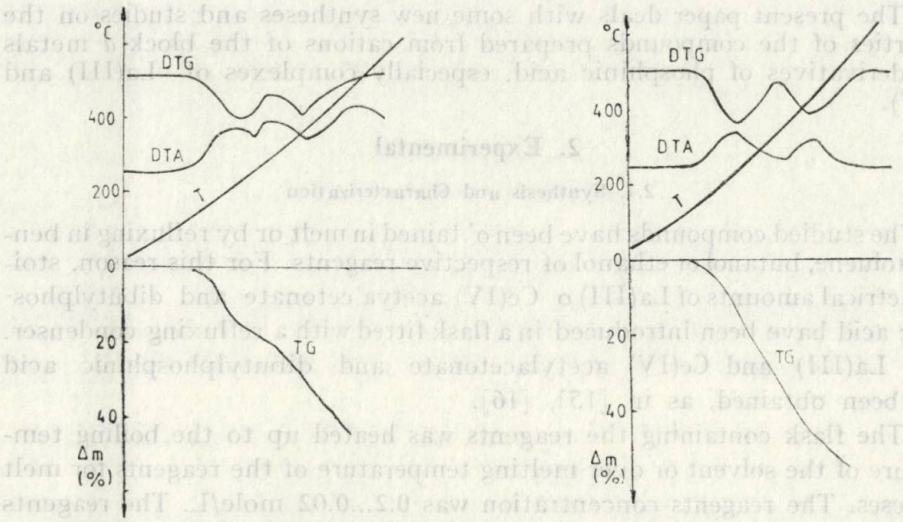

Fig. 1. — Derivatograms of complexes: 1—$\{La[(C_4H_9)_2PO_2]_3\}_n$; 2—$\{Ce[(C_4H_9)_2PO_2]_4\}_n$.

The strongest bonds in the tested compounds are La—O, Ce—O and P—O, finally found in the solid products.

The obtained compounds present a thermal stability greater than the reagents. This proves that the groups which did not resist to the thermic

effect in La(III) and Ce(IV) acetylacetonates and dibutylphosphinic acid allow the isomerization to form more stable chelate rings. The temperatures corresponding to the thermal decomposition are listed in Table 2.

Table 2

Thermal Decomposition of the Obtained Compounds

Compound	Start of decomposition °C	Temperature corresponding to a weight loss of °C		Final decomposition temperature, °C
		10%	25%	
$\{La[(C_4H_9)_2PO_2]_3\}_n$	160	217	320	480
$\{Ce[(C_4H_9)_2PO_2]_4\}_n$	190	240	295	565

Kinetical parameters of the thermal decomposition reactions, calculated by Freeman and Carol's procedure [17], for each decomposition step, are given in Table 3.

The values of the reaction order may be explained considering that the chemical reaction is defavourised by diffusion of volatile compounds through the solid, by interphase or by „vaporization" phenomena of volatile components at the free surface of the solid.

Table 3

Kinetical Parameters of the Thermal Decomposition Reactions

Compound	Temperature °C	Phase I			Phase II	
		Reaction order	Activation energy Kj/mol	Temperature °C	Reaction order	Activation energy Kj/mol
$\{La[(C_4H_9)_2PO_2]_3\}_n$	160...270	0.68	123	270...470	0.76	148
$\{Ce[(C_4H_9)_2PO_2]_4\}_n$	190...340	0.83	139	340...565	0.89	174

2.3. Spectral Analysis

The IR spectra of the synthesized products have been recorded on an UNICAM apparatus in the 400...4 000 cm^{-1} region. The most pronounced are the absorbtion bands of the $-PO_2$ group. Formation of the 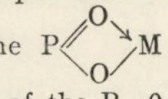 bonds causes the modification of the corresponding maxima of the P=0 group as effect of the P=0 elongation. Thus, the obtained products, show lower frequencies than the uncomplexed dibutylphosphinic acid for about 20 cm^{-1} (Fig. 2).

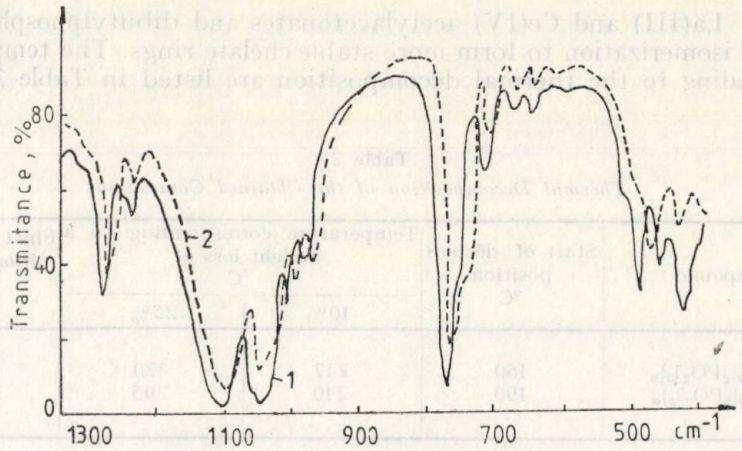

Fig. 2. — IR Spectra of the complexes:
1—$\{La[(C_4H_9)_2PO_2]_3\}_n$; *2*—$\{[(C_4H_9)_2PO_2]_4\}_n$.

X-ray diffraction spectra were recorded on a Kristalloflex-Siemens type equipment with Cu.K_α radiation and Ni filter, anodic voltage of 35 eV and a current of 12 mA. The crystallinity degree was calculated by the method presented in [18]. The found values were of 38.8% and 43.2% for La and Ce compounds, respectively. They proved to be two phase products in which, besides local ordonation proper to amorphous state, diffraction lines characteristic to crystalline phase are also exhibited.

3. Suggested Structure of the Synthesized Complexes

Data of the chemical analysis of the synthesized compounds show that for each M^{3+} ion correspond three anions of dibutylphosphinic acid. These anions being bidentate by means of oxygen atoms, the hexacoordination of M^{3+} appears (Fig. 3).

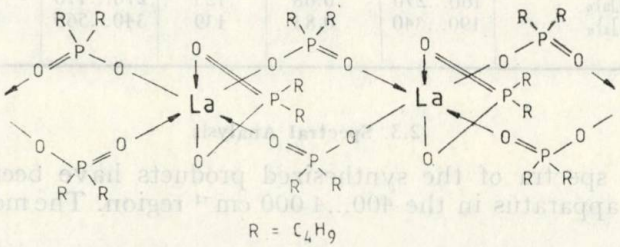

Fig. 3. — Suggested structure of the synthesised compounds:
$\{La[(C_4H_9)_2PO_2]_3\}_n$.

As known, for coordination number six, the arrangement of ligands is an octahedral one. This structure is in good agreement with the structure of some similar compounds prepared from diorganophosphinic acids and cations of the block *d* metals [4]...[12].

The values of the molecular weight reveal that these compounds are oligomers like. Therefore, the octahedral structure units, as main units in the polymer structure, will constitute configuration of the synthesized compounds. Connection of the octahedral structures is done by means of anionic groups of dibutylphosphinic acid with the phosphorous atom tetracoordinated in tetrahedral structure, which agrees with experimental and literature data.

Received, April 18, 1985

Polytechnic Institute, Jassy,
Department of Inorganic and
Analytical Chemistry and
Inorganic Technology,

REFERENCES

1. Block P.B., Simkin J., Ocone R.J., J. Am. Chem. Soc., **84**, 1 749 (1962).
2. Saraceno J.A., Block P.B., Inorg. Chem., **3**, 1 699 (1964).
3. Selwyn H., Rose H.S., Block P.B., J. Am. Chem. Soc., **87**, 2 076 (1965).
4. Crescenzi V., Giancotti V., Ropamonti A., J. Am. Chem. Soc., **88**, 391 (1966).
5. Коршак В.В., Круковский С.П., Ван Юи Хан, Высокомолек. соедин., **B 9** (1967).
6. Golgoţiu T., Roşca I., Bul. Inst. polit., Iaşi, **XVII (XXI)**, *1–2*, s. II, 1 (1971).
7. Golgoţiu T., Roşca I., Makromolek. Chemie, *160*, 59 (1972).
8. Голгоциу Т., Рошка И., Высокомолек. соедин., **9**, 2086 (1973).
9. *** Patent USA. *139 784* (1973).
10. Roşca I., *Compuşi termostabili ai Mn(II), Cr (III), Fe(III), UO_2^{2+}, Co(II) şi Ni(II) cu derivaţi ai acidului fosfinic.* Ph. D. Diss., Polyt. Inst., Jassy, 1975.
11. Roşca I., Bul Inst. polit. Iaşi, **XXIII (XXVII)**, *1–2*, s. II, 21 (1977).
12. Roşca I., Bul. Inst. polit., Iaşi, **XXI (XXV)**, *1–2*, s. II, 8 (1975).
13. Roşca I., Patent R.S.R., *68459* (1978).
14. Roşca I., Patent R.S.R., *73201* (1979).
15. Петров А. К., Близнюк К. Х., Короткова П. В., ЖОХ, **9**, 2095 (1960).
16. Brauer G., *Handbuch der präparativen anorganischen Chemie.* Ferdinand Enke Verlag, Stuttgart, 1954.
17. Freeman S.E., Carrol B., J. Phys. Chem., **62**, 394 (1958).
18. Hermans H.P., J. Polym. Sci., **4**, 709 (1960).

COMPUŞI DE COORDINAŢIE AI La(III) ŞI Ce(IV) CU ACIDUL DIBUTILFOSFINIC

(Rezumat)

Se continuă seria sintezelor şi al studiului proprietăţilor compuşilor proveniţi de la cationii blocului *d*, cu derivaţi ai acidului fosfinic, prezentîndu-se un studiu al compuşilor obţinuţi din acid dibutilfosfinic şi acetilacetonaţi de La(III) şi Ce(IV). Compuşii au fost sintetizaţi în soluţie şi în topitură. Din analiza chimică a compuşilor obţinuţi s-a putut stabili că pentru fiecare cation La^{3+} sau Ce^{4+} corespund trei şi respectiv patru anioni ai acidului dibutilfosfinic. Complecşii obţinuţi au fost studiaţi prin analiză termogravimetrică, spectre de absorbţie în IR şi spectre de raze X. Se propune în final o structură a complecşilor obţinuţi.

BULETINUL INSTITUTULUI POLITEHNIC DIN IAŞI
Tomul XXXI (XXXV), Fasc. supl., 1985
Secţia II
CHIMIE ŞI INGINERIE CHIMICĂ

D.C. 661.183.48

SYNTHETIC ZEOLITES FOR DETERGENTS CONDITIONING

I. PHYSICO-CHEMICAL PROPERTIES OF ZEOLITES

BY

EVELINE POPOVICI, M. CRUCEANU, ANGELA POPA, AURELIA VASILE and MARIA ALEXANDROAEI

1. Introduction

Last years, numerous investigations [1] ...[5], [9] ... [12] were concerned with the utilization of synthetic zeolites as subsidiary substitutes in detergents conditioning. This utilization is justified, on the one hand, by assurance of a complet security from toxicological and ecological point of view and, on the other hand, by partial diminishing of phosphates consumption, the latest ones being energointensive products.

Utilization of zeolites for this purpose is especially based on their significant property of ion exchange against Ca^{2+} and Mg^{2+}, with convenient consequences for washing steps [1]... [4] and on technical and economical estimations of Henkel and Degussa companies [6] which pointed out that utilization of zeolites for detergents conditioning do not involve essential technological modifications. This considerations explain the continuous increase of world zeolites consumption in detergents manufacture in comparison with their classical utilization, i.e. catalysis, adsorption (s. Table 1).

This paper deals with an analysis of some physico-chemical properties of certain synthetic zeolites, obtained at Polytechnic Institute of Jassy, symbolized by ZPI, in comparison with the data on the commercial product HAB-A40 Degussa in view of their utilization in detergents, as conditioning agent.

2. Experimental

The analyzed synthetic zeolites, obtained by hydrothermal procedure, [13], using as raw materials solutions of sodium silicate and aluminate of technical grade (Fig. 1), have been characterized chemically, roentgenographycally, derivatographycally and by adsorption. Their mean granula size was measured by means of optical microscope. Chemical composition was determined as follows : silicon—gravimetrically ; aluminium—complexometrically ; sodium—flamphotometrically and iron—colorimetrically with *o*-phenantroline. At the same time the comparative determinations of bulk density and powder density [14] were carried out. Adsorption of the molecular dispersed pigments was appreciated colorimetrically at $\lambda = 582$ cm^{-1} for methylene blue.

Table 1

World Consumption Estimation of Synthetic Zeolites [5]

	1975		1977		1979		1981	
	10^3t	%	10^3t	%	10^3t	%	10^3t	%
North America								
detergents	—	—	27	42	90	67	225	80
catalysts	20	64.4	23	34	28	20	35	12.5
adsorbants	11	35.6	14	22	16	13	20	7.5
Total	31		64		134		280	
Latin America								
detergents	—	—	—	—	—	—	—	—
catalysts	3	30	3	25	4	28.5	5	27.7
adsorbants	7	70	9	75	10	71.5	13	72.3
Total	10		12		14		18	
West Europe								
detergents	—	—	27	71	90	87	225	93.3
catalysts	3	37.5	4	10	4	4.3	5	2.2
adsorbants	5	62.5	7	19	9	8.7	11	4.5
Total	8		38		103		241	
Near and Far East								
detergents	—	—	—	—	29	60	90	77.6
catalysts	3	27.3	5	31.2	6	11.7	8	7.8
adsorbants	8	72.7	11	68.8	14	28.3	18	15.6
Total	11		16		49		116	
WORLD TOTAL	60		130		300		655	

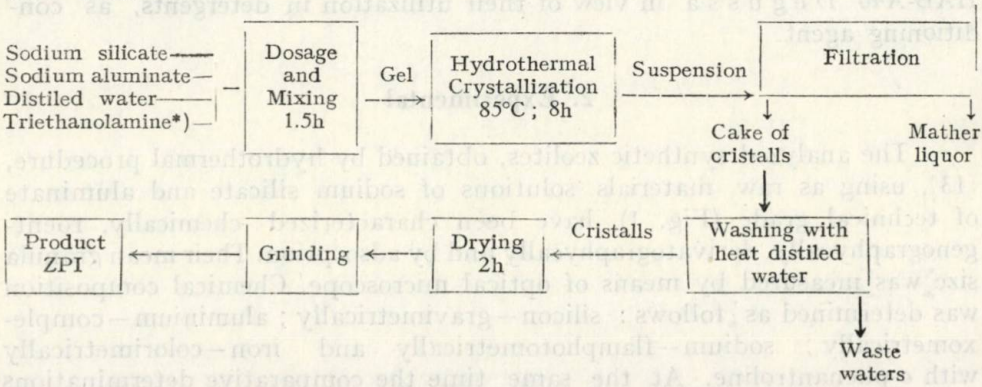

Fig. 1. — Flow diagram of hydrothermal synthesis of ZPI products.

*) Triethanolamine used only for ZPI-12 obtaining product with a significant diminishing of iron ions content.

3. Results and Discussions

Analysis of the products, done in comparison with HAB-A40 zeolite, led to the results summarized in Table 2, which shows a good agreement with principal characteristics as regards the efficient behaviour of reference product in float. Thus, roentgenographical and adsorptive measurements point out a NaA type structure, except the product ZPI-12 which is a mixture of NaA and NaX. Mean granule size is also in good agreement with the data in literature [7] referring to zeolites employed in detergents conditioning.

Table 2

Physico-chemical Properties of the Products

Characteristics	HAB A40 [6]	Present values		
		ZPI-10	ZPI-11	ZPI-12
Mean granule size, [μ]	4	4	3	3
Maximum size, [μ]	20	10	6	8
Density, [g/cm³]	2	2.12	2.08	2.09
Bulk density, [g/l]	350	381.7	371.4	369.9
Powder density, [g/l] ; [14]	450	473.5	469.9	472.1
pH [15]	12	10	10	10
Chemical composition, [%]				
Na_2O	17	17.13	16.72	14.90
Al_2O_3	28	30.63	33.63	26.46
SiO_2	33	36.22	37.70	40.62
H_2O	22	16	12.21	18
Traces of iron, [p.p.m.]	150	310	174	59
Ion exchange capacity against Ca^{2+}, [mg CaO/g]	160	171.7	161,2	169.8
Type of zeolite structure	A	A	A	A+X

It can be seen, especially, the positive influence of the synthetical procedure of ZPI-12 on its Fe content.

Since bonding capacity of Ca^{2+} and Mg^{2+} is the main property of zeolites in washing process, exchange kinetics of these ions was carried out at 22°C, for a zeolite concentration of 2 g/l (Fig. 2). As it comes from Fig. 2 all synthesized products exhibit a fast kinetics of Ca^{2+} bonding and a high exchange capacity. For a more suggestive expression of the results as for a better comparison with literature data, exchange kinetics was also expressed by variation of remanent hardness vs. time (Fig. 3). The capacity of the ZPI products is similar to that of HAB-A40. The equilibrium concentration is achieved after 10—15 min., yielding a deep softening of water.

Practical utilization of zeolites requires the knowledge of the rate of saturation degree achievement with Ca^{2+}, because their efficient behaviour in float depends on this degree ; its quantitative expression can be done according to Reichenberg [8] as Q/Q_∞, where Q is the amount of Ca^{2+} retained at any instant and Q_∞ —the maximum exchange capacity. In

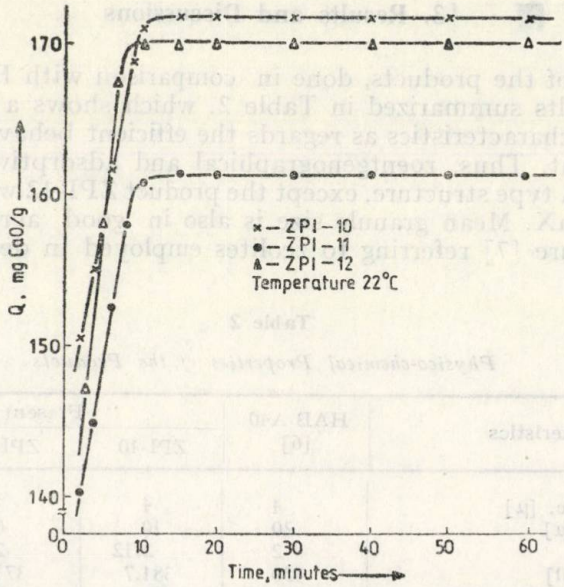

Fig. 2. — Kinetics of ion exchange for Ca^{2+} on ZPI products.

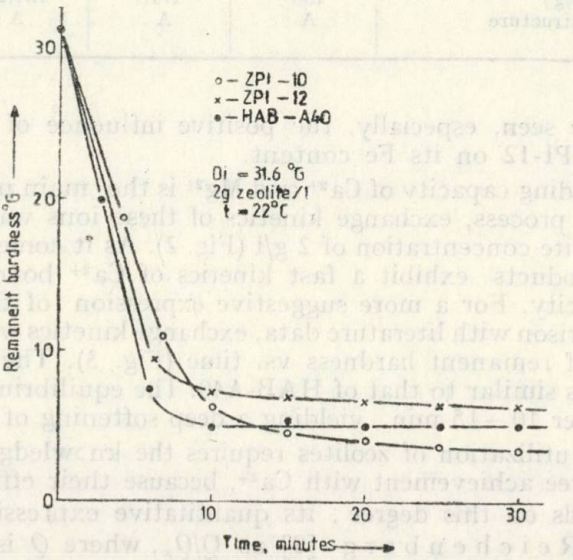

Fig. 3. — Variation of remanent hardness vs. time on tested products.

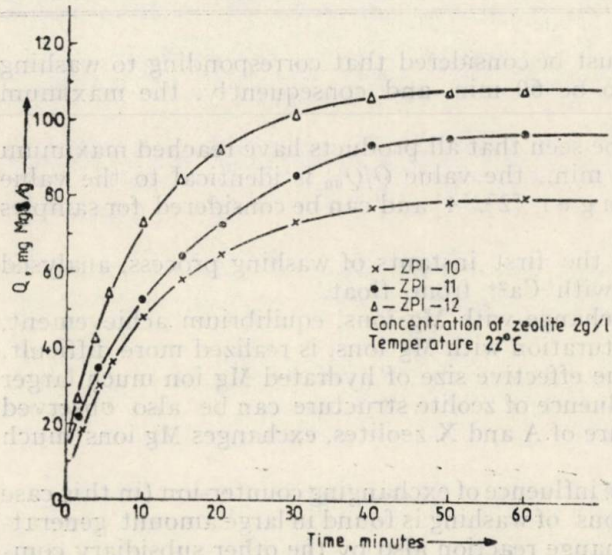

Fig. 5. — Kinetics of ion exchange for Mg^{2+} on ZPI products.

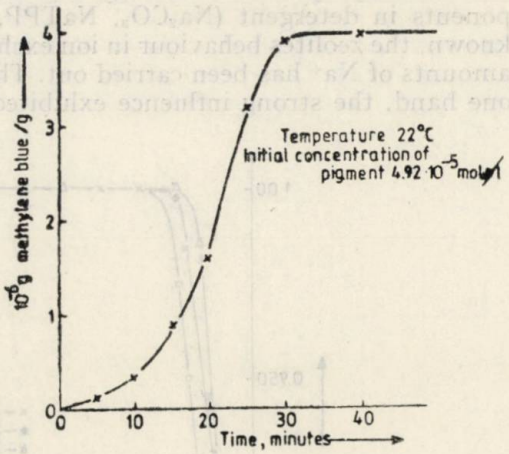

Fig. 6. — Ion exchange capacity against Ca ions on ZPI-12 vs. concentration of Na counter-ion.

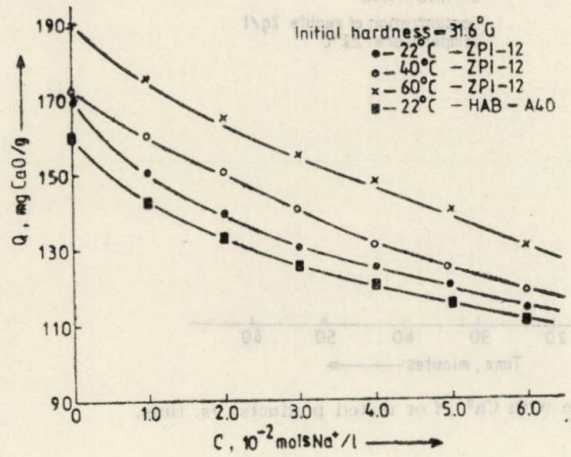

Fig. 7. — Kinetics of adsorption of methylene blue on ZPI-12.

this case the value of Q_∞ must be considered that corresponding to washing process time appreciated to be 60 min. and, consequently, the maximum value was noted Q_{60}.

Since in Fig. 4 it can be seen that all products have reached maximum exchange capacity after 60 min., the value Q/Q_{60} is identical to the value Q/Q_{70} employed by S c h w u g e r [2], [4] and can be considered for samples comparison.

It can be seen that in the first instants of washing process, analysed zeolites became saturated with Ca^{2+} from float.

As regards the ion exchange with Mg ions, equilibrium achievement, (Fig. 5) as well as zeolite saturation with Mg ions, is realized more difficult. This can be explained by the effective size of hydrated Mg ion much larger than that of Ca one. The influence of zeolite structure can be also observed the product ZPI-12, a mixture of A and X zeolites, exchanges Mg ions much faster.

Since the unfavourable influence of exchanging counter-ion (in this case Na^+, which in real conditions of washing is found in large amount generative not only by zeolite exchange reaction also by the other subsidiary components in detergent (Na_2CO_3, NaTPP, Na_2SO_4, bleaching agent, etc.)) is known, the zeolites behaviour in ion exchange process in presence of different amounts of Na^+ has been carried out. The results in Fig. 6 point out, on the one hand, the strong influence exhibited by high concentrations of Na^+ on

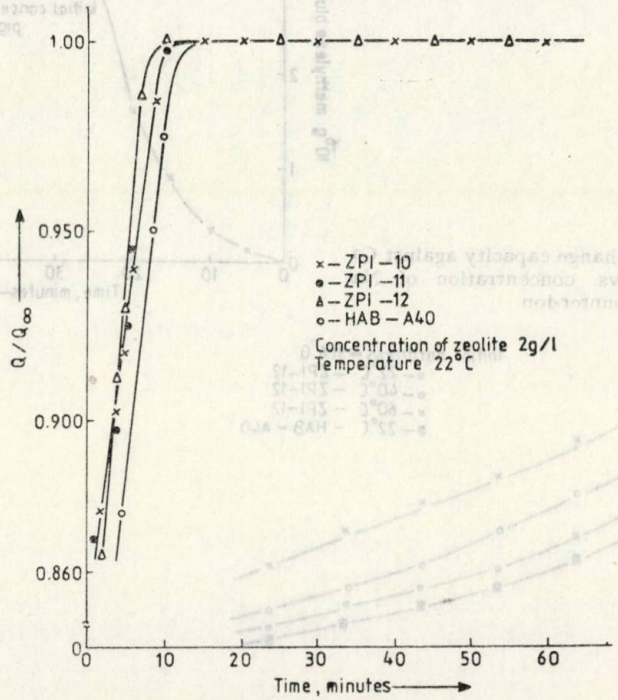

Fig. 4. — Saturation degree with Ca^{2+}, f or tested products, vs. time.

ion exchange capacity decrease, in the temperature range of 22°...60°C, and on the other hand, a very good agreement as regards the behaviour of the reference product HAB-A40.

During water softening by Ca and Mg ions retaining, zeolites exhibit in washing medium also another favourable action, i.e. adsorption of molecular dispersed pigments. To prove this fact, the adsorption of methylene blue, as reference positive charged pigment, has been studied (Fig. 7). It can be seen that methylene blue molecules are adsorbed on anionic zeolitic carcass by electrostatic forces, fact representing an advantage in washing process.

4. Conclusions

Analysis of physico-chemical properties, which are involved in efficacity of zeolites utilization in washing process, points out for the zeolite products ZPI, on the one hand, a good agreement with those of the commercial product HAB-A40 and, on the other hand, a significant diminishing of iron ions content in zeolite, due to the presence of triethanolamine in the hydrothermal synthesis medium.

Retaintion kinetics of Ca and Mg ions is influenced by concentration of sodium ions resulted from ion exchange or from the compounds, causing the ionic strenght of detergents.

Adsorption studies of the molecular dispersed pigments show a good retaintion capacity against those positively charged simultaneously, with the softening action of the water in washing float.

Received, May 10, 1985

Polytechnic Institutes, Jassy,
Department of Physical and
General Chemistry

REFERENCES

1. Berth P., J. Am. Oil Chem. Soc., **55**, 52 (1978).
2. Schwuger M.Y., Smolka H.G., Coll. Polym. Sci., *254*, 1 062 (1976).
3. Smolka H.G., Schwuger M.Y., Coll. Polym. Sci., *256*, 270 (1978).
4. Schwuger M. Y., Smolka H. G., Coll. Polym. Sci., *256*, 1 014 (1978).
5. * * * European Chemical News, 35 (1977).
6. * * * *Natriumaluminosilikat HAB-A40 Degussa.*
7. Cruceanu M., Popovici Ev., Patent R.S.R., Nr. *81 891* (1975).
8. Reichenberg D., J. Am. Chem. Soc., **76**, 579 (1953).
9. Despotovic R., Croat. Chem. Acta., **48**, 683 (1976).
10. Berth P., Jakovi G., Schmadel E., Schwuger M.Y., Krach C., Angew. Chem., **87**, 115 (1975).
11. Jakovi G., Schwuger M.Y., Chem. Z., **99**, 182 (1975).
12. Vincekovic N.F., Sekovanic L., Zitnic D., Technology, **27**, 251 (1980).
13. Cruceanu M., Popovici Ev., An. Şt. Univ. „Al. I. Cuza", Iaşi, **19**, 2, s. I,209 (1973).
14. * * * DIN 5 394, 1978.
15. * * * DIN 53 200, 1978.

ZEOLIŢI SINTETICI PENTRU CONDIŢIONAREA DETERGENŢILOR
I. PROPRIETĂŢILE FIZICO-CHIMICE ALE ZEOLIŢILOR

(Rezumat)

Cu scopul de a găsi o substituţie cît mai corespunzătoare, din punct de vedere economic, toxicologic şi ecologic, a tripolifosfatului de sodiu din amestecurile detergente, se cercetează unele proprietăţi fizico-chimice care condiţionează utilizarea zeoliţilor sintetici NaA în calitate de component subsidiar în recepturile detergente.

Utilizarea zeoliţilor în procesele de condiţionare a detergenţilor se bazează pe valoarea ridicată a capacităţii de schimb ionic faţă de ionii de calciu şi de magneziu şi pe cinetica rapidă a schimbului ionic.

Se cercetează dependenţa proprietăţilor de schimb ionic în funcţie de mărimea particulelor, de temperatură, de concentraţia ionilor de calciu şi magneziu, de pH şi de concentraţia contraionilor de sodiu.

BULETINUL INSTITUTULUI POLITEHNIC DIN IAȘI
Tomul XXXI (XXXV), Fasc. supl., 1985
Secția II
CHIMIE ȘI INGINERIE CHIMICĂ

D.C. 546.264 ; 661.521

STUDY OF THE CALCIUM CARBONATE DECOMPOSITION PROCESS WITH SOLID AMMONIUM CHLORIDE

BY

AL. SZÉP, LIVIA IFRIM, CORNELIA LEONTE and C. CALISTRU

1. Introduction

The development in sustained rate of some industries, great users of soda ash, involved relative high rates in manufacture of this product. However, due to some large disadvantages of the Solvay's procedure, its manufacture development is troubled by a series of factors such as surface water pollution and loss of raw materials [1] ... [3].

These aspects imposed the approach of investigations regarding the modification of present technology on the line of opening the classical manufacture cycle with obtention of solid ammonium chloride by different methods such as evaporation, cooling and salting out, [1], [4], [5] as a recycling procedure of „orientation agent", i.e. ammonia. The separated solid ammonium chloride can be employed to decompose calcium carbonate, a process under study in the present paper. The process allows, besides ammonia recycling, obtention also of gases product, necessary in carbonation step, with lower energy consumption than for those produced by present—day lime furnaces. In addition, the obtained solid ammonium chloride can be used in other different fields of national economy such as industry, agriculture, constructions, etc. [1], [4], [6] ... [8].

The present paper deals with macrokinetic mechanism and mathematical modelling of the process of calcium carbonate decomposition with solid ammonium chloride.

2. Macrokinetic Mechanism

If ammonium chloride of technical degree is employed to decompose different qualities of calcium carbonate, at thermical levels corresponding to „sublimation" of ammonium chloride, the macrokinetic mechanism of the process can be represented by the equations :

$$[CaCO_3 + A'']_{s_1} + [NH_4Cl + A'']_{s_2} + [A_3'']_g \rightarrow$$

$$\{[CaCO_3 + A'']_{s_1} + [NH_4Cl + A'']_{s_2} + [CaCl_2 + A'']_{s_3}\}_g + [NH_3 + \tag{1}$$

$$+ HCl + CO_2 + H_2O + NH_4Cl + A_3'']_g,$$

$$NH_4Cl_{[]_s} \rightarrow NH_4Cl_{[]_g} \tag{2}$$

$$NH_4Cl \rightleftharpoons HCl + NH_3, \tag{3}$$

$$CaCO_3 + 2HCl = CaCl_2 + H_2O + CO_2. \tag{4}$$

If the temperature is greater than that of the $CaCl_2 . nH_2O$ crystallohydrates formation, the three macroscopic elemental processes, i.e. (2), (3)

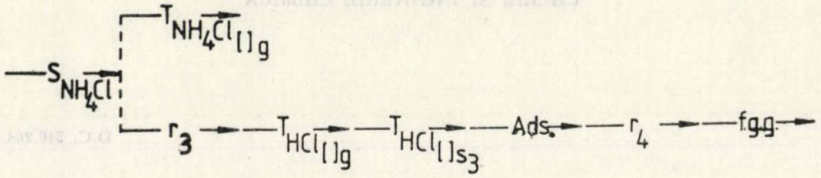

Fig. 1. — Structure of the process.

and (4), describe with enough precision the real process, so that the process structure is that given in Fig. 1.

The structure presented in Fig. 1 shows that at both the level of ammonium chloride granule as well as calcium carbonate granule the process under study can be included in unitary process of adsorption reaction formation and growing of germs type (ads. — r—f.c.g.) [9], [10].

3. Mathematical Modelling

3.1. Mathematical Models of Mass Balance

In order to develop the mathematical models of mass balance, the transformation degree of the three elemental process have been defined and, on the basis of transformation relations :

$$m^{0}_{CaCO_3[]_{s_1}}\eta_1 = \frac{M_{CaCO_3}}{M_{CaCl_2}} m_{[]_s} \bar{X}_{CaCl_2[]_s}, \tag{5}$$

$$m^{0}_{NH_4Cl[]_{s_2}}\eta_{[]} = m^{\circ}_{NH_4Cl[]_{s_2}} - m_{[]_s} \bar{X}_{NH_4Cl[]_s}, \tag{6}$$

$$m^{0}_{NH_4Cl[]_{s_2}}\eta_{[]}\eta_{NH_4Cl} = \frac{M_{NH_4Cl}}{V_M} V_{[]_g} X_{NH_3[]_g}, \tag{7}$$

the mathematical models of secondary balances for components and phases, have been established. These balances are given in Table 1.

To solve the mathematical models from Table 1, the determination of three quantities is necessary, namely : $\bar{X}_{CaCl_2[]_s}$, $X_{NH_4Cl[]_s}$ and $X_{NH_3[]_g}$. The first two quantities do not involve special problems, but determination of $X_{NH_3[]_g}$, is not possible.

If X'_{NH_3} is the content of ammonia in gaseous phase, the balance of this phase is given in Table 2.

3.2. Macrokinetical and Mathematical Models

The possible macrokinetic models of the process have been established based on the macrokinetic modelling theory [9] (s. Table 3).

Under fixed bed conditions, the macrostructural element can be made up by calcium carbonate granule surrounded by gaseous phase of HCl, CO_2, H_2O, A''_3 and NH_3.

Table 1

Mathematical Models of Mass Balance

Phase	Component	$m(V)$
Solid	$CaCO_3$	$m_{CaCO_3[]_s} = m^0_{[]_{s1}} \bar{X}_{CaCO_3[]_1} - \frac{M_{CaCO_3}}{M_{CaCl_2}} m_{[]_s} \bar{X}_{CaCl_2[]_s}$
	NH_4Cl	$m_{NH_4Cl[]_s} = m_{[]_s} \bar{X}_{NH_4Cl[]_s}$
	$CaCl_2$	$m_{CaCl_2[]_s} = m_{[]_s} \bar{X}_{CaCl_2[]_s}$
	A″	$m_{A''} = m^0_{A''_1[]_{s1}} + m^0_{A''_2[]_{s2}}$
	Total	$m_{[]_s} = \frac{m^0_{[]_{s1}} + m^0_{[]_{s2}} (1 - \bar{X}^0_{NH_4Cl[]_{s2}})}{1 - 0{,}99\bar{X}_{CaCl_2[]_s} - \bar{X}_{NH_4Cl[]_s}}$
Gaseous	NH_3	$V_{NH_3[]_g} = V_{[]_g} X_{NH_3[]_g}$
	CO_2	$V_{CO_2[]_g} = \frac{V_M}{M_{CaCl_2}} m_{[]_g} \bar{X}_{CaCl_2[]_s}$
	HCl	$V_{HCl[]_g} = V_{[]_g} X_{NH_3[]_g} - 2\frac{V_M}{M_{CaCl_2}} m_{[]_g} \bar{X}_{CaCl_2[]_s}$
	H_2O	$V_{H_2O[]_g} = \frac{V_M}{M_{CaCl_2}} m_{[]_s} \bar{X}_{CaCl\,[]_s}$
	NH_4Cl	$V_{NH_4Cl[]_g} = \frac{V_M}{M_{NH_4Cl}} (m^0_{[]_{s2}} \bar{X}^0_{NH_4Cl[]_{s2}} - m_{[]_s} \bar{X}_{NH_4Cl[]_s}) - V_{[]_g} X_{NH_3[]_g}$
	A''_3	$V_{A''[]} = V^0_{A''[]_g}$
	Total	$V_{[]_g} = \frac{\left(m^0_{[]_{s^2}} \bar{X}^0_{NH_4Cl[]_{s2}} - \frac{m^0_{[]_{s1}} + m^0_{[]_{s2}} (1 - \bar{X}^0_{NH_4Cl[]_{s2}})}{1 - 0{,}99\bar{X}_{CaCl_2[]_s} - \bar{X}_{NH_4Cl[]_s}}\right) \frac{V_M}{M_{NH_4Cl}} + V^0_{[]_g}}{1 - X_{NH_3[]_g}}$

Table 3

Macrokinetic and Mathematical Models

Controlling step	Macrokinetic model	Mathematical model for a macrostructural element
Transfer of HCl through gaseous phase	$(-\bar{q}) = K_{T_{HCl[]_g}} C_{HCl[]_g}$	$\frac{\rho^* R}{3} \cdot \frac{d\eta}{d\tau} = K_{T_{HCl[]_g}} C_{HCl[]_g}$
Transfer of HCl through crust	$(-\bar{q}) = D_{HCl} \frac{\partial C_{HCl}}{\partial X}$	$\frac{\rho^* R d\eta}{3(1-\eta)^{2/3} d\tau} = \frac{1}{2} D_{HCl} \frac{\partial C_{HCl}}{\partial X}$
Chemical reaction	$(-\bar{r}) = K C^n_{HCl}$	$\tau = \frac{2\rho^* R}{3KC^0_{HCl}} \int_0^{\eta} (1-\eta)^{n+2/3} d\eta$
Formation and growing of germs	$(-\bar{r}) = K C^n_{HCl} \tau^{-m}$	$\frac{2\rho^* R d\eta}{3 d\tau} = K(1-\eta)^{2/3+n} \tau^{-m}$ $\ln[-\ln(1-\eta)] = \ln K^* + (1-m)\ln \tau$ for $n = 1/3$

Table 2

Balance Equations of the Gaseous Phase

Component	Equation
NH_3	$V_{NH_3}=\dfrac{V^0_{A^{\sim}_3[]_g}+2(V_M/M_{CaCl_2})m_{[]_s}\overline{X}_{CaCl_2[]_s}}{1-X'_{NH_3}}X'_{NH_3}$
H_2O	$V_{H_2O}=\dfrac{V_M}{M_{CaCl_2}}m_{[]_s}\overline{X}_{CaCl_2[]_s}$
CO_2	$V_{CO_2}=\dfrac{V_M}{M_{CaCl_2}}m_{[]_s}\overline{X}_{CaCl_2[]_s}$
NH_4Cl	$V_{NH_4Cl}=\dfrac{V_M}{M_{NH_4Cl}}(m^0_{[]_{s2}}\overline{X}^0_{NH_4Cl[]_{s2}}-m_{[]_s}\overline{X}_{NH_4Cl[]_s})-\dfrac{V^0_{A^{\sim}_3[]_g}+2(V_M/M_{CaCl_2})m_{[]_s}\overline{X}_{CaCl_2[]_s}}{1-X'_{NH_3}}X'_{NH_3}$
HCl	$V_{HCl}=\dfrac{V^0_{[]_g}+2(V_M/M_{CaCl_2})m_{[]_s}\overline{X}_{CaCl_2[]_s}}{1-X'_{NH_3}}X'_{NH_3}-2V_M/M_{CaCl_2}m_{[]_s}\overline{X}_{CaCl_2[]_s}$
$A^{\sim}_3$	$V_{A^{\sim}_3}=V^0_{A^{\sim}_3}$
Total	$V_T=V^0_{A^{\sim}_3[]_g}+\dfrac{V_M}{M_{NH_4Cl}}(m^0_{[]_{s2}}\overline{X}^0_{NH_4Cl[]_{s2}}-m_{[]_s}\overline{X}_{NH_4Cl[]_s})+\dfrac{V^0_{[]_g}+2(V_M/M_{CaCl_2})m_{[]_s}\overline{X}_{CaCl_2[]_s}}{1-X'_{NH_3}}X'_{NH_3}$

In isothermic discontinuous regime, without volume variation in the Eq. (4) ($\Delta n = 0$) and, for a spherical granule, the model of macrostructural element has the form :

$$\frac{\rho^* R}{3}\cdot\frac{d\eta}{(1-\eta)^{2/3}d\tau}=-(-\dot{r}_{CaCO_3}). \tag{8}$$

The mathematical models based on macrokinetical models, developed by using Eq. (8), are presented in Table 3.

4. Mathematical Model of Real Development of the Process

4.1. Experimental

Decomposition of calcium carbonate with ammonium chloride has been carried out in a device simulating batch reactor with fixed bed. The mixture of raw materials, weighted with high precision, in short porcelain crucibles, entered the muffle furnace at constant temperature. After dif-

ferent time, the samples have been taken out and „congelated" by dissolving in bidistilled water. Then the content of $CaCl_2$ and NH_4Cl was quantitatively determined from the resulted solution.

The transformation degree has been calculated with the relation:

$$\eta = \frac{m_{CaCl_2[]L}}{\frac{M_{CaCl_2}}{M_{CaCO_3}} \overset{0}{m}_{[]_{s_1}} X^0_{CaCO_3[]s_1}} \cdot \tag{9}$$

The experiments have been performed in the temperature range of 473°...773° K, granule size $\bar{d}_{p1}=0{,}315$ mm ; $\bar{d}_{p2}=0.085$, 0.225 and 0.565 mm, the excess of ammonium chloride of 0 ; 50 and 100%, moisture content of 0 ; 10 ; 20 and 30%, reported to dried calcium carbonate, without circulation of gaseous phase.

4.2. Results and Discussion

The experimental data, presented in Figs. 2...5, show the following:

a) The temperature has a significant and favourable influence on overall rate of the process, independent of granule size, ammonium chloride excess and moisture content (Fig. 2).

b) The granule size of lime stone has also a significant influence. As granule size increases, the transformation degree decreases (Fig. 3).

The other parameters, i.e. the granule size of ammonium chloride, its excess and moisture, have no significant influence on the overall rate of the process (Figs. 4 and 5).

4.3. Determination of the Mathematical Model Describing the Real Development of the Process under Given Experimental Conditions

In order to establish the above mentioned model, the primary experimental data have been graphically processed. For this reason, the data have been plotted in coordinates proper to the equations summarized in Table 3.

The experimental data are in good agreement with the model described by the equation:

$$\ln [-\ln(1-\eta)] = \ln K^* + (1-m) \ln \tau, \tag{10}$$

plotted in Fig. 6.

Fig. 6 shows that in the investigated temperature range, these are two distinct regions.

The experimental factor $1-m$ and the constant K^* of Eq. (10), calculated graphically, are given in Table 4.

Under the conditions mentioned in Table 4, the mathematical model that describes the real development of the process is:

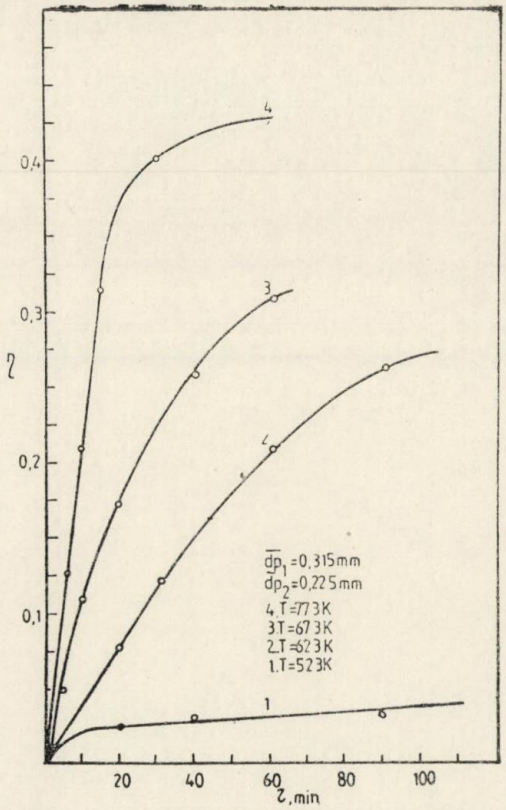

Fig. 2. — Dependence η vs. τ at different temperatures.

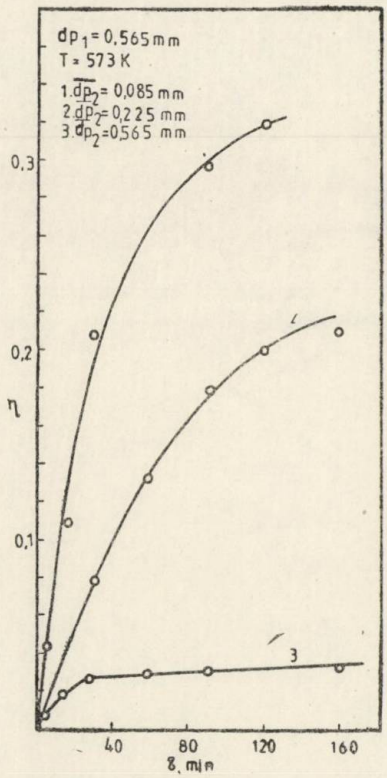

Fig. 3. — Dependence η vs. τ for different granule size of limestone.

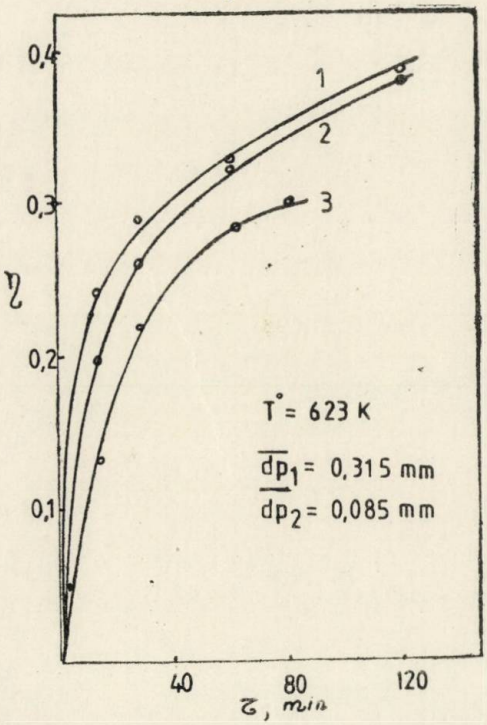

Fig. 4. — Dependence η vs. τ for different excess of ammonium chloride: *1*— 100%; *2*— 50%; *3*— 0%.

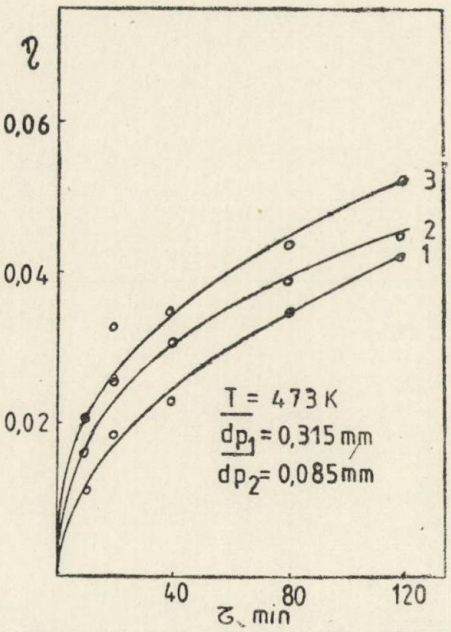

Fig. 5. — Dependence η vs. τ for different moistures: *1*— 10%; 2-20%; *3*— 30%.

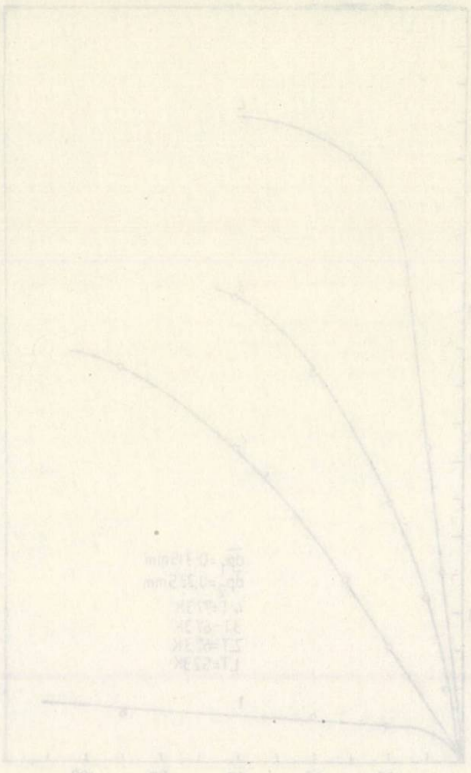

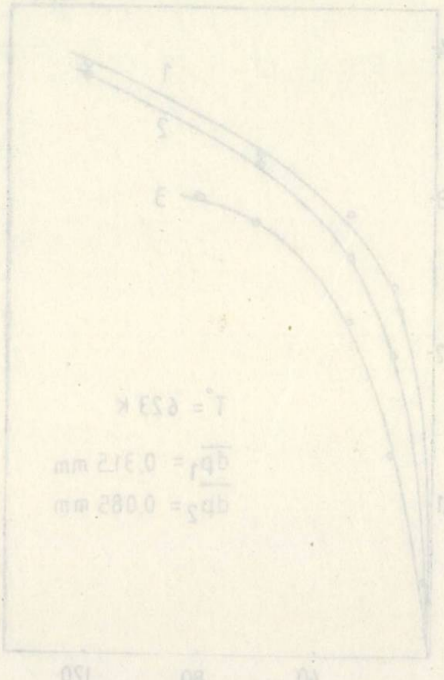

Table 4

Values of $1-m$ *and* K^* *for* $\bar{d}_{p_1}=0.315$ *mm and* $\bar{d}_{p_2}=0.225$ *mm*

Experimental conditions		Region 1		Region 2	
NH_4Cl excess, [%]	T, [°K]	$1-m$	K^*	$1-m$	K^*
0.0	773	0.952	0.0268	0.35	0.1561
	673	1.041	0.0107	—	—
	623	1.000	0.0039	0.275	0.0248
50.0	673	1.030	0.025	0.250	0.2446
	623	1.000	0.013	0.250	0.1553
	573	0.980	0.004	0.250	0.0780
	523	0.955	0.023	—	—

Table 5

Values of A *and* E *from Eq.* (13)

Conditions		Region	A	E cal/mol
NH_4Cl excess %	$\bar{d}_{p_2}$ mm			
100	0.085	1	10.3	5 001.0
		2	207.0	8 933.0
50	0.565	1	99.5	11 081.6
		2	10.88	5 129.0

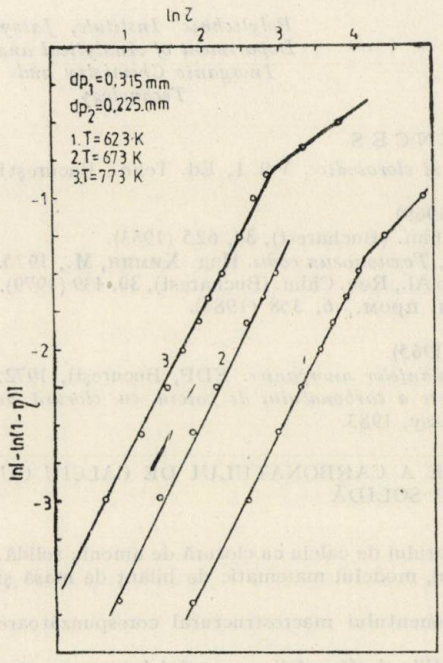

Fig. 6. — Dependence $\ln[-\ln(1-\eta)]$ vs. $\ln\tau$ at different temperatures.

$$\eta = 1 - e^{K^*\tau} \tag{11}$$

for the region 1 and

$$\eta = 1 - e^{K^*\sqrt[4]{\tau}} \tag{12}$$

for the region 2, namely equations describing the process of formation and growing of solid germs.

Dependence of K^* on temperature, under mentioned working conditions, is given by an Arrhenius' equation:

$$K^* = Ae^{-E/RT}, \tag{13}$$

where A and E depend on working conditions as shown in Table 5.

5. Conclusions

From the theoretical and experimental investigations presented above, the following conclusion may be drawn:

1. The macrokinetic mechanism, the mass balance models and mac-

rokinetic and mathematical models that describe quantitatively the development of decomposition process of calcium carbonate with ammonium chloride have been established.

2. The experimental results, obtained under the conditions of a fixed bed batch reactor, are in good agreement with mathematical model given by Eqs. (10)...(12), i.e. the controlling step of the process is the formation and growing of solid germs.

Notations

m_{A_i}, V_{A_i} — mass or volume of A_i, [Kg]; [m^3];
X_{A_i}, $\bar{X}_{A_i}$ — mass or volume fraction of A_i;
M_{A_i} — molecular weight of A_i, [Kg/Kmol];
V_M — molar volume, [m^3/Kmol];
n_{A_i} — moles of component A_i;
C_{A_i} — concentration of A_i, [mol/m^3];
τ — reaction time, [s];
ρ^* — molar density of solid, [Kmol/m^3];
R — granule radius, [m];
K_T — transfer constant, [m/s];
D — diffusion coefficient, [m^2/s];
d_{p_1} — average diameter of NH_4Cl particle, [mm];
d_{p_2} — average diameter of lime stone particle, [mm];
n — reaction order;
$1-m$ — exponential factor.

Symbols

$[\ ]_{g,s_1,\ldots_3}$ — gaseous phase 1 and solid phase 1, 2 and 3;
0 — initial instant.

Received, April 18, 1985

Polytechnic Institute, Jassy, Department of Analytical and Inorganic Chemistry and Technology

REFERENCES

1. Filipescu L., *Tehnologia produselor sodice şi clorosodice*. Vol. I, Ed. Tehn., Bucureşti, 1983, 268.
2. Peteu I., Rev. Chim. (Bucharest), **19**, 72 (1969).
3. Calistru C., Ifrim L., Szép Al., Rev. Chim. (Bucharest), **34**, 625 (1983).
4. Сокин И.Н., Красенинников С.А., *Технология соды*. Изд. Химия, М., 1975.
5. Calistru C., Ifrim L., Leonte C., Szép Al., Rev. Chim. (Bucharest), **30**, 439 (1979).
6. Ткач Г.А., Михайлов Ф.К., Хим. пром., *6*, 358 (1981).
7. Ana I., Petrol şi gaze, **24**, 205 (1973).
8. Salecki, A., Przem. Chemyczny, **45**, 555 (1965).
9. Calistru C., Leonte C., *Tehnologia substanţelor anorganice*. EDP, Bucureşti, 1972.
10. Szép Al., *Modelarea procesului de descompunere a carbonatului de calciu cu clorură de amoniu*. Ph., D. Diss., Polyt. Inst., Jassy, 1983.

STUDIUL PROCESULUI DE DESCOMPUNERE A CARBONATULUI DE CALCIU CU CLORURĂ DE AMONIU SOLIDĂ

(Rezumat)

Se cercetează procesul descompunerii carbonatului de calciu cu clorură de amoniu solidă. Se stabileşte mecanismul macrocinetic al procesului, modelul matematic de bilanţ de masă şi se indică mărimile necesare rezolvării acestuia.

Se elaborează modelele matematice ale elementului macrostructural corespunzătoare modelelor macrocinetice posibile.

Rezultatele experimentale obţinute în condiţiile desfăşurării procesului într-un reactor în strat fix şi în regim izoterm sînt verificate de modelul matematic corespunzător modelului macrocinetic transformare.

BULETINUL INSTITUTULUI POLITEHNIC DIN IAȘI
Tomul XXXI (XXXV), Fasc. supl., 1985
Secția II
CHIMIE ȘI INGINERIE CHIMICĂ

C.D. 547.792

ISOMÈRES *E* ET *Z* D'YLURES DE 1-2-4H TRIAZOLUM

PAR

MAGDA PETROVANU, GH. SURPĂȚEANU, MIRCEA CONSTANTINESCU
et ALAIN LABLACHE COMBIER

1. Introduction

Dans une Note antérieure [1] on a montré que dans les cyclimmonium ylures (1) il n'existe pas de rotation libre autour de la liaison $\overset{+}{N} - \overset{-}{C}$.

La barrière d'énergie autour de cette liaison, calculée à l'aide de la méthode de CNDO/2, [2], est de 14 Kcal/mol. Il est connu que les cycloimmonium ylures dans lesquels le carbanion et le hétérocycle sont coplanaires ont une stabilité chimique appreciable [3]. Nous rappelons dans ce sens le fait que pour la dicyanopyridine (2) les données par les spectres de diffraction des rayons X confirment la coplanarité de l'ensemble ylurique [4].

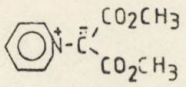

(1)

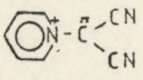

(2)

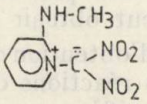

(3)

Toutefois récemment [5] on a montré qu dans l'ylure (3) cristallisé le plan du hétérocycle et le plan du carbanion ylurique font un angle de 92°. Ce résultat paraît être en contradiction avec les considérations qualitatives généralement acceptées selon lesquelles les systèmes yluriques plans sont plus stables parce que dans ces conditions tant la délocalisation prononcée de la charge négative sur le carbanion ylurique que l'interaction de résonance sont mieux assurées.

Les résultats expérimentaux ci-dessus mentionnés, tant pour l'ylure (2) que pour l'ylure (3), imposent la conclusion qu'il faut effectuer des mesures sur chaque système ylurique en particulier et en plus il faut aussi tenir compte de l'état dans lequel se trouvent les systèmes yluriques, c'est-à-dire en solution ou cristallisés.

2. Résultats et discussions

Le fait qu'il n'existe pas de rotation libre autour de la liaison ylurique nous a suggéré l'idée de synthétiser des systèmes yluriques dissymétriques qui pourraient exister sous forme des isomères *E* et *Z*. Ainsi, à partir des

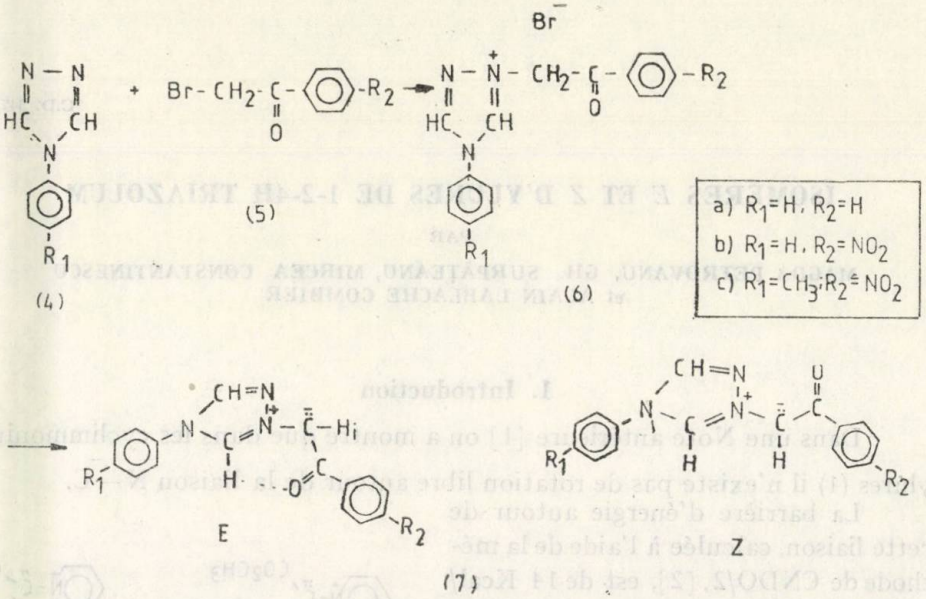

sels de cycloimmonium provenant du [1,2-4H] triazole traités par la triéthylamine on peut obtenir les triazolium ylures isomères 7*E* et 7*Z*.

Les méthodes d'obtention des ylures (7) *in situ* afin de les utiliser comme dipoles 1 3 dans des réactions de cycloaddition sont décrites dans des travaux antérieurs [7], [8].

Les ylures (7 *b*) et (7 *c*) sont stables; par contre l'ylure (7 *a*) souffre une réaction de dimérisation par cycloaddition 3 + 3 conduisant aux produit (8 *a*). Cette transformation implique une aromatisation.

Les ylures (7 *b*) et (7 *c*) existent sous forme d'isomères *E* et *Z*. Les spectres RCN-H¹ des sels (6 *a*, *b*, *c*), ceux des ylures (7 *b*, *c*) et des dimères (8) diffèrent beaucoup entre eux.

Dans les sels (6) le carbone méthylénique est tétraédrique, dans les ylures (7) le carbanion ylurique est trigonal. Le produit (8) ne possède que des protons aromatiques.

Dans le produits (7 *b*) et (7 *c*) le proton ylurique H_i et le proton H_5 résonent chacun à des fréquences différentes. Dans les deux cas la somme des intégrales des deux pics H_i et H_5 correspond à un proton.

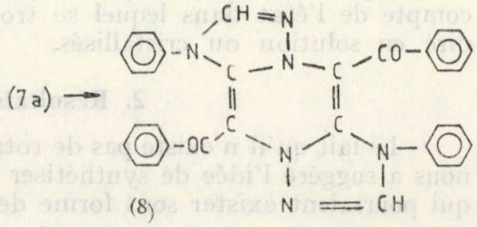

Les intensités relatives des deux pics correspondants aux pro-

Tableau 1

Caractéristiques RMN-H¹ des sels et des ylures de cycloimmonium

Composé	Valeurs (ppm)[a]	Composé	Valeurs (ppm)[a]
(6 *a*)	6.53.*s*.2H(CH_2) 7.86.*m*.10H(2Ph) 10.03.*s*.1H.(H-3) 11.09.*s*.1H(H-5)	(6 *b*)	6.53.*s*.2H(CH_2) 7.80.*m*.5H(Ph) 8.34.*j*.8.52.4h(Ph-NO_2) J_{AB}=9.23 9.93.*s*.1H(H-3) 10.83.*s*.1H(H-5)
(6 *c*)	2.44.*s*.3H(CH_3) 6.53.*s*.2H(CH_2) 7.52 ; 7.81.4H(Ph−CH_3) J_{AB}=8.58 8.33 ; 8.51.4H(Ph−NO_2) J_{AB}=9,23 9.90.*s*.1H(H-3) 10.80.*s*.1H(H-5)	(7 *b*)(*E*+*Z*)	7.09.*s*.H_i(*E*) 7.17.*s*.H_i(*Z*) 7.71.*m*.5H(Ph) 8.15 ; 8.28.4H(Ph−NO_2) J_{AB}=8,36 9.05.*s*(H-5)(*Z*) 9.52.*s*.1H.(H-3)(*E*+*Z*) 11.51.*s*.(H-5)(*E*)
(7 *c*)(*E*+*Z*)	2.44.*s*.3H(CH_3) 7.04.*s*.H_i(*E*) 7.13.*s*.H_i(*Z*) 7.42 ; 7.72.4H(Ph−CH_3) J_{AB}=8,39 8.02 ; 8.18.4H(Ph−NO_2) J_{AB}=8,36 9.02.*s*.H-5(*Z*) 9.49.*s*.1H.H-3(*E*+*Z*) 11.51.*s*.H-5(*E*)	(8 *a*)	7.50 ; 812.*m*.20H(4Ph) 9.92.*s*.2H(H-3)

s=singulet ; *m*=multiplet ; *AB*=spectre *AB* aromatique ; *a*=80 Mz ; DMSO-d_6.

tones H_5 et H_i du produit (7 *b*) sont constantes même si on varie la température entre 20°...45°C, le solvant utilisé étant le DMSO-d_6. Le spectre des ylures (7 *c*) est le mieux résolu. Dans le cas ou l'ylure (7 *c*) est obtenu à partir du sel de cycloimmonium correspondant, en présence de triéthylamine en milieu chloroformique, (synthesè (1)), le rapport entre les isomères *E* et *Z* est de 0.82. La synthèse du même ylure à partir du sel (6 *c*) et la triéthylamine dans la DMSO-d_6 comme solvant conduit à un mélange des isomères *E* et *Z* en rapport 4.55.

Il résulte des données ci-dessus que la proportion des isomères *E* et *Z* se modifie en fonction de la nature du milieu réactionnel et de la température.

Les spectres IR des ylures (7) confirment l'existence des isomères *E* et *Z*. Pour concrétiser il faut mentionner que lorsque la forme *Z* est prédominante dans le spectre de l'ylure (7 *c*) on constate l'apparition d'une bande d'absorption $\nu_{C=O}$ à 1 660 cm^{-1}, fréquence d'absorbtion classique

des groupements carbonyliques attachés à un atome de carbone ylurique [3], [9]. Par contre dans les échantillons dans lesquells la forme *E* est prédominante cette bande d'absorption se déplace vers 1 600 cm^{-1}. Ce fait met en évidence l'existence d'une très forte liaison d'hydrogène intramoléculaire.

En conclusion on peut apprécier qu'il est possible à obtenir des isomères *E* et *Z* à partir des 1, 2, 4-4H triazoles en modifiant la nature du milieu réactionnel dans le processus de transformation des sels de cycloimmoinium (6) dans les ylures correspondants (7). Comme solvants on a utilisé le chloroforme et le diméthylsulfoxyde. La température à laquelle se produit la réaction joue un rôle important dans l'établissement d'un certain rapport entre les isomères *E* et *Z*.

Dans le DMSO, des températures plus élevées contribuent à l'augmentation du contenu en isomère *Z*.

3. Partie expérimentale

a) *Variante Nr. 1.* On dissout (on suspend) 0,01 mol de sel de triazolium (6 *a, b, c*) dans 50 ml de chloroforme à une température de 10° ... 15°C. On ajoute, en agitant continuellement pendant 10 ... 15 min., 0.015 mol de triéthylamine. La solution se colore. On filtre le bromhydrate de triéthylamine. La solution chloroformique est lavée trois fois à l'eau, séchée sur Na_2SO_4 anhydre et concentrée. On ajoute de l'éther de pétrole et on précipite les ylures (7 *a, b, c*). On fait enregistrer les spectres RMN-H^1 pour les produits bruts obtenus.

b) *Variante Nr. 2.* On dissout le sel de triazolium (6 *a, b, c*) dans du DMSO-d_6, dans un tube RMN. On ajoute dans le tube la quantité équivalente de triéthylamine. On fait enregistrer le spectre RMN de l'ylure (7). On chauffe la même épreuve. Dans le cas de l'yure (7 *a*) si on chauffe pendant 20...30 min. à 65°C,on constate la formation du dimère (8 *a*). Dans le cas de l'ylure (7 *c*) en chauffant on constate l'augmentation de l'isomére (7 *c*) *Z* dans le mélange.

Reçue le 16 avril 1985

Institut Polytechnique, Jassy,
Chaire de Chimie et Technologie
organique et macromoleculaire,
Université „Al. I. Cuza", Jassy
Centre de Calcul,
et
Laboratoire de chimie organique
et macromoléculaire.
Université des Sciences et Technique, Lille, France

BIBLIOGRAPHIE

1. Surpăţeanu G., Constantinescu M., Lablache Combier A., Theor. Chem. Acta (sous presse).
2. Pople J.A., Beveridge D.L., *Aproximate Molecular Orbital Theory*. Mc. Graw-Hill, N.Y., 1970, QCPE-141.
3. Zugrăvescu I., Petrovanu M., *N-ylide Chemistry*. Mc. Graw Hill, N.Y., 1976.
4. Bugg C., Desiderato R., Sass R.L., J. Am. Chem. Soc., **86**, *3*, 157 (1964).
5. Bailey N.A., Newton C.G., Cryst. Struct. Commun., **9**, 49 (1980).
6. Surpăţeanu G., Catteau J.P., Karafiloglou P., Lablache Combier A. Tetrahedron Report, 23 (1976).

7. Petrovanu M., Luchian C., Surpățeanu G., Bărboiu V., Rev. Roum. Chim., **24**, 5, 733 (1981).
8. Petrovanu M., Luchian C., Surpățeanu G., Bărboiu V., Tetrahedron, **39**, *14*, 2 417 (1983).
9. Johnson A.W., *Ylide Chemistry*. Academic Press, N.Y., 1966.

IZOMERII *E* ȘI *Z* AI ILURILOR DE 1,2-4H TRIAZOL

(Rezumat)

S-au caracterizat izomerii *E* și *Z* ai *p*-nitrobenzoil, 4-*p*-tolil-[1,2-4H] triazolmetilidă (7 *b*) și *p*-nitrobenzoil, 4-p-fenil [1,2-4H] triazolmetilidă (7 *c*). S-au sintetizat amestecuri de izomeri în diferite condiții experimentale. Triazolilida (7 *a*) conduce la compusul (8 *a*) prin cicloadiție dimeră.

BULETINUL INSTITUTULUI POLITEHNIC DIN IAŞI
Tomul XXXI (XXXV), Fasc. supl., 1985
Secţia II
CHIMIE ŞI INGINERIE CHIMICĂ

D.C. 547.458.6 ; 542.951.3 ; 661.724 ; 677.03

STARCH ESTERS AND ETHERS AS THICKENERS IN TEXTILE PRINTING

BY

GH. MIHĂILĂ, C. CIUGUREANU, N. BÎLBĂ, P. ONU, C. LUCA and N. NAUM

1. Introduction

The hydroxylic groups in the starch structure allow its chemical modification with different inorganic or organic reagents [1] ... [3] to starch esters and ethers with new properties which can be used as thickeners in the textile printing, as improved adhesives, as emulsion stabilizers and as thickeners for food.

Useful in the textile printing are, by their thickening properties, the starch esters and ethers with low degree of substitution, products with a water solubility greater than starch and which, after dye fixation on textiles, can be removed easily by washing with water.

The present paper deals with preparation, chemical and rheological characterization as well as technological testing of starch phosphates (I), (II) and acetate (III), 2-hydroxypropylstarch (IV) and 1-chlorine-2-hydroxypropylstarch (V), written below :

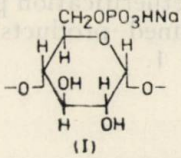

(I)

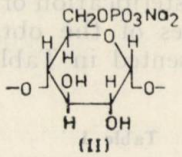

(II)

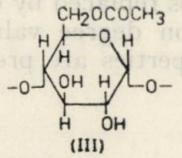

(III)

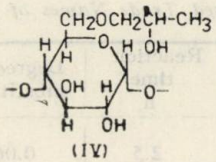

(IV)

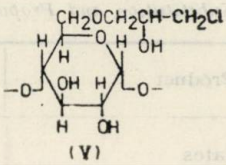

(V)

2. Experimental

The potato starch with 12...14% moisture and 0.1% ash was used in all cases.

2.1. Procedure

The starch phosphates (I) and (II) have been obtained by solid phase reaction of the starch with a mixture of sodium biphosphate and disodic phosphate at 140°...145°C for 2.5 hours. In order to realize a more uniform reaction mass, the starch was firstly impregnated in an aqueous solution of 41.5% disodic phosphate ($Na_2HPO_4 . 12 H_2O$) and 21.3% sodium biphosphate ($NaH_2PO_4 . H_2O$) with pH=6.5. The liquid/solid ratio was 2.7. After filtration, the impregnated starch dried to a remanent moisture of 8...9%, was esterified in a stainless steel reactor with mechanical stirring and heating oil jacket. During esterification, after each quarter a hour, the 30...40 g samples have been taken out, in which, after washing the excess of phosphates with a 50% methanol solution in water, the content of phosphorus and sodium has been determined. Since the molar ratio Na/P has ranged from 1.17 to 1.39, it results that a mixture of starch phosphates takes form (I) and (II) [4].

The starch acetate (III) has been obtained by treating with acetic anhydride a suspension of starch activated in acetone at 40°...45°C, in a digester with mechanical stirring, for 3.5 hours. The acetic anhydride/starch ratio was 0.4 moles to a glucose unit.

The starch ethers (IV) and (V) have been obtained by treating the starch with propenoxide and epichlorhydrin, respectively. Before etherification, the starch has been activated in acetone in the presence of sodium hydroxide, pH = 9...10, at 45°...50°C, under stirring, for 1.5 hours. After activation, the reagents were added gradually, under stirring too, at 25°...30°C for 2.5 hours. The propenoxide / starch and epichlorhydrin / starch ratios was 0.2 and 0.1 moles to a glucose unit, respectively.

2.2. Chemical Characterization

All the obtained products have been chemically characterized by means of the degree of substitution, expressed as the average number of hydroxyl groups replaced by esterification or etherification per glucose unit. The substitution degree values of the obtained products with excellent thickening properties are presented in Table 1.

Table 1

Degree of Substitution and Proposed Trade Names of the Products

Nr.	Product	Reaction time h	Degree of substitution	Trade name
1	Starch phosphates	2.5	0.060	Aglutirom *P*
2	Starch acetate	3.5	0.063	Aglutirom *Ac*
3	Hydroxypropylstarch	2.5	0.080	Aglutirom *H*
4	1-Chlorine-2-hydroxypropylstarch	2.5	0.075	Aglutirom *E*

Data of the Table 1 show that the introduction of a relatively small number of ester or ether groups (one substituent per 12...17 glucose units),

are enough to modify the colloidal properties of the starch when it is dispersed in water.

2.3. Rheological Characterization

Rheological measurements of the prepared pastes from the four products as well as those from the commercial products Indalca *PA 3* and Indalca *PZ 36* have been carried out on a rotatory viscosimeter „Rheotest type RV 2", using the coaxial cylinders S/S_2 at 25°C. The thickener pastes have been prepared by mixing a measured amounts of solid and of necessary water, at the room temperature, under stirring for 15 min., followed by heating at the temperature of 60°C on a water bath, under stirring for 15 min.

Correlation of the rheological data of the investigated pastes was done by means of Oswald and de Waele's mathematical model

$$\tau = k\dot{\gamma}^n, \tag{1}$$

where k is consistency index and n — the flow index.

By its logarithmation, an equation of straight line is obtained

$$\lg \tau = \lg k + n \lg \dot{\gamma}, \tag{2}$$

which allow to calculate the two rheological indexes.

Dependence of $\lg \tau$ vs. $\lg \dot{\gamma}$ for the pastes of studied thickeners is represented in Fig. 1.

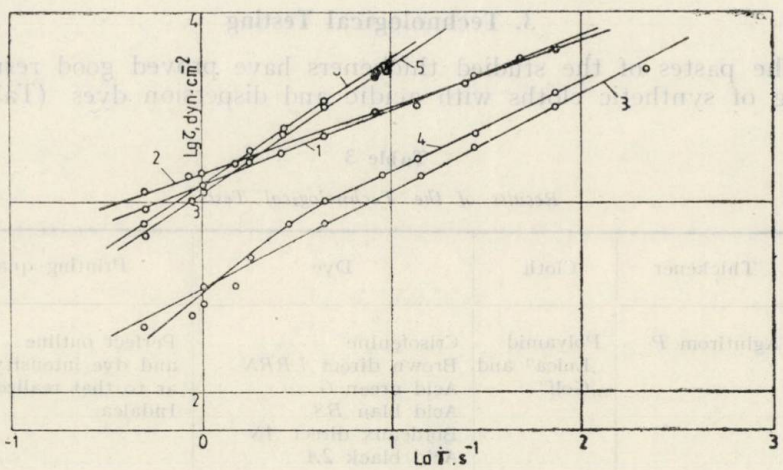

Fig. 1. — Dependence of $\lg \tau$ vs. $\lg \dot{\gamma}$: *1* — 14% Aglutirom *P*; *2* — 10% Aglutirom *Ac* ; *3* — 10% Aglutirom *H* ; *4* — 11% Aglutirom *E* ; *5* — 12% Indalca *PA 3* ; *6*-14% Indalca *PZ 36*.

The chosen model does not agree satisfactorily with the rheological data of the Aglutirom *E* paste. The rheological indexes determined from Fig. 1 are listed in Table 2.

Table 2

Indexes of the Rheological Equation

Nr.	Thickener	Paste concentration %	k, dyn. s^2. cm^{-2}	m
1	Aglutirom *P*	14	1230.2	0.400
2	Aglutirom *Ac*	10	1386.7	0.457
3	Aglutirom *H*	10	365.6	0.513
4	Indalca *PA 3*	12	1091.4	0.693
5	Indalca *PZ 36*	14	1238.8	0.662

As it comes out from Table 2, the flow index n of the pastes prepared from our thickeners have lower values then those of the commercial products Indalca *PA 3* and Indalca *PZ 36*.

Since the paste of Aglutirom *P*, without free phosphates, exhibits a flow index of 0.831 [6] , and that of unwashed product of 0.400, by repeated washings with a 50% aqueous methanol solution the flow index increases, being closer to that of Indalca type thickeners.

Since in the range of low τ and $\dot{\gamma}$, the straight lines of Aglutirom *P* and Aglutirom *Ac* intersect those of Indalca *PA 3* and Indalca *PZ 36* suggests that in this field, the pastes have an almost similar rheological behaviour, which was proved also by technical tests.

3. Technological Testing

The pastes of the studied thickeners have proved good results in printing of synthetic cloths with acidic and dispersion dyes (Table 3).

Table 3

Results of the Technological Tests

Nr.	Thickener	Cloth	Dye	Printing quality
1	Aglutirom *P*	Polyamid „Luica" and „Golf"	Crisofenine Brown direct *LBBN* Acid green *G* Acid blau *BS* Bordeaux direct *AN* Acid black *2A*	Perfect outline and dye intensity similar to that realized with Indalca
2	Aglutirom *Ac*	Polyester	Dispersion orange *GFL* Dispersion marine blau *RE*	Idem
3	Aglutirom *H*	Polyester	Dispersion dyes	Idem
4	Aglutirom *E*	Polyester	Acid and dispersion dyes	Idem

The thickeners Aglutirom *P* and *H* have been tested technologically at industrial scale at the Entreprise of Silk „Victoria", Jassy.

Preparation of the printing paste with Aglutirom *P* is reported below. First, a paste of 16% Aglutirom *P* is prepared by dispersion of thickener in cold water than addition of warm water was donne until the paste temperature rised to 60°C. After stirring for 30 min., the mixture was left for 12...24 hours to maturate and cooled down to room temperature. Secondly, the paste prepared as above, was stirred again for 15 min., followed by dye addition. The dye is added as dissolved, under boiling, in an aqueous solution of glycerine, uree and ammonium sulphate. Finally, the printing paste contains about 14% Aglutirom *P*.

4. Conclusions

1. Starch phosphate and starch acetate as well as 2-hydroxypropylstarch and 1-chlorine-2-hydroxypropylstarch with low degree of substitution have been obtained by chemical modification of the potato starch. As thickeners in the textile printing, they will be manufactured under trade names Aglutirom *P*, Aglutirom *Ac*, Aglutirom *A* and Aglutirom *E*.

2. The rheological data of the pastes prepared with thise products have been correlated by the model $\tau = k\dot{\gamma}^n$, except those of the Aglutirom *E*. For low values of τ and $\dot{\gamma}$, rheological behaviour of the products is similar to that of Indalca thickeners.

3. The pastes of the four thickeners exhibit good results in textile printing with acid and dispersion dyes on a broad variety of synthetic cloths.

Received, April 10 1985,

Polytechnic Institute, Jassy,
Department of Physical and General Chemistry

REFERENCES

1. Whistler R.L., *Starch Chemistry and Technology*. Vol. 1 and 2, Acad. Press, New York, 1965.
2. Крылова Р.Г., Усп. Хим., 36, 1615 (1967).
3. * * * *Encyclopedia of Polymer Science and Technology*. Vol. 12, John Wiley a. Sons, Inc., New York, 1967, 787.
4. Popa A., Mihăilă Gh., Bîlbă N., Onu P., Luca C., Popovici Ev., Bezdadea M., Popescu D., Ind. Uşoară-textile, tricotaje, confecţii textile, 33, 18 (1982).
5. Tudose R.Z., Volintiru T., Asandei N., Lungu M., Merică E., Ivan Gh., *Reologia compuşilor macromoleculari*. Vol. 1, Ed. Tehn., Bucureşti, 1982, 120.
6. Ioan C., Grigoriu A., Hanganu A., Popescu D., Pavel T., Ind. Uşoară-textile, tricotaje, confecţii textile, 31, 412 (1980).

ESTERI ŞI ETERI AI AMIDONULUI CU PROPRIETĂŢI AGLUTINANTE

(Rezumat)

S-au sintetizat fosfaţi şi acetat de amidon precum şi hidroxipropilamidon şi 1-clor-2-hidroxipropilamidon, cu grad mic de substituţie, utilizînd amidonul de cartofi. Produsele obţinute prezintă proprietăţi aglutinante remarcabile şi urmează a se produce sub denumirile comerciale de Aglutirom *P*, Aglutirom *Ac*, Aglutirom *H* şi Aglutirom *E*. Datele reologice ale pastelor preparate din aceste produse s-au comparat cu cele ale pastelor din produse comerciale de tip Indalca. Pastele preparate au fost testate la imprimarea textilă, cu coloranţi acizi şi cu coloranţi de dispersie, pe o largă varietate de ţesături din fibre sintetice, obţinîndu-se imprimări de bună calitate.

The thickeners Aglutinom 7 and 8 have been tested technologically at industrial scale at the Enterprise of Silk „Victoria", Jassy.

Preparation of the printing paste with Aglutinom 7 is reported below. First, a paste of 16% Aglutinom 7 is prepared by dispersion of thickener in cold water than addition of warm water was done until the paste temperature rised to 60°C. After stirring for 30 min., the mixture was left for 12...24 hours to maturate and cooled down to room temperature. Secondly, the paste prepared as above, was stirred again for 15 min., followed by dye addition. The dye is added as dissolved, under boiling, in an aqueous solution of glycerine, urea and ammonium sulphate. Finally, the printing paste contains about 11% Aglutinom 7.

4. Conclusions

1. Starch phosphate and starch acetate as well as 2-hydroxypropyl-starch and 1-chloride-2-hydroxypropylstarch with low degree of substitution have been obtained by chemical modification of the potato starch. As thickeners in the textile printing, they will be manufactured under trade names Aglutinom 7, Aglutinom 16, Aglutinom 4 and Aglutinom 8.

2. The rheological data of the pastes prepared with these products have been correlated by the model $\tau = A\gamma^n$, except those of the Aglutinom 8. For low values of τ and γ, rheological behaviour of the products is similar to that of Indalca thickeners.

3. The pastes of the four thickeners exhibit good results in textile printing with acid and dispersion dyes on a broad variety of synthetic cloths.

Received April 10, 1985,
Polytechnic Institute, Jassy,
Department of Physical and
General Chemistry

REFERENCES

1. Whistler R.L., Starch Chemistry and Technology Vol 1 and 2, Acad. Pres., New York, 1965.
2. Kuprianova P.T., Ukr. Khim. Zhur., 30, 1013 (1957).
3. * * Encyclopedia of Polymer Science and Technology Vol. 12, John Wiley & Sons Inc., New York, 1967, 787.
4. Popa A., Mihaiu Gh., Bilba N., Oana T., Lacea C., Popovici Ev., Prydan Ana M., Popescu D., Ind. Uleiuri-textile, tricotaje, confecții textile, 33, 18 (1982).
5. Teodorescu R., Voiniciuc T., Asandei S., Lungu M., Manolache I., Ivan Gh., Energia conținută macromolecule, Vol. I, Ed. Tehn., Bucureşti, 1982, 120.
6. Ioan C., Grigoriu A., Hagiopol C., Popescu D., Pavel T., Ind. Uleiuri-textile, tricotaje, confecții textile, 31, 412 (1980).

REZUMAT

Sînt descrise izolarea şi acetat de amidon precum şi hidroxipropilamidon şi 1-cloro-2-hidroxipropilamidon, ca eteri mic de substituţie, utilizînd amidonul de cartof. Produşii obţinuţi prezintă calităţi remarcabile şi urmează a se produce sub denumirile comerciale de Aglutinom 7, Aglutinom 16, Aglutinom 4 şi Aglutinom 8. Datele reologice ale pastelor preparate din acești produşi — au comparat cu cele ale tipurilor din produse comerciale de tip Indalca. Pastele preparate au fost testate la imprimarea textilă, cu coloranţi acizi şi cu coloranţi de dispersie, pe o largă varietate de ţesături din fibre sintetice, obţinîndu-se imprimări de bună calitate.

BULETINUL INSTITUTULUI POLITEHNIC DIN IAŞI
Tomul XXXI (XXXV), Fasc. supl., 1985
Secţia II
CHIMIE ŞI INGINERIE CHIMICĂ

D.K. 54-92

DER STUFENWEISE CHARAKTER DES BRUCHPROZESSES BEI POLYMEREN DURCH ZUGKRAFT UNTER KRIECHBEDINGUNGEN

VON

CLEOPATRA VASILIU-OPREA, MARCEL POPA, AL. CONSTANTINESCU
und AURELIA IOANID

1. Einführung

Die zur Zeit angenommenen Theorien hinsichtlich des Bruches von Polymeren (J u r k o w, A n d r e w s, K a u s c h) [1]...[5], die auf rein physikalischer Grundlage beruhen, erlaubten die Festlegung von Wechselbeziehungen zwischen der Belastungskraft und der Antwort auf molekularer Ebene der Polymerstruktur. Sie haben die Bedeutung, daß sie den Bruchprozeß einen mechanochemischen Vorgang zugrunde legen, der in der Aufspaltung der chemischen Verbindungen in der Hauptkette besteht. Dieser Vorgang zeigt sich bereits in den Anfangsstadien des Bruches bis hinzum makroskopischen Riß des Polymers, was jedoch nicht spontan zum Zeitpunkt der Krafteinwirkung stattfindet, sondern nur dann, wenn die gespeicherte Energie in den „Defekt- Zonen" der Struktur vergleichbare Werte mit denen der chemischen Verbindungen erreicht, wodurch ihre thermofluktuationelle Aufspaltung bewirkt wird.

Die Antwort des Polymers auf die mechanische Belastung ist bedingt sowohl durch seinen chemischen Aufbau als auch durch den physikalischen Zustand, bestimmt durch die Arbeitstemperatur ; konkret ausgedrückt, finden Verformungsprozeße und ein Reissen auf makroskopischer Ebene statt. Die komplizierte Prozeße laufen mehrstufig ab, wobei sie zuerst die Etappe der Verformung des Polymers durchlaufen (wenn dieses mechanische Energie speichert), dann primäre chemische Reaktionen und mehrere sekundäre Erscheinungen.

Der Zweck der vorliegenden Arbeit besteht in der Herausstellung der verschiedenen Stadien des Verformungsprozeßes und des Reissens von thermoplastischen Polymeren oder Elastomeren und zwar besonders die Anfangs-(Mechanokracken) und die Endetappe (Reorganisation der Struktur), wobei indirekte Techniken angewandt werden : Reaktionen mit Radikalakzeptoren, Spektralanalysen im UV-und IR-Bereich Elektronenmikroskopie (TEM).

Die UV-Strahlung beschleunigt die elementären Vorgänge des Reissens, wobei die Anhäufung der Einwirkungen den gemeinsamen Mechanismus der beiden Distruktionsprozeße beweist und ein zusätzliches Argument für ihren Verlauf durch freie Radikale darstellt. Darüber hinaus arbeiten während der Untersuchung der Polymerproben die mechanischen Faktoren unvermeidlich zusammen mit denen des Mediums, unter denen wir auch die Wirkung des Lichts zählen können, die innere Veränderungen in ihren Strukturen hervorruft und somit entsprechend die Haltbarkeit beeinflußt. So wurde im theoretischen und praktischen Sinne in der vorliegenden Arbeit bei einigen Experimenten die mechanische Belastung verbunden mit UV-Bestrahlung.

2. Experimenteller Teil

Es wurde Polyvinylchlorid (PVC) untersucht, erhalten durch das Suspensionsverfahren (KW-70), sowie ein aus 4,4-Dibenzyldiisocyanat, Polyethylenglycoladipat und Ethylenglycol synthetisiertes Polyurethan. Aus dem PVC wurden Filme mit einer Dicke von 50 μm aus Lösungen des Polymers in Tetrahydrofuran ($C = 1\%$) gewonnen. Die den Belastungen unter Kriechbedingungen unterzogenen Probestücke aus Polyurethan und PVC wurden entsprechend den Normen ISO R 527/66E hergestellt. Die mechanische Belastung wurde auf einem speziell konstruierten Stand konform der ASTM-Normen durchgeführt.

Die UV-Bestrahlung, parallel zur mechanischen Belastung unter Kriechbedingungen angewandt, wurde durch Benützung einer Quecksilberverdampfungsröhre mit mittlerem Druck bei $25° \pm 1°C$ realisiert.

Das Studium der Rißflächen wurde durch Anwendung der Zwei-Stufen-Replikationsmethode durchgeführt und zwar auf den Bruchflächen oder den anliegenden Flächen und ihre Analyse mit einem Mikroskop, Typ Tesla BS-513 A (ČSSR). Die IR-Spektren wurden durch ein Perkin—Elmer-Spektrophotometer aufgezeichnet, die UV-Spektren durch ein Spektrophotometer, Typ UNICAM, wobei direkt die PVC-Filme verwendet wurden.

3. Ergebnisse und Diskussion

Es wurden PVC-Filme analysiert, die durch Zugkräfte verschiedener Stärke belastet wurden, und zwar so, daß die Verformungen Werte zwischen 10% und 95% des Reissens hatten. Die mechanischen Belastungen wurden in DPPH-Methanollösungen oder in Lösungen von aromatischen Diaminen durchgefürt, die die Rolle von Radikalakzeptoren übernahmen. So wurde festgestellt, daß bei Streckungen bis 20% gegenüber der die zum Reissen führt, die Filme keine wesentlichen Veränderungen gegenüber der ungestreckten Probe aufweisen. In diesem Stadium der Verformungsprozeßes wird die Streckung hauptsächlich durch Aufwicklung und Ausrichtung der Makromoleküle in Richtung der Kraftwirkung vollzogen. Man kann sagen, daß das Polymer in einen mechanisch erregten Zustand übergeht, ohne daß jedoch dieses Stadium überschritten wird, wenn die mechanische Belastung aufhört zu wirken.

Bei größeren Verformungen jedoch ($> 20\%$) zeigt der aktive Sektor der Proben eine spezifische Färbung, was ein erster Beweis dafür ist, daß unter der Wirkung der mechanischen Energie homolytische molekuläre Aufspaltungen stattgefunden haben, wobei die gebildeten Radikale DPPH oder aromatishes Diamin chemisch binden. Die Färbung des Films ist ein erster experimenteller Beweis für den Ablauf der Etappe des Mechanokrackens. Der teilweise Verbrauch der gebildeten „Mechanoradikale" durch die Radikalakzeptoren wurde durch die UV-Spektren der gespannten Filme bewiesen (Abb. 1).

Bei erhöhten Streckungswerten (approx. 95% der des Reissens) wird die Anzahl der gebildeten Makroradikale sehr groß, wobei der Verbrauch von aromatischen Diamin aus dem Reaktionsmedium angewachsen ist. Infolgedessen kann die Anwesenheit der aromatischen Verbindung in dem

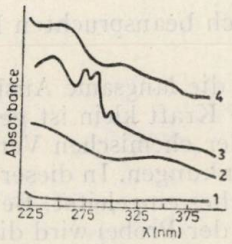

Abb. 1. — UV — Spektren von gedehnten PVC-Filmen: *1* — Vergleichsprobe; *2* — gedehntes PVC in DPPH; *3* — gedehntes PVC in *o*-PhDA; *4* — gedehntes PVC in *p*-PhDA.

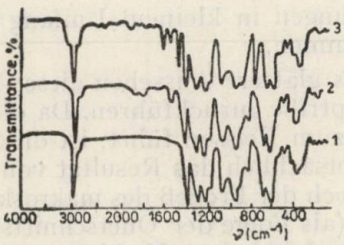

Abb. 2. — IR — Spektren von PVC-Filmen: *1* — Vergleichsprobe; *2* — gedehntes PVC in *p*-PhDA; *3* — gedehnt in Anwesenheit von Styrol.

gespannten Film auch durch eine weniger empfindliche Methode als die UV-Spektroskopie nachgewiesen werden und zwar durch die IR-Spektroskopie (Abb. 2, Kurve *2*). Die große Konzentration der Makroradikale erlaubt ebenfalls die Einleitung von Propf-Blockcopolymerisationsprozeßen in Anwesenheit eines Vinylmonomers. Das IR-Spektrum aus Abb. 2 (Kurve *3*) zeigt die chemische Bindung des Styrols an den gespannten Film durch das 775-, 1480- und 1 600 cm^{-1} Band.

Ein zusätzliches Argument für die Propf-Blockcopolymerisation des Styrols bei PVC geht aus den Mikrophotografien der gespannten Filme (Abb. 3 *a*...*c*) hervor, die ein eindeutig anderes Aussehen gegenüber denen der Vergleichsprobe haben. Auf der Oberfläche dieser bemerkt man Einschlüße, was dem Propfpolystyrol zugeschrieben wird, die jedoch auf der Oberfläche des nichtgespannten Films fehlen (Abb. 3 *a*). Besonders interessante Informationen liefern die in Abb. 4 *a*, *b* dargestellten Mikrophotografien, die das Relief der Oberfläche von gespannten Filmen nahe des Reissens festhalten, bei dem man einige Riße festtellt. Die Verformungszone, neben der des Bruches gelegen, ist charakterisiert durch das Auftreten von linearen Strukturen, gebildet aus Fibrillen senkrecht zur Kraftrichtung. In dieser Zone beobachtet man eine größere Anzahl von Propfzentren des Vinylmonomers, ein Beweis für die große Konzentration von durch das Spannen gebildeten freien Radikalen. Gleichfalls läßt sich einschätzen, daß nach dem Mechanokracken im Polymer sich das dritte Stadium des Strukturbruch und Reorganisatiosprozeßes zeigt. In der Zone des makroskopischen Bruches zeichnet sich das PVC mit globulärer Struktur durch nichtcharakteristische fibrillare Abschnitte aus, eine Folge von Veränderungen der globulären Abschnitte unter Krafteinwirkung.

Die Mikrophotografien aus Abb. 5 *a*...*c* geben das Aussehen von Zonen der Bruchfläche des unter Kriechbedingungen Beanspruchten PVC's wieder. Die Topographie dieser Zonen (Abb. 5 *a*) zeigt indirekt durch die Kavitationen die Etappe des Mechanokrackens, in der sich große Konzentrationen von freien Radikalen ansammeln, die aus den gespaltenen chemischen

Verbindungen in kleinem Umfang des mechanisch beanspruchten Festkörpers stammen.

Das glattere Aussehen dieser Fläche ist auf die langsame Ausbreitung der Hauptrisse zurückführen. Da die mechanische Kraft klein ist gegenüber der, die zum Reissen führt, ist die Aufspaltung der chemischen Verbindungen hauptsächlich das Resultat von Wärmeschwankungen. In dieser Etappe wird jedoch der Prozeß des makroskopischen Bruches eingeleitet. Bei großen Kräften (als Folge der Querschnittsverkleinerung der Probe) wird die Belastung der chemischen Verbindungen so intensiv, daß ihr Reissen sich fast ausschließlich infolge der mechanischen Energie vollzieht, wobei die Beteiligung der Wärmeschwankungen sich sehr vermindert. Die Ausbreitungsgeschwindigkeit des Rißes wächst, wobei diese den nichtelastischen Eigenschaften des Polymers unterworfen ist. Die Bruchflächen bekommen ein rauhes Aussehen (Abb. 5 *b*), weil das starre Polymer wegen seiner plastischen oder viskoelastischen Eigenschaften keine Energieverluste aufweist. Die Übergang von der ersten Phase (langsame Ausbreitung des Rißes) zur zweiten Phase (katastrophale, mit dem Bruch endende Ausbreitung) wird somit klar deutlich.

Im Falle von thermoplastischen Elastomeren des Typs Polyurethane wurden die Probestücke bei Zugkraft unter Kriechbedingungen (mit einer einheitlichen Kraft von 9,0 MPa) belastet und gleichzeitig einer UV-Älterung unterzogen.

Es wurde festgestellt, daß das Reissen der Proben nach einer Belastung von 55 Stunden stattfand, zum Unterschied zu den nichtbestrahlten, die nicht einmal nach 1 000 Belastungsstunden gerissen sind. Dem Riß vorausgehend findet eine sich verstärkende Verformung des Probestückes statt, und es wird das Mikroreissen eingeleitet, was mit Hilfe der Elektronenmikroskopie sichtbar wird.

Die mit der Zugkraftbelastung unter Kriechbedingungen gleichzeitig ausgeführte UV-Bestrah ung beschleunigt die Aufspaltung der chemischen Valenzverbindungen und die Bildung von Mikrorißen, was schließlich zum makroskopischen Bruch der Probestücke führt. Es ist bekannt, daß UV-Strahlungen mit Wellenlängen zwischen 250 und 360 nm das Reissen von Valenzverbindungen verursachen, wobei freie Radikale gebildet werden [6]. Infolge der Dehnung bei Fließbedingungen der gleichzeitigen UV-Strahlung findet durch die synergistische Wirkung dieser beiden Faktoren ein Anwachsen der Formveränderung statt, was ein Beweis dafür ist, daß diese Prozeße eine gemeinsame Ursache haben und zwar die thermofluktuationelle Aufspaltung der chemischen Valenzverbindungen. Man stellt fest, daß das makroskopische Reissen der Probestücke bei den jeweilig angewandten Experimentierbedingungen nicht durch uniaxiale Beanspruchung, nicht durch UV-Strahlung stattfindet, sondern eine Erscheinung ist, die sich erst beim gleichzeitigen Wirken dieser beiden Energieformen zeigt.

Die Wiederherstellung der gespaltenen Verbindungen nach der UV-Bestrahlung wird behindert durch die Wirkung der mechanischen Energie, was zur katastrophalen Ausbreitung des Bruchvorgangs führt bis hin zum makroskopischen Bruch des Polymers.

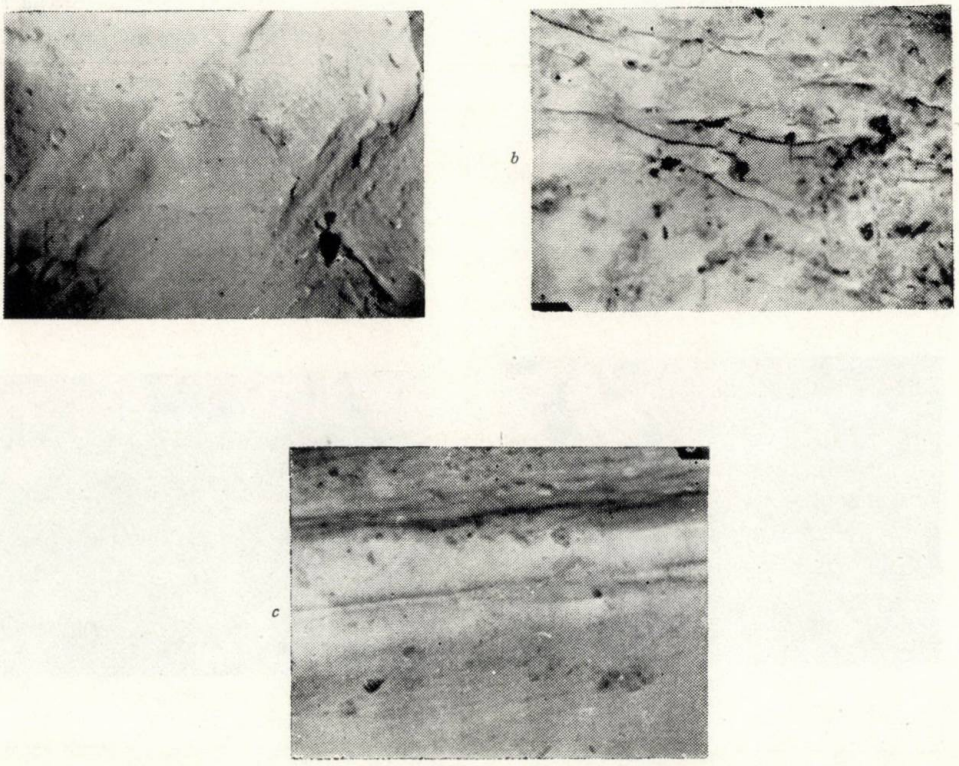

Abb. 3. — Mikrophotografien von gedehnten PVC-Filmen in Methano (*a*) oder Styrol—Methanol-Lösung.

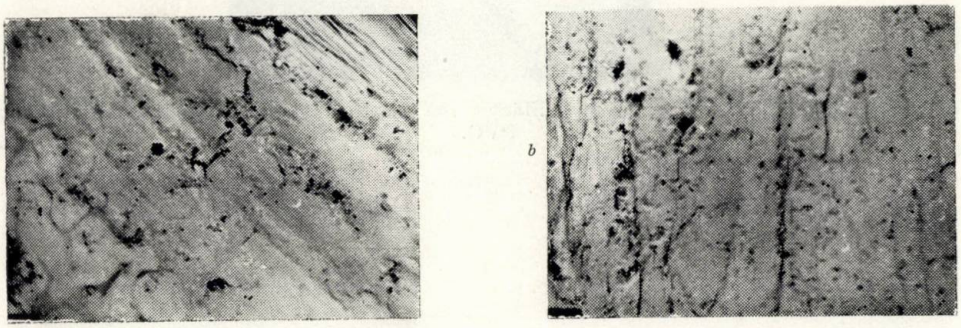

Abb. 4.— Mikrophotografien von gedehnten PVC-Filmen nahe dem Reissen ($\varepsilon = 95\%$).

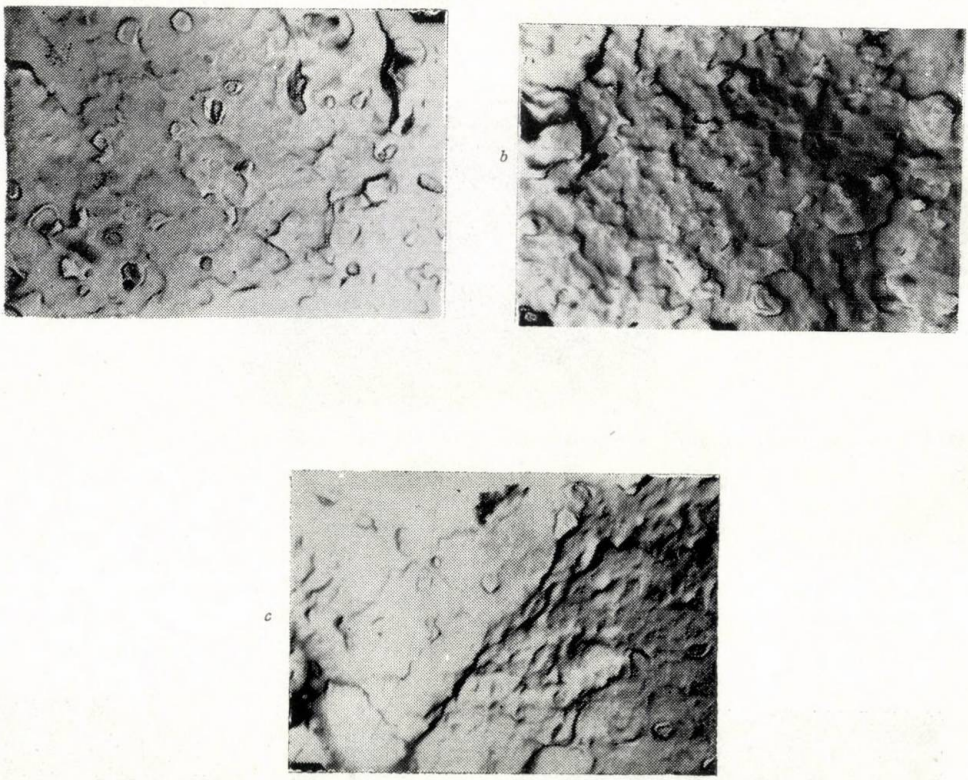

Abb. 5. — Mikrophotografien der Bruchfläche von durch Zugkraft statisch beanspruchtem PVC.

Abb. 6. — Mikrophotografie der Bruchoberfläche im Falle der nichtgedehnten und nichtbestrahlten Polyurethan-Probe, die in flüssigen Stickstoff gerissen ist (× 11 300).

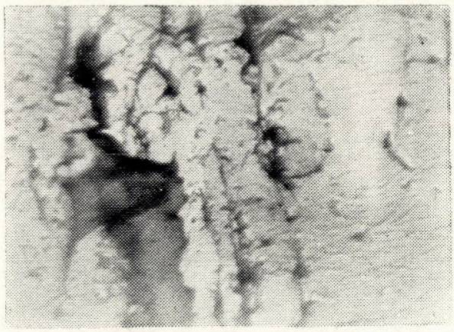

Abb. 7. — Mikrophotografie der Bruchoberfläche im Falle der unter Fließbedingungen gedehnten und gleichzeitig durch UV-Strahlung gealterten Polyurethan - Proben (× 11 300).

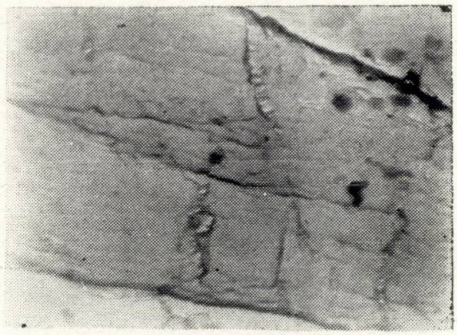

Abb. 8. — Mikrophotografie der mit der Bruchzone benachbarten deformierten Zone im Falle der unter Fließbedingungen gedehnten und gleichzeitig durch UV-Strahlung gealterten Polyurethan - Proben (× 11 300).

Als Folge der mechanischen Belastung tritt gleichzeitig eine Verringerung der Dissoziationsenergie der gedehnten Verbindungen auf, wodurch eine Beschleunigung ihrer photochemischen Spaltungsprozeße möglich wird.

Es wurde das Bruchrelief und die benachbarte Verformungszone untersucht im Vergleich zu einer nichtgedehnten und nicht UV-bestrahlten Probe, deren Bruch durch Einführung in flüßigen Stickstoff während 30 Min. realisiert wurde, während man annimmt, daß der Bruch längs der Oberfläche der suprastrukturellen Elemente stattfindet. Die erhaltenen Replikationen von der Bruchfläche der Vergleichsprobe (Abb. 6) zeigen, daß die nichtgedehnte Probe eine übermolekulare Struktur von globulären Typ aufweist, charakteristisch für amorphe Polymere. Das Studium der Mikrophotografien von der Bruchzone (Abb. 7) zeigt den rauhen Charakter dieser Zone, wobei der globuläre Aspekt nicht mehr hervortritt. Dagegen beobachtet man das Auftreten von, was Form und Abmessung anbelangt, unregelmässigen Mikrorißen.

Die der Bruchzone anliegende Verformungszone (Abb. 8) zeigt neben der Bildung von zur Belastungsrichtung querverlaufenden Mikrorißen auch einige aus eingebetteten makromolekularen Ketten gebildete fibrilläre Abschnitte. Dieser Prozeß findet durch die Auflösung der Globule und der Längsordnung der Makromoleküle statt, infolge der Wirkung der uniaxialen Zugkraft.

4. Schlussfolgerungen

1. Der Bruch von Polymeren unter Kriechbedingungen hat einen mehrstufigen Charakter, der die Mechanoaktivierung, das Mechanokracken und die Reorganisation der Struktur mit einschließt.

2. Bei jeder der einzelnen Stufen des Bruchprozeßes finden mechanochemische Vorgänge homolythischer Aufspaltung der Makromoleküle statt, die durch indirekte Techniken bewiesen werden können.

3. Durch die gleichzeitige Wirkung von mechanischer Energie und UV-Strahlungen findet eine Beschleunigung des Reissens statt, wobei eine Anhäufung der Effekte den gemeinsamen Radikalcharakter dieser beiden Abbautypen beweist.

4. Im letzten Stadium des Bruchprozeßes treten wichtige strukturelle Veränderungen auf, die in dem Übergang von der globulären in die fibrilläre Struktur bestehen.

Eingegangen am 20. April 1985

Technische Hochschule, Jassy,
Lehrstuhl fiir organische und
makromolekulare Chemie und
Technologie
und
Institut für makromolekulare Chemie
„P. Poni", Jassy

LITERATURVERZEICHNIS

1. Журков С.Н., Закревский В.А., Томашевский Е.Е., Физ. тверд. тела, 6, 1912 (1964).

2. Andrews E. H., Reed P. E., *Advances in Polymer Science*. Vol. 27, Springer-Verlag, Berlin, 1978.
3. Kausch H. H., *Polymer Fracture*. Springer-Verlag, Berlin, 1978.
4. Самоилова Г.Г., Томашевский Е.Е., Физ. рверд. тела, 10, *4*, 1094 (1968).
5. Акимбеков К., Куксенко В.С., Низамидинов С., Слуцкер А.И., Ястребинский А.А. Физ. тверд. тела, 14, *9*, 2708 (1972).
6. Rånby B., Rabek F. J., *Photodegradation, Photooxidation and Photostabilization of Polymers. Principles and Applications*. J. Wiley, New York, 1975.

CARACTERUL TREPTIFORM AL PROCESULUI DE RUPERE FRACTURARE A POLIMERILOR ÎN CONDIŢIILE FLUAJULUI LA TRACŢIUNE

(Rezumat)

Se abordează studiul etapelor procesului de rupere a polimerilor la solicitare statică la tracţiune : mecano-activarea, mecanocracarea şi reorganizarea structurii. Fiecare stadiu are la bază actul mecanochimic constînd în scindarea sub efort a unor legături chimice de pe catena de bază. Macroradicalii formaţi sînt puşi în evidenţă prin tehnici indirecte: reacţii cu acceptori radicalici, spectroscopie în ultraviolet şi infraroşu, microscopie de transmisie.

BULETINUL INSTITUTULUI POLITEHNIC DIN IAŞI
Tomul XXXI (XXXV), Fasc. supl., 1985
Secţia II
CHIMIE ŞI INGINERIE CHIMICĂ

D.C. 678-13

COPOLYMERS

VIII. STUDY ON TERPOLYMERIZATION OF ACRYLONITRILE (AN) WITH α-METHYL-STYRENE (MS) AND CINNAMIC ACID (CA)

BY

N. ASANDEI, M. NICU, M. RUSU, S. PETROVAN, VIORICA NICU and MARIA LUNGU

1. Introduction

Due to the carboxylic group the CA could confer improved tinctorial properties and lower electrostatic charge to the copolymers [1] ... [5]. Due to its high cost price it would be preferable to use it in a very low content and in ternary mixtures of a cheap termonomer.

In the present paper the characteristics of the CA copolymerization with AN and MS as a termonomer are studied.

2. Synthesis of Terpolymers

The synthesis of terpolymers was based on the reaction :

$$\text{(1)}\quad \underset{\substack{|\\ CN\\ AN(M_1)}}{CH_2{=}CH} + \underset{\substack{|\\ C_6H_5\\ MS(M_2)}}{CH_2{=}\overset{\substack{CH_3\\ |}}{C}} + \underset{\substack{|\\ C_6H_5\\ AC(M_3)}}{CH{=}\overset{\substack{COOH\\ |}}{CH}} \longrightarrow \underset{(m_1;m_2;m_3)}{\text{Terpolymers}}$$

2.1. Synthesis of Terpolymers in Methanol Medium

Since CA shows a low solubility in water (less than 2%) it had to choose a solvent for these monomers as a terpolymerization medium, namely the methanol. The compositions of the substrata as well as the recipers used are given in Table 1.

The reaction was stopped by adding a hydroquinone alcoholic solution. The obtained terpolymers were washed with acetone and then dried in an oven at 80°C.

2.2 Synthesis of Terpolymers in Aqueous Medium

Since the ternary system under study would react in aqueous medium it was necessary to verify the conclusions of the composition studies of the terpolymers synthesized in methanol on the terpolymers resulted in aqueous

medium. In this purpose the products *68* and *69* were synthesized according to the data from Table 1.

Table 1

Terpolymerization Recipers and Composition of Terpolymers

Characteristic	Symbol					
	13 128	*13 146*	*13 164*	*13 182*	*68*	*69*
	Composition substrata, [% mol]					
AN (M_1)	90	90	90	90	97.38	97.56
MS (M_2)	2	4	6	8	2.25	2.25
CA (M_3)	8	6	4	2	0.36	0.18
Reaction medium	methanol (AIBN)				water ($K_2S_2O_8$ + + $Na_2S_2O_5$)	
Reaction temperature, [°C]	60				60	
Conversion, [% weight]	2.1	2.6	2.4	2.8	63.31	60.68
Composition of terpolymers, [% mol], experimental						
AN (m_1)	88.1	86.95	86.50	89.44	96.85	95.46
MS (m_2)	7.49	7.57	10.30	7.60	1.97	2.19
CA (m_3)	4.40	5.47	3.20	2.95	1.17	0.95
Integral composition of terpolymers calculated by means of Eqs. (14)...(17), [% mol]						
AN	—	—	—	—	97.08	97.42
MS	—	—	—	—	2.38	2.33
CA	—	—	—	—	0.53	0.24
Integral compositions of terpolymers calculated by means of Eqs. (24)...(27), [% mol]						
AN	—	—	—	—	97.20	97.42
MS	—	—	—	—	2.32	2.33
CA	—	—	—	—	0.47	0.24

3. Analysis of Terpolymers

3.1. Qualitative Analyses

The synthesized terpolymers were analysed by IR and NMR spectra measurements. The IR spectra are given in Fig. 1.

The IR and NMR spectra show the absorptions and the signals, respectively, characteristic to main structural elements of the termonomers

The NMR spectroscopy was also tried for quantitative estimations (Fig. 2), but some signals are not satisfactory resolved due to the particular structure of the products, so it was not possible to use these measurements in the mentioned purpose.

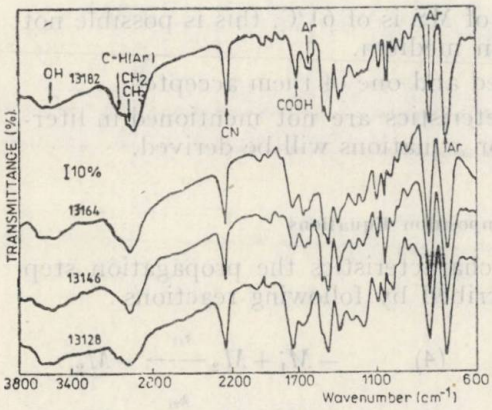

Fig. 1. — IR spectra of some terpolymers.

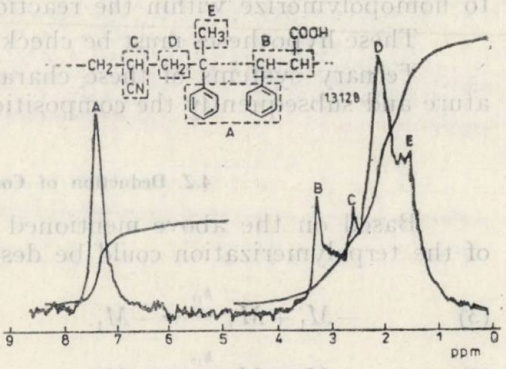

Fig. 2. — NMR spectrum of the terpolyme *13 128*.

3.2. Quantitative Analyses

In order to determine the quantitative copolymer compositions, the IR spectra were used, in which the absorptions of the —CN (2 240 cm^{-1}) —COOH (1 730 cm^{-1}) and phenyl groups (720 cm^{-1}) are well resolved.

In the IR spectra the absorptions were measured and their ratios calculated. Then the molar ratios of the terpolymers (a and b) were read on the composition — absorption ratio standard curves, and made up the following set of equations :

$$\frac{m_2+m_3}{m_1}=a, \qquad \frac{m_3}{m_1}=b, \qquad m_1+m_2+m_3=1. \tag{2}$$

By solving the system (2) the compositions of the terpolymers given in Table 1 were found.

4. Relations between Substratum and Terpolymer Compositions

4.1. Characteristics of the Terpolymerization System

The characteristics of our system may be discussed in function of those of the copolymerization in binary systems, namely :

a) Since CA must be introduced into the terpolymers in low amounts, its concentrations within the substratum will be very low ; in that limits in which it was found [6] that it might copolymerize with AN by charge transfer mechanism. This possibility must be also verified with terpolymerization.

b) CA does not homopolymerize and hence propagation reactions in which the CA molecules would add to the macroradicals terminated in AC units can not proceed.

c) CA does not copolymerize with MS and neither propagation reactions in which respective monomers would add to the macroradicals terminated in corresponding units can be assumed.

d) Since the ceiling temperature of MS is of 61°C, this is possible not to homopolymerize within the reaction medium.

These hypotheses must be checked and one of them accepted.

Ternary systems of these characteristics are not mentioned in literature and subsequently the composition equations will be derived.

4.2. Deduction of Composition Equations

Based on the above mentioned characteristics the propagation step of the terpolymerization could be described by following reactions:

(3) $-M_1^{\cdot} + M_1 \xrightarrow{k_{11}} -M_1^{\cdot}$; (4) $-M_1^{\cdot} + M_2 \xrightarrow{k_{12}} -M_2^{\cdot}$,

(5) $-M_1^{\cdot} + M_3 \xrightarrow{k_{13}} -M_3^{\cdot}$, (6) $-M_2^{\cdot} + M_1 \xrightarrow{k_{21}} -M_1^{\cdot}$,

(7) $$-M_3^{\cdot} + M_1 \xrightarrow{k_{31}} -M_1^{\cdot}.$$

The rate constants of the elemental reactions are written on the arrows.

By applying the steady state hypotheses the following equations for the monomer consumption can be written:

(8) $$-\frac{dM_1}{dt} = k_{11}M_1M_1^{\cdot} + k_{21}M_1M_2^{\cdot} + k_{31}M_1M_3^{\cdot},$$

(9) $-\frac{dM_2}{dt} = k_{12}M_2M_1^{\cdot}$, (10) $-\frac{dM_3}{dt} = k_{13}M_3M_1^{\cdot}$.

Under steady state conditions the rate of radical formation equals that of their consumption. Hence,

(11) $$k_{21}M_2^{\cdot}M_1 + k_{31}M_3^{\cdot}M_1 = k_{12}M_1^{\cdot}M_2 + k_{13}M_1^{\cdot}M_3,$$

(12) $k_{12}M_1^{\cdot}M_2 = k_{21}M_2^{\cdot}M_1$, (13) $k_{13}M_1^{\cdot}M_3 = k_{31}M_3^{\cdot}M_1$.

By combining the above relations the following set of equations results describing the correlation between the substratum and terpolymer compositions:

(14) $\frac{m_1}{m_2} = r_{12}\frac{M_1}{M_2} + 1 + \frac{1}{R}\cdot\frac{M_3}{M_2}$, (15) $\frac{m_1}{m_3} = r_{13}\frac{M_1}{M_3} + R\frac{M_2}{M_3} + 1$,

(16) $\frac{m_2}{m_3} = R\frac{M_2}{M_3}$, (17) $m_1 + m_2 + m_3 = 1$,

where m_i and M_i represent molar fractions and

$$r_{12} = \frac{k_{11}}{k_{12}}, \quad r_{13} = \frac{k_{11}}{k_{13}}, \quad R = \frac{k_{12}}{k_{13}}.$$

For the case where MS can homopolymerize the elemental reactions of the propagation step would be eq. (18)...(23)

(18) $-M_1^{\cdot} + M_1 \xrightarrow{k_{11}} -M_1^{\cdot}$, (19) $-M_1^{\cdot} + M_2 \xrightarrow{k_{12}} -M_2^{\cdot}$,

(20) $-M_1^{\cdot} + M_3 \xrightarrow{k_{13}} -M_3^{\cdot}$, (21) $-M_2^{\cdot} + M_1 \xrightarrow{k_{22}} -M_1^{\cdot}$,

(22) $-M_2^{\cdot} + M_2 \xrightarrow{k_{22}} -M_2^{\cdot}$, (23) $M_3^{\cdot} + M_1 \xrightarrow{k_{31}} -M_1^{\cdot}$

and applying the above method the composition set of equations (24)...(27) is obtained :

(24) $\frac{m_1}{m_3} = \frac{M_1}{M_3}\left(r_{13} + R\frac{M_2}{M_1} + \frac{M_3}{M_1}\right)$, (25) $\frac{m_2}{m_3} = \frac{M_2}{M_3}\left(R + r_{21} R\frac{M_2}{M_1}\right)$,

(26) $m_1 + m_2 + m_3 = 1$; (27) $r_{ij} = \frac{k_{ii}}{k_{ij}}$, $R = \frac{k_{12}}{k_{13}}$.

By means of Eqs. (14)...(17) the following values of the reactivity constants were found : $r_{12} = 0.9222$; $r_{13} = 0.5947$; $R = 0.6442$. These values suggest that the CA rather than MS pref rentially adds to the macroradicals terminated in AN.

The same conclusion is drawn from reactivity constants corresponding to Eqs. (24)...(27).

In order to find which of two proposed models reflects the real situation, more faithfully the integral compositions of the terpolymers at high conversion (*68* and *69*) were calculated by means of them. Results given in Table 1 show clearly that AN + MS + CA system forms terpolymers whose composition is described by Eqs. (14)...(17) and the terpolymerization model is given by the reactions (3)...(7).

The composition – conversion dependence calculated according to the settled model is depicted in Fig. 3.

4.3. Qualitative Appreciations on Terpolymer Sequences

Taking into account the reactivity constants and the compositions of the synthesized terpolymers from substrata of low content of MS and CA, these compounds may be considered to consist of long AN chains joined by either CA or MS units (s. (28)).

By examining the variation of the substrata and of the terpolymers as a function of conversion (Fig. 3), minor modifications in the procentual compositions are noticed which assures the compositional and sequential uniformity of terpolymers :

(28)
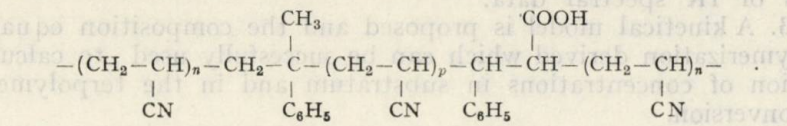

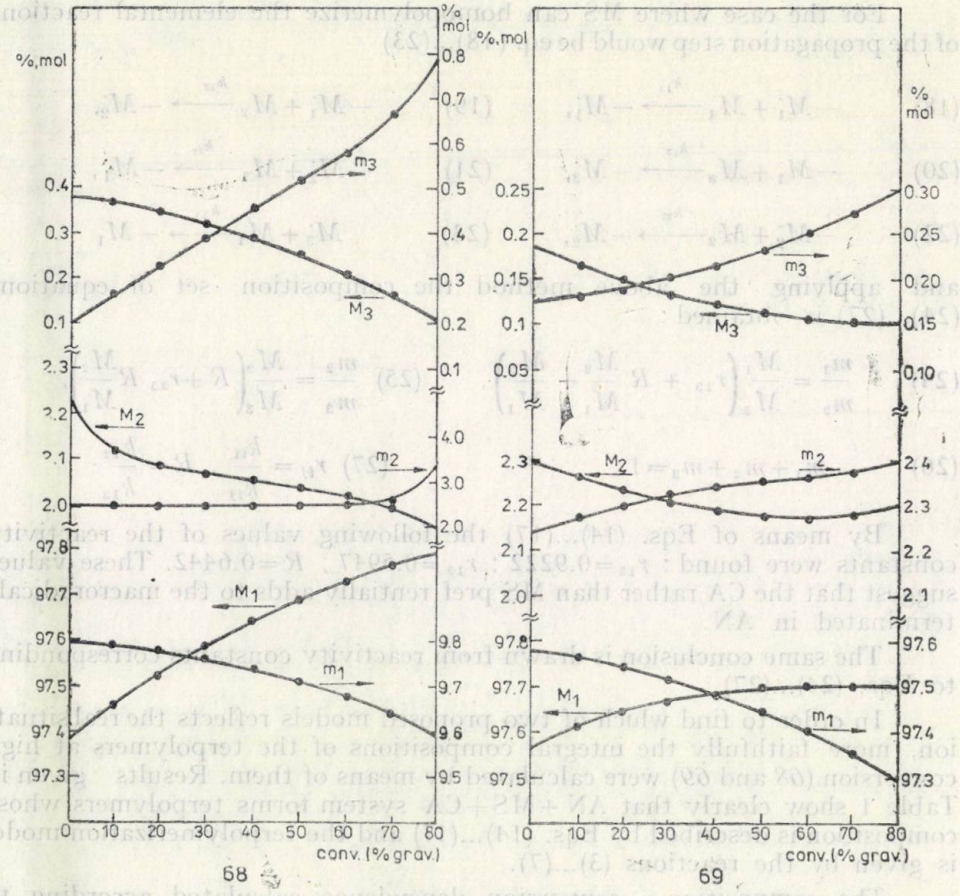

Fig. 3. — Variation of composition of substrata and terpolymers with conversion for the terpolymerizations *68* and *69*.

The proposed and verified kinetical model attests that the terpolymers do not contain CA—CA, MS—MS and CA—MS diades.

5. Conclusions

The researches on the terpolymerization of the AN + MS + CA system lead to the following conclusions:

1. By the reaction of AN with MS and CA terpolymers are formed.
2. The terpolymer composition can be estimated quantitatively by means of IR spectral data.
3. A kinetical model is proposed and the composition equations of terpolymerization derived which can be succesfully used to calculate the variation of concentrations in substratum and in the terpolymers with the conversion.

4. The synthesized terpolymers are of the statistical type and consist of the long AN sequences joined by either MS or CA units.

5. Due to the reactivity constants whose values are convenient the substratum compositions vary very little with the conversion which assures the compositional and sequential uniformity of the terpolymers.

Received, April 16, 1985

Polytechnic Institute, Jassy,
Department of Organic
and Macromolecular Chemistry and
Technology

REFERENCES

1. * * * Monsanto Chemical Co., Belg., Pat., *628 794* (1963) ; C.A. **60** (10), 12 165 g.
2. * * * Idem, U.S. Pat., *3 410 835* (1968) ; C.A. **70** (12), 48 544c, (1969).
3. * * * Idem, U.S. Pat., *3 388 189* (1968) ; C.A. **69** (8), 28 527a (1968).
4. * * * Idem, U.S. Pat., 3 310 535 (1963) ; C.A. **66**, 116 638f (1967).
5. Simionescu Cr., Vasiliu-Oprea Cl., *Tratat de chimia compuşilor macromoleculari.* Vol. I, EDP, Buc., 1973.
6. Asandei N., Nicu M., Rev. Roum. Chim., **25**, 915 (1980).

COPOLIMERI

VIII. Studiul terpolimerizării acrilonitrilului (AN) cu α -metilstirenul (MS) şi acidul cinamic (CA)

(Rezumat)

S-a studiat terpolimerizarea acrilonitrilului cu α -metilstiren şi cu acid cinamic în mediu de metanol şi în apă. Compoziţia cantitativă a terpolimerilor s-a determinat prin spectroscopie în IR. S-au stabilit ecuaţiile de compoziţie a terpolimerilor, găsindu-se că AN copolimerizează cu partenerii, dar aceştia nici nu homopolimerizează şi nici nu copolimerizează.

BULETINUL INSTITUTULUI POLITEHNIC DIN IAȘI
Tomul XXXI (XXXV), Fasc. supl., 1985
Secția II
CHIMIE ȘI INGINERIE CHIMICĂ

D.C. 547.785.5

COMPLEX COMPOUNDS OF 5-AMINO-BENZIMIDAZOLONE-2 WITH CERTAIN CATIONS OF TRANSITIONAL METALS

BY

N. FOCA, VALERIA GORDUZA and LUMINIȚA WAGNER

1. Introduction

Utilisation of 5-amino-benzimidazolone-2 in synthesis of some heterocycle azopigments of high quality rised the interest to study the structure and reactivity of the benzimidazolone derivatives (I)...(IV) [1] :

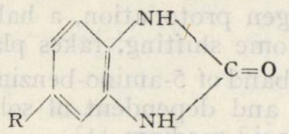

(I) – (IV)

where

R : H (I), $-NO_2$ (II), $-NH_2$ (III), $-NH-\overset{\overset{O}{\|}}{C}-CH_2-\overset{\overset{O}{\|}}{C}-CH_3$ (IV).

The benzimidazolone derivatives participate at tautomerism equilibria, which are influenced by a series of factors, such as : medium nature, temperature, the presence of transitional metal cations, etc.

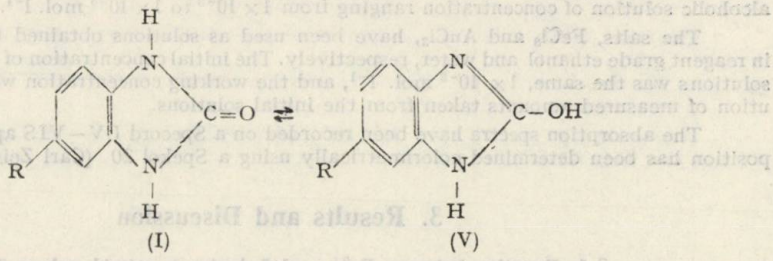

(I) (V)

Their two-fold reactivity is correlated with amphoteric character and susceptibility to react in both undisociated and ionized states [2].

The 5-amino-benzimidazolone-2 (III) can act as ligand for the Fe^{3+}, Au^{3+} and Pt^{4+} ions, due to electrodonator character correlated with the possibility of the $p-\pi$ conjugation, participation of electronic doublet of aminic nitrogen, aromatic skeleton and ureidic remainder. Thus, the

increased reactivity and implicitly coordination capacity toward the cations of transitional metals can be accepted for the structure (VI) :

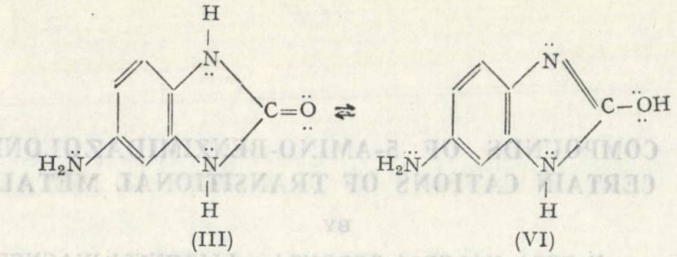

(III) (VI)

Due to the polarizability of the carbonyl group, the electrodonator character of nitrogen atoms in the ureidic remainder and phenylic nucleus, in the benzimidazolone derivatives an enlarged conjugated system is realised. Differentiation of the absorption bands is possible on the basis of solvochromic and halochromic effects [3], [4].

The possibility of the $p-\pi$ conjugation in heteroaromatic amines leads to a decrease of the bond orbital energy and to an increase of nonparticipant orbital energy, so that the $n-\pi^*$ transition energy is diminished. On the other hand, by nitrogen protonation, a halochromic effect, spectrally transposed in a hypsochrome shifting, takes place.

The characteristic band of 5-amino-benzimidazolone-2, situated between 304.4 and 318 nm, and dependent of solvent polarity, undergoes a hypsochromic shifting in acid medium [1].

It seems to be of interest the fact that by acidulation or alkalization, the absorption band characteristic to the $n-\pi^*$ transition of carbonyl group (226 nm) is shifted and modified as a shoulder in the 228...236 nm domain (acid medium) and in the 250...250.5 nm domain (in alkaline medium).

2. Experimental

The ligand (L), i.e. 5-amino-benzimidazolone-2 being water insoluble, it was employed as alcoholic solution of concentration ranging from 1×10^{-3} to 1×10^{-5} mol. l^{-1}.

The salts, $FeCl_3$ and $AuCl_3$, have been used as solutions obtained by their dissolution in reagent grade ethanol and water, respectively. The initial concentration of the $FeCl_3$ and $AuCl_3$ solutions was the same, 1×10^{-3} mol. l^{-1}, and the working concentration was attained by dilution of measured amounts taken from the initial solutions.

The absorption spectra have been recorded on a Specord UV—VIS apparatus , and composition has been determined colorimetrically using a Spekol 20 (Carl Zeiss Jena) apparatus.

3. Results and Discussion

3.1. Reaction between Fe^{2+} and 5-Amino-benzimidazolone-2

The Fe^{3+} ion easily reacts with 5-amino-benzimidazolone-2, forming a complex compound with a specific spectrum in UV and VIS regions, different from that of the reagents. The absorption spectra presented in Fig. 1 belong only to the resulted complex, the ligand alone having no absorbtion in VIS region.

The characteristics of the absorption bands of the complexes are given in Table 1.

Table 1

Characteristics of the Absorption Bands of Fig. 1

Nr.	Compound	Solvent	Concentration mol. l^{-1}	λ_{max} nm	ε_{max} $l.mol^{-1}.cm^{-1}$
1	$FeCl_3+L(1:1)$	C_2H_5OH	1×10^{-4}	640	2 350
2	$FeCl_3+2L(1:1)$	C_2H_5OH	1×10^{-4}	640	4 300
3	$FeCl_3+L(1:1)$	H_2O	1×10^{-4}	620	2 400
4	$FeCl_3+2L(1:2)$	H_2O	1×10^{-4}	620	2 650

The data from Table 1 show that, in ethanol, the complex has a band situated at 640 nm for both 1 M : 1 L and 1 M : 2 L and λ_{max}, in aqueous solution, is situated at a smaller wave length, namely 620 nm. Besides the absorption bands with $\lambda = 640$ and 620 nm, other bands occur at $\lambda_{max} = 330$ and 355 nm in ethanol and a single band with $\lambda_{max} = 350$ nm in aqueous medium, which also belongs only to the Fe^{3+}—5-amino-benzimidazolone-2 complex.

3.2. Reaction between Au^{3+} and 5-Amino-benzimidazolone-2

As in the previous case, the reaction between Au^{3+} and 5-aminobenzimidazolone-2 is a rapid one with formation of a complex whose absorption spectrum in UV and VIS region shows the interaction between Au^{3+} and 5-amino-benzimidazolone-2 (L) (Fig. 2).

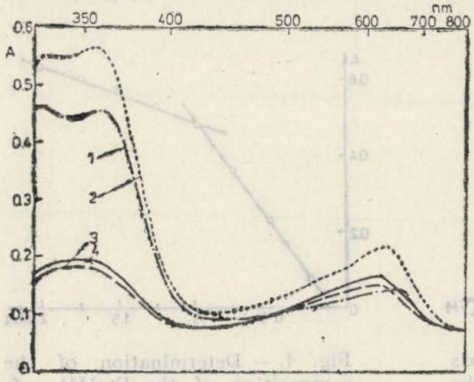

Fig. 1. — Absorption spectra of the complexes formed in the Fe^{3+} — 5-amino-benzimidazolone-2 system in VIS. region.

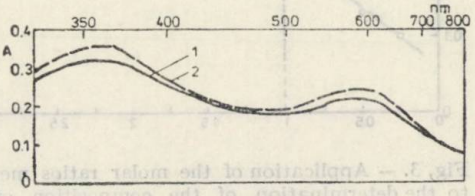

Fig. 2. — Absorption spectra in VIS region recorded for the Au^{3+} — 5-amino-benzimidazolone-2 system.

The characteristics of the bands of the absorption spectra represented in Fig. 2 are listed in Table 2.

Table 2

Characteristics of the Absorption Bands of Fig. 2

Nr.	Compound	Solvent	Concentration mol. l^{-1}	λ_{max} nm	ε_{max} $l.mol^{-1}.cm^{-1}$
1	$AuCl_3+L(1:1)$	H_2O	1.10^{-4}	365	6 800
2	$AuCl_3+L(1:1)$	H_2O	1.10^{-4}	580	4 800
3	$AuCl_3+L(1:2)$	H_2O	1.10^{-4}	365	7 600
4	$AuCl_3+L(1:2)$	H_2O	1.10^{-4}	580	5 200

As it comes out from both Fig. 2 and Table 2, the reaction of Au^{3+} with 5-amino-benzimidazolone-2 forms a complex having two bands, with $\lambda_{max}=365$ nm and respectively $\lambda_{max}=580$ nm.

4. Composition of the Complex formed in the Fe(III) — 5-Amino-benzimidazolone-2 System

The complex ions in the Fe(III) on Au(III) — 5-amino-benzimidazolone-2 systems have been investigated as regards their composition by several spectrophotometric methods.

4.1. The Molar Ratios Method [5]

The results obtained by this method show that in solution only one complex ion corresponding to the ratio $L/Fe^{3+}=1$, (Fig.3) is formed. Applying the method in the case in which the ligand concentration is maintained constant and the concentration of the metal varies, (inverse titration), one obtaines the same combination ratio, 1 M : 1 L (Fig.4).

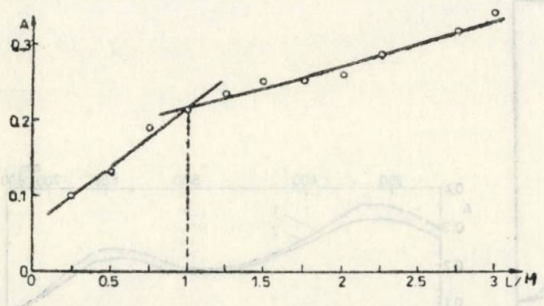

Fig. 3. — Application of the molar ratios methods to the determination of the composition of the Fe(III) — 5-amino-benzimidazolone-2 complex; $C_L = C_{FeCl_3} = 1 \cdot 10^{-3}$ mol. l^{-1} ; $V_f = 7.5$ cm³.

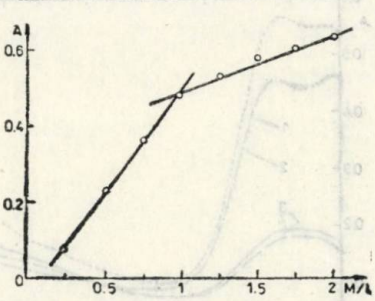

Fig. 4. — Determination of the composition of the Fe(III) — 5-amino-benzimidazolone-2 complex by inverse titration ; C_L = const. ; C_{FeCl_3} = variable ; $V_f = 5$ cm³.

4.2. The Job's Method [6]

In order to determine the composition of the formed complex, measurements of absorbance through solutions in which $FeCl_3 + L = const.$ at wavelength proper to the complex have been performed. The obtained results are presented in Fig. 5.

Fig. 5 shows that the $FeCl_3$ to 5-amino-benzimidazolone-2 combination ratio is 1 : 1, result which is in good agreement with those of previous methods.

The spectrophotometric data obtained by the above mentioned methods point out that in the Fe (III) — 5-amino-benzimidazolone-2 system, the complex with the 1 M : 1 L ratio is formed, supporting the following chemical process :

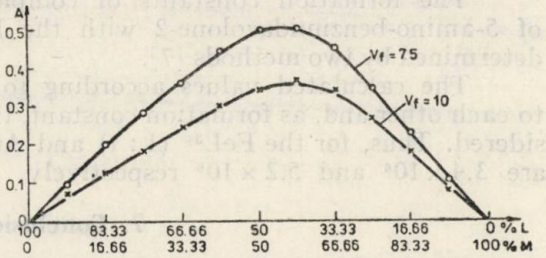

Fig. 5. — Study of composition of the $FeCl_3$ — 5-amino-benzimidazolone-2 system by Job's method.

$$Fe^{3+} + L \underset{\leftarrow}{\overset{\text{rapidly}}{\rightarrow}} FeL^{3+}.$$

The composition of the complex formed in the Au(III) — 5-amino-benzimidazolone-2 system was investigated with the same method as in previous case. The data obtained show the formation of only one complex, (Fig. 6).

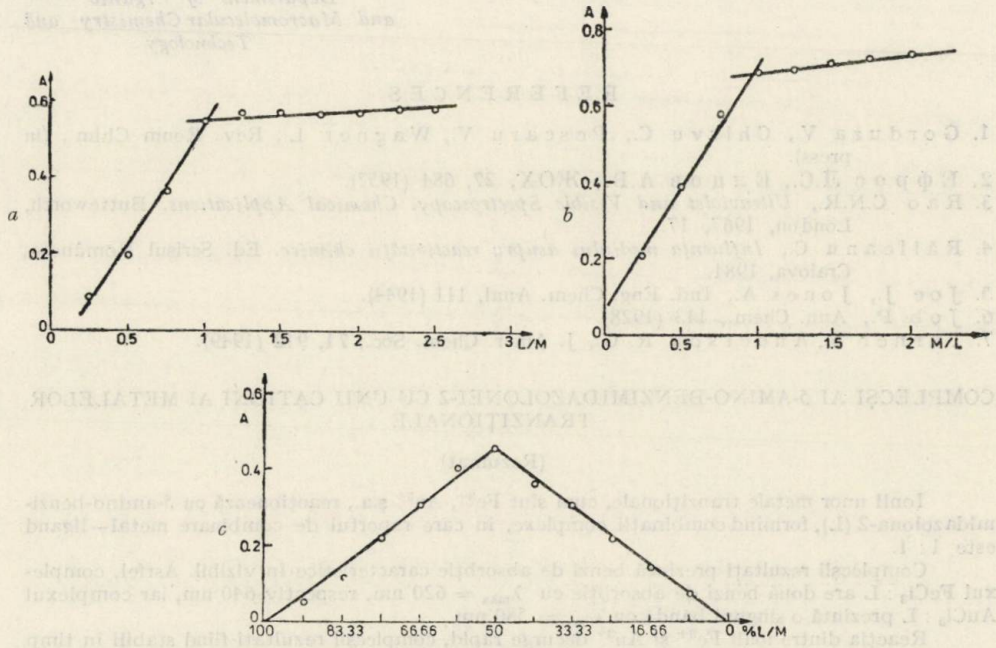

Fig. 6. — Study of the composition complex of the $AuCl_3$ — 5-amino-benzimidazolone-2 system by molar ratio (*a*), Job's method (*b*), invers titration (*c*).

The spectrophotometric data of the $AuCl_3$—5-amino-benzimidazolone-2 system, in aqueous solution, prove the formation of a single complex, $AuCl_3$—L (1 : 1).

6. Determination of the Formation Constant

The formation constants of complexes resulted from the reaction of 5-amino-benzimidazolone-2 with the Fe^{3+} and Au^{3+} ions have been determined by two methods [7].

The calculated values according to both methods are comparable to each other and, as formation constant, the mean values have been considered. Thus, for the FeL^{3+} (1 : 1) and AuL^{3+} (1 : 1) the calculated values are 3.4×10^6 and 5.2×10^6 respectively.

7. Conclusions

The results can be summarized in the following statements :

1. The Fe^{3+} and Au^{3+} ions react with 5-amino-benzimidazolone-2, forming complexes by ratio 1 M : 1 L.

2. The reaction between Fe^{3+}, Au^{3+} and ligand is a rapid one, the complex ions appearing instantaneously, when the reagents are mixed. The complex ions are stable in time.

3. The values of the formation constants show that the reaction between Fe^{3+}, Au^{3+} and ligand develops in the direction of the complex formation.

Received, April 28, 1985

Polytechnic Institute, Jassy,
Department of Organic
and Macromolecular Chemistry and
Technology

REFERENCES

1. Gorduza V., Chirvu C., Pescaru V., Wagner L., Rev. Roum Chim., (in press).
2. Ефрос Л.С., Елцов А.В., ЖОХ, 27, 684 (1957).
3. Rao C.N.R., *Ultraviolet and Visible Spectroscopy. Chemical Applications*. Butteworth, London, 1967, 17.
4. Răileanu C., *Influența mediului asupra reactivității chimice*. Ed. Scrisul Românesc, Craiova, 1981.
5. Joe J., Jones A., Ind. Eng. Chem. Anal, 111 (1944).
6. Job P., Ann. Chem., 113 (1928).
7. Turner S., Anderson R. G., J. Amer. Chem. Soc., 71, 912 (1949).

COMPLECȘI AI 5-AMINO-BENZIMIDAZOLONEI-2 CU UNII CATIONI AI METALELOR TRANZIȚIONALE

(Rezumat)

Ionii unor metale tranziționale, cum sînt Fe^{3+}, Au^{3+} ș.a., reacționează cu 5-amino-benzimidazolona-2 (L), formînd combinații complexe, în care raportul de combinare metal—ligand este 1 : 1.

Complecșii rezultați prezintă benzi de absorbție caracteristice în vizibil. Astfel, complexul $FeCl_3$: L are două benzi de absorbție cu λ_{max} = 620 nm, respectiv 640 nm, iar complexul $AuCl_3$: L prezintă o singură bandă cu λ_{max} = 580 nm.

Reacția dintre ionii Fe^{3+} și Au^{3+} decurge rapid, complecșii rezultați fiind stabili în timp și se supun legii Beer pe un domeniu larg de concentrații. Constantele de formare sînt : $3{,}40 \cdot 10^6$ și $5{,}2 \cdot 10^6$ l mol^{-1}.

BULETINUL INSTITUTULUI POLITEHNIC DIN IAȘI
Tomul XXXI (XXXV), Fasc. supl., 1985
Secția II
CHIMIE ȘI INGINERIE CHIMICĂ

D.C. 66.095.2

CATIONIC POLYMERIZATION OF 4-VINYL-1-CYCLOHEXENE

BY

IOAN I. NEGULESCU, AURA ANGELICA POPA and CAMELIA MIHĂILESCU

1. Introduction

4-Vinyl-1-cyclohexene (4-VCH) was polymerized cationically by several authors [1]...[3] and different structures were proposed for the chain units :

POSSIBLE UNITS OF 4-VINYLCYCLOHEXENE POLYMERS

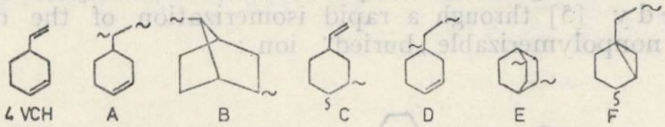

A: VINYLIC ADDITION (EXO)
B,E: CYCLOPOLYMERIZATION
C: OLEFINIC ADDITION (ENDO)
D: HYDRIDE SHIFT POLYM.

This monomer, 4-VCH, would be expected to undergo both olefinic and cyclic polymerization and, indeed, these types of enchainments, *A* and *B*, respectively, were first proposed by B u t l e r et al. [1] who eliminated the participation of the internal olefinic bond alone, to form the structure *C*, as too resistant to be opened by cationic initiators. However, in a rather old paper, H o f f m a n n [4] mentioned briefly that cyclopentene and cyclohexene can be readily oligomerized with BF_3 and some HF to dimers, trimers and tetramers as well as transparent amber solid resins.

As suggested by K e n n e d y [5], and mentioned also by H u b l e i n [3], other structural units of 1,3 addition type, *D*, could arise by intramolecular hydride shift isomerization as in cationic polymerization of vinylcyclohexane [6]. Besides the methylene bicyclo (2.2.1) heptane unit, *B*, another structural unit of bicyclo (2.2.2) octane type, *E*, could arise with some probability through the initiation at the group alone, followed by cyclization through the endo cyclic unsaturation, in a similar way to cyclization pointed out by B u t l e r et al. [7] at the polymerization of 1-methylene-4-vinylcyclohexane, but this unit would be difficult to be differentiated from the other saturated structure of *B* type.

If one considers the tertiary homoallylic carbonium ion formed by hydride shift isomerization then the condensed bicyclic structure, *F*, could appear through a mechanism similar to methylene norbornene polymerization [8].

In the present paper the cationic polymerization of 4-VCH, in the presence of $AlCl_3$, is considered and the monomer encatenation is discussed.

2. Experimental

The monomer (4-VCH) was dried over molecular sieve (4 A) and freshly distilled from sodium metal before use under purified nitrogen. Methylene chloride was kept on and distilled from molecular sieve. The initiator ($AlCl_3$) was sublimed in a flask of 25 mL in which the solution in CH_2Cl_2 was made before the use. Polymerizations were carried out in Schlenk ampoules in nitrogen.

The molecular weight was determined by GPC (Waters 200, THF solutions) and crioscopically (benzene). DSC and DTA data were obtained using a DuPont 990 Calorimeter and a Paulik-Paulik-Erdey Derivatograph, respectively.

IR spectra were recorded on a Perkin Elmer (577) Spectrophotometer. NMR spectra were recorded on a JEOL 60 MHz Spectrometer in $CDCl_3$ using TMS as standard.

3. Results and Disscusion

The fact that high polymers are not obtained at low temperatures in cationic conditions, e.g. $AlCl_3$ in ethyl chloride at $-20°C$ [9], was explained by K e n n e d y [5] through a rapid isomerization of the dimercation leading to a nonpolymerizable „buried" ion :

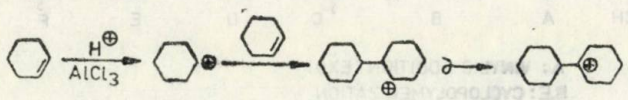

The double bond is reactive to protonation and/or cationation ; however, in the parent compound propagation is impeded because of steric congestion. It is possible that at temperatures higher than $-20°C$ the reaction continues by elimination and alkylation, as suggested by the same author [5] in the case of cyclopentene :

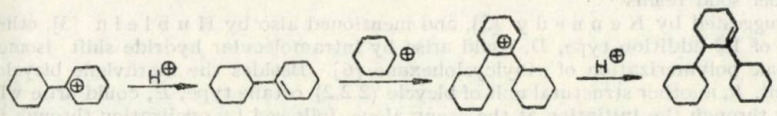

In the present work 4-VCH was polymerized with aluminum chloride in methylene chloride at $-40°$ and $20°C$ (Table 1) and the structure of the obtained products is discussed in terms of spectral and thermal data. Spectroscopic evidence indicates that the cationic polymerization of this monomer proceeds also by addition to the endo olefin bond, similarly to the cationic polymerization of 2-vinyl-5-norbornene, which proceeds predominantly by this type of addition at low temperatures especially.

Table 1

Polymerization of 4-VCH with $AlCl_3$ as Initiator) in CH_2Cl_2*

Exp.	Monomer		$AlCl_3$	T	Time	Yield		$\overline{M}_n$	Observations
	ml	mole/l	mole/l	°C	hrs	g	% conv.	by GPC	
1	8.3	2.80	0.022	−40	4	0.1017	1.65	3 430	Soluble white powder
2	16.6	2.80	0.043	−40	5	0.2085	1.52		Soluble white powder
3	4.0	0.29	0.028	*a*	20	0.7155	21.70	1 320	*a* : −40°C, 9 hrs. and to 20°C, 11 hrs; 44% ins.
4	8.0	0.42	0.089	20	48	1.0933	16.60	1 290	Light yellow ; 11% insoluble; $\overline{M}_w/\overline{M}_n = 3.1$.
5	2.0	0.30	0.206	20	48	1.4104	85.50	1 660	Light yellow ; 20% insoluble ; $\overline{M}_w/\overline{M}_n = 7.1$.
6	6.2	2.54	0.622	20	20	5.5986	total		Brown ; $AlCl_3$ added as powder at 20°C ; 98% ins. ; 6.9% Cl.
7	8.8	2.71	0.186	20	20	0.2461	2.96	2 300	Light yellow ; $AlCl_3$ added as powder at −45°C ; 5% ins.

*) $AlCl_3$ added as solution in CH_2Cl_2 if not otherwise indicated.

Thus the vinyl group is clearly evidenced in the IR spectrum (Fig. 1) of the polymer obtained at −40°C at 3 075 cm^{-1} (*m*), i.e. vinyl side chain on a ring [8] and 1 630 cm^{-1} (*m*), while the internal olefin bond absorbs at 3 020 cm^{-1} (*m*), 960 cm^{-1} (*m*) and 650 cm^{-1} (*s*).

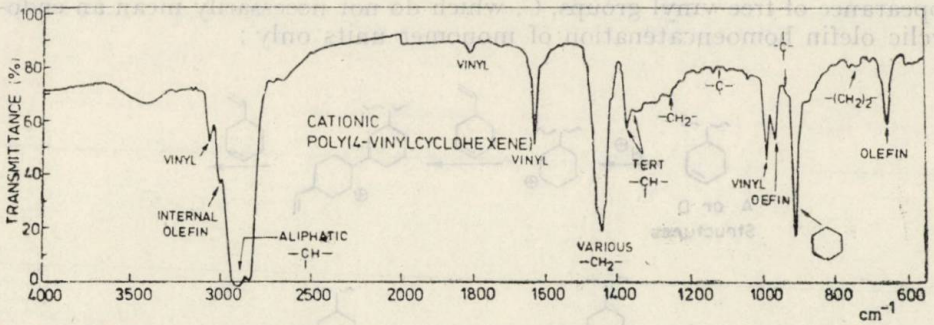

Fig. 1. — IR spectrum of poly(4—VCH) obtained at −40°C with $AlCl_3$ in CH_2Cl_2, KBr pellet.

The NMR spectrum of the same polymer was compared both with the spectrum of the monomer and with that of vinylcyclohexane. From Fig. 2 it can be seen that two of vinylic protons, *a* and *b*, as well as two olefinic protons of cyclohexene ring, *d* and *e*, from the monomer (bottom) could be differentiated easily in the spectrum of the cationic polymer.

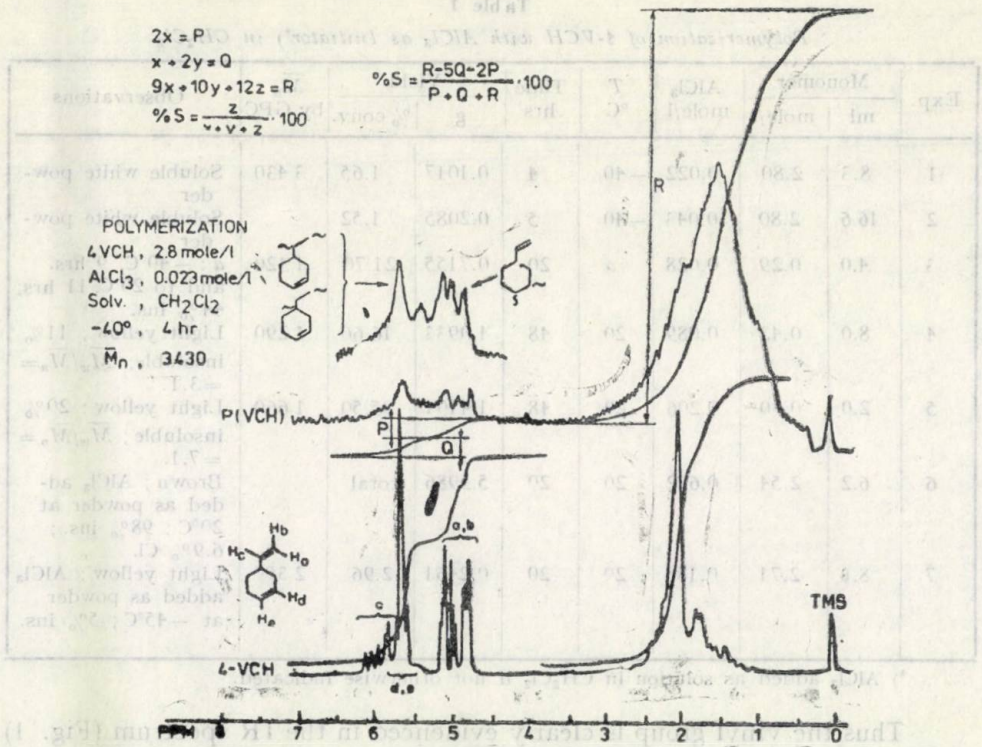

Fig. 2. — 60 MHz NMR spectra of 4-VCH and poly(4-VCH) in $CDCl_3$ at 60°C.

One can visualize the following scheme of reactions explaining the appearance of free vinyl groups, *C*, which do not necessarily mean an endocyclic olefin homoencatenation of monomer units only :

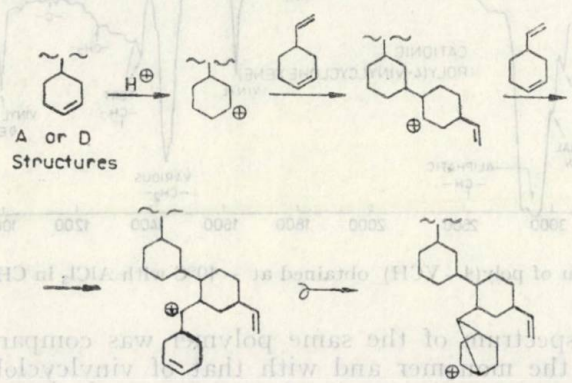

Consequently, both saturated bicyclic *B* units and free vinyl groups, *C*, can appear at the same time.

The degree of cyclization, S, given by saturated units can be readily determined from NMR data (Fig. 2):

$$\%\, S = \frac{z}{x+y+z}; \qquad \%\, S = 100\,\frac{R-5Q-2P}{P+Q+R},$$

where x, y and z represent the participation of vinyl, olefin and saturated units, respectively, and P, Q and R are the integral rise over the corresponding protons.

Not too much ground was found for the structure F from IR data, i.e. the condensed ring has no definite absorptions at 960 cm^{-1} (tert. methyne group overlaped by internal olefin band [8]) or 790 cm^{-1} (vw, bicyclic structure in a linear chain), so that it will not be taken further into consideration.

IR spectra evidentiate the other groups as follows: $>CH_2$ groups from the chain formed through an 1,3 encatenation (corresponding to D) appear between 720...750 cm^{-1} (w), in comparison with the IR spectrum of polyvinylcyclohexane [6], while the quaternary carbon, $-\overset{|}{\underset{|}{C}}-$ also from the structure D, absorbs at 1 170 cm^{-1} (w), 825 cm^{-1} (w) and 925 cm^{-1} (w, shoulder). All these bands are weak, indicating a low degree of participation of structure D ($A+D \sim 25\%$, vide infra). The absorptions from 2 920 cm^{-1} (s) and 2 860 cm^{-1} (s) corresponding to aliphatic $-\overset{\diagdown}{\underset{\diagup}{C}}-H$ groups or from 1 350 cm^{-1} (w) and 1 080 cm^{-1} (vw) corresponding to cyclic $-\overset{\diagdown}{\underset{\diagup}{C}}-H$ groups, as well as the absorptions of different $>CH_2$ groups, e.g. 1 445 cm^{-1} [5] and 1 270 cm^{-1} (w) are not particularly significant. The strong band from 895 cm^{-1} confirms the retention of the cyclohexane ring, this absorption being present in the IR spectra of linear polyvinylcyclohexene of type A [10] and cationic polyvinylcyclohexane formed by an 1,3 addition [6]. This band corresponds to the structures A, C and D.

Using the above NMR equations it was possible to estimate the ratio of structures $A...E$ for the polymer obtained at $-40°C$:

$$(A+D) : C : (B+E) = 4{,}5 : 4 : 9,$$

which gives 52% cyclization and 22% free vinyl groups.

The polymer structure, and consequently its characteristics, are very much affected by reaction conditions (Table 1). For example, the polymer prepared at 20°C, (experiment No. 4 from the Table 1) has only 7% free vinyl groups and 83% cyclized units (unfractionated soluble part of the sample), while the product formed at the same temperature but with the catalyst added as powder (quick exothermic reaction), (experiment No. 6) is practically insoluble.

The strong band at 650 cm^{-1} in IR spectra of insoluble materials show that the crosslinking occurs perhaps mainly by an intermolecular hydride transfer as proposed by H u b l e i n et al. [3].

Unlike poly(4-VCH) obtained with Z i e g l e r catalyst which is linear and crystalline [10], the corresoponding polymers synthesized in cationic conditions are amorphous materials that soften between 100° and 230°C [1] ...[3]. DSC and DTA thermograms of soluble fractions (Figs. 3, 4) evidence an exothermic effect between 120° and 240°C with $\Delta H = 103$ J/g (11.12 KJ/mol). This effect was no more registered if the analyzed sample cooled down to 20°C and re-run (Fig. 3 *C*) or if the pristine sample was annealed at 160°C for 12 min. (Fig. 4 *C*). The insoluble fraction of the

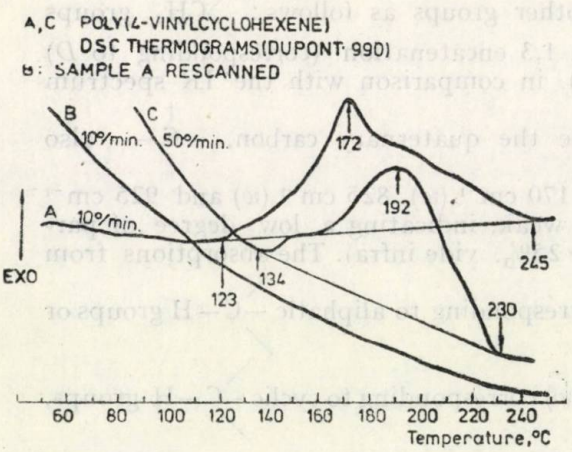

Fig. 3. — DSC thermograms of poly(4-VCH).

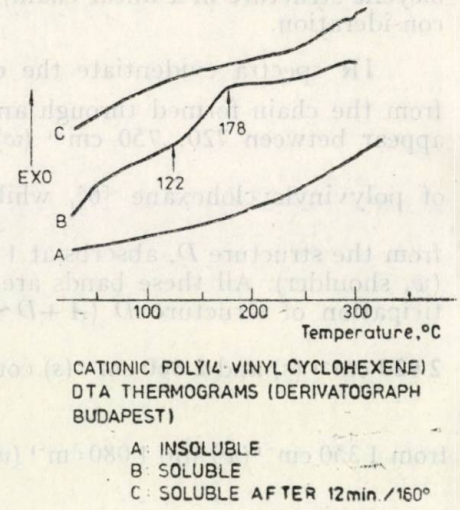

Fig. 4. — DTA thermograms of poly (4-VCH).

same polymer did not show any thermal effect in the same temperature range (Fig. 4 *B*). Based on the NMR and IR spectra of the annealed sample the exothermic effect was attributed to the reaction of free vinyl groups, i.e. the ratio of structures *A*...*D* became :

$$(A+D) : C : (B+E) = 3.5 : 2.3 : 11.3,$$

which gives 66% saturation and 13.5% free vinyl group containing units. If one takes $\Delta H \simeq 90$ KJ/mol to open the vinyl bond of 4-VCH it follows that 12.35% of the polymer units became saturated by reaction of vinyl groups alone, in good agreement with NMR calculations.

4. Conclusions

1. In the presence of $AlCl_3$ at low temperatures, besides vinyl polymerization, intramolecular hydride shift isomerization polymerization and cyclo-polymerization , 4-vinyl-1-cyclohexene can form polymers also

by initiation at the vinyl group alone followed by cyclization through the endo cyclic unsaturation.

2. Saturated structures (more than 50%) formed by cyclopolymerization and cyclization can not be differentiated.

3. Free vinyl groups (cca 20%) were evidenced especially in soluble polymers obtained at −40°C.

4. Part of free vinyl groups disappeared by annealing the sample (120°/6 min.) but the polymer remained soluble, which means that the increase of saturation (cca. 12%) was not the result of crosslinking reactions.

Received, March 26, 1985

„P. Poni" Macromolecular Chemistry Institute, Jassy

REFERENCES

1. Butler G. B., Miles M.L., J. Polymer Sci., **A 3**, 1609 (1965).
2. Альева А. Г., Стоцкая Л. Л., Кренцел Б. А., Высокомол. соедин., **A XV**, 1005 (1973).
3. Hublein G., Hublein B., Plaste u. Kautschuk, **23**, 95 (1976).
4. Hoffmann F., Chem. Ztg., **57**, 5 (1933).
5. Kennedy J. P., *Cationic Polymerization of Olefins : A Critical Inventory.* Wiley-Interscience, 1975, 150.
6. Kennedy J. P., Elliott J. J., Naegele W., J. Polymer Sci., **A 2**, 5029 (1964).
7. Butler G. B., Miles M. L., Brey W. S., J. Polymer Sci., **A 3**, 723 (1965).
8. Kennedy J. P., Makowski H. S., J. Macromol. Sci. - chem., **A-1**, 345 (1967).
9. Boor J., Youngman E. A., Dimbat M., Makromol. Chem., **90**, 26 (1966).
10. Marconi W., Cesca S., Della Fortuna G., J. Polymer Sci., **B(2)**, 301 (1964).

POLIMERIZAREA CATIONICĂ A 4-VINIL-1-CICLOHEXENEI

(Rezumat)

4-Vinil-1-ciclohexena a fost polimerizată în prezenţă de $AlCl_3$ în CH_2Cl_2 la −40°C şi 20°C. Pe lîngă structurile saturate formate prin reacţii de ciclopolimerizare şi ciclizare, în cazul fracţiilor solubile s-au evidenţiat spectral (NMR, IR) grupe vinilice libere ce pot apare prin polimerizarea cationică endociclică. Grupele vinilice libere dispar parţial în urma tratamentului termic (160°C16 min.) ce determină creşterea gradului de saturare a polimerului.

BULETINUL INSTITUTULUI POLITEHNIC DIN IAŞI
Tomul XXXI (XXXV), Fasc. supl., 1985
Secţia II
CHIMIE ŞI INGINERIE CHIMICĂ

D.C. 678 13

SYNTHESIS AND PROPERTIES OF CERTAIN NEW ACRYLIC COPOLYMERS

I. SYNTHESIS AND PROPERTIES OF ACRYLONITRILE–MONOANILIDE OF FUMARIC ACID WITH SULPHANILIC ACID Na SALT COPOLYMERS

BY

ILIE DIACONU and CARMEN CHELARU

1. Introduction

Polyacrylonitrile is considered today as one of the most important polymer in synthetic fibres industry. However, in order to improve some of its properties (e.g., the affinity for dyes and the hydrophilicity), acrylonitrile-based copolymers are used. These copolymers contain a high percent of acrylonitrile because the –CN groups determine a good intramolecular cohesion, a high thermal stability and mechanical resistance [1] ... [4].

Acrylic homopolymers and copolymers, especially polyacrylonitrile (PAN), are compounds whose structure and structural changes have remained a difficult problem to elucidate. From this reason, the origin of the thermal transitions in PAN has not been uniquely determined. The published data indicate that the glass transition temperature, T_g, of PAN is scattered over a wide range of temperature (70°...140°C) [5] ... [7] depending on the experimental method used and on the procedures of preparing the samples.

The thermally stimulated depolarization currents method commonly works in ranges of equivalent frequencies of 10^{-2}....10^{-4} Hz, and therefore could be an useful complementary tool for the molecular motion, structure and transition studies of the macromolecular compounds.

This paper reports the copolymerization of acrylonitrile (AN) with a new monomer – monoanilide of fumaric acid with sulphanilic acid – Na salt (*S*), and structural and physical characterization by IR, NMR and thermally stimulated depolarization currents (TSDC) spectroscopic analysis of the copolymer.

2. Experimental

The *S* monomer (99.9%) was used as such and AN was distilled immediately before use.

The parameters of copolymerization were determined by solution polymerization, using free radicals as initiators. Polymerizations were carried out in sealed Pyrex tubes, under argon, in aqueous solution, (at 1 M monomer concentration), at 58°C, using the redox initiators sodium metabisulfite and ammonium persulfate. The copolymerization period was established between 10...15 min. to obtain conversions less than 10%. The copolymerization period increased with the decrease of AN content in the initial mixture. The copolymers were insoluble in the reaction medium.

The purified copolymers (resolved in DMF and reprecipitated in water) were dried at 50°C, under reduced pressure, for 48 hours, for the complete removal of the solvent, (DMF), which tends to be bound to the polar groups of the polymer.

Copolymers composition were determined by elemental microanalysis for sulphur, and by ^1H-NMR spectroscopy from the ratio of aromatic to aliphatic signal integrals, the spectra being registered on a JEOL—C60 HZ spectrometer, in DMSO—d6 solutions at 60°C.

Samples used for TSDC measurements were disk-shaped, prepared by compressing the compounds powder in a mold under a pressure of 10×10^4 N/cm^2. The 16 mm - diameter disks were provided with vacuum-evaporated silver electrodes of circular form. In order to prevent current leakage on surface the electrodes had a diameter of only 14 mm and were centrally placed on both sides of the disks.

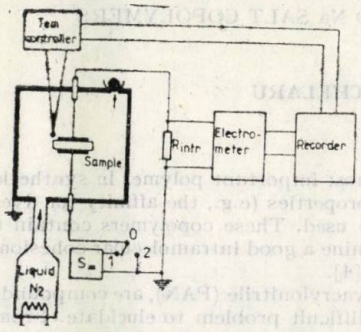

Fig. 1. — Main components of automated equipment for TSDC.

TSDC measurements were caried out in dry nitrogen using a device presented in Fig. 1.

The thermal cycles of polarization and depolarization of samples consisted of the following steps : a sample with a polarization field E_p was warmed up to the polarization temperature T_p, which was maintened constant for a polarization time t_p ; after cooling to 20°C using liquid nitrogen, E_p was removed and the sample was short circuited for 10 min. in order to eliminate the rapid depolarization currents ; then the depolarization currents were recorded by increasing the temperature. The thermal cycles were performed at a rate of 3.3° C/min.

3. Results and Discussion

The IR spectra (Fig. 2) make evident the formation of AN—S copolymers [8].

Copolymerization data are summarized in Table 1 and the copolymerization diagram is presented in Fig. 3.

Table 1

$S(M_1)$—AN(M_2) Copolymerization Data

Sample	Initial mixture $[M_1]/[M_2]$	Conversion %	Copolymer composition $d[M_1]/d[M_2]$
P(AN—S)$_I$	0.05263	8.5	0.010
P(AN—S)$_{II}$	0.17649	9.1	0.051
P(AN—S)$_{III}$	0.3333	9.5	0.089
P(AN—S)$_{IV}$	0.5385	9.0	0.150
P(AN—S)$_V$	1.00	8.7	0.220
P(AN—S)$_{VI}$	3.00	8.0	0.639

The reactivity ratio values, r_1 and r_2, were determined by K é l e n-T ü d ö s method [9], the obtained results being presented in Fig. 4.

The obtained reactivity ratio values are : $r_{AN} = 4.18$ and $r_S = 0.1$.

The straight lines in K é l e n-T ü d ö s plot indicate that no penultimate effect seems to exists for these copolymers, and that the terminal model of copolymerization could be considered to describe this system.

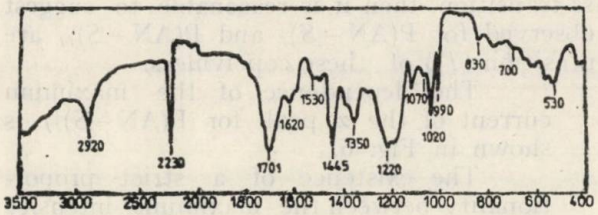

Fig. 2. — The IR spectrum of $P(AN-S)_{II}$ copolymer.

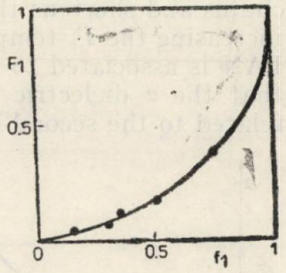

Fig. 3.—The copolymerization diagram of the $S(M_1)-AN(M_2)$ system.

The TSDC thermograms of PAN, $P(AN-S)_I$ and $P(AN-S)_{II}$ in the temperature range 50°...250°C are comparatively presented in Fig. 5.

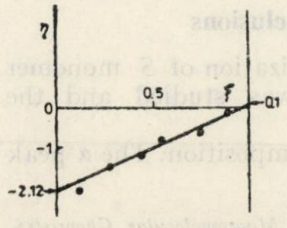

Fig. 4. — The Kélen-Tüdös plot for the $S(M_1)-AN(M_2)$ system.

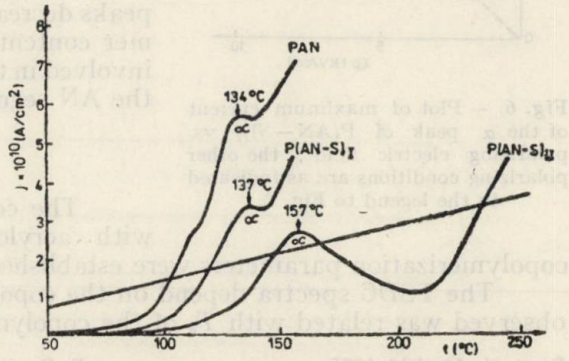

Fig. 5. — TSDC spectra of PAN, $P(AN-S)_I$ and $P(AN-S)_{II}$; polarizing conditions : $E_p=10$ KV/cm ; $t_p=30$ min ; $T_p=150$°C for PAN and $P(AN-S)_I$, and 200°C for $P(AN-S)_{II}$.

All spectra have the same general shape and are characterized by one current peak (α), more or less resolved, and an increasing current part (ρ) at higher temperatures. The α peak of $P(AN-S)_{II}$ is well resolved, whereas in the case of $P(AN-S)_I$, and especially for PAN, this peak is overlaped by ρ increasing current, which probably is the increasing portion of a new arising peak. In order to maintain unalterable the structure of the polymers, the samples were not warmed up over the temperatures shown in Fig. 5.

Fig. 5 shows that both intensity and temperature of the α peak are appreciably affected by the copolymer composition. The maximum intensity of the α peak is a decreasing function of the *S* comonomer content, whereas the corresponding temperature values increase. The α peak temperature of PAN, shown in Fig. 5, appears to be close to the glass transition temperature (140°C) reported elsewhere [5], [6]. The *S* comonomer is more bulky and more polar as compared to the AN monomer. The introduction of this comonomer enhances the dipole—dipole interactions between adiacent

chains and shortens the AN segments of chains. This two facts result in an increasing the T_g temperature of the copolymers. If the α peak observed for PAN is associated to the glass-transition, then it is reasonable to suggest that the α dielectric peaks observed for $P(AN-S)_I$ and $P(AN-S)_{II}$ are related to the second-order transition (T_g) of these copolymers.

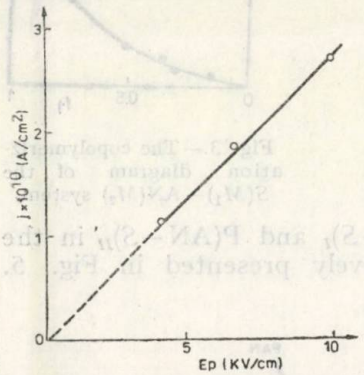

Fig. 6. — Plot of maximum current of the α peak of $P(AN-S)_{II}$ vs. polarizing electric field ; the other polarizing conditions are as indicated in the legend to Fig. 2.

The dependence of the maximum current of the α peak for $P(AN-S)_{II}$ is shown in Fig. 6.

The existence of a strict proportionality between the maximum intensity and field strength shows that a uniform volume dipolar polarization is taking place [10]. This finding also supports the fact that the observed α peaks are related with the second-order transition.

Since the maximum intensity of the α peaks decreases with increasing S comonomer content, the micro-Brownian motions involved in the polarization process occur in the AN segments of the copolymer.

4. Conclusions

The copolymerization of S monomer with acrylonitrile was studied and the copolymerization parameters were established.

The TSDC spectra depend on the copolymer composition. The α peak observed was related with T_g of the copolymers.

Received, April 24, 1985

„P. Poni" Institute of Macromolecular Chemistry, Jassy

REFERENCES

1. Goldfinger G., Steidlitz M., J. Polym. Sci., 3, 786 (1948).
2. Alfrey T.Jr., Overberger C.G., Pinner S.H., J. Amer. Chem. Soc., 75, 4221, (1953).
3. Nair A.S., Muthana M.S., Makromol. Chem., 47, 138 (1961).
4. Аскаров М.А., Банк А.С., Высокомол. Соед., 8, 1012 (1966).
5. Andrew R.D., Kimmel R.M., J. Polym. Sci., B. Polym. Lett., 3, 167 (1965).
6. Meredith R., Hsu B.S., J. Polym. Sci., **61**, 276 (1962).
7. Stupp S.I., Carr S.H., J. Polym. Sci., Polym. Phys. Ed., **18**, 13 (1978).
8. Belamy L.J., *The Infra-Red Spectra of Complex Molecules.* New-York, 1964.
9. Kélen T., Tüdös F., J. Macromol. Sci., Chem., **A9**, 1 (1975).
10. Diaconu I., Dumitrescu Sv., J. Macromol. Sci., Phys., **B21**, 555 (1982).

SINTEZA ŞI PROPRIETĂŢILE UNOR NOI COPOLIMERI ACRILICI

I. Sinteza şi proprietăţile copolimerilor acrilonitrilului cu *p*-sulfonatul de Na al anilidei acidului fumaric

(Rezumat)

Se studiază copolimerizarea acrilonitrilului cu un nou monomer — *p*-sulfonatul de Na al anilidei acidului fumaric — şi proprietăţile dielectrice ale copolimerilor prin metoda curenţilor de depolarizare termic stimulaţi.

BULETINUL INSTITUTULUI POLITEHNIC DIN IAȘI
Tomul XXXI (XXXV), Fasc. supl., 1985
Secția III
CHIMIE ȘI INGINERIE CHIMICĂ

D.C. 667.167

INFLUENCE OF FLAME-RETARDANTS ON THE BEHAVIOUR OF POLYOLEFINES AT HIGH TEMPERATURES

BY

CORNELIA VASILE, FLORIN POPESCU, OANA PETREUȘ, MIHAELA SABLIOVSCHI, ANTON AIRINEI and I. AGHERGHINEI

1. Introduction

Because of the various applications of the polyolefines, their flame-retardancy has a great practical importance. The theoretical study of polyolefine flame-retardancy points out some interesting aspects, since small structural differences determine specific behaviours at high temperatures in the presence of oxigen. Thus, the poly(propylene) sensitivity at the formation of hydro- and peroxides is of about one hundred times higher than for poly(ethylene).

The retardation of the flame and its extinction can be explained by the following complementary theories [1], [2]: gas, thermal, chemical, coating and physical interaction theory; but in the case of each polymer flame-retardant system, the interaction in solid phase or in gaseous phase is predominant.

On this theoretical basis, a classification of inorganic flame-retardants was made : chain transfer agents, which slow the free radical reactions ; ingredients which develop non-flammable gases ; compounds which are capable of forming glassy coating on the burning mass ; materials which act as catalysts for char formation ; molecules which reduce the volatility of the important components and resin formers which act as coupling agents between the substrate and flame retarding agents.

Because of the diversity of the organic flame-retardants and the synthesis of a great number of new compounds, a such classification is extremely difficult.

In the present work, the flame-retardant effect on the polyolefines of four compounds containing halogen, phosphorous and nitrogen was studied. Two of these compounds have small molecules, the others are macromolecular. The tests allowed the determination of the class of each flame-retardant.

2. Experimental

Materials. The investigated samples consisted of poly(ethylene) or poly(propylene) flame-retardants systems. The characteristics of the compounds are given in Table 1.

Mixtures were prepared by stirring the melted PE or PP with 10...16% of above mentioned flame retardants (Table 2).

Table 1

Characteristic of the Components of the Polyolefine/Flame – Retardant Systems

No.	Component	Characteristics	Symbol
1	Poly(ethylene)	I. Polymeric materials. Low-density ; $\rho = 0{,}905$ g/cm³; $\bar{M}_n = 19\,000$; $T_m = 110°...130°C$; commercial, Brazi-Petrochemical Works, Romania.	PE
2	Isotactic poly(propylene)	100% isotactic ; $\bar{M}_n = 22\,000$; $\rho = 0.90 ... 0.91$ g/cm³ ; $T_t = 166 ... 168°C$; commercial Hoechst (BDR).	IPP
3	Atactic poly(propylene)	100% atactic ; $\bar{M}_n = 38\,000$; $\rho = 0.835$ g/cm³ ; $T_t = 145°C$; commercial, Teleajen Petrochemical Works, Romania.	APP
4	Chlorendic anhydride 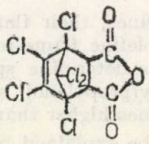	II. Flame retardants. Solid; melting point 230°...235°C; 27.78% C; 1.02% H ; 54.72% Cl	HET
5	Tris(dichloropropyl)phosphate 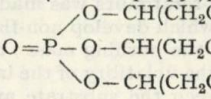	Liquid ; boiling point 250°C, with decomposition ; viscosity 1 800 cP ; 49.0% Cl ; 7.2% P.	TDF
6	Poly(phosphonate) containing chlorine 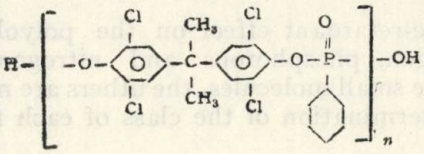	$n = 6 ... 10$; solid ; softening point 193°C ; 51.01% C ; 4.25% H ; 28.75% Cl ; 7.28% P.	PFC
7	Polymer containing phosphorous and nitrogen 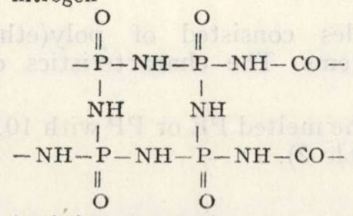 (probable structure)	solid ; crosslinked ; infusible ; 28.0% P ; 38.92% N	PNP

Table 2

TG and DTA Data of Flame Retardants, Non-Additived and Additived APP, IPP and PE

No.	Sample	Temperatures, [°C]			Residue, [%]			S_{DTA} cm^2	E_{CR} KJ/mol	n
		T_i	T_m	T_f	R_{TG}	$R_{theor.}$	R_p			
1	HET	158	209	296	0	—	0	3.72	68.85	0
2	TDF	83	287	320	12	—	—	3.92	26.59	0
3	PFC	271	433	496	20	—	—	0.0	71.10	0
4	PNP	233	320	382	15	—	—	11.47	84.35	1.4
		382	410	470					227.88	2.5
5	APP	209	430	495	0	0	0	6.95	45.46	0
6	85 APP/15 HET	183	304	540	3.5	0	1.66	9.62	50.06	0.5
			357						42.70	0
7	85 APP/15 TDF	203	305	487	4.0	1.8	0	7.13	49.26	0
			430						71.11	0.8
8	85 APP/15 PFC	242	430	490	8.0	3.0	0	6.07	51.77	0
9	85 APP/15 PNP	209	427	490	4.5	2.3	5.0	9.33	46.28	0.7
10	IPP	228	434	492	0	—	0	15.38	51.43	0
11	90 IPP/10 HET	234	447	518	4.0	0	2.8	13.52	49.93	0
12	90 IPP/10 TDF	230	310	503	3.0	1.2	1.3	15.33	86.09	1.0
			438						121.22	0.9
13	90 IPP/10 PFC	254	456	512	5.5	2.0	1.3	12.20	62.43	0
14	90 IPP/10 PNP	205	433	490	5.5	1.5	4.6	13.92	58.20	1.2
15	PE	257	462	533	0	0	0	13.40	71.22	0
16	90 PE/10 HET	273	468	524	5.0	0	4.5	13.16	55.71	0
17	90 PE/10 TDF	197	304	527	4.5	1.9	0	11.57	73.99	0.9
			468						169.54	0
18	90 PE/10 PFC	262	466	532	4.5	1.2	0	12.92	88.84	0
		308								
19	90 PE/10 PNP	226	460	524	8.5	1.5	2.6	15.83	57.99	0

R_{TG} — TG residue ; R_{theor} — theoretical residue ; R_p — pyrolysis residue.

3. Metods of Investigation

The thermooxidative behaviour was followed on a MOM-Derivatograph, Paulik-Paulik-Erdey type, using powders of mixtures. A high heating rate was chosen in order to obtain an approximative simulation of burning [3], [4].

Other conditions are : 50 mg sample weight, Al_2O_3 freshly calcined at 1 200°C as reference. The activation energies were evaluated by Coats-Redfern [5] and Reich-Levi [6] methods.

The pyrolysis studies were carried out in an autoclave type reactor, at 400°...470°C, in a self-generated atmosphere. As a consequence of the pyrolysis process gases, liquids and solids are formed. These products were analysed by convenient methods [7].

4. Results and Discussion

4.1. Thermogravimetric studies

The influence of flame-retardants on the thermal behaviour of APP, IPP and PE can be followed by the modification of characteristic decom-

position temperatures, residue amount obtained at high temperatures, the endothermicity of the decomposition process and the activation energies.

The variation of the mentioned parameters depends on the substrate / flame-retardant interaction and their compatibility.

The micromolecular compounds (HET and TDF) volatilize with decomposition at lower temperatures and two peaks or one with inflexion appear on DTG curves. Samples with polymeric flame-retardants show more simple DTG curves, with a single large peak.

The influence of the flame-retardants becomes more pronounced in the TG curves for poly(propylene) (Fig. 1), the weight losses at different temperatures being smaller for samples with HET and PFC. Differences become more proeminent together with the increasing of temperature, because of formation of decomposition residue. The residue formation in the polyolefine decomposition is supported by the fact that the experimental values are greater than the theoretical ones. The residue remains stable after 530°...600° C and can be utilized to evaluate the oxigen index [8]. The oxigen index increases from 16...17 for PE or PP to 21...23. The last value is the limit between the inflammable and noninflammable polymers and it is reached in the case of APP/PFC, IPP/PFC, IPP/PNP and PE/PNP systems.

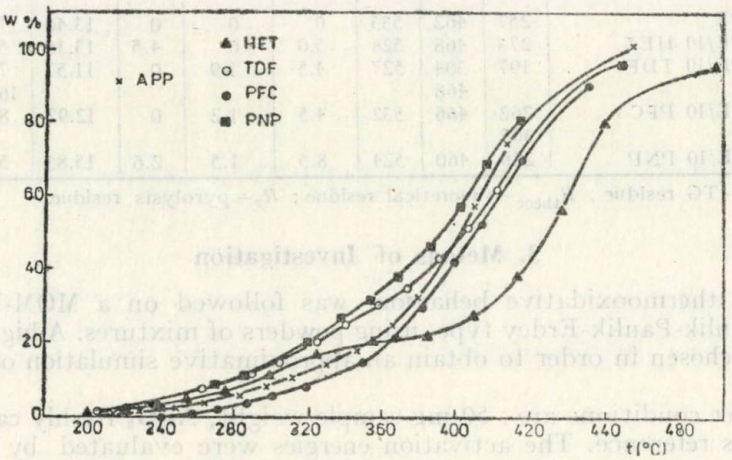

Fig. 1. — TG curves of the decomposition of additived poly(propylene) :

From Table 2 we conclude that the PFC flame-retardant leads to the increasing of thermal stability of polyolefines; PNP enhances the endothermicity of the decomposition process and TDF probably interacts with the polymer substrate, when the activation energies show great variations. The modification of thermal stability and the reaction mechanism is evidenced by the variation of activation energy against the transformation degree. The greater variations are noticed for PP (Fig. 2).

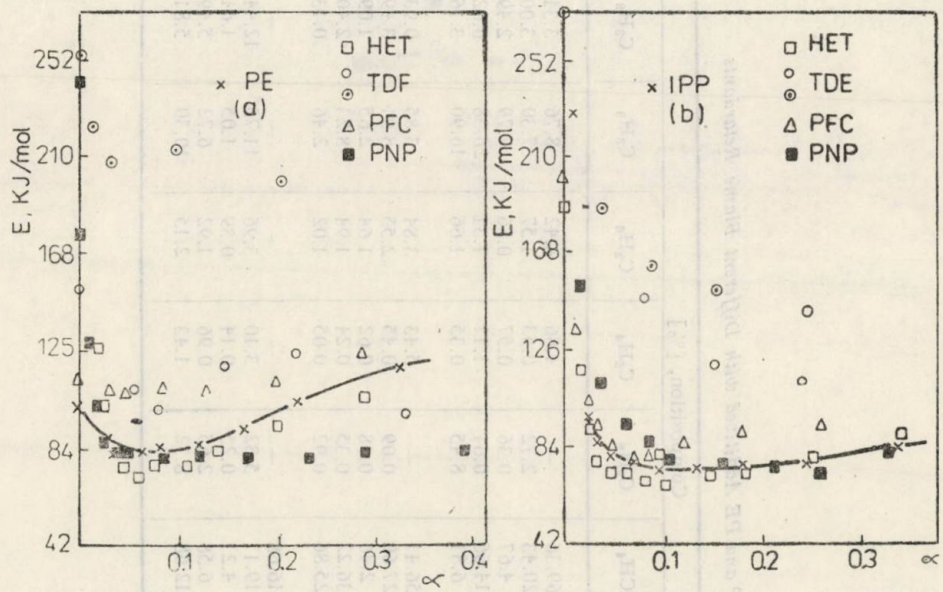

Fig. 2. — Variation of activation energy (R e i c h-L e v i method) versus conversion degree $\alpha = w_t/w_\infty$ for PE (*a*) and IPP (*b*).

HET has a catalytic action on the PE and PP decomposition and the E_{RL} values are greater than of non additived polymer. A such catalytic activity was also observed for other flame-retardants [1], [2]. Similar plots for pure flame-retardants showed that the activation energy for TDF is 42 kj/mol, characteristic value for volatilization. The pronounced increase of E_{RL} values for additived polymers reveals the interaction of components.

4.2. Pyrolysis Studies

The non-additived polymers subjected to the pyrolysis do not give carbonic residue. In the presence of flame-retardants, the residue amount varies between 1...5%, depending on the flame-retardant nature, what is supported by TG data. Adequately, variations in the amount of gases and condensable product were noticed.

a) *Gaseous Fraction.* The amount of gases and their evolving rate is smaller for almost all additived samples (Fig. 3). A marked diminution was observed for PE additived with HET and PNP, and for PP additived with HET, PFC and TDF.

The characteristics of gaseous fraction are given in Table 3. The densities and molecular weights of additived samples are smaller than those of pure polymers. Great amounts of HCl evolved from samples additived with HET and TDF, CO_2 and NH_3 result from samples with PNP. The two gaseous products are non-inflamable and dilute the combustible gases (saturated and unsaturated C_1-C_4 hydrocarbons). Acetylene results only

Table 3

General Characteristics of Gaseous Fraction Obtained by Pyrolysis of APP, IPP and PE Additived with Different Flame Retardants

No.	Sample	Density g/l	$\bar{M}$	g HCl / 100 g gas	Composition, [%]							
					CO_2	H_2	CH_4	C_2H_2	C_2H_4	C_2H_6	C_3H_3	C_3H_8
1	APP	1.9987	57.86	—	3.62	1.01	69.36	—	4.86	4.42	8.76	3.31
2	85 APP/15 HET	1.5528	44.95	1.049	3.10	1.09	20.43	2.72	0.53	1.57	7.30	3.00
3	85 APP/15 TDF	1.4643	42.29	0.052	1.30	0.89	4.67	0.36	0.57	0.86	7.79	2.49
4	85 APP/15 PFC	1.6184	46.85	0.025	0.42	0.96	14.66	0.61	1.11	1.31	26.38	6.62
5	85 APP/15 PNP	1.6677	48.27	—	39.25	0.20	6.81	8.45	0.35	1.66	16.90	3.16
6	IPP	1.7236	49.89	—	0.24	1.42	56.41	—	5.43	3.84	3.85	0.93
7	90 IPP/10 HET	1.8568	53.75	0.072	6.77	0.40	27.69	0.09	0.45	2.55	8.91	3.49
8	90 IPP/10 TDF	1.5110	43.74	0.0133	2.39	0.12	2.46	0.38	0.62	1.64	2.65	1.09
9	90 IPP/10 PFC	1.6349	47.33	0.031	8.47	1.79	36.22	0.35	0.24	1.94	8.23	2.40
10	90 IPP/10 PNP	1.7132	49.59	0.012	21.42	0.16	25.86	0.92	0.05	1.02	2.46	0.13
11	PE	1.8581	53.74	—	0.66	0.70	16.68	—	—	—	—	—
12	84 PE/16 HET	1.5976	45.73	0.225	19.17	0.72	19.17	5.32	3.10	3.96	11.75	12.44
13	90 PE/10 TDF	1.5138	43.82	2.463	7.04	0.29	4.21	0.25	0.14	0.39	1.05	1.61
14	90 PE/10 PFC	1.5143	43.84	0.012	11.09	0.48	6.58	2.65	0.96	1.92	6.72	5.49
15	90 PE/10 PNP	1.6866	48.83	—	57.42	0.60	12.68	8.32	1.43	2.15	10.30	5.81

from the pyrolysis of additived samples and its presence can explain the diminution of density and molecular weight.

b) *Liquid Fraction.* Data concerning the analysis of the liquid fraction are summarized in Table 4. It founds that each polymer/flame retardant system presents a specific behaviour. Densities are higher for the additived samples, and a marked increase takes place at flame-retardancy with TDF and PFC. The volatility decreases for IPP/flame-retardant systems and increases for PE/flame-retardant system, since the unsaturation decreases, and rise the aromaticity and the number of P—O bonds in samples with PFC and HET. The aromatic structures were also evidenced by IR-spectroscopy (1 600 cm^{-1}, 900...980 cm^{-1} and 800...885 cm^{-1}). It is well-known that the aromatic compounds burn heavier and cause the retardation of the flame by the two flame-retardants.

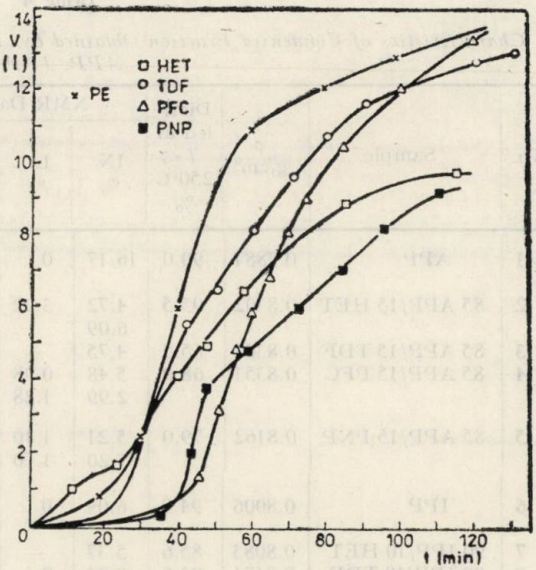

Fig. 3. — Variation of gaseous volume against reaction time (T=480...500°C, 300 g sample).

The contamination degree of the liquid fraction varies between 0.5 and 3.5%, forming compounds with N, Cl and P, which decrease also the inflammability. These compounds are in the small amounts and their structure is unknown.

The solid product or decomposition residue has the composition given in Table 5.

Phosphorous and nitrogen remain in residue, while chlorine goes into the composition of volatile fractions, in small amounts as it was shown above.

The residue structure depends especially on the flame-retardant, as it results from IR absorption spectra (Fig. 4). From the additived samples with HET a carbonic residue was obtained. The residue of the other samples contains besides carbon structures appearing from the heating modification of the P—O or P—N bonds for the samples flame-retarded with TDF, mainly with PFC and PNP.

IR absorption spectra of the residue differ from those of flame retardants heated for 15 min. at high temperatures (190°...250°C). These differences can appear from a polymer and flame-retardant chemical interaction leading to a specific structure.

Table 4

Characteristics of Condensed Fraction Obtained by Pyrolysis of Additived and Non-Additived APP, IPP and PE

No.	Sample	ρ g/cm³	Distilled at $T<$ 250°C %	NMR Data			Elemental analysis, [%]					
				IN %	IA %	NS/ 1000 C	C	H	N	Cl	P	O
1	APP	0.7881	90.0	16.17	0	74.07 21.24	84.89	14.05	—	—	—	1.06
2	85 APP/15 HET	0.8302	95.5	4.72 6.09	3.32	54.32 43.25	83.64	13.72	—	2.41	0.23	0
3	85 APP/15 TDF	0.8301	65.5	4.75	—	43.36	83.79	13.86	—	1.36	0.77	0.22
4	85 APP/15 PFC	0.8351	68.0	5.48 2.99	0.98 1.28	28.29 49.42	82.52	13.23	—	2.78	0.70	0.77
5	85 APP/15 PNP	0.8162	79.0	5.21 7.20	1.10 1.70	47.14 62.96	84.79	13.90	0.29	—	0.64	0.38
6	IPP	0.8006	94.0	6.04	0	64.90 66.40	85.28	14.15	—	—	—	0.57
7	90 IPP/10 HET	0.8083	85.6	5.37	—	48.46	84.03	13.91	—	1.36	—	0.01
8	90 IPP/10 TDF	0.8171	93.6	6.23	0	55.44	80.44	13.25	—	0.88	0.80	4.63
9	90 IPP/10 PFC	0.8129	80.9	5.80	1.84	51.99	83.78	13.29	—	1.97	0.83	0.13
10	90 IPP/10 PNP	0.7904	89.2	6.23	—	54.53	85.45	14.05	—	—	0.50	0
11	PE	0.8101	49.0	8.30	2.20	—	85.46	14.25	—	—	—	0.29
12	90 PE/10 HET	0.8102	87.9	2.19	1.09	—	84.77	13.49	—	1.39	—	0.35
13	90 PE/10 TDF	0.8463	56.1	2.99	—	—	83.79	13.86	—	1.65	0.52	0.18
14	90 PE/10 PFC	0.8400	50.6	5.43	4.77	—	82.66	13.27	—	2.37	1.17	0.53
15	90 PE/10 PNP	0.8177	70.0	4.39	1.95	—	84.43	13.73	0.40	—	0.81	0.63

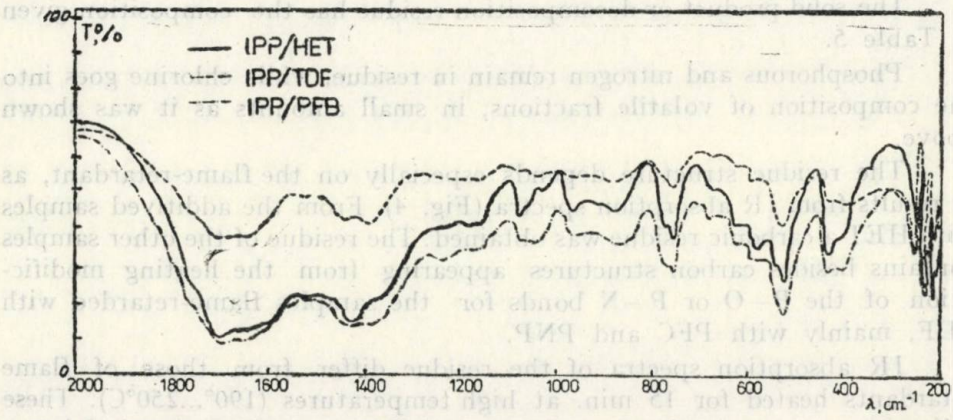

Fig. 4. — IR absorption spectra of carbonic residue resulting from the decomposition of IPP/flame-retardant system.

Table 5

Analytical Data of the Solid Product Obtained by Pyrolysis of Additived Samples

No.	Sample	Elemental analysis, [%]					
		C	H	N	Cl	P	Residue
1	85 APP/15 PNP	35.38	3.29	22.78	—	9.46	31.96
2	90 IPP/10 HET	90.69	4.38	—	1.04	—	—
3	90 IPP/10 TDF	54.87	2.27	—	0.97	12.47	21.97
4	90 IPP/10 PFC	53.75	3.36	—	1.38	10.47	38.67
5	90 IPP/10 PNP	32.77	1.87	26.42	—	20.94	17.95
6	90 PE/10 HET	90.81	4.55	—	1.18	—	1.87
7	90 PE/10 PNP	47.72	3.75	18.50	—	14.99	31.25

5. Conclusions

Finally, we can draw the following conclusions :

1. HET flame-retardant acts in vapour phase, forming dilute non-combustible gases.

2. TDF interacts with polyolefines, resulting in crosslinked structures which increase the activation energies in the second stage of decomposition. In this case, the flame retardation is achieved by forming volatile non-inflamable components (HCl, CO_2) or with diminished inflamability.

3. Like TDF, PFC has a complex action, leading to the increasing of thermal stability in solid phase. In gaseous phase, products with diminished inflamability were formed : aromatics, P and Cl containing compounds.

4. Although PNP is a crosslinked polymer, it diminishes the inflamability, by increasing of the residue amount and the interaction with the substrate, mainly with PE. Its efficiency increases at a low crosslinking degree due to the evolving of a small quantity of NH_3 and CO_2, which dilute the combustible gases.

5. The suitable behaviour of polymeric flame-retardants in the burning retardation of inflammable macromolecular compounds is in agreement with previous results [9], [10].

6. Thermogravimetrical data coupled with pyrolysis and analysis of reaction products permit to study the behaviour of polymers in burning conditions; the obtained results are confirmed by inflammability tests, what will be the object of a future work.

Received, April 8, 1985

„P. Poni" Macromolecular Chemistry Institute, Jassy

REFERENCES

1. Reeves W.A., Drake Jr. G.L., Perkins R.M., *Fire Resistant Textiles Handbook* Technomic Publ. Co., Inc., 1974, 3.
2. Mark H.F., Atlas S.M., Shalaby S.W., Pearce E.M., *Flame Retardant Polymeric Materials.* Vol. I, Plenum Press, New York, 1975, 1—29.

3. Nikolaev A.V., Gimelsheyn F. Ya., Zislin V.M., J. Therm. Anal., 6, 479 (1974).
4. Carel A.B., Cabbiness D.K., Thermochim. Acta, 44, 363 (1981).
5. Coats A.W., Redfern J.P., Nature, *201*, 68 (1964); J. Polym. Sci., B, Polym. Letters, 3, 917 (1965).
6. Reich L., Levi D.W., Makromol. Chem., 66, 102 (1963); Reich L., J. Polym. Sci., B, Polym. Letters, 2, 621 (1964).
7. Vasile C., Bărboiu V., Onu P., Sabliovschi M., Moroi G., Acta Polym. (in press).
8. Van Krevelen D.W., *Advances in the Chemistry of Thermally Stable Polymers*. Warszawa, 1977, 119.
9. Popescu Fl., Petreuş O., Agherghinei I., IMPHOS (First International Congress on Phosphorous Compounds), Rabat, Sept. 17—21, 1977, 307.
10. Petreuş O., Popescu Fl., Rev. Roumaine Chim., 28, 387 (1983).

INFLUENŢA IGNIFUGANŢILOR ASUPRA COMPORTĂRII POLIOLEFINELOR LA TEMPERATURI RIDICATE

(Rezumat)

S-a studiat influenţa ignifuganţilor conţinînd fosfor, azot şi/sau halogen asupra comportării poliolefinelor (polietilenă şi polipropilenă atactică şi izotactică) la temperaturi ridicate.

Descompunerea termică s-a efectuat prin termogravimetrie, analiză termică diferenţială, analiza gazelor degajate şi prin piroliză în atmosferă autogenerată. Produşii gazoşi, lichizi şi solizi au fost analizaţi prin următoarele metode : spectroscopie IR şi RMN, cromatografie în fază gazoasă, analiză elementară etc.

S-a stabilit eficienţa ignifuganţilor şi modificările în mecanismul reacţiei de descompunere termică.

BULETINUL INSTITUTULUI POLITEHNIC DIN IAŞI
Tomul XXXI (XXXV), Fasc. supl., 1985
Secţia II
CHIMIE ŞI INGINERIE CHIMICĂ

D.C. 678-13

REACTIVITY OF ACRYLIC MONOMERS

XII. COPOLYMERIZATION OF N,N-DIETHYLACRYLAMIDE WITH ETHYL AND *n*-BUTYL ACRILATE

BY

SPIRIDON OPREA, EMIL DUMITRIU and VASILE HULEA

1. Introduction

The previous studies on the reactivity of N,N-diethylacrylamide in the process of radical copolymerization showed some differences in the behaviour of this monomer as function of the used comonomer. Thus, the systems N,N-diethylacrylamide—methyl acrylate [1] and N,N-diethylacrylamide—acrylic acid [2] are of type $r_{1,2} < 1$, N,N-diethylacrylamide—methyl methacrylate is of type $r_1 < 1$ and $r_2 > 1$, whereas in the case of copolymerization with styrene a penultimate effect was observed [3].

Taking these into account we have studied here the reactivity of N,N-diethylacrylamide in the copolymerization process with two monomers from the acrylic esters, series, namely : ethyl acrylate and *n*-butyl acrylate.

2. Experimental

N,N-Diethylacrylamide was prepared and purified as in [1].

Ethyl acrylate (Merck) was purified by distillation under vacuum (and nitrogen) to remove the inhibitor ; the middle fraction was collected ; (b.p. = 29°C/50 mm Hg, $n^{20} = 1.404$; $d^{20} = 0.9405$).

n-Butyl acrylate (Merck) was purified in the same manner ; (b.p. = = 69°C/50 mm Hg ; $n^{20} = 1.149$; $d^{20} = 0.8986$).

2,2'-Azobis (isobutironitrile) (AIBN) was purified by recristallization from methanol.

The used solvents, dioxane and light petroleum, were purified by the common methods.

The copolymerization of N,N-diethylacrylamide with acrylic esters was carried out as previously raported [1]. The composition of copolymers was determined both by RMN analysis and by the nitrogen content analysis using micro Kjeldhal method. The reaction conditions and results are summarized in Tables 1 and 2.

Table 1

Copolymerization of N,N-diethylacrylamide (DEA) with Ethyl Acrylate (EA) in Dioxane Solution at 60°C

No.	Mole fraction of DEA in monomer feed	Mole fraction of DEA in copolymer		Nitrogen % g	Conversion % (g)
		RMN analysis	Nitrogen analysis		
1	0.123	0.073	0.071	0.97	2.47
2	0.240	0.151	0.148	2.12	2.16
3	0.352	0.227	0.214	2.30	5.41
4	0.458	0.274	0.275	3.95	3.92
5	0.559	0.335	0.353	4.51	5.13
6	0.655	0.416	0.408	5.14	4.05
7	0.747	0.496	0.482	5.98	3.22
8	0.840	0.580	0.585	7.07	1.78
9	0.919	0.703	0.710	8.34	2.18

Table 2

Copolymerization of N,N-diethylacrylamide (DEA) with n-butyl acrylate in dioxane solution at 60°C

No.	Mole fraction of DEA in monomer feed	Mole fraction of DEA in copolymer		Nitrogen % g	Conversion % (g)
		RMN analysis	Nitrogen analysis		
1	0.1	0.057	0.061	0.67	1.45
2	0.2	0.119	0.121	1.32	2.69
3	0.3	0.176	0.180	1.97	3.14
4	0.4	0.247	0.252	2.76	2.57
5	0.5	0.346	0.335	3.67	4.31
6	0.6	0.410	0.417	4.56	1.16
7	0.7	0.512	0.512	5.62	3.42
8	0.8	0.642	0.634	6.96	5.61
9	0.9	0.758	0.767	8.43	3.58

3. Results and Discussion

On the basis of the data from Tables 1 and 2 the copolymer composition vs. the monomer feed was shown in Figs. 1 and 2.

As it can be observed both systems show a similar behaviour which is characteristic to the systems having $r_1 < 1$ and $r_2 > 1$.

In order to determine the values of the reactivity ratios the F i n e m a n-R o s s and K é l e n-T ü d ö s methods were applied (Figs. 3...6). Since the experimental data are fitted on the lines it can be considered that the terminal model describes satisfactorily the copolymerization process of

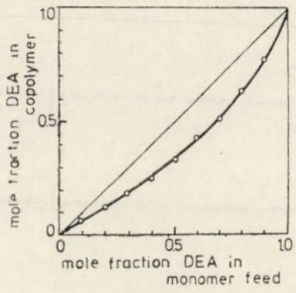

Fig. 1. — Composition diagram for copolymerization of N,N-diethylacrylamide and ethyl acrylate in dioxane solution at 60°C.

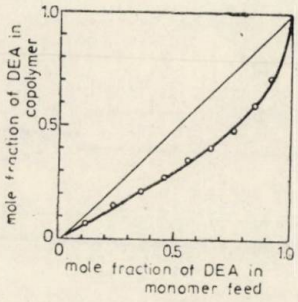

Fig. 2. — Composition diagram for copolymerization of N,N-diethylacrylamide and *n*-butyl acrylate in dioxane solution at 60°C.

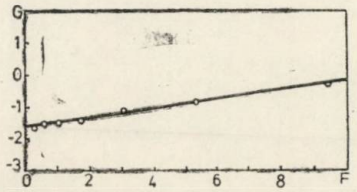

Fig. 3. — F i n e m a n-R o s s plot for copolymerization of N,N-diethylacrylamide with ethyl acrylate.

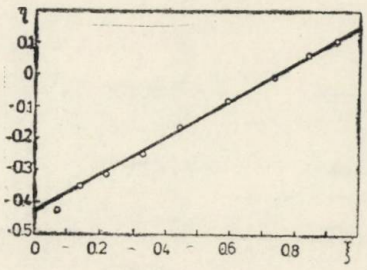

Fig. 4. — K é l e n-T ü d ö s plot for copolymerization of N,N-diethylacrylamide with ethyl acrylate.

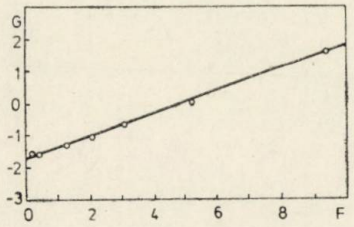

Fig. 5. — F i n e m a n-R o s s plot for copolymerization of N,N-diethylacrylamide with *n*-butyl acrylate.

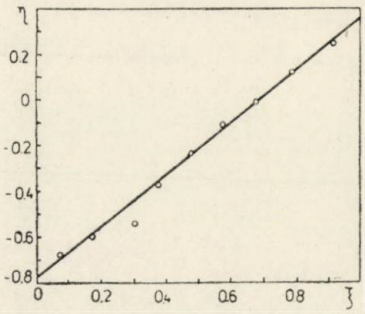

Fig. 6. — K é l e n-T ü d ö s plot for copolymerization of N,N-diethylacrylamide with *n*-butyl acrylate.

N,N-diethylacrylamide with these acrylic esters. The straightlines were plotted by the least square method and from their parameters the reactivity ratios were calculated. The values of determined reactivity ratios are shown in Table 3.

Table 3

Copolymerization Parameters for N,N-diethylacrylamide—Acrylate Systems

Monomer M_2	Fineman-Ross method		Kélen-Tüdös method	
	r_1	r_2	r_1	r_2
Ethyl acrylate	0.16	1.64	0.15	1.56
Butyl acrylate	0.33	1.63	0.34	1.69

One observs a good agreement between the obtained values by the two methods (Fineman-Ross and Kélen-Tüdös methods), and a similar behaviour of the two copolymerization systems.

On the basis of the reactivity ratios we can assert that the acrylic esters show a greater reactivity than N,N-diethylacrylamide with respect to the macroradicals present in the copolymerization system. Consequently, the copolymers have a lower content of disubstituted acrylamide than acrylic ester. Of course, this behaviour has important technological implications, especially when an homogeneous copolymer with respect to the composition, chemical and physical properties should be industrially obtained.

Taking into account the previously reported data on the copolymerization of N,N-diethylacrylamide [1], the following aspects can be underlined. The first observation consists in the different behaviour of the N,N-diethylacrylamide—methyl acrylate system when both reactivity ratios are smaller than the unity, whereas in the presence of ethyl or butyl acrylate $r_1 < 1$ and $r_2 > 1$.

The difference in reactivity can be also proved by the relative reactivities $1/r_i$ (s. Table 4).

Table 4

Relative Reactivities of the Monomers

Radical	Monomer	$1/r_1$	$1/r_2$
$-CH_2-\underset{\displaystyle CON(C_2H_5)_2}{\underset{\vert}{CH}}-\cdot$	$CH_2=CHCOOCH_3$	2.44	—
	$CH_2=CHCOOC_2H_5$	6.67	—
	$CH_2=CHCOOC_4H_9$	2.94	—
MA·	$CH_2=CHCON(C_2H_5)_2$	—	1.92
EA·		—	0.64
BA·		—	0.59

Presented data reveal that the relative reactivity of disubstituted acrylamide against the macroradicals ended in acrylic esters decreases as the alkyl chain of the ester is smaller. The relative reactivity of acrylic esters against the macroradicals ended in disubstituted acrylamide is almost the same with respect to methyl and butyl acrylate, and it is very different in the case of ethyl acrylate.

As a general conclusion we can assert that the reactivity of acrylic esters of aliphatic alcohols depends on the size of the alkyl chain.

Received, April 9, 1985

Polytechnic Institute, Jassy,
Department of Organic
and Macromolecular Chemistry and
Technology

REFERENCES

1. Dumitriu Em., Oprea Sp., Maxim S., Nathanson A., Dima M., Coll. Polymer Sci., *257* (11), 1203 (1979).
2. Oprea Sp., Dumitriu Em., Mat. Plast., **20**, *1*, 202 (1983).
3. Oprea Sp., Dumitriu Em., Dima M., Rev. Roumaine Chim., **25**, *4*, 605 (1980).

REACTIVITATEA MONOMERILOR ACRILICI

XII. Copolimerizarea N,N-dietilacrilamidei cu acrilatul de etil şi de butil

(Rezumat)

S-a studiat copolimerizarea N,N-dietilacrilamidei cu acrilatul de etil şi acrilatul de *n*-butil. Au fost stabilite valorile constantelor de copolimerizare pentru cele două sisteme şi anume: $r_1 = 0,16$ şi $r_2 = 1,64$, respectiv $r_1 = 0,37$ şi $r_2 = 1,63$. S-a constatat că reactivitatea esterilor acrilici în procesele de copolimerizare cu N,N-dietilacrilamida scade odată cu creşterea catenei alchilice din molecula acestora.

BULETINUL INSTITUTULUI POLITEHNIC DIN IAȘI
Tomul XXXI (XXXV), Fasc. supl., 1985
Secția II
CHIMIE ȘI INGINERIE CHIMICĂ

D.C. 678.746

SYNTHESIS AND PROPERTIES OF NEW POLYAZOMETHINES (II)

BY

MARIA DUMITRIU, MARIANA PĂSTRĂVANU and TATIANA LIXANDRU

1. Introduction

Among the heterochain polymers the polyazomethines are particularly important due to their good semiconducting properties and high thermal stability [1] ... [5]. They can also be used for obtaining fibers [6] and pigments for plastic materials [7].

In a previous paper a series of polyazomethines derived from acenaphthenequinone and derivatives were described [8].

In the present paper the polycondensation of 9,10-phenanthrenequinone, 9, 10-anthraquinone, 1- and 2-chloroanthraquinone with aromatic diamines as well as the properties of the obtaining polymers are studied.

2. Experimental

2.1. Materials

a) 9, 10-Phenanthrenequinone, 9, 10-anthraquinone and 1-chloroanthraquinone were Schuchard products and 2-chloroanthraquinone was a Merck product.

b) *m*- and *p* - Phenylenediamines and benzidine were laboratory reagents and were purified by the usual methods.

c) The solvent DMF was purified by double distillation.

2.2. Method

Polycondensation procedure. A mixture of 0.01 mol quinone, 0.01 or 0.02 mol. diamine and 2 g $ZnCl_2$ are solved în 40...60 ml DMF (the DMF amount depends on the quinone solubility). The solution is heated on an oil bath at 135°...140°C for 10 hours under good stirring. The reaction mixture is then cooled and filtered. A solid dark coloured mass is separated from the filtrate by water addition.

For removal of zinc chloride, the solid mass was powdered and washed twice with a hot NH_4OH/H_2O solution (1/3 ratio).

The polyazomethines obtained as complexes with $ZnCl_2$ were then purified by decomposing firstly these complexes by washing with acetic acid, in the case of the insoluble polymers, and by the dissolution followed by the precipitation in water, in case of the polymers soluble in acetic acid.

The quinone and diamine were then removed differently according to the solubilities of the obtained polymers and the initial monomers.

The phenanthrenequinone and anthraquinone soluble products were disolved in hot acetic acid, cooled, filtred and precipitated finally in water.

The phenanthrenequinone and anthraquinone insoluble products were washed repeatedly with hot acetic acid for both dissolving the uncoverted quinone and decomposing the complexed $ZnCl_2$.

The unreacted chloroanthraquinones were removed by washing with carbon tetrachloride and the anthraquinone by dissolving in hot chloroform followed by cooling, filtration and precipitation in carbon tetrachloride.

For removing the unreacted diamine components the products were washed with ethylic alcohol, benzene and chloroform, in function of monomer and polymer solubilities.

The polymers were obtained as amorphous powders of different shades, brighter for those prepared from anthraquinone and its derivatives and black for those resulting from phenanthrenequinone (Table 1).

The IR and ESR spectra were recorded on Specord IR UR 20 and ART 5 apparata, respectively.

The termograms were recorded on a Paulik-Paulik-Erdey MOM, Budapest, apparatus.

Table 1

Polycondensation of 9,10-Anthraquinone, 1-Chloro-and 2-Chloro-9,10-Anthraquinone and 9,10-Phenanthrenequinone with Aromatic Diamines

Quinone		Diamine	Yield %	m.p. °C	Aspect	IR spectra	
						$\nu_{C=N}$ cm^{-1}	$\nu_{C=O}$ cm^{-1}
9,10-Anthraquinone							
R_2	R_1						
H	H	*p*-Ph	28.20	290...300	Amorphous-grey	1 610	1 695
H	H	*m*-Ph	33.69	285...294	Amorphous-grey	1 605	1 690
H	H	Bz	36.35	276...283	Amorphous grey-bej	1 610	1 695
H	Cl	*p*-Ph	30.83	146...153	Amorphous reddish-brown	1 610	1 690
H	Cl	*m*-Ph	31.92	152...159	Amorphous-red	1 610	1 695
H	Cl	Bz	69.45	142...150	Amorphous dark-red	1 610	1 695
Cl	H	*p*-Ph	34.08	150...159	Amorphous brown-reddish	1 610	1 690
Cl	H	*m*-Ph	35.13	145...153	Amorphous brown-reddish	1 610	1 690
Cl	H	Bz	79.69	147...155	Amorphous brown-reddish	1 610	1 695
9,10-Phenanthrenequinone							
		p-Ph	66.66	330	Amorphous-black	1 620	1 690
		m-Ph	80.06	330	Amorphous-black	1 600	1 680
		Bz	79.21	330	Amorphous-black	1 650	1 700

Solvent DMF, catalyst $ZnCl_2$, quinone/diamine mole ratio 1/2, time 10 h, temperature 135° ... 140°C. Products soluble in acetic acid.

The study of the temperature dependence on the electrical conductivity was performed with disc samples of 1.0 cm diameter and 0.5 to 2.0 mm thickness. These samples were prepared by the compresion of the polymer powder at 10 t/cm². The discs were mounted between two aluminium electrodes and a good contact was achieved by a screw clamp arrangement. The temperature was measured by a Fe—constantan termocouple. The measurements were performed by an experimental arrangement similar to that described in [9], [10]. In all cases the temperature rate was 1.5°C/min.

3. Results and Discussion

3.1. Synthesis and Molecular Structure of the Polymers

By taking into account the results obtained in the syntheses of the polyazomethines derived from acenaphthenequinone [8], the facts that the 9, 10-phenanthrenequinone does not react with hydrazine hydrate in acetic acid medium with sulphuric acid as dehydrating reagent [11], and that among the Lewis acids zinc chloride was the most effective catalyst in the polycondesation of aldehydes with diamines [12], we used the DMF as a solvent and $ZnCl_2$ as a catalyst.

As regards the effect of the chlorine in 1- and 2- chloroanthraquinone on the polyazomethine yield, higher values are noticed than in case of the anthraquinone, probably due to the electron-atracting effect of the halogene which increases the reactivity of the carbonyl groups (2-chlorine > 1-chlorine).

The reactions carried out in excess of diamine led to polycondensation products in a higher yield, which is in a good agreement with previous papers [8], [13].

The yield was also found to decrease in benzidine, *m*-phenylenediamine, *p*-phenylenediamine, which is in a good agreement with the results obtained by d'Alelio for the polycondensation of isophthalaldehyde with *m*- and *p*-phenylenediamine [14].

The IR spectra of the polyazomethines obtained with different amines and ketones or aldehydes show absorption bands characteristic to $\diagdown C=N-$ and $\diagdown C=O$ end groups [15].

For different Schiff polybases types the band is to be found within the 1 630...1 640 cm^{-1} range [11], [12] although it may be also situated at values lower than 1 620 cm^{-1} for the compounds obtained from dicarbonylic derivatives and aromatic diamines [16].

In the IR spectra of polyphenanthrenequinonimine and polyanthraquinonimine, respectively, the $\nu_{\diagdown C=N-}$ vibration appears between 1 600 and 1 620 cm^{-1} (Table 1), which supports the assumed polyazomethine structure :

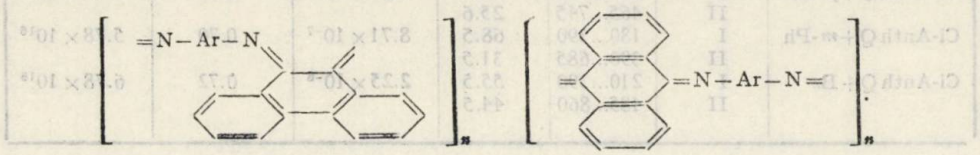

For the products resulted from anthraquinone the absorption bands of a medium intensity characteristic of the carbonyl (1 710... 1 780 cm^{-1}) and amino (3 400...3 500 cm^{-1}) groups at the chain end are found ; in all cases a decrease in the wavelength value of the $\nu_{C=O}$ for the polymer compared to the initial monomer is noticed, which is indicative of lower polycondensation degrees made also evident by the solubility and intrinsic viscosity measurements.

The IR spectra of the insoluble, black-coloured polyphenanthrenequinoneazomethines do not show the absorptions specific for the —NH— and $>C=O$ bonds which indicates either higher polycondensation degree or cyclic structures.

The thermal stability was studied by thermogravimetric and thermodifferential analyses, between 20° and 1 000°C, in air. The thermal stabilities exceeding 200°C (Table 2) are comparable to those of the polyazomethines obtained from acenaphthenequinone and derivatives [5].

Table 2

Data from TG Thermograms and Electrophysical Characteristics of Polyazomethines

Polymer	Thermogravimetric data			Electrical conductivity at 20°C $ohm^{-1}cm^{-1}$	Activation energy (E) for electrical conductivity eV	Concentration of unpaired electrons spins/g
	Degradation steps	Temperature °C	Weight losses %			
PhQ+*p*-Ph	I	90...370	63.5	3.50×10^{-7}	0.77	1.65×10^{18}
	II	370...550	36.5			
PhQ+*m*-Ph	I	190...430	14.0	1.10×10^{-7}	0.50	5.10×10^{19}
	II	430...920	86.0			
PhQ+Bz	I	215...500	17.4	4.20×10^{-8}	0.82	3.09×10^{19}
	II	500...850	82.6			
AnthQ+*p*-Ph	I	190...350	74.1	9.00×10^{-8}	0.91	0.95×10^{17}
	II	350...375	5.5			
	III	375...430	18.2			
	IV	430...540	2.2			
AnthQ+*m*-Ph	I	190...395	94.9	8.20×10^{-7}	0.86	1.57×10^{17}
	II	395...540	5.1			
AnthQ+Bz	I	190...375	44.4	2.20×10^{-6}	0.97	0.92×10^{17}
	II	375...520	18.9			
	III	520...695	30.0			
2Cl-AnthQ+*p*-Ph	I	220...440	57.8	2.12×10^{-7}	0.82	1.40×10^{17}
	II	440...815	42.2			
2Cl-AnthQ+*m*-Ph	I	220...400	62.2	6.33×10^{-8}	0.94	8.13×10^{17}
	II	460...790	36.7			
2Cl-AnthQ+Bz	I	205...400	71.1	3.47×10^{-6}	0.84	0.85×10^{17}
	II	400...730	28.9			
Cl-AnthQ+*p*-Ph	I	200...435	74.4	5.25×10^{-7}	0.66	1.17×10^{17}
	II	465...745	25.6			
Cl-AnthQ+*m*-Ph	I	180...390	68.5	8.71×10^{-7}	0.70	5.78×10^{16}
	II	390...685	31.5			
Cl-AnthQ+Bz	I	210...390	55.5	2.25×10^{-6}	0.72	6.78×10^{16}
	II	485...860	44.5			

The polyazomethines derived from anthraquinone and phenanthrenequinone show similar thermal stabilities ; the destruction process proceeds generally in two stages, with a strong exothermal effect corresponding to the maximum weight losses.

Due to the extended double bond system the synthesized polymers show electrical conductivity and paramagnetic properties (Table 2).

The electrical conductivities of the polyazomethines described here range from 10^{-6} to 10^{-8} $ohm^{-1}cm^{-1}$ at 20°C. The ln Σ vs. $1/T$ plots for the polymers are linear. The estimated values of the Σ_0 and E parameters are listed in Table 2.

All polymers show an intense ERS signal (symmetrical singlet) with a paramagnetic particle concentration of $10^{16}...10^{19}$ spin/g (Table 2).

The relative viscosities of the compounds soluble in DMF were measured. By expressing η_{sp}/C as a function of concentration the relative viscosities of 0.02...0.05 dl/g and 0.05 dl/g were obtained for the polyazomethines derived from anthraquinone and phenanthrenequinone, respectively. The obtained values are comparable with those indicated from the Schiff polybases obtained from aromatic dialdehydes and diamines [14].

4. Conclusions

The polycondensation of 9, 10-phenanthrenequinone, 9, 10-anthraquinone, 1- and 2-chloroanthraquinone with aromatic diamines such as *p*-phenylenediamine, *m*-phenylenediamine, benzidine leads to amorphous, coloured polyphenanthrenequinonimine and polyanthracenequinonimine. The obtained polymers show a high thermal stability and semiconducting properties (electrical conductivity of the $10^{-6}...10^{-8}$ ohm^{-1} cm^{-1} order and paramagnetic particle concentration of $10^{16}...19^{19}$ spin/g).

Received, April 28, 1985

Polytechnic Institute, Jassy
Department of Organic and Macromolecular Chemistry and Technology

REFERENCES

1. d'Alelio G.F., Crivello J.V., Dehner T.R., Schoenig R.T., J. Macromol Sci. Chim., **A 1** (7), 1 331 (1967).
2. Kimura Takao, Nara Shigeo, Matsuyama Kentoro, Kobunski Kagaku, **30**, 491 (1973) ; C.A. 80 : 15 366 z.
3. Межиковский С.М., Гуров А.А., Мягчилова Н.И., Лиогонкий Б.И., Берлин А.А., Высокомол. Соед.; **А 15**, 3 (1973).
4. Василенко Н.А., Правединков А.Н., Высокомол Соед., **В 19**, *6*, 162 (1977).
5. Dumitriu M., Dărângă M., Păstrăvanu M., Lixandru T., Rev. Roum. Chim., **25**, *7*, 981 (1980).
6. Moncrieff R.W., Intern. Dyer Text. Printer Bleacher and Finisher, **163**, *10*, 380 (1980); Ibid., **163**, *11*, 444 (1980).
7. Hermann H.J., Meyer G., Steffen K.D., Ger. Offen 2. 924, 944, 1981 ; C.A. 95: 8 790 g.
8. Lixandru T., Dumitriu M., Păstrăvanu M., Bul. Inst. polit., Iaşi, **XXVII (XXXI)**, *3—4*, s. II, 95 (1981).

9. Rusu G.I., Phys. Stat Sol., a, *4*, 775 (1971); An. Şt. Univ. „Al.I. Cuza", **XV**, *2*, 155 (1979).
10. Rusu G.I., et al., Angew. Makromol. Chem., *107*, 33 (1982); Polym. Bull., **6**, 243 (1982); Proc. of the IUPAC MACRO'83 Bucharest 1983, S. I, 583–586.
11. Păstrăvanu M., Dumitriu M., Lixandru T., Eur. Polym. J., **19**, 633–637 (1983).
12. d'Alelio G.F., Crivello S.V., Kurosaki T., Schoenig R.K., J. Macromol. Sci., **A 1**, *7*, 1259 (1967).
13. Берлин А.А., Лиожонкий Б.Ж., Гуров А.А., Мягчилова Н.И., Высокомол. Соед., **В 14**, 441 (1972).
14. d'Alelio G.F., Crivello J.V., Schoenig R.K., Huemmar T.F., J. Macromol. Sci., **A 1**, 7 161 (1967).
15. Bellamy L.J., *Infra-Red Spectra of Complex Molecule.* 3rd Ed., Chapman & Hall, London, 1975.
16. Patel A.A., Patel S.R., Eur. Polym. J., **19**, 561 (1983).

SINTEZA ŞI CARACTERIZAREA UNOR NOI POLIAZOMETINE (II)

(Rezumat)

S-au sintetizat noi poliazometine prin policondensarea 9,10-fenantrenchinonei, 9,10-antrachinonei, 1- şi 2-clorantrachinonei cu diamine aromatice ca *p*-fenilendiamina, *m*-fenilendiamina şi benzidina. Polimerii sînt caracterizaţi prin spectroscopie IR, măsurători de conductibilitate electrică şi termostabilitate.

BULETINUL INSTITUTULUI POLITEHNIC DIN IAȘI
Tomul XXXI (XXXV), Fasc. supl., 1985
Secția II
CHIMIE ȘI INGINERIE CHIMICĂ

D.C. 678.76

POLYMERIZATION OF 3-METHYLPENT-1-YN-3-OL BY $PdCl_2$ AND ITS TRIPHENYLPHOSPHINE COMPLEXES AS CATALYSTS

BY

VICTOR BULACOVSCHI, MARIA GROVU–IVĂNOIU, M. DĂRÂNGĂ and SVETLANA DUMITRESCU

1. Introduction

Unlike vinyl polymers, acetylenic polymers are characterized by their color, semiconductivity, paramagnetism and geometric isomerism. Acetylenic monomers, however, do not form high polymers by conventional radical, cationic or anionic polymerization [1] ... [3]. Their preparation involves some experimental shortcomings which make the investigation somewhat difficult.

Acetylene and its derivatives have been polymerized by use of several catalysts [4] ... [6]. Among these, the Z i e g l e r-type catalysts and phosphine complexes of transition metals have most often been used. In the metal halides of the 8-th group, a peculiar property was observed. They act very efficiently in polymerization of vinylic monomers in strong solvents [7] and of monosubstituted acetylenes [8]. The reaction mechanism for such promoters is not well known ; it proceeds, probably, by coordination of the monomer to the metal halide [9], [10].

In this paper we describe synthesis of soluble poly(3-methylpent-1-yn-3-ol) (poly-MP) using $PdCl_2$, $(Ph_3P)_2PdCl_2$ (TFF) and $(Ph_3Sb)_2PdCl_2$ (TFSb) as polymerization catalysts. The structure and properties of the obtained products are also reported.

2. Experimental

a) *Materials*. MP (Air Reduction Chem Co.) was dried on Na_2SO_4 and distilled at normal pressure before use (b.p. = 121°C). The solvents for polymerization were purified by usual methods. $PdCl_2$ was used as delivered. Bis(triphenylphosphine) -and bis(triphenylstibine) palladium (II) chlorides were prepared and purified according to the usual methods.

b) *Procedures*. The polymerizations were carried out under nitrogen in a two neck round bottom flask fitted with a refluxing condenser. At the end of the reaction, the resulting poly-MP was dissolved (or diluted) in acetone and precipitated by pouring the solution into a large amount of acid-containing (HCl) water. After filtration and washing with water, the polymer was dried in vacuum over P_2O_5 at room temperature.

c) *Polymer Characterization*. The molecular weights were measured cryoscopically in dioxan solution. IR-spectra (KBr pellets) were registered on a „Karl-Zeiss Jena" UR-20 spectrometer. UV-spectra were run on a „CF-4

Optica Milano" apparatus. X-ray powder spectra were obtained on a „Kristal loflex-4-Siemens" type equipment with recording goniometer and Cu—Kα radiation. Electron spin resonance (ESR) spectra were registered on a ESR-ART-5 spectrometer, IFA-Bucharest.

3. Results and Discussion

Table 1 summarizes the reaction conditions and some characteristics of the obtained polymers by bulk polymerization of MP. One can see that the monomer /catalyst ratio has no significant influence upon the overall conversion of the monomer, but an increas of the insoluble fraction in *n*-heptane was observed for $(3.0...3.7) \times 10^2$ molar ratio.

Table 1

The Bulk Polymerization of MP (Reflux Temperature; t=24 h)

No.	Catalyst	Molar ratio (MP/catalyst) $\times 10^{-2}$	Yield %	Poly-MP insoluble in *n*-heptane %	$\overline{M}_n$	Softening range °C
1	TFF—Pd	6.2	94.1	2.01	420	115...125
2	TFF—Pd	3.73	90.5	31.5	460	125...135
3	TFF—Pd	3.10	91.5	19.24	403	135...140
4	TFF—Pd	2.50	92.3	6.85	682	200...230
5	TFSb—Pd	6.2	96.05	11.2	436	118...126
6	$PdCl_2$	1.04	96.6	11.65	571	108...118

The molecular weights of the obtained polymers were not to high, they ranged from 400 to 700. The highest value was reached when 2.5×10^2 monomer/catalyst molar ratio was used, this polymer showed also a rised softening range (over 200°C). It might be that some parts of the catalyst remain bound to the polymer chain. No essential changes occured when TFSb—Pd complex was used.

It is worth mentioning that the polymerization by phosphine complexes near room temperature proceeds very slow (a month or more) and in very low yields.

Results for polymerization of MP performed in DMF solution are listed in Table 2. The polymerizations catalysed by $PdCl_2$ were carried out at 85°C for various periods of time. The conversions were usually 50...80% due, probably, to the low solubility of the catalyst in the used solvent. However, it appears an increase of the conversion with the catalyst concentration and with the reaction time.

The effect of temperature (Table 3) was studied in the range of 25°... 100°C. It is worth mentioning that the polymerization catalyzed by $PdCl_2$ proceeds in good yields even at 25°C and results in higher molecular weight polymers. It is difficult to make a correlation between molecular weight and softening points. The last ones are generally lower than those found in the preceeding case.

Table 2

Polymerization of MP in DMF Solution Catalyzed by $PdCl_2$
([MP] = 1.773 mol/L, T = 85°C)

No.	Catalyst mol/l	Time h	Conversion %	$\overline{M}_n$	Softening range °C
1	3.67×10^{-2}	7	57.1	736	100...109
2	4.94×10^{-2}	7	62.7	—	100...107
3	5.65×10^{-2}	7	67.9	702	106...115
4	6.86×10^{-2}	7	73.4	—	105...115
5	3.67×10^{-2}	12	67.7	672	88...100
6	3.67×10^{-2}	24	83.45	535	82...97

Acetylenic polymers are usually characterised by a deep color, from orange to brown, due to the conjugated double bond system. In spite of that, the visible region of the spectrum is lacking significant bands ; one can see a continuous absorbtion. In the 220...400 nm region there appear some inflections localised at about 297...299 nm (Fig. 1) without seing clear maxima.

By polymer precipitation, a soluble fraction remains in water which was subsequently extracted with ether. On removing the solvent a resinous product is abandoned which UV-spectrum is shown in Fig. 1 *c*. It reveal a distinct maximum at 240 nm and an inflection met within spectra of the all oligomers. The wavellength calculated by the empirical W o o d w a r d's method [11] taking vinyl acetylene (219 nm) as a basis, leads to a value of 239 nm which coresponds to a trimer, very close to the experimental data (240 nm). These informations are attested by cryoscopic measurements of the molecular weight ($\overline{M}_n$ = =272). Signal narrowness suggests a homogen-

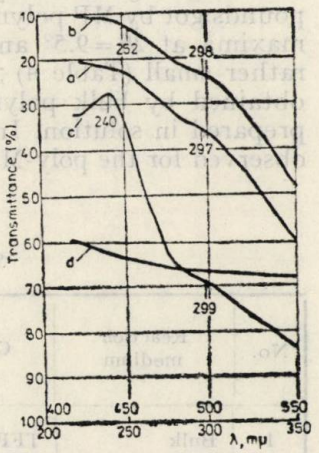

Fig. 1. — UV-spectra in MeOH for the poly-MP obtained in DMF solution ($PdCl_2$ catalyst) : *a* — at 85°C ; *b* — at 25°C ; *c* — water soluble fraction ; *d* — visible region of the spectrum.

Table 3

Polymerization of MP in DMF Solution
([MP] = 1.773 mol/L; $[PdCl_2] = 3.67 \times 10^{-2}$ mol/L)

No.	Temperature °C	Time h	Molecular weight	Softening range °C
1	100	7	623	103...105
2	85	7	736	100...109
3	25	48	1 020	110...115

eity of the product in regard to the molecular weight, which lacks at the water insoluble polymers, their spectra being wider.

The IR spectra of the obtained polymers show no bands of benzene ring (Fig. 2). This suggests a linear structure for poly-MP. Registrations are almost identical concerning the displayed bands. Both spectra show a slight maximum at 1 005 cm^{-1} which was assigned to the *trans-trans* configuration of the conjugated system. The region of 1 600...1 700 cm^{-1} is marked by a strong and broad absorbtion which corresponds to the coupling of the C=C stretching vibrations and OH bending vibrations.

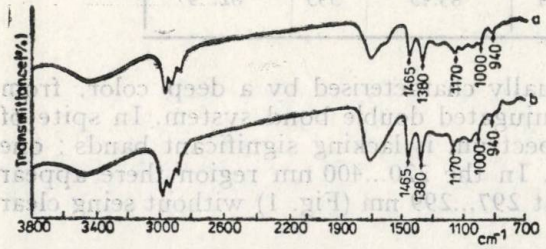

Fig. 2. — The IR spectra of the poly-MP; catalysts: *a* — TFF—Pd; *b* — $PdCl_2$.

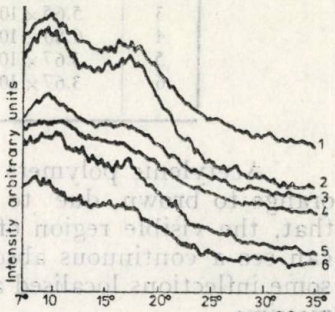

Fig. 3. — X-ray diffraction spectra of poly-MP-s (Notation follow the order in Table 4).

Fig. 3 gives X-ray diffraction patterns for the macromolecular compounds got by MP polymerization. The analyzed materials show two distinct maxima at $2\theta = 9.5°$ and $2\theta = 17°$. The calculated crystallinity indices are rather small (Table 4); they do not exceed 25%. Although, the products obtained by bulk polymerization show a higher crystallinity than those prepared in solution. In this last case, a light increase of the I_{cr} may be observed for the poly-MP obtained at room temperature. It might be that the

Table 4

Structural Properties of the Poly-MP

No.	Reaction medium	Catalyst	MP/catalyst molar ratio	Temperature °C	I_{cr} %
1	Bulk	TFF—Pd	6.2×10^2	reflux	23.70
2	Bulk	TFF—Pd	3.73×10^2	reflux	22.21
3	Bulk	TFF—Pd	2.5×10^2	reflux	19.14
4*)	DMF	$PdCl_2$	—	100	16.03
5	DMF	$PdCl_2$	—	85	15.00
6	DMF	$PdCl_2$	—	25	19.08

*) In the experiments 4...6 the catalyst concentration was 3.67×10^3 mol/L

prepared polymers are less crystalline due to the dominant *trans*-structure of the chains which does not allow their organization.

The electric and magnetic properties of poly-MP-s are shown in Table 5. The electric conductivities were in the range of $10^{-17}...10^{-15}$ ohm^{-1} cm^{-1} and are lower compared with the conductivity of polyacetylene ($10^{-9}...10^{-5}$ ohm^{-1} cm^{-1}) [12]. The ESR spectra of the studied polymers showed a structureless single lines, whose g values were very close to those of the free electron. The unpaired spin densities were $10^{-18}...10^{-19}$ g^{-1}. Compared with data obtained for other acetylene derivatives [2] it results that the presence of various groups as substituents does not affect spin density in acetylenic polymers.

Table 5

Electric and Magnetic Characteristics of Poly-MP

No.	Polymerization medium	Reaction time h	MP/catalyst, molar ratio	$\sigma_{50}°$ ohm^{-1} cm^{-1}	E_a eV	ΔH G	Unpaired spin/g
1[a]	DMF, solution	7	4.83×10^{1}	5.0×10^{-15}	1.78	7.6	7.88×10^{18}
2[a]	DMF, solution	24	4.83×10^{1}	—	—	9.8	1.23×10^{19}
3[b]	Bulk	24	3.1×10^{2}	10^{-16}	2.12	—	—
4[b]	Bulk	24	3.75×10^{2}	7.58×10^{-15}	1.49	8.0	1.02×10^{19}

a) Catalyst $PdCl_2$, temperature 85°C; b) Catalyst TFF—Pd and reflux temperature.

For the bulk polymerization of MP by TFF—Pd, the following mechanism was assumed [9], [10]:

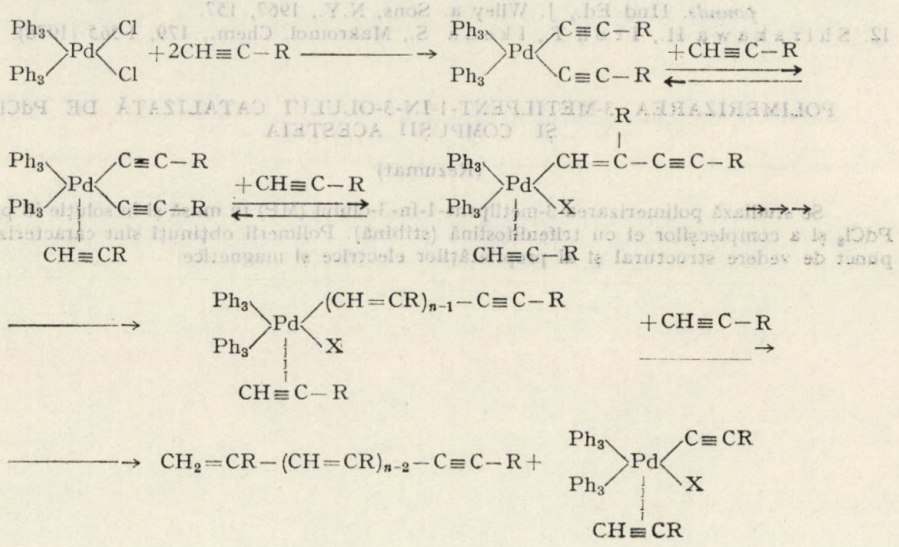

where :

$$R = -C(OH)(CH_3)-C_2H_5 \; ; \; X = -C\equiv CR, \; -Cl \text{ or polymer chain.}$$

4. Conclusions

The MP can be easely polymerized by palladium halides in polar solvents or by its phosphine (stibine) complexes. The obtained poly-MP-s are colored, soluble in common solvents and show electric conductivities and spin densities similar to those of poly-(arylacetylenes).

Received, April 12, 1985

Polytechnic Institute of Jassy,
Department of
Organic and Macromolecular
Chemistry and Technology

REFERENCES

1. Хаусер М.Г., Родионов Ю.М., Мышин М., Черкашин М.И., Усп. хим., **45**, 695 (1976).
2. Ohtori T., Masuda T., Higashimura T., Polymer J., **11**, 805 (1979); Ibid., **11**, 813 (1979).
3. Simionescu C., Grovu M., Angew. Makromol. Chem., **111**, 149 (1983).
4. Simionescu C., Dumitrescu Sv., Die Makromol. Chem., **136**, 47 (1970).
5. Itoh T., Shirakawa H., Ikeda S., J. Polymer Sci., Polymer Chem. Ed., **12**, 11 (1974).
6. Masuda T., Hasegawa K., Higashimura T., Macromolecules, **7**, 728 (1974).
7. Berger R.S., Youngman F.A., J. Polymer Sci., **A-1**, 357 (1964).
8. Kern R.J., J. Polymer Sci., **A-7**, 621 (1969).
9. Furlani A., Bicev P., Carusi P., Russo M.V., J. Polymer Sci., **B-9**, 19 (1971).
10. Bulacovschi V., Simionescu C., Acta Chim. Acad. Sci. Hungaricae, **85**, 221 (1975).
11. Silverstein R.M., Bassler B.C., *Spectrometric Identification of the Organic Compounds.* IInd Ed., J. Wiley a. Sons, N.Y., 1967, 157.
12. Shirakawa H., Itoh T., Ikeda S., Makromol. Chem., **179**, 1 565 (1978).

POLIMERIZAREA 3-METILPENT-1-IN-3-OLULUI CATALIZATĂ DE $PdCl_2$ ŞI COMPUŞII ACESTEIA

(Rezumat)

Se studiază polimerizarea 3-metilpent-1-in-3-olului (MP) în masă şi în soluţie în prezenţa $PdCl_2$ şi a complecşilor ei cu trifenilfosfină (stibină). Polimerii obţinuţi sînt caracterizaţi din punct de vedere structural şi al proprietăţilor electrice şi magnetice.

BULETINUL INSTITUTULUI POLITEHNIC DIN IAŞI
Tomul XXXI (XXXV), Fasc. supl., 1985
Secţia III
CHIMIE ŞI INGINERIE CHIMICĂ

D.C. 54-92 ; 541-24

SOLUTION PROPERTIES OF ULTRAHIGH MOLECULAR WEIGHT POLYMERS

9. SYSTEMATIC ERROR SOURCES IN LIGHT SCATTERING DETERMINATIONS AFFECTING THE DISCUSSION OF THE EXCLUDED VOLUME EFFECT[1])

BY

SILVIA IOAN, CORINA SAVA and BOGDAN C. SIMIONESCU[2])

1. Introduction

The systematic characterization of ultrahigh molecular weight polymers[3]) rises a number of problems. Along with the difficulties associated to their isolation from the reaction mixture, handling, fractionation, most problems arise during the characterization since the usual techniques of investigation have to be adapted to the new dimensions of the chains and/or new investigation methods are to be found.

The molecular weight, the mean-square radius of gyration and the second virial coefficient are the most important parameters characterizing the polymers in diluted solutions. Their determination for ultrahigh molecular weight polymers opens large area in discussing, on the base of different theoretical approximations, properties such as short- and long-range interactions, excluded volume effect, etc.

Plasma-induced polymerization (copolymerization) [1], [2] was proved to yield ultrahigh molecular weight polymers (e.g., polystyrene, poly(methyl methacrylate), poly(butyl methacrylate)) and copolymers. The obtained macromolecular compounds were analysed from the point of view of molecular weight and compositional heterogeneity [3] ... [6], and some of their solution properties (conformational changes induced by temperature and solvent nature [7], [8], determination of root-mean-square radius of gyration and second virial coefficient — molecular weight relations [5], [6], [9], [10], analysis of the excluded volume effect based on the two-parameter theory, where the second virial coefficient and the expansion factor are function of short- and long-range interactions [6], [10], [11], etc.) were considered.

The mentioned papers showed that plasma-induced polymerization yields macromolecular compounds possessing some special properties as compared to usual polymers, namely: (a) low molecular weight and compositional heterogeneity, (b) less visible and pronounced conformational changes function of temperature and solvent nature, (c) an increased rigidity of the macromolecular chains in diluted solutions, as shown by the established relations between the radii of gyration and/or the second virial coefficients and the molecular weights, and (d) for high values of the expansion factor ($\alpha_s^3 > 4$), from the theories permitting the discussion of the interpenetration function $\psi(Z)$, the experimental data are in good agreement with the Kurata-Yamakawa theory [12] and with the new theory of Douglas and Freed [13]. One has to mention that up to the synthesis of such ultrahigh molecular weight polymers no experimental data were available to interpret the asymptotic solution of the inter-

---

[1]) Part 8, submitted to Makromol. Chem.

[2]) To whom all correspondence should be addressed.

[3]) The term of „pleistomers" („pleistos" means very many, so „very many mers") has been proposed (J. Macromol. Sci., Chem., (in press)) for ultrahigh molecular weight polymers (copolymers).

penetration function for very high values of the excluded volume parameter Z. From physical considerations, one can estimate that for $Z \to \infty$ polymer molecules tend to become rigid spheres in dilute solutions, so that the interpenetration function $\psi(Z)$ becomes a constant independent of Z.

For ultrahigh molecular weights one has to consider the errors appearing during the experimental determinations, errors transmissible in further consideration of different parameters.

In this context, the present paper is concerned with the systematic error sources in light scattering determinations and with the influence of these errors in discussing the excluded volume effect for very high excluded volume parameters.

2. Results and Discussion

2.1. Experimental Errors

The experimental technique selected to determine the weight -($\overline{M}_w$) and number-average ($\overline{M}_n$) molecular weights, the root-mean-square radii of gyration ($<S^2>^{1/2}$) and the second virial coefficients (A_2) was light scattering. The method was adapted to the particular characteristics given by the very large dimensions of the macromolecular chains. It was established that the main errors could appear from: (a) the preparation of the solutions, the concentration range being $0.5 \times 10^{-4}...8 \times 10^{-4}$ g.cm^{-3}, depending on the molecular weight of the sample and on the refractive index of the solvent; (b) the purification of the solvents; (c) the processing of the solutions up to the experimental determinations, and (d) the processing of the experimental data.

These errors have been eliminated by (a) a very careful preparation of the solutions, (b) the use of high purity solvents, (c) preparation of solutions in the dark, dissolution in the dark for 4...5 days, at about 40°C, without mechanical stirring to prevent shear degradation, (d) purification of solutions by centrifuging for about 1...2 h, at 11,000 g in a J a n e t z k i centrifuge. By respecting all these precautions, reproducible experimental data (R a y l e i g h intensities for different diffusion angles and concentrations) were obtained. The experimental precision in the determination of $\overline{M}_w$ was $\pm 9\%$, and in the determination of A_2 and $<S^2>^{1/2}$, $\pm 3.4\%$ and $\pm 5.5\%$, respectively.

The processing of experimental data in order to determine $\overline{M}_w$, $\overline{M}_n$, $<S^2>^{1/2}$ and A_2 for ultrahigh molecular weight polymers is very difficult when the experimental data do not allow the observation of the R a y l e i g h intensity for diffusion angles lower than 30°. A curvature, predicted by the Gaussian theory but undetected for usual length polymers, appears in the representation of $(Kc/R_\theta)_{c=0}$ as a function of $\sin^2(\theta/2)$ (where c is the concentration, θ is the diffusion angle, K is the light scattering factor). According to B e r r y [14], this difficulty can be eliminated by plotting $(Kc/R_\theta)^{1/2}$ vs. $\sin^2(\theta/2)$, and F u j i t a [15] suggests a linearisation of the experimental curve through the representation of $[y(u)]^{-1}$ as a function of $Z(u)$, where $y(u) = (R_\theta/Kc)_{c=0}$, $Z(u) = [y(u)\, u^{4/3}]^{-1} \int_0^u y(u) u \, du$, with u defined by $u = \sin^3(\theta/2)$, and $1/y(u) = (1/M) + bZ(u)$, with $b = (32\pi^2/3\lambda^2) \times (<S^2>/M)$.

Both methods have been used in our determinations. Fig. 1 presents an example of such studies [9], [10] for two poly(butyl methacrylate) samples in ethyl methyl ketone (EMK) and CCl_4, and Table 1 gives the obtained results.

It was observed that working in the 30°...130° diffusion angles range, B e r r y's method allows a linearisation of the experimental curves up to about 50°, while F u j i t a's method up to an angle of about 80°. Also, according to Table 1, the errors in the determination of $\overline{M}_w$ and $<S^2>^{1/2}$ rise up to $\pm 9\%$ and $\pm 5.5\%$, respectively. These errors, high enough as compared to those observed in studying usual length polymers, are translated in the evaluation of different parameters characterizing high polymers in diluted solutions.

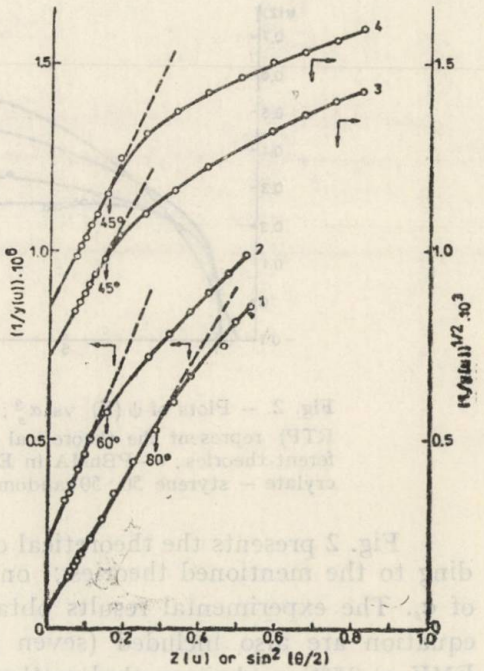

Fig. 1. — Plots of $1/y(u)$ vs. $Z(u)$ (F u j i t a's method) for PBuMA (I) in EMK (curve *1*) and PBuMA (II) in CCl_4 (curve *2*), and of $(1/y(u))^{1/2}$ vs. $\sin^2(\theta/2)$ (B e r r y's method) for PBuMA (I) in EMK (curve *3*) and PBuMA (II) in CCl_4 (curve *4*). The data points for the samples are shifted upward to the following amounts: *1* — 0; *2* — 0.2×10^{-6}; *3* — 0.5×10^{-3}; *4* — 0.7×10^{-3}.

2.2. Influence of Experimental Errors on the Excluded Volume Effect

The interpenetration function $\psi(Z)$ can be determined from different theoretical dependences with the expansion factor $\alpha_s = <S^2>^{1/2} / <S_0^2>^{1/2}$ (where $<S_0^2>^{1/2}$ is the unperturbed root-mean-square radius of gyration) obtained from experimental data (original F l o r y theory (F, *0*), modified F l o r y theory (F, *m*), K u r a t a-Y a m a k a w a theory (K-Y), renormalized group theory of D o u g l a s and F r e e d (RTP) [6], [8], [12], [13]) or directly from experimental data according to $\psi(Z) = A_2 \overline{M}^2 / 4\pi^{3/2}\, N_A <S^2>^{3/2}$.

Table 1

Light Scattering Data Obtained According to the Methods of B e r r y and F u j i t a

Sample / Method	$\overline{M}_w \cdot 10^{-6}$		$<S^2>^{1/2}(10^{-5}$ cm)	
	Berry	Fujita	Berry	Fujita
PBuMa(I)*) (EMK, 25°C)	21.633	23.256	2.204	2.057
PBuMA(II)**) (CCl_4, 20°C)	48.485	45.454	3.525	3.142

*) Fractionated sample ; **) Unfractionated sample, $\overline{M}_w/\overline{M}_n = 1.79$

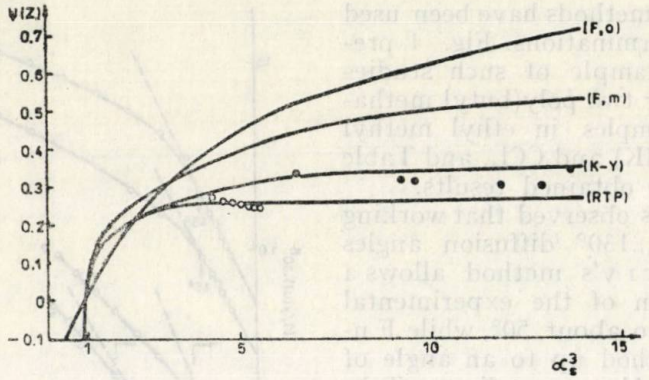

Fig. 2. — Plots of $\psi(Z)$ vs. α_s^3; the curves ($F, 0$; F, m; K-Y; RTP) represent the theoretical values calculated according to different theories; o—PBuMA in EMK at 25°C, • — methyl methacrylate — styrene 50 : 50 random copolymer in 1,4-dioxane at 20°C.

Fig. 2 presents the theoretical curves of $\psi(Z)$ as a function of α_s^3 according to the mentioned theories; one can evaluate $\psi(Z)$ for a given value of α_s. The experimental results obtained for $\psi(Z)$ according to the given equation are also included (seven poly(butyl methacrylate) samples, in EMK at 25°C, and six methyl methacrylate-styrene 50 : 50 random copolymer samples in 1,4-dioxane at 20°C [6]).

Table 2
Errors Transmitted to Z and ψ (Z) Determined According to Different Theories and Experimentally

Theory (method)	Error, [%]	
	Z	$\psi(Z)$
Original Flory theory	68	23
Modified Flory theory	68	14.6
Kurata-Yamakawa	60	8.8
Douglas-Freed theory*)	60	3.36
Domb-Barrett theory	55	—
Experimental	—	1.85

*) s. [11].

As mentioned, the experimental errors can be translated to different parameters. Starting from an error of $\pm 9\%$ ($\overline{M}_w$) and from an error of $\pm 5.5\%$ ($<S^2>^{1/2}$), errors of $\pm 11\%$ and $\pm 33\%$ are obtained for α_s and α_s^3, respectively. Table 2 presents the errors transmitted to the excluded volume parameter Z and to the interpenetration function $\psi(Z)$ (for α_s affected by the mentioned error), calculated according to different theories [11], [12].

The possible values of $\psi(Z)$ for α_s^3 affected by an error of $\pm 33\%$ (poly(butyl methacrylate) sample, EMK, 25°C, $\overline{M}_w = 1.0406 \times 10^7$) are given, as an example, in Table 3.

According to Fig. 2 and Tables 2 and 3, the evaluation of $\psi(Z)$ by different theories is affected differently by α_s^3. A minimum error appears by use of the RTP theory of Douglas and Freed for $\alpha_s^3 > 4$. It can be also seen that the values obtained directly from the experimental data

Table 3

Possible Values of $\psi(Z)$ for α_s^3 Affected by an Error of ±33% (poly(butyl methacrylate), fractionated sample, EMK, 25°C, $\bar{M}_w = 1.0406 \times 10^7$)

$\psi(Z)$	α_s^3		
	2.924	4.324	5.724
Original Flory theory	0.301	0.392	0.483
Modified Flory theory	0.318	0.372	0.426
Kurata-Yamakawa theory	0.260	0.293	0.316
Douglas-Freed theory	0.233	0.254	0.259
Experimental	0.270±0.005		

present very low errors (±1.85%) and are close to those given by K-Y theory, being in a very good agreement with the RTP theory.

3. Conclusions

In conclusion, the possible errors appearing in studying solution properties of ultrahigh molecular weight polymers by light scattering method can be very important. These errors can be minimized through specific restrictions and by applying adjusted processing techniques. The errors do not influence the values of the interpenetration function $\psi(Z)$ for expansion factors $\alpha_s^3 > 4$. In these conditions, the degree of penetration of the macromolecular chain in the diluted solution becomes constant (0.269 according to the theory of Douglas and Freed), and the chain tends to become a rigid sphere for $Z \to \infty$.

Received, May 4, 1985

„P. Poni" Institute of Macromolecular Chemistry, Jassy,
and
Polytechnic Institute, Jassy,
Department of Organic and Macromolecular Chemistry and Technology

REFERENCES

1. Simionescu C.I., Simionescu B.C., Pure Appl. Chem., **56**, *3*, 427 (1984).
2. Simionescu C.I., Simionescu B.C., Chem. Zvesti., **37**, *5*, 685 (1983).
3. Simionescu B.C., Ioan S., Simionescu C.I., Polym. Bull., **6**, 409 (1982).
4. Ioan S., Simionescu B.C., Simionescu C.I., Polym. Bull., **6**, 421 (1982).
5. Simionescu C.I., Simionescu B.C., Ioan S., Makromol. Chem., Rapid Commun., 4, 549 (1983).
6. Simionescu C.I., Simionescu B.C., Ioan S., Makromol. Chem., **184**, 829 (1983).
7. Ioan S., Simionescu B.C., Simionescu C.I., Polym. Bull., **5**, 563 (1981).
8. Simionescu C.I., Simionescu B.C., Ioan S., Macromolecules, (in press).
9. Simionescu C.I., Simionescu B.C., Ioan S., J. Polym. Sci., Polym. Lett. Ed., 3, 121 (1985).
10. Simionescu B.C., Ioan S., Simionescu C.I., Makromol. Chem., (submitted).
11. Ioan S., Simionescu B.C., Simionescu C.I., Makromol. Chem., (submitted).
12. Yamakawa H., Pure Appl. Chem., **31**, 179 (1972).
13. Douglas J.F., Freed K.F., Macromolecules (in press).
14. Berry C.G., J. Chem. Phys., **44**, 4 550 (1966).
15. Fujita H., Polym. J., **1**, *5*, **537 (1970)**.

PROPRIETĂŢILE SOLUŢIILOR DE POLIMERI CU MASE MOLECULARE FOARTE MARI

9. Surse sistematice de erori în determinări de difuzia luminii care afectează discutarea efectului volumului exclus

(Rezumat)

Se discută erorile posibile care apar în determinările de difuzia luminii la polimeri cu mase moleculare foarte mari, în soluţie diluată, minimalizate prin restricţii specifice şi tehnici de calcul adaptate, erori care sînt transmise funcţiilor termodinamice care descriu efectul volumului exclus.

S-a constatat că dacă parametrul volumului exclus Z este afectat de erori foarte importante, aceasta nu influenţează discutarea şi valorile funcţiei de interpenetrare $\psi(Z)$ pentru un factor de expansiune $\alpha_s^3 > 4$. Din teoriile existente, teoria de grup renormalizată verifică cel mai bine datele experimentale obţinute pentru $\psi(Z)$, în limitele erorilor menţionate.

BULETINUL INSTITUTULUI POLITEHNIC DIN IAŞI
Tomul XXXI (XXXV), Fasc. supl., 1985
Secţia II
CHIMIE ŞI INGINERIE CHIMICĂ

C.D. 678-13

TRANSITIONS CONFORMATIONNELLES DES TRIBLOCCOPOLYMÈRES DU TYPE *ABA*

PAR

MIRCEA GRIGORAŞ, GETA ONOFREI, ELENA BÎCU et IDIR RABIA

1. Introduction

L'étude en solution diluée des copolymères séquencés a fait l'objet de nombreux travaux au cours de ces dernières années. Le but essentiel était d'établir si ces copolymères adoptent des conformations statistiques ou si, au contraire, les séquences occupent des domaines distinctes de l'espace (forme „ségrégée"). De nombreux travaux plaident en faveur de l'existence des transitions conformationnelles dans le cas de plusieurs blocs copolymères, à savoir : poly (styrène-*b*-isoprène) [1], poly(méthacrylate de methyl-b-styrène-b-méthacrylate de methyl) [2], [3], poly(styrène-b-méthacrylate de méthyl) [4], poly(styrène-b-α-methylstyrène) [5], sous l'influence de la température ou par variation de la qualité thermodynamique du solvant par addition d'un autre solvant. L'explication de la „ségrégation" doit être basée sur l'incompatibilité qui caractérise les séquences de nature chimique différente. Or, cette incompatibilité doit diminuer lorsque la température augmente ou lorsqu'on fait varier la qualité thermodynamique du solvant. Compte tenu de l'agitation thermique croissante on peut prévoir qu'à une température donnée une interpénétration des séquences peut se produire, en passant ainsi à une conformation statistique.

Nous avons rapporté ailleurs la synthèse de quelque tribloccopolymères du type *ABA* par polymérisation cationique avec isomérisation des 2-oxazolines-2-substituées avec l'usage des initiateurs bifonctionnels. Les échantillons utilisés ont le poly-N-aciléthylènimine (partie termoplastique) comme bloc *A* et le poly-éthylèneglycoladipé ou poly-éthylèneoxyde (partie elastomère) comme bloc *B*.

Dans cet article nous allons mettre en évidence, par des études viscosimétriques, l'existence des transitions conformationnelles en solution diluée pour les tribloccopolymères synthetisés.

2. Partie expérimentale

Les bloc copolymères étudiés ont la composition et la structure suivantes :

poly(N-aciléthylènimine -b- éthylèneglycoladipé -b- N-aciléthylènimine)

$$CH_3-C_6H_4-SO_3-(CH_2-CH_2-\underset{\displaystyle C=O}{\underset{|}{N}}-)_x-[(CH_2)_2-OCO-(CH_2)_4-COO-$$

$$\underset{\displaystyle CH_3}{\underset{|}{}}$$

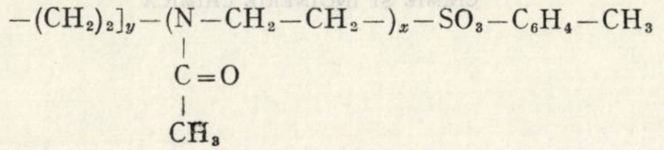

MeOxz – PEGA – MeOxz

échantillon *A* ; $x = 3{,}4$, $y = 13$
échantillon *B* ; $x = 6{,}0$, $y = 13$

poly (N-aciléthylènimine-)-b-éthylèneoxyde-b-N-aciléthylènimine)

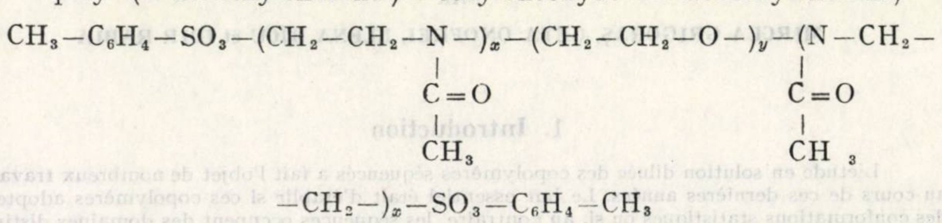

MeOxz – PEO – MeOxz

$x = 10{,}8$; $y = 52$

Leur synthèse et caracterisation a été présentée dans des travails antérieurs [6]...[8].

Les mesures de viscosité ont été effectuées avec un viscosimètre Ubbelhode. Les solvants ont été séchés et distillés.

3. Résultats et discussion

L'influence de la concentration, de la température et de la composition du mélange des solvants sur la conformation des bloccopolymères a été étudiée par voie viscosimetrique. Les solvants utilisés sont le $CHCl_3$ (solvant commun pour les deux blocs *A* et *B*) et le THF ou le benzène (solvant séléctif pour le bloc *B*).

3.1. Influence de la concentration

Dans le cas des copolymères greffés et séquencés, Dondos et Benoit [2] ont montré que dans le domaine des températures ou l'on observe des changements de conformation, la variation de la viscosité avec la concentration présente une anomalie. Les points expérimentaux se situent sur deux droites ayant des pentes différentes ui se rencontrent en un point correspondant à une concentration critique. Ultérieurement Gosa et Donescu [9] ont montré par spectrophotométrie UV que dans le cas des copolymères greffés cette concentration critique, qui est supposée marquer le passage d'une conformation „ségrégée" à une conformation pseudogaussienne, peut apparaitre à n'importe quelle température et non seulement dans le domaine des températures de transition.

En étudiant le comportement des triblocs copolymères MeOxz – PEGA – MeOxz et MeOxz – PEO – MeOxz dans un solvant commun aux deux blocs

($CHCl_3$) et dans un solvant sélectif (THF pour le PEGA et benzène pour le PEO) et dans le mélange des deux solvants, on observe l'existence des transitions conformationnelles. Celles-ci apparaissent dans un domaine de concentration voisin de celui qui a été defini par D o n d o s et B e n o i t [2] et G o s a et D o n e s c u [9], pour les blocs copolymères et les copolymères greffés.

Dans le THF les mesures ont été effectuées dans un domaine restreint de valeurs à cause de la saturation rapide de la solution du bloc copolymère étudié (Me*Oxz*—PEGA—Me*Oxz*) à partir, de la concentration $c = 0{,}16$ g/dl. Jusqu'à cette valeur de la concentration nous avons observé un comportement normal (Fig. 1, courbe *a*). Dans le $CHCl_3$ la variation de la viscosité réduite avec la concentration est conforme aux résultats de la littérature concernant le comportement des blocs copolymères en solution [2] (Fig. 1, courbe *b*).

Dans le cas du mélange binaire de solvant (solvant + solvant sélectif) on n'observe pas l'apparition d'une concentration critique mais d'un domaine d'environ 0,03 g/dl dans lequel a lieu probablement le passage graduel d'une conformation à une autre (Fig. 2).

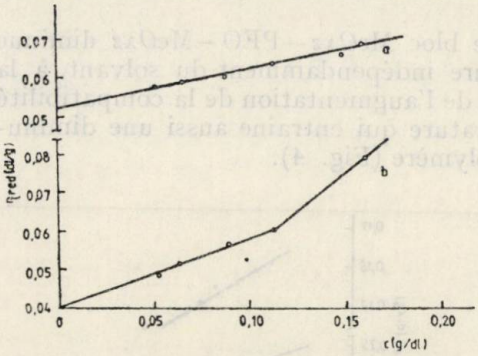

Fig. 1. — Variation de la viscosité réduite avec la concentration du bloc Me*Oxz*—PEGA—Me*Oxz* dans le THF (*a*) et dans le $CHCl_3$ (*b*).

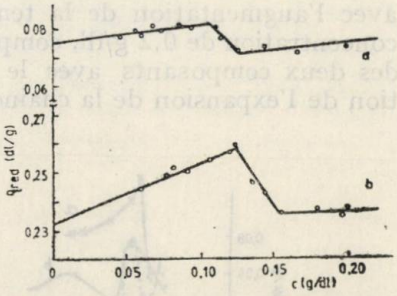

Fig. 2. — Variation de la viscosité réduite avec la concentration des blocs Me*Oxz*—PEGA—Me*Oxz* et Me*Oxz*—PEO—Me*Oxz* dans les mélanges de solvants suivants : *a* — Me*Oxz*—PEGA—Me*Oxz* dans THF/$CHCl_3$ (1/1) ; *b*—Me*Oxz*—PEO—Me*Oxz* dans benzène/$CHCl_3$ (1/1) ; température = 25°C.

C'est intéressant à remarquer que dans le cas du bloc copolymère Me*Oxz*—PEO—Me*Oxz* la température de 25°C, à laquelle ont été effectuées les mesures, n'est pas comprise dans le domaine où on enregistre une transition conformationnelle contrairement au bloc copolymère Me*Oxz*—PEGA—Me*Oxz*.

3.2. Influence de la température

L'influence de la température a été étudiée en utilisant un mélange binaire des solvants 1 : 1 (solvant/solvant séléctif). On observe une variation

non-monotone de la viscosite réduite avec la température dans le cas du tribloc Me*Oxz*—PEGA—Me*Oxz*, ce qui suppose l'existence des transitions conformationnelles. Ces transitions sont probablement dues à la nature chimique du polymère et pas à une transition d'une conformation „ségrégée" à une conformation pseudogaussienne comme il a été démontré dans le cas de certains bloccopolymères [1], [2], [10] et copolymères greffés [9], [11], [12]. Cet aspect est confirmé aussi par le fait que dans le cas de l'homopolymère PEGA apparait une transition conformationnelle dans le domaine de température étudié (Fig. 3).

D'autre part si c'était une transition conformationnelle de même nature que celles rencontrées en littérature, elle n'aurait pas pu être mise en évidence à des concentrations plus grandes que celles aux quelles a lieu le passage de la conformation „ségrégée" à la conformation pseudogaussienne. Or dans le cas des copolymères étudiés cette transition a lieu aussi dans le domaine de concentrations $c > 0{,}12$ g/dl. Cependant ces transitions sont plus évidentes dans les solutions trés diluées, à des concentrations $c < c_{critique}$ (Fig. 3). Probablement, aux concentrations plus élevées, la possibilité d'intéraction entre les différents segments augmente ce qui atténue l'effet d'intéractions du type *AA* et *BB* auxquelles on a attribué l'apparition des maximums et des minimums à 25° et 40°C.

La viscosité réduite η_{red} pour le bloc Me*Oxz*—PEO—Me*Oxz* diminue avec l'augmentation de la température indépendamment du solvant, à la concentration de 0,2 g/dl, compte tenu de l'augmentation de la compatibilité des deux composants avec le température qui entraine aussi une diminution de l'expansion de la chaine du polymère (Fig. 4).

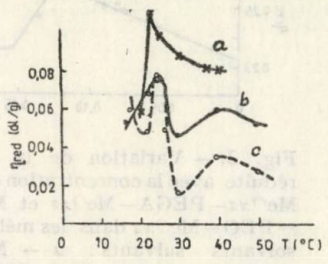

Fig. 3. — Variation de la viscosité réduite avec la température ; solvant=$CHCl_3$/THF (1/1) : *a*—PEGA ; *b*—Me⌒*xz*—PEGA—Me⌒*xz*, c = 0, 198 g/dl ; *c* — Me⌒*xz* — PEGA — —Me⌒*xz*, c=0,0495 g/dl.

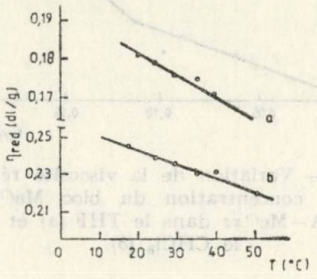

Fig. 4. — Variation de la viscosité réduite avec la température pour le bloccopolymère Me⌒*xz*—PEO—Me⌒*xz*: *a*—solvant=$CHCl_3$/THF (1/1), c=0,2 g/dl ; *b* — solvant = benzene/THF (1/1), c=0,2 g/dl.

3.3. Comportement des blocs copolymères en solution dans un mélange binaire de solvants

Pour cette étude nous avons utilisé un mélange de solvant—solvant sélectif pour le bloc principal *B* ($CHCl_3$—THF). Ayant en vue que la concentration à laquelle le bloc copolymère devient insoluble (solution saturée) dans le THF diminue avec l'augmentation du nombre d'unités structurelles

du poly-Me*Oxz*, on a étudié seulement le comportement du bloccopolymère dont $x \leqslant y$. On enregistre une variation non-monotone aussi bien de la viscosite réduite η_{red} que de la viscosité intrinsèque $[\eta_i]$ avec la composition du mélange des solvants, ce qui suppose une transition conformationnelle due au passage de l'état „ségrégée" stable dans un bon solvant ($CHCl_3$) (Fig. 5 courbe *a*) à une conformation stable dans un solvant sélectif pour le bloc central *B* (Fig. 5 courbe *b*).

Dans le THF, Z_{AA} (coefficient proportionnel à l'énergie d'interaction nécessaire au contact entre les composants *A* du polymère) diminue par suite de l'augmentation de X_{AS} (interaction très faibles entre le solvant et le bloc *A*, le THF étant un précipitant du Me*Oxz*) déterminant ainsi une diminution de l'expansion de la chaine macromoléculaire. À des concentrations du THF $<50\%$ on observe une variation négative de la viscosité (Fig. 6), conséquence de la qualite thermodynamique du couple de

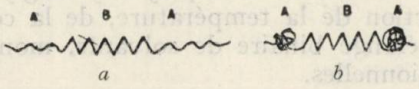

Fig. 5. — Conformation des bloccopolymères : *a* — dans le $CHCl_3$; *b* — dans le THF.

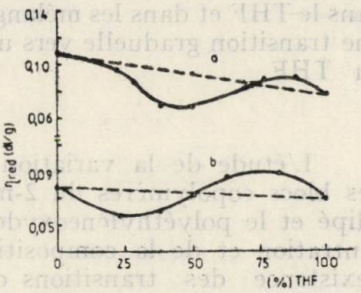

Fig. 6. — Comportement du bloc Me*Oxz* — PEGA—Me*Oxz* dans le mélange de solvants $CHCl_3$/THF, température = 25°C: *a* — échantillon *B*, $c = 0{,}12$ g/dl ; *b* — échantillon *A*, $c = 0{,}16$ g/dl.

solvants ($\Delta G^E < 0$, mélange binaire exothermique avec possibilité de formation de liaison hydrogène), comme il a été mis en évidence par Dondos et Benoit [2], [13] sur la base de la théorie de Schultz-Flory. D'après cette théorie :

$$X_{AS} = x_1 X_{A1} + x_2 X_{A2} - x_1 x_2 X_{12}, \tag{1}$$

où x_1, x_2 — fractions molaires des deux solvants du mélange ; X_{A1}, X_{A2} — coefficients d'intéraction du polymère *A* avec chaque constituant du mélange.

Les dimensions moléculaires des copolymères dépendent des trois coefficients X_{AS}, X_{BS} (qui varient avec x_1, x_2) et X_{AB}, par le paramètre global d'intéraction *Z* qui influence la valeur du coefficient d'expansion viscosimétrique.

Pour un copolymère :

$$Z = C_1 Z_{AA} + C_2 Z_{BB} + C_3 Z_{AB}, \tag{2}$$

ou : Z_{ii} — coefficients proportionnels à l'énergie d'interaction nécessaire à chaque type de contact entre les composants du polymère, dans un solvant

donné ; C_i – facteurs de fréquence caractérisant la possibilité d'existence de contacts AA, BB et AB.

Dans le cas d'un tribloccopolymère les interactions entre les blocs ont un effet mineur sur l'expansion de la chaine polymérique en comparaison aux interactions intrabloc. Pour cela on peut considérer que $C_3=0$, $Z_{ii}\approx 1/2-X_{1S}$ ce qui veut dire que dans le cas d'un solvant ayant $\Delta G^E<0$ (comme le mélange utilisé $CHCl_3$/THF), X_{12} étant négatif va déterminer une augmentation des coefficients d'interaction X_{AS} et X_{BS} et, en conséquence, une diminution des termes Z_{AA} et Z_{BB}, ce qui entraine une diminution des dimensions moléculaires.

Pour des valeurs croissantes de la concentration en THF du mélange de solvants on observe l'apparition d'un maximum qui peut être attribué à l'absorption sélective du $CHCl_3$ [14] par le bloc $MeOx_2$. Cela entraine une ségrégation accentuée des deux blocs [15] et par conséquence une augmentation des dimensions de la chaine moléculaire par rapport a celles observées dans le THF et dans les mélanges $CHCl_3$/THF antérieurs, dans lesquels a lieu une transition graduelle vers une conformation statistique due à la présence du THF.

4. Conclusions

L'étude de la variation de la viscosité réduite en solution diluée des blocs copolymères du 2-méthyl-2-oxazoline avec le polyéthylèneglycol adipé et le polyéthylèneoxyde, en fonction de la température, de la concentration et de la composition du mélange binaire de solvants, montre l'existence des transitions conformationnelles.

Reçue le 10 Avril 1985

Institut de Chimie Macromoleculaire „P. Poni", Jassy

BIBLIOGRAPHIE

1. Urwin J.R., Girolamo M., Makromol. Chem., *150*, 179 (1971).
2. Dondos A., Benoit H., Makromol. Chem., *178*, 1 089 (1977).
3. Dondos A., Makromol. Chem., *147*, 123 (1971).
4. Dondos A., Rempp P., European Polym. J., **3**, 657 (1967).
5. Dondos A., J. Polym. Sci., **B9**, 871 (1971).
6. Simionescu C.I., Rabia I., Harfas I., Polym. Bull., **7**, 129 (1982).
7. Simionescu C.I., Rabia I., Crişan Z., Polym. Bull., **7**, 217 (1982).
8. Simionescu C.I., Rabia I., Polym. Bull., **10**, 311 (1983).
9. Gosa K., Donescu D., Makromol. Chem., *182*, 1 725 (1981).
10. Dondos A., Makromol. Chem., *99*, 175 (1966).
11. Kimura S., Kurata M., Macromolecules, **14**, 1 104 (1981).
12. Petrea C., Gosa K., Donescu D., Materiale Plastice (Bucureşti), **16**, 1 (1979).
13. Dondos A., Rempp P., Benoit H., Makromol. Chem., *130*, 233 (1969).
14. Kratochvil P., Makromol. Chem., *148*, 271 (1971).
15. Skoulios A., Makromol. Chem., *148*, 305 (1971).

TRANZIŢII CONFORMAŢIONALE ÎN TRIBLOCCOPOLIMERI DE TIP *ABA*

(Rezumat)

Conformaţia în soluţie a unor tribloccopolimeri de tip *ABA*, (poli(N-acil etilenimină-b-etilenglicol adipat-b-N-acil etilenimină) şi poli(N-acil etilenimină-b-etilenoxid-b-N-acil etilenimină), unde blocul *A* are proprietăţi termoplastice iar blocul *B* proprietăţi elastice, a fost studiată prin metoda vîscozimetrică. Variaţia vîscozităţii reduse în soluţie diluată a tribloccopolimerilor funcţie de temperatură, concentraţia şi compoziţia amestecului binar de solvenţi arată existenţa unor tranziţii conformaţionale.

BULETINUL INSTITUTULUI POLITEHNIC DIN IAŞI
Tomul XXXI (XXXV), Fasc. supl., 1985
Secţia III
CHIMIE ŞI INGINERIE CHIMICĂ

D.C. 54 92

PHOTOCROSSLINKING PROCESSES IN SOLID FILMS

I. A THEORETICAL DISCUSSION OF THE METHODS TO INCREASE THE THICKNESS OF PHOTOINSOLUBILIZED LAYER

BY

VIRGIL BĂRBOIU, GEORGE ERVANT GRIGORIU, ELENA RUSU, TEODOR MARCU and EMIL BURUIANĂ

1. Introduction

It is known that the photocrosslinking polymers are used as negative photoresists. Such polymers contain ethylenic bonds which can be easily crosslinked under illumination. Many publications, especially patents, exist on this field. Many of them are refered to polymers with cinnamoyl groups, perhaps because such systems are suitable models for the study of the photocrosslinking process [1]...[10].

It was observed by studying the photocrosslinking of vinyl alcohol — vinyl acetate — vinyl cinnamate copolymers that the thickness of photoinsolubilized layer increases if the cinnamoyl group content is decreased (Fig. 1) [11], [12]. Such an observation is important to obtain photocrosslinking polymers used as negative photoresists because if the photoinsolubilized layer is too thin relative to the photoresist film then the developed image is poor or even absent due to the slide of the insoluble layer on the internal soluble layers. One of the ways to avoid such troubles would be to decrease the film thickness but this must not be smaller than 1...2 μ because otherwise the photoresist film becomes penetrable for the chemical reagents used for the processing of the support. The observation illustrated on Fig. 1 seems to lead to the supposition that the photoinsolubilized layer thickness (denoted by x_r) can be increased by decreasing the photocrosslinking group density. However it is evidently that such a decreasing is limited because it also leads to the decreasing of the probability of having pairs of two neighbouring photoactive groups.

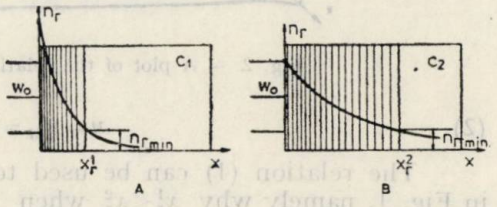

Fig. 1. — An illustration of the depth dependence of the photocrosslinked group density (n_r) for unsensitized photocrosslinking polymers. The two investigated polymers are vinyl alcohol — vinyl cinnamate copolymers with different vinyl cinnamate contents ($C_1 > C_2$). The irradiation and developing conditions were the same, and the illumination was made by the film supports which were quatz plates.

The present paper is refered to some supposed physical relationships characterizing the photocrosslinking phenomena into rigid systems (with fixed photoactive groups) developed with the purpose to find ways to increase the photoinsolubilized layer thickness.

2. Photocrosslinking due to the Normal Absorption of the Photocrosslinking Groups

Denoting the density of photocrosslinking groups by n, the probability to have two such groups in a steric arrangement favourable to the crosslinking reaction will be proportional to n^α, where α is a positive number. In addition, taking into account that the radiation intensity decreases exponentially with layer thickness, the density n_r of photocrosslinked groups at a depth x inside the film will depend on n according to :

$$n_r \sim \eta w_0 n^\alpha \exp(-\varepsilon n x), \tag{1}$$

where η is the yield of the photocrosslinking processes, w_0 — the initial irradiation energy and ε — the extinction coefficient. A plotting of the dependence of n_r on n and x is given in Fig. 2 for the case when $\alpha = 2$. It is observed that the density n_r at a depth x is maximum when

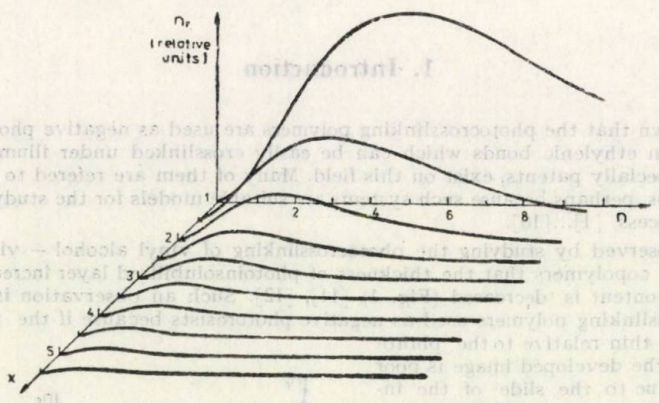

Fig. 2. — A plot of the relationship (1) for the case $\alpha = 2$.

$$n = n_M = \alpha/\varepsilon x. \tag{2}$$

The relation (1) can be used to explain the observation illustrated in Fig. 1, namely why $x_r^1 < x_r^2$ when $C_1 > C_2$. Let us suppose that $n_{r\min}$ is the lowest value of n_r for which the irradiated polymers are insoluble. Denoting by n_0 and n the initial densities of photocrosslinking groups for the two polymers in solid state (the first having a photocrosslinking group content of 100%, and the other a lower content) and by x_r^0 and x_r the photoinsolubilized layer thicknesses for the two cases, the following relations can be written :

$$n_{r\min} = \text{const.}\ n_0^\alpha \exp(-\varepsilon n_0 x_r^0) = \text{const.} n^\alpha \exp(-\varepsilon n x_r), \tag{3}$$

from where it results

$$x_r = \frac{n_0}{n} x_r^0 - \frac{\alpha}{\varepsilon n} \ln \frac{n_0}{n}. \tag{4}$$

The mathematical analysis of the relation (4) shows that x_r has a maximum value, $x_{r\max}$, when $n = n_{optim}$ (s. Fig. 3), where

$$(5) \qquad n_{optim} = n_0 \exp(1 - \varepsilon x_r^0/\alpha) \text{ and } x_{r\max} = (\alpha/\varepsilon n_0)/\exp(1 - \varepsilon n_0 x_r^0/\alpha).$$

It is observed that $n_{optim} < n_0$ and $x_{r\max} > x_r^0$ if $\varepsilon n_0 x_r^0 > \alpha$, the last condition being fulfiled if the irradiation energy is high enough.

The relation (4) with $\alpha = 2$ is plotted in Fig. 3 for the systems containing cinnamoyl groups grafted on vinyl alcohol—vinyl acetate copolymers, where $\varepsilon \approx 4 \times 10^3$ l/mol. cm ($\lambda_{max} = 280$ nm), $n_0 = 6$ mol/l and $x_r^0 = 1.5\ \mu$ ($w_0 \approx 2$ J/cm², xenon source). It is observed from this figure, or by using the relations (5), that

$$(6) \quad n_{optim} = 0.45 n_0 \text{ and } x_{r\max} = 1.25 x_r^0.$$

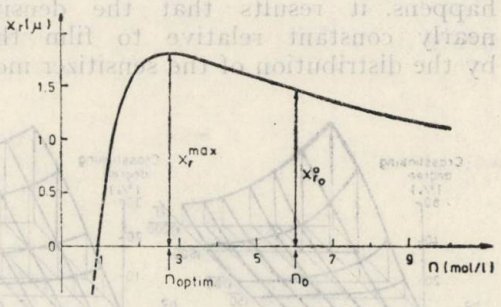

Fig. 3. — The plot of the relationship (4) fo polymers with photocrosslinking groups of cin namoyl type.

The last relations show that the cinnamoyl containing polymers are good negative photoresists if their cinnamoyl group content is equal to 40...50%. On the other hand, the increase of x_r by decreasing the cinnamoyl group concentration is theoretically quite small, therefore with no practical interest. An alternative method to increase x_r^0 and therefore $x_{r\max}$ would be to increase the irradiation energy, w_0, but such a procedure is not indicated because the photodegradation becomes important relative to the photocrosslinking in the surface layer.

The next two phenomena allow important increases of x_r^0 and $x_{r\max}$ in conditions of low photodegradation effects.

3. Sensitized Photocrosslinking

The quantum yield of photocrosslinking processes in the rigid systems can be significantly increased if some molecules known as sensitizers are present [1]...[3], [7]...[10]. The sensitizers realize both a matching between the absorption spectrum of the photoresist and the spectrum of the used ligth source, and an important increase of the photoinsolubilized layer thickness. Denoting by η', ε' and n', the quantum yield, the extinction coefficient and the density of photosensitizer molecules, the density of photocrosslinked groups at a depth x will be given by the following relationship :

$$(7) \qquad n_r^s \sim n' w_0 n^\alpha \exp(-\varepsilon' n' x),$$

if the illumination is made on the sensitizer absorption bands.

To estimate the sensitizer effect on the photoinsolubilized layer thickness (denoted by x_r' in the relation (8)), by comparison with the unsensitized photocrosslinking process, the following equalities must be used :

(8) $$n_{r\min} = \text{const.}\ \eta n^{\alpha} \exp(-\varepsilon n x_r) = \text{const.}\ \eta' n'^{\alpha} \exp(-\varepsilon' n' x_r').$$

Now it is very easy to obtain the expression of x_r' :

(9) $$x_r' = \frac{\varepsilon n}{\varepsilon' n'} x_r + \ln \frac{\eta'}{\eta}.$$

As $\eta' > \eta$, $n/n' \approx 10...10^2$ and $\varepsilon \approx \varepsilon'$,, it results that $x_r' > (10...10^2) x_r$, therefore the sensitization method assures an important increase of x_r. In addition, if $\eta' \gg \eta$ and λ_{max} (sensitizer) $> \lambda_{max}$ (photocrosslinking groups) as it usually happens, it results that the density of photocrosslinked groups is nearly constant relative to film thickness, being mainly determined by the distribution of the sensitizer molecules (which is evidently uniform).

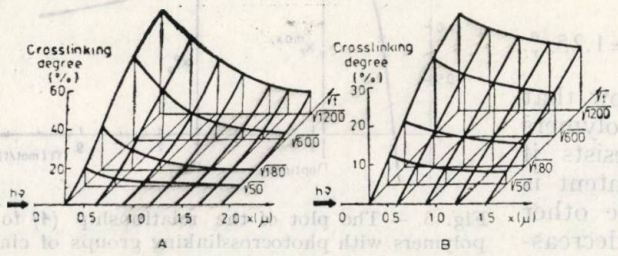

Fig. 4. — The dependence of the average photocrosslinking degree on the irradiation time and on the light penetration depth for polyvinyl alcohol 50% esterified with cinnamoyl groups : *A* — unsensitized polymer irradiated with 15...20 mW/cm² (mercury source), and *B* — sensitized polymer with 10% Michler's cetone, monocromatic illumination (360 nm) of about 0.5 mW/cm². The photocrosslinking degree was estimated from the relative decreasing of the cinnamoyl group absorption band at 280 nm ; the time is given in seconds.

For comparision, Fig. 4 shows the dependence of the photocrosslinking degree on the irradiation time and on the ligth penetration depth for a polymer containing cinnamoyl groups in two cases : unsensitized (Fig. 4 *A*) and sensitized (Fig. 4 *B*). It is observed that the sensitizer (Michler's cetone) realizes both a visible increasing of the photocrosslinking degree /irradiation energy ratio, and a weak dependence of the photocrosslinking degree on the depth of radiation penetration.

4. Photocrosslinking in Systems with Donor—Acceptor Interactions

The idea to sensitize photocrosslinking processes by interactions between electron donor and electron acceptor groups is quite recent [13], [14]. Its principle is to use a mixture of two photocrosslinking polymers, one having donor-type photoactive groups and the other having acceptor-type photoactive groups. Our observations were made using *p*-methoxycinnamoyl groups as donor groups and *p*-nitrocinnamoyl groups as acceptor groups. As expected, the complexation interactions lead to two effects which are favourable to the photocrosslinking processes : a) the increase of the probability of having pairs of two photocrosslinking groups due to the cross dimer formation, and b) the shift to the visible range of the light absorption due to the charge transfer complex band, and therefore a better matching on the actual light sources.

It was observed that the photocrosslinking appears at quite low concentrations of complexable groups (10...20%). For this reason it is expected from such a photocrosslinking to be slightly dependent on the penetration depth of radiation. Another advantage of this method is that the photoreactions are not influenced by air, while the photoreactions induced by sensitizers are inhibited by oxygen. The main disavantage of this method is the low solubility of systems with donor—acceptor interactions. For example, their solutions in common solvents are opalescent even at concentrations lower than 10% and, consequently, their dried films show a rugged surface. For this reason it would be indicated to use weak donor—acceptor interactions, but the sensitizations effects will be small in this case.

5. Conclusions

The photocrosslinking polymers can be used as negative photoresists if they are sensitized with suitable molecules. For a good matching between the photoresist absorption spectrum and the source emission spectrum it is required for sensitizer molecules to have λ_{max} in the visible range or in the near UV range. To obtain a large thickness of the photoinsolubilized layer, the sensitizer concentration must be much lower than the concentration of photocrosslinking groups on the polymer. The last concentration must be lowered up to an optimum value which is of 40...50% in the case of cinnamoyl groups. Perhaps the best results can be obtained if one sensitizer molecule complexes by weak donor—acceptor interactions with two photocrosslinking groups.

Received, April 10, 1985

„Petru Poni" Institute of Macromolecular Chemistry, Jassy

REFERENCES

1. Williams J.R.L., *Photopolymerization and Photocrosslinking of Polymers*, in *Topics in Current Chemistry*, Bd. **13**, H. 2, Springer-Verlag, Berlin-Heidelberg, 1969.
2. Finch C.A. (Ed.), *Polyvinyl Alcohol : Properties and Applications*. Wiley-Interscience, London, 1973.
3. Rånby B., Rabek J.F., *Photodegradation, Photo-oxidation and Photostabilization of Polymers* Wiley-Interscience, London, 1975.
4. Rånby B., invited lecture at the 29th Symposium on Macromolecules, Bucharest, Sept. 1983.
5. Tsuda M., Bull. Chem. Soc. Japan, **42**, 905 (1969).
6. Воскобойник Г.А., Гришанова Н.Г., Соболева Е.Б., Рябов А.В., Феодоров Ю., Высокомол. Соед., **А 14**, 2472 (1972).
7. Белякова А.П., Боков Ю.К., Лавришев В.П., Коновалов П.Г. Васкевич Д.Н., Высокомол. Соед., **А7**, 1637 (1965).
8. Nakamura K., Kikuchi S., Bull. Chem. Soc. Japan, **41**, 1977 (1968).
9. Rabek J.F., Zaleski A., Polimery, **15**, 437 (1970) ; **16**, 1 (1971) ; **18**, 57 (1971).
10. Sierocka M., Paczkowski J., Wrzyszczynski A., Zakrzewski A., Polimery, **21**, 449 (1976).
11. Bărboiu V., Grigoriu G.E., Buruiană E., Chelaru E., Materiale Plastice, **20**, 190 (1983).

12. Bărboiu V., Buruiană E., Grigoriu G.E., Chelaru E., poster at the 20th Symposium on Macromolecules, Bucharest, Sept. 1983, Abstract Volum, section VII, 371.
13. Watanabe S., Ichimura K., J. Polym. Sci., Polym. Chem. Ed., 20, 3 261 (1982).
14. Smets G., invited lecture at the 29th Symposium on Macromolecules, Bucharest, Sept. 1983.

PROCESE DE FOTORETICULARE ÎN FILME SOLIDE

I. O discuţie teoretică a metodelor de creştere a grosimii stratului fotoinsolubilizat

(Rezumat)

Este explicată dependenţa densităţii grupelor fotoreticulate de densitatea iniţială de grupe fotoreticulabile şi de adîncimea de pătrundere a luminii atît în cazul polimerilor nesensibilizaţi cît şi în cazul polimerilor sensibilizaţi. În primul caz s-a găsit că grosimea stratului fotoinsolubilizat poate fi puţin crescută printr-o micşorare adecvată a densităţii iniţiale de grupe fotoreticulabile. De asemenea, se demonstrează că această grosime poate fi mult crescută în al doilea caz dacă densitatea moleculelor de sensibilizator este mult mai mică decît densitatea grupelor fotoreticulabile. În final sînt date unele consideraţii asupra sistemelor caracterizate prin interacţii intermoleculare între grupe fotoreticulabile de tip donor şi de tip acceptor de electroni.

BULETINUL INSTITUTULUI POLITEHNIC DIN IAȘI
Tomul XXXI (XXXV), Fasc. supl., 1985
Secția II
CHIMIE ȘI INGINERIE CHIMICĂ

D.C. 541.182.6

MASS TRANSFER DURING THIN FILM FLOW OF SUSPENSIONS

BY

RADU Z. TUDOSE, ECATERINA MERICĂ and ȘT. UNGUREANU

1. Introduction

The increase of rate of mass transfer processes is a question of wide scientific interest. The development of chemical industry determined the search for new possibilities of intensifying the heat and mass transfer without having to increase the scale of apparatus.

The flow in thin films was found to be an efficient way to improve transfer processes. The advantages of this procedure are well known and a large number of researchers have devoted their studies to this type of flow [1] ... [9].

A particular attention was paid to the factors which are able to influence the film hydrodynamics, mass or heat transfer such as flow regime, rugosity, geometrical features, presence of surfactants, viscosity, etc.

However, in spite of the large number of papers in the field, the flow and mass transfer in thin films of nonnewtonian fluids are rather scarcely approached [10] .... [12]. As far as it is mentioned in the available literature, excepting for the A s t a r i t a's trial concerning the flow of suspensions, no other paper was found in literature.

The aim of the present paper was to answer to the following questions :

a) How does the solid phase influence the rate of mass transfer in thin films?

b) What fluid flow characteristics lead to higher values of individual mass transfer coefficient, k_L?

c) How does k_L vary, in the same sistem, with concentration, granulation and density of dispersed phase ?

d) How are located the experimental data within the general context of literature informations ?

2. Experimental

The absorption of carbon dioxide in water and ABS copolymer suspensions was investigated on the equipment depicted in Fig. 1.

Thr absorption column (*1...3*) is formed of two concentric pipes. The descending film flows on the external wall of the internal pipe ($\varphi = 30 \times 3$ mm, Ni—Cr-alloy steeal, $L = 2\,285$ mm). In the annular space between the external pipe (plexiglass, $\varphi - 60 \times 6$ mm) and the fluid film, the gas (carbon dioxide) flows in counter current. At the bottom the column is provided with a micrometric device allowing the column movement up and down. At the top, the column is provided with a distribution head which assures the formation of thin film on the internal pipe. The gap width is adjusted by

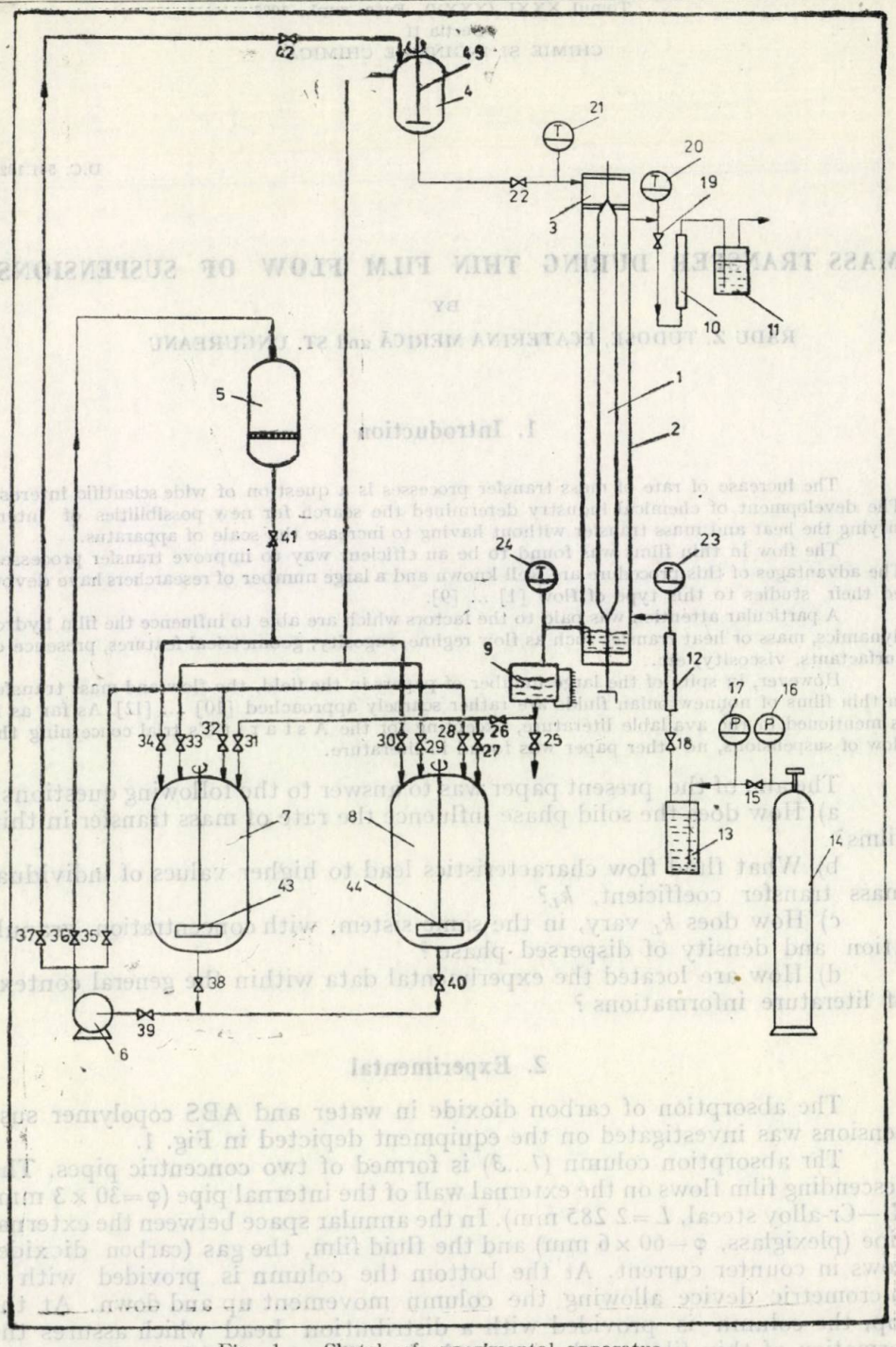

Fig. 1. — Sketch of experimental apparatus.

the internal tube displacement up and down. The liquid is taken from the supply tank with a pump and sent to the level vessel *45* from which enters the distribution head and the column. The two tanks work alternatively, one receives the liquid while from the other the column is feeded. Both tanks ($V = 300$ L) and the level vessel are provided with mixers for being able to maintain the particles in suspension.

The admission of carbon dioxide, in countercurrent, from a gas tube, was adjusted by means of two flowmeters, one for a coarse adjustement, the other for a fine one.

To prevent from water diffusion in gas, the latter was saturated by bubbling in a water vessel prior to the introduction in the column.

The flow rate at the exit was measured by timing the time required for the collection of a known volume of liquid.

The analysis for carbon dioxide was accomplished by precipitating the carbon dioxide as barium carbonate by use of a mixture of barium chloride and standard sodium hydroxide. The excess sodium hydroxide was then titrated with hydrochloric acid to a phenolpthalein end point.

The concentration of carbon dioxide in the liquid was calculated with the relation :

$$x = \frac{0.55(n_1 - n_1')T_1}{V}, \tag{1}$$

where : x denotes the concentration of carbon dioxide in liquid, [g/mL] ; n_1 — number of mL of standard NaOH solution introduced initially in sample; n_1' — number of mL of NaOH solution found in excess (determined titrimetrically) ; V — sample volume ; 0.55 — equivalent ratio.

Prior to each set of measurements a witness sample was taken (zeroth sample), the initial carbon dioxide content being thus determined.

The mass transfer coefficient in liquid phase, k_L, based on mean logarithmic driving force, was calculated, for the absorption of pure gas, at 1 atm pressure. In practical calculation the external surface of the internal pipe was assumed to be the mass transfer surface. Given the high purity of gas, the resistance of gaseous phase was neglected as well as the effect of water vapours, since the gas was previously saturated with liquid. A temperature multipoint recorder (4 points) was used (liquid and gas entrances and exits, respectively) and the physical constants used in calculations were corrected for the mean liquid temperature during the run.

The viscosity measurements for the suspensions (ABS copolymer, $0{,}12 < \varnothing < 0{,}15$ mm, 1, 2, 4 and 7% in weight) were taken on a concentric cylinder viscometer of Rheotest, DDR, type. The measurements were taken at there temperatures : 20°; 25° and 30°C. Where the readings at intermediate temperatures were not conclusive the data for 20° and 30°C were retained. Since the suspension behaviour was found to be of a Bingham plastic type the values of extrapolated viscosity were taken in calculations.

3. Results and Discussion

The experimental results obtained with water and the four suspensions are depicted in Figs. 2...6 as $Sh = f(Re)$ correlation.

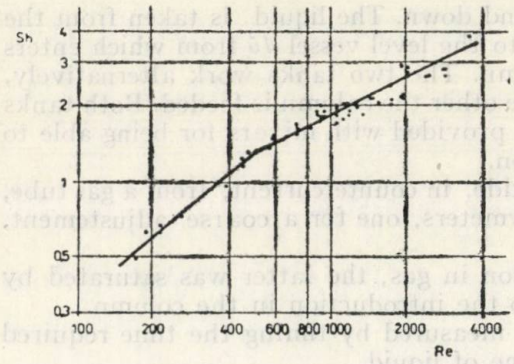

Fig. 2. — Correlation $Sh = f(Re)$ in case of water.

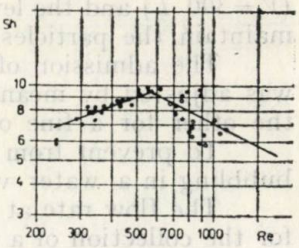

Fig. 3. — Correlation $Sh = f(Re)$ in case of ABS, 1% suspension.

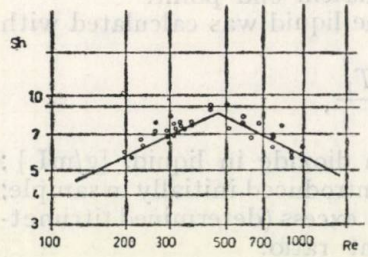

Fig. 4. — Correlation $Sh = f(Re)$ in case of ABS, 2% suspension.

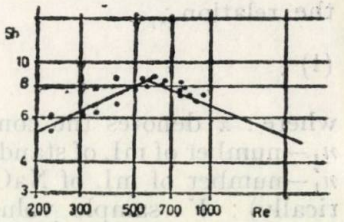

Fig. 5. — Correlation $Sh = f(Re)$ in case of ABS, 4% suspension.

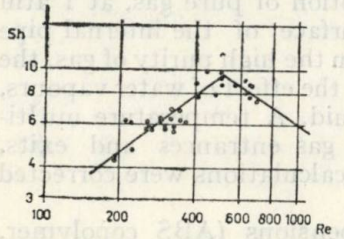

Fig. 6. — Correlation $Sh = f(Re)$ in case of ABS, 7% suspension.

As can be seen in Figs. 3...6 the introduction of solid phase strongly influences the mass transfer results. The increase of mass transfer rate up to a certain Re value is noticed in all cases, followed by a marked decrease above the critical value. The critical Re value was found to be of about 500. The difference from water is very clear.

The experimental data worked on a computer allowed to obtain the following correlations :

a) Water

$$(2)\qquad \begin{cases} Sh = 5.324 \times 10^{-3} Re^{0.89}, & (Re < 500), \\ Sh = 0.0872\, Re^{0.44}, & (Re > 500); \end{cases}$$

b) ABS, 1% suspension

$$(3)\qquad \begin{cases} Sh = 0.38\, Re^{0.15}, & (Re < 600), \\ Sh = 238\, Re^{-0.51}, & (Re > 600); \end{cases}$$

c) ABS, 2% suspension

$$(4)\qquad \begin{cases} Sh = 0.450\,Re^{0.48}, & (Re < 500), \\ Sh = 196\,Re^{-0.51}, & (Re > 500)\ ; \end{cases}$$

d) ABS, 4% suspension

$$(5)\qquad \begin{cases} Sh = 0.433\,Re^{0.47}, & (Re < 600), \\ Sh = 94.5\,Re^{-0.38}, & (Re > 600)\ ; \end{cases}$$

e) ABS, 7% suspension

$$(6)\qquad \begin{cases} Sh = 0.0848\,Re^{0.76}, & (Re < 600), \\ Sh = 6005\,Re^{-0.66}, & (Re > 600). \end{cases}$$

As seen in Figs. 5 and 6, the results for more concentrated suspensions, at higher Re values, are more dispersed. The results were generally reproducible excepting for Re values higher than 800 and larger ABS concentrations (above 7%).

Received, April 25, 1985

Polytechic Institute, Jassy,
Department of Chemical Engineering

REFERENCES

1. Emmert R.E., Pigford R.L., Chem. Eng. Process, **50** (2), 88 (1954).
2. Lamourelle P.A., Sandal C.O., Chem. Eng. Sci., 1035 (1972).
3. Blas E., Int. Chem. Eng., **19**, *2* (1972).
4. Koziol K., Broniarz L., Nowicka T., Int. Chem. Eng., **20**, *1*, 136 (1980).
5. Koziol K., Broniarz L., Int. Chem. Eng., **20**, *1*, 143 (1980).
6. Холпанов К.П., Малюсов В.А., Хаворонков М.М., Теор. осн. хим технол., **16**, *3*, 291 (1982).
7. Накоряков В.Е., Покусаев Б.Г., Алексеенко С.В., *Расчет тепломасообмена энергохимических процессах*. 1981, 23; C.A., **98**, 56298 u (1983).
8. Tudose R.Z., Zăinescu C., Sviecinski M., Mem. Secț., Șt., Acad. R.S.R., **3**, *1*, 215, 1980 (1981).
9. Ibănescu I., Tudose R.Z., Rev. chim., **23**, *2*, 114 (1972).
10. Gottifreddi J.C., Gonzo E.E., J. Non-Newtonian Fluid Mech., **10**, *3—4*, 357 (1982).
11. Astarita G., Ind. Eng. Chem. Fundls., 4, 236 (1965).
12. Mohr M.C.Jr, Williams C.M., A.I.Ch.E. Journal, **19**, *5*, 1047 (1973).

STUDIUL TRANSFERULUI DE MASĂ LA CURGEREA ÎN FILME SUBȚIRI A SUSPENSIILOR

(Rezumat)

A fost studiat transferul de masă la curgerea în filme subțiri la apă și patru suspensii în apă de copolimer ABS, 1, 2, 4 și 7% în greutate. S-a găsit că absorbția de CO_2 este puternic influențată de prezența fazei solide. Pînă la un anumit Re coeficientul de transfer în fază lichidă k_L, crește, după care scade brusc.

BULETINUL INSTITUTULUI POLITEHNIC DIN IAŞI
Tomul XXXI (XXXV), Fasc. supl., 1985
Secţia II
CHIMIE ŞI INGINERIE CHIMICĂ

SYNTHETIC FIBRE WORKS, IAŞI, a modern unit of advanced technology, much ahead in Romania chemical industry, produces and deliveries a wide range of polyester fibres and yarns as well as equipments and spare parts for chemical and textile industry as it follows:.

— Polyester staple fibre, cotton, wool and flax type, raw white, bright or dyed.
— Polyester textiles yarns.
— Polyester textiles twisted yarns for courtains and tissues.
— Polyester continuous filament drawn yarns for sewing thread.
— Polyester continuous filament textured yarns of different linear densities, twisted, bright or semidull, of round or profiled cross section, raw white or dyed suitable for knittings, tissues and cloths.

Colour card for dyed yarns includes about 100 shades classified in : light, medium and heavy shades.

Comfort, absorbency and easy care properties combined with stability and shape retention are essential qualities of the products marketed by **SYNTHETIC FIBRE WORKS, IAŞI.**

— Polyester industrial yarns (drawn, twisted, plyed) for different technical end-uses where its abrasion resistance, thermal stability and chemical proofing are highly appreciated.
— Polyester films (transparent or light dull) for electrotechnical end-uses.
— Besides its textile and chemical profile, **SYNTHETIC FIBRE WORKS, IAŞI,** is also a producer of equipments used in chemical and textile industries such as :

- precision conning machines on the basis of Schweiter licence ;
- drawing lines for polyester or polyamide fibres ;
- refrigeration plants ;
- cutting knives for tow to top converters and a host of other operations or special treatments.

The **SYNTHETIC FIBRE WORKS, IAŞI**, exports its products by :
ICE DANUBIANA, Serv. 71 Bucharest, telex 10073 (polyester yarns and fibres) ;
ICE CHIMIMPORTEXPORT, Serv. 7, Bucharest, telex 11184 (chemical products) ;
ICE INDUSTRIALEXPORT IMPORT, Serv. 42, Bucharest, telex 10052 (equipments and spare parts).

For any additional details please write directly to :

COMBINATUL DE FIBRE SINTETICE, IAŞI,

29 Ţuţora St., Code 6600

Telephone : 30020 ; Telex : 022251

CENTRALA INDUSTRIALĂ DE FIBRE CELULOZĂ ȘI HÎRTIE – BRĂILA –

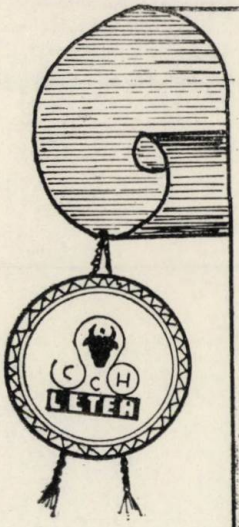

COMBINATUL DE CELULOZĂ ȘI HÎRTIE

L E T E A

B A C Ă U

PRODUCE:

- hîrtie de ziar
- hîrtie de scris si tiparit
- hîrtii ambalaj
- hîrtii speciale
- hîrtii subtiri
- hîrtii tigarete
- hîrtii absorbante pentru
- industria mobilei
- hîrtie igienică
- cartoane
- caiete școlare
- drojdie furajeră

CENTRALA INDUSTRIALĂ DE FIBRE CELULOZA ŞI HÎRTIE
– BRĂILA –

BULETINUL INSTITUTULUI POLITEHNIC DIN IAŞI
Tomul XXXI (XXXV), Fasc. supl., 1985
Secţia II
CHIMIE ŞI INGINERIE CHIMICĂ

CENTRALA INDUSTRIALĂ DE FIBRE, CELULOZĂ ŞI HÎRTIE BRĂILA

COMBINATUL DE FIBRE, CELULOZĂ ŞI HÎRTIE SUCEAVA

PRODUCE :

1. Celuloză sulfat naturală.
2. Hîrtie pentru saci, hîrtie ambalaj rezistentă, hîrtie extensibilă, hîrtie impregnată pentru filtre de aer, ulei, combustibil.
3. Fibre artificiale din vîscoză.
4. Fire mătase vîscoză.
5. Produse înnobilate : hîrtii gumate, hîrtii creponate, hîrtii acoperite cu parafină, hîrtii acoperite cu polietilenă, hîrtii bitumate, complexe anticorozive pentru ambalat piese metalice, diverse ţesături acoperite cu polietilenă, complexe suport abrazive, pînză cauşurată cu polietilenă pe hîrtie.
6. Saci şi pungi din hîrtie, confecţii din carton ondulat, confecţii din mucava, filtre auto şi industrie, sfoară din hîrtie.

CENTRALA INDUSTRIALĂ DE FIBRE, CELULOZĂ ŞI HÎRTIE BRĂILA

COMBINATUL DE FIBRE, CELULOZĂ ŞI HÎRTIE SUCEAVA

PRODUCE

1. Celuloză sulfat naturală

2. Hîrtie pentru tacî, hîrtie ambalaj ranforsată, hîrtie extensibilă, hîrtie impregnată pentru filtre de aer, ulei, combustibil.

3. Fibre artificiale din viscoză

4. Fire mătase viscoză.

5. Produse înnobilate : hîrtoi gumate, hîrtoi creponate, hîrtoi acoperite cu peralină, hîrtoi acoperite cu polietilenă, hîrtii bitumate, complexe autocolorizive pentru ambalat piese metalice, diverse texturi acoperite cu polietilenă, complexe suport adeziv, pînză cerată cu polietilenă pe hîrtie.

6. Saci şi pungi din hîrtie, conteci din carton ondulat, conteci din mucava, hîrtie autoadezivă, etuve din hîrtie.

BULETINUL INSTITUTULUI POLITEHNIC DIN IAŞI
Tomul XXXI (XXXV), Fasc. supl., 1985
Secţia II
CHIMIE ŞI INGINERIE CHIMICĂ

Combinatul de Fibre Sintetice, Săvineşti, produce şi livrează :

- **Fire şi fibre sintetice :**

— fibre acrilice Melană (R) ;
— fibre poliamidice Relon (R) ;
— fire poliamidice textile Relon (R) ;
— fire poliamidice covor Relontex (R) ;
— fire poliamidice tehnice şi cord Relon (R) ;
— corzi perii.

- **Produse chimice :**

— caprolactamă ;
— acid adipic ;
— tetracloretan ;
— clorură de cianuril ;
— dibenzildiizocianat DBDI ;
— polietilenglicoladipat PEGA ;
— granule poliamidice pentru mase plastice ;
— bare şi plăci poliamidice.

- **Utilaje şi piese de schimb pentru industria de fibre sintetice :**

— linii complete de fabricare a firelor şi fibrelor sintetice ;
— pompete de filare pentru fibre sintetice ;
— filiere pentru filare din topitură ;
— pompe de presiune pentru curăţiri de vase în industria chimică ;
— maşini de bobinat fire ;
— maşini de sculuit ;
— fuse pentru maşini textile ;
— maşini de tăiat fibre ;
— diverse piese de schimb din industria de fibre chimice.

Producător : Combinatul de Fibre Sintetice, Săvineşti — Piatra Neamţ
Telex 025221-222 ; telegraf C.F.S. Săvineşti

Exportatori :

— **Fire şi fibre sintetice : ICE Danubiana, Bucureşti,**
Spl. Independenţei 202 A
Telex 11489 ; PO BOX 3915 DANAZ

— **Produse chimice : ICE Chimimportexport, Bucureşti,**
Bd. Republicii 10
Telex 11184 ; PO BOX 1—74

— **Utilaje şi piese de schimb : ICE Industrialexport, Bucureşti,**
Str. Scaune 1—3
Telex 10052 ; PO BOX 768

BULETINUL INSTITUTULUI POLITEHNIC DIN IAŞI
Tomul XXXI (XXXV), Fasc. supl. 1985
Secţia II
CHIMIE ŞI INGINERIE CHIMICĂ

Combinatul de Fibre Sintetice, Săvineşti, produce şi livrează :

- Fire şi fibre sintetice :

— fibre acrilice Melană (R) ;
— fibre poliamidice Relon (R) ;
— fire poliamidice textile Relon (R) ;
— fire poliamidice covor Relontex (R) ;
— fire poliamidice tehnice şi cord Relon (R) ;
— corzi perii.

- Produse chimice :

— caprolactamă ;
— acid adipic ;
— tetracloretan ;
— elorură de cianuril ;
— dibenzildiizocianat DBDI ;
— polietilenglicoladipat PEGA ;
— granule poliamidice pentru mase plastice ;
— bare şi plăci poliamidice.

- Utilaje şi piese de schimb pentru industria de fibre sintetice :

— linii complete de fabricare a firelor şi fibrelor sintetice ;
— pompete de filare pentru fibre sintetice ;
— filiere pentru filare din topitură ;
— pompe de presiune pentru curăţiri de vase în industria chimică ;
— maşini de bobinat fire ;
— maşini de sculuit ;
— fuse pentru maşini textile ;
— maşini de tăiat fibre ;
— diverse piese de schimb din industria de fibre chimice.

Producător : Combinatul de Fibre Sintetice, Săvineşti — Piatra Neamţ
Telex 025221-222 ; telegraf C.F.S. Săvineşti

Exportatori :

— Fire şi fibre sintetice : ICE Danubiana, Bucureşti,
Spl. Independenţei 202 A
Telex 11489 ; PO BOX 3915 DANAZ

— Produse chimice : ICE Chimimportexport, Bucureşti,
Bd. Republicii 10
Telex 11184 ; PO BOX 1—74

— Utilaje şi piese de schimb : ICE Industrialexport, Bucureşti,
Str. Scaune 1—3
Telex 10062 ; PO BOX 768

BULETINUL INSTITUTULUI POLITEHNIC DIN IAŞI
Tomul XXXI (XXXV), Fasc. supl., 1985
Secţia II
CHIMIE ŞI INGINERIE CHIMICĂ

Synthetic Fibers Factory, Săvineşti, produces and delivres :

- **Synthetic Yarns and Fibers :**

— Melana (R) acrylic fibers ;
— Relon (R) polyamidic fibers ;
— Relon (R) polyamidic textile yarns ;
— Relontex (R) carpets polyamidic yarns ;
— Polyamidic technical yarns and Relon (R) cord ;
— Brush strings.

- **Chemical Products :**

— Caprolactam ;
— Adipic acid ;
— Tetrachlorethane ;
— Cyanuril chloride ;
— Dibenzyldiisocyanate DBDI ;
— Polyethyleneglycoladipate PEGA ;
— Polyamidic grains for plastic materials ;
— Polyamidic rods and plats.

- **Implements and Spare Parts for Synthetic Fibers Industry :**

— Full operation lines for producing synthetic yarns and fibres ;
— Spinning pumps for synthetic fibers ;
— Dies for melt spinning ;
— Pressure pumps for vessel cleaning in chemical industry ;
— Warp winding machines ;
— Shuttle sprindles ;
— Fiber-cutting machines ;
— Different spare parts for chemical fibers industry.

Producer : Combinatul de Fibre Sintetice Săvineşti, Piatra Neamţ,
Telex 025221-222 ; telegraph CFS Săvineşti.

Exporters :

— **Synthetic Yarns and Fibers : ICE Danubiana, Bucureşti,**
Spl. Independenţei 202 A
Telex 11489 ; PO BOX 3915 DANAZ

— **Chemical Products : ICE Chimimportexport, Bucureşti,**
Bd. Republicii 10
Telex 11184 ; PO BOX 1—74

— **Implements and Spare Parts : ICE Industrialexport, Bucureşti,**
Str. Scaune 1—3
Telex 10052 ; PO BOX 768

Synthetic Fibers Factory, Săvinești, produces and delivers :

- Synthetic Yarns and Fibers :

— Melana (R) acrylic fibers ;
— Relon (R) polyamidic fibers ;
— Relon (R) polyamidic textile yarns ;
— Relonyl (R) carpets polyamidic yarns ;
— Polyamidic technical yarns and Relon (R) cord ;
— Brush strings.

- Chemical Products :

— Caprolactam ;
— Adipic acid ;
— Tetrachloroethane ;
— Cyanuril chloride ;
— Dibenzyldisocyanate DIBDI ;
— Polyethyleneglycoladipate PEGA ;
— Polyamidic grains for plastic materials ;
— Polyamidic rods and plate.

- Implements and Spare Parts for Synthetic Fibers Industry :

— Full operation lines for producing synthetic yarns and fibres ;
— Spinning pumps for synthetic fibers ;
— Dies for melt spinning ;
— Pressure pumps for vessel cleaning in chemical industry ;
— Warp winding machines ;
— Shuttle spindles ;
— Fiber-cutting machines ;
— Different spare parts for chemical fibers industry.

Producer : Combinatul de Fibre Sintetice Săvinești, Piatra Neamț,
Telex 023221-222 ; telegraph CFS Săvinești.

Exporters :

— Synthetic Yarns and Fibers : ICE Danubiana, Bucureşti,
Spl. Independenţei 202 A
Telex 11489 ; PO BOX 3915 DANAZ

— Chemical Products : ICE Chimimportexport, Bucureşti,
Bd. Republicii 10
Telex 11184 ; PO BOX 1—74

— Implements and Spare Parts : ICE Industrialexport, Bucureşti,
Str. Sfaxului 1—3
Telex 10052 ; PO BOX 768

BULETINUL INSTITUTULUI POLITEHNIC DIN IAŞI
Tomul XXXI (XXXV), Fasc. supl., 1985
Secţia II
CHIMIE ŞI INGINERIE CHIMICĂ

L'Usine de Fibres Synthétiques, Săvineşti, produit et fournit :

- **Fils et fibres synthétiques :**

— fibres acryliques Melana (R) ;
— fibres polyamidiques Relon (R) ;
— fils textiles polyamidiques Relon (R) ;
— fils polyamidiques tapis Relontex (R) ;
— fils polyamidiques techniques et corde Relon (R).

- **Produits chimiques ;**

— caprolactame ;
— acide adipique ;
— éthane tétrachlorure ;
— chlorure de cyanurile ;
— dibenzylediisocyanate DBDI ;
— polyéthylèneglycoleadipate PEGA ;
— granules polyamidiques pour matériaux plastiques ;
— barres et plaques polyamidiques.

- **Outillages et pièces de réchange pour l'industrie des fibres synthétiques :**

— lignes technologiques pour la fabrication de fibres et fils synthétiques ;
— pompes de filage pour fibres synthétiques ;
— filières pour filage des mélanges coulées ;
— pompes à pression pour nétoyage de l'outillage de l'industrie chimique ;
— machines à bobiner ;
— brochettes de navette ;
— machines à trancher des fibres ;
— différentes pièces de réchange pour l'industrie des fibres chimiques.

Producteur : Combinatul de Fibre Sintetice, Săvineşti, Piatra Neamţ
Telex 025221-222 ; télégraphe C.F.S. Săvineşti

Exportateurs :

— **Fibres et fils synthétiques : ICE Danubiana, Bucureşti,**
Spl. Independenţei 202 A
Telex 11489 ; PO BOX 3915 DANAZ

— **Produits chimiques : ICE Chimimportexport, Bucureşti,**
Bd. Republicii 10
Telex 11184 ; PO BOX 1—74

— **Outillages et pièces de rechange : ICE Industrialexport, Bucureşti,**
Str. Scaune 1—3
Telex 10052 ; PO BOX 768

Coli tipo 9

Tiparul executat sub comanda nr. 125
la Întreprinderea poligrafică Iaşi,
str. 7 Noiembrie nr. 49

40822

F 1812/2
R
31. 1985.

BULETINUL INSTITUTULUI POLITEHNIC DIN IAȘI

BIBLIOTECA CENTRALĂ

Tomul XXXI (XXXV)

Fasc. supl.

Secția II

CHIMIE ȘI INGINERIE CHIMICĂ

1985

BULETINUL INSTITUTULUI POLITEHNIC DIN IAŞI

Tomul XXXI (XXXV)

Fasc. supl.

Secţia II

CHIMIE ŞI
INGINERIE CHIMICĂ

1985

1989

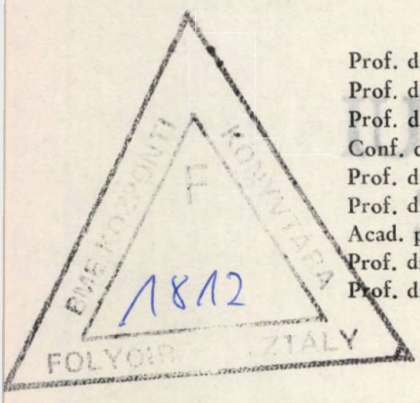

COLEGIUL DE REDACŢIE

Prof. dr. CAMELUŢA BELDIE (preşedinte)
Prof. dr. ing. ADRIAN RADU
Prof. dr. ing. M. GAFIŢANU
Conf. dr. ing. D. LIUŢE
Prof. dr. doc. D. MANGERON
Prof. dr. ing. GH. MAXIM
Acad. prof. dr. doc. CRISTOFOR SIMIONESCU
Prof. dr. doc. GH. CHIRIŢĂ
Prof. dr. doc. VALERIU BLIDARU

COMITETUL DE REDACŢIE
AL SECŢIEI
II. CHIMIE ŞI INGINERIE CHIMICĂ

Prof. dr. doc. RADU TUDOSE
Prof. dr. doc. ANGELA POPA
Conf. dr. ing. I. ROŞCA
Conf. dr. ing. SPIRIDON OPREA

REDACŢIA

Prof. dr. doc.
DUMITRU MANGERON
(redactor responsabil)
Prof. dr. ing. HUGO ROSMAN
(secretar)
Conf. dr. ing.
VICTOR BULACOVSCHI
(redactor)
ECATERINA IRIMIEA
(tehnoredactor)

BULETINUL INSTITUTULUI POLITEHNIC DIN IAŞI
BULLETIN OF THE POLYTECHNIC INSTITUTE OF JASSY
ИЗВЕСТИЯ ЯССКОГО ПОЛИТЕХНИЧЕСКОГО ИНСТИТУТА
Tom XXXI (XXXV), Fasc. supl. 1985

Secţia II

CHIMIE ŞI INGINERIE CHIMICĂ

SUMAR

Pag.

AL. DUCA, M. GĂBURICI, AL. CECAL şi M. SURPĂŢEANU, Studiul unor complecşi aminici ai cobaltului prin voltametrie anodică (engl., rez. rom.) 9

N. CALU, A. BOLD, O. VICOL, E. SAVIUC, L. BOSNEA, I. BERDAN şi I. SANDU, Metode de caracterizare fizico-chimică a coloranţilor în amestec (franc., rez. rom.) 15

C. BELDIE, A. ONU, N. AELENEI, GH. NEMŢOI, AL. RADOVICI şi AL. SAVIN, Relaţia vîscozitate—masă moleculară pentru poli(etilentereftalat) modificat cu 1,2-propandiol (engl., rez. rom.) 23

I. ROŞCA, E. ŞTEFANCU şi M. PALAMARU, Compuşi de coordinaţie ai La (III) şi Ce (IV) cu acidul dibutilfosfinic (engl., rez. rom.) 29

E. POPOVICI, M. CRUCEANU, A. POPA, A. VASILE şi M. ALEXANDROAEI, Zeoliţi sintetici pentru condiţionarea detergenţilor (I) (engl., rez. rom.) . . 35

AL. SZÉP, L. IFRIM, C. LEONTE şi C. CALISTRU, Studiul procesului de descompunere a carbonatului de calciu cu clorură de amoniu solidă (engl., rez. rom.) 41

M. PETROVANU, GH. SURPĂŢEANU, M. CONSTANTINESCU şi A. LABLACHE-COMBIER, Izomerii *E* şi *Z* ai ilurilor de 1.2-4H triazol (franc., rez. rom.) 47

GH. MIHĂILĂ, C. CIUGUREANU, N. BÎLBĂ, P. ONU, C. LUCA şi N. NAUM, Esteri şi eteri ai amidonului cu proprietăţi aglutinate (engl., rez. rom.) . . . 53

C. VASILIU-OPREA, M. POPA, AL. CONSTANTINESCU şi A. IOANID, Caracterul treptiform al procesului de rupere a polimerilor în condiţiile fluajului la tracţiune (germ., rez. rom.) 59

N. ASANDEI, M. NICU, M. RUSU, S. PETROVAN, V. NICU şi M. LUNGU, Copolimeri (VIII) (engl., rez. rom.) 65

N. FOCA, V. GORDUZA şi L. WAGNER, Complecşi ai 5-amino-benzimidazolonei-2 cu unii cationi ai metalelor tranziţionale (engl., rez. rom.) . . . 73

I.I. NEGULESCU, A.A. POPA şi C. MIHĂILESCU, Polimerizarea cationică a 4-vinil-1-ciclohexenei (engl., rez. rom.) 79

C. VASILE, FL. POPESCU, O. PETREUȘ, M. SABLIOVSCHI, A. AIRINEI și I. AGHERGHINEI, Influența ignifuganților asupra comportării poliolefinelor la temperaturi ridicate (engl., rez. rom.) 87

I. DIACONU și C. CHELARU, Sinteza și proprietățile unor noi copolimeri acrilici (I) (engl., rez. rom.) 91

S. OPREA, E. DUMITRIU și V. HULEA, Reactivitatea monomerilor acrilici (XII) (engl., rez. rom.) 101

M. DUMITRIU, M. PĂSTRĂVANU și T. LIXANDRU, Sinteza și caracterizarea unor noi poliazometine (II) (engl., rez. rom.) 105

V. BULACOVSCHI, M. GROVU-IVĂNOIU, M. DĂRÂNGĂ și S. DUMITRESCU, Polimerizarea 3-metilpent-1-in 3-olului catalizată de $PdCl_2$ și complecșii acesteia (engl., rez. rom.) 111

S. IOAN, C. SAVA și B.C. SIMIONESCU, Proprietățile soluțiilor de polimeri cu mase moleculare foarte mari (9) (engl., rez. rom.) 117

M. GRIGORAȘ, G. ONOFREI, E. BÎCU și I. RABIA, Tranziții conformaționale în tribloccopolimeri de tip *ABA* (franc., rez. rom.) 123

V. BĂRBOIU, G.E. GRIGORIU, E. RUSU, T. MARCU și E. BURUIANĂ, Proces de fotoreticulare în filme solide (I) (engl., rez. rom.) 129

R.Z. TUDOSE, E. MERICĂ și ȘT. UNGUREANU, Studiul transferului de masă la curgerea în filme subțiri a suspensiilor (engl., rez. rom.) 135

BULETINUL INSTITUTULUI POLITEHNIC DIN IAŞI
BULLETIN OF THE POLYTECHNIC INSTITUTE OF JASSY
ИЗВЕСТИЯ ЯССКОГО ПОЛИТЕХНИЧЕСКОГО ИНСТИТУТА

Том XXXI (XXXV), Supl. Fasc. 1985

Section II

CHEMISTRY and CHEMICAL ENGINEERING

CONTENTS

Pp.

AL. DUCA, M. GĂBURICI, AL. CECAL and M. SURPĂŢEANU, The Study of some Complex Amines of Cobalt by Anodic Stripping Voltammetry (English, Romanian summary) 9

N. CALU, A. BOLD, O. VICOL, E. SAVIUC, L. BOSNEA, I. BERDAN et I. SANDU, Méthodes pour la caractérisation physico-chimique des mélanges de colorants (French, Romanian summary) 15

C. BELDIE, A. ONU, N. AELENEI, GH. NEMŢOI, AL. RADOVICI and AL. SAVIN, Viscosity—Molecular Weight Relationship for Poly(ethyleneterephtalate) Modified with 1,2-Propanediol (English, Romanian summary) . . 23

I. ROŞCA, E. ŞTEFANCU and M. PALAMARU, Complexes of La (III) and Ce (IV) with Dibutylphosphinic Acid (English, Romanian summary) 29

E. POPOVICI, M. CRUCEANU, A. POPA, A. VASILE and M. ALEXANDROAEI, Synthetic Zeolites for Detergents Conditioning (I) (English, Romanian summary) 35

AL. SZÉP, L. IFRIM, C. LEONTE and C. CALISTRU, Study of the Calcium Carbonate Decomposition Process with Solid Ammonium Chloride (English, Romanian summary) 41

M. PETROVANU, GH. SURPĂŢEANU, M. CONSTANTINESCU et A. LABLACHE COMBIER, Isomères *E* et *Z* d'ylures de 1,2-4H triazolum (French, Romanian summary) 47

GH. MIHĂILĂ, C. CIUGUREANU, N. BÎLBĂ, P. ONU, C. LUCA and N. NAUM, Starch Esters and Ethers as Thickeners in Textile Printing (English, Romanian summary) 53

C. VASILIU-OPREA, M. POPA, AL. CONSTANTINESCU und A. IOANID, Der stufenweise Charakter des Bruchprozesses bei Polymeren durch Zugkraft unter Kriechbedingungen (German, Romanian summary) 59

N. ASANDEI, M. NICU, M. RUSU, S. PETROVAN, V. NICU and M. LUNGU, Copolymers (VIII) (English, Romanian, summary) 65

N. FOCA, V. GORDUZA and L. WAGNER, Complex Compounds of 5-Aminobenzimidazolone-2 with certain Cations of Transitional Metals (English, Romanian summary) 73

I.I. NEGULESCU, A.A. POPA and C. MIHĂILESCU, Cationic Polymerization of 4-Vinil-1-cyclohexene (English, Romanian summary) 79

I. DIACONU and C. CHELARU, Synthesis and Properties of certain New Acrylic Copolymers (I) (English, Romanian summary) 87

C. VASILE, FL. POPESCU, O. PETREUȘ, M. SABLIOVSCHI, A. AIRINEI and I. AGHERGHINEI, Influence of Flame-retardants on the Behaviour of Polyolefines at high Temperatures (English, Romanian summary) . . 91

S. OPREA, E. DUMITRIU and V. HULEA, Reactivity of Acrylic Monomers (XII) (English, Romanian summary) 101

M. DUMITRIU, M. PĂSTRĂVANU and T. LIXANDRU, Synthesis and Properties of new Polyazomethines (II) (English, Romanian summary) 105

V. BULACOVSCHI, M. GROVU-IVĂNOIU, M. DĂRÂNGĂ and S. DUMITRESCU, Polymerization of 3-Methylpent-1-yn-3-ol by $PdCl_2$ and its Tryphenylphosphine Complexes as Catalysts (English, Romanian summary) 111

S. IOAN, C. SAVA and B.C. SIMIONESCU, Solution Properties of Ultrahigh Molecular Weight Polymers (9) (English, Romanian summary) 117

M. GRIGORAȘ, G. ONOFREI, E. BÎCU et I. RABIA, Transitions Conformationnelles des tribloccopolymères du type *ABA* (French, Romanian summary) 123

V. BĂRBOIU, G.E. GRIGORIU, E. RUSU, T. MARCU and E. BURUIANĂ, Photocrosslinking Processes in Solid Films (I) (English, Romanian summary) 129

R.Z. TUDOSE, E. MERICĂ and ȘT. UNGUREANU, Mass Transfer during Thin Film Flow of Suspensions (English, Romanian summary) 135

BULETINUL INSTITUTULUI POLITEHNIC DIN IAŞI
BULLETIN OF THE POLYTECHNIC INSTITUTE OF JASSY
ИЗВЕСТИЯ ЯССКОГО ПОЛИТЕХНИЧЕСКОГО ИНСТИТУТА
Том XXXI (XXXV), Доп. вып. 1985

Секция II

ХИМИЯ И ХИМИЧЕСКАЯ ПРОМЫШЛЕНОСТЬ

СОДЕРЖАНИЕ

Стр.

АЛ. ДУКА, М. ГЭБУРИЧ, АЛ. ЧЕКАЛ и М. СУРПЭЦЯНИУ, Поведение некоторых комплексных амин кобальта методом инверсионной вольтаметрии (англ., рез. рум.) 9

Н. КАЛУ, А. БОЛД, О. ВИКОЛ, Е. САВИУК, Л. БОСНЯ, И. БЕРДАН и И. САНДУ, Методы физико-химического характеризования смешаных красителей (франц., рез. рум.) 15

К. БЕЛДИЕ. А. ОНУ, Н. АЕЛЕНЕЙ, Г. НЕМЦОЙ, АЛ. РАДОВИЧ и АЛ. САВИИ, Отношение вязкость—молекулярную массу для модифицированного поли(этилентерефталала) 1, 2-пропандиолом (англ., рез. рум.) 23

И. РОШКА, Е. ШТЕФАНКУ и М. ПАЛАМАРУ, Координационные La (III) и Ce (IV) дибутилфосфиновой кислотой (англ., рез. рум.) 29

Е. ПОПОВИЧ, М. КРУЧЯНУ, А. ПОПА, А. ВАСИЛЕ и М. АЛЕКСАНДРОАЕЙ, Синтетический цеолиты для моющес вещество обусловленные (I) (англ., рез. рум.) 35

АЛ. СЕП, Л. ИФРИМ, К. ЛЕОНТЕ и К. КАЛИСТРУ, Исследование процесса разложения карбоната калция с хлористым аммонием (англ., рез. рум.) 41

М. ПЕТРОВАНУ, Г. СУРПЭЦЯНУ, М. КОНСТАНТИНЕСКУ и А. Лаблаш-КОМБИЕ, Изомеры *E* и *Z* 1-2-4Н триазол илуридов (франц., рез. рум.) 47

Г. МИХЭИЛЭ, К. ЧУГУРЯНУ, Н. БЫЛБЭ, П. ОНУ, К. ЛУКА и Н. НАУМ, Эстеры и эфиры крахмала сгустители в текстильной набивке (англ., рез. рум.) 53

К. ВАСИЛИУ-ОПРЯ, М. ПОПА. АЛ. КОНСТАНТИНЕСКУ и А. ИОАНИД. Ступенчатный характер преломления полимеров в условиях растяжения (нем., рез. рум.) 59

Н. АСАНДЕЙ, М. ИНКУ, М. РУСУ, С. ПЕТРОВАН, В. НИКУ и М. ЛУНГУ, Сополимеры (VIII) (англ., рез. рум.) 65

Н. ФОКА, В. ГОРДУЗА и Л. ВАГНЕР, Комплексы 5-амино бензимидазолоны-2 с катионов переходных металлов (англ. рез. рум.) . . . 73

И.И. НЕГУЛЕСКУ, А.А. ПОПА и К. МИХЭИЛЕСКУ, Катионная полимеризация 4-винил-1-циклогексана (англ., рез. рум.) 79
И. ДИАКОНУ и К. КЕЛАРУ, Синтезис и свойства новых акриловых сополимеров (I) (анлг., рез. рум.) 87
К. ВАСИЛЕ, ФЛ. ПОПЕСКУ, О. ПЕТРЕУШ. М. САБЛИОВСКИЙ, А. АИРИНЕЙ и И. АГЕРГИНЕЙ, Влияние затушителей на свойствах полиолефинов в переделах высоких температур (англ. рез. рум.) 91
С. ОПРЯ, Е. ДУМИТРИУ и В НУЛЯ, Реактивность акриловых мономеров (XII) (англ., рез. рум.) 101
М. ДУМИТРИУ, М. ПЭСТРЭВАНУ и Т. ЛИКСАНДРУ, Синтез и характеризование полиазометин (II) (англ., рез. рум.) 105
В. БУЛАКОВСКИЙ, М. ГРОВУ-ИВЭНОЮ, М. ДЭРЫНГЭ, С. ДУМИТРЕСКУ, Полимеризация 3-метилпент-1-ин-3-ола в присуствии $PdCl_2$ и его комплексов с трифенилфосфином (англ., рез. рум.) . 111
С. ИОАН, К. САВА и Б. К. СИМИОНЕСКУ, Свойства растворов полимеров с очень болшие молекулярные веса (9) (англ., рез. рум.) . . 117
М. ГРИГОРАШ, Г. ОНОФРЕЙ, Е. БЫКУ и И. РАБИА, Конформационные переходы в триблоксополимеры типа *ABA* (франц., рез рум.) 123
В. БЭРБОЙ, Г.Е. ГРИГОРИУ, Е. РУСУ, Т. МАРКУ и Е. БУРУИАНЭ, Фотостивающие процессы в твердых плёнкак (I) (англ., рез. рум.) 129
Р.З. ТУДОСЕ, Е. МЕРИКЭ и ШТ. УНГУРЯНУ, Исследование масс передачи в течение суспензий в тонких фильмах (англ., рез. рум.) 135

BULETINUL INSTITUTULUI POLITEHNIC DIN IAȘI
Tomul XXXI (XXXV), Fasc. supl., 1985
Secția II
CHIMIE ȘI INGINERIE CHIMICĂ

D.C. 546.73 ; 537.741.3

THE STUDY OF SOME COMPLEX AMINES OF COBALT BY ANODIC STRIPPING VOLTAMMETRY

BY

AL. DUCA, MARIA GĂBURICI, AL. CECAL and MIOARA SURPĂȚEANU

1. Introduction

Anodic stripping voltammetric technique has been little used for the determination of low contents of cobalt, firstly, because the anodic stripping peaks are not well reproducible and secondly, because incomplet data are reported in literature as regards the products obtained by cobalt reduction on mercury.

The investigation of the mechanism and kinetics of Co (II) reduction is rather difficult due to the low solubility of this metal in mercury. Similar to all metals having low solubility in mercury, cobalt has the tendency to form mercuric compounds [1] :

$$Co^{2+} + 2e^- \rightleftharpoons Co(Hg),\ Co(Hg) \rightarrow CoHg_x,\ CoHg_x \rightarrow Co(Hg) \rightarrow Co_2Hg_x.$$

The first reaction is reversible, the latest two wich lead to binary or higher order compounds are not reversible.

Ivanov and Yofa [2] have indicated that dispersed cobalt is formed on mercury electrode, the process being dependent on voltage.

Perone and Gutknecht [3] studied the electroreduction of Co (II) in thiocyanate solutions and suggested the amalgamation of reduced cobalt at pre-electrolysis voltage of — 1,45 V.

Janiszewska and Galus [4] have been found that the reduction of Co (II) on hanging mercury drop electrodes with initially deposited metallic cobalt proceeds faster than on pure mercury.

This paper deals with the influence of experimental parameters on voltammetric behaviour of low amounts of cobalt, as well as with the $[Co(NH_3)_6]^{3+}$, $[Co(en)_3]^{3+}$ (en-ethylene diamine) complexes. Ammonia buffer, Na_2SO_4, KSCN and NH_4SCN were employed as supporting electrolytes.

2. Experimental

The experiments were carried out using a mercury film stationary electrode, obtained by electrolytic deposition from a solution of $Hg(NO_3)_2$ [5].

The possibility of reproducing of the same surface depends on the obtaining of homogeneous mercury thin films. Since the width of the anodic curves depends on the thickness of the mercury film, it must be rigorously standardised in order to get some sharp and easy separable peaks. All potential measurements have been made using a saturated calomel electrode. The recording of anodic stripping curves has been carried out on the LP-60 and OH-102 polarographs. The solutions were prepared using tridistilled water, carrying out a rigorous control of supporting electrolytes.

3. Results and Discussion

3.1. The Behaviour of Co^{2+}

In order to establish the optimum conditions for the determination of low contents of cobalt, the influence of voltage, preelectrolysis time, nature and concentration of supporting electrolyte have been investigated.

The optimum voltage according to experimental data is of -1.2 V (Fig. 1). At this pre-electrolysis voltage the dependence of the anodic stripping peak on Co^{2+} concentration in solution has been studied. In Fig. 2, etalonated curves for Co^{2+} in the concentration range of 5×10^{-8} to 10^{-6} M in several supporting electrolytes are represented.

For concentrations higher than 10^{-5} M, even for low pre-electrolysis times, the anodic wave is de-doubled.

There is a weak difference as regards the behaviour of Co^{2+} in both KSCN and NH_4SCN solutions 0.1 M as supporting electrolytes. The disadvantage of the latter consists in fact that it pemits the degradation of the electrode surface in a short time. This fact was established experimentally, using the same electrode for several series of determinations, without its surface area regeneration. Between experiments, the electrode was kept in tridistilled water.

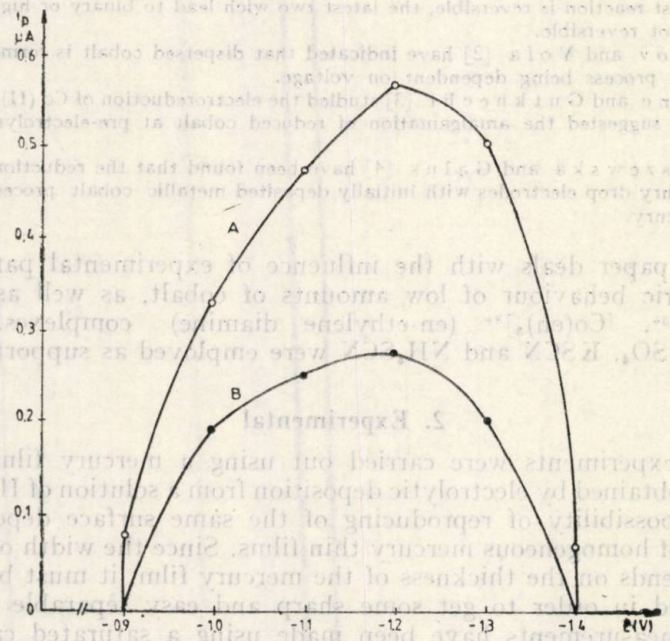

Fig. 1. — Influence of the pre-electrolysis potential over the anodic stripping peak height of Co^{2+} ($t_e=3$ min ; supporting electrolyte : KSCN 0.1 M ; $A-c=5\times10^{-7}$ M ; $B-c=2.5\times10^{-7}$ M.

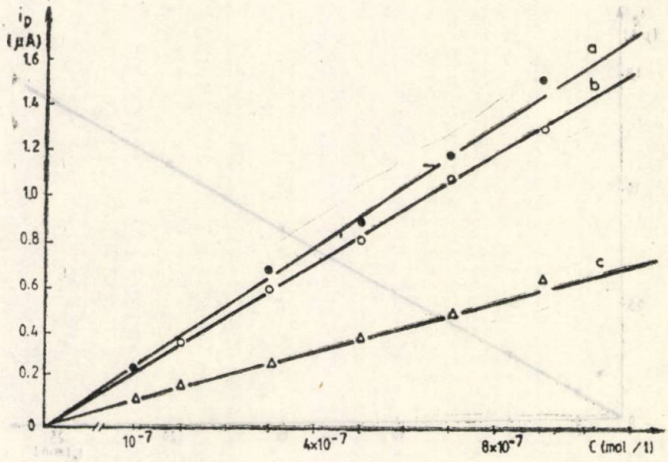

Fig. 2. — The calibration curves for determination of Co^{2+} in the concentration range $10^{-7}...10^{-6}$ M (*a* — KSCN 0.1 M ; *b* — NH_4SCN 0.1 M ; *c* — $NH_4Cl + NH_4OH$ 0.1 M ; $E_e = -1.2$ V, $t = 2$ min.).

The verification of the electrode surface area reproductibility was proved in the same solution for several days, as it can be seen in Table 1.

Table 1

The Reproductibility of the Electrode Surface Area against the Nature of the Supporting Electrolyte

Working time	Anodic stripping peak, *h*, [mm]		
	KSCN 0.1 M	NH_4SCN 0.1 M	Ammonia buffer
Fresh surface	41.5	39.2	24.0
5 hours	41.5	30.4	24.0
2 days	41.3	0	23.8
5 days	40.5	0	21.0

Another parameter that influences the anodic stripping peaks height of cobalt is the pre-electrolysis time. As it comes out from Fig. 3, as the pre-electrolysis time increases, the anodic stripping peak height increases. For pre-electrolysis times superior to 10 min. and for concentrations higher than 10^{-6} M, the anodic curves get out of shape.

The kinetics of the electrolytical deposition of Co^{60} from solutions of different concentrations on the mercury film electrode was investigated (Fig. 4).

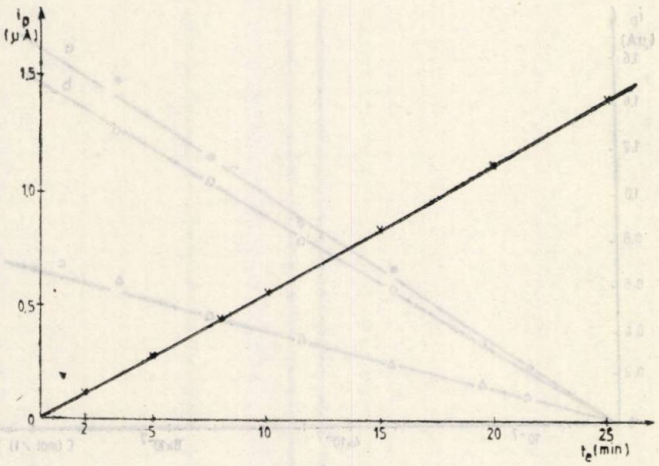

Fig. 3. — Influence of the pre-electrolysis time on the anodic stripping peak height of Co^{2+}, $C = 10^{-7}$ M, supporting electrolyte : KSCN 0.1 M.

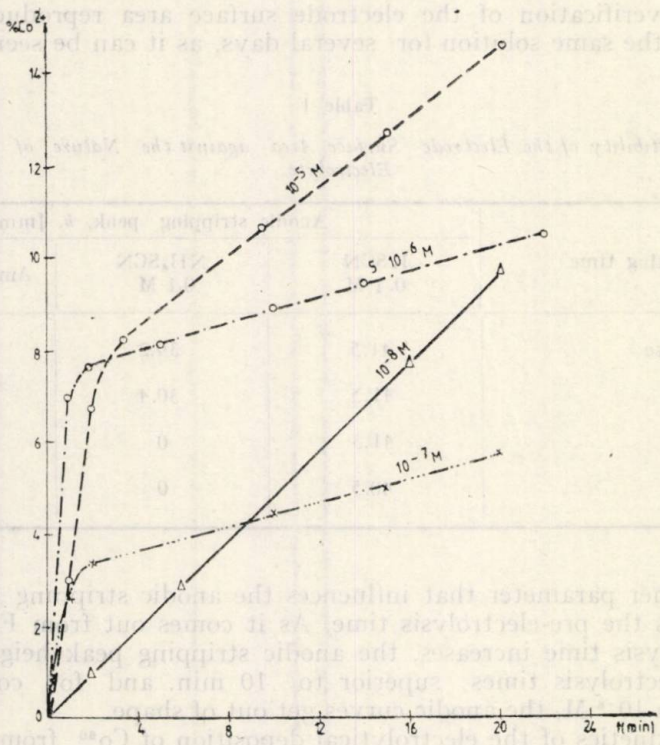

Fig. 4. — The kinetics of the electrolytical deposition of Co^{60} from the KSCN 0.1 M solution.

In order to reveal the nuclear radiations emited by Co^{60} in analysed samples, a scintilation sound with NaI (Tl) crystal connected to a NK-150 monochannel analyser apparatus was employed.

3.2. The Behaviour of $[Co(en)_3]^{3+}$

This complex has been studied in the same supporting electrolytes (KSCN, NH_4SCN) and ammonia buffer, under different concentrations. The nature of supporting electrolyte influences the potential corresponding to the maximum anodic current, as it can be seen in Table 2. This fact is of great importance, because in the case of coexistence of other foreign ions wich are reduced at potentials, other than that of complex, the basis solution allows to obtain the distinct anodic curves.

Table 2

The Potentials Corresponding to the Maximum Anodic Current against the Nature of Supporting Electrolytes Employed for Determination of $[Co(en)_3]^{3+}$

Supporting electrolyte	KSCN 0.5 M	NH_4SCN 0.5 M	Ammonia buffer
E_{an}, [V]	−0.35	−0.41	−0.42

For high concentrations of supporting electrolytes, the anodic peaks are diminished because the increasing of solution viscosity modifies the value of the diffusion coefficient and on the other hand, due to the adsorptions of ions on electrode surface take place under these conditions. Referring to the pre-electrolysis time, the linearity is not maintained for long times, when on the electrode is deposited a relatively more quantity of metal.

The optimum pre-electrolysis voltage is −1.3 V.

3.3. The Behaviour of $[Co(NH_3)_6]^3$

For this complex, the anodic peak depends on the nature of the supporting electrolyte, as observed from Table 3.

In the KSCN 0.1 M solution, the optimum pre-electrolysis voltage is −1.1 V ; for more negative potentials the anodic curves get out of shape.

Table 3

The Potentials Corresponding to the Maximum Anodic Current against the Nature of Supporting Electrolyte for Determination of $[Co(NH_3)_6]^{3+}$

Supporting electrolyte	KSCN 0.1 M	NH_4SCN 0.1 M	Ammonia buffer	Na_2SO_4 0.1 M
E_{an}, [V]	−0.42	−0.41	−0.46	−0.49

If Na_2SO_4 0.1 M solution is employed as supporting electrolyte, the optimum pre-electrolysis-potential is -1.5 V.

In Fig. 5 etalonated curves for $[Co(NH_3)_6]^{3+}$ in several supporting electrolytes are represented.

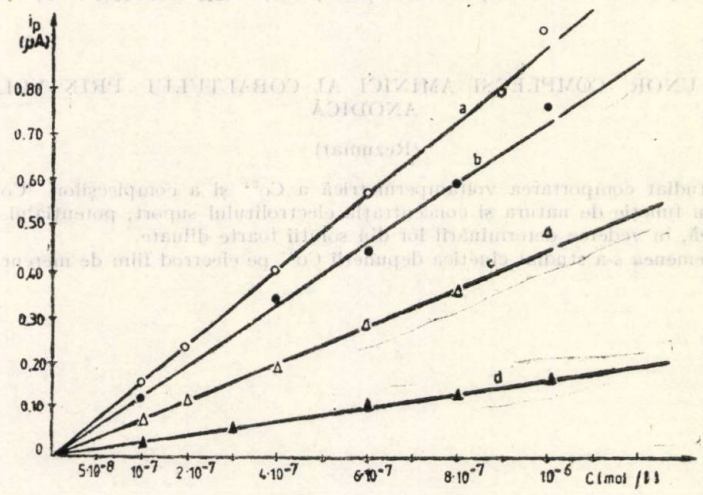

Fig. 5. — The calibration curves for determination of $[Co(NH_3)_6]^{3+}$ in the concentration range of $5\times10^{-8}...10^{-6}$ M in the following electrolytes: a — KSCN 0.1 M($E_e=-1.1$ V); b — NH_4Cl+NH_4OH 0.1 M($E_e=-1.2$ V); c — NH_4SCN 0.1 M($E_e=-1.1$ V); d — Na_2SO_4 0.1 M($E_e=-1.5$ V); $t_e=5$ min.

Although the sensitivity of determinations in Na_2SO_4 0.1 M solution is much smaller as compared to other employed electrolytes, Na_2SO_4 exhibits the advantage that the anodic curves are well defined with peaks easy to be estimated.

4. Conclusions

From the obtained results, the following conclusions can be drown:

1. Low amounts of both free and complexed cobalt can be selectively determined in the chosen concentration range on mercury film electrode.

2. In order to get a high sensitivity of the method, the optimum experimental parameters, wich alow to obtain well shaped anodic curves, have been established.

3. As regards the shape of the anodic curves obtained under the same concentration, the supporting electrolyte and other parameters being maintained constant, the differences can be explained on the basis of the different stabilities of the investigated complexes.

Received, March 18, 1985

Polytechnic Institute, Jassy,
Department of Inorganic and Analytical Chemistry and Technology

REFERENCES

1. Neeb R., *Polarographie und Voltammetrie.* Akad.-Verlag, Berlin, 1969, 139.
2. Иванов В. Ф. Иофа З. А., ДАН СССР, **140**, 1368 (3961).
3. Perone S.P., Gutknecht W.F., Anal. Chem., **39**, 892 (1967).
4. Janiszewska L., Gallus Z., Chemia Analityczna, **17**, 691 (1972).
5. Duca Al., Găburici M., Bul Inst. polit., Iaşi, **XXIII** (**XXVII**), *1—2*, s. II, 13 (1977).

STUDIUL UNOR COMPLECŞI AMINICI AI COBALTULUI PRIN VOLTAMETRIE ANODICĂ

(Rezumat)

S-a studiat comportarea voltampermetrică a Co^{2+} şi a complecşilor $[Co(NH_3)_6]^{3+}$ şi $[Co(en)_3]^{3+}$ în funcţie de natura şi concentraţia electrolitului suport, potenţialul şi timpul de pre-electroliză, în vederea determinării lor din soluţii foarte diluate.

De asemenea s-a studiat cinetica depunerii Co^{2+} pe electrod film de mercur.

BULETINUL INSTITUTULUI POLITEHNIC DIN IAŞI
Tomul XXXI (XXXV), Fasc. supl., 1985
Secţia III
CHIMIE ŞI INGINERIE CHIMICĂ

C.D. 667.21

MÉTHODES POUR LA CARACTÉRISATION PHYSICO-CHIMIQUE DES MÉLANGES DE COLORANTS

PAR

N. CALU, ANIŞOARA BOLD, OLGA VICOL, EUGENIA SAVIUC, LUCIA BOSNEA, I. BERDAN et I. SANDU

1. Introduction

D'une manière générale, l'état des mélanges de colorants, avec les composants auxiliaires ainsi que leur action dans le processus de teinture pose de nombreux problèmes d'interactions physiques et chimiques, de systèmes disperses, de thermodynamique et de cinétique.

Tout d'abord, les colorants, grâce a leurs groupements polaires, actifs (chromophores, auxochrômes, ionisables—solubilisants) mais aussi par la partie hydrophobe des molécules, conduisent à des interactions entre eux avec la formation de complexes H, complexes moléculaires, ions, polymères, etc. [1].

Par exemple, les complexes H se forment par l'établissement des liaisons d'hydrogène entre les molécules des colorants :

$$\begin{array}{c} R-H+R-H \rightleftarrows (R-H) \\ \qquad\qquad\qquad\quad \downarrow\uparrow RH \\ \qquad\qquad\qquad\quad (R-H)_2 \text{ etc.,} \end{array} \tag{1}$$

$$(R-H)_n + S_{\text{excès}} \rightleftharpoons nR-H.S\ ;\ S-\text{solvant.} \tag{2}$$

Les complexes moléculaires impliquent des liaisons de type donneur—accepteur :

$$R+R' \rightleftharpoons R \leftarrow R', \tag{3}$$

ou

$$R \leftarrow R' + S_{\text{excès}} \rightleftharpoons R \leftarrow S + R'. \tag{4}$$

Les équilibres ci-dessus sont considérablement influencés par l'excès de solvant, S, le pH et la concentration de la solution, etc.

Dans de tels équilibres, parmi les produits de réaction, ceux formés à base de liaisons plus fortes seront dominants.

D'autre part, le processus de teinture, réversible du point de vue thermodynamique, implique une série de phénomènes tels que la diffusion, le potentiel d'interface, l'échange ionique, les interactions physico-chimiques colorant—fibre etc. Les interactions colorant—fibre peuvent être de différents types : v a n d e r W a a l s, liaisons de hydrogène, etc. Quelquefois il arrive que ces interactions soient plus fortes en se manifestant dans le cadre des liaisons ioniques ou covalentes. Par conséquant les associations résultées à la suite des réactions (1)...(4) dépendent de la nature des interactions colorant—fibre et peuvent devenir transitoires dans le processus de teinture. Les colorants peuvent se fixer sur la fibre au niveau moléculaire, comme particules colloïdales, etc.

De toute manière, les associations des colorants ainsi que la charge électrostatique des colorants-ions et de la fibre — de même signe — diminuent la vitesse de teinture.

Évidemment, le problème de l'état des colorants et leur action dans le processus de teinture, présentent un intérêt particulier, surtout dans la perspective de l'assimilation de nouveaux colorants et fibres.

Dans une série de travaux antérieurs nous avons étudié quelques colorants se trouvant dans des mélanges, le dosage de ceux-ci, etc. [2] ... [4]. En poursuivant nos recherches, dans cette Note on présente de nouvelles données qui définissent les techniques de séparation et caractérisation physico-chimique des colorants préparés pour la teinture.

2. Partie expérimentale

Les déterminations ont été effectuées sur différents mélanges industriels de colorants (Tableau 1).

Tableau 1

Mélanges industriels des colorants étudiés

No.	Dénomination technique
1	Rouge de Dispersion *RR*
2	Jaune de Dispersion *G*
3	Bleu Marine de Dispersion *RE*
4	Palanyle Scharlach *RR*
5	Palanyle Violet 3 *B*
6	Cottestren Scharlach *G*
7	Cottestren Violett 3*B*
8	Cottestren Blau *SBC*
9	Indantren Brillanviolett 3*B*

Tableau 2

Les valeurs ND et NA de certains solvants [5], [6]

No.	Solvant	ND	NA
1	Benzène	0,1	8,2
2	Acétone	17,0	12,5
3	Diméthylesulfoxyde	29,8	19,3
4	Eau	33,0	54,8

Pour dissolution, les suspensions aqueuses des mélanges de colorants ont été repris par du diméthylesulfoxyde (DMSO). Les solutions ainsi obtenues ont la concentration 0,5% v/v.

On a préferé le DMSO comme solvant, puisqu'il possède une capacité donneuse comparable à celle de l'eau, conformément à ND, d'après Gutmann [5]...[6] (Tableau 2). En conséquence, il est probable que les processus de type (1)...(4), se passant en solution aqueuse (qui vise, à l'équilibre, la partie soluble) soient semblables aux processus qui ont lieu en DMSO.

Les constituants de ces mélanges de colorants ont été séparés par chromatographie en couche mince (CCM), alors que leur caractérisation a été réalisée par spectrophotométrie d'absorption dans le visible [2]...[4], [7]...[10].

2.1. Séparations par CCM

On a utilisé comme phase stationnaire le silicagel RG, auquel on y ajoute 5% $CuSO_4$. 1,5 H_2O, avec une granulation de 10...40 μ.

Les plaques pour CCM ont été préparées d'après la technique usuelle, en déposant uniformément une suspension de silicagel sur des plaques en

verre de dimensions 20 × 20 cm. La suspension avait été préparée en mélangeant 5 g de phase stationnaire avec 12 ml eau distillée. Après séchage pour une durée de 24 h à température ordinaire, les plaques ont été activées par échauffement à 110°C durant 30 min.

Comme phase mobile nous avons utilisé les mélanges d'éluants $M_i - M_j$..., dont la composition est présentée dans le Tableau 3.

Tableau 3

La composition de la phase mobile dans la séparation par CCM des mélanges industriels de colorants

No.	Mélange de solvants	Rapport des constituants (v/v)
1	Benzène – Acétone	9 : 1
2	Benzène – Chloroforme – Acétone	5 : 2 : 1
3	Benzène – Acétone – HCl	9 : 1 : 0,5
4	Toluène – Acétone	20 : 1
5	Éthanol – Eau	4 : 1
6	Benzène – Méthanol	9 : 1

On a procédé au développement ascendent – les variantes simple et double, avec le séchage intermédiaire des plaques. Les taches chromatographiques obtenues à la suite de la séparation sont colorées et par conséquent on n'a pas recouru à des réactions d'identification.

2.2. Spectres d'absorption

Les colorants, en tant que constituants des taches chromatographiques de la séparation par CCM, ont été élués par DMSO et les solutions ainsi obtenues ont été analysées par spectrophotométrie dans le visible. Parallèlement ont été analysés par voie spectroscopique et les mélanges industriels de colorants, nonséparés, dans des conditions opératoires identiques.

Les spectres ont été enregistrés à l'aide d'un spectrophotomètre Spekord UV – VIS, Carl Zeiss Jena.

3. Résultats et discussions

Parfois dans un système de colorants, une série d'interactions peuvent être estompées par le solvant à la suite de la formation de certaines associations colorant – fibre ; ceci vise surtout les processus (2) et (4). Les interactions colorant – colorant, plus fortes, restent inchangées mais elles peuvent afaiblir au fur et à mesure que le caractère donneur ou accepteur du solvant augmente et le système tend à s'uniformiser avec associations colorant – solvant.

L'état des colorants d'un système donné est donc fortement influencé par la nature du solvant. Par conséquent, dans des conditions données de pH, concentration, etc., l'état actuel des colorants d'un système est apprécié par „le niveau donneur", (ND), ou par le „niveau accepteur", (NA), imposé par le solvant.

3.1. Séparation des colorants des mélanges

En utilisant le silicagel comme phase stationnaire et le mélange benzène—acétone comme phase mobile, on a réalisé une séparation nette des colorants des mélanges. Les données expérimentales indiquent une séparation des colorants caracterisée par un grand nombre de taches chromatographiques (Fig. 1).

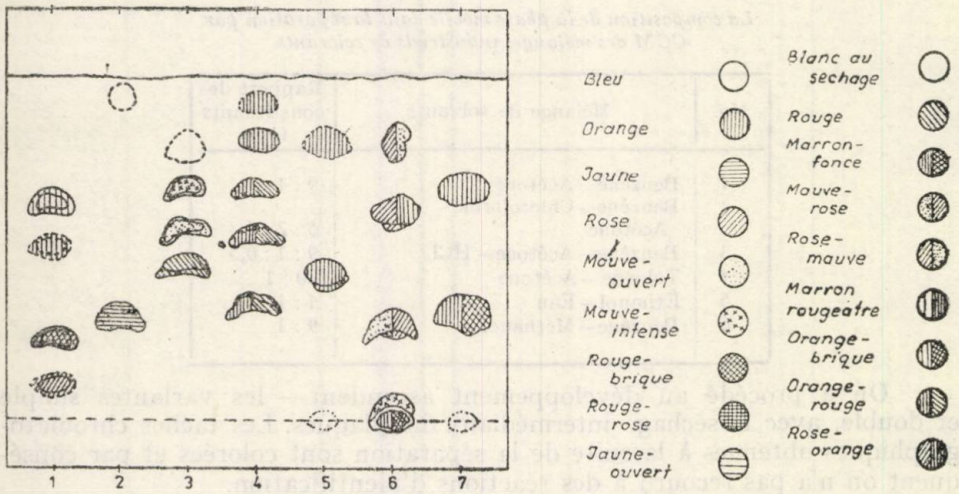

Fig. 1—Aspects de la séparation par CCM de certains colorants préparés pour la teinture: *1*—Rouge de Dispersion *RR* ; *2*—Jaune de Dispersion *G* ; *3*—Bleu Marine de Dispersion *RE* ; *4*—Palanyle Scharlach *RR* ; *5*—Palanyle Violet 3 *B* ; *6*—Cottestren Scharlach *G* ; *7*—Cottestren Violet 3*B*.

Lors de ces séparations, la dissociation des aggrégations de colorants a lieu sous l'influence de différents processus. Ainsi, le DMSO, par dissolution, favorise les processus (2) et (4). À l'équilibre, établi entre la phase stationnaire— phase mobile et les colorants constituants, le silicagel interactionne par des processus acido-basiques ou par des liaisons d'hydrogène en formant des complexes π, etc. Les deux solvants, l'acétone et le benzène, donnent lieu à des interactions plus faibles, de type donneur – accepteur (Tableau 2).

3.2. Caractérisation spectrophotométrique des mélanges de colorants

Les produits résultés lors de l'interaction des colorants, tels que les dimères et autres associations plus complexes, constituent des nouveaux systèmes d'absorption de la lumière, ce qui explique les nombreux écarts des solutions aqueuses de colorants à la loi générale de l'absorption [1].

Par exemple, pour deux molécules équivalentes, A et B, avec les fonctions d'onde Φ_a et Φ_b ou en états excités, Φ'_a et Φ'_b, l'état d'un dimère AB, formé à base de forces de dispersion London, est donné par l'équation :

(5) $$\psi_0 = \Phi_a \Phi_b .$$

Pour ses formes excitées on aura les états :

$$\Psi_{\pm} = \frac{1}{\sqrt{2}} (\Phi'_a \Phi_b \pm \Phi_a \Phi'_b), \tag{6}$$

dont les énergies sont différentes entre elles et par rapport à celle de l'état excité du monomère, ce qui explique l'apparition des modifications dans le spectre d'absorption [1].

Pour un complexe à transfert de charge, DA, l'interaction entre l'état fondamental non-liant Φ_{DA} et celui excité polaire, $\Phi_{D^+A^-}$, conduit à un état fondamental stabilisé :

$$\Psi_0 = \Phi_{DA} + \lambda \Phi_{D^+A^-}, \tag{7}$$

auquel correspond l'état (sous forme excitée, par transfert de charge) :

$$\Psi' = \Phi_{D^+A^-} + \mu \Phi_{DA}. \tag{8}$$

Le complexe moléculaire présente une bande à transfert de charge spécifique, associée à la transition électronique $\psi_0 \rightarrow \psi'$ [11].

Les investigations spectrophotométriques concernent la longueur d'onde et le coefficient molaire d'absorption de la bande caractéristique et sont effectuées plus récemment avec de la lumière polarisée [1]. Les données ainsi obtenues permettent de mettre en évidence les interactions chimiques entre les colorants, l'établissement de la composition et de la stabilité des produits formés et le dosage des colorants des mélanges.

Ces déterminations reposent sur les lois générales de l'absorption [11] :

$$A = \varepsilon c d \tag{9}$$

et

$$A_t = \sum_i A_i = d \sum_i \varepsilon_i c_i, \tag{10}$$

où : A_t — absorbance totale de la solution ; d — épaisseur de la couche de solution ; ε_i — coefficient molaire d'absorption de l'espèce i et c_i — concentration (moles/l) de l'espèce i.

a) *L'état des colorants des mélanges.* D'une manière générale, en absence des interactions entre les constituants d'un mélange de colorants, les grandeurs A_t et ΣA_i, dans des conditions expérimentales identiques, obéissent à l'équation (10). En échange, lors des interactions entre les colorants, apparaissent des effets batôchromes, hipsochromes ou hyperchromes en provoquant des écarts par rapport l'équation (10).

Dans ce qui suit on présente les données obtenues concernant l'analyse spectrophotométrique de certains mélanges de colorants dont les constituants ont été séparés par CCM (Fig. 2 et 3).

Ainsi, pour le mélange Cottestren Scharlach *G* (Fig. 2), on a :

$$A \approx \sum_i A_i \tag{11}$$

dans les limites des erreurs admises. L'effet hipsochrome qui apparait à 22...23 000 cm^{-1} sur A_t suggère que lors de la dissolution de ce mélange dans le DMSO, les interactions entre les colorants constituants n'ont pas été entièrement estompées ; mais ce dernier phénomène est réalisé lors de la séparation par CCM.

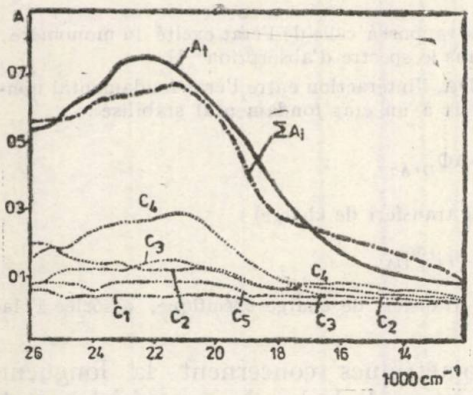

Fig. 2.— Spectres d'absorption dans le visible enregistrés sur le Cottestren Scharlach *G(CSG)* : A_t — spectre d'absorption enregistré sur le mélange technique CSG ; $C_1 \ldots C_5$ — spectres d'absorption des constituants du mélange technique CSG, séparés par CCM ; $\sum_i A_i$ — spectre résulté comme somme des absorbances des constituants $C_1 \ldots C_5$.

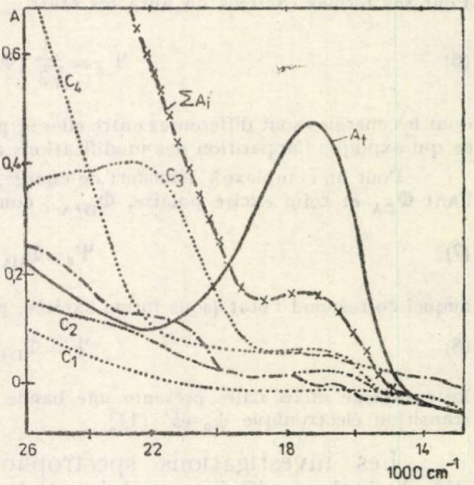

Fig. 3.— Spectres d'absorption dans le visible energistrés sur le Bleu Marine de Dispersion *RE*(AMDRE) : A_t — spectre d'absorption enregistré sur le mélange technique AMDRE ; $C_1 \ldots C_4$ — spectres d'absorption des constituants du mélange technique AMDRE, séparés par CCM ; $\sum_i A_i$ — spectre résulté comme somme des absorbances des constituants $C_1 \ldots C_4$.

En revanche, pour le mélange Bleu Marine de Dispersion *RF* (Fig. 3) :

$$A_t \neq \sum_i A_i, \tag{12}$$

ce qui indique qu'à la dissolution de celui-ci dans le DMSO, l'établissement des interactions entre les colorants se poursuit tout en permettant la séparation des constituants par CCM.

Tous ces résultats peuvent s'intégrer dans un test d'appréciation de l'état des colorants des mélanges, par rapport à un niveau donneur (ND), éventuellement accepteur (NA), imposé par le solvant. Ainsi, les mélanges qui obéissent à l'équation (10) sont considérés des systèmes summatifs pour la valeur de ND caractéristique au solvant utilisé. Dans ces mélanges le colorants se trouvent à l'état associé avec le solvant, sous forme de monomères, etc. Les mélanges pour lesquels s'applique l'inégalité (12) présentent un caractère intégral. Ces mélanges exigent des solvants à ND plus élevé qui peuvent diminuer les interactions entre les constituants.

b) *Paramètres* R_F *et* λ_{max}. De nombreux colorants avec la même formule et la même structure moléculaire ont des appélations techniques différentes. Dans une première étape ils peuvent être investigués par l'intérmediaire des paramètres R_f et λ_{max}, obtenus par l'étude des colorants par CCM et, respectivement, par spectroscopie d'absorption. Dans ce but on peut construire des diagrammes en coordonnés R_f et λ_{max} à base de valeurs déterminées dans des conditions standards (Fig. 4). Dans un tel

diagramme, parmi les colorants concentrés dans des domaines étroits on y trouve tant les colorants semblables du point de vue chimique que des colorants semblables du point de vue optique. Cet aspe t peut représenter une première étape de sélection pour mieux choisir les colorants substituants et pour définir les recettes de teinture.

c) *Dosage des colorants des mélanges.* La classification des mélanges de colorants comme summatifs et intégrals présente un grand intérêt dans le dosage spectrophotométrique des colorants des bains de teinture. Ainsi, les colorants des mélanges summatifs peuvent être simultanément dosés à base de leurs spectres d'absorption. En échange, ceux à caractère intégral nécessitent le choix d'un autre solvant à ND plus élevé qui peut diminuer les interactions du système.

Concernant le dosage, pour calculer la concentration des colorants nous avons proposé un système d'équations algébriques, avec une validité générale [2]. Ainsi, pour un mélange de deux colorants, les équations de calcul ont la forme :

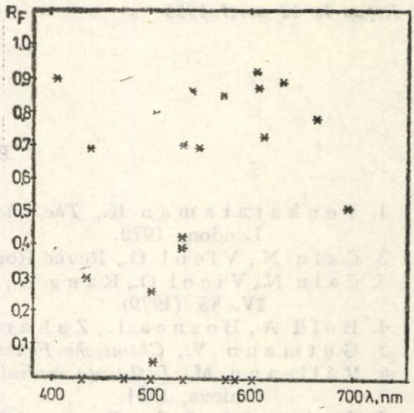

Fig. 4. — Diagramme $R_F - \lambda_{max}$ avec les paramètres caractéristiques des constituants des mélanges techniques : Rouge de Dispersion *RR* ; Bleu Marine de Dispersion *RE* ; Palanyle Violett *3B* ; Cottestren Scharlach *G* ; Cottestren Violett *3B* ; Cottestren Blau *SBC* et Indantren Brillantviolett *3B*.

$$(13)\quad \frac{A'}{d} = \operatorname{tg}\alpha_{1\lambda'} x \pm n_{1\lambda'} + \operatorname{tg}\alpha_{2\lambda'} y \pm n_{2\lambda'}, \qquad \frac{A''}{d} = \operatorname{tg}\alpha_{1\lambda''} x \pm n_{1\lambda''} + \operatorname{tg}\alpha_{2\lambda''} \pm x_{2\lambda''},$$

où : $\operatorname{tg}\alpha_i$ et n_i représentent la pente et respectivement l'ordonnée à l'origine des droites $A = f(c)$ caractéristiques de chacun des constituants i ; A' et A'' — les absorbances du mélange de colorants à λ' et respectivemment λ'' (on prend le signe + pour $n > 0$ et le signe — pour $n < 0$) ; x et y — les concentrations des deux colorants du mélange.

4. Conclusions

a) L'état des colorants d'un système est apprécié à base du caractère donneur, éventuellement accepteur des solvants.

b) Les mélanges de colorants pour lesquels l'absorbance totale A_t est égale à la somme des absorbances des constituants (ΣA_i) sont considérés, au niveau donneur imposé par le solvant, comme systèmes summatifs. Les autre mélanges, avec $A_t \neq \Sigma A_i$, à caractère intégral, peuvent devenir summatifs par rapport aux solvants avec des propriétés donneur — accepteur plus fortes.

c) Les colorants des mélanges summatifs peuvent être simultanément dosés par voie spectroscopique, à l'aide d'un système d'équations algebriques en tg α et n.

d) Les paramètres R_f et λ_{max} interviennent dans la sélection des colorants remplaçants et à l'élaboration des recettes de teinture.

Reçue le 12 avril 1985

Institut Polytechnique, Jassy,
Chaire de Chimie et Technologie
anorganique et analytique

BIBLIOGRAPHIE

1. Venkataraman K., *The Chemistry of Synthetic Dyes.* Acad. Press, New-York—London, 1970.
2. Calu N., Vicol O., Revue Roumaine de Chimie, 26, 5, 783—792 (1981).
3. Calu N., Vicol O., Rang A., Saviuc E. et collab., Bul. Șt. Stud., Inst. polit., Iași, IV, 88 (1979).
4. Bold A., Bosnea L., Zaharia E., Revista de chimie, **33**, 10, 953 (1982).
5. Gutmann V., *Chemische Fonktionslehre.* Springer Verlag, 1971.
6. Răileanu M., *Influența mediului asupra reactivității chimice.* Ed. Scrisul Românesc Craiova, 1981.
7. Brown C.J., J. Soc. Dyers and Col., **80**, 185 (1964); Ibid., **85**, 137 (1969).
8. Johnson D.C., Telesz A.L., J. Soc. Dyers ans Col., **78**, 496 (1962).
9. Sweeny D.C., American Dyestuff Reports, **61**, 70 (1972).
10. Beer A., Ann. Phys. Chem., *163*, 78 (1852).
11. Rose J., *Molecular Complexes.* Pergamon Press, Oxford-London, 1967.

METODE DE CARACTERIZARE FIZICO-CHIMICĂ A COLORANȚILOR ÎN AMESTEC

(Rezumat)

În sistemul de coloranți pregătiți pentru vopsire au loc diverse interacțiuni fizice și chimice între coloranți, cu implicații în procesul de vopsire. În același timp, solventul produce asociate colorant—solvent. Ca urmare, în lucrare este folosit conceptul de nivel donor, eventual acceptor, al solventului pentru a aprecia starea asociatelor colorant—solvent, din sistemele luate în studiu.

În fapt, coloranții din amestecuri, separați prin cromatografie în strat subțire, au fost caracterizați pe baza benzilor de absorbție în vizibil. Astfel, amestecurile la care absorbanța totală, A_t, este egală cu suma absorbanțelor coloranților componenți, $\sum_i A_i$, sînt apreciate ca sumative, la nivelul donor—acceptor impus de solvent. Pentru celelalte amestecuri, cu $A_t \neq \sum_i A_i$, se admite un caracter integral. Ele pot deveni sumative în solvenți cu o capacitate donor—acceptor mai ridicată. Coloranții din amestecurile sumative pot fi dozați pe cale spectrofotometrică, folosind un sistem de ecuații în tgα și n.

Pe de altă parte, parametrii R_f și λ_{max}. sînt utili în selectarea unor coloranți înlocuitori, la elaborarea rețetelor de vopsire.

BULETINUL INSTITUTULUI POLITEHNIC DIN IAȘI
Tomul XXXI (XXXV), Fasc. supl., 1985
Secția III
CHIMIE ȘI INGINERIE CHIMICĂ

D.C. 532.13 ; 541.24

VISCOSITY — MOLECULAR WEIGHT RELATIONSHIP FOR POLY (ETHYLENETEREPHTALATE) MODIFIED WITH 1,2-PROPANEDIOL

BY

CAMELUȚA BELDIE, ANA ONU, NICOLAE AELENEI, GH. NEMȚOI, AL. RADOVICI and AL. SAVIN

1. Introduction

To obtain certain peculiar properties (optical effects, dye adsorption, good resistance for technical use, etc.), the studies on poly(ethyleneterephtalate) were applied more and more on its copolyesters, too. Features as solubility, crystallinity, melting point, etc., can be changed inserting small amounts of a comonomer, in the chain.

The obtaining of a polyester sample with optimal properties intended to be used in a certain application depends on the molecular weight, and molecular weight distribution, so that any investigation should search these features. The value of the molecular weight polydispersity due to the existence of some low molecular weight fractions, can lead to an important modification of copolyester properties.

The evaluation of the molecular weights as well as the molecular weight distribution was performed in solution.

In our case, the solubility of these copolyesters was limited due to a high crystallinity which reduces the number of the used solvents, and it is necessary to use high temperatures in order to prepare the solutions.

This paper deals with the study of the relation between $[\eta]$ and $\overline{M}_n$ for poly(ethyleneterephtalate) modified with 1,2-propanediol on unfractionated and fractionated samples in two solvents : *o*-chlorophenol (OCPh) and phenoltetrachloroethane (Ph—TCE) mixture.

2. Experimental

Samples of poly(ethyleneterephtalate) modified with 1,2-propanediol (5.0...10.0% of 1,2-propanediol) of different molecular weights, as well as fractions obtaind from a copolyester having 10.0% 1,2-propanediol were investigated from the physico-chemical point of view.

In order to choose a proper solvent corresponding to the copolyester, the following solvents were searched: *m*-cresol, *o*-chlorophenol, and phenol/tetrachlorethane (3/2 w/w).

The solubility of the copolyester samples were studied in comparison with poly(ethyleneterephtalate). It was noticed that inserting 1,2-propanediol results in an increase of the solubility of the copolyester samples in all listed solvents. From the three investigated solvents, *m*-cresol is less proper, so the viscosimetric studies of the copolyester samples were performed using

o-chlorophenol and the phenol/tetrachloroethylene (3/2 w/w) while the cryoscopic measurements were carried out in *o*-chlorophenol.

The viscosimetric measurements of the fractions performed by the fractionation technique of copolyester were carried out using only *o*-chlorophenol, small amounts of copolyester being available.

The fractionation of poly(ethyleneterephtalate) modified with 1,2-propanediol was performed applying the known technique [1], [2] based on the distribution of copolyester between two liquid phases with reduced miscibility. The fractionation was performed at 56°C using phenol as solvent and the phenol – n-heptane mixture as eluent. The percent of phenol was increased from 45.0% up to 70.0%. The fractions were precipitated from the solution by adding acetone in exces, at 40°C.

The viscosimetric measurements were carried out on a Ubbehlode viscosimeter at 25°C. The limit viscosity index of the fractions 2...10 and unfractionated samples was determined by the H u g g i n s method [3], carrying out measurements on four different concentrations. The limit viscosity index of the fractions 1 and 11...14 was determined using the S o l o m o n - C i u t a's relation [4] when the measurements of viscosity were performed for one concentration.

The number average molecular weights were measured by the cryoscopic method on a Knauer cryometer apparatus fitted with thermoelectric cooling unit. The cooling of the sample was performed applying the Peltier's effect. The cooling degree and the cooling velocity depends on the „warm welding" thermoelement temperature and as consequence it depends on the room temperature and the working time of the apparatus. This phenomenon is not quite important for solvents which show small or moderate undercoolings ($\Delta T \leqslant 5$°C), but it is important in the case of solvents having high undercoolings (for instance, *o*-chlorophenol used in our case). In order to perform the same undercooling for all samples and solvents, the „warm welding" of the thermoelement was thermostated. For this purpose, cold water (0°C) was circulated through the thermostatic mantle of the thermoelement by means of a MK-70 Ultracryostate apparatus.

For each sample, measurements were carried out at least five different concentrations ; 20 measurements were performed for each concentrations. Polystyrene was used as standard sample (Arro Laboratories Inc., Illinois, USA), of which molecular weight (20.450) was in the average range of the measured values

3. Results and Discussion

A copolyester sample having a content of 10.0% 1,2-propanediol and $\overline{M}_n = 23\,100$ g/mol was fractionated. The experiemental data were processed and plotted as distribution curves in Fig. 1.

The results of the viscometric and cryoscopic determinations, performed in *o*-chlorophenol, at 25°C, are shown in Table 1.

The coefficients of the M a r k – H o u w i n k – S a k u r a d a (M-H-S) equation $[\eta] = KM^{\alpha}$ were calculated using these experimental data applying the least squares method :

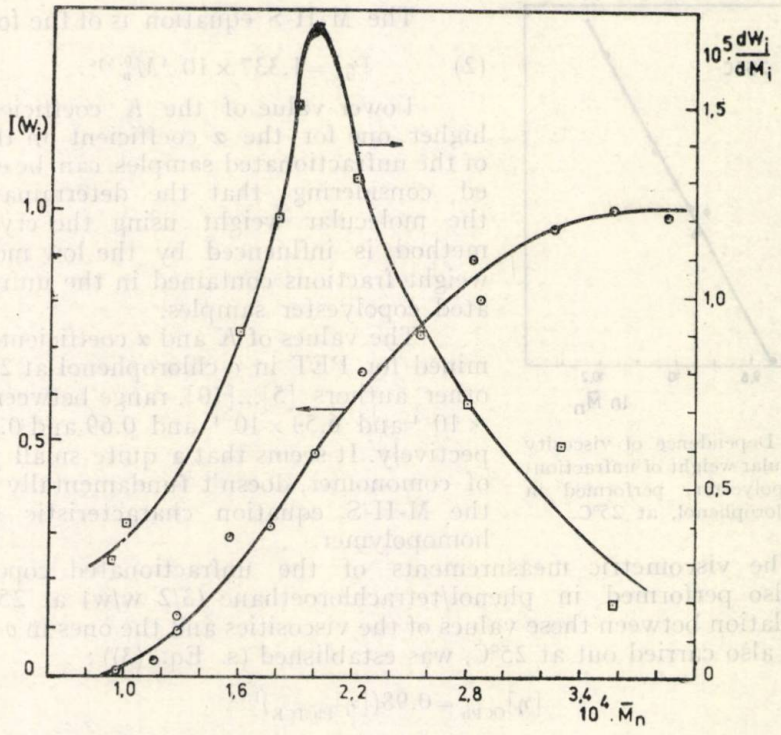

Fig. 1. — The distribution of the molecular weights for copolyester sample which contains 10.0% 1,2-propanediol.

Table 1

Number Average Molecular Weights ($\bar{M}_n$) and the Limit Viscosity Indexes ($[\eta]$) of the Copolyester Fractions, Determined in o-Chlorophenol, at 25°C

Fraction	$\bar{M}_n \times 10^{-4}$ g/mol	$[\eta]$ dl/g	Fraction	$\bar{M}_n \times 10^{-4}$ g/mol	$[\eta]$ dl/g
1	0.970	0.289	8	2.27	0.543
2	1.35	0.430	9	1.30	0.361
3	2.50	0.590	10	1.77	0.454
4	1.38	0.395	11	1.10	0.402
5	1.79	0.510	12	3.25	0.726
6	2.56	0.697	13	3.86	0.810
7	1.48	0.361	14	3.55	0.942

(1) $$[\eta] = 3.12 \times 10^{-4} \bar{M}_n^{0.75}$$

The viscometric and cryoscopic studies of unfractionated copolyester samples with 5.0...10.0% 1,2-propanediol, in *o*-chlorophenol, at 25°C show the dependence of viscosity on molecular weight represented in Fig. 2.

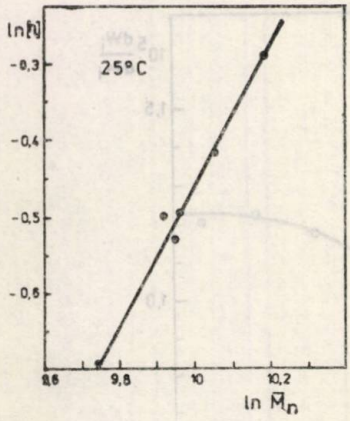

Fig. 2 — Dependence of viscosity on molecular weight of unfractionated copolyester, performed in *o*-chlorophenol, at 25°C.

The M-H-S equation is of the form:

$$[\eta] = 1.337 \times 10^{-4} \bar{M}_n^{0.816}. \quad (2)$$

Lower value of the K coefficient and higher one for the α coefficient in the case of the unfractionated samples can be explained considering that the determination of the molecular weight using the cryoscopic method is influenced by the low molecular weight fractions contained in the unfractionated copolyester samples.

The values of K and α coefficients determined for PET in *o*-chlorophenol at 25°C, by other authors [5]...[10], range between $1.6 \times \times 10^{-4}$ and 6.54×10^{-4} and 0.69 and 0.83, respectively. It seems that a quite small percent of comonomer, doesn't fundamentally change the M-H-S equation characteristic to the homopolymer.

The viscometric measurements of the unfractionated copolyester were also performed in phenol/tetrachloroethane (3/2 w/w) at 25°C and a correlation between these values of the viscosities and the ones in *o*-chlorophenol also carried out at 25°C, was established (s. Eq. (3)):

$$[\eta]_{OCPh} = 0.98([\eta]_{Ph/TCE})^{1.04} \quad (3)$$

By measuring the viscosity of the industrial copolyester samples in Ph/TCE (3/2 w/w) (the most used solvent in the laboratories of the chemical industry) and knowing the relation between this solvent mixture and *o*-chlorophenol (Eq. (3)), one can calculate $\bar{M}_n$ of the investigated sample, according to the dependence $[\eta]_{OCPh}$ vs. $\bar{M}_n$, given by Eq. (2). The experimental results are in good agreement.

The knowledge of this dependence between the viscosities in different solvents answers to a practical need, because the viscometric measurements can be easily performed in solvent mixtures, while the molecular weight measurement methods assume the utilization of a single solvent. Our results allow to widen the application possibilities of the viscosity—molecular weight relations established by different authors.

4. Conclusions

The performed studies pointed out the following conclusions:

1. The copolyester presents a better solubility than poly(ethyleneterephtalate) in *m*-cresol, *o*-chlorophenol and Ph/TCE mixture (3/2 w/w) as proved by the solubility tests as well as by viscometric determinations; *o*-chlorophenol was the best solvent for the copolyester samples.

2. The fractionation of 1,2-propanediol-ethyleneterephtalate copolyester applying the known methods for poly(ethyleneterephtalate) is not entirely adequately, because using the same solvent/nonsolvent ratio and

elution velocity, inversion of the fraction separation succession are obtained.

3. The experimental date, performed in *o*-chlorophenol at 25°C, for the 14 fractions and unfractionated copolyester, lead to a linear dependence between viscosity and molecular weight given by Eqs. (1) and (2). The K coefficient is smaller for the unfractionated samples as compared to that of the fractionated copolyester while the α exponent is higher. This behaviour is due to the existence of low molecular weight fractions which influence the number average molecular weight, while the viscosimetric measurements are influenced by the high molecular weight fractions existing in the polydisperse copolyester.

4. The determined correlation between viscosity in *o*-chlorophenol and Ph/TCE (3/2 w/w) allows the experimental determination of viscosity, in Ph/TCE (used by chemical industrial laboratories), and the calculation of $\overline{M}_n$ value by means of the viscosity—molecular weight relation. This study offers the possibility to widen the application field of the equation (2).

Received, April 18, 1985

Polytechnic Institute, Jassy,
Department of Physical and
General Chemistry

REFERENCES

1. Duveau M., J. Polymer Sci., **57**, 375 (1962).
2. Feldman D., Theil I., Călugăru E.M., Faserforschung-Textiltechnik, **23**, 123 (1972).
3. Huggins M.L., J.Am. Chem. Soc., **64**, 2716 (1942).
4. Solomon O.F., Ciuta I.Z., J. Appl. Polym. Sci., **6**, 683 (1962).
5. Ward I.M., Trans. Faraday Soc., **53**, 1406 (1957).
6. Ravens D.A.S., Ward I.M., Trans. Faraday Soc., **57**, 150 (1961).
7. Moore W.R., Sanderson D., Polymer (London), **9**, 153 (1968).
8. Marshall J., Todd A., Trans. Faraday Soc., **49**, 65 (1953).
9. Meyerhoff G., Shimotsuma S., Makromol. Chem., *135*, 195 (1970).
10. Hergenrother W.L., Nelson Ch.J., J. Polym Sci., Polymer Chem. Ed., **12**, 2905 (1974).

RELAȚIA VÎSCOZITATE—MASĂ MOLECULARĂ PENTRU POLIETILENTEREFTALAT MODIFICAT CU 1,2-PROPANDIOL

(Rezumat)

S-au determinat coeficienții K și α din ecuația Mark-Houwink-Sakurada în *o*-clorfenol (OCF) pentru poli(etilentereftalat) modificat cu 1,2-propandiol atît nefracționat cît și pentru fracțiuni. La 25°C, $[\eta] = 3{,}12 \cdot 10^{-4} \overline{M}_n^{0{,}75}$ dl/g pentru fracțiuni și $[\eta] = 1{,}337 \cdot 10^{-4} \times \overline{M}_n^{0{,}846}$ dl/g pentru probele nefracționate. Pentru probele nefracționate s-a obținut între vîscozitatea în OCF și în amestecul de solvenți fenol/tetracloretan (F/TCE) : (3/2), la 25°C relația $[\eta]_{OCF} = 0{,}98[(\eta]_{F/TCE})^{1{,}04}$. Masele molare au fost determinate prin metoda crioscopică, utilizînd un crioscop tip Knauer prevăzut cu o unitate de răcire termoelectrică bazată pe efectul Peltier.

BULETINUL INSTITUTULUI POLITEHNIC DIN IAŞI
Tomul XXXI (XXXV), Fasc. supl., 1985
Secţia II
CHIMIE ŞI INGINERIE CHIMICĂ

D.C. 546.654 ; 546.36

COMPLEXES OF La(III) AND Ce(IV) WITH DIBUTYLPHOSPHINIC ACID

BY

I. ROŞCA, ELENA ŞTEFANCU and MIRCEA PALAMARU

1. Introduction

Development of investigation in the field of the compounds prepared from cations of the block *d* metals with derivatives of phosphinic acid resulted, last years, in the synthesis and study of numerous compounds with special properties [1] ... [10].

The studies performed on these compounds have proved their high thermal stability and elastic properties which maintain at very low temperature. Besides high thermostability, some of these compounds are semiconductors or insulators, resistent in corossive media [5] ... [14]. An uncommon application of these products is their utilization in aeronautics and artificial satellites [9].

The present paper deals with some new syntheses and studies on the properties of the compounds prepared from cations of the block *d* metals with derivatives of phosphinic acid, especially complexes of La(III) and Ce(IV).

2. Experimental

2.1. Synthesis and Characterization

The studied compounds have been o' tained in melt or by refluxing in benzene, toluene, butanol or ethanol of respective reagents. For this reason, stoichiometrical amounts of La(III) o Ce(IV) acetya'cetonate and dibutylphosphinic acid have been introduced in a flask fitted with a refluxing condenser. Both La(III) and Ce(IV) acetylacetonate and dibutylphosphinic acid have been obtained, as in [15], [16].

The flask containing the reagents was heated up to the boiling temperature of the solvent or over melting temperature of the reagents for melt syntheses. The reagents concentration was 0.2...0.02 mole/L. The reagents are soluble but products are only partially soluble in the employed solvents. Separation of the products was carried out by filtration and the soluble fractions by solvent evaporation.

From the chemical composition of the obtained complexes, it appears that for each La^{3+} or Ce^{4+} cation correspond three, respectively four anions of dibutylphosphinic acid (Table 1).

Table 1

Composition and Molecular Weight of the Obtained Compounds

Compound	Molecular Weight	Composition, [%]							
		M		C		P		H	
		teor.	exp.	teor.	exp.	teor.	exp.	teor.	exp.
$\{La[(C_4H_9)_2PO_2]_3\}_n$	6 110	20.7	20.2	43.2	43.6	13.9	13.5	8.06	8.32
$\{Ce[(C_4H_9)_2PO_2]_4\}_n$	8 620	16.5	16.3	45.3	45.8	14.6	14.2	8.49	8.76

The molecular weights of the soluble fractions, determined crioscopically in benzene are summarized in Table 1.

2.2. Thermogravimetrical Analysis and Kinetics of the Thermal Decomposition Reaction

Thermogravimetrical analysis of the samples has been carried out on a Paulik-Paulik-Erdey derivatograph with amounts of 50 mg at a heating rate of 10°C/min from 20°...700°C.

The derivatograms show that the thermal decomposition occurs gradually, by releasing gaseous products (Fig. 1).

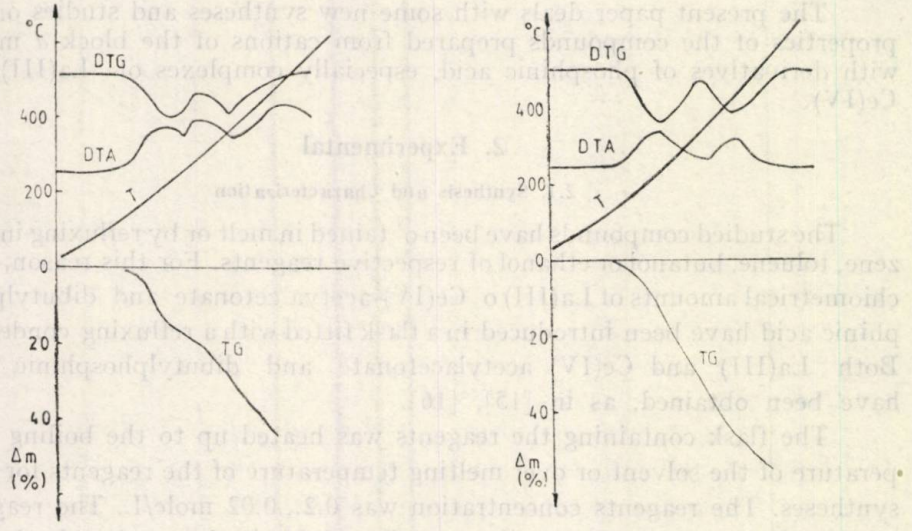

Fig. 1. — Derivatograms of complexes:
1—$\{La[(C_4H_9)_2PO_2]_3\}_n$; *2*—$\{Ce[(C_4H_9)_2PO_2]_4\}_n$.

The strongest bonds in the tested compounds are La—O, Ce—O and P—O, finally found in the solid products.

The obtained compounds present a thermal stability greater than the reagents. This proves that the groups which did not resist to the thermic

effect in La(III) and Ce(IV) acetylacetonates and dibutylphosphinic acid allow the isomerization to form more stable chelate rings. The temperatures corresponding to the thermal decomposition are listed in Table 2.

Table 2

Thermal Decomposition of the Obtained Compounds

Compound	Start of decomposition °C	Temperature corresponding to a weight loss of °C		Final decomposition temperature, °C
		10%	25%	
$\{La[(C_4H_9)_2PO_2]_3\}_n$	160	217	320	480
$\{Ce[(C_4H_9)_2PO_2]_4\}_n$	190	240	295	565

Kinetical parameters of the thermal decomposition reactions, calculated by Freeman and Carol's procedure [17], for each decomposition step, are given in Table 3.

The values of the reaction order may be explained considering that the chemical reaction is defavourised by diffusion of volatile compounds through the solid, by interphase or by „vaporization" phenomena of volatile components at the free surface of the solid.

Table 3

Kinetical Parameters of the Thermal Decomposition Reactions

Compound	Temperature °C	Phase I			Phase II	
		Reaction order	Activation energy Kj/mol	Temperature °C	Reaction order	Activation energy Kj/mol
$\{La[(C_4H_9)_2PO_2]_3\}_n$	160...270	0.68	123	270...470	0.76	148
$\{Ce[(C_4H_9)_2PO_2]_4\}_n$	190...340	0.83	139	340...565	0.89	174

2.3. Spectral Analysis

The IR spectra of the synthesized products have been recorded on an UNICAM apparatus in the 400...4 000 cm^{-1} region. The most pronounced are the absorbtion bands of the $-PO_2$ group. Formation of the 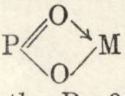 bonds causes the modification of the corresponding maxima of the P=0 group as effect of the P=0 elongation. Thus, the obtained products, show lower frequencies than the uncomplexed dibutylphosphinic acid for about 20 cm^{-1} (Fig. 2).

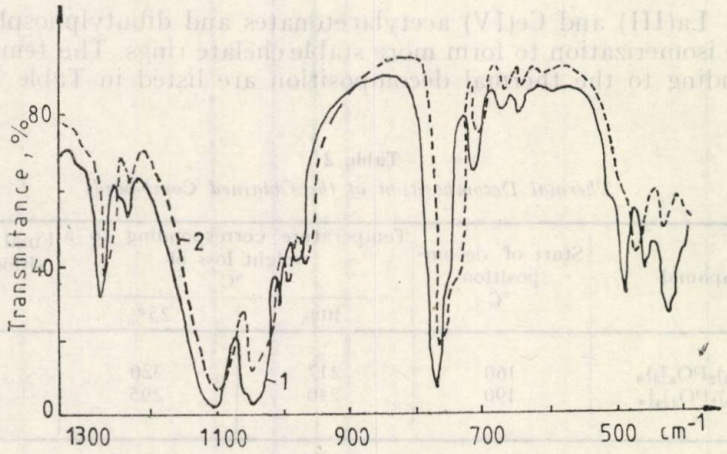

Fig. 2. — IR Spectra of the complexes:
$1-\{La[(C_4H_9)_2PO_2]_3\}_n$; $2-\{[(C_4H_9)_2PO_2]_4\}_n$.

X-ray diffraction spectra were recorded on a Kristalloflex-Siemens type equipment with Cu.K_α radiation and Ni filter, anodic voltage of 35 eV and a current of 12 mA. The crystallinity degree was calculated by the method presented in [18]. The found values were of 38.8% and 43.2% for La and Ce compounds, respectively. They proved to be two phase products in which, besides local ordonation proper to amorphous state, diffraction lines characteristic to crystalline phase are also exhibited.

3. Suggested Structure of the Synthesized Complexes

Data of the chemical analysis of the synthesized compounds show that for each M^{3+} ion correspond three anions of dibutylphosphinic acid. These anions being bidentate by means of oxygen atoms, the hexacoordination of M^{3+} appears (Fig. 3).

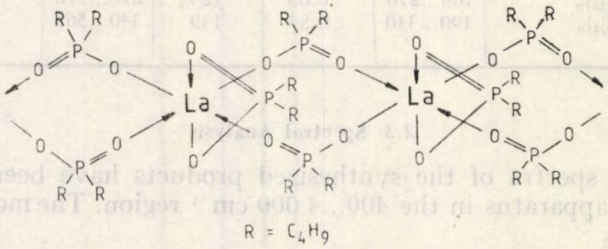

Fig. 3. — Suggested structure of the synthesised compounds:
$\{La[(C_4H_9)_2PO_2]_3\}_n$.

As known, for coordination number six, the arrangement of ligands is an octahedral one. This structure is in good agreement with the structure of some similar compounds prepared from diorganophosphinic acids and cations of the block *d* metals [4]...[12].

The values of the molecular weight reveal that these compounds are oligomers like. Therefore, the octahedral structure units, as main units in the polymer structure, will constitute configuration of the synthesized compounds. Connection of the octahedral structures is done by means of anionic groups of dibutylphosphinic acid with the phosphorous atom tetracoordinated in tetrahedral structure, which agrees with experimental and literature data.

Received, April 18, 1985

Polytechnic Institute, Jassy,
Department of Inorganic and
Analytical Chemistry and
Inorganic Technology,

REFERENCES

1. Block P.B., Simkin J., Ocone R.J., J. Am. Chem. Soc., **84**, 1 749 (1962).
2. Saraceno J.A., Block P.B., Inorg. Chem., **3**, 1 699 (1964).
3. Selwyn H., Rose H.S., Block P.B., J. Am. Chem. Soc., **87**, 2 076 (1965).
4. Crescenzi V., Giancotti V., Ropamonti A., J. Am. Chem. Soc., **88**, 391 (1966).
5. Коршак В.В., Круковский С.П., Ван Юи Хан, Высокомолек. соедин., **B 9** (1967).
6. Golgoțiu T., Roșca I., Bul. Inst. polit., Iași, **XVII** (**XXI**), *1—2*, s. II, 1 (1971).
7. Golgoțiu T., Roșca I., Makromolek. Chemie, *160*, 59 (1972).
8. Голгоциу Т., Рошка И., Высокомолек. соедин., **9**, 2086 (1973).
9. *** Patent USA. *139 784* (1973).
10. Roșca I., *Compuși termostabili ai Mn(II), Cr (III), Fe(III), UO_2^{2+}, Co(II) și Ni(II) cu derivați ai acidului fosfinic.* Ph. D. Diss., Polyt. Inst., Jassy, 1975.
11. Roșca I., Bul Inst. polit. Iași, **XXIII** (**XXVII**), *1—2*, s. II, 21 (1977).
12. Roșca I., Bul. Inst. polit., Iași, **XXI** (**XXV**), *1—2*, s. II, 8 (1975).
13. Roșca I., Patent R.S.R., *68459* (1978).
14. Roșca I., Patent R.S.R., *73201* (1979).
15. Петров А. К., Близнюк К. Х., Короткова П. В., ЖОХ, **9**, 2095 (1960).
16. Brauer G., *Handbuch der präparativen anorganischen Chemie.* Ferdinand Enke Verlag, Stuttgart, 1954.
17. Freeman S.E., Carrol B., J. Phys. Chem., **62**, 394 (1958).
18. Hermans H.P., J. Polym. Sci., **4**, 709 (1960).

COMPUȘI DE COORDINAȚIE AI La(III) ȘI Ce(IV) CU ACIDUL DIBUTILFOSFINIC

(Rezumat)

Se continuă seria sintezelor și al studiului proprietăților compușilor proveniți de la cationii blocului *d*, cu derivați ai acidului fosfinic, prezentîndu-se un studiu al compușilor obținuți din acid dibutilfosfinic și acetilacetonați de La(III) și Ce(IV). Compușii au fost sintetizați în soluție și în topitură. Din analiza chimică a compușilor obținuți s-a putut stabili că pentru fiecare cation La^{3+} sau Ce^{4+} corespund trei și respectiv patru anioni ai acidului dibutilfosfinic. Complecșii obținuți au fost studiați prin analiză termogravimetrică, spectre de absorbție în IR și spectre de raze X. Se propune în final o structură a complecșilor obținuți.

BULETINUL INSTITUTULUI POLITEHNIC DIN IAŞI
Tomul XXXI (XXXV), Fasc. supl., 1985
Secţia II
CHIMIE ŞI INGINERIE CHIMICĂ

D.C. 661.183.48

SYNTHETIC ZEOLITES FOR DETERGENTS CONDITIONING

I. PHYSICO-CHEMICAL PROPERTIES OF ZEOLITES

BY

EVELINE POPOVICI, M. CRUCEANU, ANGELA POPA, AURELIA VASILE and MARIA ALEXANDROAEI

1. Introduction

Last years, numerous investigations [1] ...[5], [9] ... [12] were concerned with the utilization of synthetic zeolites as subsidiary substitutes in detergents conditioning. This utilization is justified, on the one hand, by assurance of a complet security from toxicological and ecological point of view and, on the other hand, by partial diminishing of phosphates consumption, the latest ones being energointensive products.

Utilization of zeolites for this purpose is especially based on their significant property of ion exchange against Ca^{2+} and Mg^{2+}, with convenient consequences for washing steps [1]... [4] and on technical and economical estimations of Henkel and Degussa companies [6] which pointed out that utilization of zeolites for detergents conditioning do not involve essential technological modifications. This considerations explain the continuous increase of world zeolites consumption in detergents manufacture in comparison with their classical utilization, i.e. catalysis, adsorption (s. Table 1).

This paper deals with an analysis of some physico-chemical properties of certain synthetic zeolites, obtained at Polytechnic Institute of Jassy, symbolized by ZPI, in comparison with the data on the commercial product HAB-A40 Degussa in view of their utilization in detergents, as conditioning agent.

2. Experimental

The analyzed synthetic zeolites, obtained by hydrothermal procedure, [13], using as raw materials solutions of sodium silicate and aluminate of technical grade (Fig. 1), have been characterized chemically, roentgenographycally, derivatographycally and by adsorption. Their mean granula size was measured by means of optical microscope. Chemical composition was determined as follows : silicon—gravimetrically ; aluminium—complexometrically ; sodium—flamphotometrically and iron—colorimetrically with *o*-phenantroline. At the same time the comparative determinations of bulk density and powder density [14] were carried out. Adsorption of the molecular dispersed pigments was appreciated colorimetrically at $\lambda = 582$ cm^{-1} for methylene blue.

Table 1

World Consumption Estimation of Synthetic Zeolites [5]

	1975		1977		1979		1981	
	10^3t	%	10^3t	%	10^3t	%	10^3t	%
North America								
detergents	—	—	27	42	90	67	225	80
catalysts	20	64.4	23	34	28	20	35	12.5
adsorbants	11	35.6	14	22	16	13	20	7.5
Total	31		64		134		280	
Latin America								
detergents	—	—	—	—	—	—	—	—
catalysts	3	30	3	25	4	28.5	5	27.7
adsorbants	7	70	9	75	10	71.5	13	72.3
Total	10		12		14		18	
West Europe								
detergents	—	—	27	71	90	87	225	93.3
catalysts	3	37.5	4	10	4	4.3	5	2.2
adsorbants	5	62.5	7	19	9	8.7	11	4.5
Total	8		38		103		241	
Near and Far East								
detergents	—	—	—	—	29	60	90	77.6
catalysts	3	27.3	5	31.2	6	11.7	8	7.8
adsorbants	8	72.7	11	68.8	14	28.3	18	15.6
Total	11		16		49		116	
WORLD TOTAL	60		130		300		655	

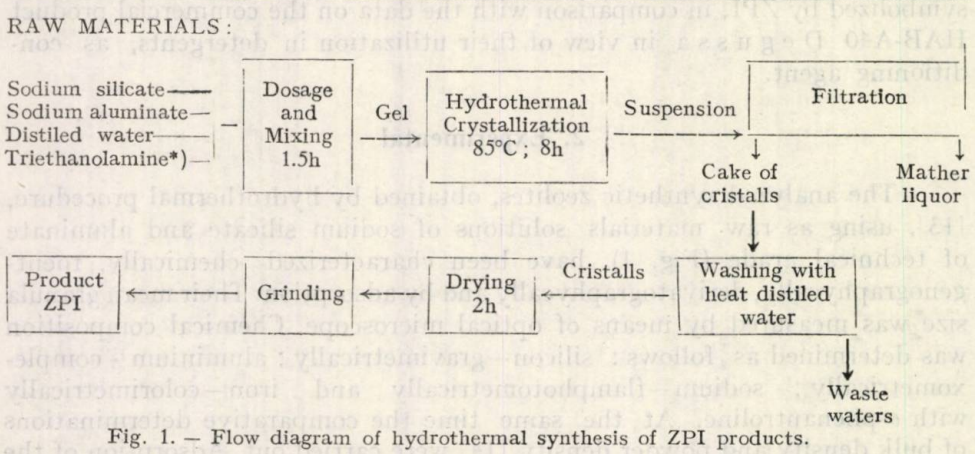

Fig. 1. — Flow diagram of hydrothermal synthesis of ZPI products.

*) Triethanolamine used only for ZPI-12 obtaining product with a significant diminishing of iron ions content.

3. Results and Discussions

Analysis of the products, done in comparison with HAB-A40 zeolite, led to the results summarized in Table 2, which shows a good agreement with principal characteristics as regards the efficient behaviour of reference product in float. Thus, roentgenographical and adsorptive measurements point out a NaA type structure, except the product ZPI-12 which is a mixture of NaA and NaX. Mean granule size is also in good agreement with the data in literature [7] referring to zeolites employed in detergents conditioning.

Table 2

Physico-chemical Properties of the Products

Characteristics	HAB-A40 [6]	Present values		
		ZPI-10	ZPI-11	ZPI-12
Mean granule size, [μ]	4	4	3	3
Maximum size, [μ]	20	10	6	8
Density, [g/cm³]	2	2.12	2.08	2.09
Bulk density, [g/l]	350	381.7	371.4	369.9
Powder density, [g/l] ; [14]	450	473.5	469.9	472.1
pH [15]	12	10	10	10
Chemical composition, [%]				
Na_2O	17	17.13	16.72	14.90
Al_2O_3	28	30.63	33.63	26.46
SiO_2	33	36.22	37.70	40.62
H_2O	22	16	12.21	18
Traces of iron, [p.p.m.]	150	310	174	59
Ion exchange capacity against Ca^{2+}, [mg CaO/g]	160	171.7	161,2	169.8
Type of zeolite structure	A	A	A	A+X

It can be seen, especially, the positive influence of the synthetical procedure of ZPI-12 on its Fe content.

Since bonding capacity of Ca^{2+} and Mg^{2+} is the main property of zeolites in washing process, exchange kinetics of these ions was carried out at 22°C, for a zeolite concentration of 2 g/l (Fig. 2). As it comes from Fig. 2 all synthesized products exhibit a fast kinetics of Ca^{2+} bonding and a high exchange capacity. For a more suggestive expression of the results as for a better comparison with literature data, exchange kinetics was also expressed by variation of remanent hardness vs. time (Fig. 3). The capacity of the ZPI products is similar to that of HAB-A40. The equilibrium concentration is achieved after 10—15 min., yielding a deep softening of water.

Practical utilization of zeolites requires the knowledge of the rate of saturation degree achievement with Ca^{2+}, because their efficient behaviour in float depends on this degree ; its quantitative expression can be done according to Reichenberg [8] as Q/Q_∞, where Q is the amount of Ca^{2+} retained at any instant and Q_∞ —the maximum exchange capacity. In

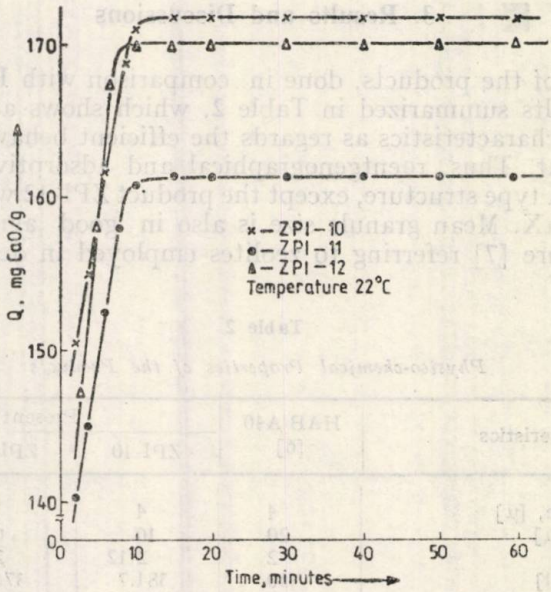

Fig. 2. — Kinetics of ion exchange for Ca^{2+} on ZPI products.

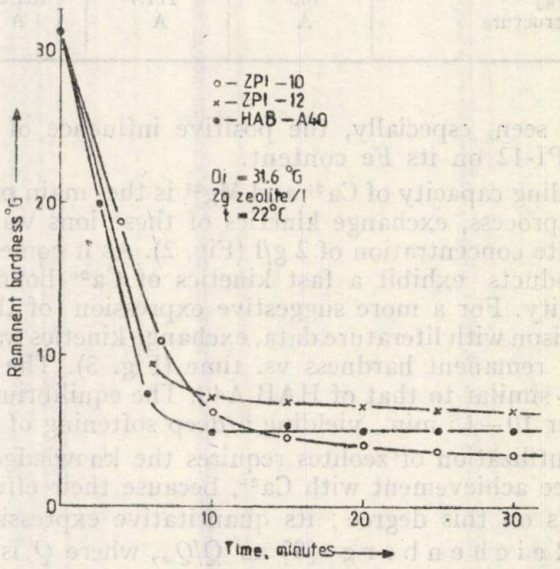

Fig. 3. — Variation of remanent hardness vs. time on tested products.

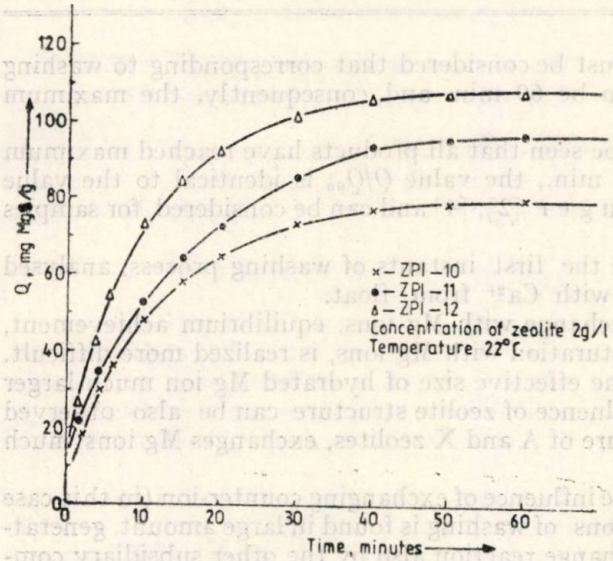

Fig. 5. — Kinetics of ion exchange for Mg^{2+} on ZPI products.

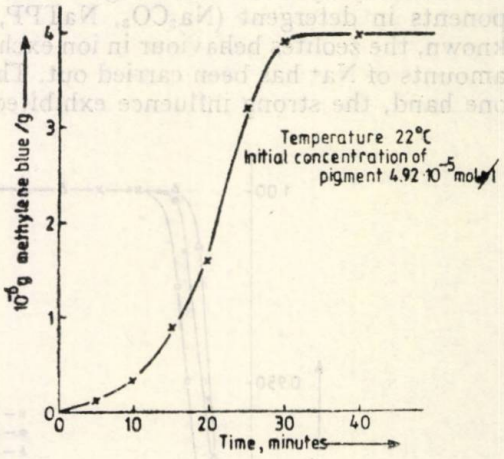

Fig. 6. — Ion exchange capacity against Ca ions on ZPI-12 vs. concentration of Na counter-ion.

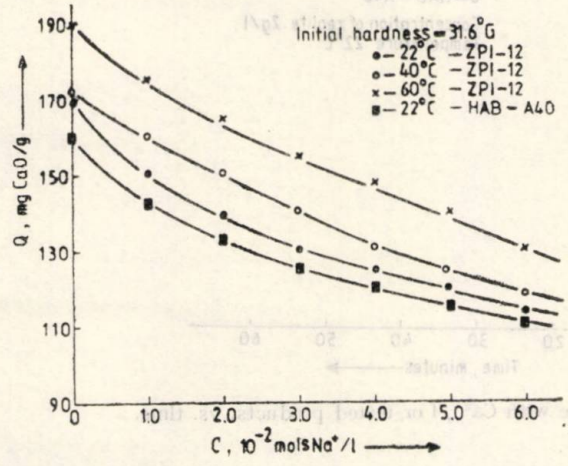

Fig. 7. — Kinetics of adsorption of methylene blue on ZPI-12.

this case the value of Q_∞ must be considered that corresponding to washing process time appreciated to be 60 min. and, consequently, the maximum value was noted Q_{60}.

Since in Fig. 4 it can be seen that all products have reached maximum exchange capacity after 60 min., the value Q/Q_{60} is identical to the value Q/Q_{70} employed by S c h w u g e r [2], [4] and can be considered for samples comparison.

It can be seen that in the first instants of washing process, analysed zeolites became saturated with Ca^{2+} from float.

As regards the ion exchange with Mg ions, equilibrium achievement, (Fig. 5) as well as zeolite saturation with Mg ions, is realized more difficult. This can be explained by the effective size of hydrated Mg ion much larger than that of Ca one. The influence of zeolite structure can be also observed the product ZPI-12, a mixture of A and X zeolites, exchanges Mg ions much faster.

Since the unfavourable influence of exchanging counter-ion (in this case Na^+, which in real conditions of washing is found in large amount generative not only by zeolite exchange reaction also by the other subsidiary components in detergent (Na_2CO_3, NaTPP, Na_2SO_4, bleaching agent, etc.)) is known, the zeolites behaviour in ion exchange process in presence of different amounts of Na^+ has been carried out. The results in Fig. 6 point out, on the one hand, the strong influence exhibited by high concentrations of Na^+ on

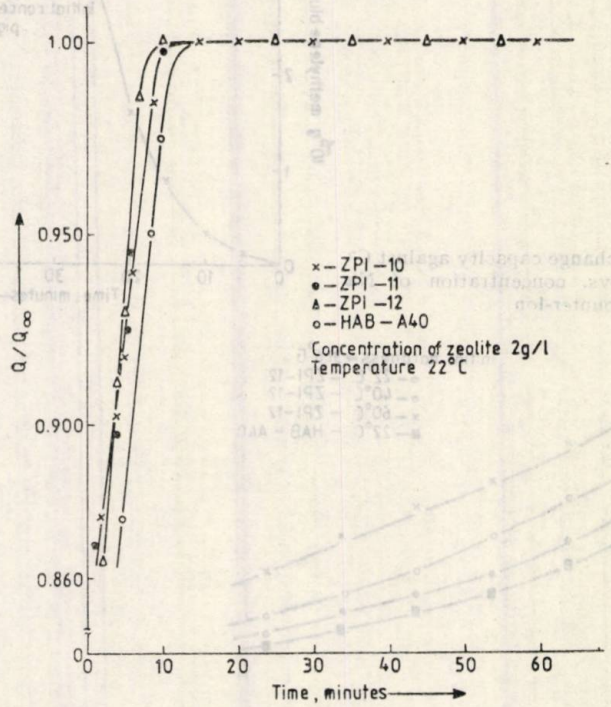

Fig. 4. — Saturation degree with Ca^{2+}, f or tested products, vs. time.

ion exchange capacity decrease, in the temperature range of 22°...60°C, and on the other hand, a very good agreement as regards the behaviour of the reference product HAB-A40.

During water softening by Ca and Mg ions retaining, zeolites exhibit in washing medium also another favourable action, i.e. adsorption of molecular dispersed pigments. To prove this fact, the adsorption of methylene blue, as reference positive charged pigment, has been studied (Fig. 7). It can be seen that methylene blue molecules are adsorbed on anionic zeolitic carcass by electrostatic forces, fact representing an advantage in washing process.

4. Conclusions

Analysis of physico-chemical properties, which are involved in efficacity of zeolites utilization in washing process, points out for the zeolite products ZPI, on the one hand, a good agreement with those of the commercial product HAB-A40 and, on the other hand, a significant diminishing of iron ions content in zeolite, due to the presence of triethanolamine in the hydrothermal synthesis medium.

Retaintion kinetics of Ca and Mg ions is influenced by concentration of sodium ions resulted from ion exchange or from the compounds, causing the ionic strenght of detergents.

Adsorption studies of the molecular dispersed pigments show a good retaintion capacity against those positively charged simultaneously, with the softening action of the water in washing float.

Received, May 10, 1985

Polytechnic Institutes, Jassy,
Department of Physical and
General Chemistry

REFERENCES

1. Berth P., J. Am. Oil Chem. Soc., **55**, 52 (1978).
2. Schwuger M.Y., Smolka H.G., Coll. Polym. Sci., *254*, 1 062 (1976).
3. Smolka H.G., Schwuger M.Y., Coll. Polym. Sci., *256*, 270 (1978).
4. Schwuger M. Y., Smolka H. G., Coll. Polym. Sci., *256*, 1 014 (1978).
5. * * * European Chemical News, 35 (1977).
6. * * * *Natriumaluminosilikat HAB-A40 Degussa.*
7. Cruceanu M., Popovici Ev., Patent R.S.R., Nr. *81 891* (1975).
8. Reichenberg D., J. Am. Chem. Soc., **76**, 579 (1953).
9. Despotovic R., Croat. Chem. Acta., **48**, 683 (1976).
10. Berth P., Jakovi G., Schmadel E., Schwuger M.Y., Krach C., Angew. Chem., **87**, 115 (1975).
11. Jakovi G., Schwuger M.Y., Chem. Z., **99**, 182 (1975).
12. Vincekovic N.F., Sekovanic L., Zitnic D., Technology, **27**, 251 (1980).
13. Cruceanu M., Popovici Ev., An. Şt. Univ. „Al. I. Cuza", Iaşi, **19**, 2, s. I,209 (1973).
14. * * * DIN 5 394, 1978.
15. * * * DIN 53 200, 1978.

ZEOLIŢI SINTETICI PENTRU CONDIŢIONAREA DETERGENŢILOR
I. PROPRIETĂŢILE FIZICO-CHIMICE ALE ZEOLIŢILOR

(Rezumat)

Cu scopul de a găsi o substituţie cît mai corespunzătoare, din punct de vedere economic, toxicologic şi ecologic, a tripolifosfatului de sodiu din amestecurile detergente, se cercetează unele proprietăţi fizico-chimice care condiţionează utilizarea zeoliţilor sintetici NaA în calitate de component subsidiar în recepturile detergente.

Utilizarea zeoliţilor în procesele de condiţionare a detergenţilor se bazează pe valoarea ridicată a capacităţii de schimb ionic faţă de ionii de calciu şi de magneziu şi pe cinetica rapidă a schimbului ionic.

Se cercetează dependenţa proprietăţilor de schimb ionic în funcţie de mărimea particulelor, de temperatură, de concentraţia ionilor de calciu şi magneziu, de pH şi de concentraţia contraionilor de sodiu.

BULETINUL INSTITUTULUI POLITEHNIC DIN IAŞI
Tomul XXXI (XXXV), Fasc. supl., 1985
Secţia II
CHIMIE ŞI INGINERIE CHIMICĂ

D.C. 546.264 ; 661.521

STUDY OF THE CALCIUM CARBONATE DECOMPOSITION PROCESS WITH SOLID AMMONIUM CHLORIDE

BY

AL. SZÉP, LIVIA IFRIM, CORNELIA LEONTE and C. CALISTRU

1. Introduction

The development in sustained rate of some industries, great users of soda ash, involved relative high rates in manufacture of this product. However, due to some large disadvantages of the Solvay's procedure, its manufacture development is troubled by a series of factors such as surface water pollution and loss of raw materials [1] ... [3].

These aspects imposed the approach of investigations regarding the modification of present technology on the line of opening the classical manufacture cycle with obtention of solid ammonium chloride by different methods such as evaporation, cooling and salting out, [1], [4], [5] as a recycling procedure of „orientation agent", i.e. ammonia. The separated solid ammonium chloride can be employed to decompose calcium carbonate, a process under study in the present paper. The process allows, besides ammonia recycling, obtention also of gases product, necessary in carbonation step, with lower energy consumption than for those produced by present—day lime furnaces. In addition, the obtained solid ammonium chloride can be used in other different fields of national economy such as industry, agriculture, constructions, etc. [1], [4], [6] ... [8].

The present paper deals with macrokinetic mechanism and mathematical modelling of the process of calcium carbonate decomposition with solid ammonium chloride.

2. Macrokinetic Mechanism

If ammonium chloride of technical degree is employed to decompose different qualities of calcium carbonate, at thermical levels corresponding to „sublimation" of ammonium chloride, the macrokinetic mechanism of the process can be represented by the equations :

$$[CaCO_3 + A'']_{s_1} + [NH_4Cl + A'']_{s_2} + [A_3'']_g \rightarrow$$

$$\{[CaCO_3 + A'']_{s_1} + [NH_4Cl + A'']_{s_2} + [CaCl_2 + A'']_{s_3}\}_g + [NH_3 + \tag{1}$$

$$+ HCl + CO_2 + H_2O + NH_4Cl + A_3'']_g,$$

$$NH_4Cl_{[]_s} \rightarrow NH_4Cl_{[]_g} \tag{2}$$

$$NH_4Cl \rightleftharpoons HCl + NH_3, \tag{3}$$

$$CaCO_3 + 2HCl = CaCl_2 + H_2O + CO_2. \tag{4}$$

If the temperature is greater than that of the $CaCl_2 . nH_2O$ crystallohydrates formation, the three macroscopic elemental processes, i.e. (2), (3)

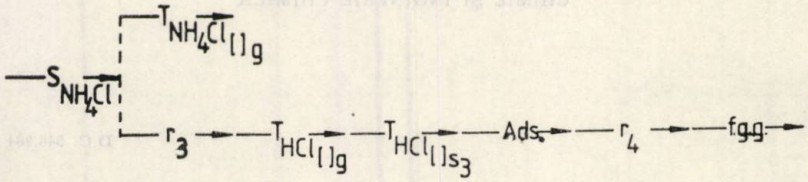

Fig. 1. — Structure of the process.

and (4), describe with enough precision the real process, so that the process structure is that given in Fig. 1.

The structure presented in Fig. 1 shows that at both the level of ammonium chloride granule as well as calcium carbonate granule the process under study can be included in unitary process of adsorption reaction formation and growing of germs type (ads. — r — f.c.g.) [9], [10].

3. Mathematical Modelling

3.1. Mathematical Models of Mass Balance

In order to develop the mathematical models of mass balance, the transformation degree of the three elemental process have been defined and, on the basis of transformation relations :

$$\overset{0}{m}_{CaCO_3[]_{s_1}}\eta = \frac{M_{CaCO_3}}{M_{CaCl_2}} m_{[]_s} \overline{X}_{CaCl_2[]_s}, \tag{5}$$

$$\overset{0}{m}_{NH_4Cl[]_{s_2}}\eta_{[]} = \overset{\circ}{m}_{NH_4Cl[]_{s_2}} - m_{[]_s} \overline{X}_{NH_4Cl[]_s}, \tag{6}$$

$$\overset{0}{m}_{NH_4Cl[]_{s_2}}\eta_{[]}\eta_{NH_4Cl} = \frac{M_{NH_4Cl}}{V_M} V_{[]_g} X_{NH_3[]_g}, \tag{7}$$

the mathematical models of secondary balances for components and phases, have been established. These balances are given in Table 1.

To solve the mathematical models from Table 1, the determination of three quantities is necessary, namely : $\overline{X}_{CaCl_2[]s}$, $\overline{X}_{NH_4Cl[]s}$ and $X_{NH_3[]g}$. The first two quantities do not involve special problems, but determination of $X_{NH_3[]g}$, is not possible.

If X'_{NH_3} is the content of ammonia in gaseous phase, the balance of this phase is given in Table 2.

3.2. Macrokinetical and Mathematical Models

The possible macrokinetic models of the process have been established based on the macrokinetic modelling theory [9] (s. Table 3).

Under fixed bed conditions, the macrostructural element can be made up by calcium carbonate granule surrounded by gaseous phase of HCl, CO_2, H_2O, A_3'' and NH_3.

Table 1

Mathematical Models of Mass Balance

Phase	Component	$m(V)$
Solid	$CaCO_3$	$m_{CaCO_3[]_s} = m^0_{[]_{s1}} \bar{X}_{CaCO_3[]_1} - \frac{M_{CaCO_3}}{M_{CaCl_2}} m_{[]_s} \bar{X}_{CaCl_2[]_s}$
	NH_4Cl	$m_{NH_4Cl[]_s} = m_{[]_s} \bar{X}_{NH_4Cl[]_s}$
	$CaCl_2$	$m_{CaCl_2[]_s} = m_{[]_s} \bar{X}_{CaCl_2[]_s}$
	A″	$m_{A''} = m^0_{A''_1[]_{s1}} + m^0_{A''_2[]_{s2}}$
	Total	$m_{[]_s} = \frac{m^0_{[]_{s1}} + m^0_{[]_{s2}} (1 - \bar{X}^0_{NH_4Cl[]_{s2}})}{1 - 0{,}99\bar{X}_{CaCl_2[]_s} - \bar{X}_{NH_4Cl[]_s}}$
Gaseous	NH_3	$V_{NH_3[]_g} = V_{[]_g} X_{NH_3[]_g}$
	CO_2	$V_{CO_2[]_g} = \frac{V_M}{M_{CaCl_2}} m_{[]_g} \bar{X}_{CaCl_2[]_s}$
	HCl	$V_{HCl[]_g} = V_{[]_g} X_{NH_3[]_g} - 2\frac{V_M}{M_{CaCl_2}} m_{[]_g} \bar{X}_{CaCl_2[]_s}$
	H_2O	$V_{H_2O[]_g} = \frac{V_M}{M_{CaCl_2}} - m_{[]_s} \bar{X}_{CaCl\,[]_s}$
	NH_4Cl	$V_{NH_4Cl[]_g} = \frac{V_M}{M_{NH_4Cl}} (m^0_{[]_{s2}} \bar{X}^0_{NH_4Cl[]_{s2}} - m_{[]_s} \bar{X}_{NH_4Cl[]_s}) - V_{[]_g} X_{NH_3[]_g}$
	A''_3	$V_{A''[]} = V^0_{A''[]_g}$
	Total	$V_{[]_g} = \frac{\left(m^0_{[]_{s^2}} \bar{X}^0_{NH_4Cl[]_{s2}} - \frac{m^0_{[]_{s1}} + m^0_{[]_{s2}} (1 - \bar{X}^0_{NH_4Cl[]_{s2}})}{1 - 0{,}99\bar{X}_{CaCl_2[]_s} - \bar{X}_{NH_4Cl[]_s}} \right) \frac{V_M}{M_{NH_4Cl}} + V^0_{[]_g}}{1 - X_{NH_3[]_g}}$

Table 3

Macrokinetic and Mathematical Models

Controlling step	Macrokinetic model	Mathematical model for a macrostructural element
Transfer of HCl through gaseous phase	$(-\bar{q}) = K_{T HCl[]_g} C_{HCl[]_g}$	$\frac{\rho^* R}{3} \cdot \frac{d\eta}{d\tau} = K_{T HCl[]_g} C_{HCl[]_g}$
Transfer of HCl through crust	$(-\bar{q}) = D_{HCl} \frac{\partial C_{HCl}}{\partial X}$	$\frac{\rho^* R d\eta}{3(1-\eta)^{2/3} d\tau} = \frac{1}{2} D_{HCl} \frac{\partial C_{HCl}}{\partial X}$
Chemical reaction	$(-\bar{r}) = K C^n_{HCl}$	$\tau = \frac{2\rho^* R}{3 K C^0_{HCl}} \int_0^\eta (1-\eta)^{n+2/3} d\eta$
Formation and growing of germs	$(-\bar{r}) = K C^n_{HCl} \tau^{-m}$	$\frac{2\rho^* R d\eta}{3 d\tau} = K(1-\eta)^{2/3+n} \tau^{-m}$ $\ln[-\ln(1-\eta)] = \ln K^* + (1-m)\ln\tau$ for $n = 1/3$

Table 1

Mathematical Models of Mass Balance

Phase	Component	$m(\Gamma)$
Solid	$CaCO_3$	$m_{CaCO_3}(\Gamma) = m_{[1]}^0 \bar{X}_{CaCO_3}(\Gamma) - \frac{M_{CaCO_3}}{M_{CaCl_2}} m_{[1]}^0 \bar{X}_{CaCl_2}(\Gamma)$
	NH_4Cl	$m_{NH_4Cl}(\Gamma) = m_{[1]}^0 \bar{X}_{NH_4Cl}(\Gamma)$
	$CaCl_2$	$m_{CaCl_2}(\Gamma) = m_{[1]}^0 \bar{X}_{CaCl_2}(\Gamma)$
	A^{α}	$m_{A^{\alpha}} = m_{A_1^{\alpha}}^0(\Gamma)_{\alpha} + m_{A_2^{\alpha}}^0(\Gamma)_{\alpha}$
	Total	$m_{[1]}^0 = \frac{m_{[1]}^0 + m_{[1]}^0(1-\bar{X}_{NH_4Cl}^0)_{\alpha}}{1 - 0{,}99\bar{X}_{CaCl_2}(\Gamma)_{\alpha} - \bar{X}_{NH_4Cl}(\Gamma)_{\alpha}}$
Gaseous	NH_3	$F_{NH_3}(\Gamma) = F_{[1]}\bar{X}_{NH_3}(\Gamma)$
	CO_2	$F_{CO_2}(\Gamma) = \frac{F_{\alpha}}{M_{CaCl_2}} m_{[1]}^0 \bar{X}_{CaCl_2}(\Gamma)$
	HCl	$F_{HCl}(\Gamma) = F_{[1]}\bar{X}_{NH_3}(\Gamma) - 2\frac{F_{\alpha}}{M_{CaCl_2}} m_{[1]}^0 \bar{X}_{CaCl_2}(\Gamma)$
	H_2O	$F_{H_2O}(\Gamma) = \frac{F_{\alpha}}{M_{CaCl_2}} m_{[1]}^0 \bar{X}_{CaCl_2}(\Gamma)$
	NH_4Cl	$F_{NH_4Cl}(\Gamma) = \frac{F_{\alpha}}{M_{NH_4Cl}}(m_{[1]}^0 \bar{X}_{NH_4Cl}^0(\Gamma) - m_{[1]}^0 \bar{X}_{NH_4Cl}(\Gamma)) = F_{[1]}\bar{X}_{NH_4Cl}(\Gamma)$
	A_3^{α}	$F_{A^{\alpha}}(\Gamma) = F_{A^{\alpha}}^0(\Gamma)$
	Total	$F_{[1]}^0 = \frac{\left(m_{[1]}^0 \bar{X}_{NH_4Cl}^0(\Gamma) - \frac{m_{[1]}^0 + m_{[1]}^0(1-\bar{X}_{NH_4Cl}^0)_{\alpha}}{1 + 0{,}99\bar{X}_{CaCl_2}(\Gamma) - \bar{X}_{NH_4Cl}(\Gamma)}\right)\frac{F_{\alpha}}{M_{NH_4Cl}} + F_{[1]}^0}{1 - \bar{X}_{NH_3}(\Gamma)}$

Table 3

Macrokinetic and Mathematical Models

Controlling step	Macrokinetic model	Mathematical model for a macrostructural element
Transfer of HCl through gaseous phase	$(-\bar{g}) = K_{HCl}^{\alpha}(\Gamma)_{\alpha} C_{HCl}^{\alpha}$	$\frac{\rho^{\alpha} R}{l}\frac{d\eta}{d\tau} = K_{HCl}^{\alpha}(\Gamma)_{\alpha} C_{HCl}^{\alpha}$
Transfer of HCl through crust	$(-\bar{g}) = D_{HCl}\frac{\partial C_{HCl}}{\partial X}$	$\frac{\rho^{\alpha} R d\eta}{(1-\eta)^2 l^2 d\tau} = \frac{1}{2} D_{HCl}\frac{\partial C_{HCl}}{\partial X}$
Chemical reaction	$(-\bar{r}) = KC_{HCl}^{\alpha}$	$\tau = \frac{2\rho^{\alpha} R}{3KC_{HCl}^0}\int_0^{\eta}(1-\eta)^{\alpha-2/3} d\eta$
Formation and growing of germs	$(-\bar{r}) = KC_{HCl}^{\alpha}\tau^{-\alpha}$	$\frac{2\rho^{\alpha} R d\eta}{3d\tau} = K(1-\eta)^{2/3+\alpha}\tau^{-\alpha}$ $\ln[-\ln(1-\eta)] = \ln K^{\alpha} + (1-\alpha)\ln\tau$ for $\alpha = 1/3$

Table 2

Balance Equations of the Gaseous Phase

Component	Equation
NH_3	$V_{NH_3} = \dfrac{V^0_{A\tilde{3}[]_g} + 2(V_M/M_{CaCl_2}) m_{[]_s} \overline{X}_{CaCl_2[]_s}}{1 - X'_{NH_3}} X'_{NH_3}$
H_2O	$V_{H_2O} = \dfrac{V_M}{M_{CaCl_2}} m_{[]_s} \overline{X}_{CaCl_2[]_s}$
CO_2	$V_{CO_2} = \dfrac{V_M}{M_{CaCl_2}} m_{[]_s} \overline{X}_{CaCl_2[]_s}$
NH_4Cl	$V_{NH_4Cl} = \dfrac{V_M}{M_{NH_4Cl}} (m^0_{[]_{s_2}} \overline{X}^0_{NH_4Cl[]_{s_2}} - m_{[]_s} \overline{X}_{NH_4Cl[]_s}) - \dfrac{V^0_{A\tilde{3}[]_g} + 2(V_M/M_{CaCl_2}) m_{[]_s} \overline{X}_{CaCl_2[]_s}}{1 - X'_{NH_3}} X'_{NH_3}$
HCl	$V_{HCl} = \dfrac{V^0_{[]_g} + 2(V_M/M_{CaCl_2}) m_{[]_s} X_{CaCl_2[]_s}}{1 - X'_{NH_3}} X'_{NH_3} - 2V_M/M_{CaCl_2} m_{[]_s} \overline{X}_{CaCl_2[]_s}$
$A\tilde{3}$	$V_{A\tilde{3}} = V^0_{A\tilde{3}}$
Total	$V_T = V^0_{A\tilde{3}[]_g} + \dfrac{V_M}{M_{NH_4Cl}} (m^0_{[]_{s_2}} \overline{X}^0_{NH_4Cl[]_{s_2}} - m_{[]_s} \overline{X}_{NH_4Cl[]_s}) + \dfrac{V^0_{[]_g} + 2(V_M/M_{CaCl_2}) m_{[]_s} \overline{X}_{CaCl_2[]_s}}{1 - X'_{NH_3}} X'_{NH_3}$

In isothermic discontinuous regime, without volume variation in the Eq. (4) ($\Delta n = 0$) and, for a spherical granule, the model of macrostructural element has the form :

$$\frac{\rho^* R}{3} \cdot \frac{d\eta}{(1-\eta)^{2/3} d\tau} = -(-\dot{r}_{CaCO_3}). \tag{8}$$

The mathematical models based on macrokinetical models, developed by using Eq. (8), are presented in Table 3.

4. Mathematical Model of Real Development of the Process

4.1. Experimental

Decomposition of calcium carbonate with ammonium chloride has been carried out in a device simulating batch reactor with fixed bed. The mixture of raw materials, weighted with high precision, in short porcelain crucibles, entered the muffle furnace at constant temperature. After dif-

ferent time, the samples have been taken out and „congelated" by dissolving in bidistilled water. Then the content of $CaCl_2$ and NH_4Cl was quantitatively determined from the resulted solution.

The transformation degree has been calculated with the relation:

$$\eta = \frac{m_{CaCl_2[]L}}{\frac{M_{CaCl_2}}{M_{CaCO_3}} \overset{0}{m}_{[]_{s1}} X^0_{CaCO_3[]s_1}} \cdot \tag{9}$$

The experiments have been performed in the temperature range of 473°...773° K, granule size $\bar{d}_{p1}=0{,}315$ mm ; $\bar{d}_{p2}=0.085$, 0.225 and 0.565 mm, the excess of ammonium chloride of 0 ; 50 and 100%, moisture content of 0 ; 10 ; 20 and 30%, reported to dried calcium carbonate, without circulation of gaseous phase.

4.2. Results and Discussion

The experimental data, presented in Figs. 2...5, show the following:

a) The temperature has a significant and favourable influence on overall rate of the process, independent of granule size, ammonium chloride excess and moisture content (Fig. 2).

b) The granule size of lime stone has also a significant influence. As granule size increases, the transformation degree decreases (Fig. 3).

The other parameters, i.e. the granule size of ammonium chloride, its excess and moisture, have no significant influence on the overall rate of the process (Figs. 4 and 5).

4.3. Determination of the Mathematical Model Describing the Real Development of the Process under Given Experimental Conditions

In order to establish the above mentioned model, the primary experimental data have been graphically processed. For this reason, the data have been plotted in coordinates proper to the equations summarized in Table 3.

The experimental data are in good agreement with the model described by the equation:

$$\ln [-\ln(1-\eta)] = \ln K^* + (1-m) \ln \tau, \tag{10}$$

plotted in Fig. 6.

Fig. 6 shows that in the investigated temperature range, these are two distinct regions.

The experimental factor $1-m$ and the constant K^* of Eq. (10), calculated graphically, are given in Table 4.

Under the conditions mentioned in Table 4, the mathematical model that describes the real development of the process is:

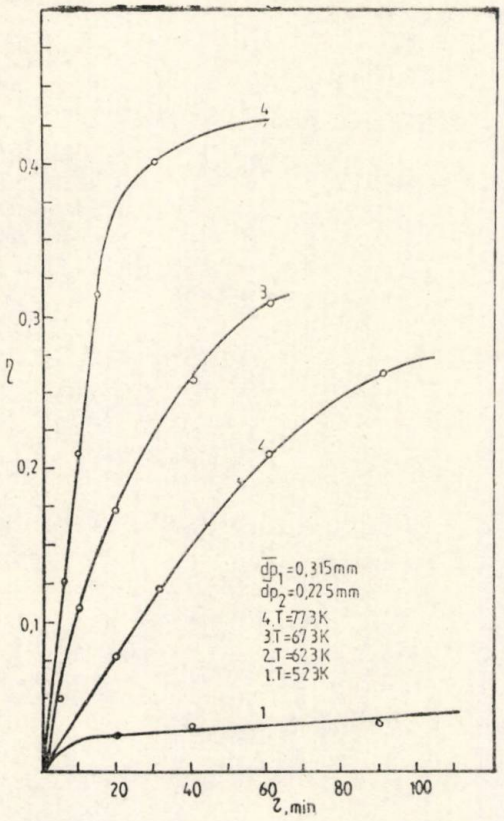

Fig. 2. — Dependence η vs. τ at different temperatures.

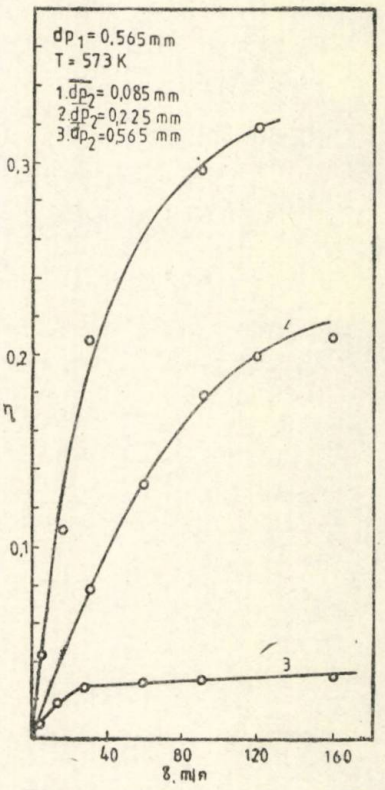

Fig. 3. — Dependence η vs. τ for different granule size of limestone.

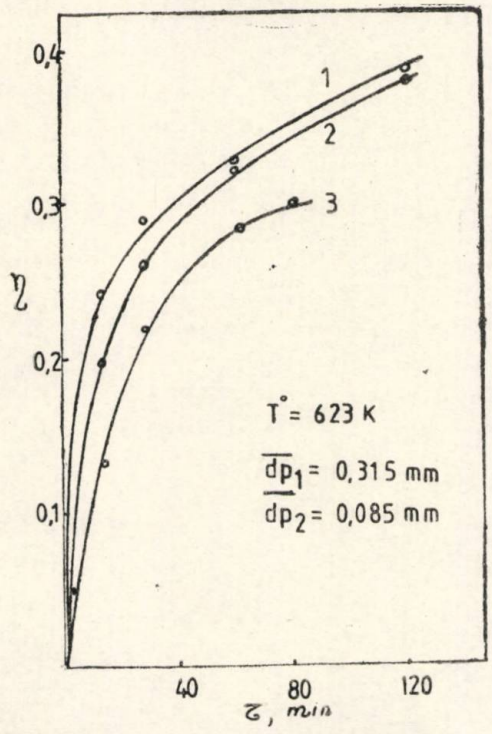

Fig. 4. — Dependence η vs. τ for different excess of ammonium chloride: *1*— 100%; *2*— 50%; *3*— 0%.

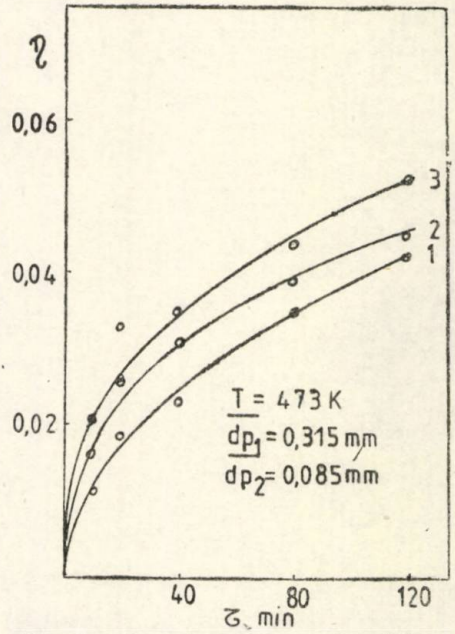

Fig. 5. — Dependence η vs. τ for different moistures : *1*— 10% ; 2-20% ; *3*— 30%.

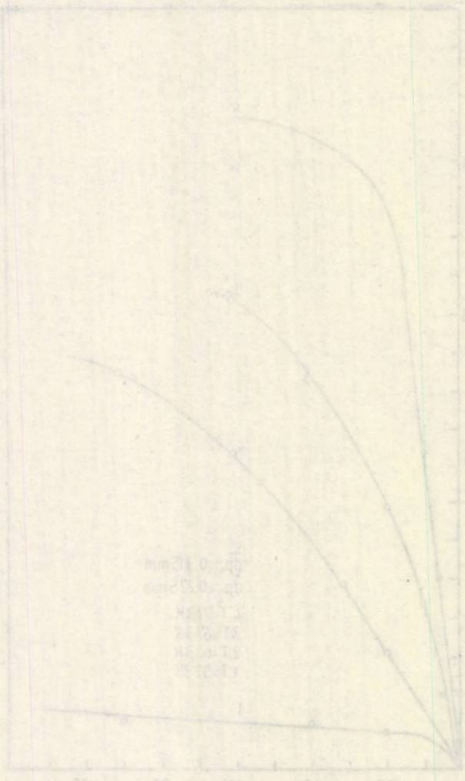

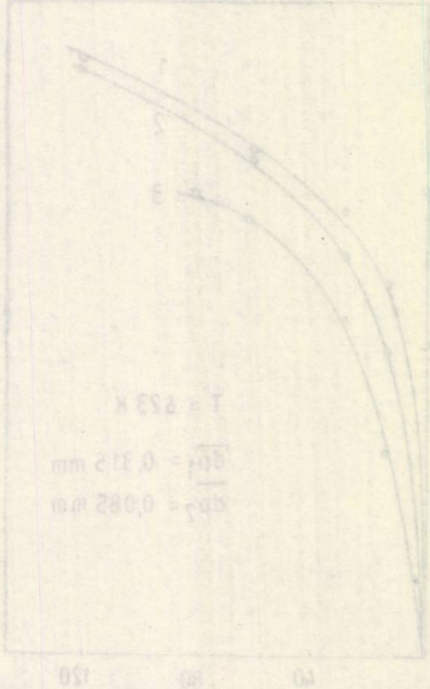

Table 4

Values of $1-m$ *and* K^* *for* $\overline{d}_{p_1}=0.315$ *mm and* $\overline{d}_{p_2}=0.225$ *mm*

Experimental conditions		Region 1		Region 2	
NH_4Cl excess, [%]	T, [°K]	$1-m$	K^*	$1-m$	K^*
0.0	773	0.952	0.0268	0.35	0.1561
	673	1.041	0.0107	—	—
	623	1.000	0.0039	0.275	0.0248
50.0	673	1.030	0.025	0.250	0.2446
	623	1.000	0.013	0.250	0.1553
	573	0.980	0.004	0.250	0.0780
	523	0.955	0.023	—	—

Table 5

Values of A *and* E *from Eq.* (13)

Conditions		Region	A	E cal/mol
NH_4Cl excess %	$\overline{d}_{p_2}$ mm			
100	0.085	1	10.3	5 001.0
		2	207.0	8 933.0
50	0.565	1	99.5	11 081.6
		2	10.88	5 129.0

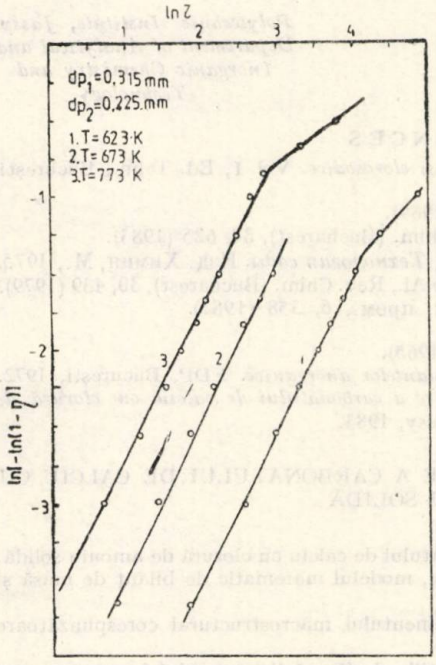

Fig. 6. — Dependence $\ln[-\ln(1-\eta)]$ vs. $\ln \tau$ at different temperatures.

(11) $$\eta = 1 - e^{K^*\tau}$$

for the region *1* and

(12) $$\eta_i = 1 - e^{K^*\sqrt[4]{\tau}}$$

for the region *2*, namely equations describing the process of formation and growing of solid germs.

Dependence of K^* on temperature, under mentioned working conditions, is given by an Arrhenius' equation:

(13) $$K^* = Ae^{-E/RT},$$

where A and E depend on working conditions as shown in Table 5.

5. Conclusions

From the theoretical and experimental investigations presented above, the following conclusion may be drawn:

1. The macrokinetic mechanism, the mass balance models and mac-

rokinetic and mathematical models that describe quantitatively the development of decomposition process of calcium carbonate with ammonium chloride have been established.

2. The experimental results, obtained under the conditions of a fixed bed batch reactor, are in good agreement with mathematical model given by Eqs. (10)...(12), i.e. the controlling step of the process is the formation and growing of solid germs.

Notations

m_{A_i}, V_{A_i} — mass or volume of A_i, [Kg]; [m^3];
X_{A_i}, $\overline{X}_{A_i}$ — mass or volume fraction of A_i;
M_{A_i} — molecular weight of A_i, [Kg/Kmol];
V_M — molar volume, [m^3/Kmol];
n_{A_i} — moles of component A_i;
C_{A_i} — concentration of A_i, [mol/m^3];
τ — reaction time, [s];
ρ^* — molar density of solid, [Kmol/m^3];
R — granule radius, [m];
K_T — transfer constant, [m/s];
D — diffusion coefficient, [m^2/s];
d_{p_1} — average diameter of NH_4Cl particle, [mm];
d_{p_2} — average diameter of lime stone particle, [mm];
n — reaction order;
$1-m$ — exponential factor.

Symbols

$[\ ]_{g,s_1,\ldots_3}$ — gaseous phase 1 and solid phase 1, 2 and 3;
0 — initial instant.

Received, April 18, 1985

Polytechnic Institute, Jassy,
Department of Analytical and Inorganic Chemistry and Technology

REFERENCES

1. Filipescu L., *Tehnologia produselor sodice şi clorosodice.* Vol. I, Ed. Tehn., Bucureşti, 1983, 268.
2. Peteu I., Rev. Chim. (Bucharest), **19**, 72 (1969).
3. Calistru C., Ifrim L., Szép Al., Rev. Chim. (Bucharest), **34**, 625 (1983).
4. Сокин И.Н., Красенинников С.А., *Технология соды.* Изд. Химия, М., 1975.
5. Calistru C., Ifrim L., Leonte C., Szép Al., Rev. Chim. (Bucharest), **30**, 439 (1979).
6. Ткач Г.А., Михаилов Ф.К., Хим. пром., *6*, 358 (1981).
7. Ana I., Petrol şi gaze, **24**, 205 (1973).
8. Salecki, A., Przem. Chemyczny, **45**, 555 (1965).
9. Calistru C., Leonte C., *Tehnologia substanţelor anorganice.* EDP, Bucureşti, 1972.
10. Szép Al., *Modelarea procesului de descompunere a carbonatului de calciu cu clorură de amoniu.* Ph., D. Diss., Polyt. Inst., Jassy, 1983.

STUDIUL PROCESULUI DE DESCOMPUNERE A CARBONATULUI DE CALCIU CU CLORURĂ DE AMONIU SOLIDĂ

(Rezumat)

Se cercetează procesul descompunerii carbonatului de calciu cu clorură de amoniu solidă. Se stabileşte mecanismul macrocinetic al procesului, modelul matematic de bilanţ de masă şi se indică mărimile necesare rezolvării acestuia.

Se elaborează modelele matematice ale elementului macrostructural corespunzătoare modelelor macrocinetice posibile.

Rezultatele experimentale obţinute în condiţiile desfăşurării procesului într-un reactor în strat fix şi în regim izoterm sînt verificate de modelul matematic corespunzător modelului macrocinetic transformare.

BULETINUL INSTITUTULUI POLITEHNIC DIN IAŞI
Tomul XXXI (XXXV), Fasc. supl., 1985
Secţia II
CHIMIE ŞI INGINERIE CHIMICĂ

C.D. 547.792

ISOMÈRES *E* ET *Z* D'YLURES DE 1-2-4H TRIAZOLUM

PAR

MAGDA PETROVANU, GH. SURPĂŢEANU, MIRCEA CONSTANTINESCU
et ALAIN LABLACHE COMBIER

1. Introduction

Dans une Note antérieure [1] on a montré que dans les cyclimmonium ylures (1) il n'existe pas de rotation libre autour de la liaison $\overset{+}{N} - \overset{-}{C}$.

La barrière d'énergie autour de cette liaison, calculée à l'aide de la méthode de CNDO/2, [2], est de 14 Kcal/mol. Il est connu que les cycloimmonium ylures dans lesquels le carbanion et le hétérocycle sont coplanaires ont une stabilité chimique appreciable [3]. Nous rappelons dans ce sens le fait que pour la dicyanopyridine (2) les données par les spectres de diffraction des rayons X confirment la coplanarité de l'ensemble ylurique [4].

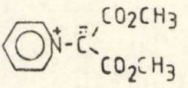

(1)

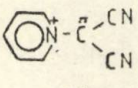

(2)

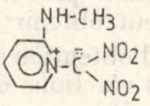

(3)

Toutefois récemment [5] on a montré qu dans l'ylure (3) cristallisé le plan du hétérocycle et le plan du carbanion ylurique font un angle de 92°. Ce résultat paraît être en contradiction avec les considérations qualitatives généralement acceptées selon lesquelles les systèmes yluriques plans sont plus stables parce que dans ces conditions tant la délocalisation prononcée de la charge négative sur le carbanion ylurique que l'interaction de résonance sont mieux assurées.

Les résultats expérimentaux ci-dessus mentionnés, tant pour l'ylure (2) que pour l'ylure (3), imposent la conclusion qu'il faut effectuer des mesures sur chaque système ylurique en particulier et en plus il faut aussi tenir compte de l'état dans lequel se trouvent les systèmes yluriques, c'est-à-dire en solution ou cristallisés.

2. Résultats et discussions

Le fait qu'il n'existe pas de rotation libre autour de la liaison ylurique nous a suggéré l'idée de synthétiser des systèmes yluriques dissymétriques qui pourraient exister sous forme des isomères *E* et *Z*. Ainsi, à partir des

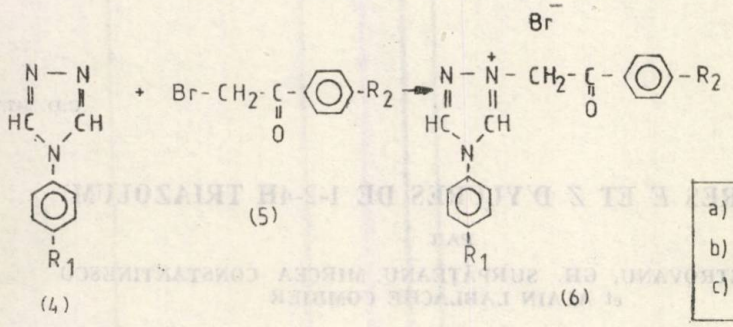

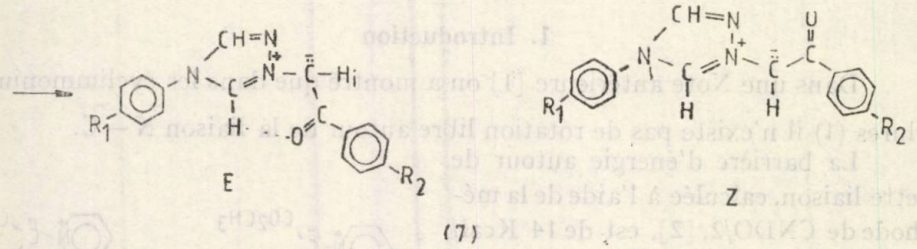

sels de cycloimmonium provenant du [1,2-4H] triazole traités par la triéthylamine on peut obtenir les triazolium ylures isomères 7*E* et 7*Z*.

Les méthodes d'obtention des ylures (7) *in situ* afin de les utiliser comme dipoles 1 3 dans des réactions de cycloaddition sont décrites dans des travaux antérieurs [7], [8].

Les ylures (7 *b*) et (7 *c*) sont stables; par contre l'ylure (7 *a*) souffre une réaction de dimérisation par cycloaddition 3 + 3 conduisant aux produit (8 *a*). Cette transformation implique une aromatisation.

Les ylures (7 *b*) et (7 *c*) existent sous forme d'isomères *E* et *Z*. Les spectres RCN-H[1] des sels (6 *a*, *b*, *c*), ceux des ylures (7 *b*, *c*) et des dimères (8) diffèrent beaucoup entre eux.

Dans les sels (6) le carbone méthylénique est tétraédrique, dans les ylures (7) le carbanion ylurique est trigonal. Le produit (8) ne possède que des protons aromatiques.

Dans le produits (7 *b*) et (7 *c*) le proton ylurique H_i et le proton H_5 résonent chacun à des fréquences différentes. Dans les deux cas la somme des intégrales des deux pics H_i et H_5 correspond à un proton.

Les intensités relatives des deux pics correspondants aux pro-

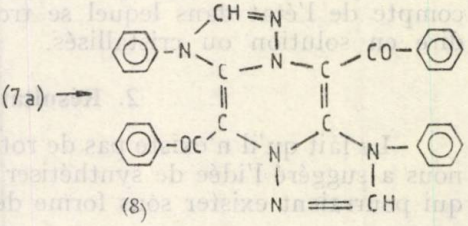

Tableau 1

Caractéristiques RMN-H¹ des sels et des ylures de cycloimmonium

Composé	Valeurs (ppm)[a]	Composé	Valeurs (ppm)[a]
(6 *a*)	6.53.*s*.2H(CH_2) 7.86.*m*.10H(2Ph) 10.03.*s*.1H.(H-3) 11.09.*s*.1H(H-5)	(6 *b*)	6.53.*s*.2H(CH_2) 7.80.*m*.5H(Ph) 8.34.*j*.8.52.4h(Ph-NO_2) J_{AB}=9.23 9.93.*s*.1H(H-3) 10.83.*s*.1H(H-5)
(6 *c*)	2.44.*s*.3H(CH_3) 6.53.*s*.2H(CH_2) 7.52 ; 7.81.4H(Ph−CH_3) J_{AB}=8.58 8.33 ; 8.51.4H(Ph−NO_2) J_{AB}=9.23 9.90.*s*.1H(H-3) 10.80.*s*.1H(H-5)	(7 *b*)(*E*+*Z*)	7.09.*s*.H_t(*E*) 7.17.*s*.H_t(*Z*) 7.71.*m*.5H(Ph) 8.15 ; 8.28.4H(Ph−NO_2) J_{AB}=8,36 9.05.*s*(H-5)(*Z*) 9.52.*s*.1H.(H-3)(*E*+*Z*) 11.51.*s*.(H-5)(*E*)
(7 *c*)(*E*+*Z*)	2.44.*s*.3H(CH_3) 7.04.*s*.H_t(*E*) 7.13.*s*.H_t(*Z*) 7.42 ; 7.72.4H(Ph−CH_3) J_{AB}=8,39 8.02 ; 8.18.4H(Ph−NO_2) J_{AB}=8,36 9.02.*s*.H-5(*Z*) 9.49.*s*.1H.H-3(*E*+*Z*) 11.51.*s*.H-5(*E*)	(8 *a*)	7.50 ; 812.*m*.20H(4Ph) 9.92.*s*.2H(H-3)

s=singulet ; *m*=multiplet ; *AB*=spectre *AB* aromatique ; *a*=80 Mz ; DMSO-d_6.

tones H_t et H_t du produit (7 *b*) sont constantes même si on varie la température entre 20°...45°C, le solvant utilisé étant le DMSO-d_6. Le spectre des ylures (7 *c*) est le mieux résolu. Dans le cas ou l'ylure (7 *c*) est obtenu à partir du sel de cycloimmonium correspondant, en présence de triéthylamine en milieu chloroformique, (synthesè (1)), le rapport entre les isomères *E* et *Z* est de 0.82. La synthèse du même ylure à partir du sel (6 *c*) et la triéthylamine dans la DMSO-d_6 comme solvant conduit à un mélange des isomères *E* et *Z* en rapport 4.55.

Il résulte des données ci-dessus que la proportion des isomères *E* et *Z* se modifie en fonction de la nature du milieu réactionnel et de la température.

Les spectres IR des ylures (7) confirment l'existence des isomères *E* et *Z*. Pour concrétiser il faut mentionner que lorsque la forme *Z* est prédominante dans le spectre de l'ylure (7 *c*) on constate l'apparition d'une bande d'absorption $\nu_{C=O}$ à 1 660 cm^{-1}, fréquence d'absorbtion classique

des groupements carbonyliques attachés à un atome de carbone ylurique [3], [9]. Par contre dans les échantillons dans lesquells la forme *E* est prédominante cette bande d'absorption se déplace vers 1 600 cm^{-1}. Ce fait met en évidence l'existence d'une très forte liaison d'hydrogène intramoléculaire.

En conclusion on peut apprécier qu'il est possible à obtenir des isomères *E* et *Z* à partir des 1, 2, 4-4H triazoles en modifiant la nature du milieu réactionnel dans le processus de transformation des sels de cycloimmoinium (6) dans les ylures correspondants (7). Comme solvants on a utilisé le chloroforme et le diméthylsulfoxyde. La température à laquelle se produit la réaction joue un rôle important dans l'établissement d'un certain rapport entre les isomères *E* et *Z*.

Dans le DMSO, des températures plus élevées contribuent à l'augmentation du contenu en isomère *Z*.

3. Partie expérimentale

a) *Variante Nr. 1.* On dissout (on suspend) 0.01 mol de sel de triazolium (6 *a*, *b*, *c*) dans 50 ml de chloroforme à une température de 10° ... 15°C. On ajoute, en agitant continuellement pendant 10 ... 15 min., 0.015 mol de triéthylamine. La solution se colore. On filtre le bromhydrate de triéthylamine. La solution chloroformique est lavée trois fois à l'eau, séchée sur Na_2SO_4 anhydre et concentrée. On ajoute de l'éther de pétrole et on précipite les ylures (7 *a*, *b*, *c*). On fait enregistrer les spectres RMN-H^1 pour les produits bruts obtenus.

b) *Variante Nr. 2.* On dissout le sel de triazolium (6 *a*, *b*, *c*) dans du DMSO-d_6, dans un tube RMN. On ajoute dans le tube la quantité équivalente de triéthylamine. On fait enregistrer le spectre RMN de l'ylure (7). On chauffe la même épreuve. Dans le cas de l'yure (7 *a*) si on chauffe pendant 20...30 min. à 65°C, on constate la formation du dimère (8 *a*). Dans le cas de l'ylure (7 *c*) en chauffant on constate l'augmentation de l'isomére (7 *c*) *Z* dans le mélange.

Reçue le 16 avril 1985

Institut Polytechnique, Jassy,
Chaire de Chimie et Technologie
organique et macromoleculaire,
Université „Al. I. Cuza", Jassy
Centre de Calcul,
et
Laboratoire de chimie organique
et macromoléculaire.
Université des Sciences et Technique, Lille, France

BIBLIOGRAPHIE

1. Surpăţeanu G., Constantinescu M., Lablache Combier A., Theor. Chem. Acta (sous presse).
2. Pople J.A., Beveridge D.L., *Aproximate Molecular Orbital Theory*. Mc. Graw-Hill, N.Y., 1970, QCPE-141.
3. Zugrăvescu I., Petrovanu M., *N-ylide Chemistry*. Mc. Graw Hill, N.Y., 1976.
4. Bugg C., Desiderato R., Sass R.L., J. Am. Chem. Soc., **86**, 3, 157 (1964).
5. Bailey N.A., Newton C.G., Cryst. Struct. Commun., **9**, 49 (1980).
6. Surpăţeanu G., Catteau J.P., Karafiloglou P., Lablache Combier A. Tetrahedron Report, 23 (1976).

7. Petrovanu M., Luchian C., Surpăţeanu G., Bărboiu V., Rev. Roum. Chim., **24**, *5*, 733 (1981).
8. Petrovanu M., Luchian C., Surpăţeanu G., Bărboiu V., Tetrahedron, **39**, *14*, 2 417 (1983).
9. Johnson A.W., *Ylide Chemistry*. Academic Press, N.Y., 1966.

IZOMERII *E* ŞI *Z* AI ILURILOR DE 1,2-4H TRIAZOL

(Rezumat)

S-au caracterizat izomerii *E* şi *Z* ai *p*-nitrobenzoil, 4-*p*-tolil-[1,2-4H] triazolmetilidă (7 *b*) şi *p*-nitrobenzoil, 4-p-fenil [1,2-4H] triazolmetilidă (7 *c*). S-au sintetizat amestecuri de izomeri în diferite condiţii experimentale. Triazolilida (7 *a*) conduce la compusul (8 *a*) prin cicloadiţie dimeră.

BULETINUL INSTITUTULUI POLITEHNIC DIN IAŞI
Tomul XXXI (XXXV), Fasc. supl., 1985
Secţia II
CHIMIE ŞI INGINERIE CHIMICĂ

D.C. 547.458.6 ; 542.951.3 ; 661.724 ; 677.03

STARCH ESTERS AND ETHERS AS THICKENERS IN TEXTILE PRINTING

BY

GH. MIHĂILĂ, C. CIUGUREANU, N. BÎLBĂ, P. ONU, C. LUCA and N. NAUM

1. Introduction

The hydroxylic groups in the starch structure allow its chemical modification with different inorganic or organic reagents [1] ... [3] to starch esters and ethers with new properties which can be used as thickeners in the textile printing, as improved adhesives, as emulsion stabilizers and as thickeners for food.

Useful in the textile printing are, by their thickening properties, the starch esters and ethers with low degree of substitution, products with a water solubility greater than starch and which, after dye fixation on textiles, can be removed easily by washing with water.

The present paper deals with preparation, chemical and rheological characterization as well as technological testing of starch phosphates (I), (II) and acetate (III), 2-hydroxypropylstarch (IV) and 1-chlorine-2-hydroxypropylstarch (V), written below :

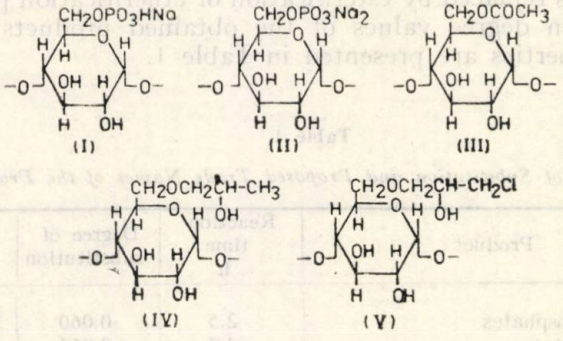

2. Experimental

The potato starch with 12...14% moisture and 0.1% ash was used in all cases.

2.1. Procedure

The starch phosphates (I) and (II) have been obtained by solid phase reaction of the starch with a mixture of sodium biphosphate and disodic phosphate at 140°...145°C for 2.5 hours. In order to realize a more uniform reaction mass, the starch was firstly impregnated in an aqueous solution of 41.5% disodic phosphate ($Na_2HPO_4 . 12 H_2O$) and 21.3% sodium biphosphate ($NaH_2PO_4 . H_2O$) with pH=6.5. The liquid/solid ratio was 2.7. After filtration, the impregnated starch dried to a remanent moisture of 8...9%, was esterified in a stainless steel reactor with mechanical stirring and heating oil jacket. During esterification, after each quarter a hour, the 30...40 g samples have been taken out, in which, after washing the excess of phosphates with a 50% methanol solution in water, the content of phosphorus and sodium has been determined. Since the molar ratio Na/P has ranged from 1.17 to 1.39, it results that a mixture of starch phosphates takes form (I) and (II) [4].

The starch acetate (III) has been obtained by treating with acetic anhydride a suspension of starch activated in acetone at 40°...45°C, in a digester with mechanical stirring, for 3.5 hours. The acetic anhydride/starch ratio was 0.4 moles to a glucose unit.

The starch ethers (IV) and (V) have been obtained by treating the starch with propenoxide and epichlorhydrin, respectively. Before etherification, the starch has been activated in acetone in the presence of sodium hydroxide, pH = 9...10, at 45°...50°C, under stirring, for 1.5 hours. After activation, the reagents were added gradually, under stirring too, at 25°...30°C for 2.5 hours. The propenoxide / starch and epichlorhydrin / starch ratios was 0.2 and 0.1 moles to a glucose unit, respectively.

2.2. Chemical Characterization

All the obtained products have been chemically characterized by means of the degree of substitution, expressed as the average number of hydroxyl groups replaced by esterification or etherification per glucose unit. The substitution degree values of the obtained products with excellent thickening properties are presented in Table 1.

Table 1

Degree of Substitution and Proposed Trade Names of the Products

Nr.	Product	Reaction time h	Degree of substitution	Trade name
1	Starch phosphates	2.5	0.060	Aglutirom *P*
2	Starch acetate	3.5	0.063	Aglutirom *Ac*
3	Hydroxypropylstarch	2.5	0.080	Aglutirom *H*
4	1-Chlorine-2-hydroxypropylstarch	2.5	0.075	Aglutirom *E*

Data of the Table 1 show that the introduction of a relatively small number of ester or ether groups (one substituent per 12...17 glucose units),

are enough to modify the colloidal properties of the starch when it is dispersed in water.

2.3. Rheological Characterization

Rheological measurements of the prepared pastes from the four products as well as those from the commercial products Indalca *PA 3* and Indalca *PZ 36* have been carried out on a rotatory viscosimeter „Rheotest type RV 2", using the coaxial cylinders S/S_2 at 25°C. The thickener pastes have been prepared by mixing a measured amounts of solid and of necessary water, at the room temperature, under stirring for 15 min., followed by heating at the temperature of 60°C on a water bath, under stirring for 15 min.

Correlation of the rheological data of the investigated pastes was done by means of Oswald and de Waele's mathematical model

$$\tau = k\dot{\gamma}^n, \tag{1}$$

where k is consistency index and n — the flow index.

By its logarithmation, an equation of straight line is obtained

$$\lg \tau = \lg k + n \lg \dot{\gamma}, \tag{2}$$

which allow to calculate the two rheological indexes.

Dependence of $\lg \tau$ vs. $\lg \dot{\gamma}$ for the pastes of studied thickeners is represented in Fig. 1.

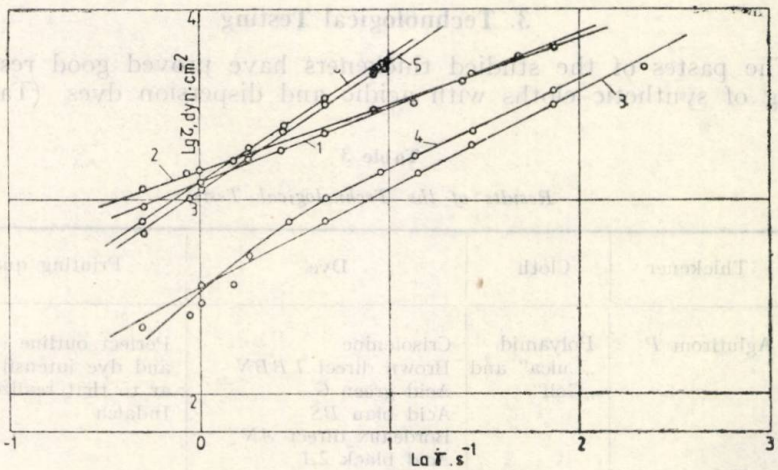

Fig. 1. — Dependence of $\lg \tau$ vs. $\lg \dot{\gamma}$: *1* — 14% Aglutirom *P*; *2* — 10% Aglutirom *Ac* ; *3* — 10% Aglutirom *H* ; *4* — 11% Aglutirom *E* ; *5* — 12% Indalca *PA 3* ; *6*-14% Indalca *PZ 36*.

The chosen model does not agree satisfactorily with the rheological data of the Aglutirom *E* paste. The rheological indexes determined from Fig. 1 are listed in Table 2.

Table 2

Indexes of the Rheological Equation

Nr.	Thickener	Paste concentration %	k, dyn. s^2. cm^{-2}	m
1	Aglutirom *P*	14	1 230.2	0.400
2	Aglutirom *Ac*	10	1 386.7	0.457
3	Aglutirom *H*	10	365.6	0.513
4	Indalca *PA 3*	12	1 091.4	0.693
5	Indalca *PZ 36*	14	1 238.8	0.662

As it comes out from Table 2, the flow index n of the pastes prepared from our thickeners have lower values then those of the commercial products Indalca *PA 3* and Indalca *PZ 36*.

Since the paste of Aglutirom *P*, without free phosphates, exhibits a flow index of 0.831 [6] , and that of unwashed product of 0.400, by repeated washings with a 50% aqueous methanol solution the flow index increases, being closer to that of Indalca type thickeners.

Since in the range of low τ and $\dot{\gamma}$, the straight lines of Aglutirom *P* and Aglutirom *Ac* intersect those of Indalca *PA 3* and Indalca *PZ 36* suggests that in this field, the pastes have an almost similar rheological behaviour, which was proved also by technical tests.

3. Technological Testing

The pastes of the studied thickeners have proved good results in printing of synthetic cloths with acidic and dispersion dyes (Table 3).

Table 3

Results of the Technological Tests

Nr.	Thickener	Cloth	Dye	Printing quality
1	Aglutirom *P*	Polyamid „Luica" and „Golf"	Crisofenine Brown direct *LBBN* Acid green *G* Acid blau *BS* Bordeaux direct *AN* Acid black *2A*	Perfect outline and dye intensity similar to that realized with Indalca
2	Aglutirom *Ac*	Polyester	Dispersion orange *GFL* Dispersion marine blau *RE*	Idem
3	Aglutirom *H*	Polyester	Dispersion dyes	Idem
4	Aglutirom *E*	Polyester	Acid and dispersion dyes	Idem

The thickeners Aglutirom *P* and *H* have been tested technologically at industrial scale at the Entreprise of Silk „Victoria", Jassy.

Preparation of the printing paste with Aglutirom *P* is reported below. First, a paste of 16% Aglutirom *P* is prepared by dispersion of thickener in cold water than addition of warm water was donne until the paste temperature rised to 60°C. After stirring for 30 min., the mixture was left for 12...24 hours to maturate and cooled down to room temperature. Secondly, the paste prepared as above, was stirred again for 15 min., followed by dye addition. The dye is added as dissolved, under boiling, in an aqueous solution of glycerine, uree and ammonium sulphate. Finally, the printing paste contains about 14% Aglutirom *P*.

4. Conclusions

1. Starch phosphate and starch acetate as well as 2-hydroxypropylstarch and 1-chlorine-2-hydroxypropylstarch with low degree of substitution have been obtained by chemical modification of the potato starch. As thickeners in the textile printing, they will be manufactured under trade names Aglutirom *P*, Aglutirom *Ac*, Aglutirom *A* and Aglutirom *E*.

2. The rheological data of the pastes prepared with thise products have been correlated by the model $\tau = k\dot{\gamma}^n$, except those of the Aglutirom *E*. For low values of τ and $\dot{\gamma}$, rheological behaviour of the products is similar to that of Indalca thickeners.

3. The pastes of the four thickeners exhibit good results in textile printing with acid and dispersion dyes on a broad variety of synthetic cloths.

Received, April 10 1985,

Polytechnic Institute, Jassy,
Department of Physical and General Chemistry

REFERENCES

1. Whistler R.L., *Starch Chemistry and Technology*. Vol. 1 and 2, Acad. Press, New York, 1965.
2. Крылова Р.Г., Усп. Хим., 36, 1615 (1967).
3. * * * *Encyclopedia of Polymer Science and Technology*. Vol. 12, John Wiley a. Sons, Inc., New York, 1967, 787.
4. Popa A., Mihăilă Gh., Bîlbă N., Onu P., Luca C., Popovici Ev., Bezdadea M., Popescu D., Ind. Uşoară-textile, tricotaje, confecţii textile, 33, 18 (1982).
5. Tudose R.Z., Volintiru T., Asandei N., Lungu M., Merică E., Ivan Gh., *Reologia compuşilor macromoleculari*. Vol. 1, Ed. Tehn., Bucureşti, 1982, 120.
6. Ioan C., Grigoriu A., Hanganu A., Popescu D., Pavel T., Ind. Uşoară-textile, tricotaje, confecţii textile, 31, 412 (1980).

ESTERI ŞI ETERI AI AMIDONULUI CU PROPRIETĂŢI AGLUTINANTE

(Rezumat)

S-au sintetizat fosfaţi şi acetat de amidon precum şi hidroxipropilamidon şi 1-clor-2-hidroxipropilamidon, cu grad mic de substituţie, utilizînd amidonul de cartofi. Produsele obţinute prezintă proprietăţi aglutinante remarcabile şi urmează a se produce sub denumirile comerciale de Aglutirom *P*, Aglutirom *Ac*, Aglutirom *H* şi Aglutirom *E*. Datele reologice ale pastelor preparate din aceste produse s-au comparat cu cele ale pastelor din produse comerciale de tip Indalca. Pastele preparate au fost testate la imprimarea textilă, cu coloranţi acizi şi cu coloranţi de dispersie, pe o largă varietate de ţesături din fibre sintetice, obţinîndu-se imprimări de bună calitate.

BULETINUL INSTITUTULUI POLITEHNIC DIN IAŞI
Tomul XXXI (XXXV), Fasc. supl., 1985
Secţia II
CHIMIE ŞI INGINERIE CHIMICĂ

D.K. 54-92

DER STUFENWEISE CHARAKTER DES BRUCHPROZESSES BEI POLYMEREN DURCH ZUGKRAFT UNTER KRIECHBEDINGUNGEN

VON

CLEOPATRA VASILIU-OPREA, MARCEL POPA, AL. CONSTANTINESCU
und AURELIA IOANID

1. Einführung

Die zur Zeit angenommenen Theorien hinsichtlich des Bruches von Polymeren (J u r k o w, A n d r e w s, K a u s c h) [1]...[5], die auf rein physikalischer Grundlage beruhen, erlaubten die Festlegung von Wechselbeziehungen zwischen der Belastungskraft und der Antwort auf molekularer Ebene der Polymerstruktur. Sie haben die Bedeutung, daß sie den Bruchprozeß einen mechanochemischen Vorgang zugrunde legen, der in der Aufspaltung der chemischen Verbindungen in der Hauptkette besteht. Dieser Vorgang zeigt sich bereits in den Anfangsstadien des Bruches bis hinzum makroskopischen Riß des Polymers, was jedoch nicht spontan zum Zeitpunkt der Krafteinwirkung stattfindet, sondern nur dann, wenn die gespeicherte Energie in den „Defekt-Zonen" der Struktur vergleichbare Werte mit denen der chemischen Verbindungen erreicht, wodurch ihre thermofluktuationelle Aufspaltung bewirkt wird.

Die Antwort des Polymers auf die mechanische Belastung ist bedingt sowohl durch seinen chemischen Aufbau als auch durch den physikalischen Zustand, bestimmt durch die Arbeitstemperatur ; konkret ausgedrückt, finden Verformungsprozeße und ein Reissen auf makroskopischer Ebene statt. Die komplizierte Prozeße laufen mehrstufig ab, wobei sie zuerst die Etappe der Verformung des Polymers durchlaufen (wenn dieses mechanische Energie speichert), dann primäre chemische Reaktionen und mehrere sekundäre Erscheinungen.

Der Zweck der vorliegenden Arbeit besteht in der Herausstellung der verschiedenen Stadien des Verformungsprozeßes und des Reissens von thermoplastischen Polymeren oder Elastomeren und zwar besonders die Anfangs-(Mechanokracken) und die Endetappe (Reorganisation der Struktur), wobei indirekte Techniken angewandt werden: Reaktionen mit Radikalakzeptoren, Spektralanalysen im UV-und IR-Bereich Elektronenmikroskopie (TEM).

Die UV-Strahlung beschleunigt die elementären Vorgänge des Reissens, wobei die Anhäufung der Einwirkungen den gemeinsamen Mechanismus der beiden Distruktionsprozeße beweist und ein zusätzliches Argument für ihren Verlauf durch freie Radikale darstellt. Darüber hinaus arbeiten während der Untersuchung der Polymerproben die mechanischen Faktoren unvermeidlich zusammen mit denen des Mediums, unter denen wir auch die Wirkung des Lichts zählen können, die innere Veränderungen in ihren Strukturen hervorruft und somit entsprechend die Haltbarkeit beeinflußt. So wurde im theoretischen und praktischen Sinne in der vorliegenden Arbeit bei einigen Experimenten die mechanische Belastung verbunden mit UV-Bestrahlung.

2. Experimenteller Teil

Es wurde Polyvinylchlorid (PVC) untersucht, erhalten durch das Suspensionsverfahren (KW-70), sowie ein aus 4,4-Dibenzyldiisocyanat, Polyethylenglycoladipat und Ethylenglycol synthetisiertes Polyurethan. Aus dem PVC wurden Filme mit einer Dicke von 50 μm aus Lösungen des Polymers in Tetrahydrofuran ($C = 1\%$) gewonnen. Die den Belastungen unter Kriechbedingungen unterzogenen Probestücke aus Polyurethan und PVC wurden entsprechend den Normen ISO R 527/66E hergestellt. Die mechanische Belastung wurde auf einem speziell konstruierten Stand konform der ASTM-Normen durchgeführt.

Die UV-Bestrahlung, parallel zur mechanischen Belastung unter Kriechbedingungen angewandt, wurde durch Benützung einer Quecksilberverdampfungsröhre mit mittlerem Druck bei $25° \pm 1°C$ realisiert.

Das Studium der Rißflächen wurde durch Anwendung der Zwei-Stufen-Replikationsmethode durchgeführt und zwar auf den Bruchflächen oder den anliegenden Flächen und ihre Analyse mit einem Mikroskop, Typ Tesla BS-513 A (ČSSR). Die IR-Spektren wurden durch ein Perkin—Elmer-Spektrophotometer aufgezeichnet, die UV-Spektren durch ein Spektrophotometer, Typ UNICAM, wobei direkt die PVC-Filme verwendet wurden.

3. Ergebnisse und Diskussion

Es wurden PVC-Filme analysiert, die durch Zugkräfte verschiedener Stärke belastet wurden, und zwar so, daß die Verformungen Werte zwischen 10% und 95% des Reissens hatten. Die mechanischen Belastungen wurden in DPPH-Methanollösungen oder in Lösungen von aromatischen Diaminen durchgefürt, die die Rolle von Radikalakzeptoren übernahmen. So wurde festgestellt, daß bei Streckungen bis 20% gegenüber der die zum Reissen führt, die Filme keine wesentlichen Veränderungen gegenüber der ungestreckten Probe aufweisen. In diesem Stadium der Verformungsprozeßes wird die Streckung hauptsächlich durch Aufwicklung und Ausrichtung der Makromoleküle in Richtung der Kraftwirkung vollzogen. Man kann sagen, daß das Polymer in einen mechanisch erregten Zustand übergeht, ohne daß jedoch dieses Stadium überschritten wird, wenn die mechanische Belastung aufhört zu wirken.

Bei größeren Verformungen jedoch ($> 20\%$) zeigt der aktive Sektor der Proben eine spezifische Färbung, was ein erster Beweis dafür ist, daß unter der Wirkung der mechanischen Energie homolytische molekuläre Aufspaltungen stattgefunden haben, wobei die gebildeten Radikale DPPH oder aromatishes Diamin chemisch binden. Die Färbung des Films ist ein erster experimenteller Beweis für den Ablauf der Etappe des Mechanokrackens. Der teilweise Verbrauch der gebildeten „Mechanoradikale" durch die Radikalakzeptoren wurde durch die UV-Spektren der gespannten Filme bewiesen (Abb. 1).

Bei erhöhten Streckungswerten (approx. 95% der des Reissens) wird die Anzahl der gebildeten Makroradikale sehr groß, wobei der Verbrauch von aromatischen Diamin aus dem Reaktionsmedium angewachsen ist. Infolgedessen kann die Anwesenheit der aromatischen Verbindung in dem

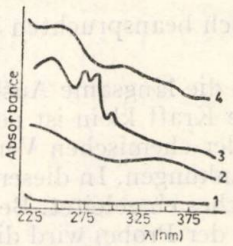

Abb. 1. — UV — Spektren von gedehnten PVC-Filmen: *1* — Vergleichsprobe; *2* — gedehntes PVC in DPPH; *3* — gedehntes PVC in *o*-PhDA; *4* — gedehntes PVC in *p*-PhDA.

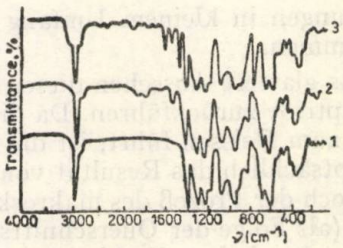

Abb. 2. — IR—Spektren von PVC-Filmen: *1*—Vergleichsprobe; *2*—gedehntes PVC in *p*-PhDA; *3*—gedehnt in Anwesenheit von Styrol.

gespannten Film auch durch eine weniger empfindliche Methode als die UV-Spektroskopie nachgewiesen werden und zwar durch die IR-Spektroskopie (Abb. 2, Kurve *2*). Die große Konzentration der Makroradikale erlaubt ebenfalls die Einleitung von Propf-Blockcopolymerisationsprozeßen in Anwesenheit eines Vinylmonomers. Das IR-Spektrum aus Abb. 2 (Kurve *3*) zeigt die chemische Bindung des Styrols an den gespannten Film durch das 775-, 1480- und 1 600 cm^{-1} Band.

Ein zusätzliches Argument für die Propf-Blockcopolymerisation des Styrols bei PVC geht aus den Mikrophotografien der gespannten Filme (Abb. 3 *a*...*c*) hervor, die ein eindeutig anderes Aussehen gegenüber denen der Vergleichsprobe haben. Auf der Oberfläche dieser bemerkt man Einschlüße, was dem Propfpolystyrol zugeschrieben wird, die jedoch auf der Oberfläche des nichtgespannten Films fehlen (Abb. 3 *a*). Besonders interessante Informationen liefern die in Abb. 4 *a*, *b* dargestellten Mikrophotografien, die das Relief der Oberfläche von gespannten Filmen nahe des Reissens festhalten, bei dem man einige Riße festtellt. Die Verformungszone, neben der des Bruches gelegen, ist charakterisiert durch das Auftreten von linearen Strukturen, gebildet aus Fibrillen senkrecht zur Kraftrichtung. In dieser Zone beobachtet man eine größere Anzahl von Propfzentren des Vinylmonomers, ein Beweis für die große Konzentration von durch das Spannen gebildeten freien Radikalen. Gleichfalls läßt sich einschätzen, daß nach dem Mechanokracken im Polymer sich das dritte Stadium des Strukturbruch und Reorganisatiosprozeßes zeigt. In der Zone des makroskopischen Bruches zeichnet sich das PVC mit globulärer Struktur durch nichtcharakteristische fibrillare Abschnitte aus, eine Folge von Veränderungen der globulären Abschnitte unter Krafteinwirkung.

Die Mikrophotografien aus Abb. 5 *a*...*c* geben das Aussehen von Zonen der Bruchfläche des unter Kriechbedingungen Beanspruchten PVC's wieder. Die Topographie dieser Zonen (Abb. 5 *a*) zeigt indirekt durch die Kavitationen die Etappe des Mechanokrackens, in der sich große Konzentrationen von freien Radikalen ansammeln, die aus den gespaltenen chemischen

Verbindungen in kleinem Umfang des mechanisch beanspruchten Festkörpers stammen.

Das glattere Aussehen dieser Fläche ist auf die langsame Ausbreitung der Hauptrisse zurückführen. Da die mechanische Kraft klein ist gegenüber der, die zum Reissen führt, ist die Aufspaltung der chemischen Verbindungen hauptsächlich das Resultat von Wärmeschwankungen. In dieser Etappe wird jedoch der Prozeß des makroskopischen Bruches eingeleitet. Bei großen Kräften (als Folge der Querschnittsverkleinerung der Probe) wird die Belastung der chemischen Verbindungen so intensiv, daß ihr Reissen sich fast ausschließlich infolge der mechanischen Energie vollzieht, wobei die Beteiligung der Wärmeschwankungen sich sehr vermindert. Die Ausbreitungsgeschwindigkeit des Rißes wächst, wobei diese den nichtelastischen Eigenschaften des Polymers unterworfen ist. Die Bruchflächen bekommen ein rauhes Aussehen (Abb. 5 *b*), weil das starre Polymer wegen seiner plastischen oder viskoelastischen Eigenschaften keine Energieverluste aufweist. Die Übergang von der ersten Phase (langsame Ausbreitung des Rißes) zur zweiten Phase (katastrophale, mit dem Bruch endende Ausbreitung) wird somit klar deutlich.

Im Falle von thermoplastischen Elastomeren des Typs Polyurethane wurden die Probestücke bei Zugkraft unter Kriechbedingungen (mit einer einheitlichen Kraft von 9,0 MPa) belastet und gleichzeitig einer UV-Älterung unterzogen.

Es wurde festgestellt, daß das Reissen der Proben nach einer Belastung von 55 Stunden stattfand, zum Unterschied zu den nichtbestrahlten, die nicht einmal nach 1 000 Belastungsstunden gerissen sind. Dem Riß vorausgehend findet eine sich verstärkende Verformung des Probestückes statt, und es wird das Mikroreissen eingeleitet, was mit Hilfe der Elektronenmikroskopie sichtbar wird.

Die mit der Zugkraftbelastung unter Kriechbedingungen gleichzeitig ausgeführte UV-Bestrah ung beschleunigt die Aufspaltung der chemischen Valenzverbindungen und die Bildung von Mikrorißen, was schließlich zum makroskopischen Bruch der Probestücke führt. Es ist bekannt, daß UV-Strahlungen mit Wellenlängen zwischen 250 und 360 nm das Reissen von Valenzverbindungen verursachen, wobei freie Radikale gebildet werden [6]. Infolge der Dehnung bei Fließbedingungen der gleichzeitigen UV-Strahlung findet durch die synergistische Wirkung dieser beiden Faktoren ein Anwachsen der Formveränderung statt, was ein Beweis dafür ist, daß diese Prozeße eine gemeinsame Ursache haben und zwar die thermofluktuationelle Aufspaltung der chemischen Valenzverbindungen. Man stellt fest, daß das makroskopische Reissen der Probestücke bei den jeweilig angewandten Experimentierbedingungen nicht durch uniaxiale Beanspruchung, nicht durch UV-Strahlung stattfindet, sondern eine Erscheinung ist, die sich erst beim gleichzeitigen Wirken dieser beiden Energieformen zeigt.

Die Wiederherstellung der gespaltenen Verbindungen nach der UV-Bestrahlung wird behindert durch die Wirkung der mechanischen Energie, was zur katastrophalen Ausbreitung des Bruchvorgangs führt bis hin zum makroskopischen Bruch des Polymers.

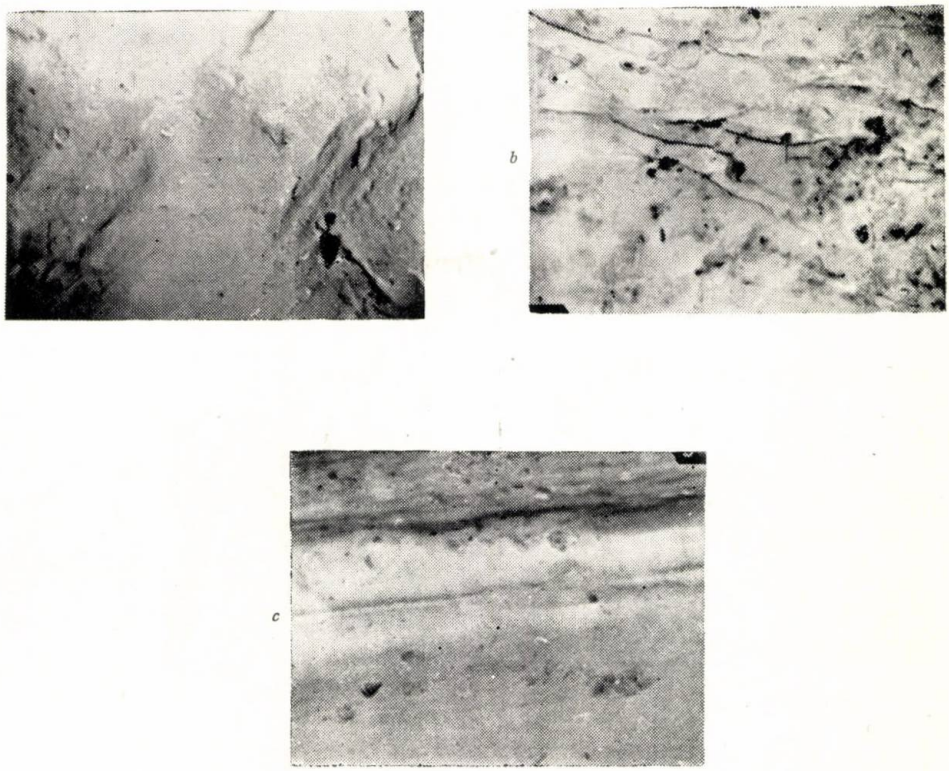

Abb. 3. — Mikrophotografien von gedehnten PVC-Filmen in Methano (*a*) oder Styrol—Methanol-Lösung.

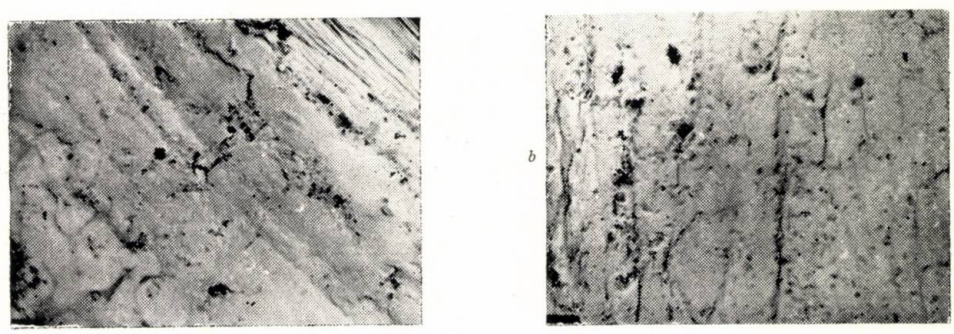

Abb. 4. — Mikrophotografien von gedehnten PVC-Filmen nahe dem Reissen ($\varepsilon = 95\%$).

a

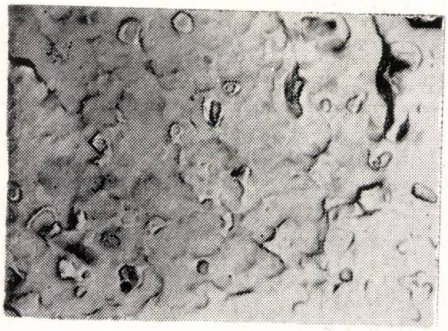

b

c

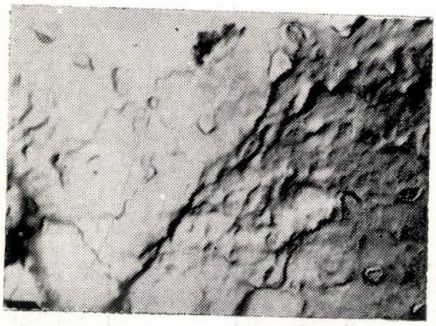

Abb. 5. — Mikrophotografien der Bruchfläche von durch Zugkraft statisch beanspruchtem PVC.

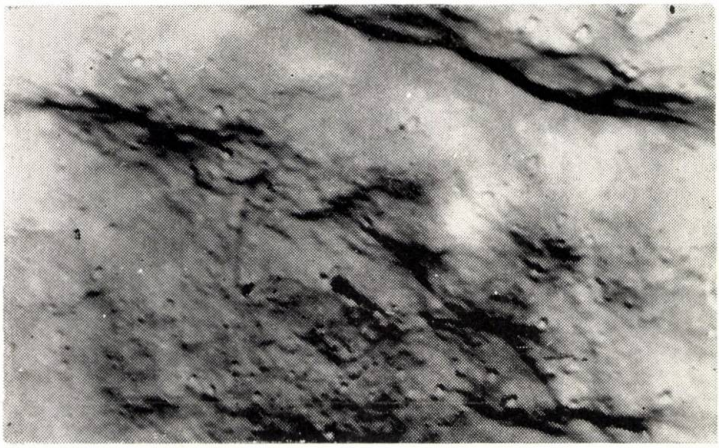

Abb. 6. — Mikrophotografie der Bruchoberfläche im Falle der nichtgedehnten und nichtbestrahlten Polyurethan-Probe, die in flüssigen Stickstoff gerissen ist (× 11 300).

Abb. 7. — Mikrophotografie der Bruchoberfläche im Falle der unter Fließbedingungen gedehnten und gleichzeitig durch UV-Strahlung gealterten Polyurethan - Proben (× 11 300).

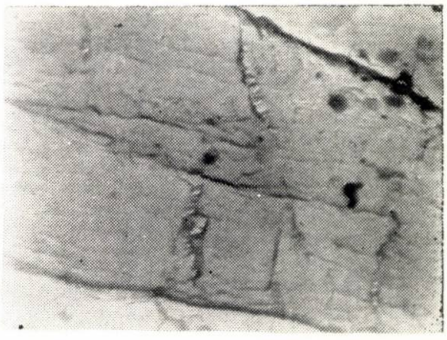

Abb. 8. — Mikrophotografie der mit der Bruchzone benachbarten deformierten Zone im Falle der unter Fließbedingungen gedehnten und gleichzeitig durch UV-Strahlung gealterten Polyurethan - Proben (× 11 300).

Als Folge der mechanischen Belastung tritt gleichzeitig eine Verringerung der Dissoziationsenergie der gedehnten Verbindungen auf, wodurch eine Beschleunigung ihrer photochemischen Spaltungsprozeße möglich wird.

Es wurde das Bruchrelief und die benachbarte Verformungszone untersucht im Vergleich zu einer nichtgedehnten und nicht UV-bestrahlten Probe, deren Bruch durch Einführung in flüßigen Stickstoff während 30 Min. realisiert wurde, während man annimmt, daß der Bruch längs der Oberfläche der suprastrukturellen Elemente stattfindet. Die erhaltenen Replikationen von der Bruchfläche der Vergleichsprobe (Abb. 6) zeigen, daß die nichtgedehnte Probe eine übermolekulare Struktur von globulären Typ aufweist, charakteristisch für amorphe Polymere. Das Studium der Mikrophotografien von der Bruchzone (Abb. 7) zeigt den rauhen Charakter dieser Zone, wobei der globuläre Aspekt nicht mehr hervortritt. Dagegen beobachtet man das Auftreten von, was Form und Abmessung anbelangt, unregelmässigen Mikrorißen.

Die der Bruchzone anliegende Verformungszone (Abb. 8) zeigt neben der Bildung von zur Belastungsrichtung querverlaufenden Mikrorißen auch einige aus eingebetteten makromolekularen Ketten gebildete fibrilläre Abschnitte. Dieser Prozeß findet durch die Auflösung der Globule und der Längsordnung der Makromoleküle statt, infolge der Wirkung der uniaxialen Zugkraft.

4. Schlussfolgerungen

1. Der Bruch von Polymeren unter Kriechbedingungen hat einen mehrstufigen Charakter, der die Mechanoaktivierung, das Mechanokracken und die Reorganisation der Struktur mit einschließt.

2. Bei jeder der einzelnen Stufen des Bruchprozeßes finden mechanochemische Vorgänge homolythischer Aufspaltung der Makromoleküle statt, die durch indirekte Techniken bewiesen werden können.

3. Durch die gleichzeitige Wirkung von mechanischer Energie und UV-Strahlungen findet eine Beschleunigung des Reissens statt, wobei eine Anhäufung der Effekte den gemeinsamen Radikalcharakter dieser beiden Abbautypen beweist.

4. Im letzten Stadium des Bruchprozeßes treten wichtige strukturelle Veränderungen auf, die in dem Übergang von der globulären in die fibrilläre Struktur bestehen.

Eingegangen am 20. April 1985

Technische Hochschule, Jassy,
Lehrstuhl fiir organische und
makromolekulare Chemie und
Technologie
und
Institut für makromolekulare Chemie
„P. Poni", Jassy

LITERATURVERZEICHNIS

1. Журков С.Н., Закревский В.А., Томашевский Е.Е., Физ. тверд. тела, 6, 1912 (1964).

2. Andrews E. H., Reed P. E., *Advances in Polymer Science*. Vol. 27, Springer-Verlag, Berlin, 1978.
3. Kausch H. H., *Polymer Fracture*. Springer-Verlag, Berlin, 1978.
4. Самоилова Г.Г., Томашевский Е.Е., Физ. рверд. тела, 10, *4*, 1094 (1968).
5. Акимбеков К., Куксенко В.С., Низамидинов С., Слуцкер А.И., Ястребинский А.А. Физ. тверд. тела, 14, *9*, 2708 (1972).
6. Rånby B., Rabek F. J., *Photodegradation, Photooxidation and Photostabilization of Polymers. Principles and Applications*. J. Wiley, New York, 1975.

CARACTERUL TREPTIFORM AL PROCESULUI DE RUPERE FRACTURARE A POLIMERILOR ÎN CONDIŢIILE FLUAJULUI LA TRACŢIUNE

(Rezumat)

Se abordează studiul etapelor procesului de rupere a polimerilor la solicitare statică la tracţiune : mecano-activarea, mecanocracarea şi reorganizarea structurii. Fiecare stadiu are la bază actul mecanochimic constînd în scindarea sub efort a unor legături chimice de pe catena de bază. Macroradicalii formaţi sînt puşi în evidenţă prin tehnici indirecte: reacţii cu acceptori radicalici, spectroscopie în ultraviolet şi infraroşu, microscopie de transmisie.

BULETINUL INSTITUTULUI POLITEHNIC DIN IAŞI
Tomul XXXI (XXXV), Fasc. supl., 1985
Secţia II
CHIMIE ŞI INGINERIE CHIMICĂ

D.C. 678-13

COPOLYMERS

VIII. STUDY ON TERPOLYMERIZATION OF ACRYLONITRILE (AN) WITH α-METHYL-STYRENE (MS) AND CINNAMIC ACID (CA)

BY

N. ASANDEI, M. NICU, M. RUSU, S. PETROVAN, VIORICA NICU and MARIA LUNGU

1. Introduction

Due to the carboxylic group the CA could confer improved tinctorial properties and lower electrostatic charge to the copolymers [1] ... [5]. Due to its high cost price it would be preferable to use it in a very low content and in ternary mixtures of a cheap termonomer.

In the present paper the characteristics of the CA copolymerization with AN and MS as a termonomer are studied.

2. Synthesis of Terpolymers

The synthesis of terpolymers was based on the reaction:

$$\underset{\substack{|\\ CN\\ AN(M_1)}}{CH_2{=}CH} + \underset{\substack{|\\ C_6H_5\\ MS(M_2)}}{CH_2{=}\overset{\substack{CH_3\\ |}}{C}} + \underset{\substack{|\\ C_6H_5\\ AC(M_3)}}{CH{=}\overset{\substack{COOH\\ |}}{CH}} \longrightarrow \underset{(m_1;m_2;m_3)}{\text{Terpolymers}} \tag{1}$$

2.1. Synthesis of Terpolymers in Methanol Medium

Since CA shows a low solubility in water (less than 2%) it had to choose a solvent for these monomers as a terpolymerization medium, namely the methanol. The compositions of the substrata as well as the recipers used are given in Table 1.

The reaction was stopped by adding a hydroquinone alcoholic solution. The obtained terpolymers were washed with acetone and then dried in an oven at 80°C.

2.2 Synthesis of Terpolymers in Aqueous Medium

Since the ternary system under study would react in aqueous medium it was necessary to verify the conclusions of the composition studies of the terpolymers synthesized in methanol on the terpolymers resulted in aqueous

medium. In this purpose the products *68* and *69* were synthesized according to the data from Table 1.

Table 1

Terpolymerization Recipers and Composition of Terpolymers

Characteristic	Symbol					
	13 128	*13 146*	*13 164*	*13 182*	*68*	*69*
	Composition substrata, [% mol]					
AN (M_1)	90	90	90	90	97.38	97.56
MS (M_2)	2	4	6	8	2.25	2.25
CA (M_3)	8	6	4	2	0.36	0.18
Reaction medium	methanol (AIBN)				water ($K_2S_2O_8$ + + $Na_2S_2O_5$)	
Reaction temperature, [°C]	60				60	
Conversion, [% weight]	2.1	2.6	2.4	2.8	63.31	60.68
Composition of terpolymers, [% mol], experimental						
AN (m_1)	88.1	86.95	86.50	89.44	96.85	95.46
MS (m_2)	7.49	7.57	10.30	7.60	1.97	2.19
CA (m_3)	4.40	5.47	3.20	2.95	1.17	0.95
Integral composition of terpolymers calculated by means of Eqs. (14)...(17), [% mol]						
AN	—	—	—	—	97.08	97.42
MS	—	—	—	—	2.38	2.33
CA	—	—	—	—	0.53	0.24
Integral compositions of terpolymers calculated by means of Eqs. (24)...(27), [% mol]						
AN	—	—	—	—	97.20	97.42
MS	—	—	—	—	2.32	2.33
CA	—	—	—	—	0.47	0.24

3. Analysis of Terpolymers

3.1. Qualitative Analyses

The synthesized terpolymers were analysed by IR and NMR spectra measurements. The IR spectra are given in Fig. 1.

The IR and NMR spectra show the absorptions and the signals, respectively, characteristic to main structural elements of the termonomers

The NMR spectroscopy was also tried for quantitative estimations (Fig. 2), but some signals are not satisfactory resolved due to the particular structure of the products, so it was not possible to use these measurements in the mentioned purpose.

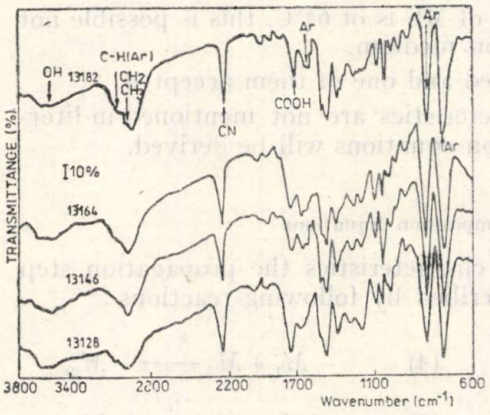

Fig. 1. — IR spectra of some terpolymers.

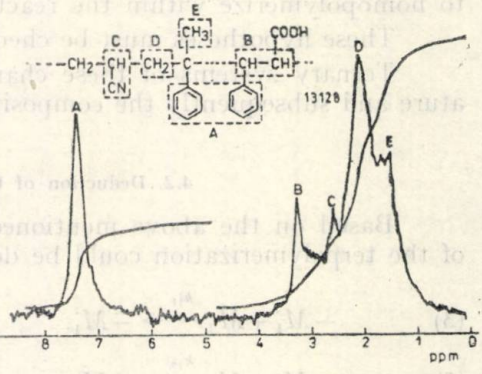

Fig. 2. — NMR spectrum of the terpolyme *13 128*.

3.2. Quantitative Analyses

In order to determine the quantitative copolymer compositions, the IR spectra were used, in which the absorptions of the —CN (2 240 cm^{-1}) —COOH (1 730 cm^{-1}) and phenyl groups (720 cm^{-1}) are well resolved.

In the IR spectra the absorptions were measured and their ratios calculated. Then the molar ratios of the terpolymers (a and b) were read on the composition — absorption ratio standard curves, and made up the following set of equations :

$$(2) \qquad \frac{m_2+m_3}{m_1}=a, \quad \frac{m_3}{m_1}=b, \quad m_1+m_2+m_3=1.$$

By solving the system (2) the compositions of the terpolymers given in Table 1 were found.

4. Relations between Substratum and Terpolymer Compositions

4.1. Characteristics of the Terpolymerization System

The characteristics of our system may be discussed in function of those of the copolymerization in binary systems, namely :

a) Since CA must be introduced into the terpolymers in low amounts, its concentrations within the substratum will be very low ; in that limits in which it was found [6] that it might copolymerize with AN by charge transfer mechanism. This possibility must be also verified with terpolymerization.

b) CA does not homopolymerize and hence propagation reactions in which the CA molecules would add to the macroradicals terminated in AC units can not proceed.

c) CA does not copolymerize with MS and neither propagation reactions in which respective monomers would add to the macroradicals terminated in corresponding units can be assumed.

d) Since the ceiling temperature of MS is of 61°C, this is possible not to homopolymerize within the reaction medium.

These hypotheses must be checked and one of them accepted.

Ternary systems of these characteristics are not mentioned in literature and subsequently the composition equations will be derived.

4.2. Deduction of Composition Equations

Based on the above mentioned characteristics the propagation step of the terpolymerization could be described by following reactions :

(3) $-M_1^{\cdot} + M_1 \xrightarrow{k_{11}} -M_1^{\cdot}$; (4) $-M_1^{\cdot} + M_2 \xrightarrow{k_{12}} -M_2^{\cdot}$,

(5) $-M_1^{\cdot} + M_3 \xrightarrow{k_{13}} -M_3^{\cdot}$, (6) $-M_2^{\cdot} + M_1 \xrightarrow{k_{21}} -M_1^{\cdot}$,

(7) $$-M_3^{\cdot} + M_1 \xrightarrow{k_{31}} -M_1^{\cdot}.$$

The rate constants of the elemental reactions are written on the arrows.

By applying the steady state hypotheses the following equations for the monomer consumption can be written :

(8) $$-\frac{dM_1}{dt} = k_{11}M_1M_1^{\cdot} + k_{21}M_1M_2^{\cdot} + k_{31}M_1M_3^{\cdot},$$

(9) $-\frac{dM_2}{dt} = k_{12}M_2M_1^{\cdot}$, (10) $-\frac{dM_3}{dt} = k_{13}M_3M_1^{\cdot}$.

Under steady state conditions the rate of radical formation equals that of their consumption. Hence,

(11) $$k_{21}M_2^{\cdot}M_1 + k_{31}M_3^{\cdot}M_1 = k_{12}M_1^{\cdot}M_2 + k_{13}M_1^{\cdot}M_3,$$

(12) $k_{12}M_1^{\cdot}M_2 = k_{21}M_2^{\cdot}M_1$, (13) $k_{13}M_1^{\cdot}M_3 = k_{31}M_3^{\cdot}M_1$.

By combining the above relations the following set of equations results describing the correlation between the substratum and terpolymer compositions :

(14) $\frac{m_1}{m_2} = r_{12}\frac{M_1}{M_2} + 1 + \frac{1}{R}\cdot\frac{M_3}{M_2}$, (15) $\frac{m_1}{m_3} = r_{13}\frac{M_1}{M_3} + R\frac{M_2}{M_3} + 1$,

(16) $\frac{m_2}{m_3} = R\frac{M_2}{M_3}$, (17) $m_1 + m_2 + m_3 = 1$,

where m_i and M_i represent molar fractions and

$$r_{12} = \frac{k_{11}}{k_{12}}, \quad r_{13} = \frac{k_{11}}{k_{13}}, \quad R = \frac{k_{12}}{k_{13}}.$$

For the case where MS can homopolymerize the elemental reactions of the propagation step would be eq. (18)...(23)

(18) $-M_1^{\cdot} + M_1 \xrightarrow{k_{11}} -M_1^{\cdot}$, (19) $-M_1^{\cdot} + M_2 \xrightarrow{k_{12}} -M_2^{\cdot}$,

(20) $-M_1^{\cdot} + M_3 \xrightarrow{k_{13}} -M_3^{\cdot}$, (21) $-M_2^{\cdot} + M_1 \xrightarrow{k_{22}} -M_1^{\cdot}$,

(22) $-M_2^{\cdot} + M_2 \xrightarrow{k_{22}} -M_2^{\cdot}$, (23) $M_3^{\cdot} + M_1 \xrightarrow{k_{31}} -M_1^{\cdot}$

and applying the above method the composition set of equations (24)...(27) is obtained :

(24) $$\frac{m_1}{m_3} = \frac{M_1}{M_3}\left(r_{13} + R\frac{M_2}{M_1} + \frac{M_3}{M_1}\right),$$ (25) $$\frac{m_2}{m_3} = \frac{M_2}{M_3}\left(R + r_{21} R\frac{M_2}{M_1}\right),$$

(26) $m_1 + m_2 + m_3 = 1$; (27) $r_{ij} = \frac{k_{ii}}{k_{ij}}$, $R = \frac{k_{12}}{k_{13}}$.

By means of Eqs. (14)...(17) the following values of the reactivity constants were found : $r_{12} = 0.9222$; $r_{13} = 0.5947$; $R = 0.6442$. These values suggest that the CA rather than MS pref rentially adds to the macroradicals terminated in AN.

The same conclusion is drawn from reactivity constants corresponding to Eqs. (24)...(27).

In order to find which of two proposed models reflects the real situation, more faithfully the integral compositions of the terpolymers at high conversion (*68* and *69*) were calculated by means of them. Results given in Table 1 show clearly that AN + MS + CA system forms terpolymers whose composition is described by Eqs. (14)...(17) and the terpolymerization model is given by the reactions (3)...(7).

The composition — conversion dependence calculated according to the settled model is depicted in Fig. 3.

4.3. Qualitative Appreciations on Terpolymer Sequences

Taking into account the reactivity constants and the compositions of the synthesized terpolymers from substrata of low content of MS and CA, these compounds may be considered to consist of long AN chains joined by either CA or MS units (s. (28)).

By examining the variation of the substrata and of the terpolymers as a function of conversion (Fig. 3), minor modifications in the procentual compositions are noticed which assures the compositional and sequential uniformity of terpolymers :

(28)
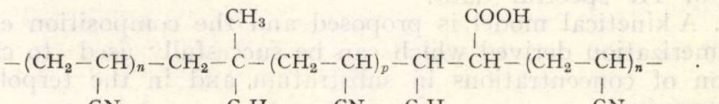

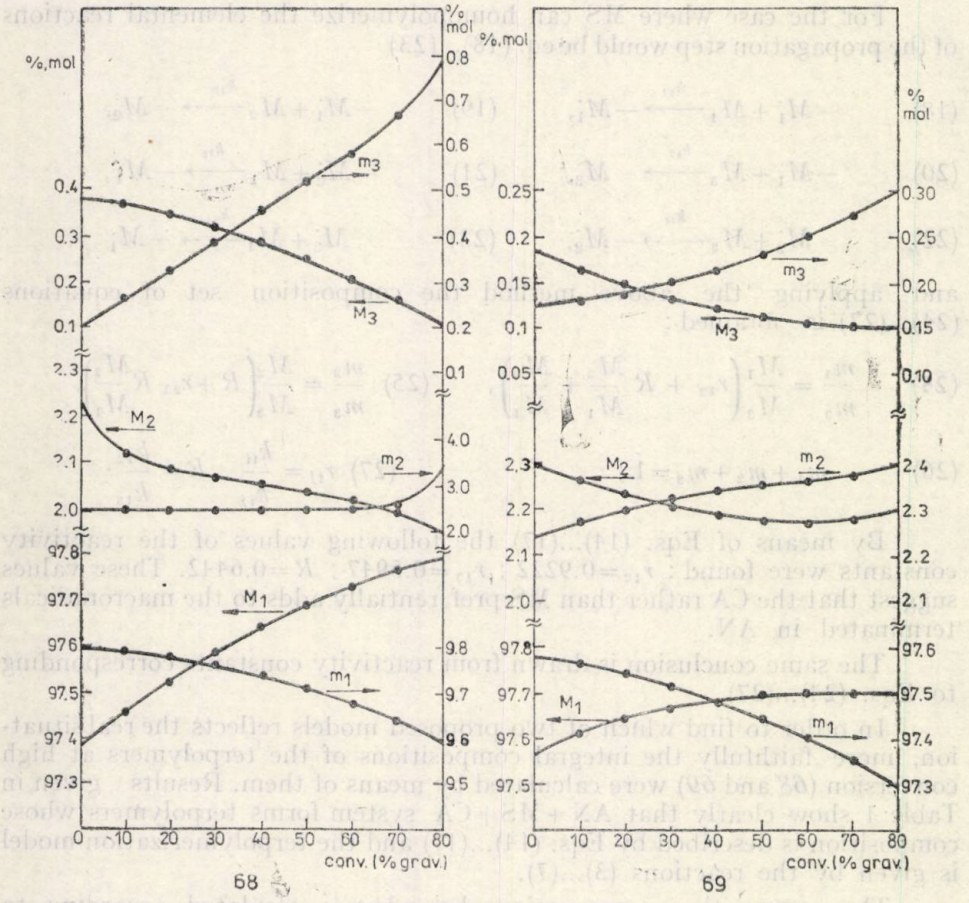

Fig. 3. — Variation of composition of substrata and terpolymers with conversion for the terpolymerizations *68* and *69*.

The proposed and verified kinetical model attests that the terpolymers do not contain CA—CA, MS—MS and CA—MS diades.

5. Conclusions

The researches on the terpolymerization of the AN + MS + CA system lead to the following conclusions:

1. By the reaction of AN with MS and CA terpolymers are formed.
2. The terpolymer composition can be estimated quantitatively by means of IR spectral data.
3. A kinetical model is proposed and the composition equations of terpolymerization derived which can be succesfully used to calculate the variation of concentrations in substratum and in the terpolymers with the conversion.

4. The synthesized terpolymers are of the statistical type and consist of the long AN sequences joined by either MS or CA units.

5. Due to the reactivity constants whose values are convenient the substratum compositions vary very little with the conversion which assures the compositional and sequential uniformity of the terpolymers.

Received, April 16, 1985

Polytechnic Institute, Jassy,
Department of Organic
and Macromolecular Chemistry and
Technology

REFERENCES

1. * * * Monsanto Chemical Co., Belg., Pat., *628 794* (1963) ; C.A. **60** (10), 12 165 g.
2. * * * Idem, U.S. Pat., *3 410 835* (1968) ; C.A. **70** (12), 48 544c, (1969).
3. * * * Idem, U.S. Pat., *3 388 189* (1968) ; C.A. **69** (8), 28 527a (1968).
4. * * * Idem, U.S. Pat., 3 310 535 (1963) ; C.A. **66**, 116 638f (1967).
5. Simionescu Cr., Vasiliu-Oprea Cl., *Tratat de chimia compuşilor macromoleculari.* Vol. I, EDP, Buc., 1973.
6. Asandei N., Nicu M., Rev. Roum. Chim., **25**, 915 (1980).

COPOLIMERI

VIII. Studiul terpolimerizării acrilonitrilului (AN) cu α-metilstirenul (MS) şi acidul cinamic (CA)

(Rezumat)

S-a studiat terpolimerizarea acrilonitrilului cu α-metilstiren şi cu acid cinamic în mediu de metanol şi în apă. Compoziţia cantitativă a terpolimerilor s-a determinat prin spectroscopie în IR. S-au stabilit ecuaţiile de compoziţie a terpolimerilor, găsindu-se că AN copolimerizează cu partenerii, dar aceştia nici nu homopolimerizează şi nici nu copolimerizează.

BULETINUL INSTITUTULUI POLITEHNIC DIN IAȘI
Tomul XXXI (XXXV), Fasc. supl., 1985
Secția II
CHIMIE ȘI INGINERIE CHIMICĂ

D.C. 547.785.5

COMPLEX COMPOUNDS OF 5-AMINO-BENZIMIDAZOLONE-2 WITH CERTAIN CATIONS OF TRANSITIONAL METALS

BY

N. FOCA, VALERIA GORDUZA and LUMINIȚA WAGNER

1. Introduction

Utilisation of 5-amino-benzimidazolone-2 in synthesis of some heterocycle azopigments of high quality rised the interest to study the structure and reactivity of the benzimidazolone derivatives (I)...(IV) [1]:

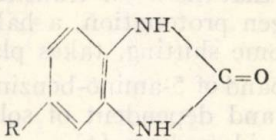

(I) – (IV)

where

R : H (I), $-NO_2$ (II), $-NH_2$ (III), $-NH-\overset{\overset{O}{\|}}{C}-CH_2-\overset{\overset{O}{\|}}{C}-CH_3$ (IV).

The benzimidazolone derivatives participate at tautomerism equilibria, which are influenced by a series of factors, such as: medium nature, temperature, the presence of transitional metal cations, etc.

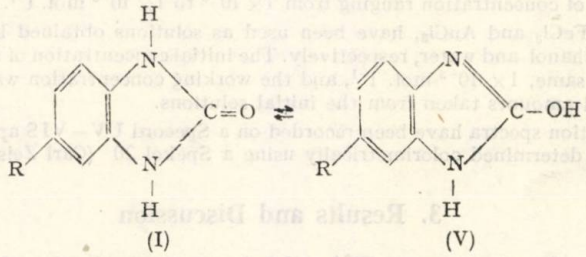

(I) (V)

Their two-fold reactivity is correlated with amphoteric character and susceptibility to react in both undisociated and ionized states [2].

The 5-amino-benzimidazolone-2 (III) can act as ligand for the Fe^{3+}, Au^{3+} and Pt^{4+} ions, due to electrodonator character correlated with the possibility of the $p-\pi$ conjugation, participation of electronic doublet of aminic nitrogen, aromatic skeleton and ureidic remainder. Thus, the

increased reactivity and implicitly coordination capacity toward the cations of transitional metals can be accepted for the structure (VI) :

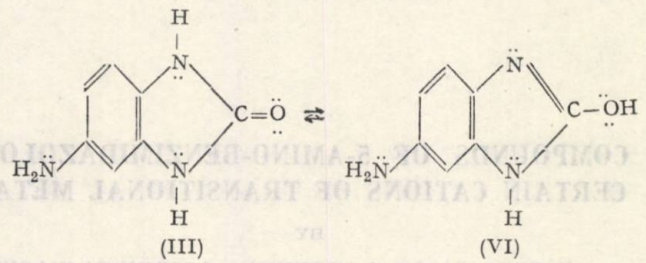

(III) (VI)

Due to the polarizability of the carbonyl group, the electrodonator character of nitrogen atoms in the ureidic remainder and phenylic nucleus, in the benzimidazolone derivatives an enlarged conjugated system is realised. Differentiation of the absorption bands is possible on the basis of solvochromic and halochromic effects [3], [4].

The possibility of the $p-\pi$ conjugation in heteroaromatic amines leads to a decrease of the bond orbital energy and to an increase of nonparticipant orbital energy, so that the $n-\pi^*$ transition energy is diminished. On the other hand, by nitrogen protonation, a halochromic effect, spectrally transposed in a hypsochrome shifting, takes place.

The characteristic band of 5-amino-benzimidazolone-2, situated between 304.4 and 318 nm, and dependent of solvent polarity, undergoes a hypsochromic shifting in acid medium [1].

It seems to be of interest the fact that by acidulation or alkalization, the absorption band characteristic to the $n-\pi^*$ transition of carbonyl group (226 nm) is shifted and modified as a shoulder in the 228...236 nm domain (acid medium) and in the 250...250.5 nm domain (in alkaline medium).

2. Experimental

The ligand (*L*), i.e. 5-amino-benzimidazolone-2 being water insoluble, it was employed as alcoholic solution of concentration ranging from 1×10^{-3} to 1×10^{-5} mol. l^{-1}.

The salts, $FeCl_3$ and $AuCl_3$, have been used as solutions obtained by their dissolution in reagent grade ethanol and water, respectively. The initial concentration of the $FeCl_3$ and $AuCl_3$ solutions was the same, 1×10^{-3} mol. l^{-1}, and the working concentration was attained by dilution of measured amounts taken from the initial solutions.

The absorption spectra have been recorded on a Specord UV—VIS apparatus , and composition has been determined colorimetrically using a Spekol 20 (Carl Zeiss Jena) apparatus.

3. Results and Discussion

3.1. Reaction between Fe^{2+} and 5-Amino-benzimidazolone-2

The Fe^{3+} ion easily reacts with 5-amino-benzimidazolone-2, forming a complex compound with a specific spectrum in UV and VIS regions, different from that of the reagents. The absorption spectra presented in Fig. 1 belong only to the resulted complex, the ligand alone having no absorbtion in VIS region.

The characteristics of the absorption bands of the complexes are given in Table 1.

Table 1

Characteristics of the Absorption Bands of Fig. 1

Nr.	Compound	Solvent	Concentration mol. l^{-1}	λ_{max} nm	ε_{max} $l.mol^{-1}.cm^{-1}$
1	$FeCl_3+L(1:1)$	C_2H_5OH	1×10^{-4}	640	2 350
2	$FeCl_3+2L(1:1)$	C_2H_5OH	1×10^{-4}	640	4 300
3	$FeCl_3+L(1:1)$	H_2O	1×10^{-4}	620	2 400
4	$FeCl_3+2L(1:2)$	H_2O	1×10^{-4}	620	2 650

The data from Table 1 show that, in ethanol, the complex has a band situated at 640 nm for both 1 M : 1 L and 1 M : 2 L and λ_{max}, in aqueous solution, is situated at a smaller wave length, namely 620 nm. Besides the absorption bands with $\lambda = 640$ and 620 nm, other bands occur at λ_{max} = 330 and 355 nm in ethanol and a single band with $\lambda_{max} = 350$ nm in aqueous medium, which also belongs only to the Fe^{3+}—5-amino-benzimidazolone-2 complex.

3.2. Reaction between Au^{3+} and 5-Amino-benzimidazolone-2

As in the previous case, the reaction between Au^{3+} and 5-aminobenzimidazolone-2 is a rapid one with formation of a complex whose absorption spectrum in UV and VIS region shows the interaction between Au^{3+} and 5-amino-benzimidazolone-2 (L) (Fig. 2).

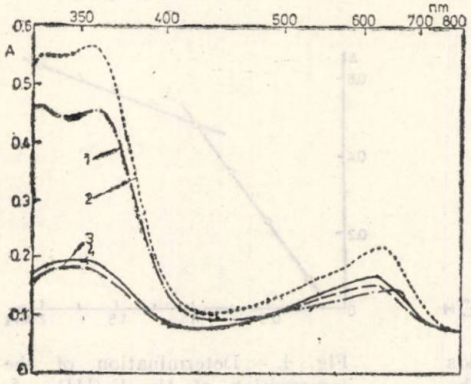

Fig. 1. — Absorption spectra of the complexes formed in the Fe^{3+} — 5-amino-benzimidazolone-2 system in VIS region.

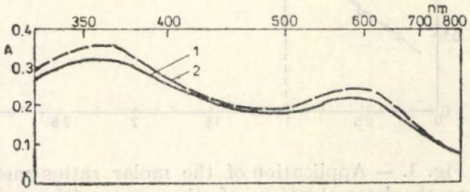

Fig. 2. — Absorption spectra in VIS region recorded for the Au^{3+} — 5-amino-benzimidazolone-2 system.

The characteristics of the bands of the absorption spectra represented in Fig. 2 are listed in Table 2.

Table 2

Characteristics of the Absorption Bands of Fig. 2

Nr.	Compound	Solvent	Concentration mol. l^{-1}	λ_{max} nm	ε_{max} $l.mol^{-1}.cm^{-1}$
1	$AuCl_3+L(1:1)$	H_2O	1.10^{-4}	365	6 800
2	$AuCl_3+L(1:1)$	H_2O	1.10^{-4}	580	4 800
3	$AuCl_3+L(1:2)$	H_2O	1.10^{-4}	365	7 600
4	$AuCl_3+L(1:2)$	H_2O	1.10^{-4}	580	5 200

As it comes out from both Fig. 2 and Table 2, the reaction of Au^{3+} with 5-amino-benzimidazolone-2 forms a complex having two bands, with $\lambda_{max}=365$ nm and respectively $\lambda_{max}=580$ nm.

4. Composition of the Complex formed in the Fe(III) —5-Amino-benzimidazolone-2 System

The complex ions in the Fe(III) on Au(III) —5-amino-benzimidazolone-2 systems have been investigated as regards their composition by several spectrophotometric methods.

4.1. The Molar Ratios Method [5]

The results obtained by this method show that in solution only one complex ion corresponding to the ratio $L/Fe^{3+}=1$, (Fig.3) is formed. Applying the method in the case in which the ligand concentration is maintained constant and the concentration of the metal varies, (inverse titration), one obtaines the same combination ratio, 1 M : 1 L (Fig.4).

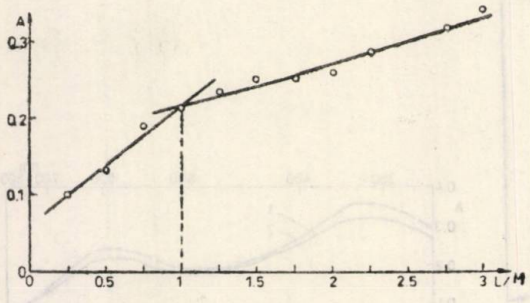

Fig. 3. — Application of the molar ratios methods to the determination of the composition of the Fe(III) — 5-amino-benzimidazolone-2 complex; $C_L = C_{FeCl_3} = 1 . 10^{-3}$ mol. l^{-1} ; $V_f = 7.5$ cm³.

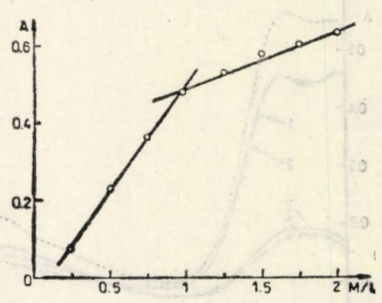

Fig. 4. — Determination of the composition of the Fe(III) — 5-amino-benzimidazolone-2 complex by inverse titration ; C_L =const. ; C_{FeCl_3} = variable ; $V_f = 5$ cm³.

4.2. The Job's Method [6]

In order to determine the composition of the formed complex, measurements of absorbance through solutions in which $FeCl_3 + L = const.$ at wavelength proper to the complex have been performed. The obtained results are presented in Fig. 5.

Fig. 5 shows that the $FeCl_3$ to 5-amino-benzimidazolone-2 combination ratio is 1 : 1, result which is in good agreement with those of previous methods.

The spectrophotometric data obtained by the above mentioned methods point out that in the Fe (III) — 5-amino-benzimidazolone-2 system, the complex with the 1 M : 1 L ratio is formed, supporting the following chemical process :

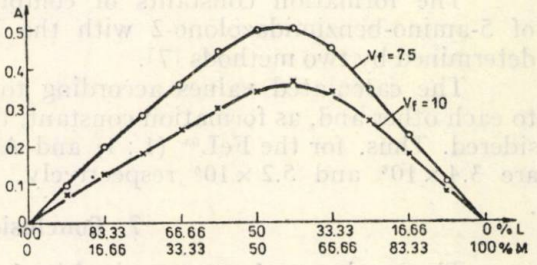

Fig. 5. — Study of composition of the $FeCl_3$ — 5-amino-benzimidazolone-2 system by Job's method.

$$Fe^{3+} + L \underset{\leftarrow}{\overset{\text{rapidly}}{\rightarrow}} FeL^{3+}.$$

The composition of the complex formed in the Au(III) — 5-amino-benzimidazolone-2 system was investigated with the same method as in previous case. The data obtained show the formation of only one complex, (Fig. 6).

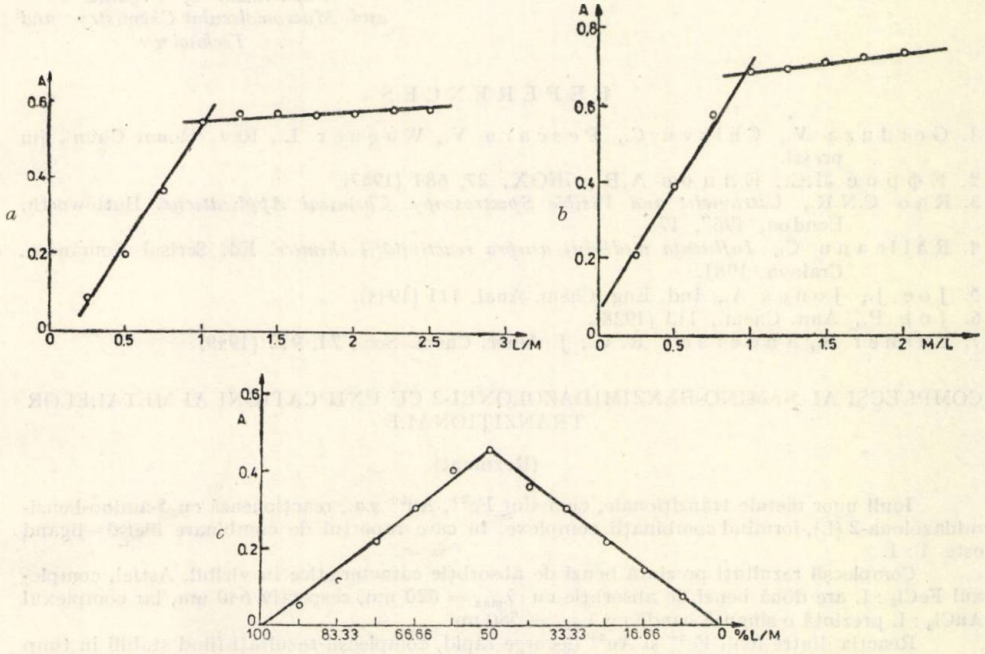

Fig. 6. — Study of the composition complex of the $AuCl_3$ — 5-amino-benzimidazolone-2 system by molar ratio (*a*), Job's method (*b*), invers titration (*c*).

The spectrophotometric data of the $AuCl_3$—5-amino-benzimidazolone-2 system, in aqueous solution, prove the formation of a single complex, $AuCl_3$—L (1 : 1).

6. Determination of the Formation Constant

The formation constants of complexes resulted from the reaction of 5-amino-benzimidazolone-2 with the Fe^{3+} and Au^{3+} ions have been determined by two methods [7].

The calculated values according to both methods are comparable to each other and, as formation constant, the mean values have been considered. Thus, for the FeL^{3+} (1 : 1) and AuL^{3+} (1 : 1) the calculated values are 3.4×10^6 and 5.2×10^6 respectively.

7. Conclusions

The results can be summarized in the following statements :

1. The Fe^{3+} and Au^{3+} ions react with 5-amino-benzimidazolone-2, forming complexes by ratio 1 M : 1 L.

2. The reaction between Fe^{3+}, Au^{3+} and ligand is a rapid one, the complex ions appearing instantaneously, when the reagents are mixed. The complex ions are stable in time.

3. The values of the formation constants show that the reaction between Fe^{3+}, Au^{3+} and ligand develops in the direction of the complex formation.

Received, April 28, 1985

Polytechnic Institute, Jassy,
Department of Organic
and Macromolecular Chemistry and
Technology

REFERENCES

1. Gorduza V., Chirvu C., Pescaru V., Wagner L., Rev. Roum Chim., (in press).
2. Ефрос Л.С., Елцов А.В., ЖОХ, 27, 684 (1957).
3. Rao C.N.R., *Ultraviolet and Visible Spectroscopy. Chemical Applications.* Butteworth, London, 1967, 17.
4. Răileanu C., *Influența mediului asupra reactivității chimice.* Ed. Scrisul Românesc, Craiova, 1981.
5. Joe J., Jones A., Ind. Eng. Chem. Anal, 111 (1944).
6. Job P., Ann. Chem., 113 (1928).
7. Turner S., Anderson R. G., J. Amer. Chem. Soc., 71, 912 (1949).

COMPLECȘI AI 5-AMINO-BENZIMIDAZOLONEI-2 CU UNII CATIONI AI METALELOR TRANZIȚIONALE

(Rezumat)

Ionii unor metale tranziționale, cum sînt Fe^{3+}, Au^{3+} ș.a., reacționează cu 5-amino-benzimidazolona-2 (L), formînd combinații complexe, în care raportul de combinare metal—ligand este 1 : 1.

Complecșii rezultați prezintă benzi de absorbție caracteristice în vizibil. Astfel, complexul $FeCl_3$: L are două benzi de absorbție cu λ_{max} = 620 nm, respectiv 640 nm, iar complexul $AuCl_3$: L prezintă o singură bandă cu λ_{max} = 580 nm.

Reacția dintre ionii Fe^{3+} și Au^{3+} decurge rapid, complecșii rezultați fiind stabili în timp și se supun legii Beer pe un domeniu larg de concentrații. Constantele de formare sînt : $3{,}40 \cdot 10^6$ și $5{,}2 \cdot 10^6$ l mol^{-1}.

BULETINUL INSTITUTULUI POLITEHNIC DIN IAȘI
Tomul XXXI (XXXV), Fasc. supl., 1985
Secția II
CHIMIE ȘI INGINERIE CHIMICĂ

D.C. 66.095.2

CATIONIC POLYMERIZATION OF 4-VINYL-1-CYCLOHEXENE

BY

IOAN I. NEGULESCU, AURA ANGELICA POPA and CAMELIA MIHĂILESCU

1. Introduction

4-Vinyl-1-cyclohexene (4-VCH) was polymerized cationically by several authors [1]...[3] and different structures were proposed for the chain units:

POSSIBLE UNITS OF 4-VINYLCYCLOHEXENE POLYMERS

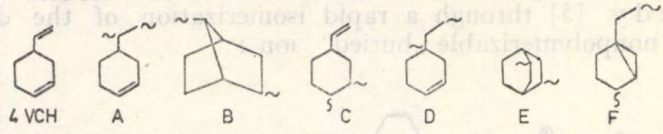

A: VINYLIC ADDITION (EXO)
B,E: CYCLOPOLYMERIZATION
C: OLEFINIC ADDITION (ENDO)
D: HYDRIDE SHIFT POLYM.

This monomer, 4-VCH, would be expected to undergo both olefinic and cyclic polymerization and, indeed, these types of enchainments, *A* and *B*, respectively, were first proposed by Butler et al. [1] who eliminated the participation of the internal olefinic bond alone, to form the structure C, as too resistant to be opened by cationic initiators. However, in a rather old paper, Hoffmann [4] mentioned briefly that cyclopentene and cyclohexene can be readily oligomerized with BF_3 and some HF to dimers, trimers and tetramers as well as transparent amber solid resins.

As suggested by Kennedy [5], and mentioned also by Hublein [3], other structural units of 1,3 addition type, *D*, could arise by intramolecular hydride shift isomerization as in cationic polymerization of vinylcyclohexane [6]. Besides the methylene bicyclo (2.2.1) heptane unit, *B*, another structural unit of bicyclo (2.2.2) octane type, *E*, could arise with some probability through the initiation at the group alone, followed by cyclization through the endo cyclic unsaturation, in a similar way to cyclization pointed out by Butler et al. [7] at the polymerization of 1-methylene-4-vinylcyclohexane, but this unit would be difficult to be differentiated from the other saturated structure of *B* type.

If one considers the tertiary homoallylic carbonium ion formed by hydride shift isomerization then the condensed bicyclic structure, *F*, could appear through a mechanism similar to methylene norbornene polymerization [8].

In the present paper the cationic polymerization of 4-VCH, in the presence of $AlCl_3$, is considered and the monomer encatenation is discussed.

2. Experimental

The monomer (4-VCH) was dried over molecular sieve (4 A) and freshly distilled from sodium metal before use under purified nitrogen. Methylene chloride was kept on and distilled from molecular sieve. The initiator ($AlCl_3$) was sublimed in a flask of 25 mL in which the solution in CH_2Cl_2 was made before the use. Polymerizations were carried out in Schlenk ampoules in nitrogen.

The molecular weight was determined by GPC (Waters 200, THF solutions) and crioscopically (benzene). DSC and DTA data were obtained using a DuPont 990 Calorimeter and a Paulik-Paulik-Erdey Derivatograph, respectively.

IR spectra were recorded on a Perkin Elmer (577) Spectrophotometer. NMR spectra were recorded on a JEOL 60 MHz Spectrometer in $CDCl_3$ using TMS as standard.

3. Results and Disscusion

The fact that high polymers are not obtained at low temperatures in cationic conditions, e.g. $AlCl_3$ in ethyl chloride at $-20°C$ [9], was explained by K e n n e d y [5] through a rapid isomerization of the dimercation leading to a nonpolymerizable „buried" ion :

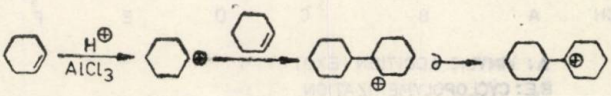

The double bond is reactive to protonation and/or cationation; however, in the parent compound propagation is impeded because of steric congestion. It is possible that at temperatures higher than $-20°C$ the reaction continues by elimination and alkylation, as suggested by the same author [5] in the case of cyclopentene :

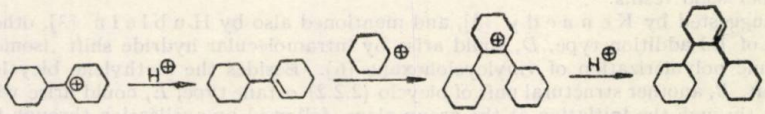

In the present work 4-VCH was polymerized with aluminum chloride in methylene chloride at $-40°$ and $20°C$ (Table 1) and the structure of the obtained products is discussed in terms of spectral and thermal data. Spectroscopic evidence indicates that the cationic polymerization of this monomer proceeds also by addition to the endo olefin bond, similarly to the cationic polymerization of 2-vinyl-5-norbornene, which proceeds predominantly by this type of addition at low temperatures especially.

Table 1

Polymerization of 4-VCH with $AlCl_3$ as Initiator) in CH_2Cl_2*

Exp.	Monomer		$AlCl_3$	T	Time	Yield		$\overline{M}_n$	Observations
	ml	mole/l	mole/l	°C	hrs	g	% conv.	by GPC	
1	8.3	2.80	0.022	−40	4	0.1017	1.65	3 430	Soluble white powder
2	16.6	2.80	0.043	−40	5	0.2085	1.52		Soluble white powder
3	4.0	0.29	0.028	*a*	20	0.7155	21.70	1 320	*a* : −40°C, 9 hrs. and to 20°C, 11 hrs; 44% ins.
4	8.0	0.42	0.089	20	48	1.0933	16.60	1 290	Light yellow ; 11% insoluble; $\overline{M}_w/\overline{M}_n = 3.1$.
5	2.0	0.30	0.206	20	48	1.4104	85.50	1 660	Light yellow ; 20% insoluble ; $\overline{M}_w/\overline{M}_n = 7.1$.
6	6.2	2.54	0.622	20	20	5.5986	total		Brown ; $AlCl_3$ added as powder at 20°C ; 98% ins. ; 6.9% Cl.
7	8.8	2.71	0.186	20	20	0.2461	2.96	2 300	Light yellow ; $AlCl_3$ added as powder at −45°C ; 5% ins.

*) $AlCl_3$ added as solution in CH_2Cl_2 if not otherwise indicated.

Thus the vinyl group is clearly evidenced in the IR spectrum (Fig. 1) of the polymer obtained at −40°C at 3 075 cm^{-1} (*m*), i.e. vinyl side chain on a ring [8] and 1 630 cm^{-1} (*m*), while the internal olefin bond absorbs at 3 020 cm^{-1} (*m*), 960 cm^{-1} (*m*) and 650 cm^{-1} (*s*).

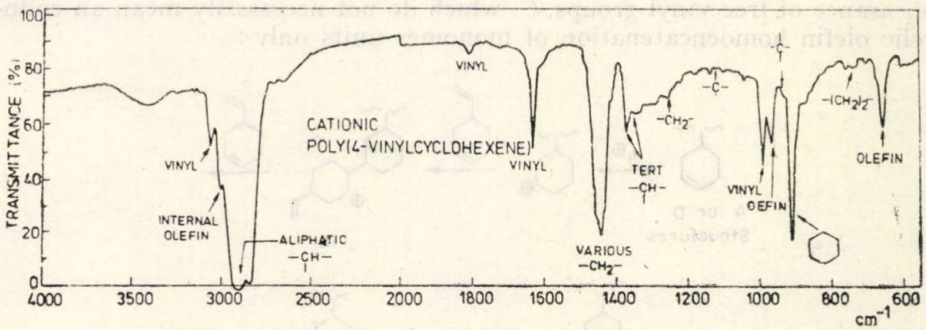

Fig. 1. — IR spectrum of poly(4—VCH) obtained at −40°C with $AlCl_3$ in CH_2Cl_2, KBr pellet.

The NMR spectrum of the same polymer was compared both with the spectrum of the monomer and with that of vinylcyclohexane. From Fig. 2 it can be seen that two of vinylic protons, *a* and *b*, as well as two olefinic protons of cyclohexene ring, *d* and *e*, from the monomer (bottom) could be differentiated easily in the spectrum of the cationic polymer.

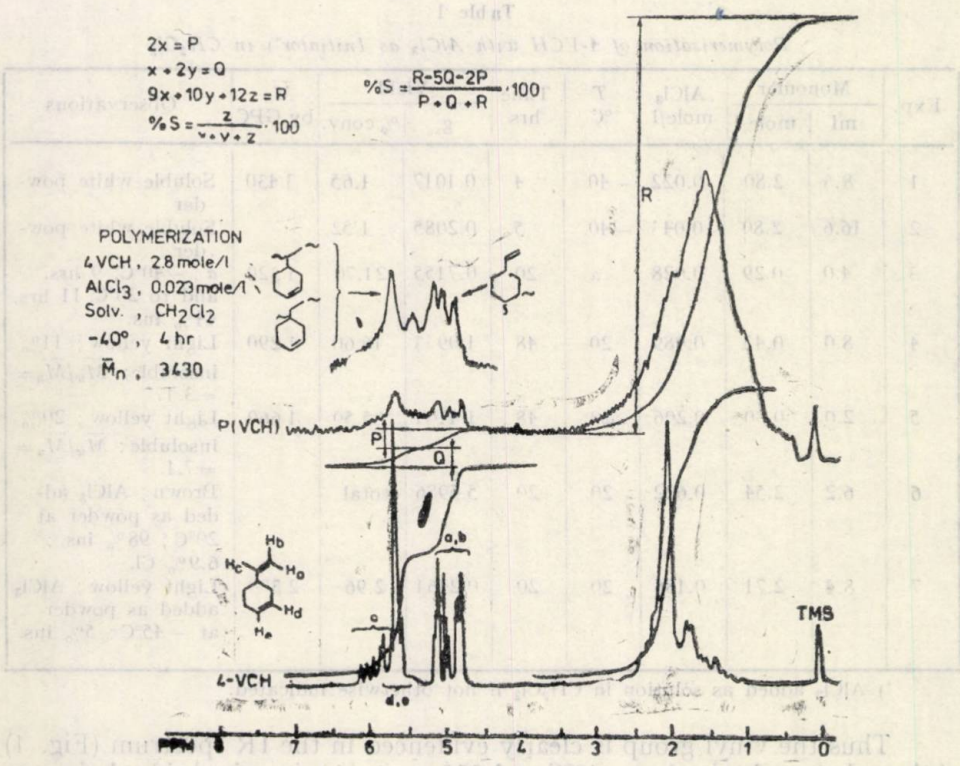

Fig. 2. — 60 MHz NMR spectra of 4-VCH and poly(4-VCH) in $CDCl_3$ at 60°C.

One can visualize the following scheme of reactions explaining the appearance of free vinyl groups, *C*, which do not necessarily mean an endocyclic olefin homoencatenation of monomer units only :

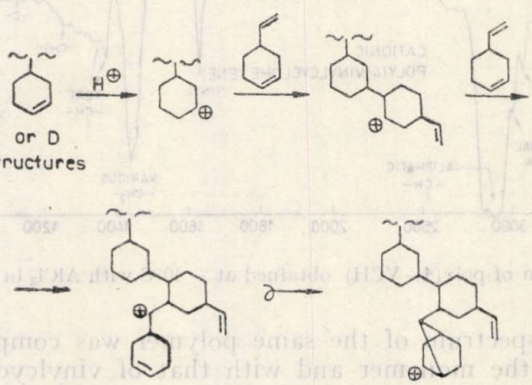

Consequently, both saturated bicyclic *B* units and free vinyl groups, *C*, can appear at the same time.

The degree of cyclization, S, given by saturated units can be readily determined from NMR data (Fig. 2):

$$\% S = \frac{z}{x+y+z}; \qquad \% S = 100\,\frac{R-5Q-2P}{P+Q+R},$$

where x, y and z represent the participation of vinyl, olefin and saturated units, respectively, and P, Q and R are the integral rise over the corresponding protons.

Not too much ground was found for the structure F from IR data, i.e. the condensed ring has no definite absorptions at 960 cm^{-1} (tert. methyne group overlaped by internal olefin band [8]) or 790 cm^{-1} (*vw*, bicyclic structure in a linear chain), so that it will not be taken further into consideration.

IR spectra evidentiate the other groups as follows: $>CH_2$ groups from the chain formed through an 1,3 encatenation (corresponding to D) appear between 720...750 cm^{-1} (*w*), in comparison with the IR spectrum of polyvinylcyclohexane [6], while the quaternary carbon, $-\overset{|}{\underset{|}{C}}-$ also from the structure D, absorbs at 1 170 cm^{-1} (*w*), 825 cm^{-1} (*w*) and 925 cm^{-1} (*w*, shoulder). All these bands are weak, indicating a low degree of participation of structure D ($A+D \sim 25\%$, vide infra). The absorptions from 2 920 cm^{-1} (*s*) and 2 860 cm^{-1} (*s*) corresponding to aliphatic $-\overset{\diagdown}{\underset{\diagup}{C}}-H$ groups or from 1 350 cm^{-1} (*w*) and 1 080 cm^{-1} (*vw*) corresponding to cyclic $-\overset{\diagdown}{\underset{\diagup}{C}}-H$ groups, as well as the absorptions of different $>CH_2$ groups, e.g. 1 445 cm^{-1} [5] and 1 270 cm^{-1} (*w*) are not particularly significant. The strong band from 895 cm^{-1} confirms the retention of the cyclohexane ring, this absorption being present in the IR spectra of linear polyvinylcyclohexene of type A [10] and cationic polyvinylcyclohexane formed by an 1,3 addition [6]. This band corresponds to the structures A, C and D.

Using the above NMR equations it was possible to estimate the ratio of structures $A...E$ for the polymer obtained at $-40°C$:

$$(A+D) : C : (B+E) = 4{,}5 : 4 : 9,$$

which gives 52% cyclization and 22% free vinyl groups.

The polymer structure, and consequently its characteristics, are very much affected by reaction conditions (Table 1). For example, the polymer prepared at 20°C, (experiment No. 4 from the Table 1) has only 7% free vinyl groups and 83% cyclized units (unfractionated soluble part of the sample), while the product formed at the same temperature but with the catalyst added as powder (quick exothermic reaction), (experiment No. 6) is practically insoluble.

The strong band at 650 cm^{-1} in IR spectra of insoluble materials show that the crosslinking occurs perhaps mainly by an intermolecular hydride transfer as proposed by H u b l e i n et al. [3].

Unlike poly(4-VCH) obtained with Z i e g l e r catalyst which is linear and crystalline [10], the corresoponding polymers synthesized in cationic conditions are amorphous materials that soften between 100° and 230°C [1] ...[3]. DSC and DTA thermograms of soluble fractions (Figs. 3, 4) evidence an exothermic effect between 120° and 240°C with $\Delta H = 103$ J/g (11.12 KJ/mol). This effect was no more registered if the analyzed sample cooled down to 20°C and re-run (Fig. 3 *C*) or if the pristine sample was annealed at 160°C for 12 min. (Fig. 4 *C*). The insoluble fraction of the

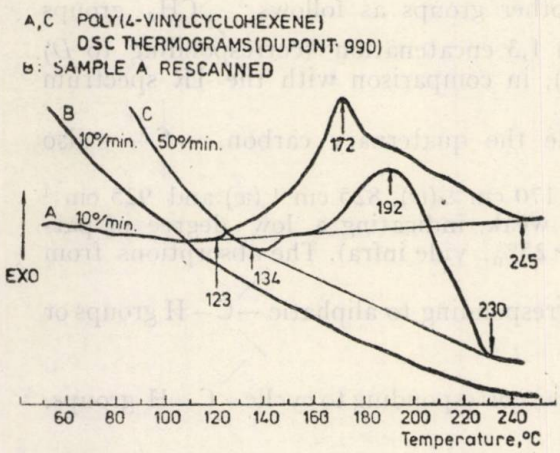

Fig. 3. — DSC thermograms of poly(4-VCH).

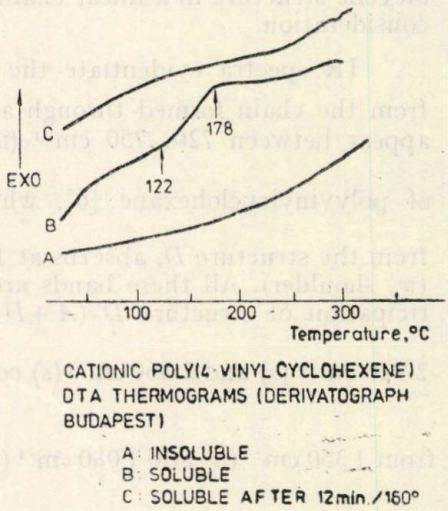

Fig. 4. — DTA thermograms of poly (4-VCH).

same polymer did not show any thermal effect in the same temperature range (Fig. 4 *B*). Based on the NMR and IR spectra of the annealed sample the exothermic effect was attributed to the reaction of free vinyl groups, i.e. the ratio of structures *A*...*D* became :

$$(A+D) : C : (B+E) = 3.5 : 2.3 : 11.3,$$

which gives 66% saturation and 13.5% free vinyl group containing units. If one takes $\Delta H \simeq 90$ KJ/mol to open the vinyl bond of 4-VCH it follows that 12.35% of the polymer units became saturated by reaction of vinyl groups alone, in good agreement with NMR calculations.

4. Conclusions

1. In the presence of $AlCl_3$ at low temperatures, besides vinyl polymerization, intramolecular hydride shift isomerization polymerization and cyclo-polymerization , 4-vinyl-1-cyclohexene can form polymers also

by initiation at the vinyl group alone followed by cyclization through the endo cyclic unsaturation.

2. Saturated structures (more than 50%) formed by cyclopolymerization and cyclization can not be differentiated.

3. Free vinyl groups (cca 20%) were evidenced especially in soluble polymers obtained at −40°C.

4. Part of free vinyl groups disappeared by annealing the sample (120°/6 min.) but the polymer remained soluble, which means that the increase of saturation (cca. 12%) was not the result of crosslinking reactions.

Received, March 26, 1985

„P. Poni" Macromolecular Chemistry Institute, Jassy

REFERENCES

1. Butler G. B., Miles M.L., J. Polymer Sci., **A 3**, 1609 (1965).
2. Альева А. Г., Стоцкая Л. Л., Кренцел Б. А., Высокомол. соедин., **A XV**, 1005 (1973).
3. Hublein G., Hublein B., Plaste u. Kautschuk, **23**, 95 (1976).
4. Hoffmann F., Chem. Ztg., **57**, 5 (1933).
5. Kennedy J. P., *Cationic Polymerization of Olefins : A Critical Inventory.* Wiley-Interscience, 1975, 150.
6. Kennedy J. P., Elliott J. J., Naegele W., J. Polymer Sci., **A 2**, 5029 (1964).
7. Butler G. B., Miles M. L., Brey W. S., J. Polymer Sci., **A 3**, 723 (1965).
8. Kennedy J. P., Makowski H. S., J. Macromol. Sci. - chem., **A-1**, 345 (1967).
9. Boor J., Youngman E. A., Dimbat M., Makromol. Chem., **90**, 26 (1966).
10. Marconi W., Cesca S., Della Fortuna G., J. Polymer Sci., **B(2)**, 301 (1964).

POLIMERIZAREA CATIONICĂ A 4-VINIL-1-CICLOHEXENEI

(Rezumat)

4-Vinil-1-ciclohexena a fost polimerizată în prezenţă de $AlCl_3$ în CH_2Cl_2 la −40°C şi 20°C. Pe lîngă structurile saturate formate prin reacţii de ciclopolimerizare şi ciclizare, în cazul fracţiilor solubile s-au evidenţiat spectral (NMR, IR) grupe vinilice libere ce pot apare prin polimerizarea cationică endociclică. Grupele vinilice libere dispar parţial în urma tratamentului termic (160°C16 min.) ce determină creşterea gradului de saturare a polimerului.

BULETINUL INSTITUTULUI POLITEHNIC DIN IAȘI
Tomul XXXI (XXXV), Fasc. supl., 1985
Secția II
CHIMIE ȘI INGINERIE CHIMICĂ

D.C. 678 13

SYNTHESIS AND PROPERTIES OF CERTAIN NEW ACRYLIC COPOLYMERS

I. SYNTHESIS AND PROPERTIES OF ACRYLONITRILE–MONOANILIDE OF FUMARIC ACID WITH SULPHANILIC ACID Na SALT COPOLYMERS

BY

ILIE DIACONU and CARMEN CHELARU

1. Introduction

Polyacrylonitrile is considered today as one of the most important polymer in synthetic fibres industry. However, in order to improve some of its properties (e.g., the affinity for dyes and the hydrophilicity), acrylonitrile-based copolymers are used. These copolymers contain a high percent of acrylonitrile because the —CN groups determine a good intramolecular cohesion, a high thermal stability and mechanical resistance [1] ... [4].

Acrylic homopolymers and copolymers, especially polyacrylonitrile (PAN), are compounds whose structure and structural changes have remained a difficult problem to elucidate. From this reason, the origin of the thermal transitions in PAN has not been uniquely determined. The published data indicate that the glass transition temperature, T_g, of PAN is scattered over a wide range of temperature (70°...140°C) [5] ... [7] depending on the experimental method used and on the procedures of preparing the samples.

The thermally stimulated depolarization currents method commonly works in ranges of equivalent frequencies of 10^{-2}....10^{-4} Hz, and therefore could be an useful complementary tool for the molecular motion, structure and transition studies of the macromolecular compounds.

This paper reports the copolymerization of acrylonitrile (AN) with a new monomer — monoanilide of fumaric acid with sulphanilic acid — Na salt (*S*), and structural and physical characterization by IR, NMR and thermally stimulated depolarization currents (TSDC) spectroscopic analysis of the copolymer.

2. Experimental

The *S* monomer (99.9%) was used as such and AN was distilled immediately before use.

The parameters of copolymerization were determined by solution polymerization, using free radicals as initiators. Polymerizations were carried out in sealed Pyrex tubes, under argon, in aqueous solution, (at 1 M monomer concentration), at 58°C, using the redox initiators sodium metabisulfite and ammonium persulfate. The copolymerization period was established between 10...15 min. to obtain conversions less than 10%. The copolymerization period increased with the decrease of AN content in the initial mixture. The copolymers were insoluble in the reaction medium.

The purified copolymers (resolved in DMF and reprecipitated in water) were dried at 50°C, under reduced pressure, for 48 hours, for the complete removal of the solvent, (DMF), which tends to be bound to the polar groups of the polymer.

Copolymers composition were determined by elemental microanalysis for sulphur, and by ^1H-NMR spectroscopy from the ratio of aromatic to aliphatic signal integrals, the spectra being registered on a JEOL–C60 HZ spectrometer, in DMSO–d6 solutions at 60°C.

Samples used for TSDC measurements were disk-shaped, prepared by compressing the compounds powder in a mold under a pressure of 10×10^4 N/cm^2. The 16 mm - diameter disks were provided with vacuum-evaporated silver electrodes of circular form. In order to prevent current leakage on surface the electrodes had a diameter of only 14 mm and were centrally placed on both sides of the disks.

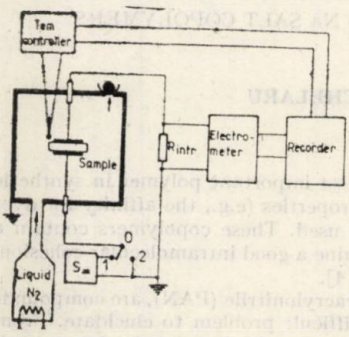

Fig. 1. – Main components of automated equipment for TSDC.

TSDC measurements were caried out in dry nitrogen using a device presented in Fig. 1.

The thermal cycles of polarization and depolarization of samples consisted of the following steps : a sample with a polarization field E_p was warmed up to the polarization temperature T_p, which was maintened constant for a polarization time t_p ; after cooling to 20°C using liquid nitrogen, E_p was removed and the sample was short circuited for 10 min. in order to eliminate the rapid depolarization currents ; then the depolarization currents were recorded by increasing the temperature. The thermal cycles were performed at a rate of 3.3° C/min.

3. Results and Discussion

The IR spectra (Fig. 2) make evident the formation of AN–S copolymers [8].

Copolymerization data are summarized in Table 1 and the copolymerization diagram is presented in Fig. 3.

Table 1

S(M_1)–AN(M_2) Copolymerization Data

Sample	Initial mixture $[M_1]/[M_2]$	Conversion %	Copolymer composition $d[M_1]/d[M_2]$
P(AN–S)$_I$	0.05263	8.5	0.010
P(AN–S)$_{II}$	0.17649	9.1	0.051
P(AN–S)$_{III}$	0.3333	9.5	0.089
P(AN–S)$_{IV}$	0.5385	9.0	0.150
P(AN–S)$_V$	1.00	8.7	0.220
P(AN–S)$_{VI}$	3.00	8.0	0.639

The reactivity ratio values, r_1 and r_2, were determined by Kélen-Tüdös method [9], the obtained results being presented in Fig. 4.

The obtained reactivity ratio values are : $r_{AN} = 4.18$ and $r_S = 0.1$.

The straight lines in Kélen-Tüdös plot indicate that no penultimate effect seems to exists for these copolymers, and that the terminal model of copolymerization could be considered to describe this system.

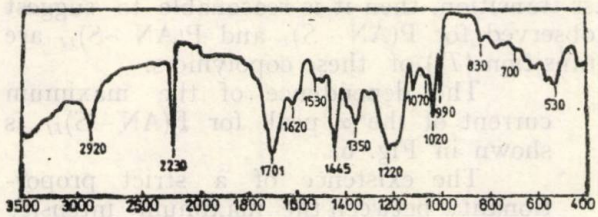

Fig. 2. — The IR spectrum of $P(AN-S)_{II}$ copolymer.

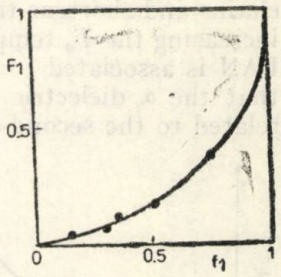

Fig. 3.—The copolymerization diagram of the $S(M_1)-AN(M_2)$ system.

The TSDC thermograms of PAN, $P(AN-S)_I$ and $P(AN-S)_{II}$ in the temperature range 50°...250°C are comparatively presented in Fig. 5.

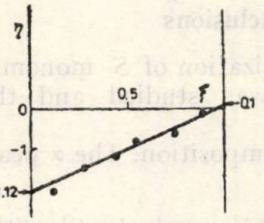

Fig. 4. — The Kélen-Tüdös plot for the $S(M_1)-AN(M_2)$ system.

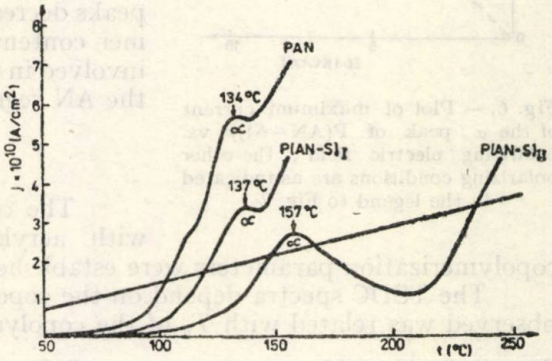

Fig. 5. — TSDC spectra of PAN, $P(AN-S)_I$ and $P(AN-S)_{II}$; polarizing conditions: $E_p = 10$ KV/cm; $t_p = 30$ min; $T_p = 150$°C for PAN and $P(AN-S)_I$, and 200°C for $P(AN-S)_{II}$.

All spectra have the same general shape and are characterized by one current peak (α), more or less resolved, and an increasing current part (ρ) at higher temperatures. The α peak of $P(AN-S)_{II}$ is well resolved, whereas in the case of $P(AN-S)_I$, and especially for PAN, this peak is overlaped by ρ increasing current, which probably is the increasing portion of a new arising peak. In order to maintain unalterable the structure of the polymers, the samples were not warmed up over the temperatures shown in Fig. 5.

Fig. 5 shows that both intensity and temperature of the α peak are appreciably affected by the copolymer composition. The maximum intensity of the α peak is a decreasing function of the *S* comonomer content, whereas the corresponding temperature values increase. The α peak temperature of PAN, shown in Fig. 5, appears to be close to the glass transition temperature (140°C) reported elsewhere [5], [6]. The *S* comonomer is more bulky and more polar as compared to the AN monomer. The introduction of this comonomer enhances the dipole—dipole interactions between adiacent

chains and shortens the AN segments of chains. This two facts result in an increasing the T_g temperature of the copolymers. If the α peak observed for PAN is associated to the glass-transition, then it is reasonable to suggest that the α dielectric peaks observed for $P(AN-S)_I$ and $P(AN-S)_{II}$ are related to the second-order transition (T_g) of these copolymers.

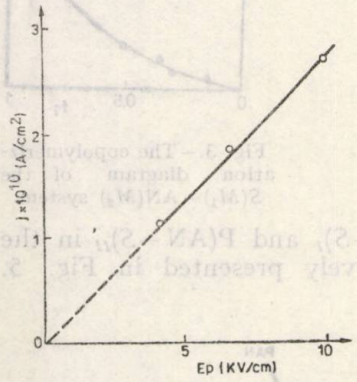

Fig. 6. — Plot of maximum current of the α peak of $P(AN-S)_{II}$ vs. polarizing electric field ; the other polarizing conditions are as indicated in the legend to Fig. 2.

The dependence of the maximum current of the α peak for $P(AN-S)_{II}$ is shown in Fig. 6.

The existence of a strict proportionality between the maximum intensity and field strength shows that a uniform volume dipolar polarization is taking place [10]. This finding also supports the fact that the observed α peaks are related with the second-order transition.

Since the maximum intensity of the α peaks decreases with increasing *S* comonomer content, the micro-Brownian motions involved in the polarization process occur in the AN segments of the copolymer.

4. Conclusions

The copolymerization of *S* monomer with acrylonitrile was studied and the copolymerization parameters were established.

The TSDC spectra depend on the copolymer composition. The α peak observed was related with T_g of the copolymers.

Received, April 24, 1985

„P. Poni" Institute of Macromolecular Chemistry, Jassy

REFERENCES

1. Goldfinger G., Steidlitz M., J. Polym. Sci., **3**, 786 (1948).
2. Alfrey T.Jr., Overberger C.G., Pinner S.H., J. Amer. Chem. Soc., **75**, 4 221, (1953).
3. Nair A.S., Muthana M.S., Makromol. Chem., **47**, 138 (1961).
4. Аскаров М.А., Банк А. С., Высокомол. Соед., **8**, 1012 (1966).
5. Andrew R.D., Kimmel R.M., J. Polym. Sci., B. Polym. Lett., **3**, 167 (1965).
6. Meredith R., Hsu B.S., J. Polym. Sci., **61**, 276 (1962).
7. Stupp S.I., Carr S.H., J. Polym. Sci., Polym. Phys. Ed., **18**, 13 (1978).
8. Belamy L.J., *The Infra-Red Spectra of Complex Molecules*. New-York, 1964.
9. Kélen T., Tüdös F., J. Macromol. Sci., Chem., **A9**, 1 (1975).
10. Diaconu I., Dumitrescu Sv., J. Macromol. Sci., Phys., **B21**, 555 (1982).

SINTEZA ȘI PROPRIETĂȚILE UNOR NOI COPOLIMERI ACRILICI

I. Sinteza și proprietățile copolimerilor acrilonitrilului cu *p*-sulfonatul de Na al anilidei acidului fumaric

(Rezumat)

Se studiază copolimerizarea acrilonitrilului cu un nou monomer — *p*-sulfonatul de Na al anilidei acidului fumaric — și proprietățile dielectrice ale copolimerilor prin metoda curenților de depolarizare termic stimulați.

BULETINUL INSTITUTULUI POLITEHNIC DIN IAŞI
Tomul XXXI (XXXV), Fasc. supl., 1985
Secţia II
CHIMIE ŞI INGINERIE CHIMICĂ

D.C. 667.167

INFLUENCE OF FLAME-RETARDANTS ON THE BEHAVIOUR OF POLYOLEFINES AT HIGH TEMPERATURES

BY

CORNELIA VASILE, FLORIN POPESCU, OANA PETREUŞ, MIHAELA SABLIOVSCHI, ANTON AIRINEI and I. AGHERGHINEI

1. Introduction

Because of the various applications of the polyolefines, their flame-retardancy has a great practical importance. The theoretical study of polyolefine flame-retardancy points out some interesting aspects, since small structural differences determine specific behaviours at high temperatures in the presence of oxigen. Thus, the poly(propylene) sensitivity at the formation of hydro- and peroxides is of about one hundred times higher than for poly(ethylene).

The retardation of the flame and its extinction can be explained by the following complementary theories [1], [2]: gas, thermal, chemical, coating and physical interaction theory ; but in the case of each polymer flame-retardant system, the interaction in solid phase or in gaseous phase is predominant.

On this theoretical basis, a classification of inorganic flame-retardants was made : chain transfer agents, which slow the free radical reactions ; ingredients which develop non-flammable gases ; compounds which are capable of forming glassy coating on the burning mass ; materials which act as catalysts for char formation ; molecules which reduce the volatility of the important components and resin formers which act as coupling agents between the substrate and flame retarding agents.

Because of the diversity of the organic flame-retardants and the synthesis of a great number of new compounds, a such classification is extremely difficult.

In the present work, the flame-retardant effect on the polyolefines of four compounds containing halogen, phosphorous and nitrogen was studied. Two of these compounds have small molecules, the others are macromolecular. The tests allowed the determination of the class of each flame-retardant.

2. Experimental

Materials. The investigated samples consisted of poly(ethylene) or poly(propylene) flame-retardants systems. The characteristics of the compounds are given in Table 1.

Mixtures were prepared by stirring the melted PE or PP with 10...16% of above mentioned flame retardants (Table 2).

Table 1

Characteristic of the Components of the Polyolefine/Flame–Retardant Systems

No.	Component	Characteristics	Symbol
1	Poly(ethylene)	I. Polymeric materials. Low-density ; $\rho = 0{,}905$ g/cm³; $\bar{M}_n = 19\,000$; $T_m = 110°...130°C$; commercial, Brazi-Petrochemical Works, Romania.	PE
2	Isotactic poly(propylene)	100% isotactic ; $\bar{M}_n = 22\,000$; $\rho = 0.90 ... 0.91$ g/cm³ ; $T_t = 166 ... 168°C$; commercial Hoechst (BDR).	IPP
3	Atactic poly(propylene)	100% atactic ; $\bar{M}_n = 38\,000$; $\rho = 0.835$ g/cm³ ; $T_t = 145°C$; commercial, Teleajen Petrochemical Works, Romania.	APP
4	Chlorendic anhydride 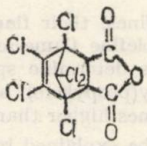	II. Flame retardants. Solid; melting point 230°...235°C; 27.78% C; 1.02% H ; 54.72%Cl	HET
5	Tris(dichloropropyl)phosphate 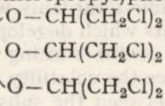	Liquid ; boiling point 250°C, with decomposition ; viscosity 1 800 cP ; 49.0% Cl ; 7.2% P.	TDF
6	Poly(phosphonate) containing chlorine 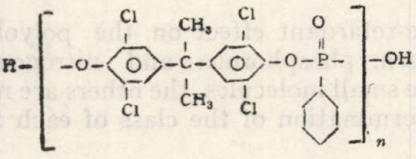	$n = 6 ... 10$; solid ; softening point 193°C ; 51.01% C ; 4.25% H ; 28.75% Cl ; 7.28% P.	PFC
7	Polymer containing phosphorous and nitrogen 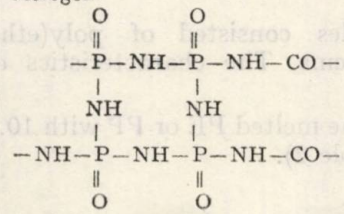 (probable structure)	solid ; crosslinked ; infusible ; 28.0% P ; 38.92% N	PNP

Table 2

TG and DTA Data of Flame Retardants, Non-Additived and Additived APP, IPP and PE

No.	Sample	Temperatures, [°C]			Residue, [%]			S_{DTA} cm²	E_{CR} KJ/mol	n
		T_i	T_m	T_f	R_{TG}	$R_{theor.}$	R_p			
1	HET	158	209	296	0	—	0	3.72	68.85	0
2	TDF	83	287	320	12	—	—	3.92	26.59	0
3	PFC	271	433	496	20	—	—	0.0	71.10	0
4	PNP	233	320	382	15	—	—	11.47	84.35	1.4
		382	410	470					227.88	2.5
5	APP	209	430	495	0	0	0	6.95	45.46	0
6	85 APP/15 HET	183	304	540	3.5	0	1.66	9.62	50.06	0.5
			357						42.70	0
7	85 APP/15 TDF	203	305	487	4.0	1.8	0	7.13	49.26	0
			430						71.11	0.8
8	85 APP/15 PFC	242	430	490	8.0	3.0	0	6.07	51.77	0
9	85 APP/15 PNP	209	427	490	4.5	2.3	5.0	9.33	46.28	0.7
10	IPP	228	434	492	0	—	0	15.38	51.43	0
11	90 IPP/10 HET	234	447	518	4.0	0	2.8	13.52	49.93	0
12	90 IPP/10 TDF	230	310	503	3.0	1.2	1.3	15.33	86.09	1.0
			438						121.22	0.9
13	90 IPP/10 PFC	254	456	512	5.5	2.0	1.3	12.20	62.43	0
14	90 IPP/10 PNP	205	433	490	5.5	1.5	4.6	13.92	58.20	1.2
15	PE	257	462	533	0	0	0	13.40	71.22	0
16	90 PE/10 HET	273	468	524	5.0	0	4.5	13.16	55.71	0
17	90 PE/10 TDF	197	304	527	4.5	1.9	0	11.57	73.99	0.9
			468						169.54	
18	90 PE/10 PFC	262	466	532	4.5	1.2	0	12.92	88.84	0
		308								
19	90 PE/10 PNP	226	460	524	8.5	1.5	2.6	15.83	57.99	0

R_{TG} – TG residue ; R_{theor} – theoretical residue ; R_p – pyrolysis residue.

3. Metods of Investigation

The thermooxidative behaviour was followed on a MOM-Derivatograph, Paulik-Paulik-Erdey type, using powders of mixtures. A high heating rate was chosen in order to obtain an approximative simulation of burning [3], [4].

Other conditions are : 50 mg sample weight, Al_2O_3 freshly calcined at 1 200°C as reference. The activation energies were evaluated by Coats-Redfern [5] and Reich-Levi [6] methods.

The pyrolysis studies were carried out in an autoclave type reactor, at 400°...470°C, in a self-generated atmosphere. As a consequence of the pyrolysis process gases, liquids and solids are formed. These products were analysed by convenient methods [7].

4. Results and Discussion

4.1. Thermogravimetric studies

The influence of flame-retardants on the thermal behaviour of APP, IPP and PE can be followed by the modification of characteristic decom-

position temperatures, residue amount obtained at high temperatures, the endothermicity of the decomposition process and the activation energies.

The variation of the mentioned parameters depends on the substrate / flame-retardant interaction and their compatibility.

The micromolecular compounds (HET and TDF) volatilize with decomposition at lower temperatures and two peaks or one with inflexion appear on DTG curves. Samples with polymeric flame-retardants show more simple DTG curves, with a single large peak.

The influence of the flame-retardants becomes more pronounced in the TG curves for poly(propylene) (Fig. 1), the weight losses at different temperatures being smaller for samples with HET and PFC. Differences become more proeminent together with the increasing of temperature, because of formation of decomposition residue. The residue formation in the polyolefine decomposition is supported by the fact that the experimental values are greater than the theoretical ones. The residue remains stable after 530°...600° C and can be utilized to evaluate the oxigen index [8]. The oxigen index increases from 16...17 for PE or PP to 21...23. The last value is the limit between the inflammable and noninflammable polymers and it is reached in the case of APP/PFC, IPP/PFC, IPP/PNP and PE/PNP systems.

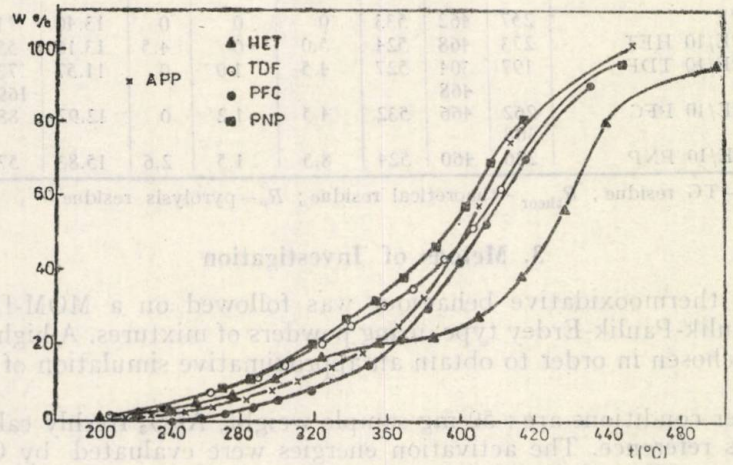

Fig. 1. — TG curves of the decomposition of additived poly(propylene) :

From Table 2 we conclude that the PFC flame-retardant leads to the increasing of thermal stability of polyolefines; PNP enhances the endothermicity of the decomposition process and TDF probably interacts with the polymer substrate, when the activation energies show great variations. The modification of thermal stability and the reaction mechanism is evidenced by the variation of activation energy against the transformation degree. The greater variations are noticed for PP (Fig. 2).

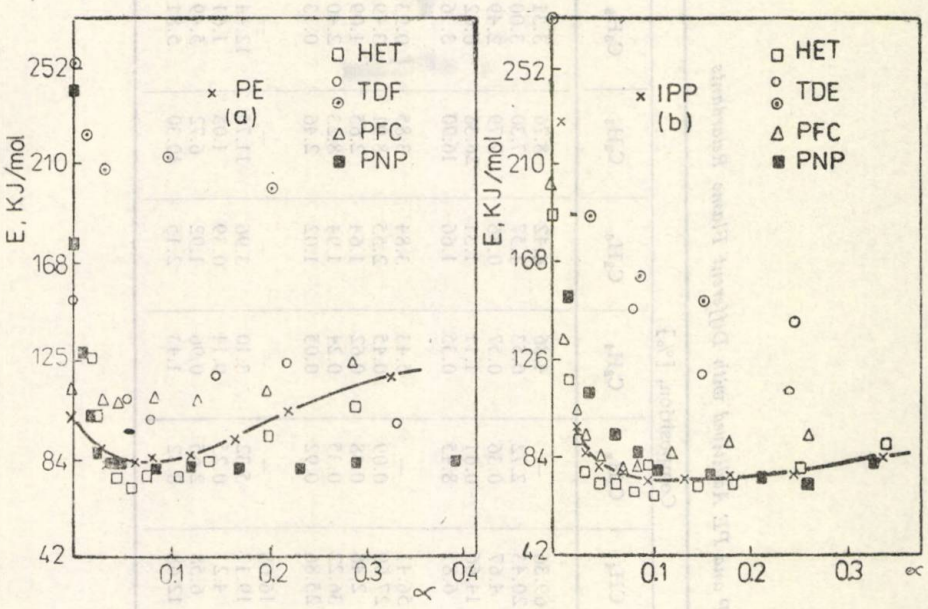

Fig. 2. — Variation of activation energy (Reich-Levi method) versus conversion degree $\alpha = w_t/w_\infty$ for PE (*a*) and IPP (*b*).

HET has a catalytic action on the PE and PP decomposition and the E_{RL} values are greater than of non additived polymer. A such catalytic activity was also observed for other flame-retardants [1], [2]. Similar plots for pure flame-retardants showed that the activation energy for TDF is 42 kj/mol, characteristic value for volatilization. The pronounced increase of E_{RL} values for additived polymers reveals the interaction of components.

4.2. Pyrolysis Studies

The non-additived polymers subjected to the pyrolysis do not give carbonic residue. In the presence of flame-retardants, the residue amount varies between 1...5%, depending on the flame-retardant nature, what is supported by TG data. Adequately, variations in the amount of gases and condensable product were noticed.

a) *Gaseous Fraction.* The amount of gases and their evolving rate is smaller for almost all additived samples (Fig. 3). A marked diminution was observed for PE additived with HET and PNP, and for PP additived with HET, PFC and TDF.

The characteristics of gaseous fraction are given in Table 3. The densities and molecular weights of additived samples are smaller than those of pure polymers. Great amounts of HCl evolved from samples additived with HET and TDF, CO_2 and NH_3 result from samples with PNP. The two gaseous products are non-inflamable and dilute the combustible gases (saturated and unsaturated C_1-C_4 hydrocarbons). Acetylene results only

Table 3

General Characteristics of Gaseous Fraction Obtained by Pyrolysis of APP, IPP and PE Additived with Different Flame Retardants

No.	Sample	Density g/l	$\bar{M}$	g HCl / 100 g gas	Composition, [%]							
					CO_2	H_2	CH_4	C_2H_2	C_2H_4	C_2H_6	C_3H_3	C_3H_8
1	APP	1.9987	57.86	—	3.62	1.01	69.36	—	4.86	4.42	8.76	3.31
2	85 APP/15 HET	1.5528	44.95	1.049	3.10	1.09	20.43	2.72	0.53	1.57	7.30	3.00
3	85 APP/15 TDF	1.4643	42.29	0.052	1.30	0.89	4.67	0.36	0.57	0.86	7.79	2.49
4	85 APP/15 PFC	1.6184	46.85	0.025	0.42	0.96	14.66	0.61	1.11	1.31	26.38	6.62
5	85 APP/15 PNP	1.6677	48.27	—	39.25	0.20	6.81	8.45	0.35	1.66	16.90	3.16
6	IPP	1.7236	49.89	—	0.24	1.42	56.41	—	5.43	3.84	3.85	0.93
7	90 IPP/10 HET	1.8568	53.75	0.072	6.77	0.40	27.69	0.09	0.45	2.55	8.91	3.49
8	90 IPP/10 TDF	1.5110	43.74	0.0133	2.39	0.12	2.46	0.38	0.62	1.64	2.65	1.09
9	90 IPP/10 PFC	1.6349	47.33	0.031	8.47	1.79	36.22	0.35	0.24	1.94	8.23	2.40
10	90 IPP/10 PNP	1.7132	49.59	0.012	21.42	0.16	25.86	0.92	0.05	1.02	2.46	0.13
11	PE	1.8581	53.74	—	0.66	0.70	16.68	—	—	—	—	—
12	84 PE/16 HET	1.5976	45.73	0.225	19.17	0.72	19.17	5.32	3.10	3.96	11.75	12.44
13	90 PE/10 TDF	1.5138	43.82	2.463	7.04	0.29	4.21	0.25	0.14	0.39	1.05	1.61
14	90 PE/10 PFC	1.5143	43.84	0.012	11.09	0.48	6.58	2.65	0.96	1.92	6.72	5.49
15	90 PE/10 PNP	1.6866	48.83	—	57.42	0.60	12.68	8.32	1.43	2.15	10.30	5.81

from the pyrolysis of additived samples and its presence can explain the diminution of density and molecular weight.

b) *Liquid Fraction.* Data concerning the analysis of the liquid fraction are summarized in Table 4. It founds that each polymer/flame retardant system presents a specific behaviour. Densities are higher for the additived samples, and a marked increase takes place at flame-retardancy with TDF and PFC. The volatility decreases for IPP/flame-retardant systems and increases for PE/flame-retardant system, since the unsaturation decreases, and rise the aromaticity and the number of P—O bonds in samples with PFC and HET. The aromatic structures were also evidenced by IR-spectroscopy (1 600 cm^{-1}, 900...980 cm^{-1} and 800...885 cm^{-1}). It is well-known that the aromatic compounds burn heavier and cause the retardation of the flame by the two flame-retardants.

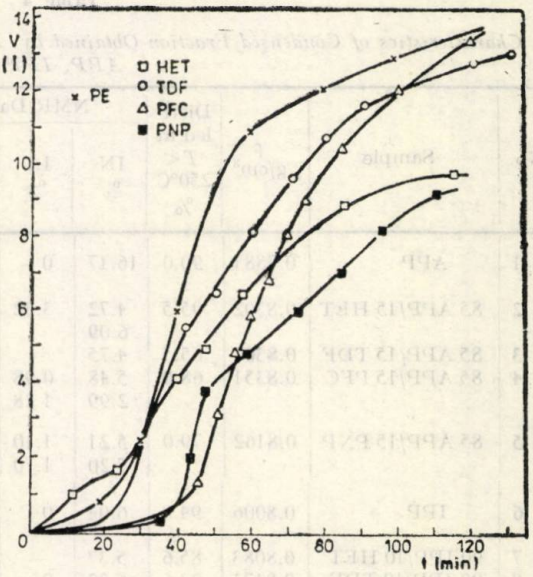

Fig. 3. — Variation of gaseous volume against reaction time (T=480...500°C, 300 g sample).

The contamination degree of the liquid fraction varies between 0.5 and 3.5%, forming compounds with N, Cl and P, which decrease also the inflammability. These compounds are in the small amounts and their structure is unknown.

The solid product or decomposition residue has the composition given in Table 5.

Phosphorous and nitrogen remain in residue, while chlorine goes into the composition of volatile fractions, in small amounts as it was shown above.

The residue structure depends especially on the flame-retardant, as it results from IR absorption spectra (Fig. 4). From the additived samples with HET a carbonic residue was obtained. The residue of the other samples contains besides carbon structures appearing from the heating modification of the P—O or P—N bonds for the samples flame-retarded with TDF, mainly with PFC and PNP.

IR absorption spectra of the residue differ from those of flame retardants heated for 15 min. at high temperatures (190°...250°C). These differences can appear from a polymer and flame-retardant chemical interaction leading to a specific structure.

Table 4

Characteristics of Condensed Fraction Obtained by Pyrolysis of Additived and Non-Additived APP, IPP and PE

No.	Sample	ρ g/cm³	Distilled at T< 250°C %	NMR Data			Elemental analysis, [%]					
				IN %	IA %	NS/ 1000 C	C	H	N	Cl	P	O
1	APP	0.7881	90.0	16.17	0	74.07	84.89	14.05	—	—	—	1.0
						21.24						
2	85 APP/15 HET	0.8302	95.5	4.72	3.32	54.32	83.64	13.72	—	2.41	0.23	0
				6.09		43.25						
3	85 APP/15 TDF	0.8301	65.5	4.75	—	43.36	83.79	13.86	—	1.36	0.77	0.2
4	85 APP/15 PFC	0.8351	68.0	5.48	0.98	28.29	82.52	13.23				
				2.99	1.28	49.42						
									—	2.78	0.70	0.7
5	85 APP/15 PNP	0.8162	79.0	5.21	1.10	47.14	84.79	13.90	0.29	—	0.64	
				7.20	1.70	62.96						0.3
6	IPP	0.8006	94.0	6.04	0	64.90	85.28	14.15	—	—	—	0.5
						66.40						
7	90 IPP/10 HET	0.8083	85.6	5.37	—	48.46	84.03	13.91	—	1.36	—	0.0
8	90 IPP/10 TDF	0.8171	93.6	6.23	0	55.44	80.44	13.25	—	0.88	0.80	4.6
9	90 IPP/10 PFC	0.8129	80.9	5.80	1.84	51.99	83.78	13.29	—	1.97	0.83	0.1
10	90 IPP/10 PNP	0.7904	89.2	6.23	—	54.53	85.45	14.05	—	—	0.50	0
11	PE	0.8101	49.0	8.30	2.20	—	85.46	14.25	—	—	—	0.29
12	90 PE/10 HET	0.8102	87.9	2.19	1.09	—	84.77	13.49	—	1.39	—	0.35
13	90 PE/10 TDF	0.8463	56.1	2.99	—	—	83.79	13.86	—	1.65	0.52	0.18
14	90 PE/10 PFC	0.8400	50.6	5.43	4.77	—	82.66	13.27	—	2.37	1.17	0.53
15	90 PE/10 PNP	0.8177	70.0	4.39	1.95	—	84.43	13.73	0.40	—	0.81	0.63

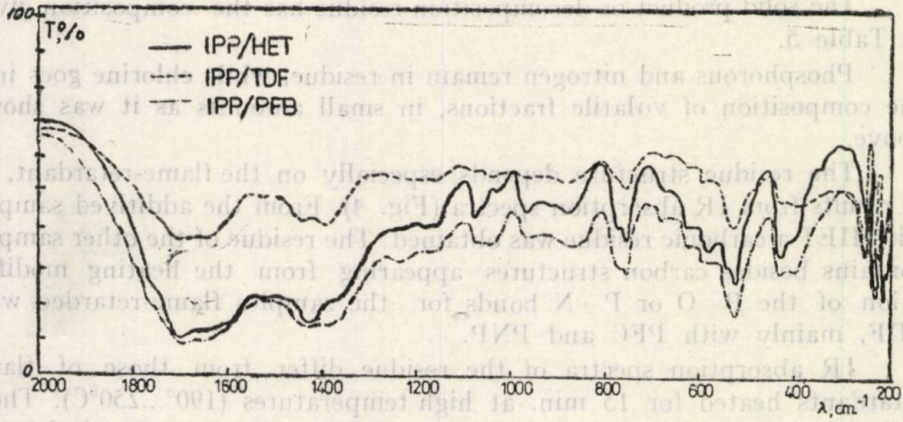

Fig. 4. — IR absorption spectra of carbonic residue resulting from the decomposition of IPP/flame-retardant system.

Table 5

Analytical Data of the Solid Product Obtained by Pyrolysis of Additived Samples

No.	Sample	Elemental analysis, [%]					
		C	H	N	Cl	P	Residue
1	85 APP/15 PNP	35.38	3.29	22.78	—	9.46	31.96
2	90 IPP/10 HET	90.69	4.38	—	1.04	—	—
3	90 IPP/10 TDF	54.87	2.27	—	0.97	12.47	21.97
4	90 IPP/10 PFC	53.75	3.36	—	1.38	10.47	38.67
5	90 IPP/10 PNP	32.77	1.87	26.42	—	20.94	17.95
6	90 PE/10 HET	90.81	4.55	—	1.18	—	1.87
7	90 PE/10 PNP	47.72	3.75	18.50	—	14.99	31.25

5. Conclusions

Finally, we can draw the following conclusions :

1. HET flame-retardant acts in vapour phase, forming dilute non-combustible gases.

2. TDF interacts with polyolefines, resulting in crosslinked structures which increase the activation energies in the second stage of decomposition. In this case, the flame retardation is achieved by forming volatile non-inflamable components (HCl, CO_2) or with diminished inflamability.

3. Like TDF, PFC has a complex action, leading to the increasing of thermal stability in solid phase. In gaseous phase, products with diminished inflamability were formed : aromatics, P and Cl containing compounds.

4. Although PNP is a crosslinked polymer, it diminishes the inflamability, by increasing of the residue amount and the interaction with the substrate, mainly with PE. Its efficiency increases at a low crosslinking degree due to the evolving of a small quantity of NH_3 and CO_2, which dilute the combustible gases.

5. The suitable behaviour of polymeric flame-retardants in the burning retardation of inflammable macromolecular compounds is in agreement with previous results [9], [10].

6. Thermogravimetrical data coupled with pyrolysis and analysis of reaction products permit to study the behaviour of polymers in burning conditions; the obtained results are confirmed by inflammability tests, what will be the object of a future work.

Received, April 8, 1985

„P. Poni" Macromolecular Chemistry Institute, Jassy

REFERENCES

1. Reeves W.A., Drake Jr. G.L., Perkins R.M., *Fire Resistant Textiles Handbook* Technomic Publ. Co., Inc., 1974, 3.
2. Mark H.F., Atlas S.M., Shalaby S.W., Pearce E.M., *Flame Retardant Polymeric Materials.* Vol. I, Plenum Press, New York, 1975, 1—29.

3. Nikolaev A.V., Gimelsheyn F. Ya., Zislin V.M., J. Therm. Anal., **6**, 479 (1974).
4. Carel A.B., Cabbiness D.K., Thermochim. Acta, **44**, 363 (1981).
5. Coats A.W., Redfern J.P., Nature, *201*, 68 (1964); J. Polym. Sci., B, Polym. Letters, **3**, 917 (1965).
6. Reich L., Levi D.W., Makromol. Chem., **66**, 102 (1963); Reich L., J. Polym. Sci., B, Polym. Letters, **2**, 621 (1964).
7. Vasile C., Bărboiu V., Onu P., Sabliovschi M., Moroi G., Acta Polym. (in press).
8. Van Krevelen D.W., *Advances in the Chemistry of Thermally Stable Polymers*. Warszawa, 1977, 119.
9. Popescu Fl., Petreuş O., Agherghinei I., IMPHOS (First International Congress on Phosphorous Compounds), Rabat, Sept. 17—21, 1977, 307.
10. Petreuş O., Popescu Fl., Rev. Roumaine Chim., **28**, 387 (1983).

INFLUENŢA IGNIFUGANŢILOR ASUPRA COMPORTĂRII POLIOLEFINELOR LA TEMPERATURI RIDICATE

(Rezumat)

S-a studiat influenţa ignifuganţilor conţinînd fosfor, azot şi/sau halogen asupra comportării poliolefinelor (polietilenă şi polipropilenă atactică şi izotactică) la temperaturi ridicate.

Descompunerea termică s-a efectuat prin termogravimetrie, analiză termică diferenţială, analiza gazelor degajate şi prin piroliză în atmosferă autogenerată. Produşii gazoşi, lichizi şi solizi au fost analizaţi prin următoarele metode : spectroscopie IR şi RMN, cromatografie în fază gazoasă, analiză elementară etc.

S-a stabilit eficienţa ignifuganţilor şi modificările în mecanismul reacţiei de descompunere termică.

BULETINUL INSTITUTULUI POLITEHNIC DIN IAŞI
Tomul XXXI (XXXV), Fasc. supl., 1985
Secţia II
CHIMIE ŞI INGINERIE CHIMICĂ

D.C. 678-13

REACTIVITY OF ACRYLIC MONOMERS

XII. COPOLYMERIZATION OF N,N-DIETHYLACRYLAMIDE WITH ETHYL AND *n*-BUTYL ACRILATE

BY

SPIRIDON OPREA, EMIL DUMITRIU and VASILE HULEA

1. Introduction

The previous studies on the reactivity of N,N-diethylacrylamide in the process of radical copolymerization showed some differences in the behaviour of this monomer as function of the used comonomer. Thus, the systems N,N-diethylacrylamide—methyl acrylate [1] and N,N-diethylacrylamide—acrylic acid [2] are of type $r_{1,2} < 1$, N,N-diethylacrylamide—methyl methacrylate is of type $r_1 < 1$ and $r_2 > 1$, whereas in the case of copolymerization with styrene a penultimate effect was observed [3].

Taking these into account we have studied here the reactivity of N,N-diethylacrylamide in the copolymerization process with two monomers from the acrylic esters, series, namely : ethyl acrylate and *n*-butyl acrylate.

2. Experimental

N,N-Diethylacrylamide was prepared and purified as in [1].

Ethyl acrylate (Merck) was purified by distillation under vacuum (and nitrogen) to remove the inhibitor ; the middle fraction was collected ; (b.p. = 29°C/50 mm Hg, $n^{20} = 1.404$; $d^{20} = 0.9405$).

n-Butyl acrylate (Merck) was purified in the same manner ; (b.p. = = 69°C/50 mm Hg ; $n^{20} = 1.149$; $d^{20} = 0.8986$).

2,2'-Azobis (isobutironitrile) (AIBN) was purified by recristallization from methanol.

The used solvents, dioxane and light petroleum, were purified by the common methods.

The copolymerization of N,N-diethylacrylamide with acrylic esters was carried out as previously raported [1]. The composition of copolymers was determined both by RMN analysis and by the nitrogen content analysis using micro Kjeldhal method. The reaction conditions and results are summarized in Tables 1 and 2.

Table 1

Copolymerization of N,N-diethylacrylamide (DEA) with Ethyl Acrylate (EA) in Dioxane Solution at 60°C

No.	Mole fraction of DEA in monomer feed	Mole fraction of DEA in copolymer		Nitrogen % g	Conversion % (g)
		RMN analysis	Nitrogen analysis		
1	0.123	0.073	0.071	0.97	2.47
2	0.240	0.151	0.148	2.12	2.16
3	0.352	0.227	0.214	2.30	5.41
4	0.458	0.274	0.275	3.95	3.92
5	0.559	0.335	0.353	4.51	5.13
6	0.655	0.416	0.408	5.14	4.05
7	0.747	0.496	0.482	5.98	3.22
8	0.840	0.580	0.585	7.07	1.78
9	0.919	0.703	0.710	8.34	2.18

Table 2

Copolymerization of N,N-diethylacrylamide (DEA) with n-butyl acrylate in dioxane solution at 60°C

No.	Mole fraction of DEA in monomer feed	Mole fraction of DEA in copolymer		Nitrogen % g	Conversion % (g)
		RMN analysis	Nitrogen analysis		
1	0.1	0.057	0.061	0.67	1.45
2	0.2	0.119	0.121	1.32	2.69
3	0.3	0.176	0.180	1.97	3.14
4	0.4	0.247	0.252	2.76	2.57
5	0.5	0.346	0.335	3.67	4.31
6	0.6	0.410	0.417	4.56	1.16
7	0.7	0.512	0.512	5.62	3.42
8	0.8	0.642	0.634	6.96	5.61
9	0.9	0.758	0.767	8.43	3.58

3. Results and Discussion

On the basis of the data from Tables 1 and 2 the copolymer composition vs. the monomer feed was shown in Figs. 1 and 2.

As it can be observed both systems show a similar behaviour which is characteristic to the systems having $r_1 < 1$ and $r_2 > 1$.

In order to determine the values of the reactivity ratios the F i n e m a n-R o s s and K é l e n-T ü d ö s methods were applied (Figs. 3...6). Since the experimental data are fitted on the lines it can be considered that the terminal model describes satisfactorily the copolymerization process of

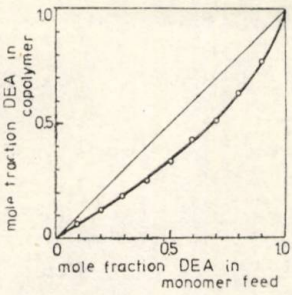

Fig. 1. — Composition diagram for copolymerization of N,N-diethylacrylamide and ethyl acrylate in dioxane solution at 60°C.

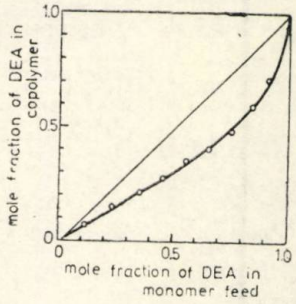

Fig. 2. — Composition diagram for copolymerization of N,N-diethylacrylamide and *n*-butyl acrylate in dioxane solution at 60°C.

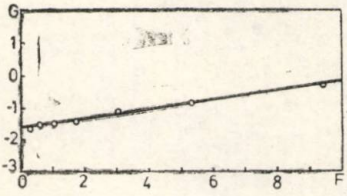

Fig. 3. — F i n e m a n-R o s s plot for copolymerization of N,N-diethylacrylamide with ethyl acrylate.

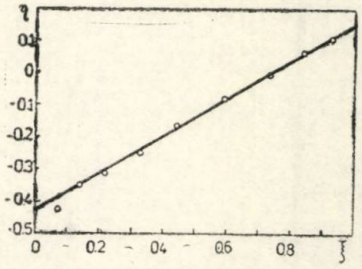

Fig. 4. — K é l e n-T ü d ö s plot for copolymerization of N,N-diethylacrylamide with ethyl acrylate.

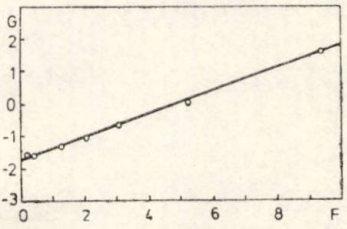

Fig. 5. — F i n e m a n-R o s s plot for copolymerization of N,N-diethylacrylamide with *n*-butyl acrylate.

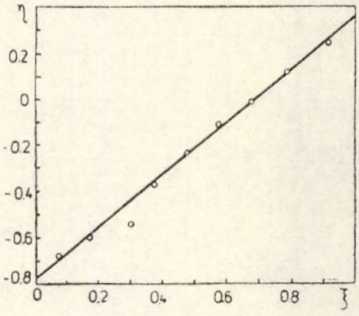

Fig. 6. — K é l e n-T ü d ö s plot for copolymerization of N,N-diethylacrylamide with *n*-butyl acrylate.

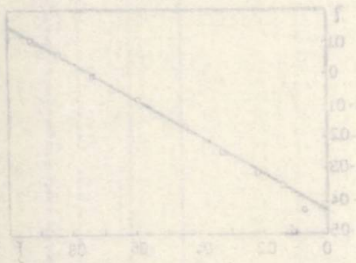

N,N-diethylacrylamide with these acrylic esters. The straightlines were plotted by the least square method and from their parameters the reactivity ratios were calculated. The values of determined reactivity ratios are shown in Table 3.

Table 3

Copolymerization Parameters for N,N-diethylacrylamide—Acrylate Systems

Monomer M_2	Fineman-Ross method		Kélen-Tüdös method	
	r_1	r_2	r_1	r_2
Ethyl acrylate	0.16	1.64	0.15	1.56
Butyl acrylate	0.33	1.63	0.34	1.69

One observs a good agreement between the obtained values by the two methods (Fineman-Ross and Kélen-Tüdös methods), and a similar behaviour of the two copolymerization systems.

On the basis of the reactivity ratios we can assert that the acrylic esters show a greater reactivity than N,N-diethylacrylamide with respect to the macroradicals present in the copolymerization system. Consequently, the copolymers have a lower content of disubstituted acrylamide than acrylic ester. Of course, this behaviour has important technological implications, especially when an homogeneous copolymer with respect to the composition, chemical and physical properties should be industrially obtained.

Taking into account the previously reported data on the copolymerization of N,N-diethylacrylamide [1], the following aspects can be underlined. The first observation consists in the different behaviour of the N,N-diethylacrylamide—methyl acrylate system when both reactivity ratios are smaller than the unity, whereas in the presence of ethyl or butyl acrylate $r_1 < 1$ and $r_2 > 1$.

The difference in reactivity can be also proved by the relative reactivities $1/r_i$ (s. Table 4).

Table 4

Relative Reactivities of the Monomers

Radical	Monomer	$1/r_1$	$1/r_2$
$-CH_2-\underset{\displaystyle CON(C_2H_5)_2}{\underset{\vert}{CH}}-$.	$CH_2=CHCOOCH_3$	2.44	—
	$CH_2=CHCOOC_2H_5$	6.67	—
	$CH_2=CHCOOC_4H_9$	2.94	—
MA·	$CH_2=CHCON(C_2H_5)_2$	—	1.92
EA·		—	0.64
BA·		—	0.59

Presented data reveal that the relative reactivity of disubstituted acrylamide against the macroradicals ended in acrylic esters decreases as the alkyl chain of the ester is smaller. The relative reactivity of acrylic esters against the macroradicals ended in disubstituted acrylamide is almost the same with respect to methyl and butyl acrylate, and it is very different in the case of ethyl acrylate.

As a general conclusion we can assert that the reactivity of acrylic esters of aliphatic alcohols depends on the size of the alkyl chain.

Received, April 9, 1985

Polytechnic Institute, Jassy,
Department of Organic
and Macromolecular Chemistry and
Technology

REFERENCES

1. Dumitriu Em., Oprea Sp., Maxim S., Nathanson A., Dima M., Coll. Polymer Sci., *257* (11), 1203 (1979).
2. Oprea Sp., Dumitriu Em., Mat. Plast., **20**, *1*, 202 (1983).
3. Oprea Sp., Dumitriu Em., Dima M., Rev. Roumaine Chim., **25**, *4*, 605 (1980).

REACTIVITATEA MONOMERILOR ACRILICI

XII. Copolimerizarea N,N-dietilacrilamidei cu acrilatul de etil şi de butil

(Rezumat)

S-a studiat copolimerizarea N,N-dietilacrilamidei cu acrilatul de etil şi acrilatul de *n*-butil. Au fost stabilite valorile constantelor de copolimerizare pentru cele două sisteme şi anume: $r_1 = 0{,}16$ şi $r_2 = 1{,}64$, respectiv $r_1 = 0{,}37$ şi $r_2 = 1{,}63$. S-a constatat că reactivitatea esterilor acrilici în procesele de copolimerizare cu N,N-dietilacrilamida scade odată cu creşterea catenei alchilice din molecula acestora.

BULETINUL INSTITUTULUI POLITEHNIC DIN IAŞI
Tomul XXXI (XXXV), Fasc. supl., 1985
Secţia II
CHIMIE ŞI INGINERIE CHIMICĂ

D.C. 678.746

SYNTHESIS AND PROPERTIES OF NEW POLYAZOMETHINES (II)

BY

MARIA DUMITRIU, MARIANA PĂSTRĂVANU and TATIANA LIXANDRU

1. Introduction

Among the heterochain polymers the polyazomethines are particularly important due to their good semiconducting properties and high thermal stability [1] ... [5]. They can also be used for obtaining fibers [6] and pigments for plastic materials [7].

In a previous paper a series of polyazomethines derived from acenaphthenequinone and derivatives were described [8].

In the present paper the polycondensation of 9,10-phenanthrenequinone, 9, 10-anthraquinone, 1- and 2-chloroanthraquinone with aromatic diamines as well as the properties of the obtaining polymers are studied.

2. Experimental

2.1. Materials

a) 9, 10-Phenanthrenequinone, 9, 10-anthraquinone and 1-chloroanthraquinone were Schuchard products and 2-chloroanthraquinone was a Merck product.

b) *m*- and *p* - Phenylenediamines and benzidine were laboratory reagents and were purified by the usual methods.

c) The solvent DMF was purified by double distillation.

2.2. Method

Polycondensation procedure. A mixture of 0.01 mol quinone, 0.01 or 0.02 mol. diamine and 2 g $ZnCl_2$ are solved în 40...60 ml DMF (the DMF amount depends on the quinone solubility). The solution is heated on an oil bath at 135°...140°C for 10 hours under good stirring. The reaction mixture is then cooled and filtered. A solid dark coloured mass is separated from the filtrate by water addition.

For removal of zinc chloride, the solid mass was powdered and washed twice with a hot NH_4OH/H_2O solution (1/3 ratio).

The polyazomethines obtained as complexes with $ZnCl_2$ were then purified by decomposing firstly these complexes by washing with acetic acid, in the case of the insoluble polymers, and by the dissolution followed by the precipitation in water, in case of the polymers soluble in acetic acid.

The quinone and diamine were then removed differently according to the solubilities of the obtained polymers and the initial monomers.

The phenanthrenequinone and anthraquinone soluble products were disolved in hot acetic acid, cooled, filtred and precipitated finally in water.

The phenanthrenequinone and anthraquinone insoluble products were washed repeatedly with hot acetic acid for both dissolving the uncoverted quinone and decomposing the complexed $ZnCl_2$.

The unreacted chloroanthraquinones were removed by washing with carbon tetrachloride and the anthraquinone by dissolving in hot chloroform followed by cooling, filtration and precipitation in carbon tetrachloride.

For removing the unreacted diamine components the products were washed with ethylic alcohol, benzene and chloroform, in function of monomer and polymer solubilities.

The polymers were obtained as amorphous powders of different shades, brighter for those prepared from anthraquinone and its derivatives and black for those resulting from phenanthrenequinone (Table 1).

The IR and ESR spectra were recorded on Specord IR UR 20 and ART 5 apparata, respectively.

The termograms were recorded on a Paulik-Paulik-Erdey MOM, Budapest, apparatus.

Table 1

Polycondensation of 9,10-Anthraquinone, 1-Chloro-and 2-Chloro-9,10-Anthraquinone and 9,10-Phenanthrenequinone with Aromatic Diamines

Quinone		Diamine	Yield %	m.p. °C	Aspect	IR spectra	
						$\nu_{C=N}$ cm^{-1}	$\nu_{C=O}$ cm^{-1}
9,10-Anthraquinone							
R_2	R_1						
H	H	*p*-Ph	28.20	290...300	Amorphous-grey	1 610	1 695
H	H	*m*-Ph	33.69	285...294	Amorphous-grey	1 605	1 690
H	H	Bz	36.35	276...283	Amorphous grey-bej	1 610	1 695
H	Cl	*p*-Ph	30.83	146...153	Amorphous reddish-brown	1 610	1 690
H	Cl	*m*-Ph	31.92	152...159	Amorphous-red	1 610	1 695
H	Cl	Bz	69.45	142...150	Amorphous dark-red	1 610	1 695
Cl	H	*p*-Ph	34.08	150...159	Amorphous brown-reddish	1 610	1 690
Cl	H	*m*-Ph	35.13	145...153	Amorphous brown-reddish	1 610	1 690
Cl	H	Bz	79.69	147...155	Amorphous brown-reddish	1 610	1 695
9,10-Phenanthrenequinone							
		p-Ph	66.66	330	Amorphous-black	1 620	1 690
		m-Ph	80.06	330	Amorphous-black	1 600	1 680
		Bz	79.21	330	Amorphous-black	1 650	1 700

Solvent DMF, catalyst $ZnCl_2$, quinone/diamine mole ratio 1/2, time 10 h, temperature 135° ... 140°C. Products soluble in acetic acid.

The study of the temperature dependence on the electrical conductivity was performed with disc samples of 1.0 cm diameter and 0.5 to 2.0 mm thickness. These samples were prepared by the compresion of the polymer powder at 10 t/cm². The discs were mounted between two aluminium electrodes and a good contact was achieved by a screw clamp arrangement. The temperature was measured by a Fe—constantan termocouple. The measurements were performed by an experimental arrangement similar to that described in [9], [10]. In all cases the temperature rate was 1.5°C/min.

3. Results and Discussion

3.1. Synthesis and Molecular Structure of the Polymers

By taking into account the results obtained in the syntheses of the polyazomethines derived from acenaphthenequinone [8], the facts that the 9, 10-phenanthrenequinone does not react with hydrazine hydrate in acetic acid medium with sulphuric acid as dehydrating reagent [11], and that among the Lewis acids zinc chloride was the most effective catalyst in the polycondesation of aldehydes with diamines [12], we used the DMF as a solvent and $ZnCl_2$ as a catalyst.

As regards the effect of the chlorine in 1- and 2- chloroanthraquinone on the polyazomethine yield, higher values are noticed than in case of the anthraquinone, probably due to the electron-atracting effect of the halogene which increases the reactivity of the carbonyl groups (2-chlorine > 1-chlorine).

The reactions carried out in excess of diamine led to polycondensation products in a higher yield, which is in a good agreement with previous papers [8], [13].

The yield was also found to decrease in benzidine, *m*-phenylenediamine, *p*-phenylenediamine, which is in a good agreement with the results obtained by d'Alelio for the polycondensation of isophthalaldehyde with *m*- and *p*-phenylenediamine [14].

The IR spectra of the polyazomethines obtained with different amines and ketones or aldehydes show absorption bands characteristic to $\diagdown C=N-\diagup$ and $\diagdown C=O$ end groups [15].

For different Schiff polybases types the band is to be found within the 1 630...1 640 cm^{-1} range [11], [12] although it may be also situated at values lower than 1 620 cm^{-1} for the compounds obtained from dicarbonylic derivatives and aromatic diamines [16].

In the IR spectra of polyphenanthrenequinonimine and polyanthraquinonimine, respectively, the $\nu_{\diagdown C=N-\diagup}$ vibration appears between 1 600 and 1 620 cm^{-1} (Table 1), which supports the assumed polyazomethine structure :

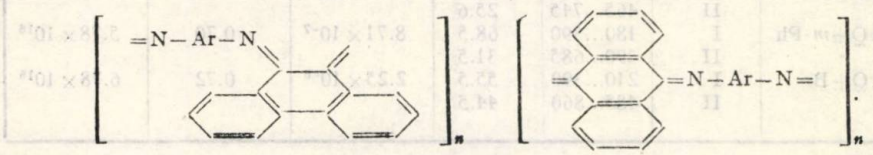

For the products resulted from anthraquinone the absorption bands of a medium intensity characteristic of the carbonyl (1 710... 1 780 cm^{-1}) and amino (3 400...3 500 cm^{-1}) groups at the chain end are found ; in all cases a decrease in the wavelength value of the $\nu_{C=O}$ for the polymer compared to the initial monomer is noticed, which is indicative of lower polycondensation degrees made also evident by the solubility and intrinsic viscosity measurements.

The IR spectra of the insoluble, black-coloured polyphenanthrenequinoneazomethines do not show the absorptions specific for the —NH— and C=O bonds which indicates either higher polycondensation degree or cyclic structures.

The thermal stability was studied by thermogravimetric and thermodifferential analyses, between 20° and 1 000°C, in air. The thermal stabilities exceeding 200°C (Table 2) are comparable to those of the polyazomethines obtained from acenaphthenequinone and derivatives [5].

Table 2

Data from TG Thermograms and Electrophysical Characteristics of Polyazomethines

Polymer	Thermogravimetric data			Electrical conductivity at 20°C $ohm^{-1}cm^{-1}$	Activation energy (E) for electrical conductivity eV	Concentration of unpaired electrons spins/g
	Degradation steps	Temperature °C	Weight losses %			
PhQ+*p*-Ph	I	90...370	63.5	3.50×10^{-7}	0.77	1.65×10^{18}
	II	370...550	36.5			
PhQ+*m*-Ph	I	190...430	14.0	1.10×10^{-7}	0.50	5.10×10^{19}
	II	430...920	86.0			
PhQ+Bz	I	215...500	17.4	4.20×10^{-8}	0.82	3.09×10^{19}
	II	500...850	82.6			
AnthQ+*p*-Ph	I	190...350	74.1	9.00×10^{-8}	0.91	0.95×10^{17}
	II	350...375	5.5			
	III	375...430	18.2			
	IV	430...540	2.2			
AnthQ+*m*-Ph	I	190...395	94.9	8.20×10^{-7}	0.86	1.57×10^{17}
	II	395...540	5.1			
AnthQ+Bz	I	190...375	44.4	2.20×10^{-6}	0.97	0.92×10^{17}
	II	375...520	18.9			
	III	520...695	30.0			
2Cl-AnthQ+*p*-Ph	I	220...440	57.8	2.12×10^{-7}	0.82	1.40×10^{17}
	II	440...815	42.2			
2Cl-AnthQ+*m*-Ph	I	220...400	62.2	6.33×10^{-8}	0.94	8.13×10^{17}
	II	460...790	36.7			
2Cl-AnthQ+Bz	I	205...400	71.1	3.47×10^{-6}	0.84	0.85×10^{17}
	II	400...730	28.9			
Cl-AnthQ+*p*-Ph	I	200...435	74.4	5.25×10^{-7}	0.66	1.17×10^{17}
	II	465...745	25.6			
Cl-AnthQ+*m*-Ph	I	180...390	68.5	8.71×10^{-7}	0.70	5.78×10^{16}
	II	390...685	31.5			
Cl-AnthQ+Bz	I	210...390	55.5	2.25×10^{-6}	0.72	6.78×10^{16}
	II	485...860	44.5			

The polyazomethines derived from anthraquinone and phenanthrenequinone show similar thermal stabilities; the destruction process proceeds generally in two stages, with a strong exothermal effect corresponding to the maximum weight losses.

Due to the extended double bond system the synthesized polymers show electrical conductivity and paramagnetic properties (Table 2).

The electrical conductivities of the polyazomethines described here range from 10^{-6} to 10^{-8} $ohm^{-1}cm^{-1}$ at 20°C. The ln Σ vs. $1/T$ plots for the polymers are linear. The estimated values of the Σ_0 and E parameters are listed in Table 2.

All polymers show an intense ERS signal (symmetrical singlet) with a paramagnetic particle concentration of $10^{16}...10^{19}$ spin/g (Table 2).

The relative viscosities of the compounds soluble in DMF were measured. By expressing η_{sp}/C as a function of concentration the relative viscosities of 0.02...0.05 dl/g and 0.05 dl/g were obtained for the polyazomethines derived from anthraquinone and phenanthrenequinone, respectively. The obtained values are comparable with those indicated from the Schiff polybases obtained from aromatic dialdehydes and diamines [14].

4. Conclusions

The polycondensation of 9, 10-phenanthrenequinone, 9, 10-anthraquinone, 1- and 2-chloroanthraquinone with aromatic diamines such as *p*-phenylenediamine, *m*-phenylenediamine, benzidine leads to amorphous, coloured polyphenanthrenequinonimine and polyanthracenequinonimine. The obtained polymers show a high thermal stability and semiconducting properties (electrical conductivity of the $10^{-6}...10^{-8}$ ohm^{-1} cm^{-1} order and paramagnetic particle concentration of $10^{16}...19^{19}$ spin/g).

Received, April 28, 1985

Polytechnic Institute, Jassy
Department of Organic and Macromolecular Chemistry and Technology

REFERENCES

1. d'Alelio G.F., Crivello J.V., Dehner T.R., Schoenig R.T., J. Macromol Sci. Chim., **A 1** (7), 1 331 (1967).
2. Kimura Takao, Nara Shigeo, Matsuyama Kentoro, Kobunski Kagaku, **30**, 491 (1973); C.A. 80: 15 366 z.
3. Межиковский С.М., Гуров А.А., Мягчилова Н.И., Лиогонкий Б.И., Берлин А.А., Высокомол. Соед.; **А 15**, 3 (1973).
4. Василенко Н.А., Правединков А.Н., Высокомол Соед., **В 19**, *6*, 162 (1977).
5. Dumitriu M., Dărângă M., Păstrăvanu M., Lixandru T., Rev. Roum. Chim., **25**, *7*, 981 (1980).
6. Moncrieff R.W., Intern. Dyer Text. Printer Bleacher and Finisher, **163**, *10*, 380 (1980); Ibid., **163**, *11*, 444 (1980).
7. Hermann H.J., Meyer G., Steffen K.D., Ger. Offen 2. 924, 944, 1981; C.A. 95: 8 790 g.
8. Lixandru T., Dumitriu M., Păstrăvanu M., Bul. Inst. polit., Iași, **XXVII (XXXI)**, *3—4*, s. II, 95 (1981).

9. Rusu G.I., Phys. Stat Sol., a, *4*, 775 (1971); An. Șt. Univ. „Al.I. Cuza", **XV**, 2, 155 (1979).
10. Rusu G.I., et al., Angew. Makromol. Chem., *107*, 33 (1982); Polym. Bull., 6, 243 (1982); Proc. of the IUPAC MACRO'83 Bucharest 1983, S. I, 583–586.
11. Păstrăvanu M., Dumitriu M., Lixandru T., Eur. Polym. J., 19, 633–637 (1983).
12. d'Alelio G.F., Crivello S.V., Kurosaki T., Schoenig R.K., J. Macromol. Sci., A 1, *7*, 1259 (1967).
13. Берлин А.А., Лиожонкий Б.Ж., Гуров А.А., Мягчилова Н.И., Высокомол. Соед., **B** 14, 441 (1972).
14. d'Alelio G.F., Crivello J.V., Schoenig R.K., Huemmar T.F., J. Macromol. Sci., A 1, 7 161 (1967).
15. Bellamy L.J., *Infra-Red Spectra of Complex Molecule.* 3rd Ed., Chapman & Hall, London, 1975.
16. Patel A.A., Patel S.R., Eur. Polym. J., 19, 561 (1983).

SINTEZA ȘI CARACTERIZAREA UNOR NOI POLIAZOMETINE (II)

(Rezumat)

S-au sintetizat noi poliazometine prin policondensarea 9,10-fenantrenchinonei, 9,10-antrachinonei, 1- și 2-clorantrachinonei cu diamine aromatice ca *p*-fenilendiamina, *m*-fenilendiamina și benzidina. Polimerii sînt caracterizați prin spectroscopie IR, măsurători de conductibilitate electrică și termostabilitate.

BULETINUL INSTITUTULUI POLITEHNIC DIN IAŞI
Tomul XXXI (XXXV), Fasc. supl., 1985
Secţia II
CHIMIE ŞI INGINERIE CHIMICĂ

D.C. 678.76

POLYMERIZATION OF 3-METHYLPENT-1-YN-3-OL BY $PdCl_2$ AND ITS TRIPHENYLPHOSPHINE COMPLEXES AS CATALYSTS

BY

VICTOR BULACOVSCHI, MARIA GROVU–IVĂNOIU, M. DĂRĂNGĂ and SVETLANA DUMITRESCU

1. Introduction

Unlike vinyl polymers, acetylenic polymers are characterized by their color, semiconductivity, paramagnetism and geometric isomerism. Acetylenic monomers, however, do not form high polymers by conventional radical, cationic or anionic polymerization [1] ... [3]. Their preparation involves some experimental shortcomings which make the investigation somewhat difficult.

Acetylene and its derivatives have been polymerized by use of several catalysts [4] ... [6]. Among these, the Z i e g l e r-type catalysts and phosphine complexes of transition metals have most often been used. In the metal halides of the 8-th group, a peculiar property was observed. They act very efficiently in polymerization of vinylic monomers in strong solvents [7] and of monosubstituted acetylenes [8]. The reaction mechanism for such promoters is not well known ; it proceeds, probably, by coordination of the monomer to the metal halide [9], [10].

In this paper we describe synthesis of soluble poly(3-methylpent-1-yn-3-ol) (poly-MP) using $PdCl_2$, $(Ph_3P)_2PdCl_2$ (TFF) and $(Ph_3Sb)_2PdCl_2$ (TFSb) as polymerization catalysts. The structure and properties of the obtained products are also reported.

2. Experimental

a) *Materials.* MP (Air Reduction Chem Co.) was dried on Na_2SO_4 and distilled at normal pressure before use (b.p. = 121°C). The solvents for polymerization were purified by usual methods. $PdCl_2$ was used as delivered. Bis(triphenylphosphine) -and bis(triphenylstibine) palladium (II) chlorides were prepared and purified according to the usual methods.

b) *Procedures.* The polymerizations were carried out under nitrogen in a two neck round bottom flask fitted with a refluxing condenser. At the end of the reaction, the resulting poly-MP was dissolved (or diluted) in acetone and precipitated by pouring the solution into a large amount of acid-containing (HCl) water. After filtration and washing with water, the polymer was dried in vacuum over P_2O_5 at room temperature.

c) *Polymer Characterization.* The molecular weights were measured cryoscopically in dioxan solution. IR-spectra (KBr pellets) were registered on a „Karl-Zeiss Jena" UR-20 spectrometer. UV-spectra were run on a „CF-4

Optica Milano" apparatus. X-ray powder spectra were obtained on a „Kristal loflex-4-Siemens" type equipment with recording goniometer and Cu – Kα radiation. Electron spin resonance (ESR) spectra were registered on a ESR-ART-5 spectrometer, IFA-Bucharest.

3. Results and Discussion

Table 1 summarizes the reaction conditions and some characteristics of the obtained polymers by bulk polymerization of MP. One can see that the monomer /catalyst ratio has no significant influence upon the overall conversion of the monomer, but an increas of the insoluble fraction in *n*-heptane was observed for $(3.0...3.7) \times 10^2$ molar ratio.

Table 1

The Bulk Polymerization of MP (Reflux Temperature; t=24 h)

No.	Catalyst	Molar ratio (MP/catalyst) $\times 10^{-2}$	Yield %	Poly-MP insoluble in *n*-heptane %	$\overline{M}_n$	Softening range °C
1	TFF – Pd	6.2	94.1	2.01	420	115...125
2	TFF – Pd	3.73	90.5	31.5	460	125...135
3	TFF – Pd	3.10	91.5	19.24	403	135...140
4	TFF – Pd	2.50	92.3	6.85	682	200...230
5	TFSb – Pd	6.2	96.05	11.2	436	118...126
6	$PdCl_2$	1.04	96.6	11.65	571	108...118

The molecular weights of the obtained polymers were not to high, they ranged from 400 to 700. The highest value was reached when 2.5×10^2 monomer/catalyst molar ratio was used, this polymer showed also a rised softening range (over 200°C). It might be that some parts of the catalyst remain bound to the polymer chain. No essential changes occured when TFSb – Pd complex was used.

It is worth mentioning that the polymerization by phosphine complexes near room temperature proceeds very slow (a month or more) and in very low yields.

Results for polymerization of MP performed in DMF solution are listed in Table 2. The polymerizations catalysed by $PdCl_2$ were carried out at 85°C for various periods of time. The conversions were usually 50...80% due, probably, to the low solubility of the catalyst in the used solvent. However, it appears an increase of the conversion with the catalyst concentration and with the reaction time.

The effect of temperature (Table 3) was studied in the range of 25°... 100°C. It is worth mentioning that the polymerization catalyzed by $PdCl_2$ proceeds in good yields even at 25°C and results in higher. molecular weight polymers. It is difficult to make a correlation between molecular weight and softening points. The last ones are generally lower than those found in the preceeding case.

Table 2

Polymerization of MP in DMF Solution Catalyzed by $PdCl_2$
([MP] = 1.773 mol/L, T = 85°C)

No.	Catalyst mol/l	Time h	Conversion %	$\overline{M}_n$	Softening range °C
1	3.67×10^{-2}	7	57.1	736	100...109
2	4.94×10^{-2}	7	62.7	—	100...107
3	5.65×10^{-2}	7	67.9	702	106...115
4	6.86×10^{-2}	7	73.4	—	105...115
5	3.67×10^{-2}	12	67.7	672	88...100
6	3.67×10^{-2}	24	83.45	535	82...97

Acetylenic polymers are usually characterised by a deep color, from orange to brown, due to the conjugated double bond system. In spite of that, the visible region of the spectrum is lacking significant bands ; one can see a continuous absorbtion. In the 220...400 nm region there appear some inflections localised at about 297...299 nm (Fig. 1) without seing clear maxima.

By polymer precipitation, a soluble fraction remains in water which was subsequently extracted with ether. On removing the solvent a resinous product is abandoned which UV-spectrum is shown in Fig. 1 *c*. It reveal a distinct maximum at 240 nm and an inflection met within spectra of the all oligomers. The wavellength calculated by the empirical W o o d w a r d's method [11] taking vinyl acetylene (219 nm) as a basis, leads to a value of 239 nm which coresponds to a trimer, very close to the experimental data (240 nm). These informations are attested by cryoscopic measurements of the molecular weight ($\overline{M}_n$ = =272). Signal narrowness suggests a homogen-

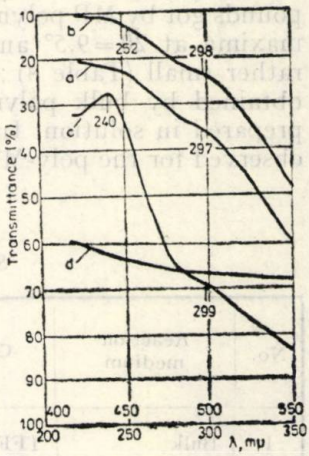

Fig. 1. — UV-spectra in MeOH for the poly-MP obtained in DMF solution ($PdCl_2$ catalyst) : *a* — at 85°C ; *b* — at 25°C ; *c* — water soluble fraction ; *d* — visible region of the spectrum.

Table 3

Polymerization of MP in DMF Solution
([MP] = 1.773 mol/L; $[PdCl_2] = 3.67 \times 10^{-2}$ mol/L)

No.	Temperature °C	Time h	Molecular weight	Softening range °C
1	100	7	623	103...105
2	85	7	736	100...109
3	25	48	1 020	110...115

eity of the product in regard to the molecular weight, which lacks at the water insoluble polymers, their spectra being wider.

The IR spectra of the obtained polymers show no bands of benzene ring (Fig. 2). This suggests a linear structure for poly-MP. Registrations are almost identical concerning the displayed bands. Both spectra show a slight maximum at 1 005 cm^{-1} which was assigned to the *trans-trans* configuration of the conjugated system. The region of 1 600...1 700 cm^{-1} is marked by a strong and broad absorbtion which corresponds to the coupling of the C=C stretching vibrations and OH bending vibrations.

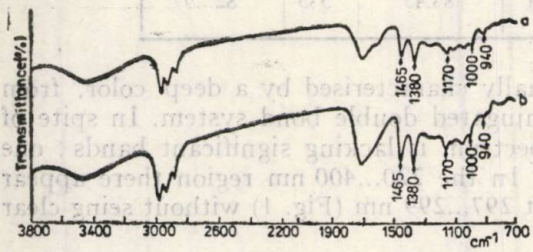

Fig. 2. — The IR spectra of the poly-MP; catalysts: *a* — TFF—Pd; *b* — $PdCl_2$.

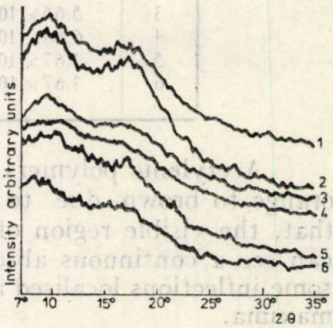

Fig. 3. — X-ray diffraction spectra of poly-MP-s (Notation follow the order in Table 4).

Fig. 3 gives X-ray diffraction patterns for the macromolecular compounds got by MP polymerization. The analyzed materials show two distinct maxima at $2\theta = 9.5°$ and $2\theta = 17°$. The calculated crystallinity indices are rather small (Table 4); they do not exceed 25%. Although, the products obtained by bulk polymerization show a higher crystallinity than those prepared in solution. In this last case, a light increase of the I_{cr} may be observed for the poly-MP obtained at room temperature. It might be that the

Table 4

Structural Properties of the Poly-MP

No.	Reaction medium	Catalyst	MP/catalyst molar ratio	Temperature °C	I_{cr} %
1	Bulk	TFF—Pd	6.2×10^2	reflux	23.70
2	Bulk	TFF—Pd	3.73×10^2	reflux	22.21
3	Bulk	TFF—Pd	2.5×10^2	reflux	19.14
4*)	DMF	$PdCl_2$	—	100	16.03
5	DMF	$PdCl_2$	—	85	15.00
6	DMF	$PdCl_2$	—	25	19.08

*) In the experiments 4...6 the catalyst concentration was 3.67×10^3 mol/L

prepared polymers are less crystalline due to the dominant *trans*-structure of the chains which does not allow their organization.

The electric and magnetic properties of poly-MP-s are shown in Table 5. The electric conductivities were in the range of $10^{-17}...10^{-15}$ ohm^{-1} cm^{-1} and are lower compared with the conductivity of polyacetylene ($10^{-9}...10^{-5}$ ohm^{-1} cm^{-1}) [12]. The ESR spectra of the studied polymers showed a structureless single lines, whose *g* values were very close to those of the free electron. The unpaired spin densities were $10^{-18}...10^{-19}$ g^{-1}. Compared with data obtained for other acetylene derivatives [2] it results that the presence of various groups as substituents does not affect spin density in acetylenic polymers.

Table 5

Electric and Magnetic Characteristics of Poly-MP

No.	Polymerization medium	Reaction time h	MP/catalyst, molar ratio	$\sigma_{50}°$ ohm^{-1} cm^{-1}	E_a eV	ΔH G	Unpaired spin/g
1[a]	DMF, solution	7	4.83×10^{1}	5.0×10^{-15}	1.78	7.6	7.88×10^{18}
2[a]	DMF, solution	24	4.83×10^{1}	—	—	9.8	1.23×10^{19}
3[b]	Bulk	24	3.1×10^{2}	10^{-16}	2.12	—	—
4[b]	Bulk	24	3.75×10^{2}	7.58×10^{-15}	1.49	8.0	1.02×10^{19}

a) Catalyst $PdCl_2$, temperature 85°C; b) Catalyst TFF—Pd and reflux temperature.

For the bulk polymerization of MP by TFF—Pd, the following mechanism was assumed [9], [10]:

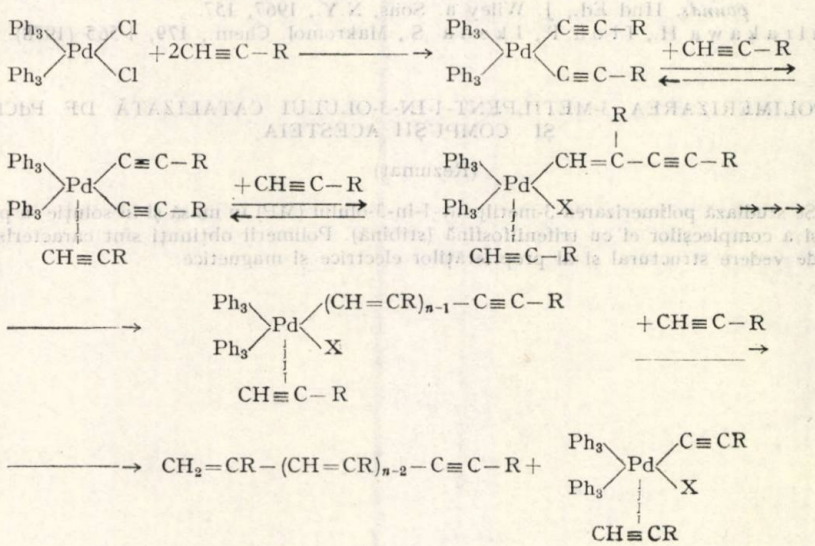

where :

$$R = -C(OH)(CH_3)-C_2H_5\ ;\ X = -C\equiv CR,\ -Cl \text{ or polymer chain.}$$

4. Conclusions

The MP can be easely polymerized by palladium halides in polar solvents or by its phosphine (stibine) complexes. The obtained poly-MP-s are colored, soluble in common solvents and show electric conductivities and spin densities similar to those of poly-(arylacetylenes).

Received, April 12, 1985

Polytechnic Institute of Jassy,
Department of
Organic and Macromolecular
Chemistry and Technology

REFERENCES

1. Хаусер М.Г., Родионов Ю.М., Мышин М., Черкашин М.И., Усп. хим., **45**, 695 (1976).
2. Ohtori T., Masuda T., Higashimura T., Polymer J., **11**, 805 (1979); Ibid., **11**, 813 (1979).
3. Simionescu C., Grovu M., Angew. Makromol. Chem., **111**, 149 (1983).
4. Simionescu C., Dumitrescu Sv., Die Makromol. Chem., **136**, 47 (1970).
5. Itoh T., Shirakawa H., Ikeda S., J. Polymer Sci., Polymer Chem. Ed., **12**, 11 (1974).
6. Masuda T., Hasegawa K., Higashimura T., Macromolecules, **7**, 728 (1974).
7. Berger R.S., Youngman F.A., J. Polymer Sci., **A-1**, 357 (1964).
8. Kern R.J., J. Polymer Sci., **A-7**, 621 (1969).
9. Furlani A., Bicev P., Carusi P., Russo M.V., J. Polymer Sci., **B-9**, 19 (1971).
10. Bulacovschi V., Simionescu C., Acta Chim. Acad. Sci. Hungaricae, **85**, 221 (1975).
11. Silverstein R.M., Bassler B.C., *Spectrometric Identification of the Organic Compounds.* IInd Ed., J. Wiley a. Sons, N.Y., 1967, 157.
12. Shirakawa H., Itoh T., Ikeda S., Makromol. Chem., **179**, 1565 (1978).

POLIMERIZAREA 3-METILPENT-1-IN-3-OLULUI CATALIZATĂ DE $PdCl_2$ ŞI COMPUŞII ACESTEIA

(Rezumat)

Se studiază polimerizarea 3-metilpent-1-in-3-olului (MP) în masă şi în soluţie în prezenţa $PdCl_2$ şi a complecşilor ei cu trifenilfosfină (stibină). Polimerii obţinuţi sînt caracterizaţi din punct de vedere structural şi al proprietăţilor electrice şi magnetice.

BULETINUL INSTITUTULUI POLITEHNIC DIN IAȘI
Tomul XXXI (XXXV), Fasc. supl., 1985
Secția II
CHIMIE ȘI INGINERIE CHIMICĂ

D.C. 54-92 ; 541-24

SOLUTION PROPERTIES OF ULTRAHIGH MOLECULAR WEIGHT POLYMERS

9. SYSTEMATIC ERROR SOURCES IN LIGHT SCATTERING DETERMINATIONS AFFECTING THE DISCUSSION OF THE EXCLUDED VOLUME EFFECT[1])

BY

SILVIA IOAN, CORINA SAVA and BOGDAN C. SIMIONESCU[2])

1. Introduction

The systematic characterization of ultrahigh molecular weight polymers[3]) rises a number of problems. Along with the difficulties associated to their isolation from the reaction mixture, handling, fractionation, most problems arise during the characterization since the usual techniques of investigation have to be adapted to the new dimensions of the chains and/or new investigation methods are to be found.

The molecular weight, the mean-square radius of gyration and the second virial coefficient are the most important parameters characterizing the polymers in diluted solutions. Their determination for ultrahigh molecular weight polymers opens large area in discussing, on the base of different theoretical approximations, properties such as short- and long-range interactions, excluded volume effect, etc.

Plasma-induced polymerization (copolymerization) [1], [2] was proved to yield ultrahigh molecular weight polymers (e.g., polystyrene, poly(methyl methacrylate), poly(butyl methacrylate)) and copolymers. The obtained macromolecular compounds were analysed from the point of view of molecular weight and compositional heterogeneity [3] ... [6], and some of their solution properties (conformational changes induced by temperature and solvent nature [7], [8], determination of root-mean-square radius of gyration and second virial coefficient — molecular weight relations [5], [6], [9], [10], analysis of the excluded volume effect based on the two-parameter theory, where the second virial coefficient and the expansion factor are function of short- and long-range interactions [6], [10], [11], etc.) were considered.

The mentioned papers showed that plasma-induced polymerization yields macromolecular compounds possessing some special properties as compared to usual polymers, namely: (a) low molecular weight and compositional heterogeneity, (b) less visible and pronounced conformational changes function of temperature and solvent nature, (c) an increased rigidity of the macromolecular chains in diluted solutions, as shown by the established relations between the radii of gyration and/or the second virial coefficients and the molecular weights, and (d) for high values of the expansion factor ($\alpha_s^3 > 4$), from the theories permitting the discussion of the interpenetration function $\psi(Z)$, the experimental data are in good agreement with the Kurata-Yamakawa theory [12] and with the new theory of Douglas and Freed [13]. One has to mention that up to the synthesis of such ultrahigh molecular weight polymers no experimental data were available to interpret the asymptotic solution of the inter-

---

[1]) Part 8, submitted to Makromol. Chem.

[2]) To whom all correspondence should be addressed.

[3]) The term of „pleistomers" („pleistos" means very many, so „very many mers") has been proposed (J. Macromol. Sci., Chem., (in press)) for ultrahigh molecular weight polymers (copolymers).

penetration function for very high values of the excluded volume parameter Z. From physical considerations, one can estimate that for $Z \to \infty$ polymer molecules tend to become rigid spheres in dilute solutions, so that the interpenetration function $\psi(Z)$ becomes a constant independent of Z.

For ultrahigh molecular weights one has to consider the errors appearing during the experimental determinations, errors transmissible in further consideration of different parameters.

In this context, the present paper is concerned with the systematic error sources in light scattering determinations and with the influence of these errors in discussing the excluded volume effect for very high excluded volume parameters.

2. Results and Discussion

2.1. Experimental Errors

The experimental technique selected to determine the weight -($\overline{M}_w$) and number-average ($\overline{M}_n$) molecular weights, the root-mean-square radii of gyration ($<S^2>^{1/2}$) and the second virial coefficients (A_2) was light scattering. The method was adapted to the particular characteristics given by the very large dimensions of the macromolecular chains. It was established that the main errors could appear from: (a) the preparation of the solutions, the concentration range being $0.5 \times 10^{-4}...8 \times 10^{-4}$ g.cm^{-3}, depending on the molecular weight of the sample and on the refractive index of the solvent; (b) the purification of the solvents; (c) the processing of the solutions up to the experimental determinations, and (d) the processing of the experimental data.

These errors have been eliminated by (a) a very careful preparation of the solutions, (b) the use of high purity solvents, (c) preparation of solutions in the dark, dissolution in the dark for 4...5 days, at about 40°C, without mechanical stirring to prevent shear degradation, (d) purification of solutions by centrifuging for about 1...2 h, at 11,000 g in a Janetzki centrifuge. By respecting all these precautions, reproducible experimental data (Rayleigh intensities for different diffusion angles and concentrations) were obtained. The experimental precision in the determination of $\overline{M}_w$ was $\pm 9\%$, and in the determination of A_2 and $<S^2>^{1/2}$, $\pm 3.4\%$ and $\pm 5.5\%$, respectively.

The processing of experimental data in order to determine $\overline{M}_w$, $\overline{M}_n$, $<S^2>^{1/2}$ and A_2 for ultrahigh molecular weight polymers is very difficult when the experimental data do not allow the observation of the Rayleigh intensity for diffusion angles lower than 30°. A curvature, predicted by the Gaussian theory but undetected for usual length polymers, appears in the representation of $(Kc/R_\theta)_{c=0}$ as a function of $\sin^2(\theta/2)$ (where c is the concentration, θ is the diffusion angle, K is the light scattering factor). According to Berry [14], this difficulty can be eliminated by plotting $(Kc/R_\theta)^{1/2}$ vs. $\sin^2(\theta/2)$, and Fujita [15] suggests a linearisation of the experimental curve through the representation of $[y(u)]^{-1}$ as a function of $Z(u)$, where $y(u) = (R_\theta/Kc)_{c=0}$, $Z(u) = [y(u)\, u^{4/3}]^{-1} \int_0^u y(u) u \, du$, with u defined by $u = \sin^3(\theta/2)$, and $1/y(u) = (1/M) + bZ(u)$, with $b = (32\pi^2/3\lambda^2) \times (<S^2>/M)$.

Both methods have been used in our determinations. Fig. 1 presents an example of such studies [9], [10] for two poly(butyl methacrylate) samples in ethyl methyl ketone (EMK) and CCl_4, and Table 1 gives the obtained results.

It was observed that working in the 30°...130° diffusion angles range, B e r r y's method allows a linearisation of the experimental curves up to about 50°, while F u j i t a's method up to an angle of about 80°. Also, according to Table 1, the errors in the determination of $\overline{M}_w$ and $<S^2>^{1/2}$ rise up to $\pm 9\%$ and $\pm 5.5\%$, respectively. These errors, high enough as compared to those observed in studying usual length polymers, are translated in the evaluation of different parameters characterizing high polymers in diluted solutions.

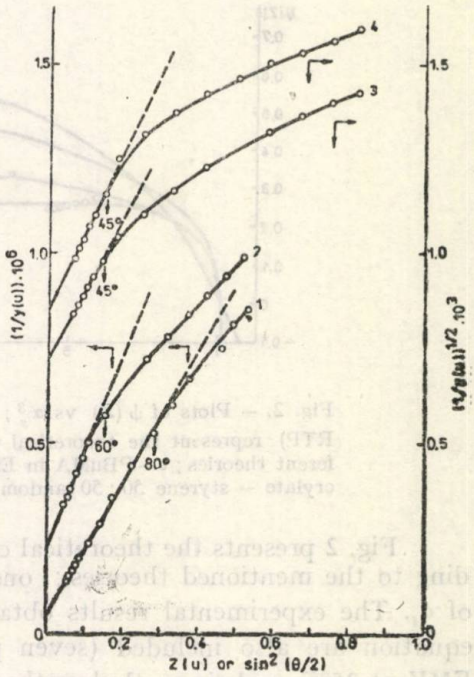

Fig. 1. — Plots of $1/y(u)$ vs. $Z(u)$ (F u j i t a's method) for PBuMA (I) in EMK (curve *1*) and PBuMA (II) in CCl_4 (curve *2*), and of $(1/y(u))^{1/2}$ vs. $\sin^2(\theta/2)$ (B e r r y's method) for PBuMA (I) in EMK (curve *3*) and PBuMA (II) in CCl_4 (curve *4*). The data points for the samples are shifted upward to the following amounts: *1* — 0; *2* — 0.2×10^{-6}; *3* — 0.5×10^{-3}; *4* — 0.7×10^{-3}.

2.2. Influence of Experimental Errors on the Excluded Volume Effect

The interpenetration function $\psi(Z)$ can be determined from different theoretical dependences with the expansion factor $\alpha_s = <S^2>^{1/2} / <S_0^2>^{1/2}$ (where $<S_0^2>^{1/2}$ is the unperturbed root-mean-square radius of gyration) obtained from experimental data (original F l o r y theory (*F*, *0*), modified F l o r y theory (*F*, *m*), K u r a t a-Y a m a k a w a theory (*K*-*Y*), renormalized group theory of D o u g l a s and F r e e d (RTP) [6], [8], [12], [13]) or directly from experimental data according to $\psi(Z) = A_2 M^2 / 4\pi^{3/2} N_A <S^2>^{3/2}$.

Table 1

Light Scattering Data Obtained According to the Methods of B e r r y and F u j i t a

Sample / Method	$\overline{M}_w \cdot 10^{-6}$		$<S^2>^{1/2}(10^{-5}$ cm)	
	B e r r y	F u j i t a	B e r r y	F u j i t a
PBuMa(I)*) (EMK, 25°C)	21.633	23.256	2.204	2.057
PBuMA(II)**) (CCl_4, 20°C)	48.485	45.454	3.525	3.142

*) Fractionated sample; **) Unfractionated sample, $\overline{M}_w/\overline{M}_n = 1.79$

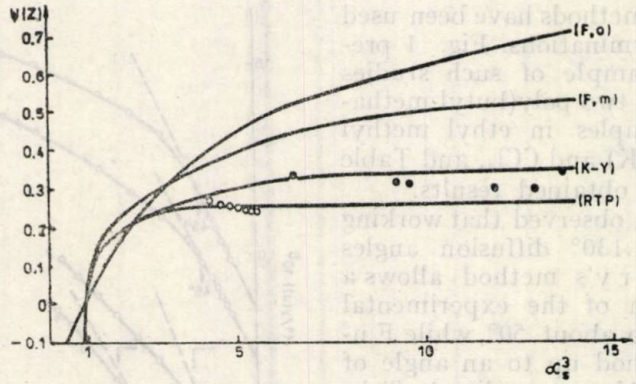

Fig. 2. — Plots of $\psi(Z)$ vs. α_s^3; the curves ($F, 0$; F, m; K-Y; RTP) represent the theoretical values calculated according to different theories; o—PBuMA in EMK at 25°C, ● — methyl methacrylate — styrene 50 : 50 random copolymer in 1,4-dioxane at 20°C.

Fig. 2 presents the theoretical curves of $\psi(Z)$ as a function of α_s^3 according to the mentioned theories; one can evaluate $\psi(Z)$ for a given value of α_s. The experimental results obtained for $\psi(Z)$ according to the given equation are also included (seven poly(butyl methacrylate) samples, in EMK at 25°C, and six methyl methacrylate-styrene 50 : 50 random copolymer samples in 1,4-dioxane at 20°C [6]).

Table 2

Errors Transmitted to Z and ψ (Z) Determined According to Different Theories and Experimentally

Theory (method)	Error, [%]	
	Z	$\psi(Z)$
Original Flory theory	68	23
Modified Flory theory	68	14.6
Kurata-Yamakawa	60	8.8
Douglas-Freed theory*)	60	3.36
Domb-Barrett theory	55	—
Experimental	—	1.85

*) s. [11].

As mentioned, the experimental errors can be translated to different parameters. Starting from an error of $\pm 9\%$ ($\overline{M}_w$) and from an error of $\pm 5.5\%$ ($<S^2>^{1/2}$), errors of $\pm 11\%$ and $\pm 33\%$ are obtained for α_s and α_s^3, respectively. Table 2 presents the errors transmitted to the excluded volume parameter Z and to the interpenetration function $\psi(Z)$ (for α_s affected by the mentioned error), calculated according to different theories [11], [12].

The possible values of $\psi(Z)$ for α_s^3 affected by an error of $\pm 33\%$ (poly(butyl methacrylate) sample, EMK, 25°C, $\overline{M}_w = 1.0406 \times 10^7$) are given, as an example, in Table 3.

According to Fig. 2 and Tables 2 and 3, the evaluation of $\psi(Z)$ by different theories is affected differently by α_s^3. A minimum error appears by use of the RTP theory of Douglas and Freed for $\alpha_s^3 > 4$. It can be also seen that the values obtained directly from the experimental data

Table 3

Possible Values of $\psi(Z)$ for α_s^3 Affected by an Error of $\pm 33\%$ (poly(butyl methacrylate), fractionated sample, EMK, 25°C, $\bar{M}_w = 1.0406 \times 10^7$)

$\psi(Z)$	α_s^3		
	2.924	4.324	5.724
Original Flory theory	0.301	0.392	0.483
Modified Flory theory	0.318	0.372	0.426
Kurata-Yamakawa theory	0.260	0.293	0.316
Douglas-Freed theory	0.233	0.254	0.259
Experimental	0.270 ± 0.005		

present very low errors ($\pm 1.85\%$) and are close to those given by K-Y theory, being in a very good agreement with the RTP theory.

3. Conclusions

In conclusion, the possible errors appearing in studying solution properties of ultrahigh molecular weight polymers by light scattering method can be very important. These errors can be minimized through specific restrictions and by applying adjusted processing techniques. The errors do not influence the values of the interpenetration function $\psi(Z)$ for expansion factors $\alpha_s^3 > 4$. In these conditions, the degree of penetration of the macromolecular chain in the diluted solution becomes constant (0.269 according to the theory of Douglas and Freed), and the chain tends to become a rigid sphere for $Z \to \infty$.

Received, May 4, 1985

„P. Poni" Institute of Macromolecular Chemistry, Jassy, and Polytechnic Institute, Jassy, Department of Organic and Macromolecular Chemistry and Technology

REFERENCES

1. Simionescu C.I., Simionescu B.C., Pure Appl. Chem., **56**, *3*, 427 (1984).
2. Simionescu C.I., Simionescu B.C., Chem. Zvesti., **37**, *5*, 685 (1983).
3. Simionescu B.C., Ioan S., Simionescu C.I., Polym. Bull., **6**, 409 (1982).
4. Ioan S., Simionescu B.C., Simionescu C.I., Polym. Bull., **6**, 421 (1982).
5. Simionescu C.I., Simionescu B.C., Ioan S., Makromol. Chem., Rapid Commun., **4**, 549 (1983).
6. Simionescu C.I., Simionescu B.C., Ioan S., Makromol. Chem., **184**, 829 (1983).
7. Ioan S., Simionescu B.C., Simionescu C.I., Polym. Bull., **5**, 563 (1981).
8. Simionescu C.I., Simionescu B.C., Ioan S., Macromolecules, (in press).
9. Simionescu C.I., Simionescu B.C., Ioan S., J. Polym. Sci., Polym. Lett. Ed., **3**, 121 (1985).
10. Simionescu B.C., Ioan S., Simionescu C.I., Makromol. Chem., (submitted).
11. Ioan S., Simionescu B.C., Simionescu C.I., Makromol. Chem., (submitted).
12. Yamakawa H., Pure Appl. Chem., **31**, 179 (1972).
13. Douglas J.F., Freed K.F., Macromolecules (in press).
14. Berry C.G., J. Chem. Phys., **44**, 4 550 (1966).
15. Fujita H., Polym. J., **1**, *5*, **537 (1970).**

PROPRIETĂŢILE SOLUŢIILOR DE POLIMERI CU MASE MOLECULARE FOARTE MARI

9. Surse sistematice de erori în determinări de difuzia luminii care afectează discutarea efectului volumului exclus

(Rezumat)

Se discută erorile posibile care apar în determinările de difuzia luminii la polimeri cu mase moleculare foarte mari, în soluţie diluată, minimalizate prin restricţii specifice şi tehnici de calcul adaptate, erori care sînt transmise funcţiilor termodinamice care descriu efectul volumului exclus.

S-a constatat că dacă parametrul volumului exclus Z este afectat de erori foarte importante, aceasta nu influenţează discutarea şi valorile funcţiei de interpenetrare $\psi(Z)$ pentru un factor de expansiune $\alpha_s^3 > 4$. Din teoriile existente, teoria de grup renormalizată verifică cel mai bine datele experimentale obţinute pentru $\psi(Z)$, în limitele erorilor menţionate.

BULETINUL INSTITUTULUI POLITEHNIC DIN IAŞI
Tomul XXXI (XXXV), Fasc. supl., 1985
Secţia II
CHIMIE ŞI INGINERIE CHIMICĂ

C.D. 678-13

TRANSITIONS CONFORMATIONNELLES DES TRIBLOCCOPOLYMÈRES DU TYPE *ABA*

PAR

MIRCEA GRIGORAŞ, GETA ONOFREI, ELENA BÎCU et IDIR RABIA

1. Introduction

L'étude en solution diluée des copolymères séquencés a fait l'objet de nombreux travaux au cours de ces dernières années. Le but essentiel était d'établir si ces copolymères adoptent des conformations statistiques ou si, au contraire, les séquences occupent des domaines distinctes de l'espace (forme „ségrégée"). De nombreux travaux plaident en faveur de l'existence des transitions conformationnelles dans le cas de plusieurs blocs copolymères, à savoir : poly (styrène-*b*-isoprène) [1], poly(méthacrylate de methyl-b-styrène-b-méthacrylate de methyl) [2], [3], poly(styrène-b-méthacrylate de méthyl) [4], poly(styrène-b-α-methylstyrène) [5], sous l'influence de la température ou par variation de la qualité thermodynamique du solvant par addition d'un autre solvant. L'explication de la „ségrégation" doit être basée sur l'incompatibilité qui caractérise les séquences de nature chimique différente. Or, cette incompatibilité doit diminuer lorsque la température augmente ou lorsqu'on fait varier la qualité thermodynamique du solvant. Compte tenu de l'agitation thermique croissante on peut prévoir qu'à une température donnée une interpénétration des séquences peut se produire, en passant ainsi à une conformation statistique.

Nous avons rapporté ailleurs la synthèse de quelque tribloccopolymères du type *ABA* par polymérisation cationique avec isomérisation des 2-oxazolines-2-substituées avec l'usage des initiateurs bifonctionnels. Les échantillons utilisés ont le poly-N-aciléthylènimine (partie termoplastique) comme bloc *A* et le poly-éthylèneglycoladipé ou poly-éthylèneoxyde (partie elastomère) comme bloc *B*.

Dans cet article nous allons mettre en évidence, par des études viscosimétriques, l'existence des transitions conformationnelles en solution diluée pour les tribloccopolymères synthetisés.

2. Partie expérimentale

Les bloc copolymères étudiés ont la composition et la structure suivantes :

poly(N-aciléthylènimine -b- éthylèneglycoladipé -b- N-aciléthylènimine)

$$CH_3-C_6H_4-SO_3-(CH_2-CH_2-\underset{\displaystyle C=O}{\underset{|}{N}}-)_x-[(CH_2)_2-OCO-(CH_2)_4-COO-$$

$$\underset{\displaystyle CH_3}{\underset{|}{}}$$

$$-(CH_2)_2]_y-(\underset{\substack{|\\ C=O\\ |\\ CH_3}}{N}-CH_2-CH_2-)_x-SO_3-C_6H_4-CH_3$$

MeOxz–PEGA–MeOxz

échantillon *A* ; $x = 3{,}4$, $y = 13$
échantillon *B* ; $x = 6{,}0$, $y = 13$

poly (N-aciléthylènimine-)-b-éthylèneoxyde-b-N-aciléthylènimine)

$$CH_3-C_6H_4-SO_3-(CH_2-CH_2-\underset{\substack{|\\ C=O\\ |\\ CH_3}}{N}-)_x-(CH_2-CH_2-O-)_y-(\underset{\substack{|\\ C=O\\ |\\ CH_3}}{N}-CH_2-$$

$$-CH_2-)_x-SO_3-C_6H_4-CH_3$$

MeOxz–PEO–MeOxz

$x = 10{,}8$; $y = 52$

Leur synthèse et caracterisation a été présentée dans des travails antérieurs [6]...[8].

Les mesures de viscosité ont été effectuées avec un viscosimètre Ubbelhode. Les solvants ont été séchés et distillés.

3. Résultats et discussion

L'influence de la concentration, de la température et de la composition du mélange des solvants sur la conformation des bloccopolymères a été étudiée par voie viscosimetrique. Les solvants utilisés sont le $CHCl_3$ (solvant commun pour les deux blocs *A* et *B*) et le THF ou le benzène (solvant séléctif pour le bloc *B*).

3.1. Influence de la concentration

Dans le cas des copolymères greffés et séquencés, Dondos et Benoit [2] ont montré que dans le domaine des températures ou l'on observe des changements de conformation, la variation de la viscosité avec la concentration présente une anomalie. Les points expérimentaux se situent sur deux droites ayant des pentes différentes ui se rencontrent en un point correspondant à une concentration critique. Ultérieurement Gosa et Donescu [9] ont montré par spectrophotométrie UV que dans le cas des copolymères greffés cette concentration critique, qui est supposée marquer le passage d'une conformation „ségrégée" à une conformation pseudogaussienne, peut apparaitre à n'importe quelle température et non seulement dans le domaine des températures de transition.

En étudiant le comportement des triblocs copolymères MeOxz–PEGA–MeOxz et MeOxz–PEO–MeOxz dans un solvant commun aux deux blocs

($CHCl_3$) et dans un solvant sélectif (THF pour le PEGA et benzène pour le PEO) et dans le mélange des deux solvants, on observe l'existence des transitions conformationnelles. Celles-ci apparaissent dans un domaine de concentration voisin de celui qui a été defini par D o n d o s et B e n o i t [2] et G o s a et D o n e s c u [9], pour les blocs copolymères et les copolymères greffés.

Dans le THF les mesures ont été effectuées dans un domaine restreint de valeurs à cause de la saturation rapide de la solution du bloc copolymère étudié (Me*Oxz*—PEGA—Me*Oxz*) à partir, de la concentration $c = 0{,}16$ g/dl. Jusqu'à cette valeur de la concentration nous avons observé un comportement normal (Fig. 1, courbe *a*). Dans le $CHCl_3$ la variation de la viscosité réduite avec la concentration est conforme aux résultats de la littérature concernant le comportement des blocs copolymères en solution [2] (Fig. 1, courbe *b*).

Dans le cas du mélange binaire de solvant (solvant + solvant sélectif) on n'observe pas l'apparition d'une concentration critique mais d'un domaine d'environ 0,03 g/dl dans lequel a lieu probablement le passage graduel d'une conformation à une autre (Fig. 2).

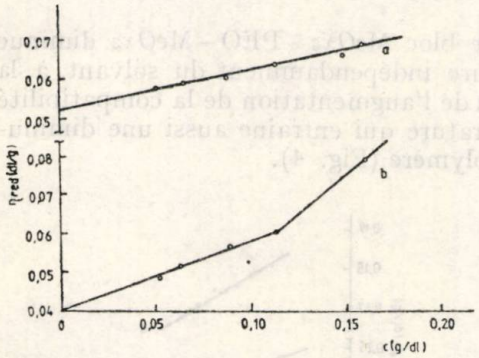

Fig. 1. — Variation de la viscosité réduite avec la concentration du bloc Me*Oxz*—PEGA—Me*Oxz* dans le THF (*a*) et dans le $CHCl_3$ (*b*).

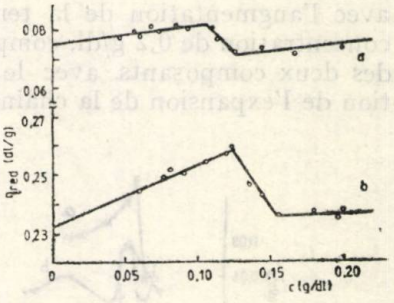

Fig. 2. — Variation de la viscosité réduite avec la concentration des blocs Me*Oxz*—PEGA—Me*Oxz* et Me*Oxz*—PEO—Me*Oxz* dans les mélanges de solvants suivants : *a* — Me*Oxz*—PEGA—Me*Oxz* dans THF/$CHCl_3$ (1/1) ; *b*—Me*Oxz*—PEO—Me*Oxz* dans benzène/$CHCl_3$ (1/1) ; température = 25°C.

C'est intéressant à remarquer que dans le cas du bloc copolymère Me*Oxz*—PEO—Me*Oxz* la température de 25°C, à laquelle ont été effectuées les mesures, n'est pas comprise dans le domaine où on enregistre une transition conformationnelle contrairement au bloc copolymère Me*Oxz*—PEGA—Me*Oxz*.

3.2. Influence de la température

L'influence de la température a été étudiée en utilisant un mélange binaire des solvants 1 : 1 (solvant/solvant séléctif). On observe une variation

non-monotone de la viscosite réduite avec la température dans le cas du tribloc Me*Oxz*—PEGA—Me*Oxz*, ce qui suppose l'existence des transitions conformationnelles. Ces transitions sont probablement dues à la nature chimique du polymère et pas à une transition d'une conformation „ségrégée" à une conformation pseudogaussienne comme il a été démontré dans le cas de certains bloccopolymères [1], [2], [10] et copolymères greffés [9], [11], [12]. Cet aspect est confirmé aussi par le fait que dans le cas de l'homopolymère PEGA apparait une transition conformationnelle dans le domaine de température étudié (Fig. 3).

D'autre part si c'était une transition conformationnelle de même nature que celles rencontrées en littérature, elle n'aurait pas pu être mise en évidence à des concentrations plus grandes que celles aux quelles a lieu le passage de la conformation „ségrégée" à la conformation pseudogaussienne. Or dans le cas des copolymères étudiés cette transition a lieu aussi dans le domaine de concentrations $c > 0{,}12$ g/dl. Cependant ces transitions sont plus évidentes dans les solutions trés diluées, à des concentrations $c < c_{critique}$ (Fig. 3). Probablement, aux concentrations plus élevées, la possibilité d'intéraction entre les différents segments augmente ce qui atténue l'effet d'intéractions du type *AA* et *BB* auxquelles on a attribué l'apparition des maximums et des minimums à 25° et 40°C.

La viscosité réduite η_{red} pour le bloc Me*Oxz*—PEO—Me*Oxz* diminue avec l'augmentation de la température indépendamment du solvant, à la concentration de 0,2 g/dl, compte tenu de l'augmentation de la compatibilité des deux composants avec le température qui entraine aussi une diminution de l'expansion de la chaine du polymère (Fig. 4).

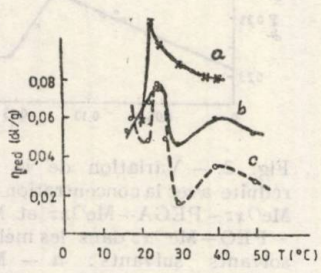

Fig. 3. — Variation de la viscosité réduite avec la température ; solvant=$CHCl_3$/THF (1/1) : *a*—PEGA ; *b*—Me*Oxz*—PEGA—Me*Oxz*, c = 0, 198 g/dl ; *c* — Me*Oxz*—PEGA—Me*Oxz*, c=0,0495 g/dl.

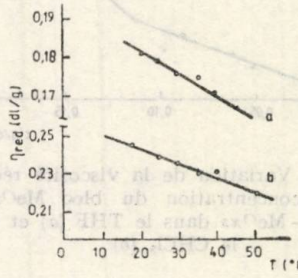

Fig. 4. — Variation de la viscosité réduite avec la température pour le bloccopolymère Me*Oxz*—PEO—Me*Oxz*: *a*—solvant=$CHCl_3$/THF (1/1), c=0,2 g/dl ; *b* — solvant = benzene/THF (1/1), c=0,2 g/dl.

3.3. Comportement des blocs copolymères en solution dans un mélange binaire de solvants

Pour cette étude nous avons utilisé un mélange de solvant—solvant sélectif pour le bloc principal *B* ($CHCl_3$—THF). Ayant en vue que la concentration à laquelle le blcc copolymère devient insoluble (solution saturée) dans le THF diminue avec l'augmentation du nombre d'unités structurelles

du poly-Me*Oxz*, on a étudié seulement le comportement du bloccopolymère dont $x \leqslant y$. On enregistre une variation non-monotone aussi bien de la viscosite réduite η_{red} que de la viscosité intrinsèque $[\eta_i]$ avec la composition du mélange des solvants, ce qui suppose une transition conformationnelle due au passage de l'état „ségrégée" stable dans un bon solvant ($CHCl_3$) (Fig. 5 courbe *a*) à une conformation stable dans un solvant sélectif pour le bloc central *B* (Fig. 5 courbe *b*).

Dans le THF, Z_{AA} (coefficient proportionnel à l'énergie d'interaction nécessaire au contact entre les composants *A* du polymère) diminue par suite de l'augmentation de X_{AS} (interaction très faibles entre le solvant et le bloc *A*, le THF étant un précipitant du Me*Oxz*) déterminant ainsi une diminution de l'expansion de la chaine macromoléculaire. À des concentrations du THF $<50\%$ on observe une variation négative de la viscosité (Fig. 6), conséquence de la qualite thermodynamique du couple de

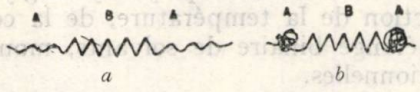

a *b*

Fig. 5. — Conformation des bloccopolymères : *a* — dans le $CHCl_3$; *b* — dans le THF.

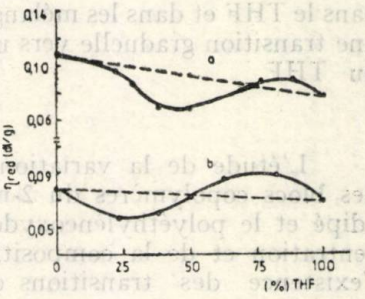

Fig. 6. — Comportement du bloc Me*Oxz* — PEGA—Me*Oxz* dans le mélange de solvants $CHCl_3$/THF, température = 25°C: *a* — échantillon *B*, $c = 0{,}12$ g/dl ; *b* — échantillon *A*, $c = 0{,}16$ g/dl.

solvants ($\Delta G^E < 0$, mélange binaire exothermique avec possibilité de formation de liaison hydrogène), comme il a été mis en évidence par Dondos et Benoit [2], [13] sur la base de la théorie de Schultz-Flory. D'après cette théorie :

$$X_{AS} = x_1 X_{A1} + x_2 X_{A2} - x_1 x_2 X_{12}, \tag{1}$$

où x_1, x_2 — fractions molaires des deux solvants du mélange ; X_{A1}, X_{A2} — coefficients d'intéraction du polymère *A* avec chaque constituant du mélange.

Les dimensions moléculaires des copolymères dépendent des trois coefficients X_{AS}, X_{BS} (qui varient avec x_1, x_2) et X_{AB}, par le paramètre global d'intéraction *Z* qui influence la valeur du coefficient d'expansion viscosimétrique.

Pour un copolymère :

$$Z = C_1 Z_{AA} + C_2 Z_{BB} + C_3 Z_{AB}, \tag{2}$$

ou : Z_{ii} — coefficients proportionnels à l'énergie d'interaction nécessaire à chaque type de contact entre les composants du polymère, dans un solvant

donné ; C_i — facteurs de fréquence caractérisant la possibilité d'existence de contacts AA, BB et AB.

Dans le cas d'un tribloccopolymère les interactions entre les blocs ont un effet mineur sur l'expansion de la chaine polymérique en comparaison aux interactions intrabloc. Pour cela on peut considérer que $C_3=0$, $Z_{ii}\approx 1/2-X_{1S}$ ce qui veut dire que dans le cas d'un solvant ayant $\Delta G^E<0$ (comme le mélange utilisé $CHCl_3$/THF), X_{12} étant négatif va déterminer une augmentation des coefficients d'interaction X_{AS} et X_{BS} et, en conséquence, une diminution des termes Z_{AA} et Z_{BB}, ce qui entraine une diminution des dimensions moléculaires.

Pour des valeurs croissantes de la concentration en THF du mélange de solvants on observe l'apparition d'un maximum qui peut être attribué à l'absorption sélective du $CHCl_3$ [14] par le bloc Me*Oxz*. Cela entraine une ségrégation accentuée des deux blocs [15] et par conséquence une augmentation des dimensions de la chaine moléculaire par rapport a celles observées dans le THF et dans les mélanges $CHCl_3$/THF antérieurs, dans lesquels a lieu une transition graduelle vers une conformation statistique due à la présence du THF.

4. Conclusions

L'étude de la variation de la viscosité réduite en solution diluée des blocs copolymères du 2-méthyl-2-oxazoline avec le polyéthylèneglycol adipé et le polyéthylèneoxyde, en fonction de la température, de la concentration et de la composition du mélange binaire de solvants, montre l'existence des transitions conformationnelles.

Reçue le 10 Avril 1985

Institut de Chimie Macromoleculaire „P. Poni", Jassy

BIBLIOGRAPHIE

1. Urwin J.R., Girolamo M., Makromol. Chem., *150*, 179 (1971).
2. Dondos A., Benoit H., Makromol. Chem., *178*, 1 089 (1977).
3. Dondos A., Makromol. Chem., *147*, 123 (1971).
4. Dondos A., Rempp P., European Polym. J., 3, 657 (1967).
5. Dondos A., J. Polym. Sci., **B9**, 871 (1971).
6. Simionescu C.I., Rabia I., Harfas I., Polym. Bull., **7**, 129 (1982).
7. Simionescu C.I., Rabia I., Crişan Z., Polym. Bull., **7**, 217 (1982).
8. Simionescu C.I., Rabia I., Polym. Bull., **10**, 311 (1983).
9. Gosa K., Donescu D., Makromol. Chem., *182*, 1 725 (1981).
10. Dondos A., Makromol. Chem., *99*, 175 (1966).
11. Kimura S., Kurata M., Macromolecules, **14**, 1 104 (1981).
12. Petrea C., Gosa K., Donescu D., Materiale Plastice (Bucureşti), **16**, 1 (1979).
13. Dondos A., Rempp P., Benoit H., Makromol. Chem., *130*, 233 (1969).
14. Kratochvil P., Makromol. Chem., *148*, 271 (1971).
15. Skoulios A., Makromol. Chem., *148*, 305 (1971).

TRANZIŢII CONFORMAŢIONALE ÎN TRIBLOCCOPOLIMERI DE TIP *ABA*

(Rezumat)

Conformaţia în soluţie a unor tribloccopolimeri de tip *ABA*, (poli(N-acil etilenimină-b-etilenglicol adipat-b-N-acil etilenimină) şi poli(N-acil etilenimină-b-etilenoxid-b-N-acil etilenimină), unde blocul *A* are proprietăţi termoplastice iar blocul *B* proprietăţi elastice, a fost studiată prin metoda viscozimetrică. Variaţia viscozităţii reduse în soluţie diluată a tribloccopolimerilor funcţie de temperatură, concentraţia şi compoziţia amestecului binar de solvenţi arată existenţa unor tranziţii conformaţionale.

BULETINUL INSTITUTULUI POLITEHNIC DIN IAŞI
Tomul XXXI (XXXV), Fasc. supl., 1985
Secţia II
CHIMIE ŞI INGINERIE CHIMICĂ

D.C. 54 92

PHOTOCROSSLINKING PROCESSES IN SOLID FILMS

I. A THEORETICAL DISCUSSION OF THE METHODS TO INCREASE THE THICKNESS OF PHOTOINSOLUBILIZED LAYER

BY

VIRGIL BĂRBOIU, GEORGE ERVANT GRIGORIU, ELENA RUSU, TEODOR MARCU and EMIL BURUIANĂ

1. Introduction

It is known that the photocrosslinking polymers are used as negative photoresists. Such polymers contain ethylenic bonds which can be easily crosslinked under illumination. Many publications, especially patents, exist on this field. Many of them are refered to polymers with cinnamoyl groups, perhaps because such systems are suitable models for the study of the photocrosslinking process [1]...[10].

It was observed by studying the photocrosslinking of vinyl alcohol — vinyl acetate — vinyl cinnamate copolymers that the thickness of photoinsolubilized layer increases if the cinnamoyl group content is decreased (Fig. 1) [11], [12]. Such an observation is important to obtain photocrosslinking polymers used as negative photoresists because if the photoinsolubilized layer is too thin relative to the photoresist film then the developed image is poor or even absent due to the slide of the insoluble layer on the internal soluble layers. One of the ways to avoid such troubles would be to decrease the film thickness but this must not be smaller than 1...2 μ because otherwise the photoresist film becomes penetrable for the chemical reagents used for the processing of the support. The observation illustrated on Fig. 1 seems to lead to the supposition that the photoinsolubilized layer thickness (denoted by x_r) can be increased by decreasing the photocrosslinking group density. However it is evidently that such a decreasing is limited because it also leads to the decreasing of the probability of having pairs of two neighbouring photoactive groups.

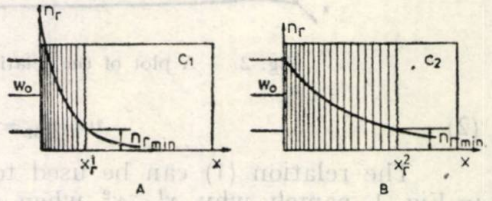

Fig. 1. — An illustration of the depth dependence of the photocrosslinked group density (n_r) for unsensitized photocrosslinking polymers. The two investigated polymers are vinyl alcohol — vinyl cinnamate copolymers with different vinyl cinnamate contents ($C_1 > C_2$). The irradiation and developing conditions were the same, and the illumination was made by the film supports which were quatz plates.

The present paper is refered to some supposed physical relationships characterizing the photocrosslinking phenomena into rigid systems (with fixed photoactive groups) developed with the purpose to find ways to increase the photoinsolubilized layer thickness.

2. Photocrosslinking due to the Normal Absorption of the Photocrosslinking Groups

Denoting the density of photocrosslinking groups by n, the probability to have two such groups in a steric arrangement favourable to the crosslinking reaction will be proportional to n^α, where α is a positive number. In addition, taking into account that the radiation intensity decreases exponentially with layer thickness, the density n_r of photocrosslinked groups at a depth x inside the film will depend on n according to :

$$n_r \sim \eta w_0 n^\alpha \exp(-\varepsilon n x), \tag{1}$$

where η is the yield of the photocrosslinking processes, w_0 — the initial irradiation energy and ε — the extinction coefficient. A plotting of the dependence of n_r on n and x is given in Fig. 2 for the case when $\alpha = 2$. It is observed that the density n_r at a depth x is maximum when

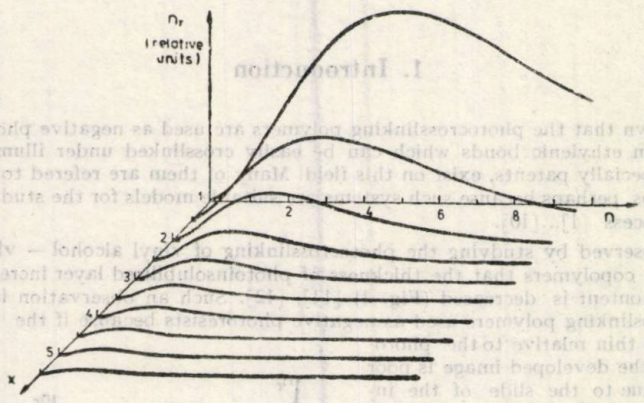

Fig. 2. — A plot of the relationship (1) for the case $\alpha = 2$.

$$n = n_M = \alpha/\varepsilon x. \tag{2}$$

The relation (1) can be used to explain the observation illustrated in Fig. 1, namely why $x_r^1 < x_r^2$ when $C_1 > C_2$. Let us suppose that $n_{r\min}$ is the lowest value of n_r for which the irradiated polymers are insoluble. Denoting by n_0 and n the initial densities of photocrosslinking groups for the two polymers in solid state (the first having a photocrosslinking group content of 100%, and the other a lower content) and by x_r^0 and x_r the photoinsolubilized layer thicknesses for the two cases, the following relations can be written :

$$n_{r\min} = \text{const.}\ n_0^\alpha \exp(-\varepsilon n_0 x_r^0) = \text{const.}\, n^\alpha \exp(-\varepsilon n x_r), \tag{3}$$

from where it results

$$x_r = \frac{n_0}{n} x_r^0 - \frac{\alpha}{\varepsilon n} \ln \frac{n_0}{n}. \tag{4}$$

The mathematical analysis of the relation (4) shows that x_r has a maximum value, $x_{r\max}$, when $n = n_{optim}$ (s. Fig. 3), where

(5) $$n_{optim} = n_0 \exp(1 - \varepsilon x_r^0/\alpha) \text{ and } x_{r\max} = (\alpha/\varepsilon n_0)/\exp(1 - \varepsilon n_0 x_r^0/\alpha).$$

It is observed that $n_{optim} < n_0$ and $x_{r\max} > x_r^0$ if $\varepsilon n_0 x_r^0 > \alpha$, the last condition being fulfiled if the irradiation energy is high enough.

The relation (4) with $\alpha = 2$ is plotted in Fig. 3 for the systems containing cinnamoyl groups grafted on vinyl alcohol—vinyl acetate copolymers, where $\varepsilon \approx 4 \times 10^3$ l/mol. cm ($\lambda_{max} = 280$ nm), $n_0 = 6$ mol/l and $x_r^0 = 1.5\ \mu$ ($w_0 \approx 2$ J/cm², xenon source). It is observed from this figure, or by using the relations (5), that

(6) $$n_{optim} = 0.45 n_0 \text{ and } x_{r\max} = 1.25 x_r^0.$$

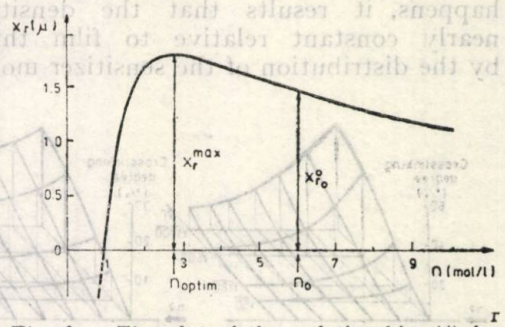

Fig. 3. — The plot of the relationship (4) fo polymers with photocrosslinking groups of cin namoyl type.

The last relations show that the cinnamoyl containing polymers are good negative photoresists if their cinnamoyl group content is equal to 40...50%. On the other hand, the increase of x_r by decreasing the cinnamoyl group concentration is theoretically quite small, therefore with no practical interest. An alternative method to increase x_r^0 and therefore $x_{r\max}$ would be to increase the irradiation energy, w_0, but such a procedure is not indicated because the photodegradation becomes important relative to the photocrosslinking in the surface layer.

The next two phenomena allow important increases of x_r^0 and $x_{r\max}$ in conditions of low photodegradation effects.

3. Sensitized Photocrosslinking

The quantum yield of photocrosslinking processes in the rigid systems can be significantly increased if some molecules known as sensitizers are present [1]...[3], [7]...[10]. The sensitizers realize both a matching between the absorption spectrum of the photoresist and the spectrum of the used ligth source, and an important increase of the photoinsolubilized layer thickness. Denoting by η', ε' and n', the quantum yield, the extinction coefficient and the density of photosensitizer molecules, the density of photocrosslinked groups at a depth x will be given by the following relationship:

(7) $$n_r^s \sim n' w_0 n^\alpha \exp(-\varepsilon' n' x),$$

if the illumination is made on the sensitizer absorption bands.

To estimate the sensitizer effect on the photoinsolubilized layer thickness (denoted by x_r' in the relation (8)), by comparison with the unsensitized photocrosslinking process, the following equalities must be used:

(8) $$n_{r\min} = \text{const.}\, \eta n^{\alpha} \exp(-\varepsilon n x_r) = \text{const.}\, \eta' n'^{\alpha} \exp(-\varepsilon' n' x'_r).$$

Now it is very easy to obtain the expression of x'_r :

(9) $$x'_r = \frac{\varepsilon n}{\varepsilon' n'} x_r + \ln \frac{\eta'}{\eta}.$$

As $\eta' > \eta$, $n/n' \approx 10...10^2$ and $\varepsilon \approx \varepsilon'$,, it results that $x'_r > (10...10^2) x_r$, therefore the sensitization method assures an important increase of x_r. In addition, if $\eta' \gg \eta$ and λ_{max} (sensitizer) $> \lambda_{max}$ (photocrosslinking groups) as it usually happens, it results that the density of photocrosslinked groups is nearly constant relative to film thickness, being mainly determined by the distribution of the sensitizer molecules (which is evidently uniform).

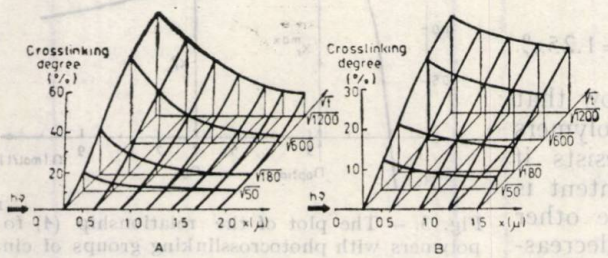

Fig. 4. — The dependence of the average photocrosslinking degree on the irradiation time and on the light penetration depth for polyvinyl alcohol 50% esterified with cinnamoyl groups : *A* — unsensitized polymer irradiated with 15...20 mW/cm² (mercury source), and *B* — sensitized polymer with 10% Michler's cetone, monocromatic illumination (360 nm) of about 0.5 mW/cm². The photocrosslinking degree was estimated from the relative decreasing of the cinnamoyl group absorption band at 280 nm ; the time is given in seconds.

For comparision, Fig. 4 shows the dependence of the photocrosslinking degree on the irradiation time and on the ligth penetration depth for a polymer containing cinnamoyl groups in two cases : unsensitized (Fig. 4 *A*) and sensitized (Fig. 4 *B*). It is observed that the sensitizer (Michler's cetone) realizes both a visible increasing of the photocrosslinking degree /irradiation energy ratio, and a weak dependence of the photocrosslinking degree on the depth of radiation penetration.

4. Photocrosslinking in Systems with Donor—Acceptor Interactions

The idea to sensitize photocrosslinking processes by interactions between electron donor and electron acceptor groups is quite recent [13], [14]. Its principle is to use a mixture of two photocrosslinking polymers, one having donor-type photoactive groups and the other having acceptor-type photoactive groups. Our observations were made using *p*-methoxycinnamoyl groups as donor groups and *p*-nitrocinnamoyl groups as acceptor groups. As expected, the complexation interactions lead to two effects which are favourable to the photocrosslinking processes : a) the increase of the probability of having pairs of two photocrosslinking groups due to the cross dimer formation, and b) the shift to the visible range of the light absorption due to the charge transfer complex band, and therefore a better matching on the actual light sources.

It was observed that the photocrosslinking appears at quite low concentrations of complexable groups (10...20%). For this reason it is expected from such a photocrosslinking to be slightly dependent on the penetration depth of radiation. Another advantage of this method is that the photoreactions are not influenced by air, while the photoreactions induced by sensitizers are inhibited by oxygen. The main disavantage of this method is the low solubility of systems with donor—acceptor interactions. For example, their solutions in common solvents are opalescent even at concentrations lower than 10% and, consequently, their dried films show a rugged surface. For this reason it would be indicated to use weak donor—acceptor interactions, but the sensitizations effects will be small in this case.

5. Conclusions

The photocrosslinking polymers can be used as negative photoresists if they are sensitized with suitable molecules. For a good matching between the photoresist absorption spectrum and the source emission spectrum it is required for sensitizer molecules to have λ_{max} in the visible range or in the near UV range. To obtain a large thickness of the photoinsolubilized layer, the sensitizer concentration must be much lower than the concentration of photocrosslinking groups on the polymer. The last concentration must be lowered up to an optimum value which is of 40...50% in the case of cinnamoyl groups. Perhaps the best results can be obtained if one sensitizer molecule complexes by weak donor—acceptor interactions with two photocrosslinking groups.

Received, April 10, 1985

„Petru Poni" Institute of Macromolecular Chemistry, Jassy

REFERENCES

1. Williams J.R.L., *Photopolymerization and Photocrosslinking of Polymers*, in *Topics in Current Chemistry*, Bd. 13, H. 2, Springer-Verlag, Berlin-Heidelberg, 1969.
2. Finch C.A. (Ed.), *Polyvinyl Alcohol: Properties and Applications*. Wiley-Interscience, London, 1973.
3. Rånby B., Rabek J.F., *Photodegradation, Photo-oxidation and Photostabilization of Polymers* Wiley-Interscience, London, 1975.
4. Rånby B., invited lecture at the 29th Symposium on Macromolecules, Bucharest, Sept. 1983.
5. Tsuda M., Bull. Chem. Soc. Japan, **42**, 905 (1969).
6. Воскобойник Г.А., Гришанова Н.Г., Соболева Е.Б., Рябов А.В., Феодоров Ю., Высокомол. Соед., **A 14**, 2472 (1972).
7. Белякова А.П., Боков Ю.К., Лавришев В.П., Коновалов П.Г. Васкевич Д.Н., Высокомол. Соед., **A7**, 1637 (1965).
8. Nakamura K., Kikuchi S., Bull. Chem. Soc. Japan, **41**, 1977 (1968).
9. Rabek J.F., Zaleski A., Polimery, **15**, 437 (1970); **16**, 1 (1971); **18**, 57 (1971).
10. Sierocka M., Paczkowski J., Wrzyszczynski A., Zakrzewski A., Polimery, **21**, 449 (1976).
11. Bărboiu V., Grigoriu G.E., Buruiană E., Chelaru E., Materiale Plastice, **20**, 190 (1983).

12. Bărboiu V., Buruiană E., Grigoriu G.E., Chelaru E., poster at the 20th Symposium on Macromolecules, Bucharest, Sept. 1983, Abstract Volum, section VII, 371.
13. Watanabe S., Ichimura K., J. Polym. Sci., Polym. Chem. Ed., **20**, 3 261 (1982).
14. Smets G., invited lecture at the 29th Symposium on Macromolecules, Bucharest, Sept. 1983.

PROCESE DE FOTORETICULARE ÎN FILME SOLIDE

I. O discuție teoretică a metodelor de creștere a grosimii stratului fotoinsolubilizat

(Rezumat)

Este explicată dependența densității grupelor fotoreticulate de densitatea inițială de grupe fotoreticulabile și de adîncimea de pătrundere a luminii atît în cazul polimerilor nesensibilizați cît și în cazul polimerilor sensibilizați. În primul caz s-a găsit că grosimea stratului fotoinsolubilizat poate fi puțin crescută printr-o micșorare adecvată a densității inițiale de grupe fotoreticulabile. De asemenea, se demonstrează că această grosime poate fi mult crescută în al doilea caz dacă densitatea moleculelor de sensibilizator este mult mai mică decît densitatea grupelor fotoreticulabile. În final sînt date unele considerații asupra sistemelor caracterizate prin interacții intermoleculare între grupe fotoreticulabile de tip donor și de tip acceptor de electroni.

BULETINUL INSTITUTULUI POLITEHNIC DIN IAȘI
Tomul XXXI (XXXV), Fasc. supl., 1985
Secția II
CHIMIE ȘI INGINERIE CHIMICĂ

D.C. 541.182.6

MASS TRANSFER DURING THIN FILM FLOW OF SUSPENSIONS

BY

RADU Z. TUDOSE, ECATERINA MERICĂ and ȘT. UNGUREANU

1. Introduction

The increase of rate of mass transfer processes is a question of wide scientific interest. The development of chemical industry determined the search for new possibilities of intensifying the heat and mass transfer without having to increase the scale of apparatus.

The flow in thin films was found to be an efficient way to improve transfer processes. The advantages of this procedure are well known and a large number of researchers have devoted their studies to this type of flow [1] ... [9].

A particular attention was paid to the factors which are able to influence the film hydrodynamics, mass or heat transfer such as flow regime, rugosity, geometrical features, presence of surfactants, viscosity, etc.

However, in spite of the large number of papers in the field, the flow and mass transfer in thin films of nonnewtonian fluids are rather scarcely approached [10] .... [12]. As far as it is mentioned in the available literature, excepting for the A s t a r i t a's trial concerning the flow of suspensions, no other paper was found in literature.

The aim of the present paper was to answer to the following questions :

a) How does the solid phase influence the rate of mass transfer in thin films?

b) What fluid flow characteristics lead to higher values of individual mass transfer coefficient, k_L?

c) How does k_L vary, in the same sistem, with concentration, granulation and density of dispersed phase ?

d) How are located the experimental data within the general context of literature informations ?

2. Experimental

The absorption of carbon dioxide in water and ABS copolymer suspensions was investigated on the equipment depicted in Fig. 1.

Thr absorption column (*1...3*) is formed of two concentric pipes. The descending film flows on the external wall of the internal pipe ($\varphi = 30 \times 3$ mm, Ni—Cr-alloy steeal, $L = 2\,285$ mm). In the annular space between the external pipe (plexiglass, $\varphi - 60 \times 6$ mm) and the fluid film, the gas (carbon dioxide) flows in counter current. At the bottom the column is provided with a micrometric device allowing the column movement up and down. At the top, the column is provided with a distribution head which assures the formation of thin film on the internal pipe. The gap width is adjusted by

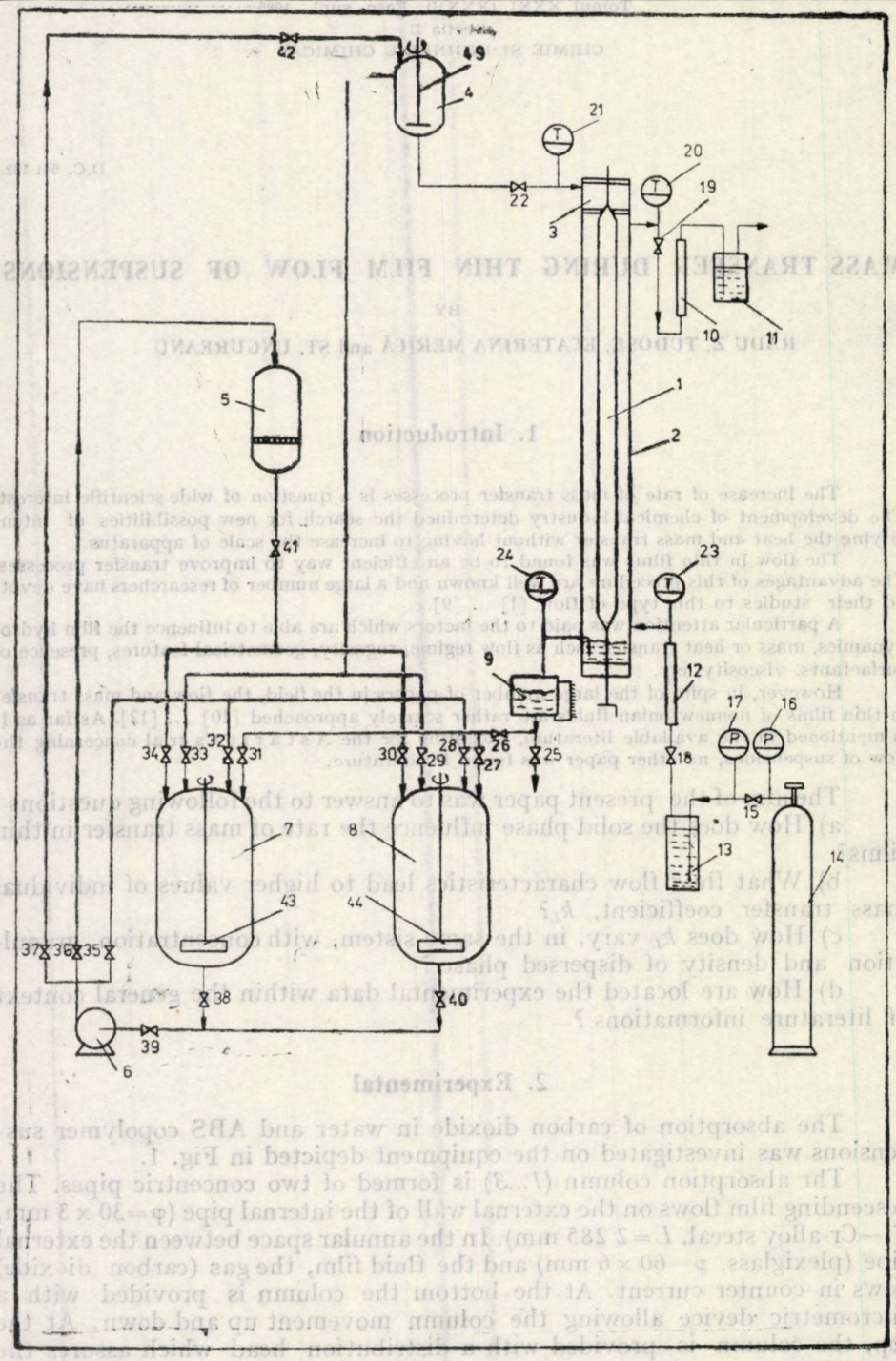

Fig. 1. — Sketch of experimental apparatus.

the internal tube displacement up and down. The liquid is taken from the supply tank with a pump and sent to the level vessel *45* from which enters the distribution head and the column. The two tanks work alternatively, one receives the liquid while from the other the column is feeded. Both tanks ($V = 300$ L) and the level vessel are provided with mixers for being able to maintain the particles in suspension.

The admission of carbon dioxide, in countercurrent, from a gas tube, was adjusted by means of two flowmeters, one for a coarse adjustement, the other for a fine one.

To prevent from water diffusion in gas, the latter was saturated by bubbling in a water vessel prior to the introduction in the column.

The flow rate at the exit was measured by timing the time required for the collection of a known volume of liquid.

The analysis for carbon dioxide was accomplished by precipitating the carbon dioxide as barium carbonate by use of a mixture of barium chloride and standard sodium hydroxide. The excess sodium hydroxide was then titrated with hydrochloric acid to a phenolpthalein end point.

The concentration of carbon dioxide in the liquid was calculated with the relation :

$$x = \frac{0.55(n_1 - n_1')T_1}{V}, \tag{1}$$

where : x denotes the concentration of carbon dioxide in liquid, [g/mL] ; n_1 — number of mL of standard NaOH solution introduced initially in sample; n_1' — number of mL of NaOH solution found in excess (determined titrimetrically) ; V — sample volume ; 0.55 — equivalent ratio.

Prior to each set of measurements a witness sample was taken (zeroth sample), the initial carbon dioxide content being thus determined.

The mass transfer coefficient in liquid phase, k_L, based on mean logarithmic driving force, was calculated, for the absorption of pure gas, at 1 atm pressure. In practical calculation the external surface of the internal pipe was assumed to be the mass transfer surface. Given the high purity of gas, the resistance of gaseous phase was neglected as well as the effect of water vapours, since the gas was previously saturated with liquid. A temperature multipoint recorder (4 points) was used (liquid and gas entrances and exits, respectively) and the physical constants used in calculations were corrected for the mean liquid temperature during the run.

The viscosity measurements for the suspensions (ABS copolymer, $0{,}12 < \varnothing < 0{,}15$ mm, 1, 2, 4 and 7% in weight) were taken on a concentric cylinder viscometer of Rheotest, DDR, type. The measurements were taken at there temperatures : 20°; 25° and 30°C. Where the readings at intermediate temperatures were not conclusive the data for 20° and 30°C were retained. Since the suspension behaviour was found to be of a Bingham plastic type the values of extrapolated viscosity were taken in calculations.

3. Results and Discussion

The experimental results obtained with water and the four suspensions are depicted in Figs. 2...6 as $\mathcal{S}h = f(\mathcal{R}e)$ correlation.

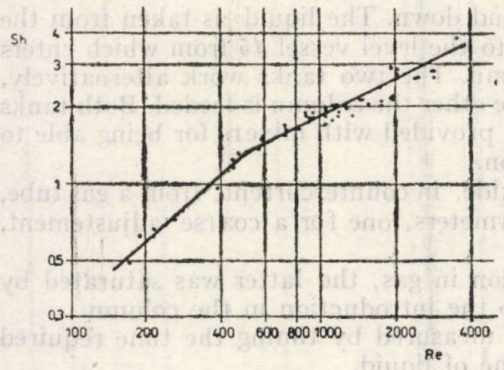

Fig. 2. — Correlation $Sh = f(Re)$ in case of water.

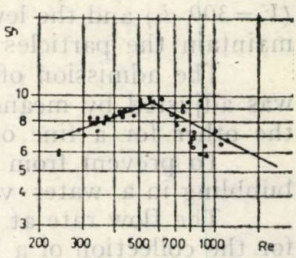

Fig. 3. — Correlation $Sh = f(Re)$ in case of ABS, 1% suspension.

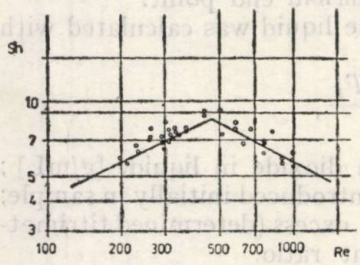

Fig. 4. — Correlation $Sh = f(Re)$ in case of ABS, 2% suspension.

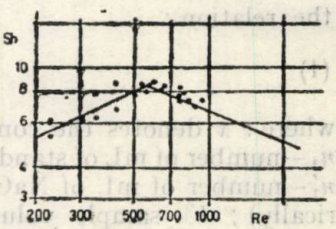

Fig. 5. — Correlation $Sh = f(Re)$ in case of ABS, 4% suspension.

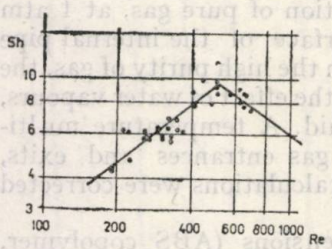

Fig. 6. — Correlation $Sh = f(Re)$ in case of ABS, 7% suspension.

As can be seen in Figs. 3...6 the introduction of solid phase strongly influences the mass transfer results. The increase of mass transfer rate up to a certain Re value is noticed in all cases, followed by a marked decrease above the critical value. The critical Re value was found to be of about 500. The difference from water is very clear.

The experimental data worked on a computer allowed to obtain the following correlations :

a) Water

$$(2)\qquad \begin{cases} Sh = 5.324 \times 10^{-3} Re^{0.89} & (Re < 500), \\ Sh = 0.0872\, Re^{0.44}, & (Re > 500)\ ; \end{cases}$$

b) ABS, 1% suspension

$$(3)\qquad \begin{cases} Sh = 0.38\, Re^{0.15}, & (Re < 600), \\ Sh = 238\, Re^{-0.51}, & (Re > 600)\ ; \end{cases}$$

c) ABS, 2% suspension

$$(4)\qquad \begin{cases} \mathcal{S}h = 0.450\,\mathcal{R}e^{0.48}, & (\mathcal{R}e < 500), \\ \mathcal{S}h = 196\,\mathcal{R}e^{-0.51}, & (\mathcal{R}e > 500)\ ; \end{cases}$$

d) ABS, 4% suspension

$$(5)\qquad \begin{cases} \mathcal{S}h = 0.433\,\mathcal{R}e^{0.47}, & (\mathcal{R}e < 600), \\ \mathcal{S}h = 94.5\,\mathcal{R}e^{-0.38}, & (\mathcal{R}e > 600)\ ; \end{cases}$$

e) ABS, 7% suspension

$$(6)\qquad \begin{cases} \mathcal{S}h = 0.0848\,\mathcal{R}e^{0.76}, & (\mathcal{R}e < 600), \\ \mathcal{S}h = 6005\,\mathcal{R}e^{-0.66}, & (\mathcal{R}e > 600). \end{cases}$$

As seen in Figs. 5 and 6, the results for more concentrated suspensions, at higher $\mathcal{R}e$ values, are more dispersed. The results were generally reproducible excepting for $\mathcal{R}e$ values higher than 800 and larger ABS concentrations (above 7%).

Received, April 25, 1985

Polytechic Institute, Jassy,
Department of Chemical Engineering

REFERENCES

1. Emmert R.E., Pigford R.L., Chem. Eng. Process, **50** (2), 88 (1954).
2. Lamourelle P.A., Sandal C.O., Chem. Eng. Sci., 1035 (1972).
3. Blas E., Int. Chem. Eng., **19**, *2* (1972).
4. Koziol K., Broniarz L., Nowicka T., Int. Chem. Eng., **20**, *1*, 136 (1980).
5. Koziol K., Broniarz L., Int. Chem. Eng., **20**, *1*, 143 (1980).
6. Холпанов К.П., Малюсов В.А., Хаворонков М.М., Теор. осн. хим технол., **16**, *3*, 291 (1982).
7. Накоряков В.Е., Покусаев Б.Г., Алексеенко С.В., *Расчет тепломасообмена энергохимических процессах*. 1981, 23; C.A., 98, 56298 u (1983).
8. Tudose R.Z., Zăinescu C., Svieciński M., Mem. Secț., Șt., Acad. R.S.R., **3**, *1*, 215, 1980 (1981).
9. Ibănescu I., Tudose R.Z., Rev. chim., **23**, *2*, 114 (1972).
10. Gottifreddi J.C., Gonzo E.E., J. Non-Newtonian Fluid Mech., **10**, *3—4*, 357 (1982).
11. Astarita G., Ind. Eng. Chem. Fundls., 4, 236 (1965).
12. Mohr M.C.Jr, Williams C.M., A.I.Ch.E. Journal, **19**, *5*, 1047 (1973).

STUDIUL TRANSFERULUI DE MASĂ LA CURGEREA ÎN FILME SUBȚIRI A SUSPENSIILOR

(Rezumat)

A fost studiat transferul de masă la curgerea în filme subțiri la apă și patru suspensii în apă de copolimer ABS, 1, 2, 4 și 7% în greutate. S-a găsit că absorbția de CO_2 este puternic influențată de prezența fazei solide. Pînă la un anumit $\mathcal{R}_e$ coeficientul de transfer în fază lichidă k_L, crește, după care scade brusc.

BULETINUL INSTITUTULUI POLITEHNIC DIN IAŞI
Tomul XXXI (XXXV), Fasc. supl., 1985
Secţia II
CHIMIE ŞI INGINERIE CHIMICĂ

SYNTHETIC FIBRE WORKS, IAŞI, a modern unit of advanced technology, much ahead in Romania chemical industry, produces and deliveries a wide range of polyester fibres and yarns as well as equipments and spare parts for chemical and textile industry as it follows:.

— Polyester staple fibre, cotton, wool and flax type, raw white, bright or dyed.
— Polyester textiles yarns.
— Polyester textiles twisted yarns for courtains and tissues.
— Polyester continuous filament drawn yarns for sewing thread.
— Polyester continuous filament textured yarns of different linear densities, twisted, bright or semidull, of round or profiled cross section, raw white or dyed suitable for knittings, tissues and cloths.

Colour card for dyed yarns includes about 100 shades classified in : light, medium and heavy shades.

Comfort, absorbency and easy care properties combined with stability and shape retention are essential qualities of the products marketed by **SYNTHETIC FIBRE WORKS, IAŞI.**

— Polyester industrial yarns (drawn, twisted, plyed) for different technical end-uses where its abrasion resistance, thermal stability and chemical proofing are highly appreciated.
— Polyester films (transparent or light dull) for electrotechnical end-uses.
— Besides its textile and chemical profile, **SYNTHETIC FIBRE WORKS, IAŞI,** is also a producer of equipments used in chemical and textile industries such as :

- precision conning machines on the basis of Schweiter licence ;
- drawing lines for polyester or polyamide fibres ;
- refrigeration plants ;
- cutting knives for tow to top converters and a host of other operations or special treatments.

The **SYNTHETIC FIBRE WORKS, IAŞI,** exports its products by :
ICE DANUBIANA, Serv. 71 Bucharest, telex 10073 (polyester yarns and fibres) ;
ICE CHIMIMPORTEXPORT, Serv. 7, Bucharest, telex 11184 (chemical products) ;
ICE INDUSTRIALEXPORT IMPORT, Serv. 42, Bucharest, telex 10052 (equipments and spare parts).

For any additional details please write directly to :

COMBINATUL DE FIBRE SINTETICE, IAŞI,

29 Ţuţora St., Code 6600

Telephone : 30020 ; Telex : 022251

CENTRALA INDUSTRIALĂ DE FIBRE CELULOZĂ ȘI HÎRTIE – BRĂILA –

COMBINATUL DE CELULOZĂ ȘI HÎRTIE

L E T E A

B A C Ă U

PRODUCE:

- hîrtie de ziar
- hîrtie de scris si tiparit
- hîrtii ambalaj
- hîrtii speciale
- hîrtii subtiri
- hîrtii tigarete
- hîrtii absorbante pentru
- industria mobilei
- hîrtie igienică
- cartoane
- caiete școlare
- drojdie furajeră

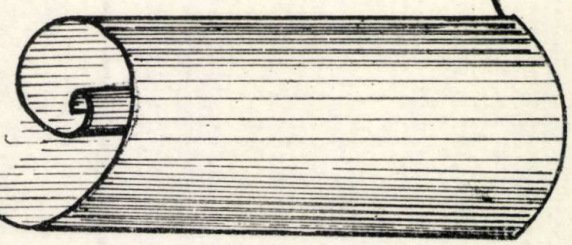

CENTRALA INDUSTRIALĂ DE FIBRE CELULOZĂ ȘI HÎRTIE
– BRĂILA –

BULETINUL INSTITUTULUI POLITEHNIC DIN IAŞI
Tomul XXXI (XXXV), Fasc. supl., 1985
Secţia II
CHIMIE ŞI INGINERIE CHIMICĂ

CENTRALA INDUSTRIALĂ DE FIBRE, CELULOZĂ ŞI HÎRTIE BRĂILA

COMBINATUL DE FIBRE, CELULOZĂ ŞI HÎRTIE SUCEAVA

PRODUCE :

1. Celuloză sulfat naturală.
2. Hîrtie pentru saci, hîrtie ambalaj rezistentă, hîrtie extensibilă, hîrtie impregnată pentru filtre de aer, ulei, combustibil.
3. Fibre artificiale din vîscoză.
4. Fire mătase vîscoză.
5. Produse înnobilate : hîrtii gumate, hîrtii creponate, hîrtii acoperite cu parafină, hîrtii acoperite cu polietilenă, hîrtii bitumate, complexe anticorozive pentru ambalat piese metalice, diverse ţesături acoperite cu polietilenă, complexe suport abrazive, pînză cauşurată cu polietilenă pe hîrtie.
6. Saci şi pungi din hîrtie, confecţii din carton ondulat, confecţii din mucava, filtre auto şi industrie, sfoară din hîrtie.

CENTRALA INDUSTRIALĂ DE FIBRE, CELULOZĂ ȘI HÂRTIE BRAILA

COMBINATUL DE FIBRE, CELULOZĂ ȘI HÂRTIE SUCEAVA

PRODUCE:

1. Celuloză sulfat naturală
2. Hârtie pentru sacî, hârtie ambalaj rezistentă, hârtie creponată, hârtie impregnată pentru filtre de aer, ulei, combustibil.
3. Fibre artificiale din viscoză.
4. Fire mătase viscoză.
5. Produse înnobilate : hârtii gumate, hârtii creponate, hârtii acoperite cu parafină, hârtii acoperite cu polietilenă, hârtii bitumate, complexe anticorosive pentru ambalaj piese metalice, diverse țesături acoperite cu polietilenă, complexe suport abraziv, pânză cauciucată cu polietilenă pe hârtie.
6. Saci și pungi din hârtie, conteiți din carton ondulat, confecții din mucava, filtre auto și industrie, stoarfă din hârtie.

BULETINUL INSTITUTULUI POLITEHNIC DIN IAȘI
Tomul XXXI (XXXV), Fasc. supl., 1985
Secția II
CHIMIE ȘI INGINERIE CHIMICĂ

Combinatul de Fibre Sintetice, Săvinești, produce și livrează :

- **Fire și fibre sintetice :**

— fibre acrilice Melană (R) ;
— fibre poliamidice Relon (R) ;
— fire poliamidice textile Relon (R) ;
— fire poliamidice covor Relontex (R) ;
— fire poliamidice tehnice și cord Relon (R) ;
— corzi perii.

- **Produse chimice :**

— caprolactamă ;
— acid adipic ;
— tetracloretan ;
— clorură de cianuril ;
— dibenzildiizocianat DBDI ;
— polietilenglicoladipat PEGA ;
— granule poliamidice pentru mase plastice ;
— bare și plăci poliamidice.

- **Utilaje și piese de schimb pentru industria de fibre sintetice :**

— linii complete de fabricare a firelor și fibrelor sintetice ;
— pompete de filare pentru fibre sintetice ;
— filiere pentru filare din topitură ;
— pompe de presiune pentru curățiri de vase în industria chimică ;
— mașini de bobinat fire ;
— mașini de sculuit ;
— fuse pentru mașini textile ;
— mașini de tăiat fibre ;
— diverse piese de schimb din industria de fibre chimice.

Producător : Combinatul de Fibre Sintetice, Săvinești — Piatra Neamț
Telex 025221-222 ; telegraf C.F.S. Săvinești

Exportatori :

— **Fire și fibre sintetice : ICE Danubiana, București,**
Spl. Independenței 202 A
Telex 11489 ; PO BOX 3915 DANAZ

— **Produse chimice : ICE Chimimportexport, București,**
Bd. Republicii 10
Telex 11184 ; PO BOX 1—74

— **Utilaje și piese de schimb : ICE Industrialexport, București,**
Str. Scaune 1—3
Telex 10052 ; PO BOX 768

BULETINUL INSTITUTULUI POLITEHNIC DIN IAŞI
Tomul XXXI (XXXV), Fasc. supl., 1985
Secţia II
CHIMIE ŞI INGINERIE CHIMICĂ

Combinatul de Fibre Sintetice, Săvineşti, produce şi livrează :

- Fire şi fibre sintetice :

— fibre acrilice Melană (R) ;
— fibre poliamidice Relon (R) ;
— fire poliamidice textile Relon (R) ;
— fire poliamidice covor Relontex (R) ;
— fire poliamidice tehnice şi cord Relon (R) ;
— corzi perii.

- Produse chimice :

— caprolactamă ;
— acid adipic ;
— tetracloretan ;
— clorură de cianuril ;
— dibenzildiizocianat DBDI ;
— polietilenglicoladipat PEGA ;
— granule poliamidice pentru mase plastice ;
— bare şi plăci poliamidice.

- Utilaje şi piese de schimb pentru industria de fibre sintetice :

— linii complete de fabricare a firelor şi fibrelor sintetice ;
— pompete de filare pentru fibre sintetice ;
— filiere pentru filare din topitură ;
— pompe de presiune pentru curăţiri de vase în industria chimică ;
— maşini de bobinat fire ;
— maşini de sculuit ;
— fuse pentru maşini textile ;
— maşini de tăiat fibre ;
— diverse piese de schimb din industria de fibre chimice.

Producător : Combinatul de Fibre Sintetice, Săvineşti — Piatra Neamţ
Telex 025221-222 ; telegraf C.F.S. Săvineşti

Exportatori :

— Fire şi fibre sintetice : ICE Danubiana, Bucureşti,
Spl. Independenţei 202 A
Telex 11489 ; PO BOX 3915 DANAZ

— Produse chimice : ICE Chimimportexport, Bucureşti,
Bd. Republicii 10
Telex 11184 ; PO BOX 1—74

— Utilaje şi piese de schimb : ICE Industrialexport, Bucureşti,
Str. Szamos 1—3
Telex 10052 ; PO BOX 768

BULETINUL INSTITUTULUI POLITEHNIC DIN IAŞI
Tomul XXXI (XXXV), Fasc. supl., 1985
Secţia II
CHIMIE ŞI INGINERIE CHIMICĂ

Synthetic Fibers Factory, Săvineşti, produces and delivres :

- **Synthetic Yarns and Fibers :**

— Melana (R) acrylic fibers ;
— Relon (R) polyamidic fibers ;
— Relon (R) polyamidic textile yarns ;
— Relontex (R) carpets polyamidic yarns ;
— Polyamidic technical yarns and Relon (R) cord ;
— Brush strings.

- **Chemical Products :**

— Caprolactam ;
— Adipic acid ;
— Tetrachlorethane ;
— Cyanuril chloride ;
— Dibenzyldiisocyanate DBDI ;
— Polyethyleneglycoladipate PEGA ;
— Polyamidic grains for plastic materials ;
— Polyamidic rods and plats.

- **Implements and Spare Parts for Synthetic Fibers Industry :**

— Full operation lines for producing synthetic yarns and fibres ;
— Spinning pumps for synthetic fibers ;
— Dies for melt spinning ;
— Pressure pumps for vessel cleaning in chemical industry ;
— Warp winding machines ;
— Shuttle sprindles ;
— Fiber-cutting machines ;
— Different spare parts for chemical fibers industry.

Producer : Combinatul de Fibre Sintetice Săvineşti, Piatra Neamţ,
Telex 025221-222 ; telegraph CFS Săvineşti.

Exporters :

— **Synthetic Yarns and Fibers : ICE Danubiana, Bucureşti,**
Spl. Independenţei 202 A
Telex 11489 ; PO BOX 3915 DANAZ

— **Chemical Products : ICE Chimimportexport, Bucureşti,**
Bd. Republicii 10
Telex 11184 ; PO BOX 1—74

— **Implements and Spare Parts : ICE Industrialexport, Bucureşti,**
Str. Scaune 1—3
Telex 10052 ; PO BOX 768

BULETINUL INSTITUTULUI POLITEHNIC DIN IAŞI
Tomul XXXI (XXXV), Fasc. supl., 1985
Secţia II
CHIMIE ŞI INGINERIE CHIMICA

Synthetic Fibers Factory, Săvineşti, produces and delivres :

- Synthetic Yarns and Fibers :

— Melana (R) acrylic fibers ;
— Relon (R) polyamidic fibers ;
— Relon (R) polyamidic textile yarns ;
— Relontex (R) carpets polyamidic yarns ;
— Polyamidic technical yarns and Relon (R) cord ;
— Brush strings.

- Chemical Products :

— Caprolactam ;
— Adipic acid ;
— Tetrachlorethane ;
— Cyanuril chloride ;
— Dibenzyldiisocyanate DBDI ;
— Polyethyleneglycoladipate PEGA ;
— Polyamidic grains for plastic materials ;
— Polyamidic rods and plats.

- Implements and Spare Parts for Synthetic Fibers Industry :

— Full operation lines for producing synthetic yarns and fibres ;
— Spinning pumps for synthetic fibers ;
— Dies for melt spinning ;
— Pressure pumps for vessel cleaning in chemical industry ;
— Warp winding machines ;
— Shuttle sprindles ;
— Fiber-cutting machines ;
— Different spare parts for chemical fibers industry.

Producer : Combinatul de Fibre Sintetice Săvineşti, Piatra Neamţ,
Telex 025221-222 ; telegraph CFS Săvineşti.

Exporters :

— Synthetic Yarns and Fibers : ICE Danubiana, Bucureşti,
Spl. Independenţei 202 A
Telex 11489 : PO BOX 3913 DANAZ

— Chemical Products : ICE Chimimportexport, Bucureşti,
Bd. Republicii 10
Telex 11184 : PO BOX 1—74

— Implements and Spare Parts : ICE Industrialexport, Bucureşti,
Str. Scaune 1—3
Telex 10052 : PO BOX 768

BULETINUL INSTITUTULUI POLITEHNIC DIN IAŞI
Tomul XXXI (XXXV), Fasc. supl., 1985
Secţia II
CHIMIE ŞI INGINERIE CHIMICĂ

L'Usine de Fibres Synthétiques, Săvineşti, produit et fournit :

- **Fils et fibres synthétiques :**

— fibres acryliques Melana (R) ;
— fibres polyamidiques Relon (R) ;
— fils textiles polyamidiques Relon (R) ;
— fils polyamidiques tapis Relontex (R) ;
— fils polyamidiques techniques et corde Relon (R).

- **Produits chimiques ;**

— caprolactame ;
— acide adipique ;
— éthane tétrachlorure ;
— chlorure de cyanurile ;
— dibenzylediisocyanate DBDI ;
— polyéthylèneglycoleadipate PEGA ;
— granules polyamidiques pour matériaux plastiques ;
— barres et plaques polyamidiques.

- **Outillages et pièces de réchange pour l'industrie des fibres synthétiques :**

— lignes technologiques pour la fabrication de fibres et fils synthétiques ;
— pompes de filage pour fibres synthétiques ;
— filières pour filage des mélanges coulées ;
— pompes à pression pour nétoyage de l'outillage de l'industrie chimique ;
— machines à bobiner ;
— brochettes de navette ;
— machines à trancher des fibres ;
— différentes pièces de réchange pour l'industrie des fibres chimiques.

Producteur : Combinatul de Fibre Sintetice, Săvineşti, Piatra Neamţ
Telex 025221-222 ; télégraphe C.F.S. Săvineşti

Exportateurs :

— **Fibres et fils synthétiques : ICE Danubiana, Bucureşti,**
Spl. Independenţei 202 A
Telex 11489 ; PO BOX 3915 DANAZ

— **Produits chimiques : ICE Chimimportexport, Bucureşti,**
Bd. Republicii 10
Telex 11184 ; PO BOX 1—74

— **Outillages et pièces de rechange : ICE Industrialexport, Bucureşti,**
Str. Scaune 1—3
Telex 10052 ; PO BOX 768

Coli tipo 9

Tiparul executat sub comanda nr. 125
la Întreprinderea poligrafică Iaşi,
str. 7 Noiembrie nr. 49